The Scientific World Journal

Plant Abio-Stress and Bioresources Utilization for Sustainable Development

Guest Editors: Hong-bo Shao, Marian Brestic, Si-Xue Chen, Zhao Chang-Xing, and Xu Gang

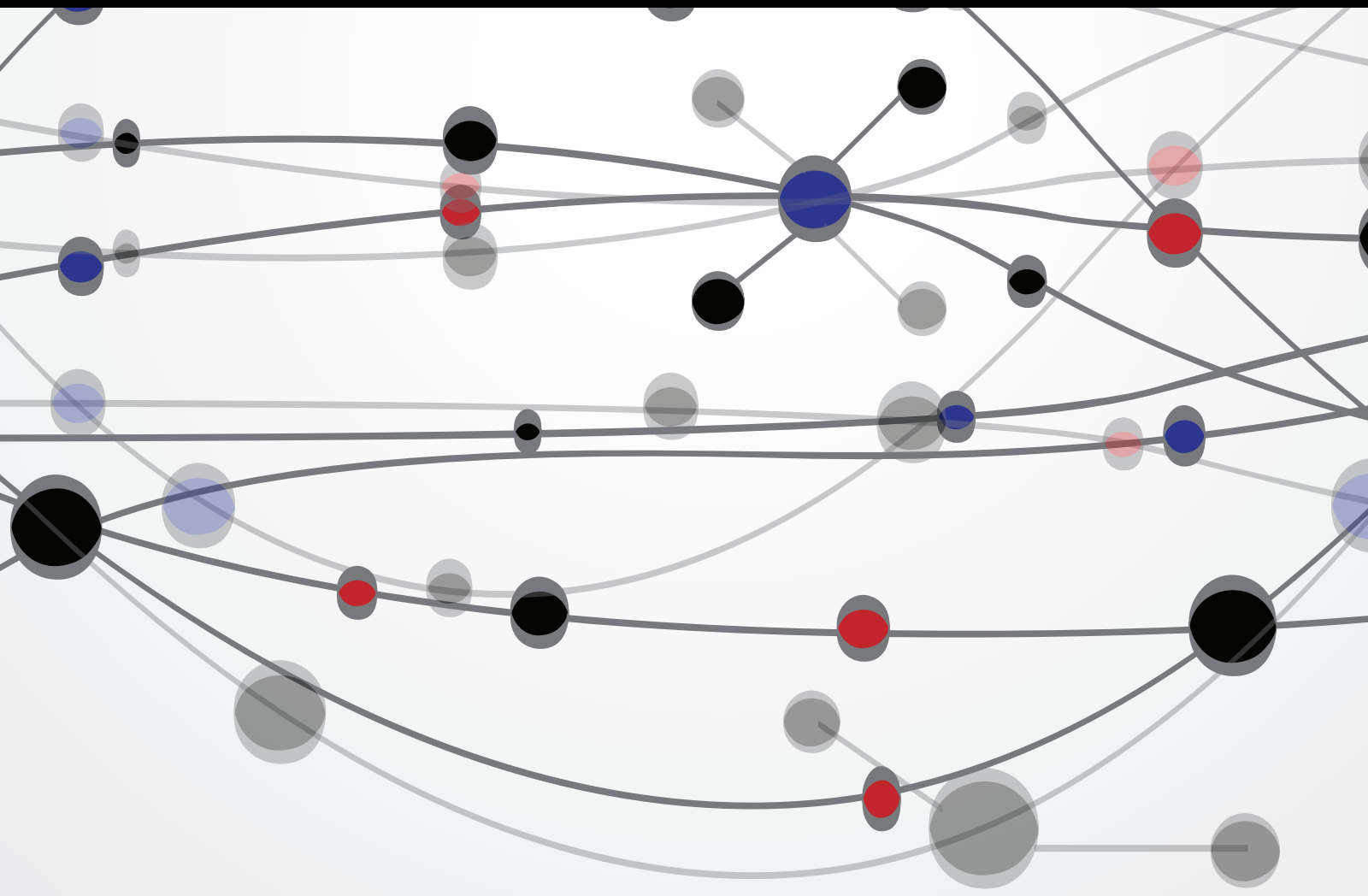

Plant Abio-Stress and Bioresources Utilization for Sustainable Development

The Scientific World Journal

Plant Abio-Stress and Bioresources Utilization for Sustainable Development

Guest Editors: Hong-bo Shao, Marian Brestic, Si-Xue Chen, Zhao Chang-Xing, and Xu Gang

Contents

Hindawi Publishing Corporation
The Scientific World Journal
Volume 2014, Article ID 163123, 2 pages
http://dx.doi.org/10.1155/2014/163123

Editorial

Plant Abio-Stress and Bioresources Utilization for Sustainable Development

Hong-bo Shao,[1,2] Marian Brestic,[3] Si-Xue Chen,[4] Zhao Chang-Xing,[5] and Xu Gang[2]

[1] *Institute of Biotechnology, Jiangsu Academy of Agricultural Sciences, Nanjing 210014, China*
[2] *Yantai Institute of Coastal Zone Research (YIC), Chinese Academy of Sciences (CAS), Yantai 264003, China*
[3] *Department of Plant Physiology, Slovak Agricultural University, Tr. A. Hlinku 2, 949 01 Nitra, Slovakia*
[4] *Cancer and Genetics Research Complex, University of Florida, 2033 Mowry Road, Room 438, Gainesville, FL 32610, USA*
[5] *College of Agronomy and Plant Protection, Qingdao Agricultural University, Qingdao 266109, China*

Correspondence should be addressed to Hong-bo Shao; shaohongbochu@126.com

Received 24 December 2014; Accepted 24 December 2014; Published 31 December 2014

Resources, environment, food, and sustainable development (REFS) are the topics of the world. There are many factors in the current world that limit plant productivity and resources utilization including objective and subjective aspects. More efforts should be made to know the physiological mechanisms for plants responding to abiotic stresses such as salt, heat, drought, cold, and UV-B, which have been extensively investigated under increasing global climate change. How to efficiently use bioresources and protect and construct eco-environment for sustainable development is the greatest challenge. As known, plants can provide human beings with renewable energy, food, and materials and are the base for sustainable development in different forms around the world. The other related issues are bioresources efficient utilization and eco-environmental construction. So, these major global challenges are the precondition of our sustainable survival.

Plants have evolved different mechanisms for adapting themselves to different stress during long-term natural evolution and domestic pressure, which at least include molecular, biochemical, physiological, cellular, organ, tissue, anatomy, individual, and ecological scales. The physiological level is very important as it is the key for farmers to fertilize and manage crops. More recent progress related with molecular biology and metabolism and bioresources and eco-environment has also taken place for the past 20 years. How to regulate plant-soils relationship for sustainable plant productivity at precise level has a long way to go not only in agriculture but also in environmental sciences. In the topic issue, many papers are devoted to this field such as soil, microbiological organisms, green-house gas, vegetation restoration, and salt soil improvement with more potential measures. Soil resources utilization is another important aspect. In soil P bioavailability is a key issue. In this special issue, some papers have been devoted to this issue and its role in eco-restoration. Partial papers about salt-resistant genes characterization and functional analysis will be of great value to further gene resources utilization in agriculture and salt soil improvement. We hope that readers of this special issue will find not only accurate data and updated articles that are involved in REFS, but also important questions to be resolved, for example, by different biomeasures. Related relationship can be referenced to Figure 1.

Hong-bo Shao
Marian Brestic
Si-Xue Chen
Zhao Chang-Xing
Xu Gang

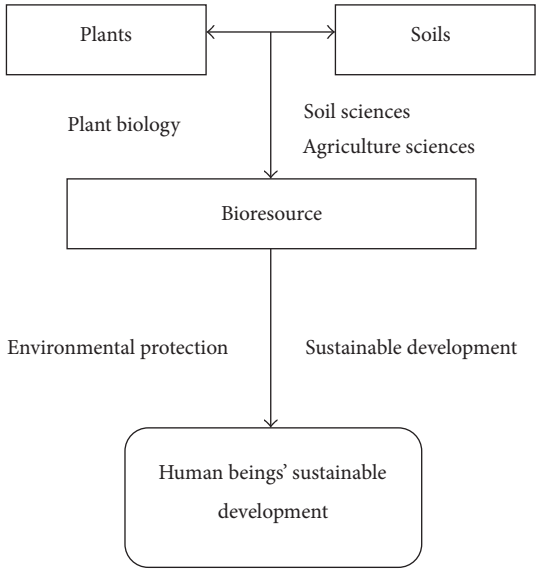
Plants
Soils
Plant biology
Soil sciences
Agriculture sciences
Bioresource
Environmental protection
Sustainable development
Human beings' sustainable development

Figure 1

Hindawi Publishing Corporation
The Scientific World Journal
Volume 2014, Article ID 618421, 9 pages
http://dx.doi.org/10.1155/2014/618421

Research Article

Effect of Continuous Cropping Generations on Each Component Biomass of Poplar Seedlings during Different Growth Periods

Jiangbao Xia,[1] Shuyong Zhang,[2] Tian Li,[1] Xia Liu,[3] Ronghua Zhang,[2] and Guangcan Zhang[2]

[1] *Shandong Provincial Key Laboratory of Eco-Environmental Science for Yellow River Delta, Binzhou University, Binzhou 256603, China*
[2] *Shandong Province Key Laboratory of Soil Erosion and Ecological Restoration, Forestry College, Shandong Agricultural University, Taian 271018, China*
[3] *Forestry College, Nanjing Forestry University, Nanjing, Jiangsu 210037, China*

Correspondence should be addressed to Jiangbao Xia; xiajiangbao2012@126.com and Guangcan Zhang; zhgc@sdau.edu.cn

Received 7 June 2014; Revised 30 June 2014; Accepted 30 June 2014; Published 23 October 2014

Academic Editor: Xu Gang

In order to investigate the change rules and response characteristics of growth status on each component of poplar seedling followed by continuous cropping generations and growth period, we clear the biomass distribution pattern of poplar seedling, adapt continuous cropping, and provide theoretical foundation and technical reference on cultivation management of poplar seedling, the first generation, second generation, and third generation continuous cropping poplar seedlings were taken as study objects, and the whole poplar seedling was harvested to measure and analyze the change of each component biomass on different growth period poplar leaves, newly emerging branches, trunks and root system, and so forth. The results showed that the whole biomass of poplar seedling decreased significantly with the leaf area and its ratio increased, and the growth was inhibited obviously. The biomass aboveground was more than that underground. The ratios of leaf biomass and newly emerging branches biomass of first continuous cropping poplar seedling were relatively high. With the continuous cropping generations and growth cycle increasing, poplar seedling had a growth strategy to improve the ratio of root-shoot and root-leaf to adapt the limited soil nutrient of continuous cropping.

1. Introduction

Due to the characteristics of fast growth, early lumber, easy to update, and so forth, the poplar is one of the most appropriate management species for industrial timber with short rotation [1]. Poplar is also a good tree species for afforestation and plains in north China, with the characteristics of long planting history, big planting area, and intensive planting measure [2] and had high stand volume per unit area and significant economic and social effect [3]. Long time monoculture and continuous cropping led to the deterioration of soil ecological environment, exhaustion of soil fertility [4], and the decrease of forest growth and productivity [2, 3]. As early as 1869, Germany had found soil fertility exhaustion which was called by a joint name "second effect," then many countries including Norway, India, France, South Africa, and former Soviet Union, also found the question of plantation soil fertility exhaustion and the decline of productivity, the referred trees included *Picea abies*, *Pinus pinaster*, and *Pinus radiate* [2, 3]. In the 1990s, the research on poplar plantation mainly focused on the mechanism of degradation and the technology of soil fertility holding on continuous cropping poplar forest land [2, 3], the biological characteristics of forest land [5], the rhizosphere effect of continuous cropping poplar plantation [4], and so forth. The research on how the continuous cropping generations led to the change of each component growth was little, and how the continuous cropping effects the distribution of each component biomass of poplar plantation was not clear, resulted in the morphology mechanism of poplar seedling adapting continuous cropping unclear, which limited the cultivation management and pattern allocation of continuous cropping poplar to some extent.

Phytocoenosium biomass, which embodies the combined action of community structure, environment, human activity, and so forth and reflects the matter production, the community structure feature, and growth status of the producer of ecological system, were an important reflection of ecological system productivity [6]. Single tree biomass is one of the main measurement indexes of community structure and function, which can indicate the capacity of plant to fix and accumulate space resource. Each tissue and organ of plant is a unified whole, and the aboveground part has important effect on underground part. The competitive capacity of plant to light resource, underground water, and mineral nutrition was achieved through comparing the biomass distribution ratio of aboveground organic and underground organic [7].

The comprehensive performance of plant growth in all environments is the response of plant biology characteristic. The distribution of plant resource is the centre content on the theoretical research of life history [8] and has important ecological and evolutionary sense, while the division of each component biomass is the response of the limited resource distribution in plant [7]. The variation of biomass distribution pattern, not only is an important way for plant to adapt divergent habitat, but also reflects the change of available resource in environment [9]. The level of each component biomass of plant can reflect the level of photosynthate accumulate in each function part, and the ratio of each component biomass can be used to analyze the change rules of plant biomass distribution patterns [7, 10]. Biomass ratio is the important indicator of plants fitness and reflects trade-off idea [7, 10]. The variation of absolute biomass in plant components reflects the distribution states and optimal distribution pattern of biomass directly, while the relative biomass embodies the dynamic balance of plant physiological metabolism and the circulation of materials, the balance included not only the balance of circulation of materials in plants, but also the balance of plant and environment. Therefore, under the condition of environment variation and stress, the study on the distribution pattern of photosynthetic carbon in plant is more meaningful than that on the accumulation of photosynthate in plant [11]. The growth situation and morphological characteristics of trees during seedling period can preferably reflect the growth potential of plant. The level of each component biomass of plant seedling can comprehensively express the influence of external factor on seedling growth and the adaptive capacity of seedling to external environment [10]. Therefore, the first generation, second generation, and third generation continuous cropping poplar seedlings were taken as study objects, and the whole poplar seedling was harvested to measure and analyze the change of each component biomass of poplar leaves, newly emerging branches, and trunks and root system during different growth period. The purpose was to investigate the response characteristics of growth status on each component of poplar seedling following by continuous cropping generations and growth period, and illuminate the change rules of biomass distribution pattern adapting continuous cropping, thereby to provide theoretical foundation and technical reference on cultivation management of poplar seedling.

2. Materials and Methods

2.1. Plant Material and Experimental Design. The experimental site is located in Dahesha forest farm, Shan County, Shandong Province, China, which is part of Yellow river delta, and the soil is yellow alluvial soil with light loamy and low organic matter content. It lies at north latitude 34°26′ and east longitude 116°04′. Four-year-old, *Populus deltoids* "I-69" cutting poplar seedlings were selected as the study material and planted in the middle of March 2012. Every tree was selected before explanting to ensure consistent seedling height, diameter at breast height, and growth situations, and the density was 2.0 m × 2.0 m. Under the same site condition, selected sample plot under the condition of first generation, second generation, and third generation continuous cropping, respectively, and the area of each sample plot was 20 m × 20 m with 120 poplar seedlings. In June, August, and the end of October, 30 poplar seedlings were selected every time, and the whole poplar seedling was harvested to measure and analyze the poplar seedling biomass accumulation and distribution. The methods were as follows: dig up the whole seedling and clean it, and four parts were divided, including leaf, one-year-old emerging branches, trunks, and root system. Inactivate enzymes under 105°C, and put them in 80°C to constant weight 30 min latter. Use CID-CI 203 to measure leaf area index (LAI), weigh dry weight of each component and calculate leaf area ratio (LAR), specific leaf area (SLA), leaf mass ratio (LMR), stem mass ratio (SMR), branch mass ratio (BMR), root/shoot ratio (R/S), and root/leaf ratio (RLR).

2.2. Statistical Analysis. All statistical analyses were performed with SPSS 16.0 and Excel 2007 for Windows. Repeated measurement analysis of variance (ANOVA) was used and differences were considered significant at $P < 0.05$.

3. Results and Discussion

3.1. The Biomass of Poplar

3.1.1. Total Biomass. Biomass is the best index of forest ecosystem productivity and the most direct expression on the level of forest ecosystem structure and function, which can reflect the comprehensive environment quality of forest ecosystem [6, 10, 11]. Single tree biomass is the main expression on accumulating energy of plant, and the distribution pattern is limited by external environment, plant age, and plant size [12, 13]. As shown in Figure 1, there were no significant difference between the total biomass of first generation and second generation continuous cropping poplar ($P > 0.05$) in the early growth period, but there was significant difference in the middle growth period and the late growth period ($P < 0.05$). With the plant growing, the differences of total biomass among the first generation, second generation, and third generation were gradually enlarged, totally followed by first generation, second generation, and third generation. Seeming from the same generation, the difference of biomass of first generation and second generation was significant ($P < 0.05$) in the middle and the late growth periods, while there

were no significant difference in the third generation biomass ($P > 0.05$); namely, the August later, the growth of third generation poplar was slow. In the middle growth period, the total biomass of first generation and second generation increased by 56.1% and 30.1% compared with that of third generation, respectively, while in the late growth period, the total biomass increased by 140.2% and 65.0% respectively. The related research showed that under the condition of continuous cropping, the tree height and the growth of volume of seven-year-old and ten-year-old I-69 poplar and I-72 poplar expressed a down trend with the increasing generation [1]. The stand biomass of the third generation and fourth generation poplar decreased significantly, and the serious spike top, putrid root, and death of whole plant appeared [3], which was similar to the conclusion that with the increasing generation, the total biomass of poplar decreased. In the period of seedling growth, the adjacent plants competed for sunshine, water, and nutrient [14]. Continuous cropping can lead to lack of soil nutrient, while the decrease of soil nutrient was most significant when the continuous cropping just had single poplar species. The above analysis showed that continuous cropping can inhibit the growth of poplar seedling, and the sequence of the biomass of poplar seedling in each growth period was followed by the first generation, the second generation, and the third generation. With the generation and growth cycle increasing, the inhibition influence was more and more significant, which might be related to the exhaustion of soil caused by continuous cropping [1].

3.1.2. Aboveground and Underground Biomass. The plasticity of biomass distribution, which runs through the whole life history of plant and decides the acquiring ability to different resources, has an important ecological significance [15]. Plant made respond to compete recourse through regulating the biomass distribution aboveground and underground, in order to ensure maximizing the limited resource [7]. As shown in Figure 2, the biomass of poplar seedling aboveground was higher than that underground; the change rules of biomass aboveground showed good consistency with the total biomass; namely, with the generation and growth cycle increasing, the growth aboveground was inhibited. In different growth periods, the sequence of the biomass aboveground was followed by the first generation, the second generation, and the third generation. In early growth period, the growth underground had no significant difference among three generations ($P > 0.05$). In middle growth period, the biomass underground had significant difference ($P < 0.05$), and the sequence was followed by the first generation, the second generation, and the third generation. In late growth period, the biomass underground had significant difference ($P < 0.05$), with the sequence followed by the second generation, the first generation, and the third generation, and the first generation poplar grew slowly. In late growth period, the biomass aboveground and underground of first generation and second generation poplar was 2.78 and 1.61 times, 1.63 and 1.74 times that of third generation, respectively. The analysis showed that the growth aboveground and underground of poplar was inhibited by continuous cropping, but the influence aboveground of continuous cropping was higher than that of underground, indicating that the inhibition aboveground was mainly caused by continuous cropping. In early growth period, the influence of continuous cropping on the growth was less, but with the growth cycle increasing, the inhibition was more obvious. In middle and late growth periods, the influence of continuous cropping on the growth underground of first generation and second generation poplars had no significant difference ($P > 0.05$) but had significant difference ($P < 0.05$) aboveground, while the growth of third generation was obviously inhibited by continuous cropping.

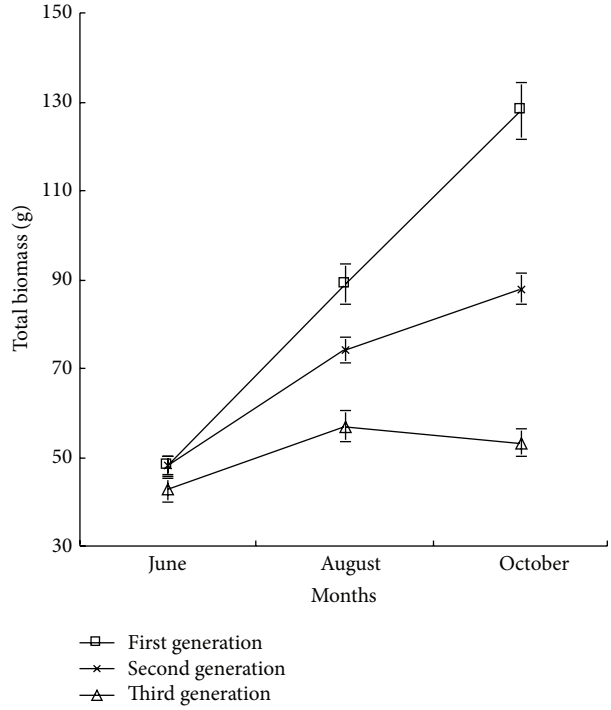

Figure 1: The growth dynamics of total biomass of poplar under different continuous croppings.

3.2. The SLA and LAR of Poplar Seedling. SLA and LAR are the important indexes to the regulation of the function of plant. With the adversity stress decreasing, the leaf assimilation rate in unit area was higher, meanwhile major LAR and SLA ensured higher light resource capture area, and both interactions ensured high biomass accumulation [11, 13–15]. As shown in Figure 3, in early growth period, there was no significant difference ($P > 0.05$) among the SLA of first generation, second generation, and third generation. In middle growth period, the SLA of first generation and second generation poplars was obviously higher than that of third generation poplar and was 2.31 and 2.21 times that of third generation poplar, respectively. In late growth period, the SLA of third generation poplar increased significantly and was 5.40 times that of the first generation poplar and 1.33 times that of the second generation poplar, respectively. To the same

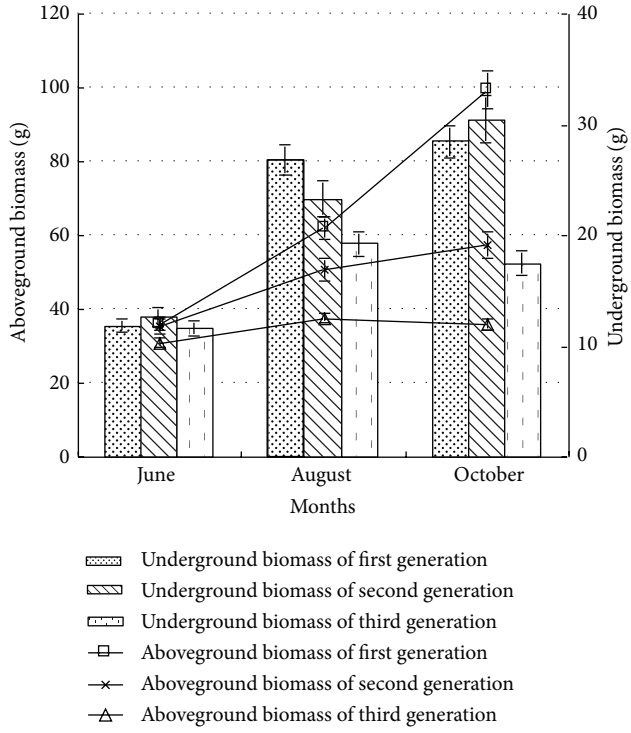

Figure 2: The aboveground and underground biomass of poplar under different continuous croppings.

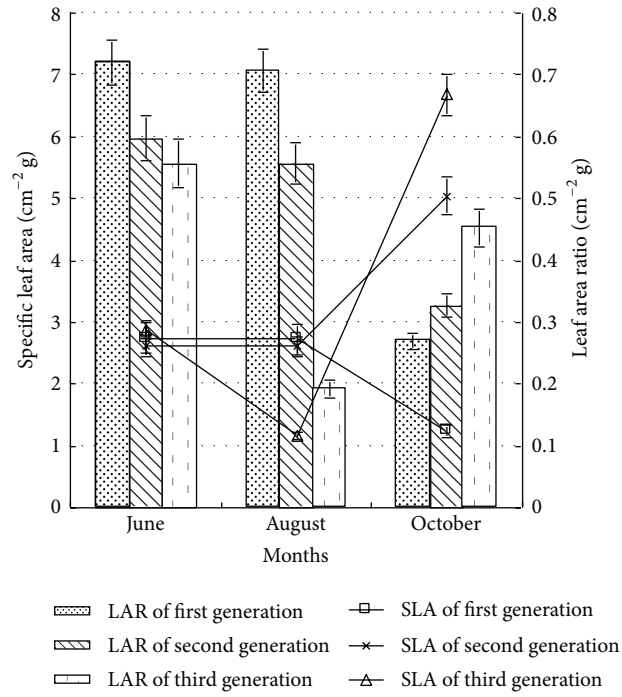

Figure 3: The specific leaf area and leaf area ratio of poplar under different continuous croppings.

generation, in middle growth period, there was no significant difference ($P > 0.05$) between the SLA of first generation and second generation poplars. With the growth cycle increasing, the SLA of third generation poplar decreased first and then increased. According to the optimal distribution theory, plant could use the most restrictive resource to acquire component of organic under stress condition, which would get the first priority configuration [16]. Therefore, the SLA of the third generation poplar in late growth period showed increasing trend, in order to get higher light resource capture area sufficiently, indicating that the photosynthetic rate of plant unit mass leaf and the relative growth rate of leaf expressed increasing trend [7].

As shown in Figure 3, in early and middle growth periods, the sequence of LAR was the first generation, the second generation, and the third generation, but in early growth period, there was no significant difference ($P > 0.05$) between that of the second generation and the third generation. In late growth period, the LAR of third generation increased by 40.35% and 27.79%, respectively, comparing with that of first generation and second generation. The LAR of the third generation increased, while that of first generation decreased, which was mainly related to the biomass increasing of the first generation, and that decreasing of the third generation. To the same generation, the LAR of first generation and second generation poplar changed rarely in early and middle growth periods, while decreasing significantly in late growth period. The fluctuation of LAR of third generation was larger and lowest in middle growth period. The above analysis showed that the influence of first generation and second generation on the SLA was rarely in early and middle growth periods. With the growth cycle increasing, the influence of continuous cropping on the SLA and LAR increased; namely, with the generation increasing, the leaf biomass of poplar seedling decreased, and the SLA and LAR increased, indicating that poplar showed some morphological adaptation strategy to maintain self-survival or biomass accumulation, in accordance with the optimal distribution theory [16].

3.3. The Distribution Ratio of Each Component Biomass of Poplar Seedling. The adjustment to the biomass distribution pattern, which was able to let plant balance the relation of resource acquisition and using better, had important significant for plant to maintain regular physiological activity under stress condition. The response of the biomass distribution pattern to environment was the key factor for plant resource acquisition, competition, and reproductive capacity, which was also the key index to reflect the plant competitive capacity, and affected the conformity of organic. The influence of individual development on the biomass of plant organs, which was different to different species and could reflect the sequence change of priority selection on growth, reproduction, defense, and so forth, in the whole growth and development stages, generally was decided by genotype [17] but closely related to heterogeneity habitat [18].

3.3.1. The Ratios of Aboveground Biomass and Underground Biomass. The ratios of biomass aboveground and underground could reflect the relative materiality on competition

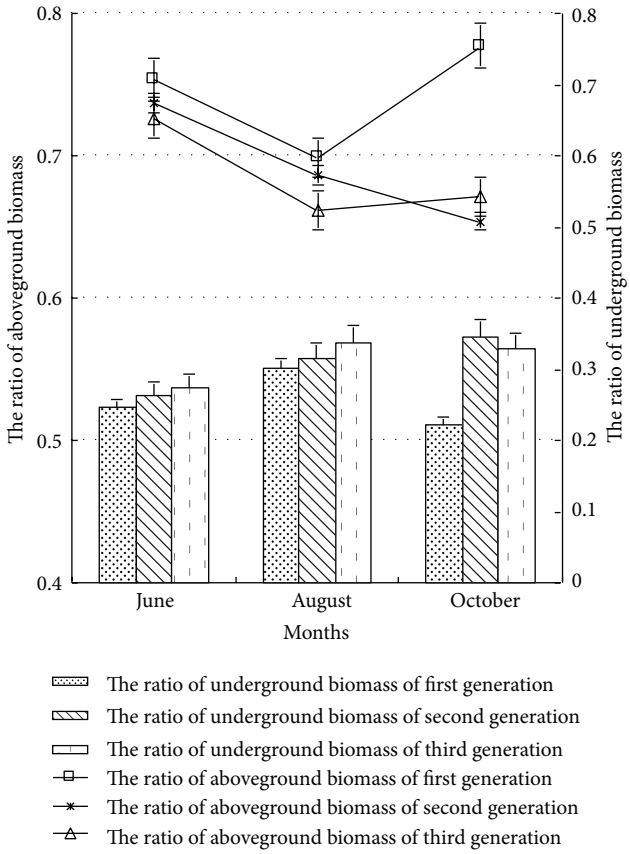

Figure 4: The ratio of aboveground and underground biomass of poplar under different continuous croppings.

aboveground and underground, as well as reflecting the competitive capacity of plant to environmental resources, such as light, water, and mineral nutrition [7]. As shown in Figure 4, the ratio of biomass aboveground of poplar seedling was higher than that of underground in different continuous generation and growth stages, and the ratios of biomass aboveground and underground showed opposite change rules with the continuous generation and growth cycle increasing. In early and middle growth periods, the ratio of biomass aboveground of first, second, and third generation poplar had significant difference ($P < 0.05$), and the sequence was the first generation, the second generation, and the third generation. In late growth period, the ratio of biomass aboveground of the second and third generation poplars decreased significantly, and that of first generation poplar increased significantly. The ratio of biomass aboveground of the first generation poplar increased by 18.88% and 15.78%, respectively, comparing with that of the second and third generations. In the early and middle growth periods, the ratio of biomass underground of first and second generation poplars had no significant difference ($P > 0.05$), and the sequence was third generation, second generation, and first generation. In late growth period, the ratio of biomass underground of second and third generation poplars was significantly higher than that of first generation ($P < 0.05$) and was 1.55 times and 1.48 times that of the first generation, respectively. For the same generation poplar, the ratio of biomass aboveground of poplar showed decrease trend, but that of biomass underground showed increase trend in middle growth period. Analysis showed that with the generations and growth cycle increasing, the ratio of biomass underground of poplar decreased significantly; while in late growth period, the ratio of biomass aboveground of first generation poplar was obviously higher than that of the second and third generations. The ratio of biomass underground of the second and third generations influenced by continuous cropping was rare, but with the growth cycle increasing, the ratio of biomass underground increased, while that of first generation decreased.

3.3.2. The Ratio of Main Component Biomass. The ratio of each component biomass of plant to total biomass was the result of interaction of self-hereditary character and external environment [10]. The biomass distribution was the key driving factor for plant to acquire net carbon, and the distribution on stem, leaf, and root had direct influence on plant future growth and reproduction [11]. Poorter and Nagel pointed out [19] that not all plants had changeless biomass distribution pattern, which depended on species type, individual development, and habitat environment. The optimal distribution theory predicted that the response of plant to environment was achieved through adjusting the biomass distribution of each organic, in order to maximize acquiring limitation resources, such as light, nutrition, and water [7]. According to the optimal distribution theory and function balance hypothesis, plant should increase the distribution of organics by acquiring limitation resources and reduce the distribution of organics by acquiring nonrestriction resources [20, 21].

(1) The Ratio of Leaves Biomass. As shown in Figure 5, in early and middle growth periods, the ratio of leaf biomass had significant difference ($P < 0.05$) with the sequence of first generation, second generation, and third generation. In late growth period, the ratio of leaf biomass of first generation was obviously higher than that of the second and third generations, and was 3.35 times and 3.21 times that of the second and third generations, respectively, indicating that in the first generation continuous cropping with the soil nutrient sufficient, poplar seedling tended to distribute more organic to leaves, in order to satisfy the demand of seedling to immobilization nutrient through photosynthesis. The rate of leaf biomass of the same generation poplar had no significant difference ($P > 0.05$) in the early and middle growth periods, and that decreased in the late growth period, especially for the second and third generation poplars, indicating that with the generation and growth cycle increasing, the proportion of leaf biomass decreased.

(2) The Ratio of Newly Emerging Branches Biomass. As shown in Figure 5, the influence of continuous cropping on the ratio of newly emerging branches biomass of first and second generation was little, but the ratio of third generation decreased significantly. In the late growth period, the ratio of newly emerging branches biomass of the first and second generation

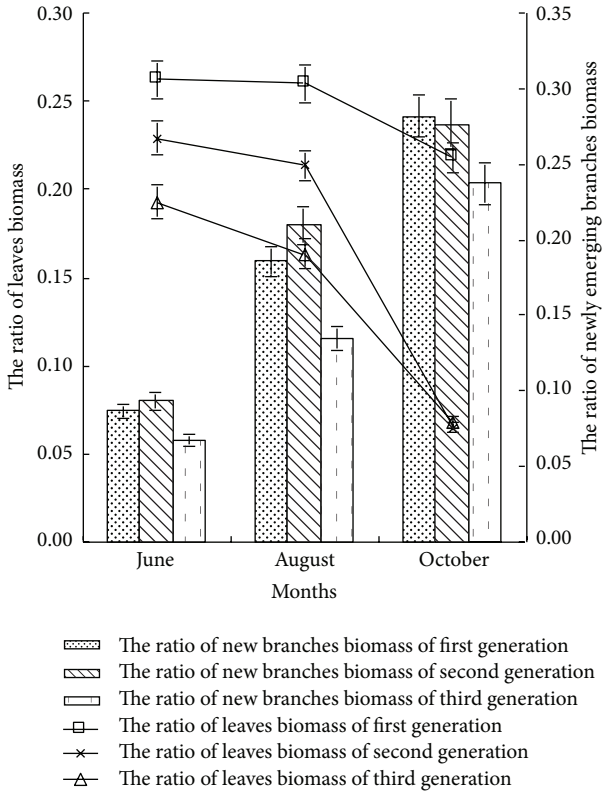

Figure 5: The ratio of leaves and newly emerging branches biomass of poplar under different continuous croppings.

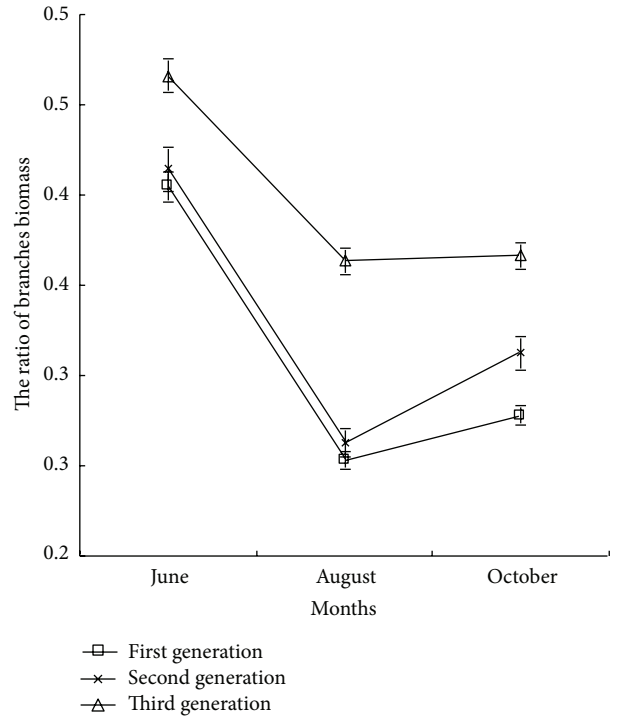

Figure 6: The ratio of branches biomass of poplar under different continuous croppings.

poplars increased by 18.99% and 16.88%, comparing with that of the third generation, respectively, indicating that the poplar seedling of the first and second generation had the characteristics of enlarging stems and leaves biomass, increasing the photosynthesis area, and improving the accumulation of substance accumulation, to ensure the demand of seedling growth. With the growth cycle increasing, the ratio of newly emerging branches biomass increased significantly under different continuous cropping conditions. Analysis showed that the third generation continuous cropping obviously inhibited the newly emerging branches growth: with the growth cycle increasing, the inhibited effect of continuous cropping on newly emerging branches growth increased.

(3) The Ratio of Branches Biomass. As shown in Figure 6, the ratio of branches biomass of poplar was followed by third generation, second generation, and first generation, but the difference of first generation and second generation was not significant ($P > 0.05$), and the ratio of branches biomass of third generation was significantly higher than that of first and second generations. In the early growth period, the ratio of branches biomass of the second and third generations increased by 2.48% and 15.53%, respectively, and in the late growth period, increased by 12.23% and 32.01%, respectively, comparing with that of first generation. With the growth cycle increasing, the ratio of branches biomass of poplar decreased rapidly first and then increased. Analysis showed that the growth of poplar branches was slow comparing with other organics, and the growth of plant height had no difference in short continuous cropping; thus the ratio of branches of third generation was higher, further indicating that the growth of leaves and newly emerging branches of third generation was slow.

(4) The Ratio of Root-Shoot and Root-Leaf. The plant root-shoot ratio, which affected the ecotype of plant individual and the capture strategy to slight resource, and reflected the balance aboveground and underground well, and the function of assimilation and balance of plant to water and nutrient, was one of the main indexes in the analysis of biomass distribution [10]. As shown in Figure 7, in the early and middle growth periods, the root-shoot ratio of poplar was followed by first generation, second generation, and third generation, indicating that the competitive capacity of third generation to soil water and nutrient was strong [10], in order to adapt the poor and severe environment due to continuous cropping. The root-shoot ratio of first generation poplar was the lowest, indicating that the poplar seedling could use major sunlight energy and had high production capacity under first generation continuous cropping condition [7]. In the late growth period, the plant root-shoot ratio of second generation was highest with 0.53, while that of first generation decreased obviously with 0.29, the reason was probably that under first generation condition, in the growth process, the poplar seedling used light resource by enhancing the distribution of tern and leaf, resulting in the plant root-shoot ratio decreasing. To the same generation continuous cropping

poplar, with the growth cycle increasing, the root-shoot ratio of first generation increased first and then decreased, while that of the second generation poplar increased all the time. Analysis showed that in order to adjust the soil fertility exhaustion due to continuous cropping, the root system of poplar seedling showed obvious plasticity to assimilate more nutrients. In the early growth period, the influence of continuous cropping on the biomass aboveground was bigger than that on the root system. With the generation increasing, the inhibition effect on the biomass aboveground was higher than that on the growth of root system. Continuous cropping led to the biomass aboveground decreasing, and root-shoot ratio increasing, which was in accordance with the optimal distribution theory. When the plant growth was inhibited by the lack material assimilation by root, the growth of root would show relative advantage, and would lead to the root-shoot ratio increasing [7, 22], which could make the plant under stress condition to increase the most limited resources or organics be distributed optimally [21, 23]. This was similar to the conclusion that the whole biomass and biomass aboveground decreased, but the distribution ratio of photosynthetic production to root and plant root-shoot ratio gradually increased under adversity conditions [22, 24–26].

Root-leaf ratio is the important index to reflect the balance between water absorption and water loss of plant. As shown in Figure 7, in the early and middle growth periods, the root-leaf ratio of poplar seedling was followed by third generation, second generation, and first generation. In late growth period, the root-leaf ratio of second generation poplar was 5.34, while the root-leaf ratio of first generation poplar was 1.02. With the growth cycle increasing, the variation of root-leaf ratio of first generation poplar was rare, while that of second and third generation all showed increased trend, indicating that the poplar seedling distributed more biomass to root, in order to relief the lack of nutrients caused by generation cropping and gain more nutrients from soil, which was in accordance with the optimal distribution theory [24, 27]. In the process of plant growth, plant adjusted the biomass distribution to adapt the change of nutrient condition, when the nutrient was lacking, plant distributed more biomass to roots, and the root-leaf ratio increased; when the nutrient was sufficient, plant distributed more biomass to leaf, and the ratio of leaf biomass increased [26], which was similar to the rules of root system and leaves growth of continuous cropping poplar in the study.

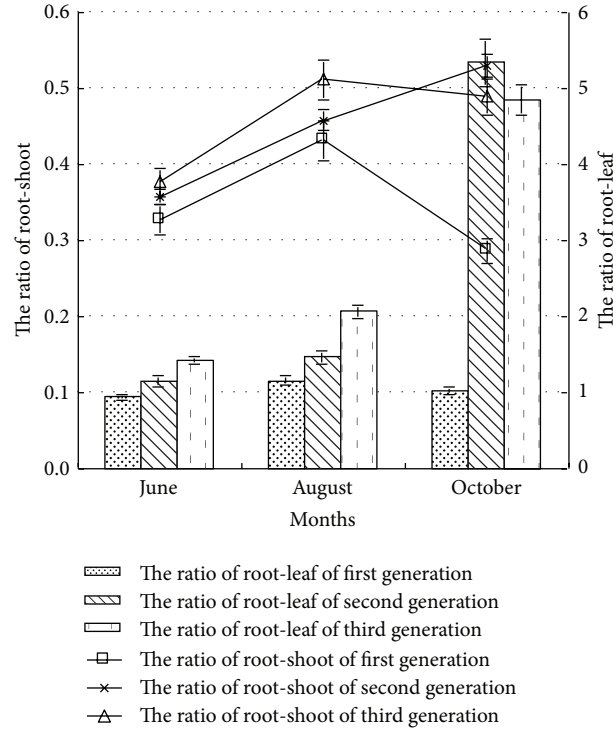

Figure 7: The ratio of root-shoot and root-leaf of poplar under different continuous croppings.

4. Conclusions

With the generation and growth cycle increasing, the total biomass of poplar significantly decreased, and the inhibition effect of growth was significant. The growth aboveground of continuous cropping poplar was significantly higher than that underground, indicating that continuous cropping led to slow growth of plant, increment decline, and significant lack of growth potential.

With the generation increasing, both the SLA and LAR of poplar seedling increased, and with the growth cycle increasing, the SLA and LAR of third generation poplar seedling increased significantly. The ratio of biomass aboveground was higher than that underground under continuous cropping condition. With the generation and growth cycle increasing, except in late growth period, the ratio of biomass aboveground increased significantly and the ratio of biomass underground decreased significantly, and the ratio of biomass aboveground of second generation and third generation decreased significantly, while the ratio of biomass underground increased significantly.

The ratio of leaves biomass and newly emerging branches biomass of first generation poplar was higher, and poplar seedling distributed more biomass to the leaves growth and branches growth, which could improve the photosynthetic yield and satisfy the demand of the maximum growth potential of poplar. But with the generation and growth cycle increasing, the ratio of leaves biomass and newly emerging branches biomass decreased significantly. With the growth cycle increasing, the ratio of branches biomass decreased first and then increased in different growth stages with the sequence of third generation, second generation, and first generation.

With the generation and growth cycle increasing, the ratio of poplar root-shoot and root-leaf increased significantly, and more resources were distributed to root system growth, in order to adapt the degeneration of forest soil ecological environment due to continuous cropping, which was in accordance with the optimal distribution theory. Poplar seedling had the growth strategy to improve the ratio

of root-leaf and root-shoot to adapt the limited soil nutrient due to continuous cropping.

Conflict of Interests

The authors declare that there is no conflict of interests regarding the publication of this paper.

Authors' Contribution

Jiangbao Xia and Shuyong Zhang contributed equally to this work.

Acknowledgments

This study was supported by the Major State Basic Research Development Program (no. 2012CB416904), the National Natural Science Foundation of China (nos. 31370702, 31100468, and 31100196), Science and Technology Plan of Universities in Shandong Province [no. J13LC03], and the Promotive Research fund for Excellent Young and Middle-aged Scientists of Shandong Province (no. BS2013NY010).

References

[1] L. Fang, J. Yu, and J. L. Chen, "Effect of continuous cropping on leaf nutrient and growth of different species of poplar plantation," *Agricultural Science & Technology*, vol. 12, no. 2, pp. 224–227, 2011.

[2] F. D. Liu, L. G. Kong, S. Q. An, H. T. Wang, Y. Z. Jiang, and H. L. Gao, "Characteristics of soi l micro-ecological environment at different growth stages of poplar plantation under continuous cropping," *Journal of Soil and Water Conservation*, vol. 22, no. 2, pp. 121–125, 2008.

[3] F. D. Liu, Y. Z. Jiang, H. T. Wang, Y. Wang, and L. G. Kong, "Soil productivity maintenance technique of poplar plantation under continuous cropping," *Scientia Silvae Sinicae*, vol. 43, no. 1, pp. 58–63, 2007.

[4] Y. Wang, H. Wang, X. Tan, Y. Jiang, and L. Kong, "Comparison on rhizosphere effect of cultivar alternation and non-alternation continuous cropping poplar (*Populus deltoids*) plantation," *Acta Ecologica Sinica*, vol. 30, no. 5, pp. 1379–1389, 2010.

[5] D. Baniulyte, E. Favila, and J. J. Kelly, "Shifts in microbial community composition following surface application of dredged river sediments," *Microbial Ecology*, vol. 57, no. 1, pp. 160–169, 2009.

[6] L. Lei, X. D. Liu, S. L. Wang, Y. Li, and X. L. Zhang, "Assignment rule of alpine shrubs biomass and its relationships to environmental factors in Qilian Mountains," *Ecology and Environmental Sciences*, vol. 20, no. 11, pp. 1602–1607, 2011.

[7] L. Li, D.-W. Zhou, and L.-X. Sheng, "Density dependence-determined plant biomass allocation pattern," *Chinese Journal of Ecology*, vol. 30, no. 8, pp. 1579–1589, 2011.

[8] I. Müller, B. Schmid, and J. Weiner, "The effect of nutrient availability on biomass allocation patterns in 27 species of herbaceous plants," *Perspectives in Plant Ecology, Evolution and Systematics*, vol. 3, no. 2, pp. 115–127, 2000.

[9] D. W. Hilbert and J. Canadell, "Biomass partitioning and resource allocation of plants from Mediterranean-type ecosystems: possible response to elevated atmospheric CO_2," in *Global Change and Mediterranean-Type Ecosystems*, J. M. Moreno, Ed., pp. 76–101, Springer, New York, NY, USA, 1995.

[10] C. B. Xu, Q. L. Zhong, D. L. Cheng, and S. Z. Zhu, "Comparison of leaf phenotypic traits and biomass allocation of different provenances of Machilus pauhoi," *Journal of Anhui Agricultural University*, vol. 39, no. 6, pp. 920–924, 2012.

[11] B. Yang, J. Wang, and Y. Zhang, "Effect of long-term warming on growth and biomass allocation of *Abies faxoniana* seedlings," *Acta Ecologica Sinica*, vol. 30, no. 21, pp. 5994–6000, 2010.

[12] K. Mokany, R. J. Raison, and A. S. Prokushkin, "Critical analysis of root: shoot ratios in terrestrial biomes," *Global Change Biology*, vol. 12, no. 1, pp. 84–96, 2006.

[13] I. Schmid, "The influence of soil type and interspecific competition on the fine root system of Norway spruce and European beech," *Basic and Applied Ecology*, vol. 3, no. 4, pp. 339–346, 2002.

[14] S. L. Lewis and E. V. J. Tanner, "Effects of above-and below-ground competition on growth and survival of rain forest tree seedlings," *Ecology*, vol. 81, no. 9, pp. 2525–2538, 2000.

[15] M. J. Hutchings, "Resource allocation patterns in clonal herbs and their consequences for growth," in *Plant Resource Allocation*, F. A. Bazzaz and J. Grace, Eds., chapter 7, pp. 161–189, Academic Press, New York, NY, USA, 1997.

[16] A. J. Bloom, F. S. Chapin III, and H. A. Mooney, "Resource limitation in plants—an economic analogy," *Annual Review of Ecology and Systematics*, vol. 16, pp. 363–392, 1985.

[17] J. Weiner, "Allocation, plasticity and allometry in plants," *Perspectives in Plant Ecology, Evolution and Systematics*, vol. 6, no. 4, pp. 207–215, 2004.

[18] C. Wang, "Biomass allometric equations for 10 co-occurring tree species in Chinese temperate forests," *Forest Ecology and Management*, vol. 222, no. 1–3, pp. 9–16, 2006.

[19] H. Poorter and O. Nagel, "The role of biomass allocation in the growth response of plants to different levels of light, CO_2, nutrients and water: a quantitative review," *Australian Journal of Plant Physiology*, vol. 27, no. 6, pp. 595–607, 2000.

[20] R. G. Bloom and A. U. Mallik, "Indirect effects of black spruce (*Picea mariana*) cover on community structure and function in sheep laurel (*Kalmia angustifolia*) dominated heath of Eastern Canada," *Plant and Soil*, vol. 265, no. 1-2, pp. 279–293, 2004.

[21] A. J. Bloom, F. S. Chapin III, and H. A. Mooney, "Resource limitation in plants: an economic analogy," *Annual Reviews of Ecology and Systematics*, vol. 16, pp. 363–392, 1985.

[22] S. A. Greco and J. B. Cavagnaro, "Effects of drought in biomass production and allocation in three varieties of *Trichloris crinita* P. (Poaceae) a forage grass from the arid Monte region of Argentina," *Plant Ecology*, vol. 164, no. 1, pp. 125–135, 2003.

[23] W. Guo, B. Li, X. Zhang, and R. Wang, "Architectural plasticity and growth responses of *Hippophae rhamnoides* and *Caragana intermedia* seedlings to simulated water stress," *Journal of Arid Environments*, vol. 69, no. 3, pp. 385–399, 2007.

[24] M. L. Wang, D. X. Kong, R. Zou, S. F. Chai, Z. Y. Chen, and H. Tang, "Effect of different soil conditions on the growth and biomass allocation of *Illicium difengpi* K.I.B. et K.I.M seedlings," *Crops*, no. 3, pp. 67–71, 2013.

[25] H.-X. Yan, L.-B. Fang, and D.-Z. Huang, "Effects of drought stress on the biomass distribution and photosynthetic characteristics of cluster mulberry," *Chinese Journal of Applied Ecology*, vol. 22, no. 12, pp. 3365–3370, 2011.

[26] K. D. M. McConnaughay and J. S. Coleman, "Can plants track changes in nutrient availability via changes in biomass partitioning?" *Plant and Soil*, vol. 202, no. 2, pp. 201–209, 1998.

[27] H. Y. Lu and Y. M. Zhang, "Response of growth and biomass allocation of *Haloxylon persicum* seedlings to different salt treatments," *Arid Zone Research*, vol. 29, no. 2, pp. 194–202, 2012.

Hindawi Publishing Corporation
The Scientific World Journal
Volume 2014, Article ID 765840, 7 pages
http://dx.doi.org/10.1155/2014/765840

Research Article

Effects of Salt-Drought Stress on Growth and Physiobiochemical Characteristics of *Tamarix chinensis* Seedlings

Junhua Liu,[1,2] Jiangbao Xia,[2] Yanming Fang,[1] Tian Li,[2] and Jingtao Liu[2]

[1] *College of Biological and Environmental Sciences, Nanjing Forest University, Nanjing 210037, China*
[2] *Shandong Provincial Key Laboratory of Eco-Environmental Science for Yellow River Delta, Binzhou University, Binzhou 256603, China*

Correspondence should be addressed to Jiangbao Xia; xiajiangbao2012@126.com and Yanming Fang; jwu4@njfu.edu.cn

Received 9 June 2014; Revised 3 July 2014; Accepted 3 July 2014; Published 22 July 2014

Academic Editor: Hongbo Shao

The present study was designed to clarify the effects of salinity and water intercross stresses on the growth and physiobiochemical characteristics of *Tamarix chinensis* seedlings by pots culture under the artificial simulated conditions. The growth, activities of SOD, POD, and contents of MDA and osmotic adjusting substances of three years old seedlings of *T. chinensis* were studied under different salt-drought intercross stress. Results showed that the influence of salt stress on growth was greater than drought stress, the oxidation resistance of SOD and POD weakened gradually with salt and drought stresses intensified, and the content of MDA was higher under severe drought and mild and moderate salt stresses. The proline contents increased with the stress intensified but only significantly higher than control under the intercross stresses of severe salt-severe drought. It implied that *T. chinensis* could improve its stress resistance by adjusted self-growth and physiobiochemical characteristics, and the intercross compatibility of *T. chinensis* to salt and drought stresses can enhance the salt resistance under appropriate drought stress, but the dominant factors influencing the physiological biochemical characteristics of *T. chinensis* were various with the changing of salt-drought intercross stresses gradients.

1. Introduction

Tamarix chinensis belongs to the Tamarix family (Tamaricaceae), which are mainly xerophytes. It is native to China and Korea, and it is known in many other parts of the world as an introduced species and sometimes an invasive noxious weed. It easily inhabits moist habitat with saline soils. *T. chinensis* as an ornamental plant was introduced into North America at the beginning of nineteenth Century and later into the southwest American desert regions for windbreak and sand fixation. *Tamarix chinensis* receives more attention amongst different Tamarix species [1]. Because of its strong adaptability to the local environment, *T. chinensis* replaced the native species, and as the rapid invasion to many rivers and desert edges results in the loss of biodiversity in arid area, water consumption increased and a series of related problems are listed as USA ten alien invasive species [2, 3]. As a native species in China, *T. chinensis* is mainly distributed in the northwest arid area of Xinjiang, Inner Mongolia and Gansu, and it is also the main species for vegetation restoration of ecological restoration and protection for the coastal wetlands of Bohai Gulf. The Yellow River Delta is the most concentrated distribution area of *T. chinensis* [4], but this area is being threatened by hydrological changes [1]. In recent years, due to the large amount of groundwater exploitation of local area, seawater intrusion led to soil salinity and the evaporation to precipitation ratio increased. Due to the lack of freshwater resources, the salt and drought stress became the two major effect factors on local *T. chinensis* seedlings growth [4, 5].

As known, soil is an essential component of wetland ecosystem, which can support, hold, and regulate water and

nutrients [6]. However, the effects of drought stress and salt stress on the growth and development of plants are coupled together, by reducing the soil solution water potential. Many of the previous studies are focused on the interaction between salt and drought and its effect on plant growth and physiological and biochemical characteristics [7–10]. The effects of salt and drought stress on plant physiological and biochemical properties are mainly concentrated in the *Ammodendron bifolium* [7, 10], *Gleditsia sinensis* [8], and *Cercis chinensis Bunge* seedlings [9]. But the stress physiology researches of *T. chinensis* mainly concentrated on single salt stress [11–14] or drought stress [15, 16], such as salt stress on the growth of *T. chinensis* [11], physiological and biochemical characteristics during the leaf expansion period [17], photosynthesis and osmotic adjustment substances [12], and salt secretion characteristics and influence factor under saline habitats [13]. Furthermore, the drought resistance mechanism under different stress levels [15] and physiological and ecological characteristics [16] under different environment had been carried out. But the physiological and biochemical characteristics response of *T. chinensis* to the salt-drought intercross stress conditions has not been reported. This study was aimed at analyzing the change dynamic of biomass, superoxide dismutase (SOD), peroxidase (POD), malondialdehyde (MDA), and osmotic adjusting substances under different gradients of salinity stress-drought intercross stresses treatment, simulating the soil moisture and soil salinity conditions of sea-side and land-side and clarifying the growth and physiobiochemical characteristics of *T. chinensis* under different salt-drought stresses conditions.

2. Materials and Methods

2.1. Plants. Three-year-old *Tamarix chinensis* seedlings were selected from National Marine Ecological Conservation Region at Changyi county in Shandong Province, China. Previous works indicated that these seedlings had homogenesis traits in physiological and morphological aspects.

2.2. Experimental Setup. The experiments were carried out in a greenhouse at Binzhou University, Binzhou, China, from March 21, 2013, to June 15, 2013. *T. chinensis* seedlings of 3a old had been transplanted to research greenhouse, cocultivated using pots diameter 30 cm, high 50 cm, 1 plants per pot, a total of 24 plants, potted matrix for sandy loam soil (salt content 0.02%). *T. chinensis* seedlings normal growth after April 20th 2013 to salt and drought stress treatment. Drought stress treatment using Hsiao [14] moisture gradient design method, includes high soil moisture (mild drought stress) and low soil moisture (serve drought stress); the soil relative water content was 55%~60% and 30%~35%. Salinity (soil salinity/soil dry weight) by NaCl solution configuration of different gradient times irrigation to control, set up 2 levels, the salt concentrations were 0.4%, 1.2% and 2.5%, and the salt content of 0.02% as control. The pot bottom is provided with a tray whose depth is 8 cm, the leakage water into the pot and the cleaning tray, clean water is poured into the pot to prevent salt loss [18]. The experiment consists of 8 (2×4) salt-drought treatments. Each treatment was repeated 3 times and was designed by randomized block arrangement. Salt and drought stress treatment for 8 weeks (From April 20th to June 15th), determination of sample indexes.

2.3. Plant Sampling and Analysis. The same position of *T. chinensis* seedlings mature leaves was collected and dried, ground and sieved through a 120 mesh sieve, and sealed with plastic bags to be measured.

2.3.1. Physiological and Biochemical Indexes. The SOD activity was determined by nitro blue tetrazolium [19, 20] four photochemical reduction method; the activity of POD [21] was measured using guaiacol colorimetric method; MDA was measured by TBA colorimetric method [19].

2.3.2. Determination of Proline Content. Take 0.05 g of dry sample into a centrifuge tube, sulfosalicylic acid with 10 mL 3%, sealing bag seal affixed after boiling water bath extraction for 30 min; after cooling centrifugal (3000 r/min, 10 min), 1 mL supernatant fluid, 1 mL 3% sulfosalicylic acid, acetic acid, and 2 mL 2.5% acid indene ketone were added to three glass test tubes (tube with glass balls) in boiling water bath for 60 min chromogenic reaction; then we cool them to room temperature to join the 4 mL toluene and shake extracted red material, still taking the toluene layer, in the 520 nm absorbance (OD) [19].

2.4. Statistical Analysis. All statistical tests were performed using SPSS 18.0. Two-way ANOVA was used to determine the significance of different salt and drought treatment effects on growth and the physiological characteristics. Mean treatment differences were separated by the LSD test ($P < 0.05$ and $P < 0.01$) if F-tests were significant.

3. Results

3.1. Effect of Salt and Drought Stresses on the Growth Traits of T. chinensis. As can be seen from Table 1, *T. chinensis* plant height increased more significantly ($P < 0.05$) in the salt content at 0.4% level, respectively, 34.7% and 15.0%, than CK under high and low soil moisture, but the plants died under the stress condition with salinity 2.5% and high soil moisture (see Figure 2). The main root length of *T. chinensis* showed no significant difference ($P > 0.05$) between 0.4% salt stress treatment and CK under high soil moisture level, but the main root length of 1.2% salt stress treatment was shorter obviously than CK ($P < 0.05$). Under low soil moisture condition, the main root length increased first and then decreased, and the main root length of 1.2% salt stress treatment was significantly longer than CK ($P < 0.05$). The basal diameter of *T. chinensis* increased first and then decreased with the increase of the salt content in the two kinds of soil moisture conditions and reached the maximum at 0.4%, and the salt content of 1.2% was significantly decreased ($P < 0.05$).

Under the mild and severe drought stress, aboveground parts and underground parts dry weight of *T. chinensis* was both increased first and then decreased with the salt

Table 1: Effects of *Tamarix chinensis* growth and biomass conditions with different salt and drought stresses treatment.

Treatment		Plant height (cm)	Main root length (cm)	Stem basal diameter (cm)	Overground biomass (g)	Underground biomass (g)
Water condition	Salinity content					
High soil moisture (mild drought)	CK	85.93 ± 7.65^{b}	14.54 ± 1.25^{a}	0.51 ± 0.12^{a}	13.12 ± 2.89^{b}	5.01 ± 0.97^{b}
	0.4%	115.76 ± 10.28^{a}	15.58 ± 1.67^{a}	0.63 ± 0.26^{a}	18.01 ± 3.35^{a}	9.52 ± 2.71^{a}
	1.2%	87.29 ± 5.96^{b}	11.56 ± 1.87^{b}	0.37 ± 0.14^{b}	9.04 ± 3.02^{c}	4.13 ± 1.85^{b}
	2.5%	—	—	—	—	—
Low soil moisture (severe drought)	CK	85.70 ± 5.37^{b}	11.51 ± 1.12^{b}	0.47 ± 0.14^{a}	12.89 ± 1.18^{b}	4.86 ± 0.92^{b}
	0.4%	98.58 ± 4.72^{a}	12.57 ± 1.25^{b}	0.49 ± 0.22^{a}	15.67 ± 1.37^{a}	7.03 ± 1.15^{a}
	1.2%	74.43 ± 5.01^{c}	15.68 ± 1.67^{a}	0.35 ± 0.09^{b}	6.95 ± 1.86^{c}	3.72 ± 0.89^{b}
	2.5%	86.24 ± 3.97^{b}	10.89 ± 1.02^{b}	0.36 ± 0.08^{b}	5.26 ± 0.98^{c}	2.63 ± 0.76^{c}

The different letters within the same row indicate the significant difference at 0.05 level. "—" stands for plant individual death.

stress increase, and reached the maximum value at the salt content of 0.4%. In addition, plant individuals of *T. chinensis* still alive under the severe drought stress, while died in mild drought under severe salt stress, it may be appropriate drought stress can improved *T. chinensis* to a certain extent of salt tolerance to water logging and saline habitats. The above results showed that the effects of salt stress on the growth of *T. chinensis* were more than drought stress, although there are certain inhibitory effects of drought stress on *T. chinensis*. In the meanwhile, the variation degree of aboveground dry weight was higher than those of the underground parts under the drought stress and salt stress treatments.

3.2. Effects of Salt and Drought Stresses on SOD and POD Enzymes Activities of T. chinensis Seedlings. We can see from Figure 1, under mild drought stress, SOD activity in leaves of *T. chinensis* increased with the salt content decrease, and the difference between the salt stress treatment was significant ($P < 0.05$); compared with CK, SOD activity of leaves decreased significantly in the salt content of 0.4% ($P < 0.05$) and decreased obviously in the salt content of 1.2% and 2.5% ($P < 0.01$). Under low soil moisture conditions, the SOD activity in leaves increased first and then decreased with the salinity increasing, and the activity of SOD increased about 30% and 80%, respectively, compared with CK in the salinity of 0.4% and 1.2%, then reached the maximum value at salinity 1.2%, and was significantly lower in the salt content of 2.5% ($P < 0.05$). Under the same salt stress, the effects of different drought stress and salt stress effect on SOD activity were significant ($P < 0.01$). By the double factor variance analysis, SOD activity in leaves of *T. chinensis* by containing salt and salt drought intercross stress was significant ($P < 0.01$).

Under mild drought stress condition, the leaf POD activity decreased first and then increased and then decreased with the increase of soil salt content; the difference among all treatments was extremely significant ($P < 0.01$). Under severe drought stress, POD activity in leaves is increased first and then decreased with the increasing of salinity, and the salt content of 0.4% and 1.2% was increased 20% and 50%, respectively, more than those of CK and decreased approximately 15% compared to those in the salt content 2.5% ($P < 0.05$). Under the same salt stress, the effects of different drought stress and salt effect on POD activity also reached extremely significant level. Double factor variance analysis showed that salt stress, drought stress, and salt drought intercross stress had significant effects on POD activity of *T. chinensis* leaf.

3.3. Effects of Salt and Drought Stresses on MDA Content. MDA content in leaves of *T. chinensis* was firstly decreased and then increased under mild drought stress and reached the minimum value in the salt content of 1.2% and 0.4%. Under severe drought stress, the content of MDA in leaves increased first and then decreased and reached the maximum ($11.96\ \text{nmol} \cdot \text{mg}^{-1}$ prot) at salinity 0.4%, 3.75 times of CK ($P < 0.01$). The content of MDA in leaves decreased in the salinity 1.2% but is still significantly higher than that of control. At the salinity of 2.5%, MDA content significantly decreased compared to other treatments but had no significant difference compared to the control. Double factor variance analysis showed that the effect of salt stress on the content of MDA was significant ($P < 0.05$), and drought stress or salt drought intercross stress effect on the MDA content reached extremely significant level ($P < 0.01$). Under the severe drought and light salt stress, the content of MDA reached a maximum value.

3.4. Effect of Salt Stress and Drought Stress on Proline Content in Leaves. As seen from Figure 3, the proline content in the leaves of *T. chinensis* increased at different extent with the increase of salt and drought stress in this study.

Under light drought stress condition, the proline content increased gradually with salt stress increases, but the had no significant difference compared with CK ($P > 0.05$); under the severe drought, the proline content in leaves decreased first and then increased with the enhancement of salt stress intensity, and the content at the salinity of 2.5% was significantly higher than that of CK ($P < 0.05$). When the salt concentration was below 2.5%, the proline content under different drought stress had no significant difference ($P > 0.05$). Double factor variance analysis showed that both salt stress and drought stress had significant effects on the content of proline in leaves of *Tamarix* seedlings ($P < 0.05$), and the mild drought stress is able to enhance accumulation

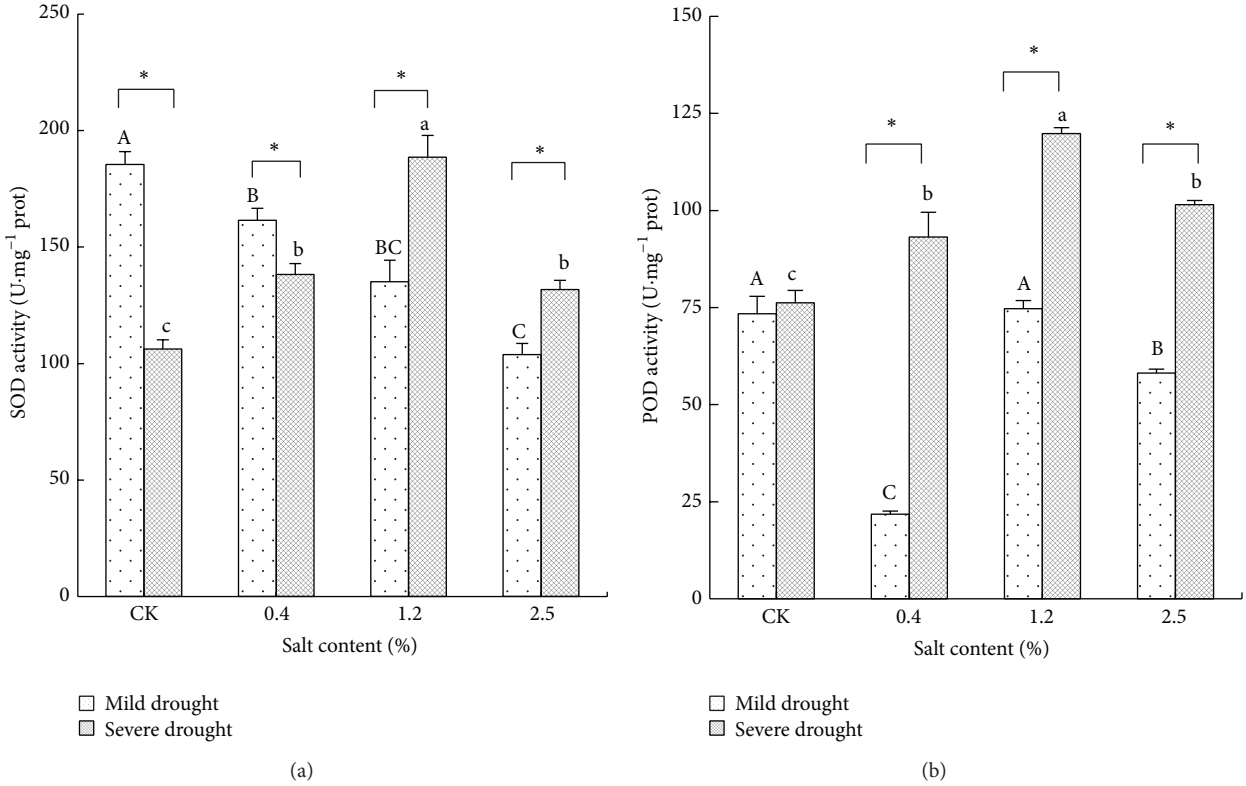

Figure 1: The changes of SOD and POD activity under different salt and drought stresses. The different letters within the same treatment indicate the significant difference at 0.05 level. The "∗" stands for the significant difference at 0.01 level between two treatments under the same salt stress.

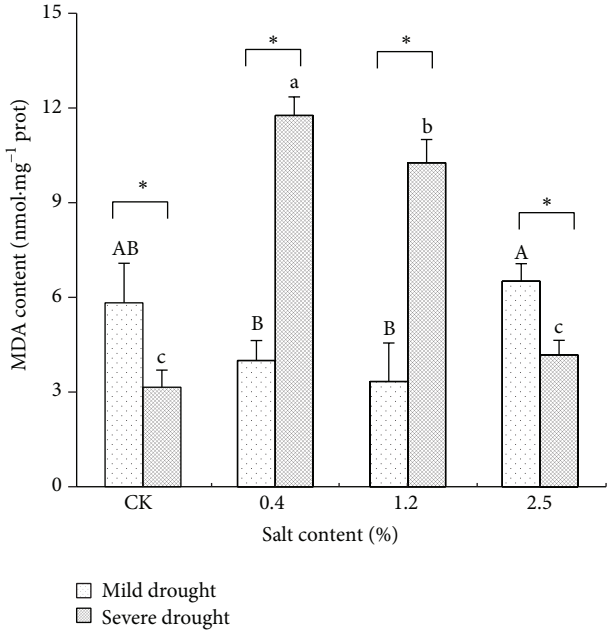

Figure 2: The changes of MDA contents under different salt and drought stresses. The different letters within the same treatment indicate the significant difference at 0.05 level. The "∗" stands for the significant difference at 0.01 level between two treatment under the same salt stress.

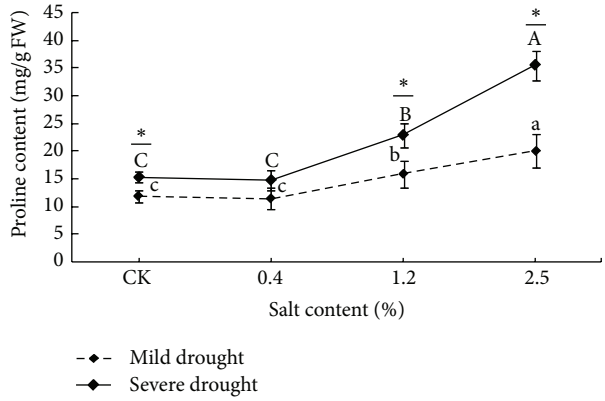

Figure 3: The changes of proline contents under different salt and drought stresses. The different letters within the same treatment indicate the significant difference at 0.05 level. The "∗" stands forthe significant difference at 0.01 level between two treatments under the same salt stress.

of proline in leaves of *T. chinensis*, to adapt to the saline environment.

4. Discussion

4.1. Salt-Drought Intercross Stress Affected Plant Growth and Biomass Allocation. As usually, salt-drought stress can delay plants growth and inhibit differentiation of plant tissue and reduce fresh weight of leaf, stem, and root with the salt stress increase [22]. Previous study showed that soils along the coastal area could form gradients of salinity and vegetation development during the desalinization process [23]. With the salt content increasing, *Tamarix hispida* stress symptoms become more obvious, survival rate decreased, and high growth was inhibited [11]. *Xanthoceras sorbifolia* seedlings adapt to drought stress by adjusting the biomass allocation and modified shape to achieve efficient use of existing habitat resources [24]. This study showed that *T. chinensis* had stronger tolerance of drought stress, but its growth was affected significantly by salt stress. Furthermore, the changing of *T. chinensis* biomass is obvious with the salt stress intensified and to adapt to high sanity environment by reducing plant height, basal diameter, and dry matter weight. In a word, *T. chinensis* maintained the normal growth under salt and drought conditions by adjusting the biomass allocation and its form.

4.2. Salt-Drought Stress Affected Enzyme System. SOD and POD are the main antioxidant enzymes in plants [7–9, 16] and play an important role in scavenging superoxide ion, resisting lipid peroxidation, reducing membrane damage, and so forth. The previous research results showed that, under stress conditions, the intensity and rise or fall of drought resistance related enzymes activity were related closely to plant species or varieties [25]. During experiment progress, enzyme activity increased with the stress increasing or first increased and then decreased. Like *Gleditsia sinensis* Lam, its SOD and POD activity first increased and then decreased under salt drought intercross stress condition, and in the same treatment condition, both SOD and POD activities were decreased along with the extension of treatment time. This study showed that leaf SOD and POD activity of *T. chinensis* had different change patterns under different intercross salt and drought stress. Under light drought stress, SOD activity decreased; POD activity decreased first and then increased and then decreased; this dynamic progress was related to that the low concentration of salt stress is able to alleviate the effects related to drought stress. In contrast, under severe salt stress, protective enzyme system was breached and enzyme activity was inhibited strongly, leading to further reduce in the moderate activity. Under the severe drought condition, the activities of SOD and POD decreased so obviously that it was not enough to clear free radicals in the body; then it resulted in lipid peroxidation and the damage of membrane system [8, 16].

4.3. Hydraulic-Salt Stress Affected MDA Contents. MDA is often used as a major index to judge the membrane lipid peroxidation, and its content represents the degree of damage [7, 8, 26]. Researchers found that MDA content of *Ammodendron bifolium* and *Gleditsia sinensis* seedlings membrane permeability increased along with the salt and drought intercross stress intensified. This study showed that appropriate salt drought intercross stress can weaken the peroxidation of membrane lipid, and then MDA content is relatively low, with less damage to the membrane system. However, under severe drought and mild to moderate salt stress, *T. chinensis* accumulated so much free radical that initiated peroxidation of membrane lipid and then injured cell membrane. But in severe salt and drought stress, MDA content decreased significantly, which may be a dominant factor and its salt drought intercross stress adaptive regulation; its mechanism still needs further analysis and discussion.

4.4. Salt-Drought Stress Affected Osmotic Adjusting Substances Contents. Osmotic adjusting substances play an important role for plants during the progress of growth, development, and reproduction in salt and drought stress [27]. Under

natural conditions, plants frequently suffer multiple environmental stresses, and the combined effects of environmental stresses on plants are complex and are not equal to the sum by simply adding the effect of each single factor [28]. Under the salt and drought stress conditions, large accumulation of intracellular soluble sugar and proline improves the cell sap concentration, maintains normal cell turgor, prevents excessive water loss, and enhances the resistance of plants [29]. A large number of studies showed that the soluble sugar is one kind of important organic osmotic regulators under adversity condition; it not only has a stabilizing effect on cell membrane and protoplast and providing carbon skeletons and energy for the synthesis of protein but also indirectly transmuted into proline [30]. This study showed that, in the salt drought intercross stress, soluble sugar contents in the leaves of *T. chinensis* seedlings gradually increased with the stress degree enhancement, and in severe salt and drought stress, the soluble sugar content began to decrease. That is to say that the soluble sugar plays an important role in osmotic adjustment, but the permeability of soluble sugar regulation has certain limitations; for example, under serve drought stress, the osmotic adjustment ability of *T. chinensis* reduced greatly or was lost. Proline is usually considered as one of main osmotic substances for plants used to regulate potential balance of cytoplasmic and vacuolar infiltration under salt stress [31]. This study showed that proline of *T. chinensis* increased gradually with increasing of salt and drought stress, but under mild drought stress it did not increase significantly; the cumulative amount of proline was low, only significantly increased in severe salt stress and severe drought stress conditions.

5. Conclusion

In summary, research on the relationships between plants and their environmental conditions has become a hotspot in present ecology studies. In this study, the growth and physiobiochemical characteristics of *T. chinensis* is able to adapt to the stress environment by adjusting the growth pattern and alternating soluble sugar and proline content, protective enzyme activity, and other physiobiochemical indexes to improve the ability to adapt to adversity. *T. chinensis* showed strong drought resistance and salt tolerance, and its growth conditions and physiobiochemical characteristics were related closely to the outside environmental factors, such as soil salinity and soil moisture status. On the other hand, the intercross compatibility of *T. chinensis* to salt and drought stresses can enhance the salt resistance under appropriate drought stress, and the dominant factor influencing the physiological biochemical characteristics of *T. chinensis* shows some differences with the changing of salt-drought intercross stress gradients. As *Tamarix chinensis* communities degrades in the Yellow River Delta, due to environment change and anthropogenic activities, then, the results of this study has certain theoretical and practical significance for the evaluation of *T. chinensis* resistance and reproductive technology, but the internal adjustment mechanism and adaptation mechanism need to be further researched in future.

Conflict of Interests

The authors declare that there is no conflict of interests regarding the publication of this paper.

Authors' Contribution

Junhua Liu and Jiangbao Xia contributed equally to this work.

Acknowledgments

This study was supported by the National Natural Science Foundation of China (nos. 31370702, 31100468, and 41201023), by Science and Technology Plan of Universities in Shandong Province (no. J13LC03), by the promotive research fund for excellent young and middle-aged scientists of Shandong Province (no. BS2013NY010), and by the Priority Academic Program Development of Jiangsu High Education Institutions, PAPD.

References

[1] B. Cui, Q. Yang, K. Zhang, X. Zhao, and Z. You, "Responses of saltcedar (*Tamarix chinensis*) to water table depth and soil salinity in the Yellow River Delta, China," *Plant Ecology*, vol. 209, no. 2, pp. 279–290, 2010.

[2] G. L. Anderson, R. I. Carruthers, S. Ge, and P. Gong, "Monitoring of invasive Tamarix distribution and effects of biological control with airborne hyperspectral remote sensing," *International Journal of Remote Sensing*, vol. 26, no. 12, pp. 2487–2489, 2005.

[3] C. R. Whitcraft, D. M. Talley, J. A. Crooks, J. Boland, and J. Gaskin, "Invasion of tamarisk (*Tamarix* spp.) in a southern California salt marsh," *Biological Invasions*, vol. 9, no. 7, pp. 875–879, 2007.

[4] X. Zhang, Y. Zhang, H. Sun, and D. Xia, "Changes of hydrological environment and their influences on coastal wetlands in the Southern Laizhou Bay, China," *Environmental Monitoring and Assessment*, vol. 119, no. 1–3, pp. 97–106, 2006.

[5] M. Yang, *Study on the Coastal Zone Environment Degradation in the Southern Coastal of the Laizhou Bay and Its Control Policy*, Ocean University of China, 2005.

[6] C. Huang, J. Bai, H. Shao et al., "Changes in soil properties before and after wetland degradation in the Yellow River Delta, China," *Clean-Soil, Air, Water*, vol. 40, no. 10, pp. 1125–1130, 2012.

[7] W. W. Zhuang, J. Li, and M. H. Cao, "Effects of salt- drought intercross stress on physiological and biochemical characteristics of *Ammodendron argenteum* (Pall.) kuntze seedlings," *Journal of Wuhan Botanical Research*, vol. 28, no. 6, pp. 730–736, 2010.

[8] Z. Q. Yu, M. G. Sun, H. X. Wei et al., "Effects of salt and drought intercross stresses on activity of cell defense enzymes in leaves of *Gleditsia sinedsis* Lam. Seedlings," *Journal of Central South University of Forestry & Technology*, vol. 27, no. 6, pp. 29–32, 2007.

[9] T. L. Lv, M. G. Sun, S. H. W. Song et al., "Study on photosynthesis characteristics of *Cercis chinensis* Bunge under drought and

salt stress," *Journal of Shandong Agricultural University (Natural Science)*, vol. 41, no. 2, pp. 191–195, 2010.

[10] W. W. Zhuang, J. Li, M. H. Cao et al., "Changes of osmotic adjusting substances in leaves of Ammodendron argenteum seedlings under salt and drought stress," *Acta Botanica Boreali-Occidentalia Sinica*, vol. 30, no. 10, pp. 2010–2015, 2010.

[11] X. H. Dong and G. Z. H. Yue, "Effects on growth of *Tamarix hispida willd* under salt stress," *Acta Agriculturae Boreali-Sinica*, vol. 25, pp. 154–155, 2010.

[12] W. H. Wang, X. M. Zhang, H. L. Yan et al., "Effects of salt stress on photosynthesis and smoregulation Substances of *Tamarix ramosissima Ledeb*," *Arid Zone Research*, vol. 26, no. 4, pp. 561–568, 2009.

[13] Y. Chen, H. Wang, F. S. Zhang, J. Xi, and Y. He, "The characteristic of salt excretion and its affected factors on *Tamarix ramosissima ledeb* under desert saline-alkali habitat in Xinjiang Province," *Acta Ecologica Sinica*, vol. 30, no. 2, pp. 511–518, 2010.

[14] T. C. Hsiao, "Physiological effects of plant in response to water stress," *Plant Physiology*, vol. 24, pp. 519–570, 1973.

[15] M. Chen, Y. N. Chen, and W. H. Li, "Physiological response of *Tamarix* spp.for different groundwater depths in the middle reaches of Tarim river in China," *Acta Botanica Boreali Occidentalia Sinica*, vol. 28, no. 7, pp. 1415–1421, 2008.

[16] W. Q. Zhao, L. Zhuang, F. Yuan et al., "Physiological and ecological characteristic of *Haloxylon ammodendron* and *Tamarix ramosissim*a in different habitatas on the southern edge of Zhunger Basin," *Journal of Shihezi University(Natural Science)*, vol. 28, no. 3, pp. 285–289, 2010.

[17] P. P. Xue, Ch. H. Cao, X. D. He et al., "Physiological and biochemical properties of Fraxinus velutina and Tamarix chinensis during the leaf expansion period under heavy salt stress," *Acta Scientiarum Naturalium Universitis Nankaiensis*, vol. 42, no. 4, pp. 18–23, 2009.

[18] G. B. Wang, F. L. Cao, and Q. Wang, "The effect of soil salt contents on uptake of nutrients of baldcypress," *Journal of Fujian College of Forestry*, vol. 24, no. 1, pp. 58–62, 2004.

[19] H. S. Li, *Principle and Technology of Plant Physio—Biochemical Experiment*, Higher Education Press, Beijing, China, 2000.

[20] G. H. Luo and A. G. Wang, *Guideline for Modern Plant Physiology Experiments*, Science Press, Beijing, China, 1999.

[21] A. J. Mao and Y. J. Wang, "Variation of polyphenoloxidase, peroxidase and phenylalanine ammonialylase in hot pepper seedlings infected by *Phytophthora capsici* L.," *Acta agricultural Boreali-Sinica*, vol. 18, no. 2, pp. 66–69, 2003.

[22] Sh. H. Yang, J. Ji, and G. Wang, "Effects of salt stress on plants and the mechanism of salt tolerance," *World Science-Technology Rearch & Development*, vol. 28, no. 4, pp. 70–76, 2006.

[23] G. Xu, H. B. Shao, J. N. Sun, and S. X. Chang, "Phosphorus fractions and profile distribution in newly formed wetland soils along a salinity gradient in the Yellow River Delta in China," *Journal of Plant Nutrition and Soil Science*, vol. 175, no. 5, pp. 721–728, 2012.

[24] Z. Y. Xie, W. H. Zhang, X. C. Liu et al., "Growth and physiological characteristics of *Xanthoceras sorbifolia* seedlings under soil drought stress," *Acta Botany Boreal-Occident Sinica*, vol. 30, no. 5, pp. 948–954, 2010.

[25] R. S. Dhindsa, P. Plumb-dhindsa, and T. A. Thorpe, "Leaf senescence: correlated with increased levels of membrane permeability and lipid peroxidation, and decreased levels of superoxide dismutase and catalase," *Journal of Experimental Botany*, vol. 32, no. 1, pp. 93–101, 1981.

[26] Y. Li, "Effect of salt and PEG to antioxidant enzymes activity and MDA concentration of *Luffa cylindrical* Roem," *Agricultural Research in the Arid Areas*, vol. 27, no. 2, pp. 159–162, 2009.

[27] S. Y. Rong, S. G. Guo, and T. Zhang, "Effects of drought stress on osmoregulation substances in sweet sorghum seedlings," *Journal of Henan Agricultural Sciences*, vol. 40, no. 4, pp. 56–59, 2011.

[28] K. Yan, P. Chen, H. Shao et al., "Responses of Photosynthesis and Photosystem II to higher temperature and salt stress in sorghum," *Journal of Agronomy and Crop Science*, vol. 198, no. 3, pp. 218–225, 2012.

[29] J.-X. Liu, J.-C. Wang, R.-J. Wang, and H.-Y. Jia, "Interactive effects of drought and salinity stresses on growth and osmotica of naked oat seedlings," *Journal of Soil and Water Conservation*, vol. 26, no. 3, pp. 244–248, 2012.

[30] Y. W. Shi, Y. L. Wang, and W. B. Li, "Effects of water stress on soluble protein, soluble sugar and praline content in Tamarix hispida," *Journal of Xinjiang Agricultural University*, vol. 30, no. 2, pp. 5–8, 2007.

[31] G. R. Stewart and J. A. Lee, "The role of proline accumulation in halophytes," *Planta*, vol. 120, no. 3, pp. 279–289, 1974.

Hindawi Publishing Corporation
The Scientific World Journal
Volume 2014, Article ID 183457, 10 pages
http://dx.doi.org/10.1155/2014/183457

Research Article

Impacts of Groundwater Recharge from Rubber Dams on the Hydrogeological Environment in Luoyang Basin, China

Shaogang Dong,[1] Baiwei Liu,[2] Huamin Liu,[3] Shidong Wang,[4] and Lixin Wang[1]

[1] *College of Environment and Resources, Inner Mongolia University, Hohhot 010021, China*
[2] *School of Environmental Studies, China University of Geosciences, Wuhan 430074, China*
[3] *College of Life Sciences, Inner Mongolia University, Hohhot 010021, China*
[4] *National Secondary Occupation School, Xilingol Vocational College, Xilinhot 026000, China*

Correspondence should be addressed to Huamin Liu; huaminliu@126.com and Lixin Wang; lxwimu@foxmail.com

Received 9 June 2014; Revised 21 June 2014; Accepted 21 June 2014; Published 14 July 2014

Academic Editor: Hongbo Shao

In the rubber dam's impact area, the groundwater total hardness (TH) has declined since 2000, ultimately dropping to 100–300 mg/L in 2012. pH levels have shown no obvious changes. NH_4-N concentration in the groundwater remained stable from 2000 to 2006, but it increased from 2007 to 2012, with the largest increase up to 0.2 mg/L. NO_3-N concentration in the groundwater generally declined in 2000–2006 and then increased from 2007; the largest increase was to 10 mg/L in 2012. Total dissolved solids (TDS) of the groundwater showed a general trend of decline from 2000 to 2009, but levels increased after 2010, especially along the south bank of the Luohe River where the largest increase recorded was approximately 100 mg/L. This study has shown that the increases in the concentrations of NH_4-N and NO_3-N were probably caused by changes in groundwater levels. Nitrates adsorbed by the silt clay of aeration zone appear to have entered the groundwater through physical and chemical reactions. TDS increased because of groundwater evaporation and some soluble ions entered the groundwater in the unsaturated zone. The distance of the contaminant to the surface of the aquifer became shorter due to the shallow depth of groundwater, resulting in the observed rise in pollutant concentrations more pronounced.

1. Introduction

Groundwater is an important water resource because of its wide distribution, good quality, ease of access, and small seasonal shifts. It becomes critical especially in arid and semiarid areas, as it may often be the only water source. The chemical compositions of the natural groundwater developed during the long geological history. It is affected by the types and characters of rocks to which the water is exposed, the feature of the replenishment water, and the water-rock interactions. As human actions on the environment have intensified, they have become a primary cause of the impact on the chemical characteristics of the groundwater in certain locations. For example, groundwater has been overpumped for industrial use and agriculture, which has caused the groundwater levels to decline and quality to deteriorate [1]. The concentration of nitrogen of the regional groundwater was raised by over fertilization in agriculture [2–4]. Insecticide residue polluted the surface water and shallow groundwater [5, 6]. Solid municipal waste and industrially manufactured solid waste increased the organic, heavy metals, and inorganic groundwater ions [7–9]. Excess discharge of domestic and industrial wastewater has also polluted the groundwater [10]. Groundwater overpumping in coastal areas has caused seawater intrusion [11–13].

Since 1965, more than 1000 rubber dams have been built in China for various purposes, such as irrigation, hydropower, groundwater replenishment, flood control, beautification of the environment, and recreation [14]. There are still a certain number of rubber dams under construction and being planned, especially in the arid and semiarid parts of China. The construction of rubber dams has changed the characteristics of the regional groundwater flow system and increased the amount of groundwater. It has also caused a series of

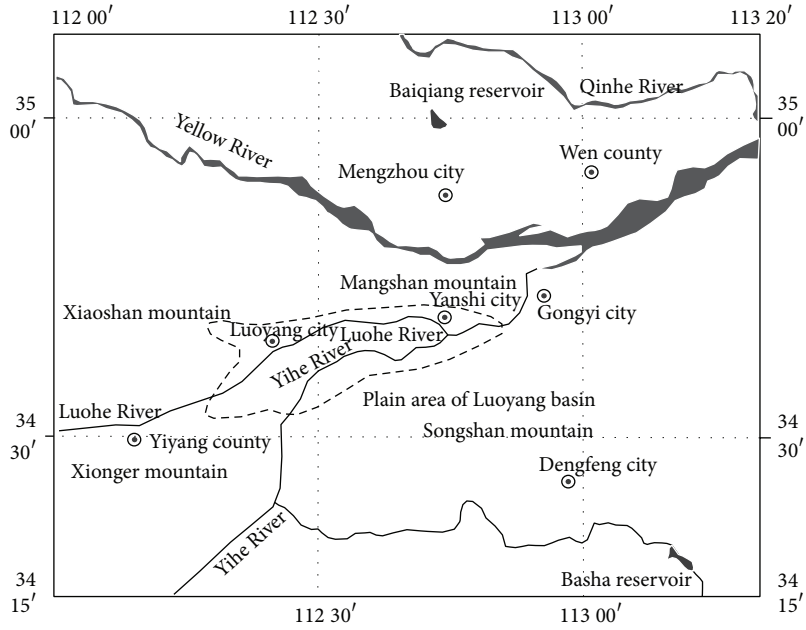

Figure 1: Luoyang Basin map.

environmental problems. The rise in the groundwater table has increased groundwater evaporation capacity, caused soil salinization, and increased groundwater salinity [15].

The groundwater recharge quantity of Luoyang Basin is 3.3–4.1 × 10^8 m^3/a (from 1995 to 1999) and the exploitation quantity is 3.8–4.3 × 10^8 m^3/a (from 1996 to 2000). The substantial decline in groundwater levels and the deterioration in quality were due to annual local overexploitation. In order to meet needs for groundwater as a resource and beautify the urban environment, five rubber dams were built on the Luohe River from 2000 to 2008. This paper discusses the impact of the rubber dam construction on groundwater and provides references for groundwater environment management and protection of Luoyang Basin.

2. Regional Physical Geography and Hydrogeology

2.1. Regional Physical Geography. The Luoyang Basin is located in western Henan Province, surrounded by Mang Shan, Xiao Shan, Xionger Shan, and Song Shan (Figure 1). It has a warm-temperate and monsoon climate. According to meteorological data, the perennial average temperature is 14.3°C and multiyear evaporation is 1451.7 mm. The multiyear average precipitation is 545.98 mm and this is subject to considerable temporal and spatial change. Precipitation is concentrated in July, August, and September, accounting for about 50% of annual precipitation.

2.2. Regional Hydrogeology. The Luoyang Basin formed in the late Mesozoic. It is a complete hydrogeological unit, surrounded by mountainous and loess hills. The Yi-luohe River alluvial plain is in the middle of it. Distribution and occurrence regulations of groundwater were dominated primarily by meteorology, hydrology, topography, formation lithology, and geological structure. Precipitation infiltration is the main supplement to groundwater.

The south side of the Basin is wildly composed, with carbonate rocks, and the north and west side are a loess hilly area with a steep slope and developed a deep clough. This kind of landform lends itself easily to runoff and discharge. The groundwater in this area can run very short.

The Yi-luohe River alluvial plain has subsided since the Quaternary period. It was the lowest part of this area and became a catchment area for surface water and groundwater. The aquifer of the whole Yi-luohe River alluvial plain area, especially in the massif and overbank, is thick. The aquifer is either directly exposed to the surface or covered by a minimal layer of earth or rock. This area has abundant groundwater resources. Generally, a single well can yield over 3000 m^3/d. The first and second terraces are mostly presented with a dual structure, an upper layer covered with sandy clay, and a lower layer stock with coarse sand and sandy gravel. Here, a single well can yield 1000–3000 m^3/d (Figure 2).

3. Primary Environmental Geological Problems before and after the Rubber Dam Construction

From 1957 to present, there have been thirteen groundwater source fields found in the Luoyang Basin, the total yield reached 280–300 million m^3/a. According to the monitoring data, the groundwater depth of the Luohe Riverside was 5.9–11.5 m in the middle and late 1980s. Because of overexploitation, the groundwater table has declined since the early 1990s. The Luohe River became a suspended river. Until 1999,

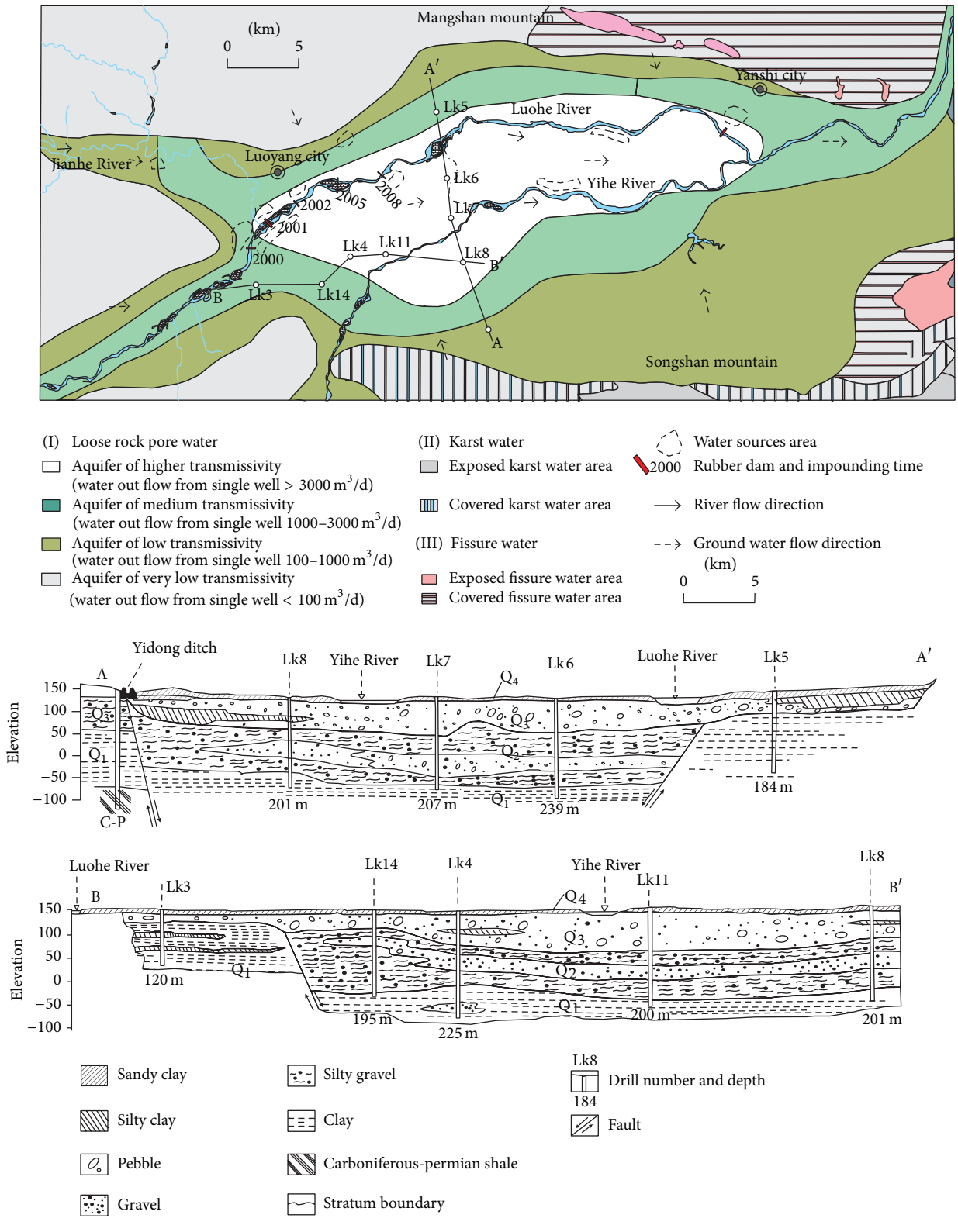

Geological profiles A-A′ and B-B′ in the study area

FIGURE 2: Hydrogeological plan fig. and profiles A–A′ and B–B′ in the Luoyang Basin.

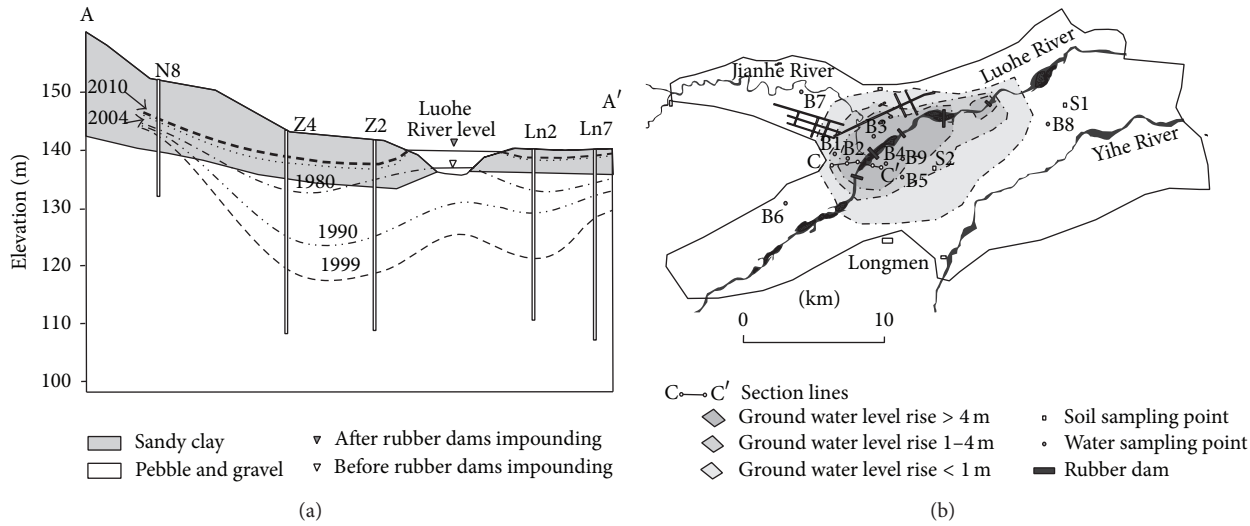

Figure 3: Changes of water tables before and after the rubber dam's construction.

groundwater depth was as low as to 13–19 m and even reached 30 m in some places (Figure 3(a)).

Due to long-term excessive exploitation of groundwater, the Luoyang Basin has suffered a serious environmental problem, including depression of the water table, deterioration of water quality, and land subsidence. In order to alleviate the increasingly intense groundwater shortages and improve the city landscape, the Luoyang city government built five rubber dams from 2000 to 2008 (Table 1 and Figure 3(b)).

Construction of Luohe River rubber dams has changed the regional groundwater flow system tremendously. The groundwater table along the river began to rise when the first rubber dam was built in April 2000. In addition, the cone of depression which had been caused by overpumping of groundwater along the river has already dispersed, resembling the state recorded in 2004. The main replenishment of the Luohe River to groundwater has changed from vertical seepage to lateral one (Figure 3(a)). As the groundwater level has risen, its quality has changed as well.

4. Materials and Methods

Nine observation wells were selected in Luoyang Basin, China, to study the variations in pH, total hardness (TH), total dissolved solids (TDS), nitrate nitrogen (NO_3-N), and ammonium nitrogen (NH_4-N) before and after the construction of the Luohe River rubber dams. The data were gathered over the course of 24 years from 1989 to 2012 and sampled in the dry period (October to December of each sampling year).The positions of the observation wells are shown in Figure 3(b) and the vertical dimension of the observation to the Luohe River is shown in Table 2. Observation wells number B6, number B7, and number B8 are located in an area largely unaffected by rubber dams. First, the water was left to run from sampling source for 4-5 min, before taking the final sample. Samples were collected in precleaned sterilized polyethylene bottles of 3 L capacity. The pH of the collected water samples was measured in the field using portable pH meter. TH was determined using ethylenediaminetetraacetic acid (EDTA) titration method. TDS were estimated by gravimetric method. NO_3^- was determined in inductively coupled plasma mass spectrometry (ICP-MS). NH_4^+ was determined in ultraviolet-visible spectrophotometer.

To analyze characteristics of nitrogen distribution in the vadose zone, two undisturbed sediment cores were collected in October 2011. The cores were accomplished by drilling and sampling with a 7.5 cm diameter hollow stem hand auger. Two cores (core S1 and core S2) from two locations (Figure 3(b)) were taken continuously from the ground surface to a depth of 6.5 m. Bulk soil samples of w400 g were collected at different depths (Table 3). Samples were homogenized over the sampling interval and immediately sealed in polyethylene bags. Gravimetric moisture content was determined by drying a minimum of 100 g of soil sample at 110°C for 12 h. For the unsaturated zone moisture extracts, 200 g of sediment was combined with 200 mL of deionized water and shaken for 30 min at room temperature, after which a mixture of deionized water and soil water was produced using centrifuge at a rotational speed of 4000 rpm [16]. All of the samples were kept at 4°C prior to analysis.

5. Results

The pH values and NH_4-N concentrations for observation wells number B6, number B7, and number B8 did not show marked variations when compared with values prior to the construction of the Luohe River rubber dams (Figures 4(a) and 4(e)). However, TH (Figure 4(b)), TDS (Figure 4(c)), and NO_3-N (Figure 4(d)) were slightly higher than before the dam had been constructed. The average concentrations of TH, TDS, and NO_3-N were 34.7–120.1 mg/L, 71.5–178.3 mg/L, and 4.6–6.9 mg/L, respectively, after the rubber dams were built (Table 4). Number B7 was located in the Jianhe River area and all its indexes went up the fastest. Number B6 and

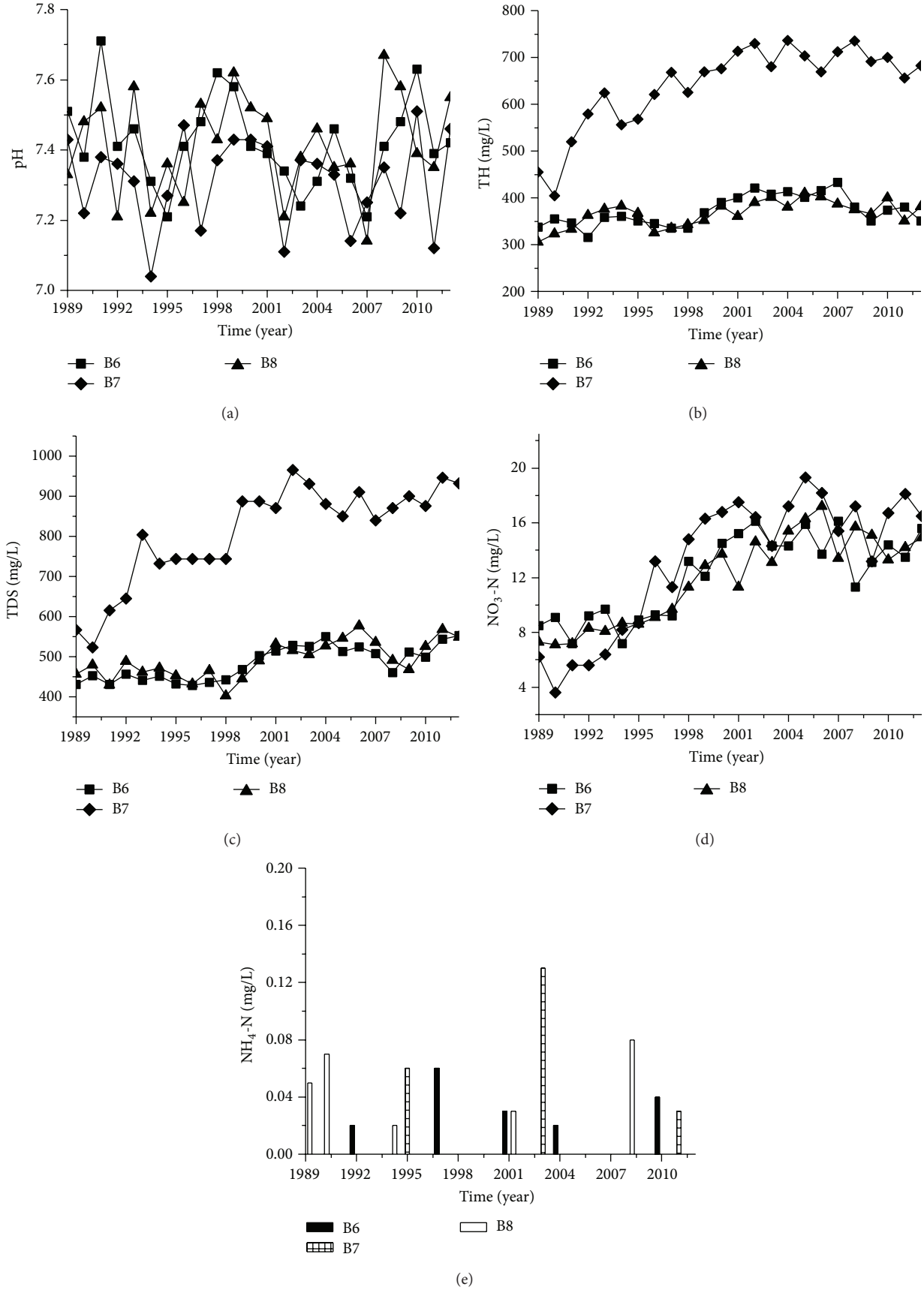

Figure 4: Concentration changes of pH, TH, TDS, NO_3-N, and NH_4-N of wells B6, B7, and B8.

Table 1: Basic information regarding rubber dams in Luoyang.

Stage	Locations	Storage time	Water surface elevation (m)	Bottom elevation (m)	Maximum dam height (m)	Backwater length (m)	Water area $\times 10^4$ m^2	Water storage $\times 10^4$ m^3
First stage	Shangyang gong	April, 2000	140.5	136.5	4	3200	148	369
Second stage	Tongleyuan	April, 2001	135.6	132.1	3.5	2330	128	327
Third stage	Luoshenpu	April, 2002	131.6	127.6	4	3270	184	504
Forth stage	Zhoushan	April, 2005	130.3	126	4.3	2200	219	468
Fifth stage	Hualinyuan	April, 2008	127.7	123	4.5	3200	148	500

Table 2: Locations of observation wells along the Luohe River.

Well number	Vertical dimension to Luohe River (m)	Location	Well depth (m)
B1	1850	Second terrace	40
B2	960	First terrace	45
B3	700	First terrace	30
B4	800	Flood plain	27
B5	2330	Flood plain	29
B6	1820	Second terrace	33
B7	6410	Jianhe river watershed	76
B8	2730	Flood plain	35
B9	1160	Flood plain	21

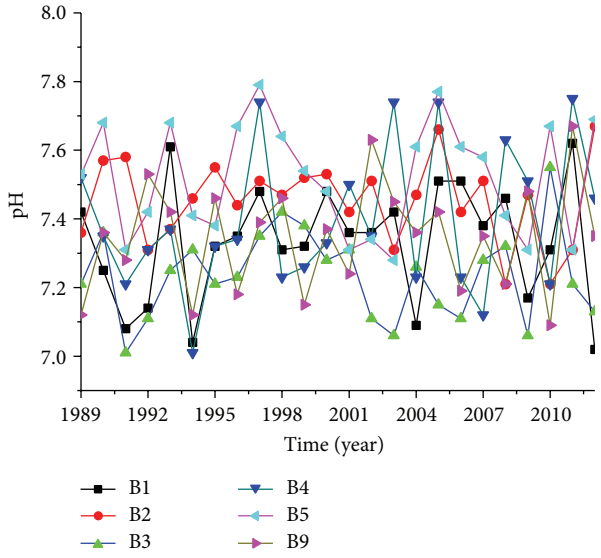

Figure 5: pH values change of groundwater of rubber dams affected area.

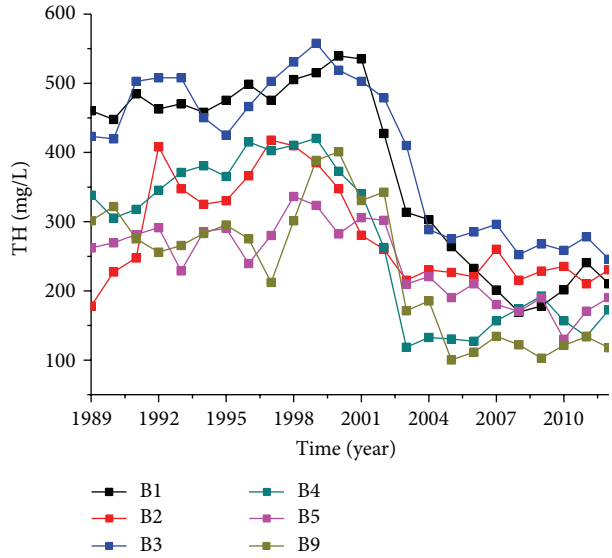

Figure 6: TH concentration changes of groundwater of the rubber dams affected area.

number 8 were in the Luohe River area, which showed similar changes. In all, regional groundwater tended to deteriorate because of overexploitation and human activity.

Observation wells number B1, number B2, number B3, number B4, number B5, and number B9 were located in the areas affected by rubber dams, and concentrations of TH, TDS, NO_3-N, and NH_4-N presented showed significant changes after the rubber dams were built but pH values did not change very much (Figure 5).

The annual average concentration of TH, TDS, and NO_3-N declined within a range of 75.0–209.8 mg/L, 49.8–244.6 mg/L, and 0.2–14.0 mg/L, respectively, but the concentration of NH_4-N increased within the range of 0.01–0.07 mg/L (Table 4). TH concentration of above wells obviously declined from 2000 and was then kept relatively stable (Figure 6).

Observation wells number B1, number B2, and number B3 are located on the first and second terraces of the north

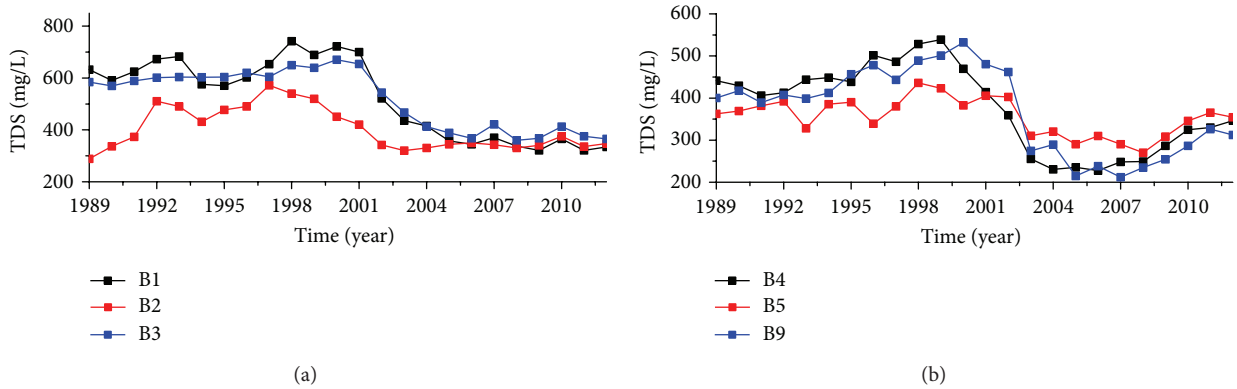

Figure 7: TDS concentration changes of groundwater of the rubber dams affected area.

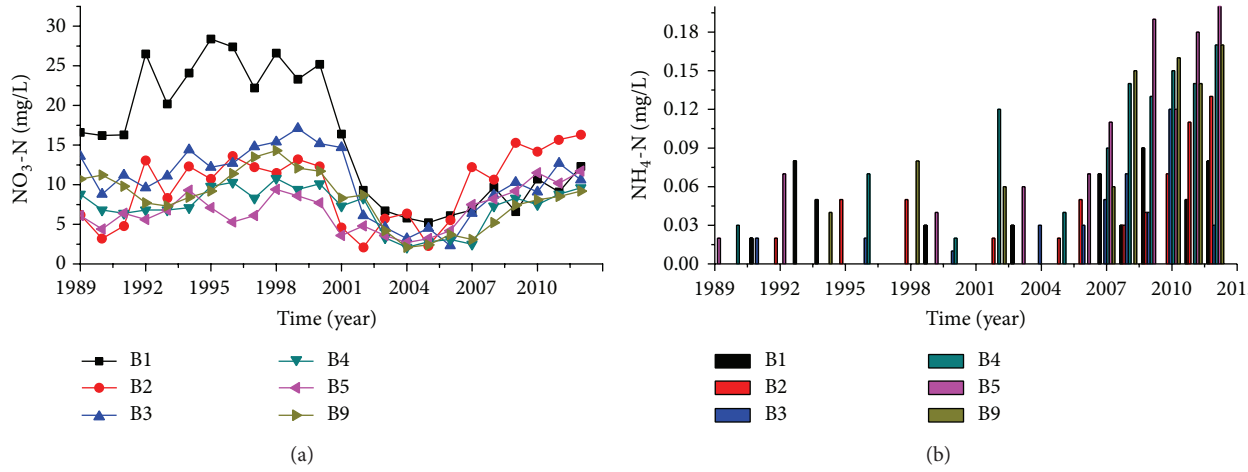

Figure 8: NO_3-N and NH_4-N concentration changes of groundwater of rubber dams affected area.

side of the Luohe River. The TDS concentration of these wells decreased from 2000, after which it became stable (Figure 7(a)). Number B4, number B5, and number B9 wells are located in the south bank of Luohe River floodplain. These rebounded after 2010 (Figure 7(b)).

The concentration of NO_3-N declined after 2000, following the construction of the rubber dam (Figure 8(a)). In most places, concentration was restored to its previous level since 2007. Number B2 well had higher levels during the study period than it had before the rubber dams were constructed.

The NH_3-N concentration of the groundwater in this area was extremely low before the rubber dam was built. There have been twelve monitors from 1989 to 2000. Only number B1 was assessed four times and all other wells were assessed two or three times. The maximum concentration was 0.08 mg/L (Figure 8(b)). From 2000 to 2006, ammonia in the groundwater showed only small changes but it has increased since 2007, and the entire groundwater recovery has been mapped out (Figure 8(b)). The concentration peaked at 0.22 mg/L (number B5).

6. Discussions

6.1. Water Quality in Luohe River versus Regional Groundwater. The degree to which the water of the Luohe River has replenished the groundwater increased greatly after the construction of the rubber dams, so the water quality of the Luohe River has had a significant impact on that of the groundwater. According to the monitoring data of Luohe River water quality from 1998 to 2012, the values of TH, TDS, and NO_3-N were lower than that of the regional groundwater, but the concentration of NH_4-N and pH values were higher (Table 5). If the only action that takes place is mixing, then the concentrations of TH, NO_3-N, and TDS in the groundwater would have exhibited similar changes and the concentration of NH_4-N would be lower in groundwater than in the river. This may explain the concentration anomalies observed for NO_3-N, TDS, and NH_4-N in the groundwater following the rubber dam construction. This indicates that those changes not only had a close relationship with river replenishment but also had a close relationship with the local hydrogeological conditions and land use changes.

Table 3: Analysis of the chemical composition of water-soluble NH_4-N and NO_3-N in different soil depth. Unit: mg/kg dry soil.

Sample		S1			S2	
Buried depth	NH_4-N	NO_3-N	Soil type	NH_4-N	NO_3-N	Soil type
0–10 cm	32.1	14.36	Sandy clay	28.1	18.25	Sandy clay
20–30 cm	27.2	7.53	Sandy clay	21.4	14.34	Sandy clay
50–60 cm	29.1	5.88	Sandy clay	20.1	7.21	Sandy clay
110–120 cm	41.6	2.43	Sandy clay	32.3	4.32	Sandy clay
240–250 cm	25.3	6.12	Sandy clay	28.1	8.44	Sandy clay
310–320 cm	36.7	4.32	Sandy clay	19.6	6.21	Sandy clay
450–460 cm	3.2	0.36	Sandy gravel	22.6	5.21	Sandy clay
550–560 cm	2.5	0.25	Sandy gravel	4.1	0.32	Sandy gravel
610–620 cm				2.3	0.18	Sandy gravel
650–660 cm				2.6	0.11	Sandy gravel

Table 4: Each index of annual average concentration before and after the rubber dams construction.

Well number		B1	B2	B3	B4	B5	B9	B6	B7	B8
pH	Average of 1989 to 2000	7.32	7.47	7.26	7.33	7.54	7.32	7.46	7.32	7.42
	Average of 2001 to 2012	7.35	7.43	7.21	7.46	7.49	7.37	7.38	7.30	7.41
	Difference	0.03	−0.04	−0.05	0.12	−0.05	0.05	−0.07	−0.02	−0.01
TH (mg/L)	Average of 1989 to 2000	482.9	332.6	484.5	370.5	280.9	298.1	349.8	580.6	348.9
	Average of 2001 to 2012	273.1	234.5	320.0	174.9	206.0	164.4	393.9	700.8	383.6
	Difference	−209.8	−98.2	−164.5	−195.6	−75.0	−133.7	44.1	120.1	34.7
TDS (mg/L)	Average of 1989 to 2000	646.6	456.8	611.6	462.0	380.9	443.8	447.6	719.5	456.1
	Average of 2001 to 2012	402.0	348.4	428.1	292.3	331.1	298.9	519.1	897.8	528.4
	Difference	−244.6	−108.4	−183.5	−169.7	−49.8	−145.0	71.5	178.3	72.3
NO_3-N (mg/L)	Average of 1989 to 2000	22.8	10.1	13.0	8.5	6.9	10.6	9.8	9.7	9.3
	Average of 2001 to 2012	8.7	9.2	7.8	5.9	6.7	5.9	14.5	16.7	14.5
	Difference	−14.0	−0.9	−5.2	−2.5	−0.2	−4.7	4.6	6.9	5.2
NH_4-N (mg/L)	Average of 1989 to 2000	0.02	0.01	0.00	0.01	0.01	0.01	0.01	0.01	0.01
	Average of 2001 to 2012	0.03	0.04	0.03	0.08	0.08	0.06	0.01	0.01	0.01
	Difference	0.01	0.03	0.03	0.07	0.07	0.05	0.00	0.01	0.00

6.2. Concentrations of NO_3-N and NH_4-N in Groundwater. The concentration of nitrate in groundwater is affected by many factors, such as land use change groundwater replenishment, vadose zone lithology, nitrogen transformation in saturated zone and aeration zone, groundwater table depth, surface water and groundwater exchange, and groundwater dynamics [17–21].

The urbanization of Luohe River south bank has proceeded rapidly since 2005. A great deal of farmland has disappeared. Observation wells number B4, number B5, and number B9 are located in this area, which was farmland before 2007 and was replaced by buildings, parks, and wetlands as of 2010. This shows that the high levels of ammonia nitrogen and nitrate nitrogen in the groundwater could be more related to point sources of pollution than to agricultural activity.

According to soil sample analysis (Table 3), the difference in water-soluble NH_4^+ and NO_3^- was enormous in the upper sandy clay and lower sandy gravel, which is in the vadose zone of the Luoyang Basin plain. Water-soluble NO_3-N in the upper sandy clay was 2.43–18.25 mg/kg (dry soil), which was 0.11–0.36 mg/kg (dry soil) in the lower gravel. Water-soluble NH_4-N in the upper sandy clay was found to be 19.6–41.6 mg/L (dry soil), and it was 2.3–4.1 mg/kg (dry soil) in the lower gravel.

Soil characteristics dictate nitrogen kinetics. In well-drained soils, infiltration is considerable, so the rate of nitrification is high and denitrification may be insignificant. Soil depth controls the time lag between the on-ground application of nitrogen and nitrate leaching and it influences the time span of soil nitrogen transformations [17].

The groundwater table rose from sandy gravel layer to the sandy clay layer after the rubber dams were built (Figure 3(a)). Water-soluble NO_3^- and NH_4^+ in the vadose zone dissolved into the groundwater as the water table ascended, so the concentration of NO_3^- and NH_4^+ increased gradually. The groundwater table is also subject to seasonal changes. Part of the sandy clay layer is in alternating drying-wetting situation that can accelerate nitrification. A part of NH_4^+ was converted to NO_3^- in oxidizing atmospheres, causing a decrease in ammonia nitrogen in the groundwater, and the NO_3^- concentration increased further. This process

Table 5: Analysis of surface water quality.

Time	pH	TH (mg/L)	TDS (mg/L)	NO_3-N (mg/L)	NH_4-N (mg/L)
Oct. 1998	7.65	207.4	265.3	2.25	0.14
Oct. 1999	7.43	189.3	212.7	1.75	0.07
Oct. 2000	7.51	211.3	237.6	2.56	0.11
Oct. 2002	7.52	194.3	256.1	1.87	0.05
Nov. 2003	7.81	250.7	344.6	3.07	0.27
Oct. 2004	7.58	215.2	310.5	3.14	0.19
Nov. 2005	7.62	245.2	320.1	2.98	0.23
Oct. 2007	7.42	237.1	312.1	4.12	0.21
Nov. 2008	7.35	225.2	330.4	2.73	0.16
Nov. 2010	7.36	232.6	310.7	2.58	0.15
Oct. 2011	7.41	253.2	338.9	2.32	0.17
Nov. 2012	7.63	211.5	289.4	3.15	0.22

is affected by groundwater table depth, water level, and lithology of the water transition area. The nitrogen of Earth's surface reaches the groundwater in a shorter time due to superficial groundwater burial depth and speeds up the increasing rate of NO_3^- [22].

The changes in NO_3-N and NH_4-N in this area are presented mainly in two phases: from 2000 to 2006, rivers replenished the groundwater in abundance, and the NO_3-N and NH_4-N of the groundwater were mainly influenced by the quality of river water, presenting a depressed tendency. As the groundwater table rose, the river water replenished to groundwater decreasingly. After 2007, the NH_4^+ and NO_3^- of the aeration zone and Earth's surface were the primary causes of the increase in the concentration of NO_3-N and NH_4-N in groundwater.

6.3. Analysis of TDS Changes in the Groundwater. The concentration of TDS in the groundwater was controlled by the types and characteristics of the rock, the properties of the replenishing water, human activities, water-rock interactions, and evaporation. The south bank (location of observation wells number 1, number 2, and number 3) and north bank (location of observation wells number 4, number 5, and number 9) of the Luohe River had the same lithology distribution and were subject to similar human activities, so the main cause of the different concentrations of TDS may be attributed mainly to different groundwater burial depths. Groundwater evaporation capacity is affected by burial depth, lithology, and meteorological conditions, and evaporation generally increases as depth becomes shallower.

The plain area of Luoyang Basin is with a double structure, the upper layer is sandy clay, and the lower layer is sand and gravel. When the groundwater table rises to the sandy clay layer, which consists of small granules, capillary elevation and groundwater evaporation both increase.

A groundwater evaporation simulation was performed before and after a four-grade rubber dam system was constructed on Bai River of Nanyang City [23]. This area has hydrology and meteorology conditions similar to those of the Luohe River. After the four rubber dams were finished, the evaporation loss reached 5.02 million m^3, about 3 times of the amount of evaporation prior to the construction of the dam. Observation wells number 1, number 2, and number 3 were located on the first and second terraces, and regional groundwater burial depth was 5–15 m. Observation wells number 4, number 5, and number 9 were on the flood plain of the Yi-luohe River. The groundwater burial depth there is 0.3–4 m. There was much more evaporation of the south bank than on the north bank of the Luohe River. The TDS concentration has definitely increased over the ten years since the rubber dams were built under strong evaporation conditions and water-rock interactions caused by wet-dry season changes. Surface pollutants discharged by human activities entered the aquifer in a shorter time than rubber dam constructed before due to the shallow groundwater burial depth. This might be another reason why the concentration of TDS increased.

7. Conclusions

The present study revealed that five rubber dams built in Luohe River from 2000 to 2008 have affected the groundwater environment a great deal. With the construction of the first rubber dam in 2000 and 4 additional dams built later, groundwater overdraft problem caused by groundwater exploitation was almost completely alleviated. The groundwater table ascended 30 m in some places, even as early as 2004. Concentrations of TH, TDS, and NO_3-N decreased considerably after river water began to replenish the groundwater.

In 2007, seven years after the rubber dam was constructed, the amount of NH_4^+ and NO_3^- that had been adsorbed in the aeration zone was instead turned into the aquifer. As a result, the concentrations of NH_4-N and NO_3-N in this area were elevated. TDS of the south side of the Luohe River increased under strong evaporation and water-rock interactions in the sandy clay layer starting in 2010. With the rise of the groundwater level, pollutants discharged by human activities reached the aquifer in a shorter time than before. This is another reason why the concentration of TDS, NH_4-N, and NO_3-N increased.

Developing means of exerting reasonable control over groundwater resource management to prevent groundwater

overdraft should be the focus of groundwater research in this region.

Conflict of Interests

There is no conflict of interests regarding the publication of the paper.

Authors' Contribution

Shaogang Dong and Baiwei Liu are cofirst authors who contributed to the work in the paper equally.

Acknowledgments

This study was supported by the National Key Basic Research Program of China (no. 2014CB138802), the National Key Technology R&D Program (no. 2011BAC02B03), and the National Natural Science Funds, China (nos. 41002129, 31060076, 41261009, and 40901029).

References

[1] N. J. Lambrakis, K. S. Voudouris, L. N. Tiniakos, and G. A. Kallergis, "Impacts of simultaneous action of drought and overpumping on quaternary aquifers of Glafkos basin (Patras region, western Greece)," *Environmental Geology*, vol. 29, no. 3-4, pp. 209–215, 1997.

[2] Y. Jiang and G. Somers, "Modeling effects of nitrate from non-point sources on groundwater quality in an agricultural watershed in Prince Edward Island, Canada," *Hydrogeology Journal*, vol. 17, no. 3, pp. 707–724, 2009.

[3] J. B. Aguilar, P. Orban, A. Dassargues, and S. Brouyère, "Identification of groundwater quality trends in a chalk aquifer threatened by intensive agriculture in Belgium," *Hydrogeology Journal*, vol. 15, no. 8, pp. 1615–1627, 2007.

[4] G. Stamatis, K. Parpodis, A. Filintas, and E. Zagana, "Groundwater quality, nitrate pollution and irrigation environmental management in the Neogene sediments of an agricultural region in central Thessaly (Greece)," *Environmental Earth Sciences*, vol. 64, no. 4, pp. 1081–1105, 2011.

[5] F. Worrall and T. Besien, "The vulnerability of groundwater to pesticide contamination estimated directly from observations of presence or absence in wells," *Journal of Hydrology*, vol. 303, no. 1–4, pp. 92–107, 2005.

[6] K. L. Knee, R. Gossett, A. B. Boehm, and A. Paytan, "Caffeine and agricultural pesticide concentrations in surface water and groundwater on the north shore of Kauai (Hawaii, USA)," *Marine Pollution Bulletin*, vol. 60, no. 8, pp. 1376–1382, 2010.

[7] R. Vijay, P. Khobragade, and P. K. Mohapatra, "Assessment of groundwater quality in Puri City, India: an impact of anthropogenic activities," *Environmental Monitoring and Assessment*, vol. 177, no. 1–4, pp. 409–418, 2011.

[8] G. T. Rao, V. V. S. G. Rao, K. Ranganathan, L. Surinaidu, J. Mahesh, and G. Ramesh, "Assessment of groundwater contamination from a hazardous dump site in Ranipet, Tamil Nadu, India," *Hydrogeology Journal*, vol. 19, no. 8, pp. 1587–1598, 2011.

[9] J. Ngo Michel, V. Gujisaite, A. Latifi, and M. O. Simonnot, "Parameters describing nonequilibrium transport of polycyclic aromatic hydrocarbons through contaminated soil columns: estimability analysis, correlation, and optimization," *Journal of Contaminant Hydrology*, vol. 158, pp. 93–109, 2014.

[10] A. Mukhopadhay, A. Akber, and E. Al-Awadi, "Evaluation of urban groundwater contamination from sewage network in Kuwait City," *Water, Air, and Soil Pollution*, vol. 216, no. 1–4, pp. 125–139, 2011.

[11] A. Baghvand, T. Nasrabadi, G. N. Bidhendi, A. Vosoogh, A. Karbassi, and N. Mehrdadi, "Groundwater quality degradation of an aquifer in Iran central desert," *Desalination*, vol. 260, no. 1–3, pp. 264–275, 2010.

[12] S. Sankaran, S. Sonkamble, K. Krishnakumar, and N. C. Mondal, "Integrated approach for demarcating subsurface pollution and saline water intrusion zones in SIPCOT area: A case study from Cuddalore in Southern India," *Environmental Monitoring and Assessment*, vol. 184, no. 8, pp. 5121–5138, 2012.

[13] A. H. D. Cheng, L. F. Konikow, and D. Ouazar, "Special issue of transport in porous media on 'seawater intrusion in coastal aquifers'," *Transport in Porous Media*, vol. 43, pp. 1–2, 2001.

[14] W.-H. Lu and Z.-Q. Hou, *Design and Management of Rubber Dam*, Water Power Press, Beijing, China, 2005, (Chinese).

[15] G. Zarei, M. Homaee, and A. Liaghat, "Modeling transient evaporation from descending shallow groundwater table based on Brooks-Corey retention function," *Water Resources Management*, vol. 23, no. 14, pp. 2867–2876, 2009.

[16] L. Yuan, Z. Pang, and T. Huang, "Integrated assessment on groundwater nitrate by unsaturated zone probing and aquifer sampling with environmental tracers," *Environmental Pollution*, vol. 171, pp. 226–233, 2012.

[17] M. N. Almasri, "Nitrate contamination of groundwater: a conceptual management framework," *Environmental Impact Assessment Review*, vol. 27, no. 3, pp. 220–242, 2007.

[18] T. Darwish, T. Atallah, R. Francis et al., "Observations on soil and groundwater contamination with nitrate: a case study from Lebanon-East Mediterranean," *Agricultural Water Management*, vol. 99, no. 1, pp. 74–84, 2011.

[19] M. M. R. Jahangir, P. Johnston, M. I. Khalil, and K. G. Richards, "Linking hydrogeochemistry to nitrate abundance in groundwater in agricultural settings in Ireland," *Journal of Hydrology*, vol. 448-449, pp. 212–222, 2012.

[20] T. Hosono, T. Tokunaga, M. Kagabu et al., "The use of δ^{15}N and δ^{18}O tracers with an understanding of groundwater flow dynamics for evaluating the origins and attenuation mechanisms of nitrate pollution," *Water Research*, vol. 47, no. 8, pp. 2661–2675, 2013.

[21] R. Kent and M. K. Landon, "Trends in concentrations of nitrate and total dissolved solids in public supply wells of the Bunker Hill, Lytle, Rialto, and Colton groundwater subbasins, San Bernardino County, California: influence of legacy land use," *Science of the Total Environment*, vol. 452-453, pp. 125–136, 2013.

[22] H. Guo, G. Li, D. Zhang, X. Zhang, and C.-A. Lu, "Effects of water table and fertilization management on nitrogen loading to groundwater," *Agricultural Water Management*, vol. 82, no. 1-2, pp. 86–98, 2006.

[23] X. Chen, M. Ling, Q. Zhou, Z. Zhang, and Q. Cheng, "Numerical modeling the role of rubber dams on groundwater recharge and phreatic evaporation loss in riparian zones," *Environmental Earth Sciences*, vol. 65, no. 1, pp. 345–352, 2012.

Hindawi Publishing Corporation
The Scientific World Journal
Volume 2014, Article ID 868391, 9 pages
http://dx.doi.org/10.1155/2014/868391

Research Article

Expression Profiles of 12 Late Embryogenesis Abundant Protein Genes from *Tamarix hispida* in Response to Abiotic Stress

Caiqiu Gao,[1,2] Yali Liu,[3] Chao Wang,[1] Kaimin Zhang,[1] and Yucheng Wang[1]

[1] *State Key Laboratory of Tree Genetics and Breeding, Northeast Forestry University, 26 Hexing Road, Harbin 150040, China*
[2] *Key Laboratory of Forest Genetics & Biotechnology, Nanjing Forestry University, Ministry of Education, Nanjing 210037, China*
[3] *Northeast Forestry University Library, 26 Hexing Road, Harbin 150040, China*

Correspondence should be addressed to Yucheng Wang; ychngwang@yahoo.com

Received 23 February 2014; Revised 21 June 2014; Accepted 21 June 2014; Published 10 July 2014

Academic Editor: Hongbo Shao

Twelve embryogenesis abundant protein (*LEA*) genes (named *ThLEA-1 to -12*) were cloned from *Tamarix hispida*. The expression profiles of these genes in response to NaCl, PEG, and abscisic acid (ABA) in roots, stems, and leaves of *T. hispida* were assessed using real-time reverse transcriptase-polymerase chain reaction (RT-PCR). These *ThLEAs* all showed tissue-specific expression patterns in roots, stems, and leaves under normal growth conditions. However, they shared a high similar expression patterns in the roots, stems, and leaves when exposed to NaCl and PEG stress. Furthermore, *ThLEA-1, -2, -3, -4*, and *-11* were induced by NaCl and PEG, but *ThLEA-5, -6, -8, -10*, and *-12* were downregulated by salt and drought stresses. Under ABA treatment, some *ThLEA* genes, such as *ThLEA-1, -2*, and *-3*, were only slightly differentially expressed in roots, stems, and leaves, indicating that they may be involved in the ABA-independent signaling pathway. These findings provide a basis for the elucidation of the function of *LEA* genes in future work.

1. Introduction

Adverse environmental conditions, such as salt, drought, and high temperatures, severely limit the growth and geographical distribution of many plants. At the same time, plants have evolved many mechanisms to tolerate these adverse conditions [1–5], and the regulation of gene expression is critical for these processes [6]. *Late embryogenesis abundant* (*LEA*) genes play important roles in stress tolerance, especially in drought stress. In wheat, there are several genes which are responsible for drought stress tolerance and produce different types of enzymes and proteins, for instance, late embryogenesis abundant (LEA) protein, responsive to abscisic acid (Rab), rubisco, helicase, proline, glutathione-S-transferase (GST), and carbohydrates during drought stress [7]. The LEA proteins to be firstly identified were from cotton, and they were highly synthesized during the later stages of embryogenesis [8].

To date, hundreds of *LEA*s have been cloned from different plant species [9]. Some *LEA* genes are highly induced by various abiotic or biotic stress treatments including salt [10, 11], drought or osmotic stress [12, 13], heat [14], cold [15, 16], and wounding [17]. In addition, the expression of *LEA* genes are also modulated by abscisic acid (ABA) [10, 18] and ethylene [17]. Transformed plants that overexpress *LEA* genes show improved tolerance to salt stress [19, 20], water deficit or drought conditions [10, 21], and cold [16, 22], but they are hypersensitive to ABA [23].

However, to date the true functions of *LEA*s are not fully understood. Therefore, analyzing the expression patterns of *LEA* genes will be beneficial to understanding their role in stress responses. *Tamarix hispida*, a woody halophyte, is widely distributed in drought-stricken areas and saline or saline-alkali soil in Central Asia and China. This species is highly tolerant to salt, drought, and high temperature, which makes it the desirable tree special to study the salt tolerance mechanism and clone the genes involved in salt tolerance.

In the present study, 12 *ThLEA* genes were cloned from *T. hispida*, and the expression patterns of these genes were determined in response to salt (NaCl), drought (PEG), and abscisic acid (ABA) treatments in the roots, stems, and leaves by using real-time reverse transcriptase-polymerase chain

Table 1: Primers used for quantitative real-time RT-PCR analysis.

Gene	GenBank accession number	Forward primer (5′-3′)	Reverse primer (5′-3′)
ThLEA-1	KF801660	CAGCGAAGTTTGGATGGAATG	ACCTGTCGCCAATCAGAAGAT
ThLEA-2	KF801661	CACACAATAGAAACCGTAGAG	CCTCCATGGTCTCCTTAACT
ThLEA-3	KF801662	CGAGATCCTTGGTGGAGCTCG	TCACGTATGTGTCATGACTAC
ThLEA-4	KF801663	GTGGCTATCTCGATTCGTAGT	GCAACAGACACCAACCAAGAT
ThLEA-5	KF801664	GTTCGCAGCAGGAAAGAGCAG	ACTCCGTCAACACGGTACTACT
ThLEA-6	KF801665	GTTGAGGATGTGGATATCAAG	CGAGTTCATAATCGATATCC
ThLEA-7	KF801666	TCATGATATTGGTGAGAAG	AGTGGTATCTTAACAGTCTCT
ThLEA-8	KF801667	GATGACGACACATGATGAAGC	AGCCTCCACAGTCCCTTCCGT
ThLEA-9	KF924555	GTGGTTGTGGAGATGAACGGAG	GGTAGCAGCATCATCAGCAATG
ThLEA-10	KF924556	AGAGTCAGCAACCGATACAGC	TCTCTGCCTTGCTGATTCCTC
ThLEA-11	KF924557	ACGGAGGAAGCTAGGCACGAAG	CTGCTGCGTCCTTGTATTCC
ThLEA-12	KF924558	CAAGATGCAGGAGGTGGTGAT	ATCTGCTATTCTTCTGCCTGT
Actin	FJ618517	AAACAATGGCTGATGCTG	ACAATACCGTGCTCAATAGG
α-Tubulin	FJ618518	CACCCACCGTTGTTCCAG	ACCGTCGTCATCTTCACC
β-Tubulin	FJ618519	GGAAGCCATAGAAAGACC	CAACAAATGTGGGATGCT

reaction (RT-PCR). Our study may provide the fundament data for studying the function of *LEA* genes.

2. Materials and Methods

2.1. Plant Materials and Treatments. Seedlings of *T. hispida* were grown in pots with a mixture of turf peat and sand (2 : 1 v/v) in a greenhouse at 70–75% relative humidity, light/dark cycle of 14/10 h, and the temperature of 24°C. Two-month-old seedlingswere used for experimental analyses. The seedlings were watered at the roots with one of the following solutions: 0.4 M NaCl, 20% (w/v) PEG_{6000}, or 100 μM ABA for 0, 3, 6, 9, 12, and 24 h. In controls, the seedlings were watered with the same volume of fresh water. Following these treatments, the leaves, stems, and roots from at least 20 seedlings were harvested and pooled, frozen immediately in liquid nitrogen, and stored at −80°C for RNA preparation. Three samples were used for real-time RT-PCR biological repeats.

2.2. Cloning of the LEA Genes from T. hispida. In a previous study, 11 cDNA libraries of *T. hispida* treated with $NaHCO_3$ were constructed using Solexa technology, which were the 8 libraries, respectively, from roots of *T. hispida* treated with $NaHCO_3$ for 0, 12, 24, and 48 h (2 libraries were built from each treatment as biological replication) and 3 libraries from leaves of *T. hispida* treated with $NaHCO_3$ for 0, 12, and 24 h. In total 94,359 nonredundant unigenes of >200 nt in length were generated using the SOAP de novo software. Subsequently, these unigenes were searched against the Nr database and the Swiss-Prot database using blastx (http://blast.ncbi.nlm.nih.gov/) with a cut-off *E*-value of 10^{-5} [24, 25]. The unigenes representing the "*LEA*" genes were queried and identified from these libraries according to the functional annotation. Then, primers for the *LEA* genes were designed according to these sequences. RT-PCR and resequencing were used to confirm the *LEA* sequences.

2.3. Sequence Alignments and Phylogenetic Analysis. Firstly, the open reading frames (ORFs) of all the *LEA* unigenes (named as *ThLEA-1* to *-12*) were identified using the ORF finder tools from the NCBI (http://www.ncbi.nlm.nih.gov/gorf/gorf.html). Subsequently, the *LEA*s with complete ORFs were subjected to molecular weight (MW) and isoelectronic point (pI) predictions using the Compute pI/Mw tool (http://www.expasy.org/tools/protparam.html). Subcellular location predictions for these genes were undertaken using the Target *P*1.1 Server (http://www.cbs.dtu.dk/services/TargetP/). All the LEA proteins from *T. hispida* and 51 Arabidopsis LEA proteins were subjected to phylogenetic analysis by constructing a phylogenetic tree by the neighbor-joining (NJ) method in ClustalX.

2.4. RNA Extraction and Reverse Transcription (RT). Total RNA was isolated from the roots, stems, and leaves using the CTAB method. Total RNA was digested with DNase I (Promega) to remove any residual DNA. Approximately 1 μg of total RNA was reverse transcribed to cDNA in a 10 μL volume using oligodeoxythymidine and 6-bp random primers following the PrimeScript RT reagent kit (TaKaRa) protocol. The synthesized cDNAs were diluted 10-fold with sterile water and used as templates for real-time RT-PCR.

2.5. Quantitative Real-Time RT-PCR. Real-time RT-PCR was carried out in an Opticon machine (Biorad, Hercules, CA) using a real-time PCR MIX Kit (SYBR Green as the fluorescent dye, TOKOBO) and the primers used are shown in Table 1. The *alpha tubulin* (FJ618518), *beta tubulin* (FJ618519), and *actin* (FJ618517) genes were used as internal controls (reference genes) to normalize the total RNA amount present in each reaction. The reaction mixture (20 μL) contained 10 μL of SYBR Green Real-Time PCR Master Mix (Toyobo), 0.5 μM of forward and reverse primer, and 2 μL of cDNA template (equivalent to 20 ng of total RNA). The amplification was performed using the following cycling parameters: 94°C

Table 2: Characteristics of the 8 *ThLEAs* from *T. hispida* that had full ORFs.

Gene name	Deduced number of amino acids	MW (kDa)	pI	Predicted subcellular localization*
ThLEA-1	584	65.40	8.18	Other
ThLEA-2	435	46.70	8.67	Secreted
ThLEA-3	462	51.31	8.02	Chloroplast
ThLEA-4	212	23.55	9.60	Secreted
ThLEA-5	114	12.29	5.54	Other
ThLEA-6	151	16.31	4.97	Other
ThLEA-7	318	35.31	4.75	Other
ThLEA-8	171	17.49	8.02	Other

*Subcellular localization was predicted from protein sequence analysis using the targetP algorithm.

for 30 s, followed by 45 cycles of 94°C for 12 s, 60°C for 30 s, 72°C for 40 s, and then at 81°C for 1 s for plate reading. A melting curve was generated for each sample at the end of each run to assess the purity of the amplified product. Real-time RT-PCR was carried out in triplicate to ensure the reproducibility of the results. The expression levels were calculated from the threshold cycle according to $2^{-\Delta\Delta Ct}$ [26].

3. Results

3.1. Characterization of ThLEAs. In total, 12 unique *ThLEA*s (*ThLEA-1-8*, respectively, with the GenBank numbers KF801660 to KF801667; *ThLEA-9-12*, respectively, with the GenBank numbers KF924555 to KF924558) that are expressed differentially in response to at least one stress were identified from the *T. hispida* cDNA libraries. Among these, eight ThLEA proteins had complete ORFs that encoded deduced polypeptides of 114–584 amino acids with predicted molecular masses of 12.29–65.4 kDa and pIs of 4.75–9.6 (Table 2). Subcellular locations were predicted from protein sequence analysis using the targetP algorithm. The results suggested that ThLEA-3 may be located in the chloroplast, ThLEA-2 and -4 may be secreted proteins, and the locations of the other five *ThLEA* genes with full ORFs may be classified as "other."

Hunault and Jaspard [9] identified 51 LEA protein encoding genes in Arabidopsis genome and classified them into nine distinct groups (LEA-1, -2, -3, -4, -5, Atm, SMP, dehydrin, and PvLEA18). According to this classification, the phylogenetic relationships showed that ThLEA-1, -3, -6, and -7 are in the LEA-2 group and ThLEA-2, -4, -9, -10, -11, and -12 are in the LEA-1 group, while ThLEA-8 and -5 are in the Atm and LEA-5 groups, respectively (Figure 1).

3.2. Relative Transcript Abundances of ThLEAs under Normal Growth Conditions. In order to study the tissue specificity of *ThLEA* gene expression, the relative transcript abundances of the *ThLEA* genes in *T. hispida* roots, stems, leaves, and seeds under normal growth conditions were monitored by real-time RT-PCR. The transcript level of the *actin* gene was assigned as 100, while the transcript levels of *ThLEA* genes were plotted relative to transcript level of *actin* gene (Table 3). The results indicated that *ThLEA-4* is the gene with the highest expression in stems and leaves and in the roots

Table 3: Relative transcript abundance of the 12 *ThLEA*s in different tissues of *T. hispida*. The transcript levels of the 12 *ThLEA* genes were plotted relative to expression of the *actin* gene. Transcript levels of the *actin* gene in roots, stems, leaves, and seeds were all assigned as 100.

Gene	Relative abundance			
	Roots	Stems	Leaves	Seeds
ThLEA-1	6.8	11.6	36.2	10
ThLEA-2	5.3	26.4	12.1	230
ThLEA-3	8.2	23.2	64.8	4
ThLEA-4	188.1	365.6	355.5	161
ThLEA-5	1.5	0.2	0.3	20
ThLEA-6	0.1	1.4	0.7	3
ThLEA-7	0.8	19.5	27.9	10
ThLEA-8	8.5	0.8	1.5	770
ThLEA-9	17.7	61.7	26.2	180
ThLEA-10	198.3	2.0	5.1	1240
ThLEA-11	161.8	4.1	23.7	6050
ThLEA-12	9.9	0.1	0.1	1220

only *ThLEA-10* had greater expression, while the transcript levels of *ThLEA-5* and *-6* were very low in all four tissues (roots, stems, leaves, and seeds). The expressions of *ThLEA-8* and *-12* were very high in seeds while those were very low in the other three tissues. In the roots, the transcript level of *ThLEA-6* was lowest and only 0.1 (equivalent to 1/1000 of *actin*). Meanwhile, in stems and leaves, the transcript level of *ThLEA-12* was lowest and less than 1/1000 of *actin*. Moreover, the transcript level of the *ThLEA* genes highly differed among each other and also strongly differed among the four tissues. For instance, *ThLEA-10*, *-11,* and *-12* were expressed mainly in the roots and seeds, and their transcript levels were all exceeded 1220-fold in the seeds. *ThLEA-2* and *-9* were expressed mainly in the stems and seeds, while *ThLEA-1*, *-3,* and *-7* showed relatively high transcript level in the leaves.

3.3. The Expression Profiles of ThLEAs in Response to NaCl, PEG, and ABA Treatments

3.3.1. NaCl Stress. The transcript patterns of all of the *ThLEA* genes were quite similar among the roots, stems, and leaves

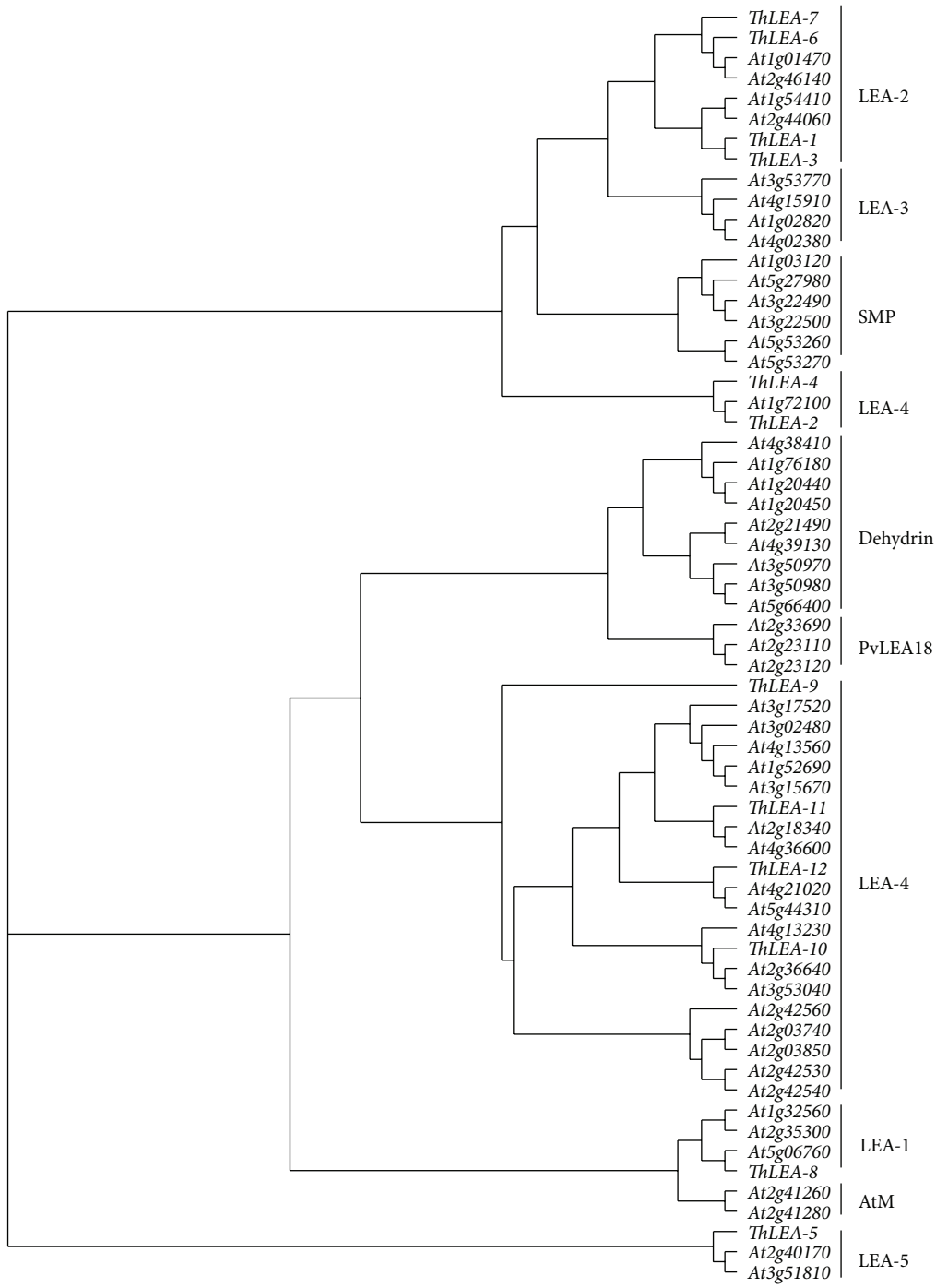

Figure 1: Phylogenetic tree of the 12 *ThLEA*s and 51 Arabidopsis *LEA*s based on sequence alignments of the predicted proteins. All the 12 ThLEA proteins from *T. hispida* and 51 Arabidopsis LEA proteins were subjected to phylogenetic analysis by constructing a phylogenetic tree by the neighbor-joining (NJ) method in ClustalX. According to the classification of Hunault and Jaspard [9], the LEA proteins were classified into nine groups.

under NaCl stress. Furthermore, *ThLEA-2*, *-3*, *-4,* and *-11* were induced (>2-fold) during NaCl stress period. *ThLEA-7* was also upregulated during most treatment period, and six *ThLEA* genes reached their peak expression level in the leaves at 24 h of stress. The most highly induced gene was *ThLEA-1*, which was induced 1596-fold. However, *ThLEA-5, -6*, *-8*, *-10,* or *-12* were highly downregulated at almost each stress time point. Except for *ThLEA-5*, the other four downregulated genes reached lowest transcript levels at 9 h in stems and leaves. Interestingly, distinct from these genes, the transcript pattern of *ThLEA-9* was different among the three tissues. In the roots, it was induced at 3 h but downregulated at the

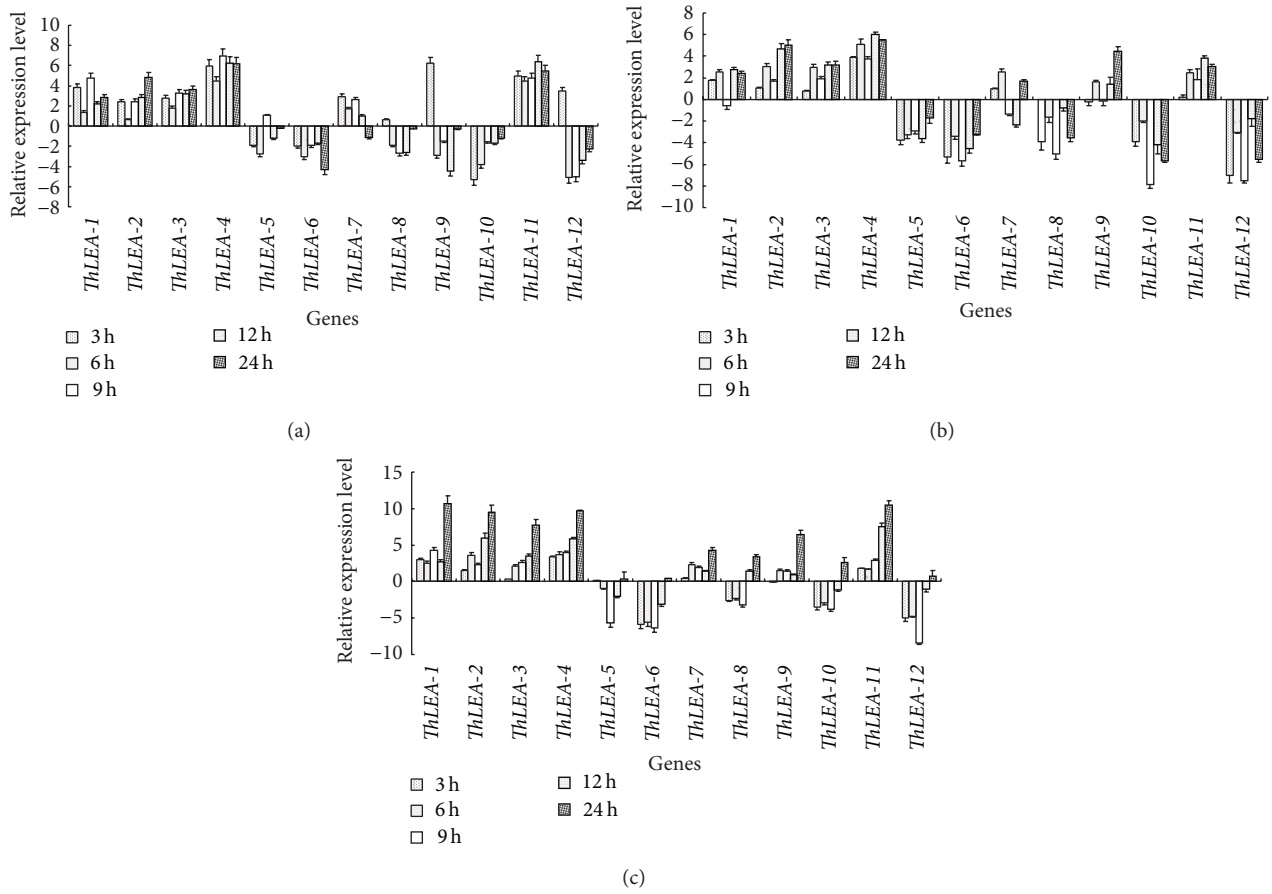

Figure 2: Expression analysis of the 12 *ThLEA*s in response to 0.4 M NaCl stress. Relative expression level = transcription level under stress treatment/transcription level under control conditions. All relative expression levels were $\log_2$ transformed and error bars (SD) were obtained from multiple replicates of the real-time RT-PCR. (a), (b), (c): expression of *ThLEA*s in roots, stems, and leaves, respectively.

other time points, while in stems and leaves it was mainly upregulated. Similar with the other upregulated *ThLEA*s, *ThLEA-9* reached greatest expression at 24 h in the leaves (Figure 2).

3.3.2. PEG Stress. Consistent with NaCl stress, the transcript patterns of these *ThLEA* genes under PEG stress were divided into two distinct groups (Figure 3). One group was composed of *ThLEA-1*, *-2*, *-3*, *-4,* and *-11*, and these genes were mainly upregulated. The second group included *ThLEA-5*, *-6*, *-8*, *-9*, *-10*, and *-12* that were largely downregulated during the PEG treatment period.

3.3.3. ABA Treatment. After application of exogenous ABA, *ThLEA-1*, *-2,* and *-3* were only slightly differentially regulated in the roots, stems, and leaves, indicating that they may be regulated via the ABA-independent signaling pathway. However, the genes that were downregulated by PEG and/or NaCl stress were also highly downregulated by ABA treatment. In contrast, *ThLEA-4*, *-7*, and *-11* were mainly upregulated, especially *ThLEA-4*, whose transcript levels in the stem at 6 h were increased by 38-fold compared with the control (Figure 4).

4. Discussion

In the present study, 12 *ThLEA* genes were identified from *Tamarix* RNA-seq data base, and the transcript abundance of each gene was assessed in normal growth conditions by real-time RT-PCR. Furthermore, NaCl and PEG were used to simulate salinity and drought conditions, respectively, and the expression levels of the *ThLEA* genes were investigated in roots, stems, and leaves in response to these stress environments.

Many studies have shown that members of the plant *LEA* family displayed tissue-specific expression and are involved in various processes in plant growth and development. For example, in Arabidopsis, 22 of the 51 *LEA* genes (43%) showed high expression levels (relative expression >10) in the nonseed organs in the absence of a stress or hormone treatment [27]. The *OsLEA3-2* gene is not expressed in vegetative tissues under normal conditions and it is thought to play an important role in the maturation of the embryo [10]. Moreover, the transcripts of *MsLEA3-1* were strongly enriched in leaves compared with roots and stems of mature alfalfa plants [20]. Expression profiles of the 12 *ThLEA* genes in different tissues of *T. hispida* were determined under normal growth conditions and this showed that most of

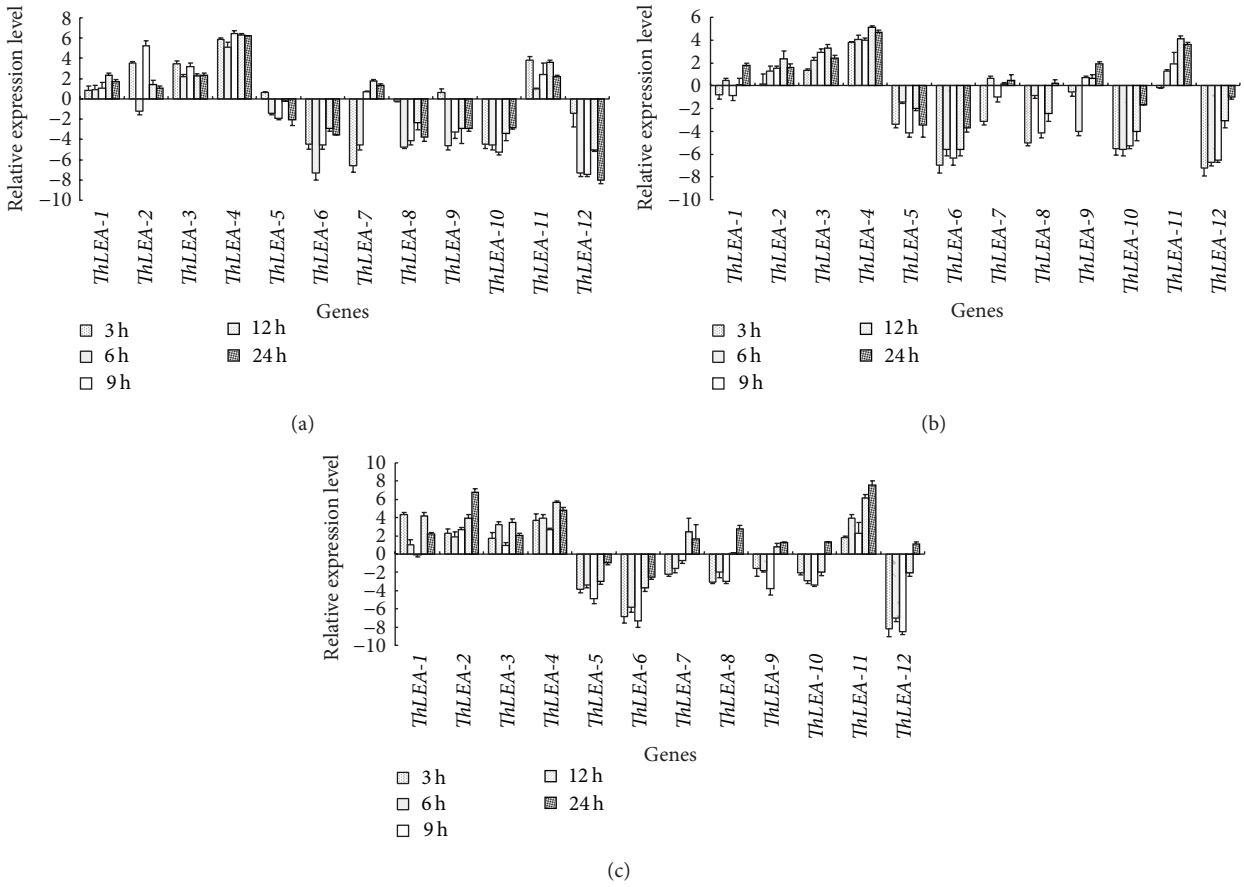

Figure 3: Expression analysis of the 12 *ThLEA*s in response to 20% PEG6000 stress. Relative expression level = transcript level under stress treatment/transcript level under control conditions. All relative expression levels were $\log_2$ transformed and error bars (SD) were obtained from multiple replicates of the real-time RT-PCR. (a), (b), (c): expression of *ThLEA*s in roots, stems, and leaves, respectively.

the *ThLEA*s were expressed in various organs and tissues. However, they displayed different expression levels between the different tissue types and this may reflect the complexity of functions performed by this gene family [28]. Among the 12 *ThLEA*s, *ThLEA-10*, *-11*, and *-12* were mainly expressed in the roots, suggesting that these genes may play roles in root stress response. *ThLEA-2* and *-9* were highly expressed in the stem, while *ThLEA-1*, *-3*, and *-7* may play important roles in the leaves as these genes are highly and specifically expressed in leaves. Moreover, *ThLEA-4* has very high expression level in the roots, stems, and leaves, suggesting that it might play important roles in all of these tissues. The expression levels of *ThLEA-5*, *-6*, *-8*, and *-12* were very low in each of the tissues examined, indicating that these genes may play a relatively unimportant role in these tissues under normal growth conditions.

There is increasing evidence suggesting that *LEA* genes are associated with abiotic stress tolerance, particularly in plant responses to dehydration, salt, and cold stresses [18, 29]. In Arabidopsis, of the 22 genes highly expressed in nonseed tissues, 12 were induced by more than 3-fold in response to cold, drought, and salt stresses [27]. In sweet potato plants, *IbLEA14* expression was strongly induced by dehydration and NaCl [30]. In the present study, half of the 12 *ThLEA* genes (*ThLEA-1*, *-2*, *-3*, *-4*, *-7*, and *-11*) were induced under salt and drought stress, indicating that these genes might play important roles in response to salt and drought stresses in *T. hispida*. Bies-Ethève et al. [31] reported that *LEA* genes from the same group do not show identical expression profiles and regulation of *LEA* genes that show apparently similar expression patterns does not systematically involve the same regulatory pathway. Consistent with this, the six upregulated *ThLEA*s in *T. hispida* belong to two *LEA*s groups (*LEA-2* and *LEA-4*), while *LEA*s in the same group (such as *LEA-4*) showed completely different expression patterns.

There are ABA-dependent and ABA-independent regulatory networks controlling plant responses to abiotic stresses. *LEA* genes are often considered as being ABA-regulated and previous studies have shown that some *ThLEA* genes can be induced by exogenous ABA [10, 30]. However, our study shows that some *ThLEA* genes, including *ThLEA-1*, *-2*, and *-3*, were highly induced by abiotic stresses but were not regulated by ABA. Consistent with this, Bies-Ethève et al. [31] reported that most of the *LEA* genes in Arabidopsis seedlings show no response at all following exogenous ABA treatment. Hundertmark and Hincha [27] deduced the presence of different signal transduction pathways in different Arabidopsis tissues (vegetative plants and seeds) by comparing the expression of

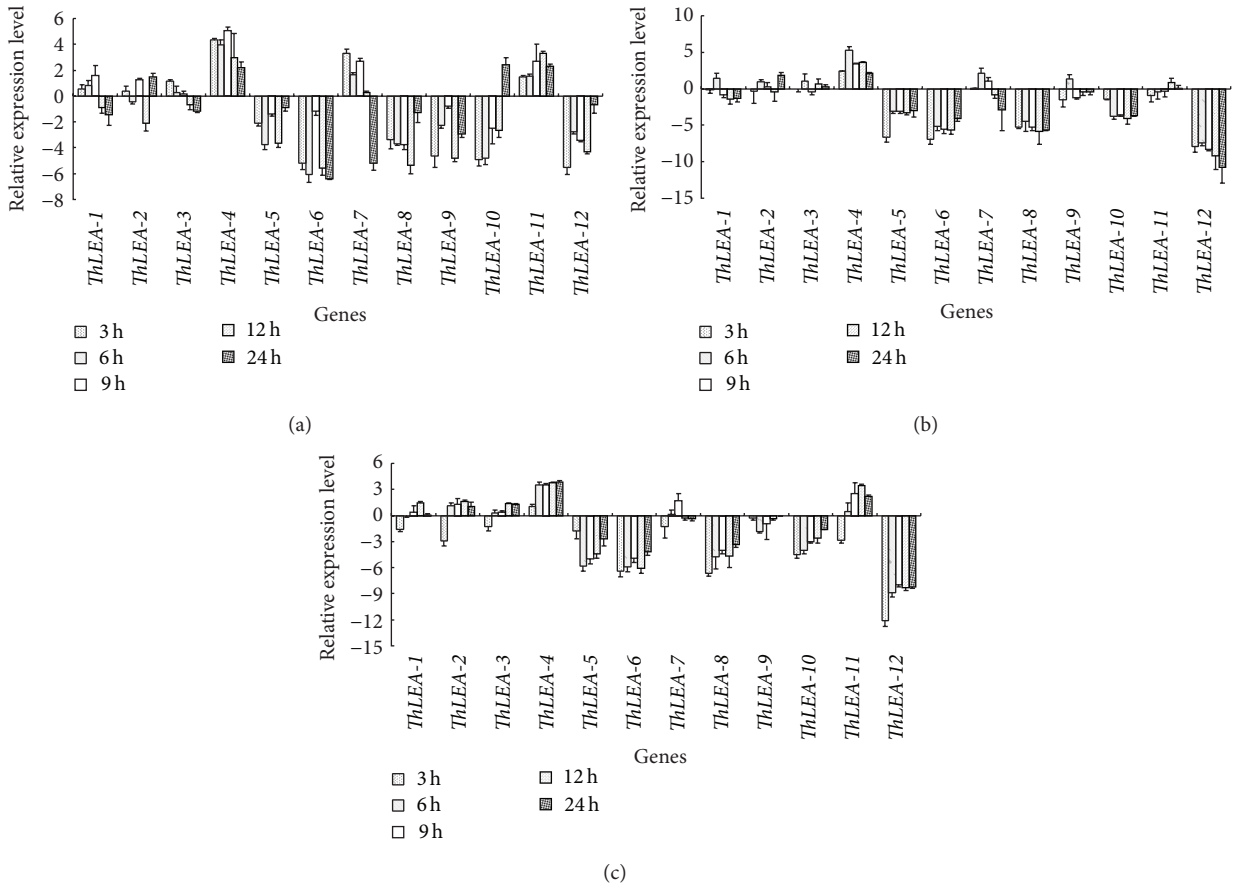

Figure 4: Expression analysis of the 12 *ThLEA*s in response to 100 μM ABA treatment. Relative expression level = transcript level under stress treatment/transcript level under control conditions. All relative expression levels were $\log_2$ transformed and error bars (SD) were obtained from multiple replicates of the real-time RT-PCR. (a), (b), (c): expression of *ThLEA*s in roots, stems, and leaves, respectively.

LEA genes after ABA treatment. In contrast, we found that expression patterns were highly similar in the three tissues examined after ABA treatment. Expression analyses showed that nine *ThLEA* genes in three tissues of *T. hispida* were upregulated or downregulated by ABA, which suggests that these *ThLEA* genes are regulated by ABA-dependent stress resistance pathways. These findings demonstrate that the *ThLEA* genes involved in salt and drought stress resistance in *T. hispida* are probably regulated by two different pathways (ABA-dependent and ABA-independent). Further studies are required to elucidate the functions of the *ThLEA*s in response to the abiotic stress and to fully characterize the signaling pathways that regulate their expression.

5. Conclusion

In summary, we identified 12 *ThLEA* genes from *T. hispida*, which belong to three groups. The LEA-1 group includes ThLEA-2, -4, -9, -10, -11, and -12 proteins, the LEA-2 group contains ThLEA-1, ThLEA-3, ThLEA-6, and ThLEA-7, and ThLEA-8 and -5 are in the Atm and LEA-5 groups. The *ThLEA* genes displayed tissue-specific expression patterns under normal growth conditions. *ThLEA-10*, *-11*, and *-12* were expressed mainly in the roots and seeds. *ThLEA-2* and *-9* were preferentially expressed in the stems and seeds, while *ThLEA-1*, *-3*, and *-7* showed high transcript level in the leaves. Furthermore, real-time RT-PCR analysis showed that the *ThLEA* genes were regulated by salt and drought stresses. *ThLEA-1*, *-2*, *-3*, *-4*, *-7*, and *-11* were mainly induced by salt and drought stress. But *ThLEA-5*, *-6*, *-8*, *-9*, *-10*, and *-12* were largely downregulated during the NaCl and PEG treatment. After the application of exogenous ABA, the expression levels of all *ThLEA* genes (except for the *ThLEA-1*, *-2*, and *-3*) were obviously different under the ABA treatment. Our studies will contribute to a better understanding of the functions of *ThLEA* genes involved in stress response in *T. hispida*.

Conflict of Interests

The authors declare that there is no conflict of interests regarding the publication of this paper.

Authors' Contribution

Caiqiu Gao and Yali Liu have the same contribution to this paper.

Acknowledgments

This work was supported by Key Laboratory of Forest Genetics & Biotechnology (Nanjing Forestry University), Ministry of Education (FGB200902), and The Program for Young Top-Notch Talents of Northeast Forestry University (PYTT-1213-09).

References

[1] H. B. Shao, L. Y. Chu, M. A. Shao, C. A. Jaleel, and M. Hongmei, "Higher plant antioxidants and redox signaling under environmental stresses," *Comptes Rendus—Biologies*, vol. 331, no. 6, pp. 433–441, 2008.

[2] H. Shao, L. Chu, C. A. Jaleel, and C. Zhao, "Water-deficit stress-induced anatomical changes in higher plants," *Comptes Rendus—Biologies*, vol. 331, no. 3, pp. 215–225, 2008.

[3] F. T. Ni, L. Y. Chu, H. B. Shao, and Z. H. Liu, "Gene expression and regulation of higher plants under soil water stress," *Current Genomics*, vol. 10, no. 4, pp. 269–280, 2009.

[4] H. Shao, L. Chu, C. A. Jaleel, P. Manivannan, R. Panneerselvam, and M. Shao, "Understanding water deficit stress-induced changes in the basic metabolism of higher plants-biotechnologically and sustainably improving agriculture and the ecoenvironment in arid regions of the globe," *Critical Reviews in Biotechnology*, vol. 29, no. 2, pp. 131–151, 2009.

[5] H. Cao, Z. Zhang, P. Xu et al., "Mutual physiological genetic mechanism of plant high water use efficiency and nutrition use efficiency," *Colloids and Surfaces B: Biointerfaces*, vol. 57, no. 1, pp. 1–7, 2007.

[6] E. Mazzucotelli, A. M. Mastrangelo, C. Crosatti, D. Guerra, A. M. Stanca, and L. Cattivelli, "Abiotic stress response in plants: When post-transcriptional and post-translational regulations control transcription," *Plant Science*, vol. 174, no. 4, pp. 420–431, 2008.

[7] A. Nezhadahmadi, Z. H. Prodhan, and G. Faruq, "Drought tolerance in wheat," *The Scientific World Journal*, vol. 2013, Article ID 610721, 12 pages, 2013.

[8] L. Dure III, S. C. Greenway, and G. A. Galau, "Developmental biochemistry of cottonseed embryogenesis and germination: changing messenger ribonucleic acid populations as shown by in vitro and in vivo protein synthesis," *Biochemistry*, vol. 20, no. 14, pp. 4162–4168, 1981.

[9] G. Hunault and E. Jaspard, "LEAPdb: a database for the late embryogenesis abundant proteins," *BMC Genomics*, vol. 11, no. 1, article 221, 2010.

[10] J. Duan and W. Cai, "OsLEA3-2, an abiotic stress induced gene of rice plays a key role in salt and drought tolerance," *PLoS ONE*, vol. 7, no. 9, Article ID e45117, 2012.

[11] Y. Zhang, Y. Li, J. Lai et al., "Ectopic expression of a LEA protein gene TsLEA1 from *Thellungiella salsuginea* confers salt-tolerance in yeast and Arabidopsis," *Molecular Biology Reports*, vol. 39, no. 4, pp. 4627–4633, 2012.

[12] Y. Olvera-Carrillo, F. Campos, J. L. Reyes, A. Garciarrubio, and A. A. Covarrubias, "Functional analysis of the group 4 late embryogenesis abundant proteins reveals their relevance in the adaptive response during water deficit in arabidopsis," *Plant Physiology*, vol. 154, no. 1, pp. 373–390, 2010.

[13] S. Cui, J. Hu, S. Guo et al., "Proteome analysis of Physcomitrella patens exposed to progressive dehydration and rehydration," *Journal of Experimental Botany*, vol. 63, no. 2, pp. 711–726, 2012.

[14] D. Naot, G. Ben-Hayyim, Y. Eshdat, and D. Holland, "Drought, heat and salt stress induce the expression of a citrus homologue of an atypical late-embryogenesis of *Lea5* gene," *Plant Molecular Biology*, vol. 27, no. 3, pp. 619–622, 1995.

[15] N. Ukaji, C. Kuwabara, D. Takezawa, K. Arakawa, and S. Fujikawa, "Cold acclimation-induced WAP27 localized in endoplasmic reticulum in cortical parenchyma cells of mulberry tree was homologous to group 3 late-embryogenesis abundant proteins," *Plant Physiology*, vol. 126, no. 4, pp. 1588–1597, 2001.

[16] C. NDong, J. Danyluk, K. E. Wilson, T. Pocock, N. P. A. Huner, and F. Sarhan, "Cold-regulated cereal chloroplast late embryogenesis abundant-like proteins. Molecular characterization and functional analyses," *Plant Physiology*, vol. 129, no. 3, pp. 1368–1381, 2002.

[17] H. Zegzouti, B. Jones, C. Marty et al., "ER5, a tomato cDNA encoding an ethylene-responsive LEA-like protein: characterization and expression in response to drought, ABA and wounding," *Plant Molecular Biology*, vol. 35, no. 6, pp. 847–854, 1997.

[18] M. Dalal, D. Tayal, V. Chinnusamy, and K. C. Bansal, "Abiotic stress and ABA-inducible Group 4 LEA from *Brassica napus* plays a key role in salt and drought tolerance," *Journal of Biotechnology*, vol. 139, no. 2, pp. 137–145, 2009.

[19] A. RoyChoudhury, C. Roy, and D. N. Sengupta, "Transgenic tobacco plants overexpressing the heterologous lea gene Rab16A from rice during high salt and water deficit display enhanced tolerance to salinity stress," *Plant Cell Reports*, vol. 26, no. 10, pp. 1839–1859, 2007.

[20] Y. Bai, Q. Yang, J. Kang, Y. Sun, M. Gruber, and Y. Chao, "Isolation and functional characterization of a *Medicago sativa* L. gene, MsLEA3-1," *Molecular Biology Reports*, vol. 39, no. 3, pp. 2883–2892, 2012.

[21] B. J. Park, Z. Liu, A. Kanno, and T. Kameya, "Increased tolerance to salt- and water-deficit stress in transgenic lettuce (*Lactuca sativa* L.) by constitutive expression of LEA," *Plant Growth Regulation*, vol. 45, no. 2, pp. 165–171, 2005.

[22] X. Zhao, L. Zhan, and X. Zou, "Improvement of cold tolerance of the half-high bush Northland blueberry by transformation with the LEA gene from *Tamarix androssowii*," *Plant Growth Regulation*, vol. 63, no. 1, pp. 13–22, 2011.

[23] P. Zhao, F. Liu, M. Ma et al., "Overexpression of AtLEA3-3 confers resistance to cold stress in Escherichia coli and provides enhanced osmotic stress tolerance and ABA sensitivity in Arabidopsis thaliana.," *Molekuliarnaia Biologiia*, vol. 45, no. 5, pp. 851–862, 2011.

[24] C. Wang, C. Gao, L. Wang, L. Zheng, C. Yang, and Y. Wang, "Comprehensive transcriptional profiling of $NaHCO_3$-stressed *Tamarix hispida* roots reveals networks of responsive genes," *Plant Molecular Biology*, vol. 84, no. 1-2, pp. 145–157, 2014.

[25] L. Wang, C. Wang, D. Wang, and Y. Wang, "Molecular characterization and transcript profiling of NAC genes in response to abiotic stress in *Tamarix hispida*," *Tree Genetics & Genomes*, vol. 10, pp. 157–171, 2014.

[26] K. J. Livak and T. D. Schmittgen, "Analysis of relative gene expression data using real-time quantitative PCR and the $2^{-\Delta\Delta C}$T method," *Methods*, vol. 25, no. 4, pp. 402–408, 2001.

[27] M. Hundertmark and D. K. Hincha, "LEA (Late Embryogenesis Abundant) proteins and their encoding genes in *Arabidopsis thaliana*," *BMC Genomics*, vol. 9, article 118, 2008.

[28] I. A. Paponov, M. Paponov, W. Teale et al., "Comprehensive transcriptome analysis of auxin responses in Arabidopsis," *Molecular Plant*, vol. 1, no. 2, pp. 321–337, 2008.

[29] J. Boudet, J. Buitink, F. A. Hoekstra et al., "Comparative analysis of the heat stable proteome of radicles of Medicago truncatula seeds during germination identifies late embryogenesis abundant proteins associated with desiccation tolerance," *Plant Physiology*, vol. 140, no. 4, pp. 1418–1436, 2006.

[30] S. Park, Y. Kim, J. C. Jeong et al., "Sweetpotato late embryogenesis abundant 14 (*IbLEA14*) gene influences lignification and increases osmotic- and salt stress-tolerance of transgenic calli," *Planta*, vol. 233, no. 3, pp. 621–634, 2011.

[31] N. Bies-Ethève, P. Gaubier-Comella, A. Debures et al., "Inventory, evolution and expression profiling diversity of the LEA (late embryogenesis abundant) protein gene family in *Arabidopsis thaliana*," *Plant Molecular Biology*, vol. 67, no. 1-2, pp. 107–124, 2008.

Hindawi Publishing Corporation
The Scientific World Journal
Volume 2014, Article ID 834630, 8 pages
http://dx.doi.org/10.1155/2014/834630

Research Article

Responses of Seed Germination, Seedling Growth, and Seed Yield Traits to Seed Pretreatment in Maize (*Zea mays* L.)

Yu Tian,[1] Bo Guan,[2] Daowei Zhou,[3] Junbao Yu,[2] Guangdi Li,[4] and Yujie Lou[1]

[1] *College of Animal Science and Technology, Jilin Agricultural University, Changchun, Jilin 130118, China*
[2] *Key Laboratory of Coastal Environmental Processes and Ecological Remediation, Yantai Institute of Coastal Zone Research, Chinese Academy of Sciences, Yantai, Shandong 264003, China*
[3] *Northeast Institute of Geography and Agricultural Ecology, Chinese Academy of Sciences, Changchun, Jilin 130102, China*
[4] *Graham Centre for Agricultural Innovation (Alliance between NSW Department of Primary Industries and Charles Sturt University), Wagga Wagga Agricultural Institute, Pine Gully Road, Wagga Wagga, NSW 2650, Australia*

Correspondence should be addressed to Bo Guan; guanb627@gmail.com

Received 3 June 2014; Accepted 12 June 2014; Published 26 June 2014

Academic Editor: Hongbo Shao

A series of seed priming experiments were conducted to test the effects of different pretreatment methods to seed germination, seedling growth, and seed yield traits in maize (*Zea mays* L.). Results indicated that the seeds primed by gibberellins (GA), NaCl, and polyethylene glycol (PEG) reagents showed a higher imbibitions rate compared to those primed with water. The final germination percentage and germination rate varied with different reagents significantly ($P < 0.05$). The recommended prime reagents were GA at 10 mg/L, NaCl at 50 mM, and PEG at 15% on account of germination experiment. 15% PEG priming reagent increased shoot and root biomass of maize seedling. The shoot biomass of seedlings after presoaking the seeds with NaCl reagent was significantly higher than the seedlings without priming treatment. No significant differences of plant height, leaf number, and hundred-grain weight were observed between control group and priming treatments. Presoaking with water, NaCl (50 mM), or PEG (15%) significantly increased the hundred-grain weight of maize. Therefore, seed pretreatment is proved to be an effective technique to improve the germination performance, seedling growth, and seed yield of maize. However, when compared with the two methods, if immediate sowing is possible, presoaking is recommended to harvest better benefits compared to priming method.

1. Introduction

In semiarid area, seasonal drought is often frequent in spring and autumn, especially in the sowing season. Soil evaporation will lead to a large amount of moisture loss, of which 90%–95% occurred in 5–10 cm soil layer [1], that is, the optimum depth for crop sowing. Under this condition, it is important to improve the water use efficiency of crop seedlings or find some ways to increase crop yield under drought conditions [2].

Maize (*Zea mays* L.) is an important crop in the world; it is widely used for feed and industrial raw material. Maize ranks the third in world production following wheat and rice for the area and production. It is also the main crop in northern China, where the climate is a combination of temperate and semiarid monsoon. Rapid and uniform field emergence is an important factor to achieve high yield to meet the growing demand for food [3].

Seed priming is a presowing treatment that exposes seeds to a certain solution that allows partial hydration but not germination [4], and redried to original moisture content. Although the germination is not completed, metabolic activities that prepare seeds for radicle protrusion may be initiated during priming [4, 5]. Many evidences have shown seed priming could improve germination and early seedling growth under stress conditions compared to plants grown from untreated seed [6–8].

Various priming treatments have been developed to increase the speed and synchrony of seed germination [6, 9, 10]. Common priming techniques include hydropriming (soaking seed in water), osmopriming (soaking seed in osmotic solutions such as PEG), halopriming (soaking seed

in salt solutions), and priming with plant growth hormones. However, different priming effects were reported with different priming reagents and species. For instance, when *Lolium perenne* seeds were primed with PEG solution, the germination was significantly improved, but no obvious effects were observed with *Festuca rubra*, *Festuca ovina,* and *Poa trivialis* [11]. Seed priming with optimal concentrations of plant growth hormones, such as auxin (IAA), gibberellins (GA), abscisic acid, and ethylene, has proven that germination performance as well as growth and yield of many crop species under both normal and stress conditions could be improved effectively [12, 13]. By soaking seeds (sorghum, rice, or wheat) in water and planting the same day (so-called presoaking treatment), the germination rate could also be increased and seedling emergence improved [14].

In recent years, numerous studies were devoted to the physiological responses of seed germination and seedlings stages to chilling or osmotic stress [8, 13]; the ecological responses of the whole growing season remain largely unknown. To elucidate the ecological responses of different pretreatment to maize species, it may be useful to investigate the changes in not only germination stage, but also seedling growth and yield responses. Few studies to date have attempted to test the whole growing season response to different pretreatments. In this study, we choose water, PEG, NaCl, and GA as different priming reagents, to investigate the dynamics of seed water uptake during seed priming, germination and seedling growth responses after seed priming and presoaking, and yield response to different pretreatment.

2. Materials and Methods

Four experiments were conducted at Jilin Agricultural University. Seeds of maize (*Zea mays* L.) cv. Jinong 610 were used as test materials. All seeds were pretreated with 0.1% H_2O_2 solution for 5 min and then thoroughly washed for 5 min prior to seed treatments.

2.1. Experiment 1: Seed Priming Experiment. There were 10 treatments with 4 seed pretreatment reagents, namely, water, NaCl (50, 150, 250 mmol/L), PEG (10%, 15%, 20%), and Gibberellin (GA) (5, 10, 15 mg/L), and unprimed seeds were used as control, replicated 4 times.

Thirty seeds were placed in two layers of filter paper in a 12 cm Petri dish. The filter paper was moistened with about 30 mL of different priming reagents, ensuring that the seeds were immerged with solutions. Seeds were primed in different priming reagent solution in the lab with room temperature 14°C to 21°C and relative humidity 48% to 64% at night and during day, respectively.

At the hydration stage, the seeds were weighted every 4 h after the surface solutions were dried with filter paper until the weight of seeds was not changed (seeds were saturated). On the dehydration stage, seeds were placed in dry Petri dishes and weighted every 4 h to original weight [15].

The water content of seeds and rate of hydration was calculated with the following formula:

$$\text{Water content} = W_1 - W_0,$$
$$\text{Imbibition rate} = \frac{(W_1 - W_0)}{W_0}, \quad (1)$$

where W_1 is the weight when the seed was saturated with different solutions and W_0 is the original weight.

2.2. Experiment 2: Germination Experiment. The germination experiment was conducted at growth chambers (HPG-400, Haerbin, China) at relative humidity of 60% with 12 h photoperiod (Sylvania cool white fluorescent lamps, 200 mmol m^{-2} s^{-1}, 400–700 nm, 25/15°C).

The primed seeds under different priming reagents from Experiment 1 were germinated in Petri dishes (12 cm diameter) containing two layers of filter paper with 15 mL of distilled water. Each Petri dish contained 30 seeds representing an experimental unit. The seeds were considered to have germinated after radicle emergence. Germination test was ended when no seeds have germinated for 3 days. The germination period was 12 days.

The rate of germination was estimated using a modified Timson's index of germination velocity = $\Sigma G/t$, where G is the percentage of seed germination at one-day intervals and t is the total germination period [16]. The maximum value possible for our data using this index was 100 (i.e., 1000/10). The greater the value, the more rapid the rate of germination.

2.3. Experiment 3: Seedling Response to Seed Treatments. There were two seed treatment methods (priming and presoaking) and 4 seed treatment regents (water, 50 mM NaCl, 15% PEG, or 10 mg/L GA) with untreated seeds as control. The experiment was a 2 × 4 factorial design, replicated 5 times.

Seeds were either primed as described in Experiment 1 or presoaked using regents mentioned above. Those solutions were selected based on the results from Experiments 1 and 2, which were the best expressive concentrations of each reagent to prime the seeds.

The experiment was conducted in a glasshouse but partially shaded under maximum photosynthetically active radiation of 1000 μmol m^{-2} s^{-1}, day/night temperature of 30/24 ± 3°C. Seeds were sown in 25 cm diameter plastic pots that contained 4 kg of native loamy soils. Ten seeds were sown with 3 cm depth in each pot and then thin to 5 seedlings after geminating. Pots were destructively harvested 40 days after seed germinated.

Seedling height, root length, and the biomass of different organ parts were measured at harvest.

2.4. Experiment 4: Yield Response to Seed Treatments. The experiment was conducted in the field. Seeds were pretreated as mentioned in Experiment 3. The experimental design was identical to Experiment 3, but replicated 3 times.

Two or three seeds were sown every 40 cm at the bottom of the ridge and then covered with about 5 cm of soil in

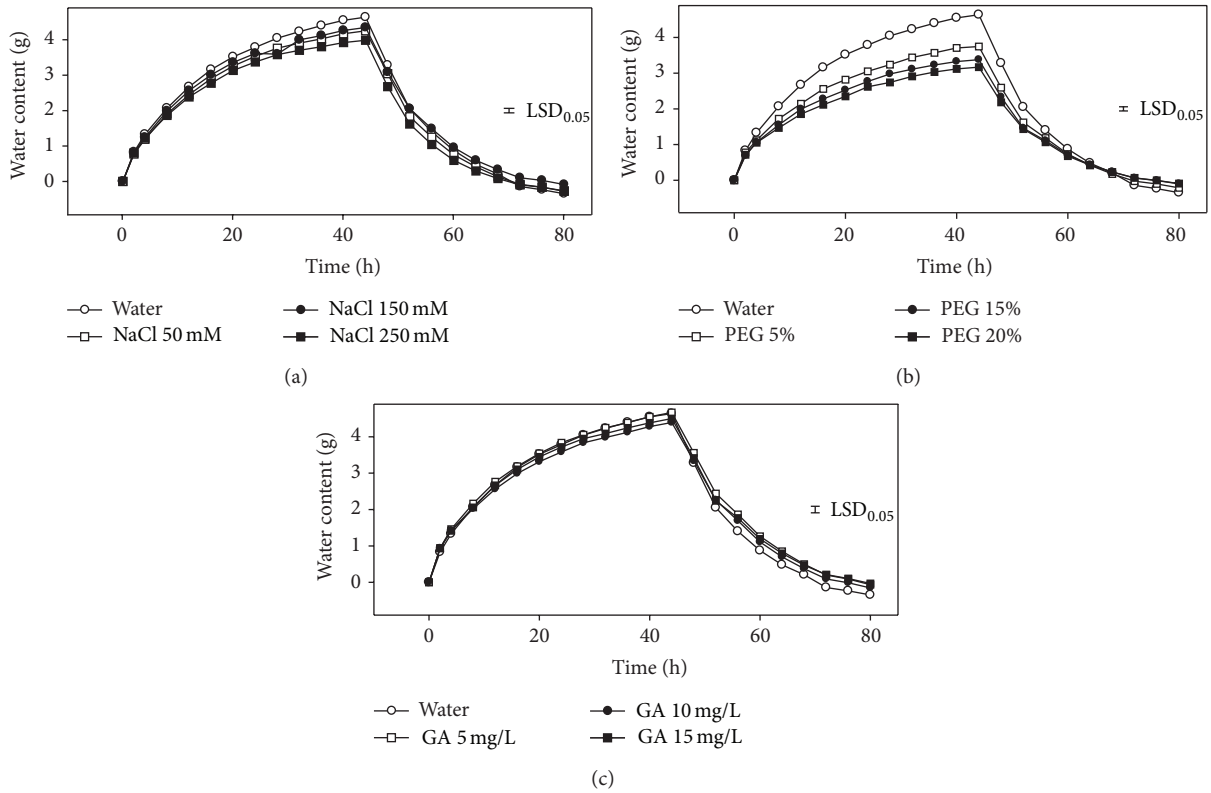

Figure 1: Effects of pretreatment reagents on water intake under priming cycle ($n = 4$).

a 50 m long row as one plot. At the three-leaf stage plants were thinned to one per hole. Each plant received 5.3 g urea/per plant (200 kg urea/ha) on the surface of the soil 10 cm from the plant when it reached the eighth leaf stage. Weeds, insects, and diseases were controlled adequately when necessary.

Ten successive plants per plot were randomly selected at physiological maturity stage. The leaf number and shoot height were measured before harvest. Grain yield and 100-grain weight were determined by oven drying samples at 65°C. Yield was expressed as t/ha.

2.5. Data Analysis. Analysis of variance (ANOVA) was conducted using Statistics SPSS 19.0. Water intake and imbibition rate in Experiment 1 were analyzed using repeated measures. One-way ANOVA was performed for data from Experiment 2 and two-way ANOVA was employed for data from Experiments 3 and 4. The treatment mean values were compared with the least significant difference (LSD) at the 5% level.

3. Results

3.1. Experiment 1: Seed Water Intake under Priming Cycle. The water intake of maize seed showed similar trends in different priming reagents. The percentage of water intake was greater at the first 12 hours then slowed down. It took about 44 h for the seeds to be saturated (Figure 1). When comparing different concentrations of different solutions with water (control), the water intake with 250 mM NaCl was significantly lower than control, and all the three concentrations of PEG showed slower water intake than control. No significant differences were observed between GA and control. One hydration-dehydration cycle lasted about 84 h.

The imbibitions rate of seeds was increased after one hydration-dehydration cycle (Figure 2). Compared with water priming, the seeds showed a higher imbibitions rate when primed by GA, NaCl, and PEG reagents. The imbibitions rates were significantly higher when primed with NaCl (150 and 250 mM), GA (15 mM), and all the three concentrations of PEG compared with those primed in water (Figure 2).

3.2. Experiment 2: Germination Responses after Seed Pretreatment. The seed pretreatment of different reagents had significant ($P < 0.05$) effects on the final germination percentage and germination rate (Figures 3(a) and 3(b)). Primed seeds had significantly higher germination percentage than those in control, but no significant differences were observed among priming reagents. The germination rate was also significantly increased by seed priming except 20% PEG. GA showed greater effect on germination rate, and PEG had slightly increased germination rate when compared with other reagents. No statistical differences were observed between water and NaCl priming methods ($P > 0.05$).

Within each reagent, the concentration of different priming reagents also showed different effects to germination percentage and germination rate. The optimum germination

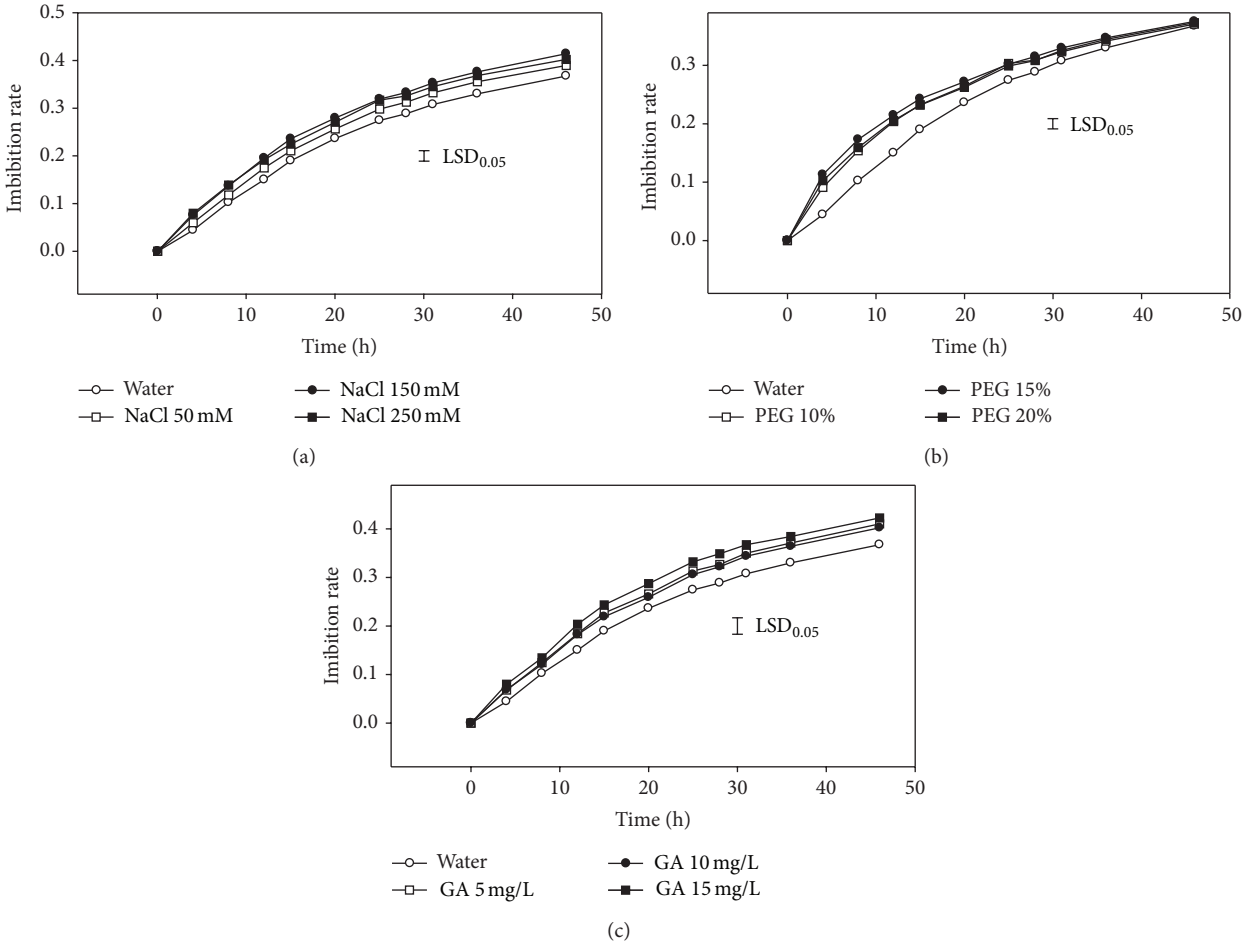

Figure 2: Effects of pretreatment reagents on imbibition rate after seed priming ($n = 4$).

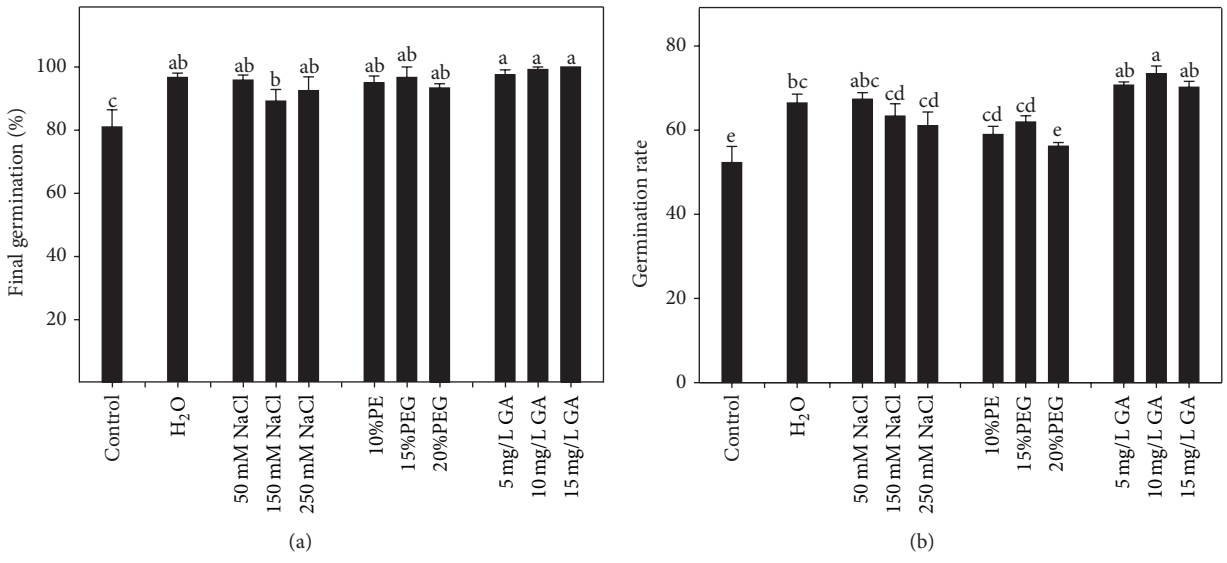

Figure 3: Effects of pretreatment reagents on final germination percentage and germination rate of maize ($n = 4$).

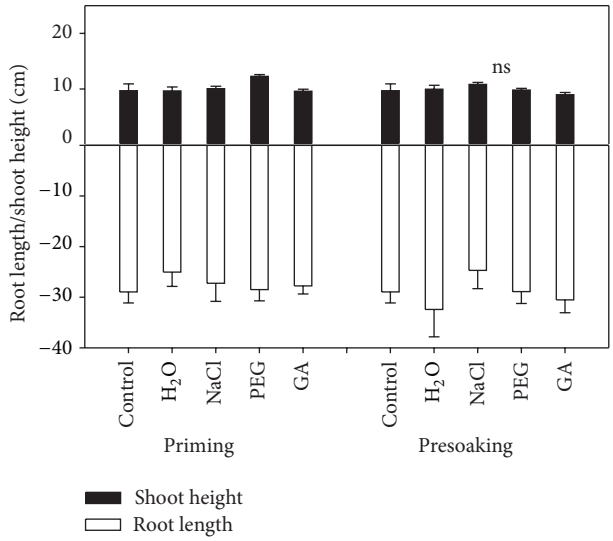

Figure 4: Effects of pretreatment reagents and priming methods on seedling shoot height and root length of maize ($n = 10$; ns: not significant).

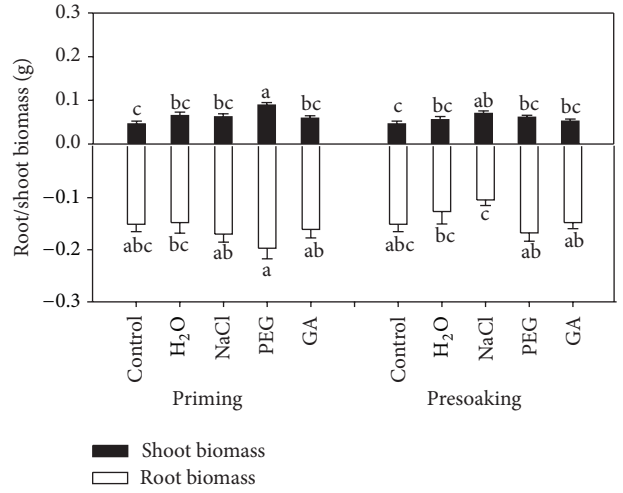

Figure 5: Effects of pretreatment reagents and priming methods on seedling shoot and root biomass of maize ($n = 10$).

performance was observed after priming with 10 mg/L GA, 50 mM NaCl, and 15% PEG, which were used for Experiments 3 and 4.

3.3. Experiment 3: Seedling Response to Seed Pretreatments. No significant differences were observed in plant height and root length after priming by different reagents (Figure 4). The shoot and root biomass of maize seedlings were significantly affected by priming reagents (Figure 5 and Table 1). Pretreatment methods (priming and presoaking) also significantly affected the root biomass ($P < 0.05$). The shoot and root length showed no remarkable differences by the interaction of priming reagents and pretreatment methods in this pot experiment. Priming treatment with PEG reagent significantly increased shoot biomass compared to the control group. The shoot biomass was also significantly higher when presoaking with NaCl reagent compared to control. However, no significant differences were observed in root biomass between treatments.

3.4. Yield Response to Seed Pretreatment. There was no significant difference in plant height between seed pretreatments. Presoaking with PEG and GA significantly increased the leaf number when compared with control. No significant differences were observed to the seed yield and hundred grain weight between different priming reagents (Table 1). But compared with priming methods, presoaking with water, NaCl, or PEG significantly increased the hundred-grain weight of maize (Table 2).

4. Discussion

The study revealed that seed priming and presoaking techniques using different solutions can significantly improve maize plant performance by increasing seed germination rate, seedling biomass, and seed yield, although response varied with different solutions and concentrations. Seed priming with different concentrations of solutions significantly improved germination performance, but no remarkable differences were observed for seedling growth and seed yield, while seed presoaking with some solution dramatically improved seedling growth and seed yield of maize.

Germination and seedling establishment are critical stages which affected both quality and quantity of crop yields [17]. Soil water content is the key factor affecting seed germination and plant establishment in the semiarid area. The present study showed that, compared with the control group, the rate of hydration increased dramatically after seed primed by reagents. This implies that seed priming may improve seed germination of maize seeds by speeding up imbibition, which could contribute to facilitate emergence phage of maize after raining in the semiarid area. Similar results were also reported that priming improved germination of sunflower cultivars by accelerating imbibitions [18].

Generally, seed germination entails three distinct phases: (i) imbibition, (ii) lag phase, and (iii) radicle growth and emergence [19]. The purpose of priming is to prolong the lag phase, which allows some pregerminative physiological and biochemical processes to take place but prevents germination [20]. The results of our germination tests indicated that seed priming significantly increased the final germination percentage and germination rate of maize. The increment in seed germination due to seed priming treatment is in conformity with other researchers [21, 22]. When compared with different priming reagents, GA of all concentrations showed greater influence on germination rate. It was reported earlier that GA participated in regulation of many growth and developmental processes in plants [23, 24] and was particularly important in regulating stem elongation [25]. GA treated seed was closely associated with their rapid utilization in the synthesis of various amino acids and amides [26], which could be the reason for the increased germination rate.

Table 1: Analysis of variance for seed priming effects on maize for seedling growth and yield composition ($n = 10$, $P < 0.05$).

Source	Seedling growth (pot experiment)				
	df	Shoot height	Root length	Shoot biomass	Root biomass
Priming reagents	4	0.152	0.588	0.000*	0.012*
Treatment methods	1	0.366	0.366	0.074	0.005*
PR × TM	4	0.206	0.206	0.074	0.394
	Yield composition (field experiment)				
	df	Seed yield per plant		Hundred-grain weight	
Priming reagents	4	0.569		0.071	
Treatment methods	1	0.180		0.001*	
PR × TM	4	0.673		0.047*	

* $P < 0.05$.

Table 2: Effects of pretreatment reagents and priming methods on yield composition of maize ($n = 10$).

Pretreatment methods	Reagents	Plant height (cm)	Leaf number	Yield (*t*/hr)	Hundred-grain weight (g)
	Control	185.11 ± 3.36^{a}	9.00 ± 0.49^{bcd}	13.24 ± 1.57	18.64 ± 2.55^{d}
Priming	Water	178.84 ± 3.34^{ab}	7.80 ± 0.51^{d}	13.94 ± 1.09	20.78 ± 3.22^{cd}
	NaCl	183.41 ± 4.96^{a}	8.25 ± 0.59^{cd}	10.88 ± 1.01	16.43 ± 2.18^{d}
	PEG	182.28 ± 4.13^{a}	9.44 ± 0.37^{abc}	12.35 ± 0.96	21.29 ± 4.32^{cd}
	GA	169.43 ± 5.19^{b}	8.70 ± 0.26^{bcd}	11.14 ± 0.93	25.72 ± 4.56^{bcd}
Presoaking	Water	178.03 ± 5.20^{ab}	8.90 ± 0.40^{ab}	13.57 ± 1.11	29.23 ± 4.38^{abc}
	NaCl	178.87 ± 4.53^{ab}	9.40 ± 0.37^{ab}	13.02 ± 0.64	32.17 ± 4.26^{ab}
	PEG	183.78 ± 3.68^{a}	10.30 ± 0.36^{a}	13.07 ± 0.79	37.13 ± 4.70^{a}
	GA	182.16 ± 4.11^{a}	9.55 ± 0.44^{a}	13.58 ± 1.08	24.23 ± 2.57^{bcd}

Different letters indicate significant differences from different pretreatments ($P < 0.05$).

Priming reagents (especially for PEG priming) had the beneficial effects on shoot and root biomass. This was mainly due to the accelerated metabolism occurring in primed seeds, which increases the imbibition speed as compared to unprimed seeds. Similar results were also reported by Guan et al. [27] on sorghum seeds. Farooq et al. [28] reported that presoaking with inorganic salts improved seedling emergence, shoot and root length, and biomass. In contrast, no significant differences were observed for plant height, root length, and biomass in the present study. Only presoaking with NaCl solution increased shoot biomass, which had a similar trend with the study by Farooq et al. [28].

Increasing evidence suggests that seed priming could change the crop performance from physiological, biochemical, and molecular aspects [8, 29]. There are several studies arguing that the priming itself could be a stress, for the water uptake activates previously quiescent cellular events in primed seeds while compromising the desiccation tolerance [30, 31]. Chen and Arora [31] also concluded that primed seeds, no matter what the priming scheme that was chosen, would inevitably endure some injury by the dehydration treatment. Only few studies reported that seed priming could increase the grain yield as shown by Sharifi and Khavazi [6] with plant growth promoting Rhizobacteria (PGPR). However, in the current study, no significant difference in grain yield was observed in priming treatments while presoaking with water, NaCl, and PEG solutions did significantly increase the grain yield. Harris et al. [32, 33] also reported that presoaking followed by surface drying has more advantages to yield in many field crops.

5. Conclusions

The results indicated that the final germination percentage and germination rate varied with different reagents significantly ($P < 0.05$). The GA at 10 mg/L, NaCl at 50 mM, and PEG at 15% were recommended on account of germination experiment. 15% PEG priming reagent increased shoot and root biomass of maize seedling. The shoot biomass of seedlings after presoaking the seeds with NaCl reagent was significantly higher than the seedlings without priming treatment. No significant differences of plant height, leaf number, and hundred-grain weight were observed between control group and priming treatments, while presoaking with water, NaCl, and PEG solutions did significantly increase the hundred-grain weight of maize. Our results confirmed that seed pretreatment is an effective technique to improve the germination percentage, germination rate, seedling growth, and seed yield. However, if immediate sowing is possible, presoaking is recommended to harvest better benefits compared to hydration–dehydration method.

Conflict of Interests

The authors declare that there is no conflict of interests regarding the publication of this paper.

Authors' Contribution

Yu Tian, Daowei Zhou, and Bo Guan contributed equally to this work.

Acknowledgments

The authors were grateful to all the laboratory members for continuous technical advice and helpful discussion. This project was financially supported by Shandong Province Natural Science Fund (no. ZR2012CQ017) and National Natural Science Foundation for Distinguished Young Scholar of Shandong Province(no. JQ201114). The authors would like to thank the editor and the anonymous reviewers for their helpful comments.

References

[1] J. T. Ritchie and A. Johnson, " Soil and plant factors affecting evaporation," in *Irrigation of Agricultural Crops*, B. A. Stewart and D. R. Nielsen, Eds., pp. 369–390, American Society of Agronomy, Madison, Wis, USA, 1990.

[2] H. Budak, M. Kantar, and K. Yucebilgili Kurtoglu, "Drought tolerance in modern and wild wheat," *The Scientific World Journal*, vol. 2013, Article ID 548246, 16 pages, 2013.

[3] M. W. Rosegrant, M. Agcaoili-Sombilla, and N. D. Perez, *Food, Agriculture and the Environment Discussion Paper 5. Global Food Projections to 2020: Implications for Investment*, IFPRI, Washington, DC, USA, 1995.

[4] W. Heydecker, J. Higgins, and R. L. Gulliver, "Accelerated germination by osmotic seed treatment," *Nature*, vol. 246, no. 5427, pp. 42–44, 1973.

[5] H. C. Passam and D. Kakouriotis, "The effects of osmoconditioning on the germination, emergence and early plant growth of cucumber under saline conditions," *Scientia Horticulturae*, vol. 57, no. 3, pp. 233–240, 1994.

[6] R. S. Sharifi and K. Khavazi, "Effects of seed priming with Plant Growth Promoting Rhizobacteria (PGPR) on yield and yield attribute of maize (Zea mays L.) hybrids," *Journal of Food, Agriculture and Environment*, vol. 9, no. 3-4, pp. 496–500, 2011.

[7] J. Bakht, M. Shafi, Y. Jamal, and H. Sher, "Response of maize (*Zea mays* L.) to seed priming with NaCl and salinity stress," *Spanish Journal of Agricultural Research*, vol. 9, no. 1, pp. 252–261, 2011.

[8] K. Chen, A. Fessehaie, and R. Arora, "Dehydrin metabolism is altered during seed osmopriming and subsequent germination under chilling and desiccation in *Spinacia oleracea* L. cv. Bloomsdale: possible role in stress tolerance," *Plant Science*, vol. 183, pp. 27–36, 2012.

[9] P. Dahal and K. J. Bradford, "Effects of priming and endosperm integrity on seed-germination rates of tomato genotypes. 2. Germination at reduced water potential," *Journal of Experimental Botany*, vol. 41, no. 11, pp. 1441–1453, 1990.

[10] W. E. Finch-Savage, K. C. Dent, and L. J. Clark, "Soak conditions and temperature following sowing influence the response of maize (*Zea mays* L.) seeds to on-farm priming (pre-sowing seed soak)," *Field Crops Research*, vol. 90, no. 2-3, pp. 361–374, 2004.

[11] E. Adegbuyi, S. R. Cooper, and R. Don, "Osmotic priming of some herbage grass seed using polyethylene glycol (PEG)," *Seed Science and Technology*, vol. 9, no. 3, pp. 867–878, 1981.

[12] R. F. Hurly, J. Van Staden, and M. T. Smith, "Improved germination in seeds of guayule (*Parthenium argentatum* Gray) following polyethylene glycol and gibberellic acid pretreatments," *Annals of Applied Biology*, vol. 118, pp. 175–184, 1991.

[13] H. P. Anosheh, Y. Emam, and M. Ashraf, "Impact of cycocel on seed germination and growth in some commercial crops under osmotic stress conditions," *Archives of Agronomy and Soil Science*, vol. 60, no. 9, pp. 1277–1289, 2014.

[14] D. Harris, A. K. Pathan, P. Gothkar, A. Joshi, W. Chivasa, and P. Nyamudeza, "On-farm seed priming: using participatory methods to revive and refine a key technology," *Agricultural Systems*, vol. 69, no. 1-2, pp. 151–164, 2001.

[15] F. J. Sundstrom, R. B. Reader, and R. L. Edwards, "Effect of seed treatment and planting method on Tabasco pepper," *Journal of American Society for Horticultural Science*, vol. 112, pp. 641–644, 1987.

[16] M. A. Khan and I. A. Ungar, "The effect of salinity and temperature on the germination of polymorphic seeds and growth of *Atriplex triangularis* Willd," *American Journal of Botany*, vol. 71, pp. 481–489, 1984.

[17] K. D. Subedi and B. L. Ma, "Seed priming does not improve corn yield in a humid temperate environment," *Agronomy Journal*, vol. 97, no. 1, pp. 211–218, 2005.

[18] H. A. Farahani, P. Moaveni, and K. Maroufi, "Effect of hydropriming on germination percentage in sunflower (*Helianthus annus* L.) cultivars," *Advances in Environmental Biology*, vol. 5, no. 8, pp. 2253–2257, 2011.

[19] K. J. Bradford, "Water relations in seed germination," in *Seed Development and Germination*, J. Kigel and G. Galili, Eds., pp. 351–396, Marcel Dekker, New York, NY, USA, 1995.

[20] K. J. Bradford, "Manipulation of seed water relations via osmotic priming to improve germination under stress conditions," *HortScience*, vol. 21, pp. 1105–1112, 1986.

[21] F. S. Murungu, C. Chiduza, P. Nyamugafata, L. J. Clark, W. R. Whalley, and W. E. Finch-Savage, "Effects of on-farm seed priming on consecutive daily sowing occasions on the emergence and growth of maize in semi-arid Zimbabwe," *Field Crops Research*, vol. 89, no. 1, pp. 49–57, 2004.

[22] A. S. Basra, M. Farooq, I. Afzal, and M. Hussain, "Influence of osmopriming on the germination and early seedling growth of coarse and fine rice," *International Journal of Agricultural Biology*, vol. 8, pp. 19–21, 2006.

[23] P. Hedden and A. L. Phillips, "Gibberellin metabolism: new insights revealed by the genes," *Trends in Plant Science*, vol. 5, no. 12, pp. 523–530, 2000.

[24] H. Sevik and K. Guney, "Effects of IAA, IBA, NAA, and GA_3 on rooting and morphological features of *Melissa officinalis* L. stem cuttings," *The Scientific World Journal*, vol. 2013, Article ID 909507, 5 pages, 2013.

[25] Y. Zhang, Z. Ni, Y. Yao, X. Nie, and Q. Sun, "Gibberellins and heterosis of plant height in wheat (*Triticum aestivum* L.)," *BMC Genetics*, vol. 8, article 40, 2007.

[26] P. Gupta and D. Mukherjee, "Influence of GA3 pre-soaking of seeds on biochemical changes in seedling parts of *Pennisetum typhoides* Rich," *Proceedings of Indian National Science Academy B*, vol. 48, no. 5, pp. 642–648, 1982.

[27] B. Guan, D. Cao, and J. B. Yu, "Eco-physiological responses of seed germination of sweet sorghum to seed priming," *Chinese Journal of Ecology*, vol. 33, no. 4, pp. 982–988, 2014, (Chinese).

[28] M. Farooq, T. Aziz, H. ur Rehman, A. ur Rehman, and S. A. Cheema, "Evaluating surface drying and re-drying for wheat

seed priming with polyamines: effects on emergence, early seedling growth and starch metabolism," *Acta Physiologiae Plantarum*, vol. 33, no. 5, pp. 1707–1713, 2011.

[29] M. Farooq, S. M. A. Basra, R. Tabassum, and I. Afzal, "Enhancing the performance of direct seeded fine rice by seed priming," *Plant Production Science*, vol. 9, no. 4, pp. 446–456, 2006.

[30] P. Yang, X. Li, X. Wang, H. Chen, F. Chen, and S. Shen, "Proteomic analysis of rice (*Oryza sativa*) seeds during germination," *Proteomics*, vol. 7, no. 18, pp. 3358–3368, 2007.

[31] K. Chen and R. Arora, "Priming memory invokes seed stress-tolerance," *Environmental and Experimental Botany*, vol. 94, pp. 33–45, 2013.

[32] D. Harris, R. S. Tripathi, and A. Joshi, "On-farm seed priming to improve crop establishment and yield in dry direct-seeded rice," in *Proceedings of International Workshop on Dry-Seeded Rice Technology*, pp. 25–28, Bangkok, Thailand, January 2000.

[33] D. Harris, R. S. Tripathi, and A. Joshi, "On-farm seed priming to improve crop establishment and yield in dry direct-seeded," in *Direct Seeding: Research Strategies and Opportunities*, S. Pandey, M. Mortimer, L. Wade, T. P. Tuong, K. Lopes, and B. Hardy, Eds., pp. 231–240, International Research Institute, Manila, Philippines, 2002.

Hindawi Publishing Corporation
The Scientific World Journal
Volume 2014, Article ID 164732, 8 pages
http://dx.doi.org/10.1155/2014/164732

Research Article

N_2O Emissions from an Apple Orchard in the Coastal Area of Bohai Bay, China

Baohua Xie,[1] Junbao Yu,[1] Xunhua Zheng,[2] Fanzhu Qu,[1] Yu Xu,[3] and Haitao Lin[3]

[1] *Key Laboratory of Coastal Zone Environmental Processes and Ecological Remediation, Yantai Institute of Coastal Zone Research (YIC), Chinese Academy of Sciences (CAS), Shandong Provincial Key Laboratory of Coastal Zone Environmental Processes, YICCAS, Yantai Shandong 264003, China*

[2] *State Key Laboratory of Atmospheric Boundary Layer Physics and Atmospheric Chemistry, Institute of Atmospheric Physics, Chinese Academy of Sciences, Beijing 100029, China*

[3] *Agricultural Resources and Environment Institute, Shandong Academy of Agricultural Sciences, 202 Gongyebei Road, Jinan 250100, China*

Correspondence should be addressed to Junbao Yu; jbyu@yic.ac.cn

Received 1 June 2014; Accepted 8 June 2014; Published 23 June 2014

Academic Editor: Hongbo Shao

Using static chambers and gas chromatography, nitrous oxide (N_2O) fluxes from an apple orchard soil in the Bohai Bay region of China were measured from February 2010 to February 2011. In this study, two nitrogen (N) fertilizer treatments were designed—without (CK) or with (SN) synthetic N fertilizers (800 kg N ha^{-1}). The annual cumulative N_2O emissions from CK and SN were 34.6 ± 3.0 (mean ± standard error) and 44.3 ± 6.0 kg N_2O–N ha^{-1}, respectively. Such high emissions resulted from the intensive N fertilization in the experimental and previous years. The direct emission factor (EF_d) of N_2O induced by the applied synthetic N fertilizers was 1.2%. The EF_d is within the range of previous studies carried out in other croplands, which suggests that it is reasonable to estimate regional N_2O emissions from apple orchards using the EF_d obtained in other croplands. In addition, significant positive correlations existed between N_2O fluxes and soil temperatures or soil dissolved organic carbon contents.

1. Introduction

Nitrous oxide (N_2O) is an important atmospheric trace gas that contributes to global warming and stratosphere ozone depletion [1]. Mainly due to the use of nitrogen (N) fertilizer, agricultural soils are a major source of atmospheric N_2O, releasing about 1.7–4.8 Tg N_2O–N yr^{-1} [1]. Despite an increase in the number of N_2O measurements from agricultural soils in recent years, there is still a great uncertainty in the current estimates of the total global N_2O emission [2]. The uncertainty mainly originates from errors in measurements underlying emission factors and a lack of knowledge of emission processes [2, 3].

China currently consumes almost one-third of the world's N fertilizers (http://faostat.fao.org/default.aspx), in which the highest application rates of N fertilizers are in vegetable and fruit production [4, 5]. Many scientists have shown strong interest in the emissions of N_2O from various Chinese croplands including the croplands of rice-wheat rotation, paddy rice, maize-wheat rotation, tea, and vegetables [5–12]. However, few investigations have been conducted in Chinese orchards, including apple, peach, and orange fields [13–15]. In other countries, studies on N_2O emission from orchards are limited as well [2, 16]. The apple is the leading fruit in China and the area of apple orchards was 2.1×10^6 ha in 2010 [17]. China has become the world's largest apple producing country, accounting for two-fifths and one-third of the total world apple acreage and yield, respectively (http://faostat.fao.org). The Bohai Bay region and the northwest Loess Plateau are the major apple producing areas and account for 86% and 90% of the Chinese apple acreage and yield, respectively [18]. Ju et al. [4] reported that the average application rate of N fertilizers in the apple orchards and greenhouse vegetables in the northeast of Shandong Province, located in the Bohai

Bay region, was 882 and 3239 kg N ha^{-1} $year^{-1}$, respectively. The highest rate of organic fertilizers in China is also applied in fruit production [19]. The direct emission factor (EF_d) of N_2O, that is, the ratio of the fertilizer induced N_2O–N to the applied N fertilizers, is often used to estimate regional N_2O emissions from agroecosystems. However, there are few studies which reported the emission factors obtained from orchards. The intensive N fertilization is likely to lead to a lot of N_2O emissions [10]. Does the EF_d rise with the increased rate of N fertilization? Few researches were reported on it. Therefore, understanding the characteristics and quantifying the EF_d of N_2O from intensively fertilized orchards will provide a scientific basis for better estimation of regional or global N_2O emissions and developing mitigation options.

The objectives of this study were to determine the temporal variations of N_2O fluxes and the EF_d of N_2O induced by the applied synthetic N fertilizer in an apple orchard in the Bohai Bay region and to investigate the relationships between N_2O fluxes and environmental factors, such as soil temperature, soil moisture, soil carbon, and nitrogen contents.

Table 1: Details of fertilization events in the apple orchard.

Fertilizers[a]	Total amount (kg ha^{-1})	Date of fertilizations		
		2010-4-2	2010-6-24	2010-8-16
N	800	400	120	280
P	175	175	0	0
K	664	332	0	332

[a]Synthetic fertilizers of N, P, and K were urea, calcium biphosphate, and potassium sulfate, respectively.

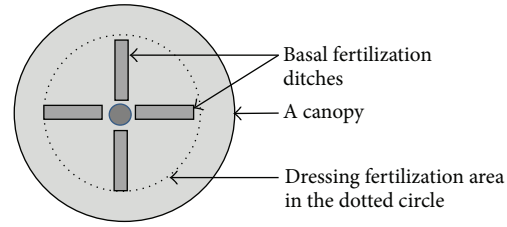

Figure 1: The diagram of fertilization area in the canopy projection area of an apple tree.

2. Materials and Methods

2.1. Site Description. The experimental site is located in the suburb (37°49′N, 120°45′E) of Penglai County in Shandong Province, neighboring the Bohai Bay. The investigated area is representative of the major apple production areas in China. This region displays a warm temperate continental monsoon climate. The annual precipitation is 664 mm. The annual mean air temperature is 11.9°C, and the annual frost-free period is approximately 206 days. The soil at the experimental site is Argosols (Cooperative Research Group on Chinese Soil Taxonomy, 2001) with 7.0% clay (<0.002 mm), 39.6% silt (0.002–0.02 mm), and 53.4% sand (0.02–2 mm). Other soil properties of the soil sample before the experiment beginning at a 0–20 cm depth are as follows: bulk density 1.39 g cm^{-3}, soil organic carbon (SOC) 10.0 g kg^{-1}, total nitrogen 1.2 g kg^{-1}, total phosphorous 1.9 g kg^{-1}, total potassium 15.8 g kg^{-1}, available phosphorous 50.7 mg kg^{-1}, available potassium 155.2 mg kg^{-1}, and pH 6.7 (water).

2.2. Experiment Design. The experiment was performed in an apple orchard from February 2010 to February 2011. The apple orchard, which was converted from the former winter wheat field in 2002, was dominated by Fuji apple trees. The plant density is 670 plants ha^{-1}, and the apples are usually harvested in mid-October. In the study, two N fertilization treatments, that is, without and with the addition of synthetic N fertilizer (hereinafter referred to as CK and SN, resp.), were applied. Both treatments were replicated three times. During 2010, urea (800 kg N ha^{-1}), calcium biphosphate (175 kg P ha^{-1}), and potassium sulfate (664 kg K ha^{-1}) were applied in SN treatment, including the basal fertilization in early April and two dressing fertilizations in late June and mid-August (Table 1). The CK treatment was added with the same rates of P and K as SN but none synthetic N fertilizers. Several pesticides and fungicides were foliar sprayed two or three times per year in both SN and CK to prevent pests and diseases. Although the application rate of N fertilizers was very high, it was representative in Shandong Province. Ju et al. [4] reported that the average application rate of N fertilizers in the apple orchards in the northeast of Shandong Province was 882 kg N ha^{-1}.

On April 2, 2010, the basal fertilizers were buried in ditches (length ∗ breadth ∗ depth = 1 ∗ 0.3 ∗ 0.2 m). Four ditches evenly scattered around an apple tree. The dressing fertilizations were evenly broadcasted on the ground under the trees one day after a rainfall or irrigation event in June and August 2010. The fertilization area for a tree is smaller than its canopy area. Figure 1 showed the fertilization area for an apple tree. Both the basal and dressing fertilizers were applied inside the dotted circle of Figure 1. Due to the specific fertilization mode in the orchard, we separated a canopy projection area into two subplots, that is, inside and outside the dotted circle of Figure 1 (hereinafter referred to as site A and site B). Thus, SN and CK plots were separated to SN-A, SN-B, CK-A, and CK-B subplots for the sampling of gas and soil. The area ratio of sites A and B was 0.38.

2.3. Measurement of N_2O Flux. The measurements of the N_2O exchange flux *in situ* were performed from February 2010 to February 2011. Both of the CK and SN treatments were randomly set up with three replicates, and each replicate was separated to site A and site B subplots. The fluxes were generally measured once every 3-4 days, using static opaque chamber method in combination with gas chromatography techniques [21]. The sampling frequency was doubled in one week after a fertilization event and was reduced to once a week in cold winter.

For the sampling of N_2O gas, a 0.25 m^2 stainless-steel frame was permanently installed in the soil. A 0.5 m high, gas-tight chamber with water seals was temporarily mounted on the frame when the sampling occurred. The sampling process

Table 2: Average concentrations (mean ± SE) of soil DOC (mg C kg^{-1}) and IN (mg N kg^{-1}) during the experimental period.

Items	N treatment	Site A	Site B	Weighted average
DOC	SN	153.9 ± 13.0	145.4 ± 12.3	151.4 ± 12.8
	CK	140.9 ± 16.7	121.0 ± 17.2	135.0 ± 16.8
NO_3^-–N	SN	73.7 ± 14.1	29.7 ± 9.0	60.5 ± 12.6
	CK	42.4 ± 12.4	24.1 ± 9.2	36.9 ± 12.9
NH_4^+–N	SN	113.6 ± 22.8	10.7 ± 4.2	82.8 ± 17.2
	CK	42.0 ± 14.4	13.8 ± 7.5	33.5 ± 12.3

SN means the synthetic N fertilizer treatment. CK means the treatment without synthetic N fertilizer. Site A means the fertilization area in an apple tree canopy projection area. Site B means the nonfertilization area in an apple tree canopy projection area. The weighted averages were calculated from the emissions from site A and site B according to their area ratio.

was completed between 09:00 and 11:00. Five gas samples were taken with 60 mL plastic syringes at 6 min intervals. Immediately after taking the fifth gas sample, the chamber was removed from the frame. Within at most 10 hours after sampling, the gas samples in the syringes were analyzed using a gas chromatograph with an electron capture detector (ECD) [21].

The nitrous oxide flux was calculated by the rate of the change in the N_2O concentration in the chamber, estimated as the slope of linear regression between N_2O concentration and time. The data on air pressure and chamber headspace air temperature were used to correct the N_2O density at 273 K and 1,013 hPa to the actual headspace air conditions. Flux rates were discarded if the coefficient of determination (r^2) was less than 0.85. Single flux from the measurement between 9:00 and 11:00 was regarded as the daily mean flux and directly extrapolated to the cumulative emission for the observational period [22, 23]. The annual cumulative N_2O emissions were calculated by linear interpolations between adjacent observations. The cumulative N_2O emission from SN or CK treatment was determined by weighting the emissions from sites A and B on the basis of their area ratio of 0.38.

2.4. Auxiliary Measurements. Soil temperature, WFPS, inorganic nitrogen (IN, including NO_3^-– and NH_4^+–N), and dissolved organic carbon (DOC) were measured to determine the main factors that influence the emission of N_2O.

Daily precipitation and air temperature were observed by a nearby automatic climate station. Soil temperatures and volumetric moisture at 10 cm depth were recorded automatically once an hour, though only the daily averages are reported here. Soil volumetric moisture values, which were measured with FDR sensor, were converted into values of water-filled pore space (%WFPS) by the following formula:

$$\%\text{WFPS} = \frac{\theta}{1 - \text{BD}/\text{PD}}, \quad (1)$$

where θ is the volumetric soil water content (%), BD is the bulk density (g m^{-3}), and PD is the particle density constant (2.65 g m^{-3}).

The surface soil (0–10 cm) was sampled biweekly using a 2 cm diameter gauge auger. At each sampling date, one sample, containing three bulked subsamples, was collected from each subplot. To measure NO_3^- and NH_4^+ contents, fresh soil samples were extracted with a KCl solution (2 mol, soil : solution = 1 : 10) by shaking for 1 h. The extracts were analyzed with a continuous flow analyzer (Seal Bran-Lubbe AA3, Germany). Soil samples were extracted with deionized water (soil : water = 1 : 4) and the extracts were immediately analyzed for DOC with a total organic carbon analyzer (Shimadzu TOC-VCPH, Japan).

2.5. Statistical Analysis. In order to examine the relationships between the measured N_2O fluxes and environmental parameters, exponential and linear regression analyses were performed. Differences in IN and DOC concentrations and N_2O emissions among SN-A, SN-B, CK-A, and CK-B were determined using one-way ANOVA.

3. Results and Discussion

3.1. Environmental Conditions and Soil Parameters. The annual average air temperature was 12.0°C and the total precipitation was 752 mm (Figure 2(a)). Figure 2(b) showed soil temperature and WFPS at 10 cm depth. The variation pattern of soil temperatures was similar to that of air temperatures. Soil WFPS was 62% on average.

Table 2 listed the averages of soil DOC and IN concentrations during the experimental period. Both DOC and IN concentrations in SN-A were significantly higher than those in the other subplots. The average DOC concentration in SN-A was 153.9 mg kg^{-1}, which was higher than that in SN-B, CK-A, and CK-B by 6% ($P < 0.01$), 9% ($P < 0.01$), and 27% ($P < 0.01$), respectively. The difference in DOC concentration in SN-B and CK-B was also significant ($P < 0.05$).

The average NO_3^-–N concentration in SN-A was 73.7 mg kg^{-1}, which was higher than that in SN-B, CK-A, and CK-B by 148% ($P < 0.01$), 74% ($P < 0.01$), and 206% ($P < 0.01$), respectively. The average NH_4^+–N concentration in SN-A was 113.6 mg kg^{-1}, which was higher than that in SN-B, CK-A, and CK-B by 963% ($P < 0.01$), 171% ($P < 0.01$), and 725% ($P < 0.01$), respectively. Due to the previous N fertilizations in CK-A in the previous years before the experiment, the concentrations of both NO_3^-–N and

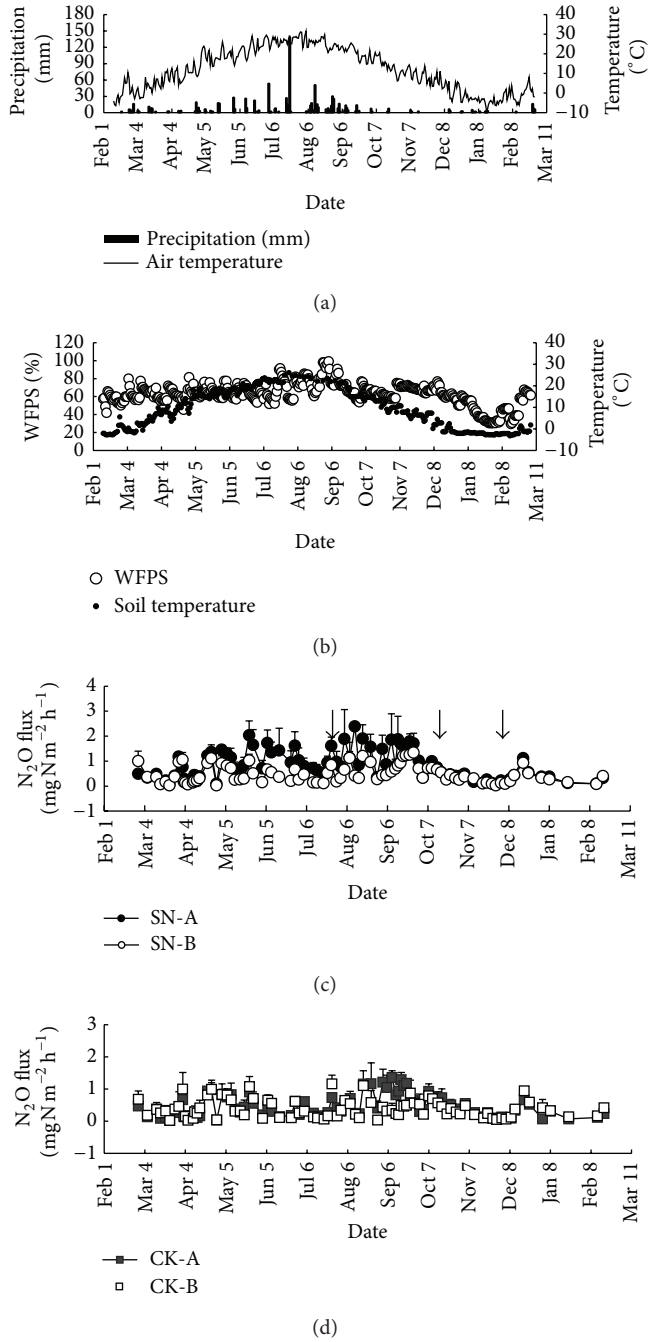

Figure 2: (a) Daily precipitation and average air temperature, (b) soil moisture (WFPS, i.e., the water-filled pore space) and soil temperature at 10 cm depth in site A (under the middle of an apple tree canopy), (c) N_2O fluxes from SN, and (d) N_2O fluxes from CK. The N_2O data are the means and standard errors (the vertical bars) of three replicates. SN-A means site A (the fertilization area in an apple tree canopy projection area) in SN treatment. SN-B means site B (the unfertilization area in an apple tree canopy projection area) in SN treatment. CK-A and CK-B mean sites A and B in CK treatment, respectively. The downward arrows indicate the time of fertilization.

NH_4^+–N in CK-A were significantly higher than those in CK-B ($P < 0.01$).

3.2. N_2O Fluxes and Annual Cumulative Emissions. The seasonal variation of N_2O fluxes in SN-A was very large, followed by SN-B, CK-A, and CK-B in sequence (Figures 2(c) and 2(d)). In the fall and winter, N_2O fluxes were low and varied only slightly in the four types of subplots. From May to October, N_2O fluxes in SN-A were remarkably higher than those in the other subplots. Immediately after a synthetic N fertilization event, N_2O fluxes usually increased temporarily in SN-A. The flux range in all the subplots was from 0.02 to

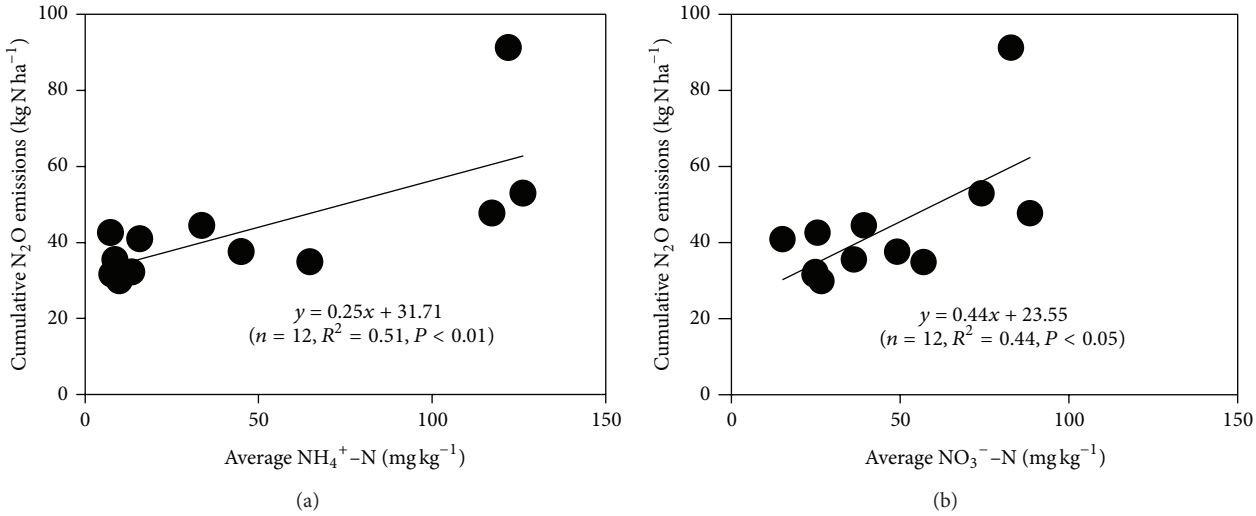

Figure 3: Relationships between the annual cumulative N_2O emissions and the annual average (a) NH_4^+–N and (b) NO_3^-–N contents. The given data are obtained from all of the 12 subplots.

2.39 mg N_2O–N m^{-2} h^{-1}. The annual average N_2O flux in SN-A was 0.83 mg N_2O–N m^{-2} h^{-1}, significantly higher than that in SN-B, CK-A, and CK-B by 79% ($P < 0.05$), 70% ($P < 0.05$), and 113% ($P < 0.01$), respectively.

Table 3 presented the annual cumulative N_2O emissions. Mainly due to the application of synthetic N fertilizers, the annual cumulative N_2O emissions in SN-A, 63.9 kg N_2O–N ha^{-1}, were higher than those in SN-B, CK-A, and CK-B by 74% ($P < 0.01$), 77% ($P < 0.05$), and 87% ($P < 0.01$), respectively. The weighed annual N_2O emissions were 44.3 ± 6.0 and 34.6 ± 3.0 kg N_2O–N ha^{-1} from SN and CK, respectively. The EF_d of N_2O induced by the applied synthetic N fertilizer was 1.2 ± 0.4%.

3.3. Relationships between N_2O Fluxes and Soil Temperature, WFPS, DOC, and IN. Because N fertilizers were added only to site A, we analyzed the relationships between N_2O fluxes and soil parameters on sites A and B, respectively. Except for CK-B, N_2O fluxes exhibited a significant exponential correlation with soil temperatures ($n = 85$, $P < 0.01$) and the determination coefficient (R^2) in site A was higher than that in site B (Table 4), which was in good agreement with the results from other studies [14, 15, 20]. Although a large number of previous studies suggested that N_2O emission was significantly correlated with WFPS [20, 24, 25], there was no significant correlation between N_2O fluxes and soil WFPS in this study. The possible reason is that the specific farm management such as fertilization and irrigation mode may conceal the relationship between N_2O emissions and soil WFPS. Lin et al. [14] reported that N_2O emissions from an orange orchard were positively correlated with soil temperature but not correlated with WFPS. Pang et al. [15] also reported a similar finding in a study which was performed in an apple orchard.

Table 3: Annual cumulative emissions of N_2O (mean ± SE, kg N_2O–N ha^{-1}).

N treatment	Site A	Site B	Weighted average
SN	63.9 ± 13.7	36.7 ± 3.1	44.3 ± 6.0
CK	36.1 ± 1.9	34.1 ± 3.4	34.6 ± 3.0

The meanings of SN, CK, site A, and site B can be found in the text and the footnote in Table 2. The weighted averages were calculated from the emissions of site A and site B according to their area ratio.

N_2O emissions increase with the increase of SOC contents [24]. N_2O fluxes exhibited a significant positive correlation with soil DOC in both CK and SN treatments (Table 4). The determination coefficients in CK were higher than those in SN, in which DOC contents were higher than those in CK (Table 2). The results suggested that the effect of DOC on N_2O emissions might become weak when DOC content was higher than some threshold value.

Nitrous oxide is mainly produced in soil by nitrification and denitrification, which are particularly controlled by the amount of ammonium and nitrate [26, 27]. Although the seasonal variations of N_2O fluxes were not significantly correlated with the dynamics of soil NO_3^-–N or NH_4^+–N contents, the annual cumulative N_2O emissions in all of the subplots exhibited significant positive correlations with the annual average contents of soil NO_3^-–N and NH_4^+–N (Figure 3). The results suggested that the contents of soil inorganic N should be one of the major reasons controlling the annual N_2O emissions from various subplots.

3.4. Comparison with Other Studies on N_2O Emissions from Orchard Soils. To date, there were few reports on N_2O emissions from orchard soils. Table 5 listed soil properties, annual N fertilizations, and N_2O emissions from some orchard soils. Pang et al. [15] reported that N_2O emission

Table 4: Summary of regression analysis.

N treatment	Variables	Regressions	R^2	n	P
CK-A	ST	$y = 0.167e0.05x$	0.25	85	<0.01
SN-A	ST	$y = 0.229e0.07x$	0.49	85	<0.01
SN-B	ST	$y = 0.209e0.07x$	0.15	85	<0.01
CK-A	DOC	$y = 0.004x - 0.202$	0.23	26	<0.05
SN-A	DOC	$y = 0.005x - 0.139$	0.08	26	<0.1

The variable y means N_2O fluxes. The variable x means the environmental factor including soil temperature and soil DOC.

Table 5: Soil properties, annual N fertilizations, and N_2O emissions from orchard soils.

Land use	TN ($g\,kg^{-1}$)	SOC ($g\,kg^{-1}$)	C/N ratio	NH_4^+–N ($mg\,kg^{-1}$)	NO_3^-–N ($mg\,kg^{-1}$)	N fertilizer ($kg\,N\,ha^{-1}$)	N_2O emissions ($kg\,N\,ha^{-1}$)	References
Apple	1.42	10.0	6.9	82.8	60.5	800	44.3	This study
Apple	1.36	10.0	7.4	33.5	36.9	0[a]	34.6	This study
Apple	1.00	6.3				312	3.2	[15]
Orange	1.10			7.4	27.1	597	2.03	[14]
Orange	1.06			8.5	65.2	579	1.55	[14]
Peach	1.38	6.3				210	1.4	[13]
Longan	1.49	13.4	10.0			0[a]	8.64	[20]

[a]Nitrogen fertilizers were applied before the experimental years (Liu et al. [20] and this study).

from an apple orchard was $2.05\,kg\,N_2O–N\,ha^{-1}\,year^{-1}$. Lin et al. [14] found that N_2O emissions were 1.55–$2.03\,kg\,N_2O–N\,ha^{-1}\,year^{-1}$ from orange orchard soils. Lin et al. [13] reported that the annual cumulative N_2O emission was $1.4\,kg\,N_2O–N\,ha^{-1}$ from a peach orchard. Liu et al. [20] reported a high N_2O emission of $8.64\,kg\,N_2O–N\,ha^{-1}$ from a longan orchard without fertilization. The annual cumulative N_2O emissions in these previous studies were only 0.1%–24.9% of the emissions from SN in the present study. There may be two major reasons leading to such a great distinction. The first one is the enormous difference in the nitrogen fertilizer application rates; the rates in the above literatures were $0–597\,kg\,N\,ha^{-1}$, only 0%–74.6% of that in the present study. Many previous studies suggested that N_2O emissions from fertilized soils were positively correlated with the nitrogen fertilization rates [28–30]. N_2O emissions were found to be very high in cultivated soils which were incorporated with high amount of N fertilizers. For example, Mei et al. [5] reported that the annual cumulative N_2O emissions from the vegetable fields incorporated with N fertilization rates of $1195 \pm 63\,kg\,N\,ha^{-1}\,year^{-1}$ were $36.7 \pm 14\,kg\,N_2O–N\,ha^{-1}$. The second reason is the very low measurement frequencies in the previous studies, that is, biweekly [13, 15] or even monthly [14] interval, which probably led to missing some peak fluxes of N_2O in case of significant changes in soil moistures or nitrogen fertilization events [5, 8, 16, 31]. Liu et al. [20] measured N_2O fluxes at the same frequency as this study, that is, twice a week, and found that N_2O emission from a longan orchard without fertilization was $8.64\,kg\,N_2O–N\,ha^{-1}$, which was severalfold of those values obtained from much lower frequency of measurements in orchards [13–15].

It should be noted that N_2O emission from CK was as high as $33.1 \pm 3.8\,kg\,N_2O–N\,ha^{-1}$. Nitrous oxide is mainly produced in soil by nitrification and denitrification, and N_2O emissions were particularly controlled by the amount of ammonium and nitrate [26, 27]. The CK treatment received a large amount of N fertilizers in previous years before the experiment, resulting in high amounts of both NO_3^-–N and NH_4^+–N in the experimental period (Table 2). In CK-A, the content of soil NO_3^-–N and NH_4^+–N was up to 42.4 ± 12.4 and $42.0 \pm 14.4\,mg\,kg^{-1}$, respectively. Even in CK-B, the content of soil NO_3^-–N and NH_4^+–N was up to 24.1 ± 9.2 and $13.8 \pm 7.5\,mg\,kg^{-1}$, respectively. The high contents of IN in CK probably resulted in high emissions of N_2O. Liu et al. [20] reported that N_2O emission was up to $8.64\,kg\,N_2O–N\,ha^{-1}$ from a none-N fertilization longan orchard which was fertilized before the experimental year.

3.5. Emission Factor of N_2O Induced by the Applied Synthetic N Fertilizer. Based on the available site-scale data sets of N_2O emissions in annual paddy rice-wheat rotation systems, Zou et al. [28] reported that the EF_d of N_2O induced by the applied synthetic fertilizer averaged 1.02% for the rice season, 1.65% for the wheat season, and 1.25% for the annual season. Xiong et al. [32] reported that the EF_d of N_2O was 0.73% from a greenhouse vegetable field which was added with N fertilizers at the rate of $1636\,kg\,N\,ha^{-1}\,year^{-1}$. Bouwman et al. [33] reported that the EF_d of N_2O induced by the applied synthetic N fertilizer averaged 1.0% and the value was renewed as 0.91% [2]. Due to the high amount of N fertilizer application, the annual cumulative emission of N_2O was very high in the present study, though the EF_d was 1.2%, close to the previous studies. The result suggests that the EF_d of the apple orchard is close to other croplands, and it may be reasonable to estimate N_2O emissions from the apple orchard soil using the EF_d obtained from other croplands.

4. Conclusions

Mainly due to the high application rate of N fertilizers, the annual N_2O emission from an apple orchard in the Bohai Bay region, China, was up to $44.3 \pm 6.0\,kg\,N_2O–N\,ha^{-1}$, which indicated that the apple orchard is an important source of atmospheric N_2O. Apple production must be taken into account when estimating N_2O emissions from agroecosystems. The EF_d of N_2O induced by the applied synthetic N fertilizer in the present study was 1.2%, which was within the range of EF_d obtained in other croplands. Thus, it may be reasonable to estimate N_2O emissions from apple orchard soils using the EF_d obtained in other croplands.

Conflict of Interests

The authors declare that there is no conflict of interests regarding the publishing of this paper.

Acknowledgments

The authors are grateful for the financial support provided by the Non-Profit Research Foundation for Agriculture (Grant no. 201103039), the National Natural Science Foundation of China (Grant nos. 41205118, 41021004), and the National Natural Science Foundation for Distinguished Young Scholar of Shandong Province (no. JQ201114). They also thank Mr. Yunzhao Li for the contribution to the field measurements.

References

[1] IPCC, "Climate change 2007, the physical science basis," in *Contribution of Working Group I to the Fourth Assessment Report of the Intergovernmental Panel on Climate Change*, pp. 131–236, Cambridge University Press, New York, NY, USA, 2007.

[2] E. Stehfest and L. Bouwman, "N_2O and NO emission from agricultural fields and soils under natural vegetation: summarizing available measurement data and modeling of global annual emissions," *Nutrient Cycling in Agroecosystems*, vol. 74, no. 3, pp. 207–228, 2006.

[3] L. Nol, P. H. Verburg, and E. J. Moors, "Trends in future N_2O emissions due to land use change," *Journal of Environmental Management*, vol. 94, no. 1, pp. 78–90, 2012.

[4] X. T. Ju, C. L. Kou, F. S. Zhang, and P. Christie, "Nitrogen balance and groundwater nitrate contamination: comparison among three intensive cropping systems on the North China Plain," *Environmental Pollution*, vol. 143, no. 1, pp. 117–125, 2006.

[5] B. Mei, X. Zheng, B. Xie et al., "Characteristics of multiple-year nitrous oxide emissions from conventional vegetable fields in southeastern China," *Journal of Geophysical Research: Atmospheres*, vol. 116, no. 12, Article ID D12113, 2011.

[6] W. Sun and Y. Huang, "Synthetic fertilizer management for China's cereal crops has reduced N_2O emissions since the early 2000s," *Environmental Pollution*, vol. 160, no. 1, pp. 24–27, 2012.

[7] J. W. Zou, Y. Huang, Y. M. Qin et al., "Changes in fertilizer-induced direct N_2O emissions from paddy fields during rice-growing season in China between 1950s and 1990s," *Global Change Biology*, vol. 15, no. 1, pp. 229–242, 2009.

[8] X. Zheng, M. Wang, Y. Wang et al., "Impacts of soil moisture on nitrous oxide emission from croplands: a case study on the rice-based agro-ecosystem in Southeast China," *Chemosphere—Global Change Science*, vol. 2, no. 2, pp. 207–224, 2000.

[9] W. Ding, L. Meng, Z. Cai, and F. Han, "Effects of long-term amendment of organic manure and nitrogen fertilizer on nitrous oxide emission in a sandy loam soil," *Journal of Environmental Sciences*, vol. 19, no. 2, pp. 185–193, 2007.

[10] J. Zou, Y. Huang, X. Zheng, and Y. Wang, "Quantifying direct N_2O emissions in paddy fields during rice growing season in mainland China: dependence on water regime," *Atmospheric Environment*, vol. 41, no. 37, pp. 8030–8042, 2007.

[11] Z. Cai, G. Xing, X. Yan et al., "Methane and nitrous oxide emissions from rice paddy fields as affected by nitrogen fertilisers and water management," *Plant and Soil*, vol. 196, no. 1, pp. 7–14, 1997.

[12] S. Xu, X. Fu, S. Ma et al., "Mitigating nitrous oxide emissions from tea field soil using bioaugmentation with a *Trichoderma viride* biofertilizer," *The Scientific World Journal*, vol. 2014, Article ID 793752, 9 pages, 2014.

[13] S. Lin, J. Iqbal, R. Hu et al., "Differences in nitrous oxide fluxes from red soil under different land uses in mid-subtropical China," *Agriculture, Ecosystems and Environment*, vol. 146, no. 1, pp. 168–178, 2012.

[14] S. Lin, J. Iqbal, R. Hu, and M. Feng, "N_2O emissions from different land uses in mid-subtropical China," *Agriculture, Ecosystems and Environment*, vol. 136, no. 1-2, pp. 40–48, 2010.

[15] J. Pang, X. Wang, Y. Mu, Z. Ouyang, and W. Liu, "Nitrous oxide emissions from an apple orchard soil in the semiarid Loess Plateau of China," *Biology and Fertility of Soils*, vol. 46, no. 1, pp. 37–44, 2009.

[16] E. Veldkamp and M. Keller, "Nitrogen oxide emissions from a banana plantation in the humid tropics," *Journal of Geophysical Research D: Atmospheres*, vol. 102, no. 13, pp. 15889–15898, 1997.

[17] *China Rural Statistical Yearbook*, China Statistics Press, 2011.

[18] H. Zhai, S. Dachuang, and S. Huairui, "Current status and developing trend of apple industry in China," *Journal of Fruit Science*, vol. 24, no. 3, pp. 355–360, 2007 (Chinese).

[19] X. Yan, *Study on present status of chemical fertilizer application and high efficient utilization of nutrition [Ph.D. thesis]*, Chinese Academy of Agricultural Sciences, 2008, (Chinese).

[20] H. Liu, P. Zhao, P. Lu, Y. Wang, Y. Lin, and X. Rao, "Greenhouse gas fluxes from soils of different land-use types in a hilly area of South China," *Agriculture, Ecosystems and Environment*, vol. 124, no. 1-2, pp. 125–135, 2008.

[21] W. Yuesi and W. Yinghong, "Quick measurement of CH_4, CO_2 and N_2O emissions from a short-plant ecosystem," *Advances in Atmospheric Sciences*, vol. 20, no. 5, pp. 842–844, 2003.

[22] Y. S. Lou, Z. P. Li, and T. L. Zhang, "Carbon dioxide flux in a subtropical agricultural soil of China," *Water, Air, and Soil Pollution*, vol. 149, no. 1–4, pp. 281–293, 2003.

[23] X. Zheng, M. Wang, Y. Wang et al., "Comparison of manual and automatic methods for measurement of methane emission from rice paddy fields," *Advances in Atmospheric Sciences*, vol. 15, no. 4, pp. 569–579, 1998.

[24] T. Harrison-Kirk, M. H. Beare, E. D. Meenken, and L. M. Condron, "Soil organic matter and texture affect responses to dry/wet cycles: effects on carbon dioxide and nitrous oxide emissions," *Soil Biology & Biochemistry*, vol. 57, pp. 43–55, 2013.

[25] D. W. Rowlings, P. R. Grace, R. Kiese, and K. L. Weier, "Environmental factors controlling temporal and spatial variability in the soil-atmosphere exchange of CO_2, CH_4 and N_2O from an Australian subtropical rainforest," *Global Change Biology*, vol. 18, no. 2, pp. 726–738, 2012.

[26] E. A. Davidson and L. V. Verchot, "Testing the hole-in-the-pipe model of nitric and nitrous oxide emissions from soils using the TRAGNET database," *Global Biogeochemical Cycles*, vol. 14, no. 4, pp. 1035–1043, 2000.

[27] B. Kachenchart, D. L. Jones, N. Gajaseni, G. Edwards-Jones, and A. Limsakul, "Seasonal nitrous oxide emissions from different land uses and their controlling factors in a tropical riparian ecosystem," *Agriculture, Ecosystems & Environment*, vol. 158, pp. 15–30, 2012.

[28] J. Zou, Y. Huang, Y. Lu, X. Zheng, and Y. Wang, "Direct emission factor for N_2O from rice-winter wheat rotation systems in Southeast China," *Atmospheric Environment*, vol. 39, no. 26, pp. 4755–4765, 2005.

[29] J. P. Hoben, R. J. Gehl, N. Millar, P. R. Grace, and G. P. Robertson, "Nonlinear nitrous oxide (N_2O) response to nitrogen fertilizer in on-farm corn crops of the US Midwest," *Global Change Biology*, vol. 17, no. 2, pp. 1140–1152, 2011.

[30] X. Gao, M. Tenuta, A. Nelson et al., "Effect of nitrogen fertilizer rate on nitrous oxide emission from irrigated potato on a clay loam soil in manitoba, Canada," *Canadian Journal of Soil Science*, vol. 93, no. 1, pp. 1–11, 2013.

[31] C. Werner, X. Zheng, J. Tang et al., "N_2O, CH_4 and CO_2 emissions from seasonal tropical rainforests and a rubber plantation in Southwest China," *Plant and Soil*, vol. 289, no. 1-2, pp. 335–353, 2006.

[32] Z. Q. Xiong, Y. X. Xie, G. X. Xing, Z. L. Zhu, and C. Butenhoff, "Measurements of nitrous oxide emissions from vegetable production in China," *Atmospheric Environment*, vol. 40, no. 12, pp. 2225–2234, 2006.

[33] A. F. Bouwman, L. J. M. Boumans, and N. H. Batjes, "Modeling global annual N_2O and NO emissions from fertilized fields," *Global Biogeochemical Cycles*, vol. 16, no. 4, 2002.

Hindawi Publishing Corporation
The Scientific World Journal
Volume 2014, Article ID 483862, 9 pages
http://dx.doi.org/10.1155/2014/483862

Review Article

Mine Land Reclamation and Eco-Reconstruction in Shanxi Province I: Mine Land Reclamation Model

Hao Bing-yuan and Kang Li-xun

Taiyuan University of Technology, Taiyuan, Shanxi 030024, China

Correspondence should be addressed to Hao Bing-yuan; haobingyuan@126.com

Received 29 May 2014; Accepted 31 May 2014; Published 22 June 2014

Academic Editor: Hongbo Shao

Coal resource is the main primary energy in our country, while Shanxi Province is the most important province in resource. Therefore Shanxi is an energy base for our country and has a great significance in energy strategy. However because of the heavy development of the coal resource, the ecological environment is worsening and the farmland is reducing continuously in Shanxi Province. How to resolve the contradiction between coal resource exploitation and environmental protection has become the imperative. Thus the concept of "green mining industry" is arousing more and more attention. In this assay, we will talk about the basic mode of land reclamation in mine area, the engineering study of mine land reclamation, the comprehensive model study of mine land reclamation, and the design and model of ecological agricultural reclamation in mining subsidence.

1. Introduction

As is well known, coal is the foundation of national economic development and is also one of the main primary energies in China. In our country the coal production shows rapid growth rate. For example, the output was 2960 million tons in 2001, while the yield grew up to 1381 million tons in 2009 with an average annual growth rate at 175 million tons [1]. The rapid development of the coal production meets the requirements of social and economic development and is the important foundation of national economic development [2]. It accounts for about 75.6% and 68.7%, respectively, in energy production and consumption structure in 2008.

The main position of coal remained unchanged for nearly 50 years. The coal plays special important roles in the process of industrialization, urbanization, and modernization in our country. However, the mining, transportation, and utilization of coal bring up a series of environment problems, as is the trouble we have to confront and solve in building a well-off society and achieving good ecological mining area [3].

All the mining activities will lead to subside, exert an effluence on surface structures and environment such as reduction in farmland output, flatlands ponding, road crack, and house collapse [4]. According to statistics, the forest broken directly by mining added up to 1060 thousand hectares, the destroyed grassland 263 thousand hectares [5]. In addition, the area of collapse due to the mining industry reached 5000–6000 thousand mu including farm land 1300 thousand mu, about 40 cities. The cities all suffered from mining subsidence and 25 cities of them were seriously damaged. Every year, the loss on account of mining subsidence reached more than 400 million. In short, the damage brought about by mining subsidence is more serious than earthquake [6]. Shanxi Province is an important coal resource province in our country. It was reported that its coal reserves accounts for 1/3 in the total reserve in our country, the coal production for 1/4 in national total output, coal transfer volume per year for 3/4 in national inter provincial volume and coal export volume for 1/2 in the national total exports [7]. In face of the narrow agricultural base, worse circumstance, and lack of arable land and resource per person in Shanxi province, how to resolve the contradiction among coal resource exploitation, subsidence, and environmental protection have become the urgent affairs [8].

Recently, the idea of green mining and mining industry were proposed in succession and got widely recognized. One

of the core concepts of the "friendly mining industries" was to achieve the "green mining" [9]. The connotation of the green mining was to strive to follow the principle of the green industry in economy, forming a "low mining-high use-low emissions" production technology [10]. Namely, we should make full use of the available resource exploitation and ecological environmental protection technology as well as geological conditions to realize the mining development model with optimal economic benefits and minimal ecological environmental impact [11]. In this model the main point focuses on the scientific and reasonable control of the subsidence in coal mining. The unreasonable exploitation of the coal district will lead to a series of environmental problems in the following.

(1) The mining subsidence in coal field severely damaged the mining area environment, resulting in the house crack, farmland ponding, road fracture, pond dried up, and so on. All the damages make a great difference and loss to daily life and production. The destruction of floorscape is specially difficult to recover.

(2) The subsidence caused damages to buildings, roads, railways, bridges, underground pipe network, and urban infrastructure, leading to railroad and road diversion, reconstruction of the buildings, and huge economic losses.

(3) The subsidence destructed the groundwater level and water system, forming low-lying area and pools zone and even wetland. The destroyed land neither can be used for planting nor breeding turning into wasteland in the end. The destruction of the underground water system and the run off of the underground water are unrecoverable.

(4) The subsidence disrupted the natural forest, grasslands, vegetation, and massif, affecting the ecological balance [12].

(5) The subsidence can also influence the industry-agriculture relation and social stability, sharpening the contradiction between enterprise and local regions and aggravating social instability.

Based on the above problems, this paper conducted the study about the utilization model of mine land reclamation.

2. The Basic Mode of Land Reclamation in Mine Area

The use of mine land reclamation mainly includes agriculture, forestry, fishery, construction, and entertainment [13].

2.1. The Reclamation for Agriculture. According to the Land Administrative Laws, the reclaimed land should on a priority basis be used for agriculture. The agricultural reclamation can adopt different management methods in accordance with different situations. On account of the rugged areas in mountainous regions, the shallow subside can be used for reclamation directly with a little proper adjustment [14]. In plain areas, the shallow subside which was formed can be transformed into dry land or paddy field, respectively, according to the water table [15]. As for the deep collapse with a low water table, we should take the fill and overlying transformation methods. Finally, with regard to the extensive, deep, and low water table collapse, we have to do comprehensive treatment. Generally, we took the method of digging, filling, and filling the rimland before reclamation.

2.2. The Reclamation for Forestry. The reclamation of sank land for forestry is decided by the terrain and the soil property [16]. In general, the asperous land in hill and mountainous regions, and the irregular reclaimed land are suitable for garden. In these gardens we can cultivate cash crops or do afforestation. The land which is barren, elevated, and steep should be reclaimed into forest or meadowland [17]. For the collapse in low mountains and hills or overlying land after strip mining, they are fit for planting forages or trees [18].

2.3. The Reclamation for Fishery. It is cheaper and faster to perform fishing reclamation. Normally, the land sank in plain with ponding at the 2 meter or more deep can be transformed into a fish farm. The water accumulated area for all year round can carry out fish farming in the depth of the subsidence [19]. The subsidence areas which are excavating coal are still collapsing, so we can adopt the extensive reclamation mode to do fish-duck polyculture.

2.4. The Reclamation for Construction. The leveled mining area in the subsidence region can be used for building. The areas after foundation treatment can be used to construct residential houses and industry building. This measure on the one hand can relax our country land to be extensive to some degree, and on the other hand can offer nearby place for the countryside transfer, getting around the move again, relieving the relationship between industry and agriculture, saving compensation for damages and the cost of relocating again [20].

2.5. The Reclamation for Tourist. The filled collapse should be smartly planned. We can set tourist attractions, plant trees and flowering straws with ornamental value, and build ponticulus and lakes for fish and sightseeing [21]. The collapse with large water surface, deep water, and good water quality can build underwater park or amusement center.

2.6. The Reclamation for Headwaters. The subsidence basin should be able to store and block up water as much as possible under the rational development and utilization. The deposit water can supply underground water or conduct aquaculture or irrigate land. For the north which lacks water, this mode is a very good development approach for water source. The collapse areas with good quality water can be developed into a newly waterhead area. We can also build water works in these regions. The purification treated hydrops is transformed into drinking water to relieve the lack of water in urban, residential areas and company.

Technical requirements of the land reclamation mode are shown in Table 1.

Table 1: Technical requirements of the land reclamation mode.

Reclamation mode	Application	Technical requirements
Agriculture	Plantation, garden	Land leveling spread topsoil. For the food crops, the topsoil should not be less than 0.5 meter, of which the humus layer should not be less than 0.2-0.3 meter. The filling material should not contain harmful element, if any the isolation layer is needed and the thickness should not be less than 0.4 meter. The hydraulic condition should be good. The demand of topsoil: the soil mass density should not be more than 1.5 g/cm^3. The proportion of clay and sand is 1 : 3 or 1 : 2. The porosity is no less than 40%–50%. The content of the soluble sodium sulfate and magnesium sulfate is no more than 5%. Sodium oxide is no more than 0.01% and the pH value should be 6–8.
Forestry	Planting trees, orchard	The terrain may have appropriate grade and the topsoil is needed. For planting trees, the topsoil is no less than 0.3 meter and the plant pit needs more than 1 meter. The isolated layer is needed if the filling material contains harmful elements. The thickness of the filling material is no less than 0.4 meter and filling material should be punning.
Fishery	Reservoir, fish-farming	The gradient of the shoreside should not be too steep. The area of the water should not be too large. The quality of the water should meet the water quality standard for fisheries.
Construction	Civilian, industry	The land needs to be punned well and the houses need antideformation measure.
Tourist	Stadium, park, swimming pool	The land needs to be punned well and the houses need antideformation measure.
Headwaters	Irrigation, drinking	The land needs to be punned well. The isolated layer is needed and its thickness is no less than 0.5 meter. In addition, cement to harden the surface is needed if necessary.

3. Engineering Study of Mine Land Reclamation

Since the mid-1980s, the reclamation technologies including gangue filling, flyash filling, and digging deep to fill shallow achieved success in Huaibei coal mine area. The Xuzhou coal mine also acquired the successful experiences in land formation, drainage, reducing immersing, and ecological engineering reclamation [22]. The other coal mines obtained technology experiences such as salt marsh governance, waste heap reclamation for afforestation, collapse pit for open mine, and building reclamation [23]. For example, the comprehensive treatment technology method study of subsidence reclamation in Huaibei coal mine, the mine land reclamation study in Tongshan county, and the study of waste heap reclamation in Hegang mining area.

The acquirement of all the above experience and achievement can be said to set the style for mine land reclamation in our country, making a pioneered contribution.

3.1. Land Formation and Gradient Technology. This technology is suitable for low water table mining areas or the middle-high water mining areas which are implemented with drainage and reducing immersing measures [24]. The following should be noticed in applying this method: the stripping and preserve of the topsoil, the determination of the elevation after land leveling, the determination of elements in the terrace section, the mating of the irrigation-drainage methods, and so forth.

As for the collapse areas without hydrops, the side of the ponding collapse and the collapse areas in hills, the reclamation methods of land formation and transformation into terrace or greenbelt are suitable for all. Slope-to-terrace sectional view is shown in Figure 1. Commonly, the additional gradient produced by mining subsidence is minor. The

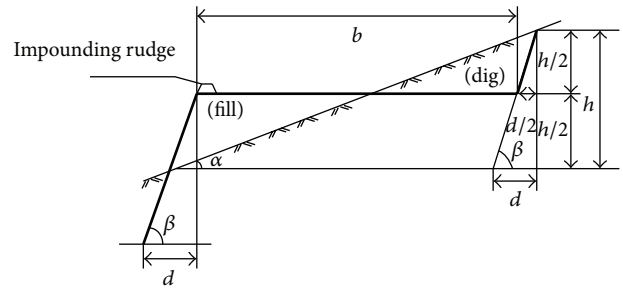

Figure 1: Slope-to-terrace sectional view.

collapsed ground with the slope gradient within 2° can be used for farming after land leveling. The collapsed ground with the slope gradient between 2°–6° can be transformed into terrace according to the topographic contour and it should be cambered inwards to dam up water for soil moisture. Adopting contour ploughing mode in farming is in favor of soil and water conservation.

3.2. Elevating Land-Reclamation Technology. The main stuffing in elevating reclamation includes gangue, fly ash, hydraulic clay, household refuse, industrial refuse, and out-soil backfill. The better choice of elevating reclamation is to use mud in pond, lake and river, industrial refuse, out-soil, and so on. The measure should be taken to prevent secondary pollution if the gangue, fly ash, and industrial refuse were used [25].

3.2.1. Gangue Filling Reclamation Technology. The approach of gangue filling reclamation technology is appropriate for all kinds of mining areas [26]. The gangue can not only act as the filling material to renew the destructive land, but

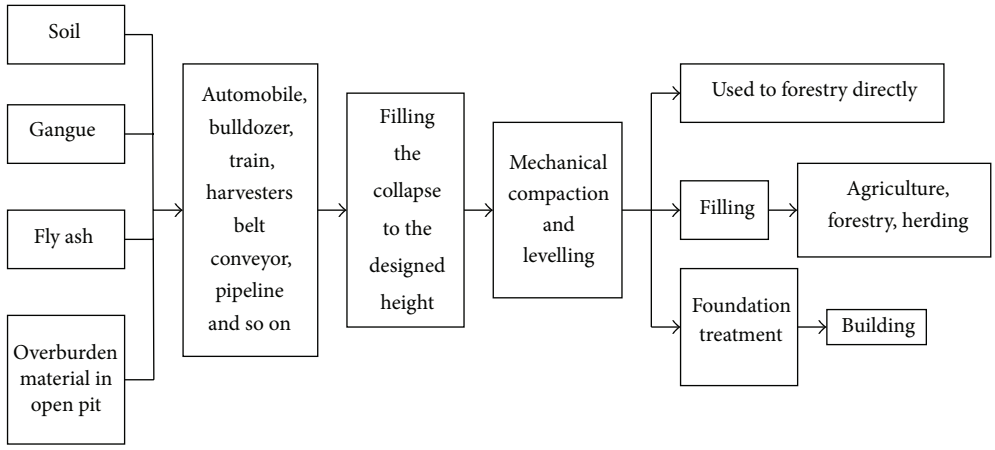

Figure 2: The industrial and mining area filling reclamation process flow diagram.

also can reduce the covering and pollution of gangue. The reclaimed land can be used for agricultural as well as building land.

The steps of gangue reclamation are as follows: in the stable subsidence areas, the superficial mellow soil should be peeled and stacked around at first, and then the gangue is filled. Once the filled gangue reaches horizontal, the mellow soil should be covered on the gangue, acting as plowing layer. Isolation treatment is required in the reclamation if the gangue is poisonous and harmful. Namely, lay the waterproof layer of clay in the collapse pit to prevent the drain of the poisonous and harmful material in gangue. The gangue can be set directly in the collapse for reclamation when the collapse is not taking shape or stable. That is, predict the areas to submerge and take out the topsoil to pile up around, and then set the gangue by the dumping equipment in advance according to the predicted subsidence depth and scope. Finally, cover the topsoil which is stacked all around on the gangue layer to backfill when the gangue is filled to the anticipated level.

For the gangue reclaimed land which is used for farming, the filled gangue should be dense at the bottom and loose at the upper part so as to conserve soil moisture and nutrient to facilitate plant growth. For the gangue reclaimed land which is used for building, the handling should be performed in accordance with demand.

The elevation of the land reclamation in collapse should be determined by the application, groundwater elevation, and flood elevation. Generally, the reclaimed elevation of the building land should be higher than the local flood elevation or the restored original elevation. With an eye on the decline of the surface and the water table after exploit, the reclaimed elevation of agriculture and forestry is always lower than the original elevation in order to facilitate the soil moisture, water and fertilizer preserving, as well as the growth of crops. Therefore, the reclaimed elevation of agriculture and forestry is decided by the water table in the reclamation area. If the reclaimed surface exceeds the elevation of the water table, it should be confirmed by the water logging tolerance of the crops.

The technological process of industrial and mining area filling reclamation is shown in Figure 2.

3.2.2. Drainage Reclamation Technology. In the diggings which are plain or have higher water table, the land surface subsidence is always accompanied by ponding or undischarged water, hindering cultivation. The surface ponding can be divided into two cases as follows.

(1) The flood level of the outside river is higher than the surface elevation, and thus the water in the collapse cannot drain out automatically. Filling reclamation or exhausting the ponding in the collapse can be applied to remould the areas for farming.

(2) The flood level of the outside river is lower than the surface elevation, and thus the water in the collapse can flow automatically. Now a suitable drain system is needed to automatically discharge the ponding in the collapse. In addition, if the groundwater table is overtop, draining channel is needed to lower the underwater level to guarantee the normal growth of the crops.

The key of the drainage reclamation is the design of the drainage system. Due to the integrality of the water, the situation of the whole mine or even the whole digging should be taken into consideration to form a comprehensive drainage system in designing the drainage system. Therefore, we should design the drainage system with a global idea.

Normally, the drainage system is made up of drainage ditch and impounding facility, drainage receiver outside the drainage area, and the drainage hub. The fixed channel of drainage ditch is divided into four levels according to the scope and effect of the discharge. The impounding facilities can be lake, swag, reservoir, and so on, and the drainage ditch can also be used for water impounding. The drainage receiver

is the so-called outside river. The drainage hub is referred to the drain valve, powerful drainage station, and so on.

3.2.3. The Utilization of Water Surface and Eco-Engineering Technology. The mining areas with high ground-water level have higher probability of hydrops, and thus the commercial and effective reclamation technology for these regions are to combine the utilization of water surface and ecological engineering. The significance of this technology manifested on one hand in that we need not to invest a huge sum of money on eliminate stagnant water and on the other hand in that the reserved water surface has great ecological value in maintaining the ecological balance of mining areas. For example, the collapse pit can be used for flood storage for irrigation. The water park has ornamental value and the scientific utilization of the water surface is able to acquire high economic benefit and so on [27].

It should be noticed in applying this technology that we should take advantage of the ecological engineering technology as much as possible to increase the production of the aquatic animals and plants, and thereby the production capacity of the waters and the productivity of the reclaimed land are improved.

3.3. The Dynamic Prereclamation Technology in Industrial and Mining Areas. This technology is mainly used to settle the problems of the reclamation in unstable collapse areas [28]. It is performed when the collapse is not complete and the hydrops has not formed. This technology designed according to the scale, scope, and goal of the reclamation is composed of two stages: the calculation of the engineering design and the implement of the engineering. The calculation of the engineering design includes the calculation of the expected deflection, the partition of the construction field, and the determination of the construction parameter. Compared to the commonly used technology "destruction first, government later," this technology has the following advantages: the dynamic prereclamation achieves the effective combination of mining and reclamation, reducing the reclamation input, shortening the reclamation cycle, augmenting the reclamation benefit, promoting the sustainable utilization of the land resource in mining areas, and achieving the sustainable development of the mine areas. All the advantages can effectively relieve vegetation deterioration in mining, ecological deterioration resulted from water loss, and soil erosion, protecting the land resources at the maximum level.

The dynamic prereclamation drawing is as shown in Figures 3 and 4.

3.4. The Technology for Combing Reclamation Measures with Mineral Engineering. The combing of reclamation measure and mineral engineering may take the following forms: the field with bad coal seam occurrence conditions and coal quality should take the local mining to reduce the damage to fertile farmland. Construct a reasonable system of discharging gangue to transport gangue directly to the collapse. Underground mining should make a good mining project (such as the mining sequence and mining area partition) to

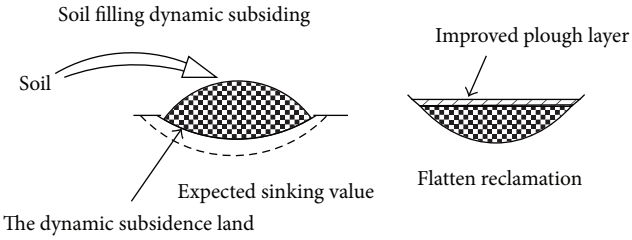

Figure 3: The dynamic prereclamation schematic diagram of soil backfilled collapse.

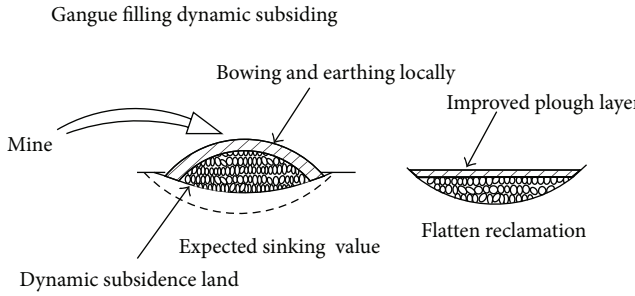

Figure 4: The dynamic prereclamation schematic diagram of gangue backfilled collapse.

reduce the loss on the floor. The opencast working should optimize the mining technology by casting mining to reduce the dumping coving and to do the reclamation for farming. The mining waste land should be used for coal mine capital construction as much as possible.

3.5. The Land Improvement and Utilization Technology following Reclamation. The primary mission of the biological reclamation is to improve the reclaimed soil and optimize the direction of land use. The method of improving the reclaimed soil should consider the forms and physicochemical property of the reclaimed soil, material, and technological conditions in diggings. Moreover, the methods should combine with planting strategies, too. The land-using technology not only includes the primary determination of the land utilization but also contains the planting plan and cultivation methods in recovery period of soil fertility.

The improvement measures for different reclaimed soil are displayed in Table 2.

4. The Comprehensive Model Study of Mine Land Reclamation

4.1. The Model of Gangue Filling Reclamation for Farmland in Mining Subsidence. In this model, the stowed discharge of gangue is transformed into pile up in stable collapse for filling reclamation, or to pile up in unstable collapse for prefilling reclamation. Finally, the agriculture is performed on it.

In this model the filled reclamation should be partitioned and reasonable, realizing divisional filling and divisional backfill cycle.

Table 2: The improvement measures for three typical reclaimed soils.

Reclaimed soil	Defect	Improved measures
Fly ash	Short of organic matter and nitrogenous fertilizer, bad field water performance, powerful heat absorptivity, fast heat, high pH value	Returning straw to field, rotation of green manure, the cooperation of organic and inorganic nitrogenous fertilizer, to transform pouring to sprinkling irrigation, laid straw interval, application of acid fertilizer
Mud	More clay particle, weak permeability, low content of organic matter	Returning straw to field, fly ash improvement, increment in humic and acid fertilizer
Rotten gangue	Low content of available water, strong endothermic character, fast heat, low content of nutrient element	Regular irrigation, keep a full stand of seedlings, laid straw interval, increment in humic and acid fertilizer

4.2. The Model of Fly Ash-Filling Reclamation and Eco-Reclamation in Subsidence Area. Now, the fly ash reclaimed land is mainly used for agroforestry planting. The covered earth should be over 0.3 meter at the thickness and the planted crops grow well [29]. Generally, the bore fruit on the land meets the demand of the sanitary standard. For the reclaimed land with higher fluorine, it should be used for cultivating trees which do not take part in the food cycle. With the comprehensive development of relocated pressing coal villages, more and more fly ash reclaimed land is used for resetting village foundation. In order to endow the fly ash reset village with long-term stability, we should study the fly ash processing technology actively [30]. We can predict that relocating the pressing coal village on the fly ash reclaimed land is going to be an important approach to settle the coal mining in village with high underground water level.

4.3. The Comprehensive Model of Agroforestry Reclamation in Nonponding Collapse. The nonponding collapse on plain has deep layers, fertile soil, and abundant ground water resources. Although the surface is rugged, the soil layer does not change significantly and the change in soil nutrition is small. The reclaimed land can restore the intrinsic value-in-use as long as we take engineering measures to level land and improve the water conservancy conditions. The specific engineering measures are (1) land leveling project, and (2) restore road, conservancy conditions, and agroforestry net.

The nonponding collapse in mountains and hills is usually reclaimed by land leveling, transforming into terrace or terrace green belt along the topographic contour. The key of the technology is the determination of the terrace section element, the determination of the land leveling elevation, the mating of the drainage and irrigation facilities, as well as the delamination peeling, deposit, and backfill of the topsoil.

4.4. The Reclamation Model of the Eco-Agriculture Overall Development in Shallow Ponding Collapse. The comprehensive development direction of the shallow ponding collapse is to make full use of the ponding conditions to develop fishing, turning the simple planting agriculture before collapse into an ecological agriculture combing planting and breeding [31].

The major measure is digging deep to fill shallow.

According to the food cycle theory in ecology in this model, many diggings allocate the agriculture, forestry, and herding reasonably, achieving the comprehensive operating for ecological agriculture. In this system, the crops and fodder can be used as feed for stock-raising. The feces of herding can be used as fish bait for aquaculture and also can be used as fertilizer for farmland directly. The pond sludge in fish pond is a good organic fertilizer. Ultimately, the multistage circulation utilization of the material is formed.

4.5. The Model of Developing Park Scenery Traveling Reclamation in Collapse. Generally the diggings are developed into mining cities of energy and heavy industry. The mining around is densely populated and residential quarters. Programming reasonably and investing to rest, afforest, and construct recreational facilities for the local collapse to become the place for recreation can not only improve life equality of people in mining but also expand the urban green area [32]. Therefore this model has great significance on improving local environment and biodiversity in mining area.

4.6. The Comprehensive Reclamation of Eco-Agriculture in Mining Subsidence. The subsidence of the diggings is the inevitable results of the impaired surface. Multidestruction forms appear on the surface, especially for the adverse effect for agricultural environment and the damage is also obvious. The comprehensive treatment for ecological agriculture in mining is not the simple reclamation but the integrated reclamation process of agriculture, forestry, herding, fishing, and processing industries. It is the combination and assembling according to ecology principle. It makes full use of the symbiotic relationship to allocate plant, animal, and microorganism reasonably to perform vertical farming and aquaculture reclamation. In terms of multilevel energy exploitation and circulating and regenerating mechanism, it is the recycle utilization of waste in agricultural industry, making the agricultural organic wastes to become resources and increasing products. It makes full use of modern science and technology to plan rational to achieve the unification of economy and social and ecological benefit [10]. Therefore, the comprehensive treatment of ecological agriculture in mining collapse is the key link in the comprehensive treatment of the whole mining area of ecological agriculture.

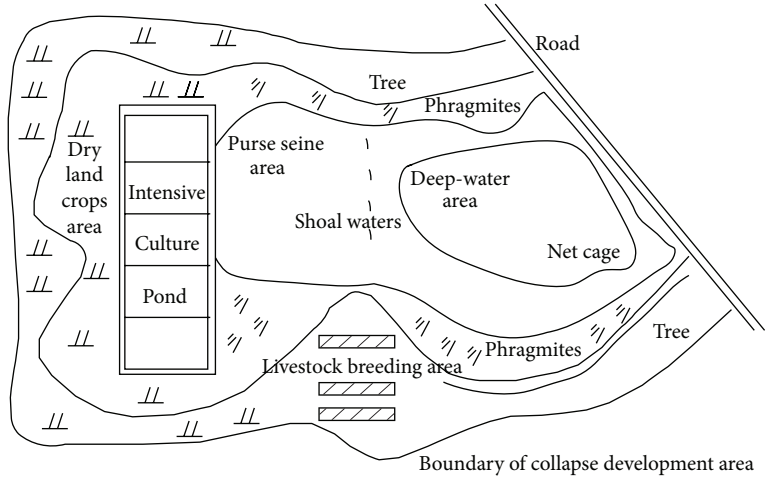

Figure 5: Example of graphic design for ecological agricultural reclamation in mining subsidence.

5. The Design and Model for Eco-Agricultural Reclamation in Mining Subsidence

5.1. The Design of Eco-Agricultural Reclamation in Mining Subsidence. The design of ecological agricultural reclamation in mining subsidence includes graphic design, vertical design, food chain design, time design, and engineering design [27]. In the graphic design and vertical design, it should be noticed that make full use of the specific terrain and land form produced by mining and realize the local hydrogeological and climate conditions to distribute rationally [33]. The spatial arrangement has to meet the requirements for light, heat, water, and air, living up to reasonable, effective, and economic. In the food chain design, we should keep away from the populations which can degrade harmful substance and the populations which do not absorb and enrich harmful substance [9]. In the time design, we should have a good standing of the local resources time rhythm following the ecological agriculture suitability analysis.

The graphic design for ecological agricultural reclamation in mining subsidence is to determine biotic population or ecotype and the proportion distributions occupied by the industrial in a certain reclamation area to achieve the optimal utilization of various resources in horizontal space.

The example of graphic design for ecological agricultural reclamation in mining subsidence is as shown in Figure 5.

5.2. The Model of Eco-Agricultural Reclamation in Mining Subsidence. The model of ecological agricultural reclamation in mining subsidence is a grade separation between time and space. It is a rational combination ecological agricultural reclamation system according to the mutually beneficial relationship between biology and ecology characteristic and biology [34].

Based on the biological form, habitat heterogeneity, and the numbers of abiological factors, the three-dimensional symbiosis of ecological agricultural reclamation can be divided into the following types and modes.

(1) The stereoscopic plantation type:

① the intercropping, interplanting, and rotation mode, such as grain-cotton, grain-oil, and grain-vegetable;

② the stereoscopic plantation mode of forest crops. With the different species, the combinations are different;

③ the stereoscopic plantation mode of tree-crop intercropping, such as paulownia-grain intercropping, jujube-grain intercropping, and fruit tree-vegetable intercropping;

④ the stereoscopic plantation mode of tree-medicine intercropping. It refers to the spatial organization of forest, fruiter, and pharmaceutical plant.

(2) The stereoscopic aquaculture type: the stereoscopic aquaculture means the hierarchical configuration of the farmed animals in a certain space or the integrate of products in a certain period of time. The dominate modes are as follows.

① The stereoscopic captive breeding mode on land: it is a stereoscopic aquaculture of interspace symbiosis so as to make full use of space, save material, and make use of waste. For example, bee barrel (upper layer)—hen house (middle layer)—pigsty (under layer)—earthworm (bottom layer).

② The stereoscopic aquaculture mode in water: it is a spatial configuration mode in order to make full use of space, nutrition, and dissolved oxygen in water. The usual combinations are chub (upper layer)—grass carp (middle layer)—black carp (under layer); duck (upper layer)—fish (middle layer)—oyster (under layer); fish (upper layer)—trionychidae (under layer).

(3) The stereoscopic cropping and raising as follows.

It refers to planting botany and farming animals in a certain space. It is to form a simple food chain among animals

Table 3: The suitable tree species and the standard of planting density in Shanxi.

Terrain	Chief species	Planting density (plant/mu)
Mountainous and hilly area	Larch, birch	220–330
	Picea meyeri, picea wilsonii, chinese pine, pinus armandi, pinus bungeana, fir, platycladus, oak	330–440
	Sumac	40–70
	Pecan	10–25
	Jujube	16–56
Basin and plain	Poplar, willow, catalpa	80–150
	Paulownia	40–70
	Elm, locust tree	220–330
Remarks	Species of pygmyism and minor, fit for growth in line spacing	

and is characterized by the symbiotic relationship among organisms. The upper plant offers concealment conditions and living environment for the animal and plant in under layer. The free-ranging creature in under layer is able to clear weeds and pests under the crops promoting the growth of upper plant. Meanwhile, the plant or animal waste in under layer provides bait for fish in bottom water, while the activities of fish increase the dissolved oxygen in water, promoting the permeability of plant roots. The dominate modes of this type are as follows: rice—duckweed—fish, rice—duck—fish, forest—livestock—earthworm, reed (as well as other swamp crops)—birds—fish, and so on.

Totally, the suitable tree species and the standard of planting density in Shanxi Province are summarized in Table 3.

Conflict of Interests

The authors declare that there is no conflict of interests regarding the publication of this paper.

Acknowledgments

The work in this paper has been supported by the Project supported by the National Key Technology R&D Program of China (Grant no. 2009BAB48B03) and the Project supported by Key Technology R&D Program of Shanxi Province, China (Grant no. 20121101009-03).

References

[1] X.-X. Miao and M.-G. Qian, "Research on green mining of coal resources in China: current status and future prospects," *Journal of Mining & Safety Engineering*, vol. 26, no. 1, pp. 1–14, 2009.

[2] M. Jiehua and X. Huilong, "China's coal resource distribution and perspective prediction," *Coal Geology and Exploration*, vol. 27, pp. 1–4, 1999.

[3] J. Zobrist, M. Sima, D. Dogaru et al., "Environmental and socioeconomic assessment of impacts by mining activities—a case study in the Certej River catchment, Western Carpathians, Romania," *Environmental Science and Pollution Research International*, vol. 16, no. 1, pp. 14–26, 2009.

[4] M. Balat, "Influence of coal as an energy source on environmental pollution," *Energy Sources A: Recovery, Utilization and Environmental Effects*, vol. 29, no. 7, pp. 581–589, 2007.

[5] J. Groninger, J. Skousen, P. Angel, C. Barton, J. Burger, and C. Zipper, *Mine Reclamation Practices to Enhance Forest Development through Natural Succession*, Forest Reclamation Advisory, 2007.

[6] X. Huang, M. Sillanpää, E. T. Gjessing, S. Peräniemi, and R. D. Vogt, "Environmental impact of mining activities on the surface water quality in Tibet: Gyama valley," *Science of the Total Environment*, vol. 408, no. 19, pp. 4177–4184, 2010.

[7] W. Yinghong, G. Dazhi, and Z. Hairong, "Spatial distribution and applications of coal resource potential in China," *Journal of Natural Resources*, vol. 21, pp. 225–231, 2006.

[8] S. Jiping, "Mine safety monitoring and control technology and system," *Coal Science and Technology*, vol. 38, pp. 1–4, 2010.

[9] Q. Ming-Gao, "Technological system and green mining concept," *Coal Science & Technology Magazine*, no. 4, pp. 1–3, 2003.

[10] M.-G. Qian, X.-X. Miao, and J.-I. Xu, "Green mining of coal resources harmonizing with environment," *Journal of China Coal Society*, vol. 32, no. 1, pp. 1–7, 2007.

[11] J. R. Pichtel, W. A. Dick, and P. Sutton, "Comparison of amendments and management practices for long-term reclamation of abandoned mine lands," *Journal of Environmental Quality*, vol. 23, no. 4, pp. 766–772, 1994.

[12] C. E. Zipper, J. A. Burger, J. G. Skousen et al., "Restoring forests and associated ecosystem services on appalachian coal surface mines," *Environmental Management*, vol. 47, no. 5, pp. 751–765, 2011.

[13] Q. Shi, Y. Lin, E. Zhang, H. Yan, and J. Zhan, "Impacts of cultivated land reclamation on the climate and grain production in Northeast China in the future 30 years," *Advances in Meteorology*, vol. 2013, Article ID 853098, 8 pages, 2013.

[14] M. J. Shipitalo and J. V. Bonta, "Impact of using paper mill sludge for surface-mine reclamation on runoff water quality and plant growth," *Journal of Environmental Quality*, vol. 37, no. 6, pp. 2351–2359, 2008.

[15] Z. Bang-Jun, "Land reclamation and environmental changes in Sichuan during the Qing dynasty: focusing on the problem of soil erosion," *Journal of Southwest Jiaotong University (Social Sciences)*, no. 3, pp. 87–92, 2006.

[16] J. A. Simmons, W. S. Currie, K. N. Eshleman et al., "Forest to reclaimed mine land use change leads to altered ecosystem structure and function," *Ecological Applications*, vol. 18, no. 1, pp. 104–118, 2008.

[17] J. Burger, D. Graves, P. Angel, V. Davis, and C. Zipper, "The forestry reclamation approach," *Forest Reclamation Advisory*, no. 2, 2005.

[18] P. N. Angel, J. A. Burger, V. M. Davis et al., "The forestry reclamation approach and the measure of its success in appalachia," in *Proceedings of the 26th Annual Meetings of the American Society of Mining and Reclamation and 11th Billings Land Reclamation Symposium (MT '09)*, pp. 18–36, Billings, June 2009.

[19] P. Breber, R. Povilanskas, and A. Armaitienė, "Recent evolution of fishery and land reclamation in Curonian and Lesina lagoons," *Hydrobiologia*, vol. 611, no. 1, pp. 105–114, 2008.

[20] C. R. Tamanini, A. C. V. Motta, C. V. Andreoli, and B. H. Doetzer, "Land reclamation recovery with the sewage sludge use," *Brazilian Archives of Biology and Technology*, vol. 51, no. 4, pp. 643–655, 2008.

[21] J. Wang, Y. Chen, X. Shao, Y. Zhang, and Y. Cao, "Land-use changes and policy dimension driving forces in China: present, trend and future," *Land Use Policy*, vol. 29, no. 4, pp. 737–749, 2012.

[22] F . Shan-Shan, C. Jiang, Y. Bo, and D. Zhong-Shu, "Re-use strategy of subsided land based on urban space ecological compensation: case study for Xuzhou mining area for example," *Procedia Earth and Planetary Science*, vol. 1, no. 1, pp. 982–988, 2009.

[23] J.-M. Nicolau, "Trends in relief design and construction in opencast mining reclamation," *Land Degradation & Development*, vol. 14, no. 2, pp. 215–226, 2003.

[24] JJ. Jiao, "Modification of regional groundwater regimes by land reclamation," *Hong Kong Geologist*, vol. 6, pp. 29–36, 2000.

[25] X.-M. Wang, B. Zhao, C.-S. Zhang, and Q.-L. Zhang, "Paste-like self-flowing transportation backfilling technology based on coal gangue," *Mining Science and Technology*, vol. 19, no. 2, pp. 137–143, 2009 (Chinese).

[26] X.-X. Miao and J.-X. Zhang, "Analysis of strata behavior in the process of coal mining by gangue backfilling," *Journal of Mining Safety Engineering*, vol. 45, no. 5, pp. 618–627, 2007.

[27] K. Krolikowska, A. Dunajski, P. Magnuszewski, and M. Sieczka, "Institutional and environmental issues in land reclamation systems maintenance," *Environmental Science and Policy*, vol. 12, no. 8, pp. 1137–1143, 2009.

[28] J.-X. Xu, G.-G. Li, G. Chen, and H. Zhao, "Dynamic changes and evaluation of land ecological quality in coal mining area," *Journal of the China Coal Society*, vol. 38, no. 1, pp. 180–186, 2013.

[29] J.-M. Xu, J.-X. Zhang, Y.-L. Huang, and F. Ju, "Experimental research on the compress deformation characteristic of waste-flyash and its application in backfilling fully mechanized coal mining technology," *Journal of Mining and Safety Engineering*, vol. 28, no. 1, pp. 158–162, 2011.

[30] Z. Hu, M. Zhang, B. Ma, P. Wang, and J. Kang, "Fly ash for control pollution of acid and heavy metals from coal refuse," *Journal of the China Coal Society*, vol. 34, no. 1, pp. 79–83, 2009.

[31] L. Fei and L. Lin, "Progress in the study of ecological restoration of coal mining subsidence areas," *Journal of Natural Resources*, vol. 4, article 007, 2009.

[32] F. López Gayarre, M. Alvarez-Fernández, C. González-Nicieza, A. Álvarez-Vigil, and G. Herrera García, "Forensic analysis of buildings affected by mining subsidence," *Engineering Failure Analysis*, vol. 17, no. 1, pp. 270–285, 2010.

[33] W. Yuehan, D. Kazhong, W. Kan, and G. Guangli, "On the dynamic mechanics model of mining subsidence," *Chinese Journal of Rock Mechanics and Engineering*, vol. 22, no. 3, pp. 352–357, 2003.

[34] Y. Xiaoyan, J. Changsheng, and W. Xiuli, "Ecological restoration and reconstruction of abandoned land in mines of China," *Express Information of Mining Industry*, vol. 10, article 10, pp. 22–24,48, 2008.

Hindawi Publishing Corporation
The Scientific World Journal
Volume 2014, Article ID 239279, 11 pages
http://dx.doi.org/10.1155/2014/239279

Research Article

Regulating N Application for Rice Yield and Sustainable Eco-Agro Development in the Upper Reaches of Yellow River Basin, China

Aiping Zhang,[1] Ruliang Liu,[2] Ji Gao,[1] Shiqi Yang,[1] and Zhe Chen[1]

[1] *Institute of Agro-Environment and Sustainable Development, CAAS/Key Laboratory of Agro-Environment and Climate Change, Ministry of Agriculture, Beijing 100081, China*
[2] *Ningxia Academy of Agriculture and Forestry Sciences, Ningxia 75000, China*

Correspondence should be addressed to Aiping Zhang; aipingzhang1980@163.com

Received 13 April 2014; Accepted 18 April 2014; Published 17 June 2014

Academic Editor: Hongbo Shao

High N fertilizer and flooding irrigation applied to rice on anthropogenic-alluvial soil often result in N leaching and low recovery of applied fertilizer N from the rice fields in Ningxia irrigation region in the upper reaches of the Yellow River, which threatens ecological environment, food security, and sustainable agricultural development. This paper reported the regulating N application for rice yield and sustainable Eco-Agro development in the upper reaches of Yellow River basin. The results showed that reducing and postponing N application could maintain crop yields while substantially reducing N leaching losses to the environment and improving the nitrogen use efficiency. Considering the high food production, the minimum environmental threat, and the low labor input, we suggested that regulating N application is an important measure to help sustainable agricultural development in this region.

1. Introduction

The large world population creates a huge demand for food. To meet the challenge, more grains must be produced which requires more chemical fertilizer nitrogen. From 1960 to 2000, the use of nitrogen fertilizers increased by 800%, with wheat, rice, and maize accounting for almost half of current fertilizer use [1]. At 81.7 million tons (Mt), chemical fertilizer nitrogen (N) accounts for approximately half of all N reaching global croplands today and supplies basic food needs for at least 40% of the population [2]. As the largest consumer of chemical N in the world, China accounts for 32% of the world's total consumption, and approximately 18% of the chemical N is applied to rice paddies [3]. However, the nitrogen use efficiency is typically below 40% with these crops, indicating that most applied fertilizer is either washed out of root zone, which will result in increased N losses as leachate to freshwater and marine systems [4–7].

Located in the upper reaches of the Yellow River, Ningxia Irrigation Region with an irrigation area of 9697 km^2 is one of the oldest and largest irrigation areas in northwest China and sustains over 60% of the Ningxia population. From 1980 to 2011, total annual grain production increased from 1.20 to 3.59 billion kg (an increase of 2.99 times), and chemical fertilizer application increased from 171,000 tons to 1033,000 tons (an increase of 6.04 times), of which chemical N fertilizer application was 533,000 tons [8] (Ningxia Statistical Yearbook, 2012). Ningxia Irrigation Region is located in the arid and semiarid zones, with the average annual precipitation of 180–220 mm, which is extremely lower compared to the 1000–1550 mm evaporation. The fertile alluvial soil is formed by accumulated sediments transferred by the Yellow River with abundant transboundary water about 32.5 billion m^3 in Ningxia segment annually. In this region, agriculture essentially relies on irrigation water. About 7 billion m^3 water from the Yellow River is drawn and 2.5 billion m^3 is returned annually [9] (Ningxia Water Source Bulletin, 2008). Over 93–95% of the water is used for agriculture. Rice is a major crop grown in the anthropogenic-alluvial soil and is often perceived as the largest water and fertilizer consumer in the basin. In the rice fields, the application rate of fertilizer is as high as 300 kg ha^{-1} due to flooding irrigation. Large amounts

of N fertilizer into the land will inevitably leach N into the water bodies, and thus becoming one of the nonpoint source pollution to the Yellow River.

Cui et al. [10] surveyed the water quality between the upstream station where the Yellow River flows in Ningxia boundary and the downstream station where Yellow River flows out Ningxia boundary during the 2005-2006. He estimated that N washed out from farmland into the Yellow River was 41.1 thousand tons, which is 1.52 times higher than those from the point source pollution during the same time period. de Data and Buresh [11] analyzed the correlation between N fertilizer application rates and total N contents of the river water and found that N contents in outboundary station in the downstream reaches coincidently increased with the N application rates in the Irrigation Region. Fixen and West [12] found that both total N and ammonium N contents were increasing significantly with the increase of fertilizer application rates, especially since 1990s in Ningxia segment of the Yellow River. Total N and ammonium N contents in water samples taken from the outboundary station were obviously higher than those from the upstream station. This clearly indicates the influence of fertilizer application in the Irrigation Region on the water quality of the Yellow River. Zhang et al. [13] also demonstrated that fertilizer and pesticide were the main nonpoint source pollutants of underground water.

Nitrogen leaching from agricultural soils can represent a substantial loss of fertilizer N and put pressure on the surrounding environment. Studies have already showed that N discharged into the Yellow River in Ningxia Irrigation Region was estimated to be 20–65% of the total N lost from the fertilizer [11], and the annual N loss from the rice field in Region was 28,865 tons [14]. The challenge is to continue to help meet food need while minimizing the risk of negative environmental impacts through improved N use efficiency [15–19].

In Ningxia, the pattern applying N fertilizer to a single-seasonal rice consists mostly of 50~70% base fertilization and 50~30% green-turning and tillering fertilization. Traditionally, farmers hold that topdressing additional N fertilizer in the booting stage would make for the fact that the paddy remains green when it is due to become yellow and ripe. The truth is that application of excessive base N fertilizer would not only make it hard to meet the demand of the currently prevailing high-yield breed of rice on nitrogen but also lead to more nitrogen loss from leaching because rice needs less N-nutrition for its growth before the jointing stage [20–23].

Therefore, there is a need for looking for optimizing N application amount and time that will improve N efficiency and reduce N leaching loss while maintaining rice yield. The objectives of this study were (1) to quantify the leaching amount of inorganic N during different rice growth stages as affected by RPN and (2) to estimate the effects of RPN on N use efficiency and rice yields (Table 3). We hope to recommend alternative N application techniques that will reduce N losses while maintaining crop yields.

2. Materials and Methods

2.1. Study Area. Our field experiment was conducted at Lingwu Farm (106°17′43 E, 38°07′14 N), in the upper reaches of the Yellow River basin during 2010 and 2011. In spite of the effort to promote water saving, farmers are following the old traditional way by blindly increasing the amount of chemical fertilizers, especially fertilizers N. The application rate of fertilizer N is as high as 300 kg ha^{-1}, which was found after a survey of 200 farmers on over 113 ha rice field. High input of N fertilizer causes out-of-proportion soil N, P, and K. The residual N can be stored in the soil as nitrate, which flows into the Yellow River or leaches into the groundwater with the irrigation water. The soil is classified as anthropogenic-alluvial soil, which is the main soil type of Ningxia Irrigation Region, with a soil texture of 18.25% clay, 53.76% silt, and 27.99% sand (Table 1). The soil fertility is at the mid to high yield levels with a high fertilizer application rate. Soil organic matter and total N concentrations in the tillage layer (0–30 cm) of soil profile are 13.97 g kg^{-1} and 0.98 g kg^{-1} irrigation drawn from the Yellow River. The soil bulk density of the tillage layer is 1.39 g cm^{-3}. Three main crop rotations occur in Ningxia Irrigation Region, namely, rice-wheat, summer maize-wheat, and rice-rice. Of these, large amount of N fertilizer has been applied into rice-rice system leach into the water bodies [16] and is therefore the focus of this study.

Beginning on June 11, the rice field remained submerged with flooding irrigation and irrigation was on August 28, putting in 1365 m^3 water per ha in 2010 and the precipitation is 130.9 mm (Figure 1). In 2011, beginning on May 20 and stopping irrigation on August 12 and thereafter the same as that of 2010, water per ha were put in the rice field and the precipitation is 171.1 mm during the rice-growing stage. Irrigation was mainly done during the early reproductive season from returning green to tillering and jointing-booting stages. About 80% of total irrigation water was applied before the rice heading stage. Less than 20% was used at flowering, booting, and mature stages.

2.2. The Field Experiment. The experiments were arranged in a randomized complete block design. The five fertilizer N treatments included (1) CK (No N fertilizer application treatment: 0 kg N ha^{-1}), (2) N300 (300 kg N·ha^{-1}, 50% used as base fertilizer, 25% as tillering fertilizer, and 25% as booting fertilizer), (3) N240 (240 kg N·ha^{-1}, 50% used as base fertilizer, 25% as tillering fertilizer, and 25% as booting fertilizer), (4) RPN I (240 kg N·ha^{-1}, divide the fertilizer into 3 equal amounts, each about 80 kg, used as base fertilizer, tillering fertilizer, and booting fertilizer), and (5) RPN II (240 kg N·ha^{-1}, divide the fertilizer into 4 equal amounts, each about 60 kg, used as base fertilizer, tillering fertilizer, booting fertilizer, and panicle fertilizer). The nitrogen fertilizer is urea which contains 46% N. In all of the treatments, phosphorus (90 kg P_2O_5 ha^{-1}) and potassium (90 kg K_2O ha^{-1}) fertilizers were ploughed into the soil tillage layer in one time before flooding the field as a basal fertilizer. The experiment design is shown in Table 2.

The rice cultivar for the 2-year experiment was 96D10. In 2010, rice seedlings were transplanted on June 14th, and the rice harvesting was on October 10th. In 2011, rice seedlings were transplanted on May 21th, and the rice harvesting was on September 21th. Each treatment had three replicates. Each

Table 1: Properties of the anthropogenic-alluvial soil in the study site.

Soil depths (cm)	Bulk density ($g \cdot kg^{-1}$)	Organic matter ($g \cdot kg^{-1}$)	Total N ($g \cdot kg^{-1}$)	Porosity (%)	Soil particle size (%)		
					Clay	Silt	Sand
0–15	1.35	15.21	0.98	44.25	18.25	53.76	27.99
15–30	1.43	13.07	0.99	42.04	17.33	51.07	26.59
30–45	1.55	10.12	0.86	40.71	17.70	52.15	25.74
45–60	1.59	8.30	0.73	42.07	28.04	67.71	4.26
60–90	1.50	5.56	0.34	44.82	12.11	31.96	55.93
90–100	1.52	4.48	0.31	43.72	15.96	42.05	42.00
100–120	1.48	3.55	0.25	45.28	6.41	26.93	66.67

Table 2: Reducing and postponing N application experiment design.

Treatments	Total N input (kg/hm^2)	N input/(kg/hm^2)			
		Base fertilizer	Tillering fertilizer	Booting fertilizer	Panicle fertilizer
CK	0	0	0	0	0
N300	300	150	75	75	0
N240	240	120	60	60	0
RPN I	240	80	80	80	0
RPN II	240	60	60	60	60

Note: basic fertilizer buried in soil preparation, top dressing application in surface water.

plot area was 60 m^2 and there were 15 plots in total. Trenches of 130 cm in depth were dug between the experimental plots. The field was mulched with plastic film, and double layers were installed to the inner side to prevent water interchange. Ditches and ridges were also dug. The whole experimental was separated by 2 m wide protection rows. Each treatment plot was irrigated separately, but equal amount of water was applied for all plots.

2.3. Sample Collection and Laboratory Analysis. During 2010 and 2011 seasons, soil water samples used for the leaching calculations were collected from lysimeters [24, 25]. Four PPR (polypropylene random) equilibrium-tension lysimeters (ETLs) (0.19 m^2) were installed at 1.2 m below the soil surface in each treatment. The regulated vacuum system was adjusted manually several times a week to provide suction that was slightly more negative than the matric potential recorded in the surrounding bulk soil with the heat dissipation sensors. The purpose was to avoid ponding above and bypass flow around the porous plate of the lysimeters to recreate as natural a drainage pattern as possible [25].

Leaching samples were collected 1, 3, 5, 7, and 9 days after transplanting and topdressing. The subsequent sampling was conducted at 7-day intervals. We collected water sample for 21 times in 2010 and 22 times in 2011. The water samples were transferred to a plastic tube and stored at 4°C until analysis in the laboratory. At maturity, plants were removed from the field to calculate the N use efficiency (NUE) and partial factor productivity (PFP).

The NUE is defined as the ratio of the crop N uptake to the total input of N fertilizer [26]. The PFP is the ratio of grain yield to the applied N rate [27]. They were calculated as below, respectively:

$$\mathrm{NUE} = \frac{\mathrm{N}_{\text{uptake with N application}} - \mathrm{N}_{\text{uptake without N application}}}{\mathrm{N}_{\text{applied}}} \times 100\%, \quad (1)$$

$$\mathrm{PFP} = \frac{Y}{\mathrm{N}_{\text{applied}}}, \quad (2)$$

where Y is grain yield, $kg \cdot ha^{-1}$, and $N_{applied}$ is the amount of N applied, kg ha^{-1}.

The N leaching loss during the rice grow stage was calculated using the following formula [25]:

$$Q_n = C_n Q_w. \quad (3)$$

Here, C_n is the N concentration (TN, NH_4^+, and NO_3^-) from leaching water collected from lysimeter in the different rice growing stage, kg N m^{-3}; Q_w is the quantity of leaching water in the corresponding stage collected from lysimeter, $m^3 \cdot ha^{-1}$; and Q_n is the quantity of N leaching loss, kg ha^{-1}.

Total N content of soil and rice plants was calculated by using the Kjeldahl N method, total P content using Mo-Sb colorimetric method, and total K content using flame photometry. The total N concentration of soil water sample was determined by Persulfate-UV spectrophotometry [28], and the concentrations of NH_4^+ and NO_3^- were measured by flow injection analysis (FIA) made in France. One-way

Table 3: Effect of RPN on rice yield and its components.

Year	Treatment	Panicle length (cm)	Panicle number	Grain number per panicle ($\times 10^4 \cdot ha^{-1}$)	1000 grain weight (g)	Average yield (kg/hm^2)	Increased yield (kg/hm^2)	Ratio (%)
2010	CK	16.2 b	112 c	76.7 c	25.7 a	3990 b	—	—
	N300	16.5 b	169 a	109.3 a	21.9 b	9634 a	5644	141.5
	N240	19.0 a	141 b	98.6 b	22.0 b	9631 a	5641	141.4
	RPN I	19.5 a	152 ab	105.7 a	22.8 ab	10326 a	6336	158.8
	RPN II	19.0 a	148 b	92.5 b	23.4 a	10727 a	6737	168.8
2011	CK	12.1 b	105 b	71.8 c	26.1 a	3366 b	—	—
	N300	15.4 a	147 a	111.8 a	23.7 b	8676 a	5310	157.8
	N240	15.0 a	138 a	106.4 a	23.9 b	8498 a	5132	152.5
	RPN I	15.1 a	145 a	109.7 a	24.8 a	8778 a	5412	160.8
	RPN II	14.8 a	138 a	99.4 b	24.1 ab	8612 a	5246	155.9

Figures followed by the same letters within a column for different treatments are not significantly different at the significance level $P < 0.05$ based on one-way analysis of variance (ANOVA).

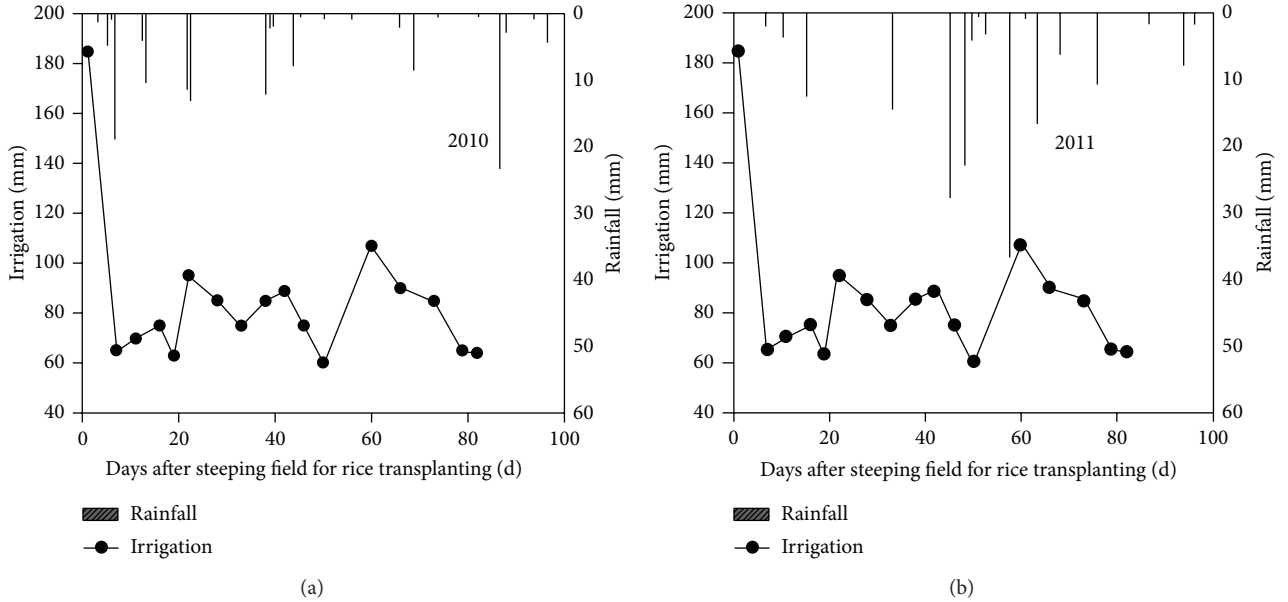

Figure 1: Precipitation and irrigation amount during whole growth period of rice.

analysis of variance (ANOVA) at $\alpha = 0.05$ probability was conducted to test the significance in different treatments. All statistiN300l analyses were performed using statistiN300l analysis System (SAS) General Linear Model procedures [29].

3. Results

3.1. Effects of Reducing and Postponing N Application on Rice Yield and Its Components. All N treatments could significantly improve rice yield compared with CK (Table 2). In 2010, the highest yield was from RPN II, which was 6737 kg/hm^2 higher than that of CK, and then RPN I. In 2011, the highest yield was from the field of RPN I treatment, which were 5412 kg/hm^2 higher than CK. There was no significant different between all of the N treatments in both 2010 and 2011. This indicated the nitrogen fertilizer application level of N240 kg $N \cdot ha^{-1}$ can allow current N application rates to reduce by 20% while still maintain crop yields. Because of the continuous rainfall of more than 10 days in middle and late September 2011 in Ningxia Irrigation Area, the weather was cooler than usual and rice yield reduced by about 20% in the whole irrigation area compared to the normal years, and thus the rice yield of all treatments was lower than in 2010.

The rice yield is composed of spikes number per unit area, grain number per spike, and thousand kernel weights. In 2010 and 2011, the panicles of all N treatments were higher than that of CK, but there was no significant difference among other N treatments except N300 in 2010. The grain number per panicle showed an increasing trend with N levels as follows: N300 > RPN I > N240 > RPN II > CK. The grain

Table 4: Total N accumulative leaching at rice growth stages (kg·ha^{-1}).

Year	Treatment	Growth stage						
		Seedling stage	Tillering stage	Booting stage	Flowering stage	Heading stage	Harvest stage	Sum
2010	CK	1.58 d	5.11 d	2.76 b	2.42 c	1.22 c	0.50 c	13.60 d
	N300	11.24 a	19.31 a	8.45 a	3.15 b	1.47 c	0.89 bc	44.51 a
	N240	8.24 b	13.98 b	7.42 a	2.98 bc	1.12 c	0.45 c	34.19 b
	RPN I	5.14 c	10.34 c	8.16 a	3.35 b	2.47 b	1.32 b	30.78 c
	RPN II	5.22 c	7.96 c	8.24 a	4.14 a	3.72 a	2.04 a	31.32 bc
2011	CK	1.07 d	3.45 e	1.87 d	1.64 d	0.82 e	0.34 d	9.19 d
	N300	8.96 a	17.45 a	6.86 a	3.25 b	1.97 c	1.31 b	39.8 a
	N240	6.03 b	14.47 b	5.56 b	2.47 c	1.43 d	0.62 c	30.58 b
	RPN I	3.42 c	8.91 c	4.67 c	3.87 a	3.12 b	1.36 b	25.35 c
	RPN II	3.08 c	6.74 d	6.52 a	4.07 a	4.94 a	2.36 a	27.71 bc

numbers per panicle of N300 treatment and RPN I treatment were significantly higher than those of the CK and RPN II treatments. With regard to differences among treatments, CK and RPN had the higher thousand grain weight while N300 and N240 had the lower.

3.2. Effects of Reducing and Postponing N Application on N Leaching Losses. High N fertilizer and irrigation amounts applied to rice on anthropogenic-alluvial soil often result in severe nitrogen loss from leaching. There is a significant correlation between N leaching losses and the N application amount. During the whole rice growing period, in each treatment, the TN leaching loss increased as the N fertilizer application amount goes up (Table 4). The total N leaching loss was 13.60 kg/hm^2 and 9.19 kg/hm^2 under CK treatment in 2010 and 2011, while it was 44.51 and 39.8 kg·ha^{-1} under the N300 treatment, respectively. The results from the two-year experiment showed that TN leaching loss under the N300 treatment was the highest and then the N240 treatment. The total N leaching loss under the RPN I treatment was substantially lower than that under N300 and N240, but there was no significant difference with RPN II. In 2010, total N leaching loss of RPN I and RPN II treatment were 30.78 and 31.32 kg·ha^{-1}, 30.85% and 29.63% lower than the N300 treatment. In 2011, total N leaching loss of RPN I and RPN II treatment were 25.53 and 27.71 kg·ha^{-1}, 36.31% and 30.38% lower than N300 treatment. These results indicated that RPN treatments can significantly reduce TN leaching loss. Net total N leaching loss of N fertilizers under N300, N240, RPN I, and RPN II was 30.91, 20.59, 16.18, and 17.72 kg/hm^2 in 2010 and 30.61, 21.39, 16.16, and 18.52 kg/hm^2 in 2011. The two-year average leaching loss of total N accounted for 10.3%, 8.75%, 6.74%, and 7.48% of applied N fertilizer.

The main leaching period of total N was delayed under the RPN treatments. Total N leaching loss under CK, N300, and N240 treatment mainly happened in the tillering stage while that of RPN I and RPN II treatments mainly happened from tillering stage to booting stage. The tillering stage was the main stage for total N leaching loss that might be due to two reasons, firstly, the higher irrigation volume at this stage for promoting tillering [30]. In addition, during this period, the basal and top dressing N inputs accounted for 50%–75% of the entire growth period with flood irrigation, which resulted in a huge leaching loss of total N.

Nitrogen loss by leaching is the major problem in rice field. Under normal conditions, soil N is leached mainly as nitrate-N (NO_3^--N) which forms a major contaminant of ground water. The NO_3^--N leaching losses under N300 treatment during rice growing stage were higher those that of other treatments during 2010 and 2011. The NO_3^--N leaching loss of different treatments shared the same changing trend with the total N, N300 > N240 > RPN II > RPN I > CK (Table 5). The majority of leaching losses of NO_3^--N under N300 and N240 treatment occurred during seedling stage and tillering stage and then booting stage while those of the RPN treatments occurred during tillering stage and booting stage and then seedling stage. The NO_3^--N leaching losses of all nitrogen treatments reached the peak at tillering stage, accounting for 33.6–43.4% and 35.1–47.3% of the total loss during the rice growing stages in 2010 and 2011, respectively. The NO_3^--N leaching losses of CK also mainly occurred in tillering stage, accounting for 25.4% in 2010 and 24.3% in 2011 of the total NO_3^--N loss. In 2010, 35.49 and 22.08 kg NO_3^--N ha^{-1} (representing about 79.7% and 71.7% of the TN leaching losses) leached below the root zone in N300 and RPN I, respectively. Thus, RPN I reduced the NO_3^--N leaching loss by about 37.8% compared to N300. In 2011, 30.02 and 19.63 kg NO_3^--N ha^{-1} (representing about 75.4% and 70.84% of the TN leaching losses) leached out of the root zone in N300 and RPN I, respectively. In this year, RPN I reduced NO_3^--N leaching losses by about 34.6% compared to N300.

Nitrogen can also be lost as NH_4^+-N, but the quantity is very small compared to NO_3^--N. The NH_4^+-N losses ranked from greatest to smallest were N300 > N240 > RPN II > RPN I > CK. The major stages of NH_4^+-N leaching losses (Table 6) were similar to the stage of NO_3^--N. Under N300 treatment, 3.58 and 3.21 kg NH_4^+-N ha^{-1} (representing about 8.04% and 8.07% of the TN leaching losses) leached below the root zone in 2010 and 2011, respectively. In RPN I, 2.76 and 2.94 kg NH_4^+-N ha^{-1} (representing about 12.5% and 14.9% of the TN leaching losses) leached out of the root zone in 2010 and 2011, respectively. From the two-year average results, RPN I

Table 5: NO_3^--N accumulative leaching at rice growth stages (kg·ha^{-1}).

Year	Treatment	Growth stage						
		Seedling stage	Tillering stage	Booting stage	Flowering stage	Heading stage	Harvest stage	Sum
2010	CK	1.52 d	5.31 d	1.34 c	0.56 d	0.22 d	0.09 e	9.04 d
	N300	9.03 a	15.74 a	6.37 a	2.82 b	1.07 c	0.53 c	35.49 a
	N240	6.02 b	10.97 b	5.48 b	2.21 c	0.84 c	0.29 d	25.81 b
	RPN I	3.92 c	8.12 c	5.21 b	1.94 c	1.87 b	1.02 b	22.08 c
	RPN II	3.62 c	6.12 d	6.35 a	3.41 a	2.54 a	1.21 a	23.25 bc
2011	CK	0.81 d	2.12 e	1.45 d	1.28 e	0.52 d	0.17 d	6.35 d
	N300	7.02 a	12.84 a	5.21 a	2.52 c	1.45 c	0.98 b	30.02 a
	N240	4.83 b	10.84 b	4.76 ab	1.83 d	1.12 c	0.35 c	23.73 b
	RPN I	2.73 c	7.08 c	3.61 c	3.23 b	2.14 b	0.84 b	19.63 c
	RPN II	2.47 c	5.21 d	4.38 b	4.98 a	3.67 a	1.69 a	22.4 b

Table 6: NH_4^+-N accumulative leaching at rice growth stages (kg·ha^{-1}).

Year	Treatment	Growth stage						
		Seedling stage	Tillering stage	Jointing stage	Flowering stage	Heading stage	Harvest stage	Sum
2010	CK	0.15 a	0.35 c	0.15 d	0.11 c	0.26 b	0.06 d	1.09 c
	N300	0.18 a	1.09 a	0.77 a	0.53 a	0.67 a	0.34 b	3.58 a
	N240	0.14	1.23 a	0.71 ab	0.27 b	0.23 b	0.28 c	2.86 b
	RPN I	0.14 a	0.82 b	0.62 b	0.25 b	0.62 a	0.31 bc	2.76 b
	RPN II	0.13 a	0.84 b	0.41 c	0.43 a	0.57 a	0.43 a	2.81 b
2011	CK	0.08 c	0.23 d	0.17 c	0.12 d	0.16 d	0.08 d	0.84 b
	N300	0.18 a	1.27 a	0.65 ab	0.44 b	0.48 c	0.19 b	3.21 a
	N240	0.17 a	1.12 a	0.68 ab	0.32 c	0.72 b	0.14 c	3.15 a
	RPN I	0.15 ab	0.89 b	0.71 a	0.34 bc	0.64 b	0.21 b	2.94 a
	RPN II	0.10 c	0.64 c	0.51 b	0.62 a	0.81 a	0.36 a	3.04 a

reduced the NH_4^+-N leaching loss by about 16.1% compared to N300. There were no significant differences of the NH_4^+-N leaching losses at the N-fertilization level of 240 kg/hm^2. Our results indicated that the NH_4^+-N leaching losses contributed very little to the total N leaching losses during rice growth stage.

3.3. Effects of Reducing and Postponing N Application on N Use Efficiency. Under the conditions applied in this experiment, when more N fertilizer is applied the upper soil absorbs more nitrogen but N fertilizer uses efficiency drops with increasing applied quantity of N fertilizer, and the result from two-year experiment is consistent (Table 7). Compared with CK treatment, N fertilizer application can help the rice grains and stems to absorb more nitrogen though the N fertilizer use efficiency declines with rising quantity of N fertilizer applied. The two-year average use efficiency of N fertilizer treated with N300 is merely 32.0%, and that of N fertilizer treated with N240, RPN I, and RPN II is 36.8%, 40.0%, and 39.6%, respectively, among which that of N fertilizer treated with RPN I and RPN II is higher than that with N300 by 8.0 and 7.6 percentages, and RPN I results in the highest use efficiency, 8% higher than what N300 treatment results in.

As the N applied rate increased, there was a decrease in PFP. The absolute values for PFP were higher in 2010 compared to in 2011 at all the levels of N application. The RPN I treatment had highest PFP while the N300 had the lowest both in 2010 and 2011. There was no significant difference of PFP among N240, RPN I, and RPN II. The PFP of RPN I was 20.94% and 25.38% higher than that of N300 in 2010 and 2011, respectively.

4. Discussions

Nitrogen loss by leaching is the major problem in rice field. Under normal conditions, soil N is leached mainly as NO_3^--N which forms a major contaminant of ground water. Nitrogen can also be lost as NH_4^+-N, but the quantity is very small compared to the former one. A study by Yun et al. [31] revealed that N loss by leaching was not so pronounced in arid and semiarid soil, but it could be 20 to 30 kg ha^{-1} in the wet temperate zone or as high as 50 kg ha^{-1} in Europe and middle states of USA. Nitrogen enters a unique environment in anthropogenic-alluvial soil, in which losses of fertilizer N and mechanisms of losses vary greatly from those in upland situations. The study showed that the N lost was 152 to 155 kg ha^{-1}, of which N lost by leaching was 78 kg ha^{-1} under the conventional fertilizer rate of 300 kg ha^{-1} [32]. It is higher than our 2-year average results of 42.16 kg ha^{-1}. With the excessive application amount of fertilizer N during the

Table 7: Effects of RPN on NUE and PFP.

Year	Treatment	Straw N uptake (kg/hm^2)	Grain N uptake (kg/hm^2)	Total N uptake (kg/hm^2)	NUE (%)	PFP (kg grain kg^{-1}N)
2010	CK	37.0	43.5	80.5 b	—	—
	N300	62.2	113.3	175.5 a	31.7 b	32.11 b
	N240	61.8	108.3	170.1 a	37.3 a	40.13 a
	RPN I	63.2	114.6	177.8 a	40.5 a	43.03 a
	RPN II	68.7	110.4	179.1 a	41.1 a	44.7 a
2011	CK	16.2	37.4	53.6 b	—	—
	N300	54.3	95.8	150.1 a	32.2 b	28.92 b
	N240	50.4	90.2	140.6 a	36.3 a	35.41 a
	RPN I	53.6	94.8	148.4 a	39.5 a	36.58 a
	RPN II	49.5	95.3	144.8 a	38.0 a	35.88 a

flooding irrigation, NO_3^--N leaching was most prevalent in the rice filed of the study area. Our results showed that the 2-year average NO_3^--N leaching loss under the fertilizer rate of 300 kg ha^{-1} accounted for 77.54% of the total N loss. As SAS Institute [33] stated, a close relationship existed between the amount of NO_3^--N leached and the amount of fertilizer N used in most cases. The treatment of N240, which is still higher than that for the currently grown rice cultivars in the United States, ranging from 134 to 202 kg ha^{-1} [29–31, 34–38], would maintain crop yields while substantially reducing N losses to the environment [39–42].

In Ningxia Irrigation Region, there appeared a large quantity of nitrogen leaching loss at the early stage of rice growth due to excessive N fertilizer application, improper timing of topdressing and, heavier irrigation early on. Irrigation was mainly done during the early reproductive season, and the base fertilizer and the tillering fertilizer that were applied just after about 10 days of rice seedling accounted for 80% of total N fertilizer throughout the rice growth stage; large amount of N fertilizer with flood irrigation led to massive nitrogen leaching loss [43, 44]. In the RPN I and RPN II treatments, the N fertilizer was divided into three and four equal parts and applied in three or four times; however, the resulting rice yield was similar to those with the traditional N fertilizer application and N300 treatment used by farmers, while less quantity of N fertilizer was applied at the early stage of rice growth, obviating the peak period of leaching. This led not only to increased N fertilizer use efficiency but also to reduced nitrogen leaching loss. Liu et al. [22] discovered from his study that with RPN technology, even under the condition that the quantity of N fertilizer used was 30% less compared to traditional farming, the corn yield, the surface dry matter accumulation, and N accumulation rate did not drop, and N fertilizer use efficiency rose significantly instead [20]. In this way the supply of inorganic nitrogen kept pace with crop absorption and accumulation of inorganic nitrogen in soil in the depth up to 100 cm reduced to a considerable degree, thus the field apparent loss of nitrogen mitigated. Li et al. [20] found in her investigation that, even under the condition that the quantity of N fertilizer was used 30% less than used in traditional farming, RPN did not lead to reduced wheat yield, but increased N fertilizer use efficiency with extremely low nitrogen apparent loss and enabled increasing nitrate-N's accumulation in soil in the depth 0~20 cm and reducing its accumulation in soil in the depth 20~80 cm [21]. Many researches indicated that excessive quantity of N fertilizer application, unsynchronization of demand and supply, and improper fertilization pattern are main cause of low N fertilizer use efficiency [30, 34, 35]. In this study, under the RPN I and RPN II treatment, part of nitrogen fertilizer was postponed, which maintained the sufficient supply of nitrogen need at the later stage of rice growth, and thus the rice yield remained basically unchanged when using 20% less nitrogen fertilizer. This indicated that the RPN worked to synchronize the nutrition supply and crop absorption and improved both the yield and N use efficiency. The result was consistent with Yi's research [36].

Excess application of N on the field is one of the major factors of N leaching. The amount of N leached and the amount of fertilizer N used showed a close relationship [33]. The N leaching amount is in linear relationship with the fertilizer application rate ($P < 0.05$) (Figure 2). The soil texture and irrigation practice are considered other major factors of N leaching, especially in flooded irrigation area. With the excessive amount of fertilizer N application during the flooding irrigation, large amounts of N fertilizer into the land will inevitably leach N into the water bodies, and thus becoming one of the nonpoint source pollution to the Yellow River. There were about 28,500 tons of NO_3^--N, 5,500 tons of NH_4^+-N, and 41,100 tons of TN that were lost every year due to leaching in Ningxia irrigation region. In the conditions of this experiment, total nitrogen leaching loss was 6.7%~10.3% of total N fertilizer applied and treated with various methods and the leaching is mainly in the form of NO_3^--N which accounts for more than 80% in TN loss, which is consistent with the results from previous researches [14, 37]. For comparison, on the south of the Yangtze River, the predominant soil types in rice field are the yellow mud soil, red loam soil, and red purple soil. When N fertilizer was applied at a rate of 300 kg ha^{-1}, no leaching of NO_3^--N was found in the paddy field during rice growing season [38]. However in the Ningxia irrigation zone, a total of 18–23 times

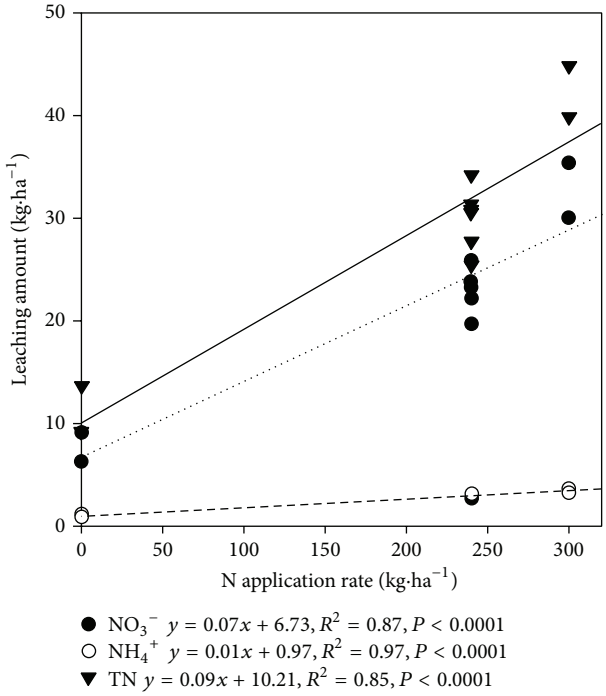

Figure 2: Linear regression relationships between N application rate and leaching amount of TN, NO_3^- and NH_4^+.

and about 1400–1600 m^3 water per ha was put into the rice filed during the rice growing season, and the soil in the study site has a high silt percentage of 53.76%. NO_3^--N leaching was most prevalent on sandy soils that received heavy irrigation. It has been shown that NO_3^--N may travel with gravitational water that moves quickly down these holes during heavy flooding [33]. Zhang et al. [45] reported in their literature review that nitrate leaching was most prevalent on sandy soils that received heavy irrigation. Zhao et al. [46] reported in their literature review that irrigation practices would possibly overwhelm any recommended fertilizer application rates.

High N fertilizer and irrigation amounts applied to rice on sandy soils often result in N leaching and low use efficiency of applied fertilizer N. The RPN I treatment could allow current N use efficiency to increase. Fertilizer N use efficiency of irrigated rice is relatively low due to rapid losses of applied N through volatilization and denitrification in the soil-flood-water system [47–49]. In this 2-year study, the average N use efficiency under N300 treatment was 31.95%. The average N utilization rate reached 40.0% for RPN I treatment, which greatly reduced the amount of N fertilizer and increased the N use efficiency. It not only saved fertilizer resources, but also effectively reduced other forms of N losses. Compared with N300 treatment, RPN I could reduce 20% N application and 34.61% TN leaching loss while the yield did not significantly reduce. de Datta and Buresh [50] reported that proper timing and rate of N applications are crucial to minimize N losses [27, 28, 32, 33, 39, 40]. RPN could reduce N leaching loss because less N fertilizer was used in the early stage of rice growth and thus reduces the level of N fertilizer in the leaching solution. Because the base fertilizer, if applied excessively at one time, would accumulate nitrogen in soil and because rice needs less nitrogen at the early stage, there is great possibility for nitrogen leaching with heavy irrigation to begin [51–53]. In the later stage of rice growth when N fertilizer was applied, its root system has developed its ability to absorb more nitrogen that will cause the nitrogen concentration in the leaching solution to decline. It improved the congruence between crop N demand and the available N supply from soil and applied fertilizer, and thus increased the N use efficiency [54, 55]. The result is accordance with Cassman's report [56]. It was generally believed that under planting conditions of lower N levels (e.g., 150 kg·ha^{-1}), the N use efficiency could be significantly improved [57]. Shi et al. [58] found that after rice flowering, while N application was higher than 200 kg·ha^{-1}, the N translocation rate and fertilizer use efficiency would reduce with the increase of N application. High input but low utilization efficiency of chemical fertilizer N also resulted in a decrease in partial factor productivity [59, 60]. The low efficiency of fertilizer use suggests that N was not the only major limiting resource in this Region. Management interventions, particularly those that address competitive water, will likely be critical to the success of this system. A combination of careful irrigation and N management needs to be studied to improve N uptake efficiency and to minimize fertilizer N loss.

5. Conclusions

Achieving synchrony between N supply and crop demand without excess or deficiency is the key to optimizing tradeoffs between yield and environmental protection. The RPN I can allows current N application rates to reduce by 20% and maintain crop yields. This would significantly improve the N use efficient and thereby substantially reduce the N leaching loss.

Optimization of fertilizer application gave chance to increase nitrogen use efficiency while the rice yield was maintained. In the condition of optimized fertilizer application (nitrogen applied reduced by 20%), rice yield under RPN treatment did not decline compared with traditional fertilizer application (N300 treatment), and the two-year average yield of rice under RPN I treatment was 397 kg/hm^2 higher than that of under N300. The average use efficiency of N300 treatment was 32.0% while the N240, RPN I, and RPN II were 36.8%, 40.0%, and 39.6%, respectively, among which RPN I treatment delivered the maximal use efficiency, 8% higher than N300 treatment.

RPN made it possible to drop nitrogen leaching loss at paddies in the irrigation region significantly. The two-year average net TN leaching loss under N300, N240, RPN I, and RPN II were 10.3%, 8.75%, 6.74%, and 7.48% of total N fertilizer applied, respectively. RPN I treatment had the minimal TN leaching loss, at 16.17 kg/hm^2, 14.64 kg/hm^2 less than N300 treatment. The two-year average NH_4^+-N leaching loss due to various treatments were 7.9%, 10.15%, 11.63%, and 10.82% and this suggested that NH_4^+-N was not the major nitrogen leaching loss; NO_3^--N leaching loss accounted for more than 80% in TN leaching loss, regardless of the treatment. RPN I can give the same yields and lead to using

less nitrogen fertilizer by 20% while it did not increase labor intensity, and thus it is one way to continue to help meet food need while minimizing the risk of negative environmental impacts. Considering the high food production, the minimum environmental threat, and the low labor intensive, we should fully take into account the RPN I by reducing fertilizer N inputs and N leaching loss. Since irrigation regimes have remarkable affects fertilizers uptake, the interaction between irrigation management and N application rate on N use efficiency in alkaline anthropogenic-alluvial soil is needed to be further studeied.

Conflict of Interests

There is no conflict regarding the publication of the paper.

Authors' Contribution

Aiping Zhang and Ruliang Liu contributed equally to this work and should be considered co-first authors.

Acknowledgments

The paper has been supported by Special Foundation for Basic Scientific Research of Central Public Welfare Institute (BSRF201306) and Innovation Capital of Agricultural Clean Watershed.

References

[1] S. D. Bao, *Soil and Agricultural Chemistry Analysis*, China Agriculture Press, Beijing, China, 2000.

[2] L. Bergstrom, "Use of lysimeters to estimate leaching of pesticides in agricultural soils," *Environmental Pollution*, vol. 67, no. 4, pp. 325–347, 1990.

[3] K. R. Brye, J. M. Norman, L. G. Bundy, and S. T. Gower, "An equilibrium tension lysimeter for measuring drainage through soil," *Soil Science Society of America Journal*, vol. 63, no. 3, pp. 536–543, 1999.

[4] N. R. Burgos, R. J. Norman, D. R. Gealy, and H. Black, "Competitive N uptake between rice and weedy rice," *Field Crops Research*, vol. 99, no. 2-3, pp. 96–105, 2006.

[5] D. E. Canfield, A. N. Glazer, and P. G. Falkowski, "The evolution and future of earth's nitrogen cycle," *Science*, vol. 330, no. 6001, pp. 192–196, 2010.

[6] X. M. Cao and H. Liu, "Quality analysis of groundwater in Ningxia," *Ningxia Engineering and Technology*, vol. 3, pp. 385–388, 2004.

[7] K. G. Cassman, M. J. Kropff, and Z. D. Yan, "A conceptual framework for nitrogen management of irrigated rice in high-yield environments," in *Hybrid Rice Technology: New Developments and Future Prospects*, pp. 81–96, 1994.

[8] K. G. Cassman, S. K. de Datta, S. T. Amarante, S. P. Liboon, M. I. Samson, and M. A. Dizon, "Long-term comparison of the agronomic efficiency and residual benefits of organic and inorganic nitrogen sources for tropical lowland rice," *Experimental Agriculture*, vol. 32, no. 4, pp. 427–444, 1996.

[9] Y. Conrad and N. Fohrer, "Modelling of nitrogen leaching under a complex winter wheat and red clover crop rotation in a drained agricultural field," *Physics and Chemistry of the Earth*, vol. 34, no. 8-9, pp. 530–540, 2009.

[10] Z. Cui, F. Zhang, X. Chen et al., "On-farm estimation of indigenous nitrogen supply for site-specific nitrogen management in the North China plain," *Nutrient Cycling in Agroecosystems*, vol. 81, no. 1, pp. 37–47, 2008.

[11] S. K. de Datta and R. J. Buresh, "Integrated nitrogen management in irrigated rice," in *Advances in Soil Science*, pp. 143–169, Springer, New York, NY, USA, 1989.

[12] P. E. Fixen and F. B. West, "Nitrogen fertilizers: meeting contemporary challenges," *Ambio*, vol. 31, no. 2, pp. 169–176, 2002.

[13] F. Zhang, Z. Cui, J. Wang, and C. Li X, "Current status of soil and plant nutrient management in China and improvement strategies," *Chinese Bulletin of Botany*, vol. 24, no. 6, pp. 687–694, 2007.

[14] P. Heffer, *Assessment of Fertilizer Use by Crop at the Global Level: 2006/07–2007/08*, International Fertilizer Industry Association, Paris, France, 2009.

[15] X. T. Ju, G. X. Xing, X. P. Chen et al., "Reducing environmental risk by improving N management in intensive Chinese agricultural systems," *Proceedings of the National Academy of Sciences of the United States of America*, vol. 106, no. 9, pp. 3041–3046, 2009.

[16] D. R. Keeney, "Nitrogen management for maximum efficiency and minimum pollution," in *Nitrogen in Agricultural Soils*, pp. 605–649, 1982.

[17] M. R. Kenna and G. L. Horst, "Turfgrass water conservation and quality," *International Turfgrass Society Research Journal*, vol. 7, pp. 99–113, 1993.

[18] P. J. Lea and R. A. Azevedo, "Nitrogen use efficiency. 1: uptake of nitrogen from the soil," *Annals of Applied Biology*, vol. 149, no. 3, pp. 243–247, 2006.

[19] Q. K. Li, H. E. Li, Y. W. Hu, and J. Sun, "Nitrogen loss in Qingtongxia irrigation area," *Journal of Agro-Environment Science*, vol. 27, pp. 683–686, 2008.

[20] W. J. Li, Y. Q. Xia, X. Y. Yang, M. Guo, and X. Y. Yan, "Effects of applying nitrogen fertilizer and fertilizer additive on rice yield and rice plant nitrogen uptake, translocation, and utilization," *Chinese Journal of Applied Ecology*, vol. 22, no. 9, pp. 2331–2336, 2011.

[21] X. Q. Liang, Y. X. Chen, H. Li, G. Tian, and Q. G. Yu, "Effect of rainfall intensity and rain-fertilization interval on N export by runoff in oilseed rape land," *Journal of Soil and Water Conservation*, vol. 20, no. 6, pp. 14–17, 2006.

[22] J. Liu, L. You, M. Amini et al., "A high-resolution assessment on global nitrogen flows in cropland," *Proceedings of the National Academy of Sciences of the United States of America*, vol. 107, no. 17, pp. 8035–8040, 2010.

[23] T. Liu, J. Tang, S. Jiang et al., "Effect of postponing nitrogen fertilizer application on yield and nitrogen using efficiency of super rice Yangliangyou6," *Journal of Northeast Agricultural University*, vol. 43, no. 7, pp. 57–60, 2012.

[24] *Ningxia Statistical Yearbook*, China Statistics Press, Beijing, China, 2012.

[25] Ningxia Water Conservancy Bureau, *Ningxia Water Resource Bulletin No. 22*, Water Resources Bureau of Ningxia press, Ningxia, China, 2008.

[26] X. X. Pei, X. B. Wang, P. He et al., "Effect of postponing N application on soil N supply, plant N uptake and utilization in winter wheat," *Plant Nutrition and Fertilizer Science*, vol. 15, no. 1, pp. 9–15, 2009.

[27] S. Peng, F. V. Garcia, R. C. Laza, A. L. Sanico, R. M. Visperas, and K. G. Cassman, "Increased N-use efficiency using a chlorophyll meter on high-yielding irrigated rice," *Field Crops Research*, vol. 47, no. 2-3, pp. 243–252, 1996.

[28] L. Prunty and R. Greenland, "Nitrate leaching using two potato-corn N-fertilizer plans on sandy soil," *Agriculture, Ecosystems and Environment*, vol. 65, no. 1, pp. 1–13, 1997.

[29] T. Yu and J. S. Chen, "Impacts of the agricultural development on the water quality and nitrogen pollution of the Yellow River-case of Ningxia irrigation area," *Journal of Arid Land Resources & Environment*, vol. 18, pp. 2–9, 2004.

[30] J. Yi, *Study on the characteristics of nitrogen migration in rice fields in Ningxia irrigation region [M.S. thesis]*, Chinese Academy of Agricultural Sciences, 2011.

[31] F. Yun, Y. Li, and J. N. Yang, "Investigation on simulation of dynamic distribution of COD and ammonia-nitrogen pollution in Ningxia segment of the Yellow River," *Journal of Ningxia University: Natural Science Edition*, vol. 26, pp. 83–287, 2005.

[32] W. J. Riley, I. Ortiz-Monasterio, and P. A. Matson, "Nitrogen leaching and soil nitrate, nitrite, and ammonium levels under irrigated wheat in Northern Mexico," *Nutrient Cycling in Agroecosystems*, vol. 61, no. 3, pp. 223–236, 2001.

[33] SAS Institute, *SAS User's Guide: Statistics*, Statistical Analysis System Institute Inc., Cary, NC, USA, 1990.

[34] S. J. Yang, A. P. Zhang, Z. L. Yang, and S. Q. Yang, "Agricultural non-point source pollution in Ningxia irrigation district and preliminary study of load estimation methods," *Scientia Agricultura Sinica*, vol. 42, no. 11, pp. 3947–3955, 2009.

[35] Q. Yi, S. C. Zhao, X. Z. Zhang, L. Yang, G. Y. Xiong, and P. He, "Yield and nitrogen use efficiency as influenced by real time and site specific nitrogen management in two rice cultivars," *Plant Nutrition and Fertilizer Science*, vol. 18, no. 4, pp. 777–785, 2012.

[36] B. J. Zebarth, C. F. Drury, N. Tremblay, and A. N. Cambouris, "Opportunities for improved fertilizer nitrogen management in production of arable crops in eastern Canada: a review," *Canadian Journal of Soil Science*, vol. 89, no. 2, pp. 113–132, 2009.

[37] H. Zhang, Z. Yang, L. Luo et al., "The feature of N_2O emission from a paddy field in irrigation area of the yellow river," *Acta Ecologica Sinica*, vol. 31, no. 21, pp. 6606–6615, 2011.

[38] Q. Zhang, H. Zhang, J. Yi et al., "The fate of fertilizer-derived nitrogen in a rice field in the Qingtongxia irrigation area," *Acta Scientiae Circumstantiae*, vol. 30, no. 8, pp. 1707–1714, 2010.

[39] Y. Shi and Z. W. Yu, "Effects of nitrogen fertilizer rate and ratio of base and topdressing on yield of wheat, content of soil nitrate and nitrogen balance," *Acta Ecologica Sinica*, vol. 26, no. 11, pp. 3661–3669, 2006.

[40] T. R. Turner and N. W. Hummel, "Nutritional requirements and fertilization," *Turfgrass-Agronomy Monograph*, vol. 32, pp. 385–439, 1992.

[41] P. M. Vitousek, R. Naylor, T. Crews et al., "Nutrient imbalances in agricultural development," *Science*, vol. 324, no. 5934, pp. 1519–1520, 2009.

[42] Y. Wang and S. Yang, "The nitrate-nitrogen leachingamount in paddy winter-spring fallow period," *Acta Ecologica Sinica*, vol. 31, no. 16, pp. 4653–4660, 2011.

[43] X. Xiaoliang, S. Zuliang, J. Qi, D. Tingbo, J. Dong, and C. Weixing, "Effects of nitrogen fertilization on spatial-temporal distributions of soil nitrate and nitrogen utilization in wheat season of rice-wheat systems," *Acta Pedologica Sinica*, vol. 47, no. 3, pp. 490–496, 2010.

[44] C. H. Xing, Y. S. Zhang, X. Y. Lin, S. T. Du, and C. Y. Yu, "Study on decreasing ammonia volatilization and leaching rates by NDSA fertilization method," *Journal of Zhejiang University: Agriculture and Life Sciences*, vol. 32, no. 2, pp. 155–161, 2006.

[45] Q. Zhang, Z. Yang, H. Zhang, and J. Yi, "Recovery efficiency and loss of 15N-labelled urea in a rice-soil system in the upper reaches of the Yellow River basin," *Agriculture, Ecosystems and Environment*, vol. 158, pp. 118–126, 2012.

[46] S. C. Zhao, X. X. Pei, P. He et al., "Effects of reducing and postponing nitrogen application on soil N supply, plant N uptake and utilization of summer maize," *Plant Nutrition and Fertilizer Science*, vol. 16, no. 2, pp. 492–497, 2010.

[47] X. L. Tang, X. M. Mu, H. B. Shao, H. Y. Wang, and M. Brestic, "Global plant-responding mechanisms to salt stress: physiological and molecular levels and implications in biotechnology," *Critical Reviews in Biotechnology*, 2014.

[48] G. Xu, H. B. Shao, J. N. Sun, and S. X. Chang, "Phosphorus fractions and profile distribution in newly formed wetland soils along a salinity gradient in the Yellow River Delta in China," *Journal of Plant Nutrition and Soil Science*, vol. 175, no. 5, pp. 721–728, 2012.

[49] J. N. Sun, G. Xu, H. B. Shao, and S. H. Xu, "Potential retention and release capacity of phosphorus in the newly formed wetland soils from the Yellow River Delta, China," *Clean—Soil, Air, Water*, vol. 40, no. 10, pp. 1131–1136, 2012.

[50] G. Xu, Y. Lv, J. Sun, H. Shao, and L. Wei, "Recent advances in biochar applications in agricultural soils: benefits and environmental implications," *Clean—Soil, Air, Water*, vol. 40, no. 10, pp. 1093–1098, 2012.

[51] H. B. Shao, B. S. Cui, and J. H. Bai, "Wetland ecology in China," *Clean—Soil, Air, Water*, vol. 40, no. 10, pp. 1009–1010, 2012.

[52] K. Yan, P. Chen, H. Shao et al., "Responses of photosynthesis and photosystem II to higher temperature and salt stress in Sorghum," *Journal of Agronomy and Crop Science*, vol. 198, no. 3, pp. 218–225, 2012.

[53] K. Yan, P. Chen, H. Shao, C. Shao, S. Zhao, and M. Brestic, "Dissection of photosynthetic electron transport process in sweet Sorghum under heat stress," *PLoS ONE*, vol. 8, no. 5, Article ID e62100, 2013.

[54] K. Yan, H. Shao, C. Shao et al., "Physiological adaptive mechanisms of plants grown in saline soil and implications for sustainable saline agriculture in coastal zone," *Acta Physiologiae Plantarum*, vol. 35, no. 10, pp. 2867–2878, 2013.

[55] L. Wei, G. Xu, H. Shao, J. Sun, and S. X. Chang, "Regulating environmental factors of nutrients release from wheat straw biochar for sustainable agriculture," *Clean—Soil, Air, Water*, vol. 41, no. 7, pp. 697–701, 2013.

[56] K. Yan, P. Chen, H. B. Shao, and S. J. Zhao, "Characterization of photosynthetic electron transport chain in bioenergy crop Jerusalem artichoke (Helianthus tuberosus L.) under heat stress for sustainable cultivation," *Industrial Crops and Products*, vol. 50, pp. 809–815, 2013.

[57] Z. Huang, L. Zhao, D. Chen et al., "Salt stress encourages proline accumulation by regulating proline biosynthesis and degradation in Jerusalem Artichoke plantlets," *PLoS ONE*, vol. 8, no. 4, Article ID e62085, 2013.

[58] Y. Shi, Y. Ge, J. Chang, H. Shao, and Y. Tang, "Garden waste biomass for renewable and sustainable energy production in China: potential, challenges and development," *Renewable and Sustainable Energy Reviews*, vol. 22, pp. 432–437, 2013.

[59] S. Jin, L. Liu, Z. Liu, X. Long, H. Shao, and J. Chen, "Characterization of marine Pseudomonas spp. antagonist towards three tuber-rotting fungi from Jerusalem artichoke, a new industrial crop," *Industrial Crops and Products*, vol. 43, no. 1, pp. 556–561, 2013.

[60] H. B. Shao and L. Y. Chu, "Some progress in the study of plant-soil interactions in China," *Plant Biosystems*, vol. 147, no. 3, pp. 1163–1165, 2013.

Hindawi Publishing Corporation
The Scientific World Journal
Volume 2014, Article ID 248792, 10 pages
http://dx.doi.org/10.1155/2014/248792

Research Article

The Static Breaking Technique for Sustainable and Eco-Environmental Coal Mining

Hao Bing-yuan, Huang Hui, Feng Zi-jun, and Wang Kai

Taiyuan University of Technology, Taiyuan, Shanxi 030024, China

Correspondence should be addressed to Hao Bing-yuan; haobingyuan@126.com

Received 13 April 2014; Revised 18 April 2014; Accepted 18 April 2014; Published 3 June 2014

Academic Editor: Hongbo Shao

The initiating explosive devices are prohibited in rock breaking near the goaf of the highly gassy mine. It is effective and applicable to cracking the hard roof with static cracking agent. By testing the static cracking of cubic limestone (size: 200 × 200 × 200 mm) with true triaxial rock mechanics testing machine under the effect of bidirectional stress and by monitoring the evolution process of the cracks generated during the acoustic emission experiment of static cracking, we conclude the following: the experiment results of the acoustic emission show that the cracks start from the lower part of the hole wall until they spread all over the sample. The crack growth rate follows a trend of "from rapidness to slowness." The expansion time is different for the two bunches of cracks. The growth rates can be divided into the rapid increasing period and the rapid declining period, of which the growth rate in declining period is less than that in the increasing period. Also, the growth rate along the vertical direction is greater than that of the horizontal direction. Then the extended model for the static cracking is built according to the theories of elastic mechanics and fracture mechanics. Thus the relation formula between the applied forces of cracks and crack expansion radius is obtained. By comparison with the test results, the model proves to be applicable. In accordance with the actual geological situation of Yangquan No. 3 Mine, the basic parameters of manpower manipulated caving breaking with static crushing are settled, which reaps bumper industrial effects.

1. Introduction

Coal energy is the most important source of energy in China. Safe coal mining under the condition of protecting eco-environment is more necessary [1–9]. Taiyuan, China, is one of the most resource-consuming coal cities, facing serious eco-environmental issues [10–19]. How to find sustainable and eco-environmental coal mining methodology is the challenge. Currently, the fully mechanized coal mining face, when exploited, gradually enters the mining roadway of the goaf. However, due to the influence of the dynamic pressure and some other factors generated during the service term, it is difficult to haul off and dismantle the anchor; therefore it is still in suspension and is being a part of reinforcement [1, 2]. Meanwhile, it is positioned at triangle area of the stope roof arch, thus the tunnel roof cannot inbreak along with the mining face roof caving, and also a hanging arch is formed on the back of the work face, which becomes universally encountered hidden danger across the sector of exploitation [5–9].

By far, the main method of tackling the issue the hanging arch are on other than hydraulic fracturing and pre splitting blasting [3]. The first method requires high-quality top tray, coupled with long processing period and does not render satisfying result, which is basically at the testing stage [4–7]. The second method, being time efficient, convenient, viable, and cost effective and having good effect, is the best way to tackle the issue of top tray and is widely utilized all over the world [6–9]. However, due to the prohibition of utilizing the explosive device for rock breaking in the goaf of highly gassy mine, it is inappropriate to tackle the issue in this way.

In this paper, the static crushing technique is first introduced to provide solution to the issue of top tray. It is a way to place the gob side roof of the roadway with manpower and shorten the spacing in between the goaf roadway, thereby solving the problems of methane accumulation in the upper

Table 1: The main mechanical parameters of limestone needed for the experiment.

Number	Specification			Max. compressing force/KN	Compressive strength/MPa	Poisson's ratio	Modulus of elasticity E/GPa
	Diameter/mm	Basal area/mm^2	Height/mm				
1	50.90	2034.76	104.60	98.70	48.51	0.23	28.4
2	51.00	2042.76	106.60	113.05	55.34	0.26	30.2
3	50.94	2037.96	102.46	102.73	50.41	0.22	25.9
Average				104.83	51.42	0.237	28.12

corner, air leak on the work face, and great pressure in the supporting roadway. Therefore it promotes the safety management of mines.

As a well-developed technology, static breaking has been applied in several sectors and has yielded bumper harvest. Ruiping and Yongqi have studied on expansion mechanism and controllability of the static cracking agent [10]. Yujie researched into the expansion mechanism and rock breaking mechanism under the effect of static breaking techniques [11]. Furthermore, Tang et al., by carrying out physical and data analog tests on the destruction process of concrete model under the influence of static cracking agent, conclude that the destruction pattern of the crack is formed before the unstable expansion process occurs [12]. However, the above illustrated documents have never extended to the evolution principles of cracks, which also do not appear in other documents that are available to me.

This paper will report the crack evolution pattern in the process of crushing limestone with static cracking agent by monitoring the crack evolution details in the process of static destruction with acoustic emission instrument, thereby giving you a clear depiction of the three-dimensional coordinates of the location of the crack events, which is an eco-environmental sustainable method for coal mining in heavy-metal polluted region. By combining the theoretical analysis and experimental data, we acquire the calculation formula of crack expansion radius. As per this, the relationship between crack expansion radius and the expansive pressure of the static cracking agent is revealed. Also, according to the practical geological conditions of K8113 Yangquan No. 3 Mine, we determine the basic parameters of manpower forced static breaking technique. Based on the practical application, the industrial result is excellent.

2. The Experiment Acoustic Emission

2.1. Experimental Equipment and the Sample. This experiment employs the multichannel sound emission instrument with the AEwin data processing software produced by The America Physical Acoustics Co (PAC).

The breaking material used is K2 limestone, hexahedron limestone with side length of 200 mm, as is shown in Figure 1. Along the center position on the side perpendicular to the stretch of rock bedding, the rock core with 50 mm diameter and 150 mm length shall be chosen to be processed into standard test sample with height of 100 mm. The basic parameters needed for dynamic experiment are provided as in Table 1.

Figure 1: Limestone sample.

Mix the static cracking agent with water at the mass ratio of 7 : 3. After stirring evenly, drip it into the hole. To simulate a practical working condition of the mine roadway, the temperature during acoustic emission experiment shall be controlled at about 10°C.

2.2. Calibration of the Detecting Points. Select two fine parallel planes. On the two ends of the diagonal line of one plane calibrate points 1 and 2, the other points 3 and 4. Points 1 and 3 shall be upward and points 2 and 4 shall be downward, and the four points calibrated shall be 70 mm away from their nearest corresponding endpoint, as shown in Figure 2.

2.3. Pressurization and Filling. After the debug of the acoustic emission instrument, check to make sure the press machine works properly. In the beginning of the experiment, prepare the agent first and then apply pressure to axial and lateral side, respectively, till 5 MPa (Figure 3).

When pressurized operation is completed, click on the "reacquisition" button on the interface of AEwinTM, filter off the acoustic emission data collected during the pressurizing process to initiate the data collection process, and record the start time of the data acquisition.

2.4. Experimental Results. Figure 4 is a reflection of the relationship between the three-dimensional coordinates of the acoustic emission events and time, as can be seen from the figure.

(1) Within 0 to 15 min, the number of acoustic emission events remains approximately unchanged; from 15 min to 20 min, the number of events significantly increases and the static cracking agent begins to react;

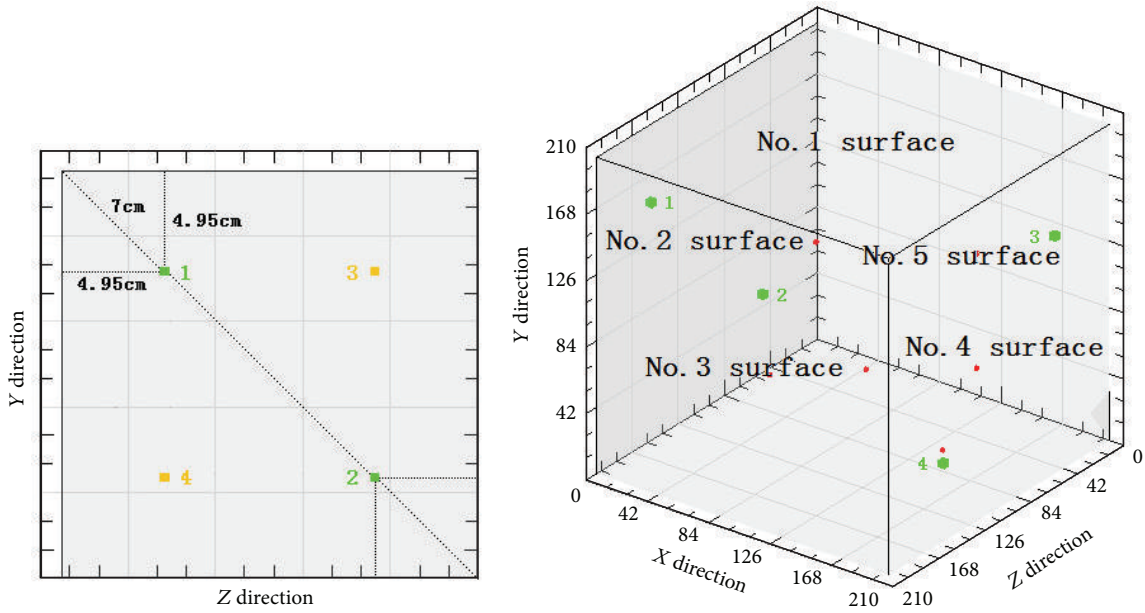

(a) (b)

Figure 2: The position of the calibrated points.

Figure 3: Pressurization.

at 30 min, the number of events continues to rise; at the same time in the lower part of the hole wall, the events are more dense; therefore, it can be inferred that the first occurring crack begins there and then expands outward.

(2) At 40 min, the cracks continue to expand all around, and the expansion velocity at the hole bottom is greater than that at the orifice; at about 50 min, the first two cracks have basically expanded through the whole limestone sample, and meanwhile, the two latter occurring cracks begin to take shape; after 60 min, the first two cracks continue to expand as ever and the latter two gradually begin to grow clear; from 60 min to 300 min, the first two and the latter ones continue to expand. The comparison between the graphs at 240 min and at 300 min reveals no obvious differences. As per this, it can be concluded that, from 240 min, the formation process of the cracks basically completed for the reaction velocity of the static cracking agent is minimal.

Seen from the overall status of the three-dimensional coordinates of the acoustic emission events, from 0 min to 300 min, the number of events increases along with the elapsing of time and the growth rate is greater at first than later on and finally becomes stable; the swelling pressure of the static cracking agent breeds cracks and the cracks formed at first are approximately vertical to the latter occurring ones.

Figure 5 describes the expansion status of the first occurring cracks A and B. It reveals that the cracks start from the hole wall and extend vertically and horizontally till they go through the whole limestone sample. Select the coordinates of the main areas where events concentrate from the acoustic emission data recorded during the process to calculate the range of the occurring events and regard the result as the growth length of the cracks. According to the data distributed along directions X and Y in Figure 5, the curve reflected in Figure 6 can be obtained.

On the basis of the expansion lengths' changes over time reflected in Figure 6, the curves in Figure 7 can be obtained. A combination analysis of Figures 6 and 7 demonstrates the following.

(1) The swelling agent begins to react after about 20 min, and within the 20 min prereaction period, no cracks occur.

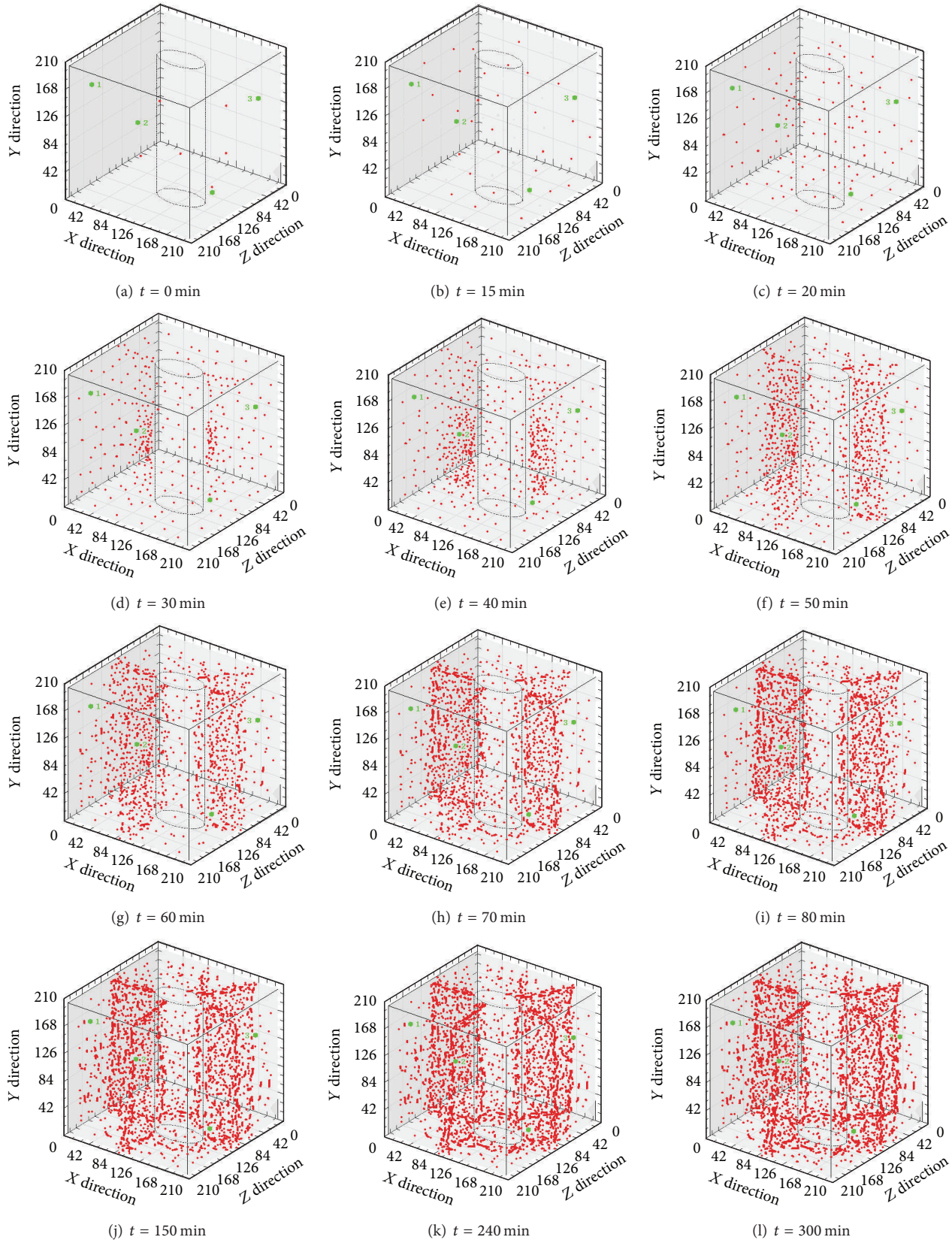

(a) $t = 0$ min (b) $t = 15$ min (c) $t = 20$ min

(d) $t = 30$ min (e) $t = 40$ min (f) $t = 50$ min

(g) $t = 60$ min (h) $t = 70$ min (i) $t = 80$ min

(j) $t = 150$ min (k) $t = 240$ min (l) $t = 300$ min

Figure 4: The three-dimensional coordinates graph of the acoustic emission events.

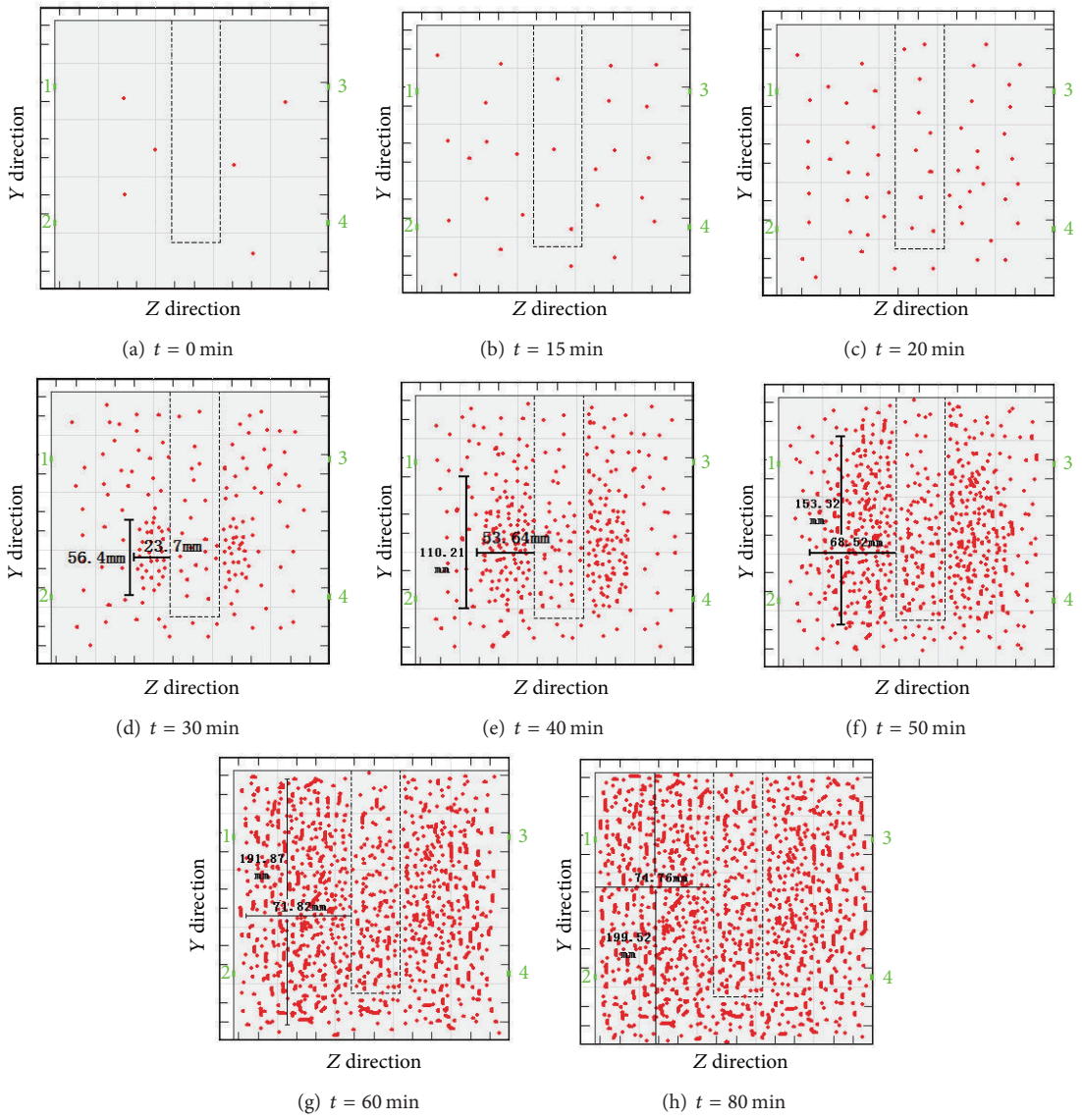

(a) t = 0 min (b) t = 15 min (c) t = 20 min

(d) t = 30 min (e) t = 40 min (f) t = 50 min

(g) t = 60 min (h) t = 80 min

Figure 5: The expansion status of the first occurring cracks A and B.

(2) After the swelling agent takes chemical reaction, the reaction rate rises over time gradually till it reaches the maximum level at 40 min. At 40 min, the growth rate of the cracks also reaches its peak.

(3) The growth rate of the cracks presents a trend of "from rapidness to slowness, and to be steady finally"; from 20 min to 30 min, the growth rate of the vertical cracks increases rapidly. After 30 min, the growth rate drops radically, and the growth rate during the declining period is less than that of the growth period. From 20 min to 40 min, the growth rate of the cracks along the horizontal bedding direction rises greatly until 40 min, when it begins to decline rapidly. Also, the growth rate during the declining period is less than that of the growth period.

(4) The growth rate along the horizontal direction is greater than that of the vertical direction.

(5) At 80 min, the cracks almost spread all over the whole limestone sample.

Figure 8 reveals the expansion status of the latter occurring cracks C and D. It shows that after 40 min from the occurrence of cracks A and B, cracks C and D appear. Based on the data on X and Y from Figure 8, the curves in Figures 9 and 10 can be obtained.

From the curves in Figures 9 and 10, we can see that the following occur.

(1) Cracks C and D have no obvious changes from 0 to 40 min.

(2) The growth rate of cracks C and D presents a trend of "from rapidness to slowness"; from 40 min to 60 min, the growth rate of the vertical cracks increases rapidly. After 60 min, the growth rate drops radically, and the growth rate during the declining period is less than

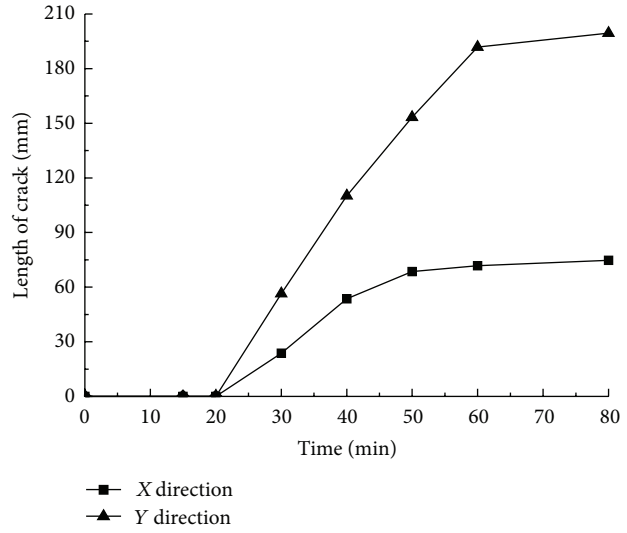

Figure 6: The relation curves between the expansion lengths of cracks A and B and time.

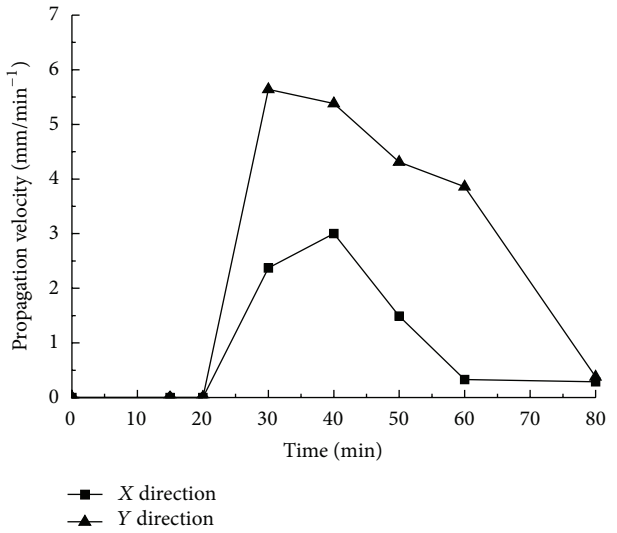

Figure 7: The relation curves between the average expansion velocities of cracks A and B and time.

that of the previous period. From 40 min to 50 min, the growth rate of the cracks along the horizontal direction rises greatly until 50 min, when it begins to decline rapidly. Again, the growth rate during the declining period is less than that of the growth period.

(3) The growth rate along the vertical direction is greater than that of the horizontal direction; at 240 min, the cracks almost spread all over the whole limestone sample.

3. Establishment of Crack Expansion Model

According to the acoustic emission experiment and based on existing data, the crack expansion model is obtained as Figure 11 shows.

When the first occurring crack length is minimal enough, the drill hole can be regarded as part of the cracks. Then if the whole model is regarded as an infinite medium, the stress intensity factor of the swelling pressure $q(t)$ which changes over time should be [13]

$$K^* = 2\sqrt{\frac{a}{\pi}}q(t)\arcsin\left(\frac{d}{a}\right). \quad (1)$$

In the formula: K^* is the stress intensity factor of first occurring cracks, N/mm$^{3/2}$; d is the diameter of the drill hole; a is the crack length, mm.

When a is greater than d, the model can be regarded as the cracks generated by a couple of concentrated stress P, which acts on the central, upper, and lower surfaces. $P = \lim_{r\to 0} 2q(t)d$; in this formula, r stands for the distance from any point to the center of the drill hole. Therefore, the stress intensity factor can be expressed as

$$K_a^* = \frac{P}{\sqrt{\pi a}}, \quad (2)$$

$$K_b^* = \frac{P}{\sqrt{\pi b}}. \quad (3)$$

4. Calculating the Expansion Radius of the Cracks

When the static cracking agent expands its volume due to hydration, the swelling pressure exerted on the drill hole rises correspondingly. Thus the stress intensity factor around the hole increases accordingly. When it rises to the fracture toughness of the rock, the cracks begin to expand all around. From formulas (2) and (3), we can see that when stress P remains unchanged, the less length a is, the greater the stress intensity factor is. When K^* reaches fracture toughness K_{IC}, the cracks begin to expand and along with the increasing of the crack length, the stress intensity factor drops rapidly until it is less than K_{IC}, when the crack expansion stops. When P rises constantly, the above illustrated crack expansion will not take place. Through the measurement of the uniaxial compressive strength σ_c, the corresponding fracture toughness K_{IC} can be obtained [14] by

$$K_{IC} = 0.0265\sigma_c + 0.0014. \quad (4)$$

Because $a < b$, therefore $K_a^* < K_b^*$. The formula of minimum crack expansion should be [15]

$$K^* = K_{IC}. \quad (5)$$

Bring the formulas (2) and (4) into formula (5), we can obtain the following formula (6):

$$a = \frac{q^2(t)}{\pi\left(0.0256\sigma_c + 0.0014\right)^2}. \quad (6)$$

Theoretically speaking, formula (6) should be the expansion radius of the cracks. On the basis of it, the appropriate spacing between the drill holes during the process of utilizing static breaking method to tackle the issue of hanging arch should be $2a$.

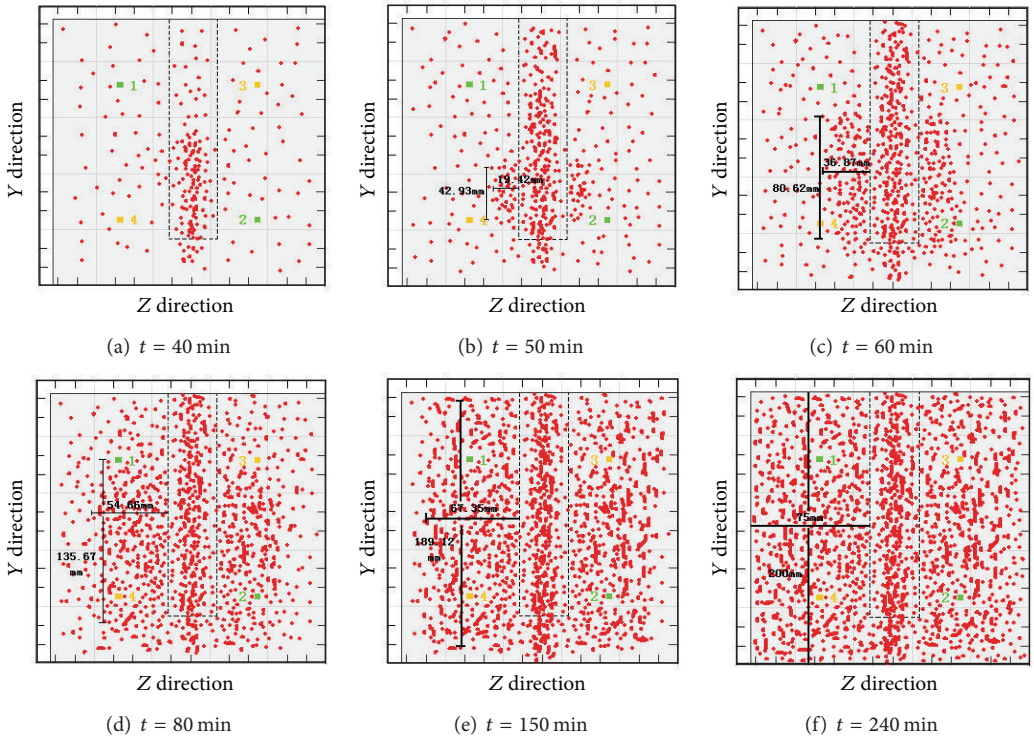

Figure 8: The expansion status of the latter occurring cracks C and D over time.

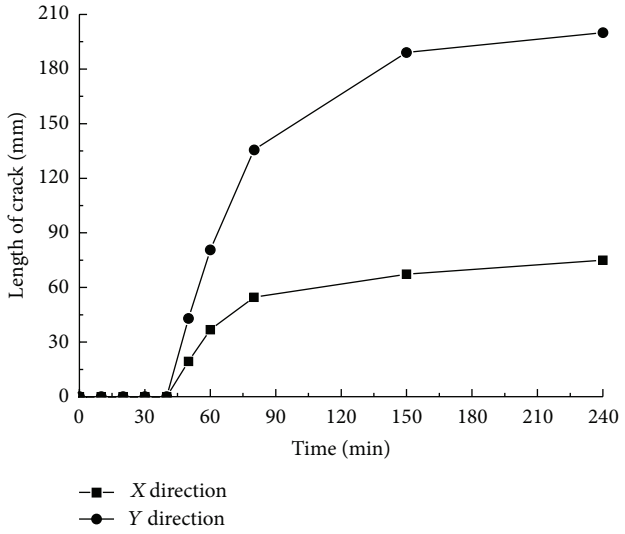

Figure 9: The relation curves between the growth lengths of C and D and time.

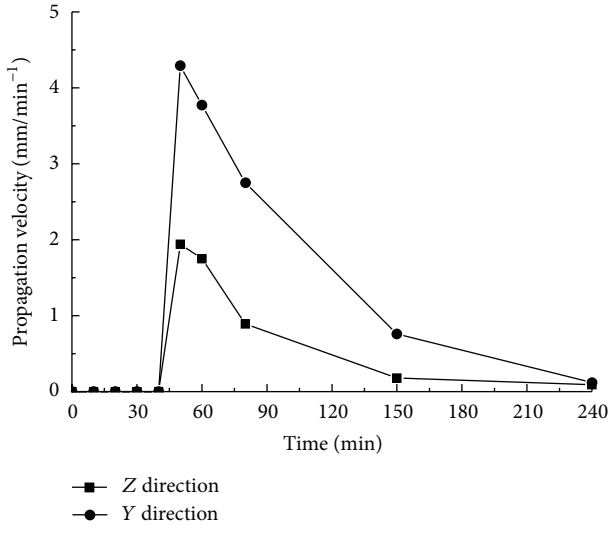

Figure 10: The relation curves between the average growth rate of C and D and time.

5. Analysis and Discussion

The following results can be concluded from the acoustic emission experiment.

(1) The crack expands outward from down the middle part of the hole wall till it spreads all over the whole sample.

(2) After certain time when the first occurring cracks A and B show up, cracks C and D appear. It can be inferred that the latter occurring cracks always appear later than the first cracks.

(3) The expansion process of crack A is in conformity to that of crack B. It is also true for cracks C and D.

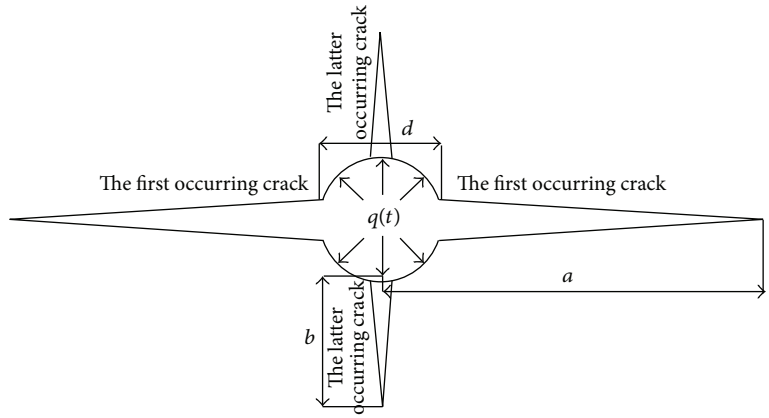

Figure 11: The crack expansion model.

(4) The growth rate of the cracks presents a trend of "from rapidness to slowness"; the growth rate can be divided into two parts, namely, period of rapid increasing and period of rapid declining. The growth rate during the declining period is less than that of the growth period.

(5) The growth rate along the vertical direction is greater than that of the horizontal direction.

The result of crack expansion during the acoustic emission experiment is shown in Figure 12.

By comparing Figure 12 with Figures 4, 5, 8, and 11, we can see that the result of the crack expansion monitored from the acoustic emission experiment is in conformity with the actual situation and the crack expansion model is in accordance with the practical situation. Thus the model proves to be reasonable.

6. Application in Project

6.1. General Situation of the Project. Yangquan No. 3 Mine is a highly gassy mine. Number 15 coal seam to be mined is in K8113 working face. The average thickness is 7.18 m and the uniaxial comprehensive strength is about 50 MPa.

Static crushing material used in this study is "high efficiency coal mine static expanding agent"; the maximum swelling pressure is 80 MPa.

6.2. Scheme Design. In static crushing technology, the spacing between holes remains a problem. At present, there are only some certain empirical methods, which have not been studied scientifically in a systematical fashion. On the basis of the crack expansion model built according to result from the acoustic emission experiment, this paper offers the formula for calculating the spacing in between drill holes so as to provide theoretical support for properly designing the hole spacing.

By putting the maximum swelling pressure and the uniaxial compressive strength on the immediate roof into formula (6), we can obtain such formula as $a \approx 400$ mm; then $2a \approx 800$ mm; namely, the most reasonable spacing between drill holes should be 800 mm. Other parameters needed are mainly the hole depth 4.5 m; the horizontal contained angle with the worked out section 45°; specification of the hole sealing machine ZF-A22; the grout amount can be calculated as $Q = K\pi\gamma(\Phi/2)^2(H - h)$; in the formula, K is grouting coefficient, and put it between 1.4 and 1.5; γ stands for material volume-weight, unit: kg/m3; Φ is diameter of the drill hole, unit: m; H stands for hole depth, unit: m; h is hole sealing length, unit: m; Q is mass of the swelling agent, unit: kg.

6.3. Test Results. Before the industrial test was taken, when the hauling-off anchor and net cut are completed on working face K8113, the hanging arch is still as long as 20 m. Several hours after the grouting is completed, an obvious sound of fracture can be heard in the rock of the top tray. When working face and nose move 4 coal cutters, namely, 3.2 m forward, the coals on top inside the setting roadway begin to inbreak. Meanwhile, the limestone on the upper roof gradually starts to collapse. With further moving forward of 12 coal cutters, namely, 9.6 m, the whole test area will have already collapsed thoroughly. By being processed with the static crushing method, the length of the hanging arch lessens by 7.2 m, which improves the safety production environment of the working face effectively.

7. Conclusion

(1) The experiment results of the acoustic emission show that the cracks start from the lower part of the hole wall. The processes of expansion for the first occurring cracks are in conformity with each other, which is also true of the latter occurring cracks. Expansion time for the two bunches of cracks is distinct. The crack growth rate follows a trend of "from rapidness to slowness." The growth rates can be divided into the rapid increasing period and the rapid declining period, of which the growth rate in declining period is less than that of the increasing period. Also, the growth rate along the vertical direction is greater than that of the horizontal direction.

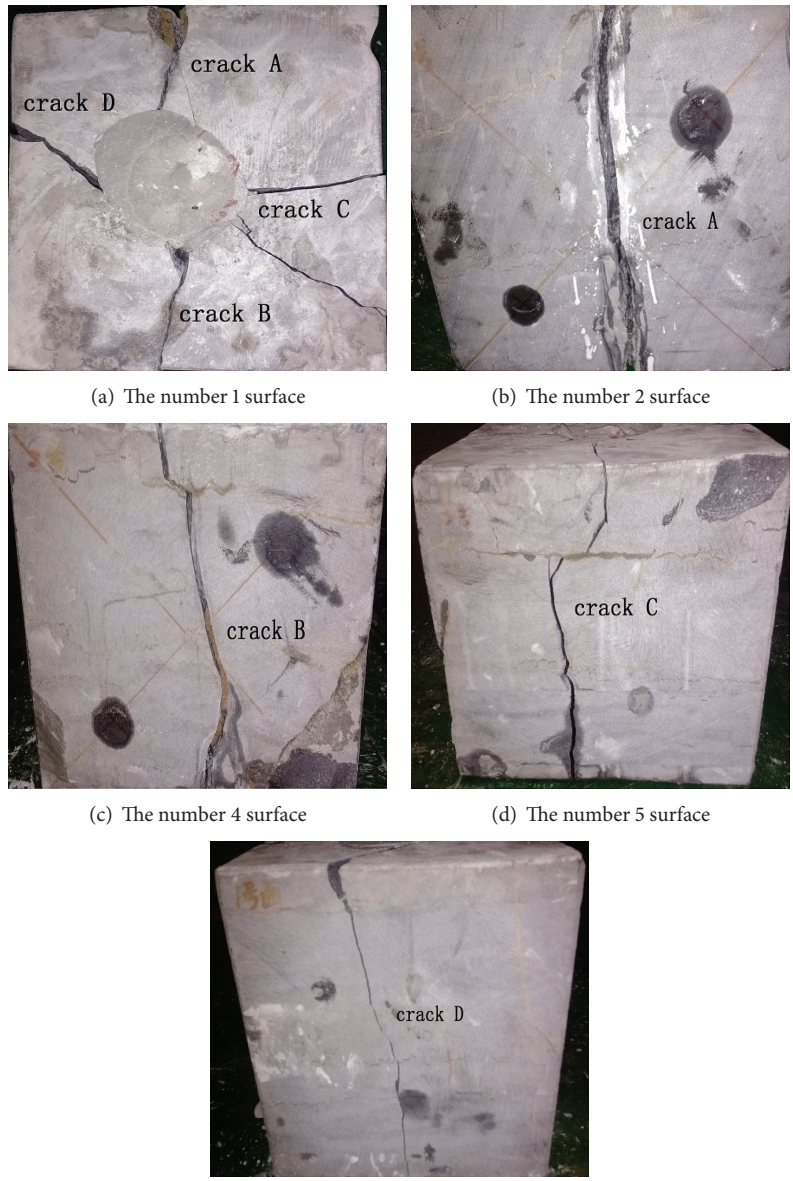

(a) The number 1 surface

(b) The number 2 surface

(c) The number 4 surface

(d) The number 5 surface

(e) The number 3 surface

Figure 12: Crack expansion actual results.

(2) Based on the acoustic emission test results, the extended model of the static breaking crack, by comparison, is in conformity with the actual situation, which indicates that the model is reasonable; the fracture radius in static crushing can be calculated through the formula

$$a = \frac{q^2(t)}{\pi\left(0.0256\sigma_c + 0.0014\right)^2}. \quad (7)$$

(3) Research on the crack expansion principles and the static technique, combined with application in the project of Yangquan Coal Group, demonstrates that the static crushing technique satisfies the demand for tackling the issue of hanging arch on highly gassy mine working face.

Conflict of Interests

The authors declare that there is no conflict of interests regarding the publication of this paper.

Acknowledgments

The study has been supported by National Key Technology R&D Program of China, (Grant no. 2009BAB48B03) and Key Technology R&D Program of Shanxi Province, China (Grant no. 20121101009-03).

References

[1] K. Hongpu and W. Jinhua, *Theories of Anchor Bolt Support and Technology*, China Coal Industry Publishing House, Beijing, China, 2007.

[2] C. Li, J. H. Xu, R. Wu, and J. T. Dong, "Mechanism and practice of support release of mining roadway about fully-mechanized top-coal caving mining stope," *Journal of the China Coal Society*, vol. 36, no. 12, pp. 2018–2023, 2011.

[3] K. Wang, T. H. Kang, H. T. Li, and W. Han, "Study of control caving methods and reasonable hanging roof length on hard roof," *Chinese Journal of Rock Mechanics and Engineering*, vol. 28, no. 11, pp. 2320–2327, 2009.

[4] S. H. Yan, Y. Ning, L. J. Kang, Y. W. Shi, Y. G. Wang, and Y. F. Li, "The mechanism of hydrobreakage to control hard roof and its test study," *Journal of China Coal Society*, vol. 25, no. 1, pp. 32–35, 2000.

[5] Y. Feng and H. Kang, "Test on hard and stable roof control by means of directional hydraulic fracturing in coal mine," *Chinese Journal of Rock Mechanics and Engineering*, vol. 31, no. 6, pp. 1148–1155, 2012.

[6] X. J. Yang and Z. P. Shen, "Application of softening hard roof with deep bore explosion in full-mechanized mining face with large mining height," *Coal Mining Technology*, vol. 12, no. 6, pp. 30–32, 2007.

[7] C. R. Li, L. J. Kang, Q. X. Qi, D. B. Mao, and G. Xu, "Numerical simulation of deep-hole blasting and its application in mine roof weaken," *Journal of the China Coal Society*, vol. 34, no. 12, pp. 1632–1636, 2009.

[8] Y. P. Wu, K. F. Li, and Y. L. Zhang, "Simulation of hard roof weakening ahead of working face with fully mechanized caving," *Journal of Mining and Safety Engineering*, vol. 26, no. 3, pp. 273–277, 2009.

[9] D. Y. Guo, D. Y. Shang, P. F. Lv, S. Y. Wang, and J. M. Wang, "Experimental research of deep-hole cumulative blasting in hard roof weakening," *Journal of the China Coal Society*, vol. 38, no. 7, pp. 1149–1153, 2013.

[10] G. Ruiping and Y. Yongqi, "Swelling mechanism and controllability of SCA," *Journal of China Coal Society*, vol. 19, no. 5, pp. 478–485, 1994.

[11] W. Yujie, *Research on Mechanism and Technology of Non-Explosive Demolition*, Wuhan University of Technology, Wuhan, China, 2009.

[12] L. Tang, C. Tang, S. Tang, Y. Cui, and L. Song, "Physical experiment and numerical simulation on effect of soundless cracking agent," *Chinese Journal of Geotechnical Engineering*, vol. 27, no. 4, pp. 437–441, 2005.

[13] C. Jin and Z. Shushan, *Fracture Mechanics*, Science Press, Beijing, China, 2012.

[14] L. Jiangteng, G. Desheng, C. Ping et al., "Interrelated law between mode-I fracture toughness and compression strength of rock," *Journal of Central South University (Science and Technology)*, vol. 40, no. 6, pp. 1695–1699, 2009.

[15] L. Shiyu and Y. Xiangchu, *Introduction of Rock Fracture Mechanics*, Press of University of Science and Technology of China, Beijing, China, 2010.

[16] G. Xu, Y. C. Lv, J. N. Sun, H. B. Shao, and L. L. Wei, "Recent advances in biochar applications in agricultural soils: benefits and environmental implications," *Clean—Soil, Air, Water*, vol. 40, no. 10, pp. 1093–1098, 2012.

[17] G. Wu, H. B. Kang, X. Y. Zhang, H. B. Shao, L. Y. Chu, and C. J. Ruan, "A critical review on the bio-removal of hazardous heavy metals from contaminated soils: issues, progress, eco-environmental concerns and opportunities," *Journal of Hazardous Materials*, vol. 174, no. 1–3, pp. 1–8, 2010.

[18] H. B. Shao, Ed., *Metal Contamination: Sources, Detection and Environmental Impact*, NOVA Science Publishers, New York, NY, USA, 2012.

[19] H. B. Shao and L. Y. Chu, "Some progress in the study of plant-soil interactions in China," *Plant Biosystems*, vol. 147, no. 4, pp. 1163–1165, 2013.

Hindawi Publishing Corporation
The Scientific World Journal
Volume 2014, Article ID 843764, 7 pages
http://dx.doi.org/10.1155/2014/843764

Research Article

Hydrogen Peroxide Is Involved in Salicylic Acid-Elicited Rosmarinic Acid Production in *Salvia miltiorrhiza* Cell Cultures

Wenfang Hao, Hongbo Guo, Jingyi Zhang, Gege Hu, Yaqin Yao, and Juane Dong

State Key Laboratory of Crop Stress Biology for Arid Areas, College of Life Sciences, Northwest A&F University, Yangling 712100, China

Correspondence should be addressed to Juane Dong; dzsys@nwsuaf.edu.cn

Received 4 April 2014; Revised 7 May 2014; Accepted 7 May 2014; Published 29 May 2014

Academic Editor: Hongbo Shao

Salicylic acid (SA) is an elicitor to induce the biosynthesis of secondary metabolites in plant cells. Hydrogen peroxide (H_2O_2) plays an important role as a key signaling molecule in response to various stimuli and is involved in the accumulation of secondary metabolites. However, the relationship between them is unclear and their synergetic functions on accumulation of secondary metabolites are unknown. In this paper, the roles of SA and H_2O_2 in rosmarinic acid (RA) production in *Salvia miltiorrhiza* cell cultures were investigated. The results showed that SA significantly enhanced H_2O_2 production, phenylalanine ammonia-lyase (PAL) activity, and RA accumulation. Exogenous H_2O_2 could also promote PAL activity and enhance RA production. If H_2O_2 production was inhibited by NADPH oxidase inhibitor (IMD) or scavenged by quencher (DMTU), RA accumulation would be blocked. These results indicated that H_2O_2 is secondary messenger for signal transduction, which can be induced by SA, significantly and promotes RA accumulation.

1. Introduction

Salicylic acid (SA) is often used to regulate plant growth and development, seed germination, and fruit formation and to enhance the capability of the plants to respond to abiotic and biotic stresses [1, 2]. Exogenous application of SA can promote the thermo tolerance of mustard seedlings [3], chilling tolerance of cucumber [4], salt stress of *Arabidopsis* seedlings [5], and toxicity tolerance of cadmium of barley seedlings [6]. In recent years, SA has been used as an elicitor to induce the biosynthesis of secondary metabolites in plants. Exogenous application of SA induces the biosynthesis of coumarins in *Matricaria chamomilla* [7], taxane in *Taxus chinensis* [8], saponins in ginseng [9], phenolic acids in *Salvia miltiorrhiza* [10], artemisinin in *Artemisia annua* [11], and sinapyl alcohol in ulmus cells [12].

The biosynthesis of secondary metabolites in plant cells is regulated by specific signal transduction pathways. Under the stimulation of elicitors, some biochemical events related to signal transduction can be activated, such as ion transmembrane transport, active oxide species (AOS) burst, and protein phosphorylation and dephosphorylation [13, 14]. AOS are signal molecules that widely exist in plant cells [13–15]. Hydrogen peroxide (H_2O_2), one of the AOS, has been considered as the most significant signal molecules [14, 16]. Generally, when plants are under stress, H_2O_2 is produced rapidly to activate systemic acquired resistance [13, 17, 18] and acts as a signal molecule mediating the biosynthesis of secondary metabolites in plants. For example, H_2O_2 is the key signal molecule for oligosaccharides to induce the biosynthesis of taxol in *T. chinensis* cells [19], for the cell wall of *Aspergillus niger* to elicit *Catharanthus roseus* cells to synthesize catharanthine [20], for ABA to induce rice seedling leaves to synthesize anthocyanidins [21], and for the cell cultures of *Rubia tinctorum* to produce anthraquinone [22], and so forth.

Rosmarinic acid (RA) is one of effective compounds of Danshen, the root and rhizome of *Salvia miltiorrhiza* Bunge, which is used as a traditional Chinese herbal drug which removes blood stasis, stops pain, and activates blood flow and is heart-relieving [23]. RA shows a great intensity for free radical scavenging and antioxidant activity. The

phenylalanine ammonia-lyase (PAL) is the first enzyme for accumulating phenolic acid compounds in *S. miltiorrhiza* cell cultures [10], and SA could induce the production of rosmarinic acid [24]. The aim of this work is to reveal the effects of SA and H_2O_2 on the accumulation of RA in *S. miltiorrhiza* cell cultures. For this purpose, imidazole (IMD, NADPH oxidase inhibitor) is used to inhibit the enzyme activity of NADPH oxidase, and dimethylthiourea (DMTU, H_2O_2 scavenger) is employed as scavenger of H_2O_2.

2. Results

2.1. Effects of SA on PAL Activity, H_2O_2 Production, and RA Accumulation. The PAL activity increased from 20 min after treating with 22.5 mg/L SA and reached the peak at 16 h, when the activity was 5.46 folds of that of control, followed by subsequent decrease (Figure 1(a)). The H_2O_2 production induced by SA also exhibited continuous increase at the beginning with two peaks, but decreased rapidly after 2-h elicitation. The first peak occurred at 20 min and the second did at 2 h, when 8.51 folds H_2O_2 production was found in SA-treated cells (Figure 1(b)). In terms of RA accumulation, continuous increase was found till the 2nd day when RA content reached the highest with 2.15 folds and then it decreased gradually (Figure 1(c)).

2.2. Effects of Exogenous H_2O_2 on the PAL Activation and RA Production. The effects of H_2O_2 on activation of PAL activity and RA production were investigated, after applying exogenous H_2O_2 with concentration ranging from 1 to 70 mM. The activity of PAL and RA content were enhanced with the increase of H_2O_2 concentration ranging from 1 to 10 mM, whereas both decreased if the concentration was more than 10 mM (Figure 2). This result suggests that 10 mM is an appropriate concentration to enhance PAL activity and RA accumulation.

To further estimate the suitable treatment time of H_2O_2, continuous 6-day treatment was performed to confirm the best time point. Both PAL activity and RA accumulation were increased at early stage with time extension and then decreased at the late stage (Figure 3). The activity of PAL reached the highest peak at 8 h, followed by drastic decrease. The RA content reached the peak at 1 d and decreased drastically after 2 d.

2.3. Influences of CAT on SA-Induced RA Production. CAT is a scavenger of H_2O_2, which can not pass through cell membrane, and thus the exogenous CAT cannot scavenge H_2O_2 within cells. Both contents of H_2O_2 (Figure 4(a)) and RA (Figure 4(b)) were slightly lower than those of control after adding CAT, whereas both contents showed no significant difference between CAT + SA-treated and SA-elicited cells. The application of CAT did not affect the production of endogenous H_2O_2 and RA accumulation in cells that were subjected to SA elicitation. However, CAT can scavenge the exogenous H_2O_2, thereby eliminating the production of H_2O_2 and RA synthesis due to H_2O_2 regulation. This indicates that the RA biosynthesis is mediated by intracellular H_2O_2 elicited by SA.

2.4. Influences of DMTU on SA-Induced RA Production. DMTU is a H_2O_2 quencher that can effectively remove H_2O_2 within cells. The results showed that H_2O_2 was released and RA accumulated due to SA elicitation (Figure 1(b)). In order to further explain whether endogenous H_2O_2 was involved in the activation of PAL and the synthesis of RA, DMTU was employed to quench endogenous H_2O_2, and under such condition, both contents of H_2O_2 and RA in cells were measured (Figure 5).

The production of endogenous H_2O_2 (Figure 5(a)) and the accumulation of RA (Figure 5(b)) within cells were partially inhibited by 100 μM DMTU, and they were significantly inhibited with the concentration of 500 μM. If the cells were treated by 500 μM DMTU + 22.5 mg/L SA or 500 μM DMTU + 10 mM H_2O_2, DMTU would significantly inhibit the production of endogenous H_2O_2 and the accumulation of RA. Application of exogenous H_2O_2 and/or SA could partially reverse the inhibition of DMTU on RA synthesis. The treatment of 700 μM DMTU also completely inhibited the production of H_2O_2 in cells, and the inhibition could not be reversed by application of exogenous SA or H_2O_2. These results showed DMTU treatment slightly decreased both contents of RA and H_2O_2, when compared with the H_2O control. Meanwhile, DMTU + SA treatment would significantly block both contents if compared with those SA-elicited cells. These results indicated that H_2O_2 produced from SA elicitation is necessary for triggering the biosynthesis of RA.

2.5. Influences of IMD on SA-Induced RA Production. NADPH oxidase is one of the key enzymes for the generation of intracellular H_2O_2 [25, 26]. IMD is the specific inhibitor of NADPH oxidase on plasma membrane, which can inhibit the production of H_2O_2 through inactivating NPDPH oxidase [16, 17, 25]. For instance, IMD scavenged H_2O_2 produced from NADPH oxidase elicited by ABA and decreased the synthesis of anthocyanins in rice leaves [21]. In this study, IMD was used to inhibit the activity of NADPH oxidase to examine its influence on the biosynthesis of RA elicited by exogenous H_2O_2 and/or SA.

When IMD (100 μM) was used solely, IMD treatment slightly decreased the contents of RA and H_2O_2 when compared with the control, while IMD + SA and IMD + H_2O_2 treatments significantly decreased both contents when compared with SA-elicited cells (Figure 6). The results indicated that IMD inhibited the effects of SA elicitation, and the inhibition of IMD to the synthesis of RA in cell cultures depended on H_2O_2 generated from NADPH oxidase.

3. Discussion

This investigation shows SA can induce the burst of H_2O_2, and the elicited H_2O_2 enhances the PAL activity and RA accumulation in *S. miltiorrhiza* cell cultures. SA signaling

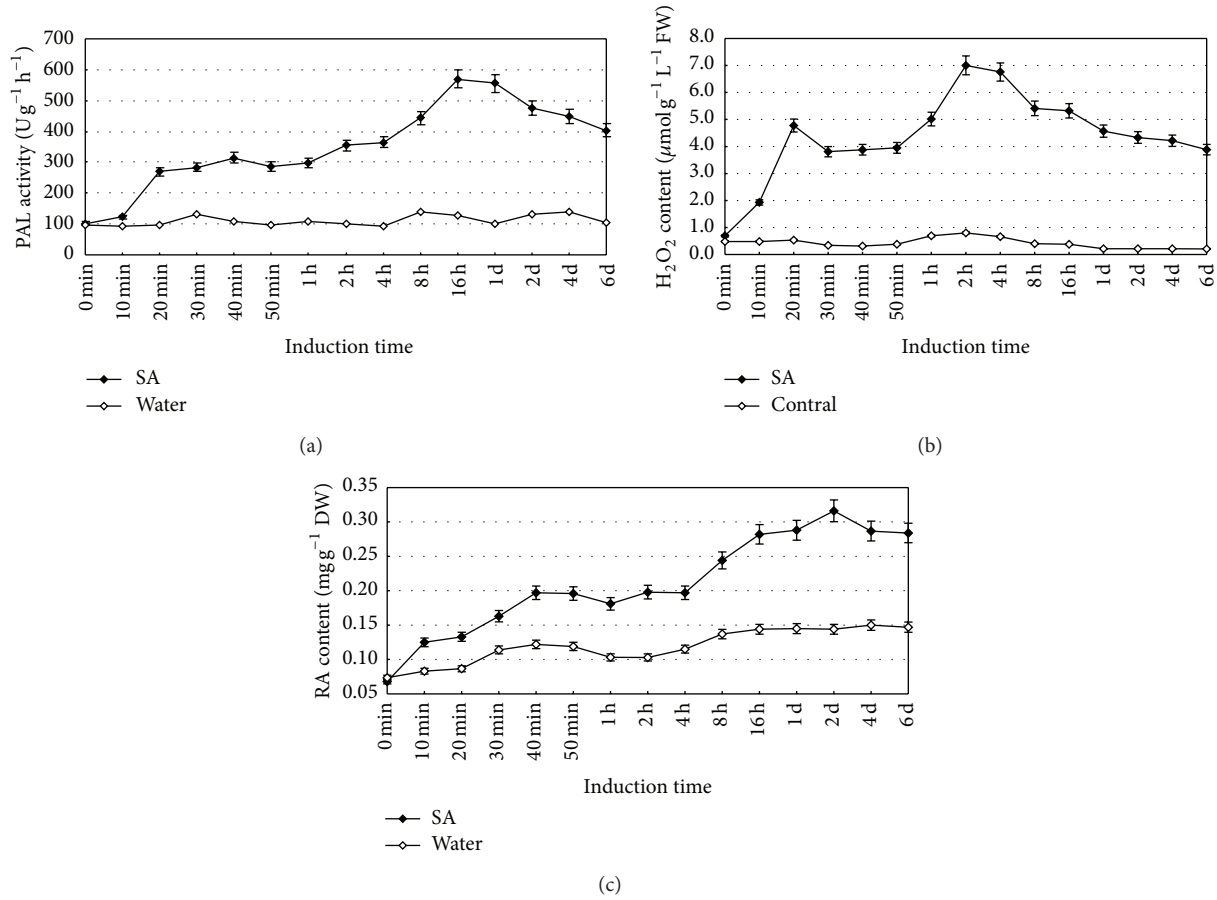

Figure 1: Exogenous SA promotes PAL activity (a), H_2O_2 production (b) and RA synthesis (c) in the suspension cultured cells of *S. miltiorrhiza*. 6-day-old suspension cultured cells treated with 22.5 mg/L SA were harvested at the time indicated. The PAL activity and contents of H_2O_2 and RA were determined. Values are means of three independent experiments. Bars represented standard errors.

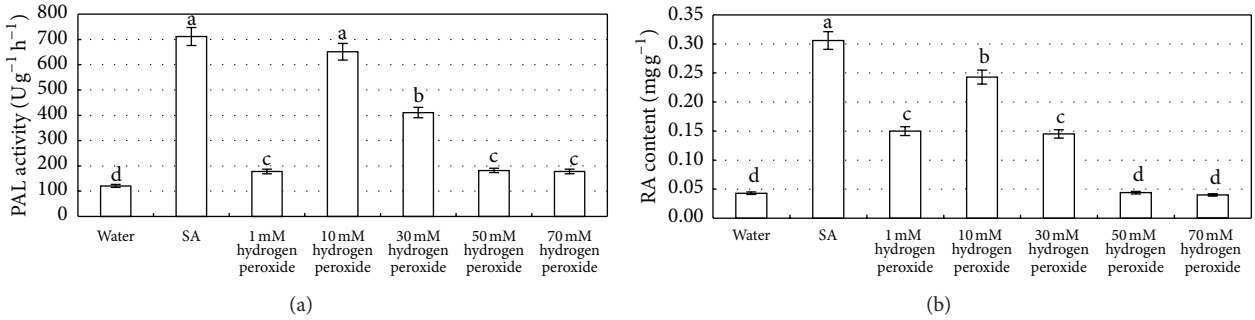

Figure 2: Effects of exogenous hydrogen peroxide with different concentrations on PAL activity (a) and RA accumulation (b) in the *S. miltiorrhiza* suspension cultured cells. The salicylic acid concentration is 22.5 mg/L. Values are means of three independent experiments. Bars represented standard errors. Different lowercase letters represent the significant differences between PAL activity (a) and RA content (b) after each treatment at the level of 5%.

pathways in plant defense network have been widely investigated during the past two decades [27, 28], but their role in secondary metabolism is rather limited. Zitta et al. [29] reports that 10 μM SA leads to a significant 4-fold increase in H_2O_2 concentrations, which may be attributed to the fact that SA can directly reduce the activity of catalase that decompose of H_2O_2 (Figure 4). As in our study, the content of H_2O_2 in SA-elicited cells was 8.51-fold higher than that of water control (Figure 1), which is consistent with these reports. Although low level (<10 μM) of H_2O_2 is thought to result in the induction of various intracellular signaling pathways [28, 29], application of either exogenous H_2O_2 (10 mM) or endogenous H_2O_2 elicited by SA (22 mg/L) showed its capacity to enhance both PAL activity and RA accumulation

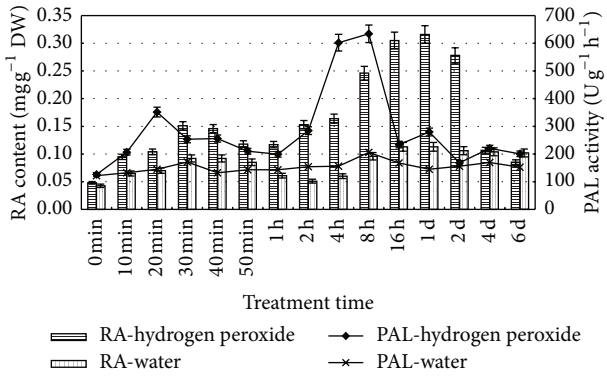

Figure 3: Exogenous hydrogen peroxide promotes PAL activity and RA production in the *S. miltiorrhiza* suspension cell cultures. 6-d-old cells treated with 10 mM H_2O_2 were harvested at the time as indicated, and RA contents and PAL activities were then determined. Values are means of three independent experiments. Bars represented standard errors.

in our experiments. PAL is the first key enzyme in the phenylpropanoid pathway for the biosynthesis of RA [30], which has been reported to be enhanced by SA in the colonization of arbusclular mycorrhizal fungus [28] and in the interaction between tomato plants and *Fusarium oxysporum* f. sp. *lycopersici* [31]. H_2O_2 comes to light as a second messenger involved in SA-elicited pathway. In this paper, both PAL activity and RA accumulation were significantly increased when exogenous 10 mM H_2O_2 was applied (Figure 2). On the other hand, H_2O_2 could be elicited by SA even though it was treated by catalase or DMTU (Figures 4 and 5), and the elicited H_2O_2 also could significantly promote RA accumulation. Our results are consistent with those reports in the fact that H_2O_2 is involved in many elicitor-induced processes to produce secondary metabolites, for instance, the biosynthesis of taxol [19], catharanthine [20], anthocyanidins [21], and anthraquinone [22].

Increasing evidence proved that plant responses to elicitors, including enzymes activation and the production of secondary metabolites, are not only regulated by signaling pathway, but also a cross-talk process. The mechanism about cross-talk among SA, H_2O_2, enzyme activity, and synthesis of secondary metabolites has gained some attention recently, but related studies are rare [32]. According to the latest progress in our lab, both nitric oxide (NO) and increase of intracellular Ca^{2+} are also involved in this cross-talk during SA induction.

Taken together, H_2O_2 production can be elicited by SA and the elicited H_2O_2 can promote PAL activity and RA accumulation, in which H_2O_2 plays an important role as a second messenger in signal transduction when SA is applied.

4. Experimental Section

4.1. Cell Culture. The detailed protocols of *S. miltiorrhiza* cell culture were provided by Dong et al. [10]. The seeds were collected from Shangluo, Shaanxi Province, and then soaked in water for 2–4 h. The wax coat was removed by gauze, followed by washing with water. The seeds were soaked in 70% ethanol for 30 s. After washing by sterile water for 3 times, the seeds were sterilized by 0.1% $HgCl_2$ for 10–15 min. They were sown in the autoclaved MS solid media after washing with sterile water for three times, supplemented with 5.5 g/L agar (Beijing Kangbeisi Sci & Tech Company) and 30 g/L sucrose (Guangzhou Jinhuada Chemical Company) to induce the germ free seedlings. The leaves of germ free seedlings were cut into 0.5 cm × 0.5 cm pieces and inoculated on the autoclaved MS solid medium supplemented with 1.0 mg/L NAA (Tianjin Bodi Chemical Company), 1.0 mg/L 6-BA (Beijing Kangbeisi Sci & Tech Company), 1.0 mg/L 2,4-D (Beijing Kangbeisi Sci & Tech Company), 5.5 g/L agar, and 30 g/L sucrose. Calli were induced and cultured at 25 ± 2°C with light intensity of 2000–3000 Lx for 12–16 h per day. After 15-day culture, the calli would be subcultured till two months when their morphological characteristics and growth rates were stable. The stable calli were collected and inoculated in MS liquid media (containing 30 g/L sucrose) with the ratio of callus to culture medium 1 : 15 (W/V). The suspension cells were cultured in the dark at 25°C with shaking speed of 125 rpm.

4.2. Elicitation and Chemical Treatments. Stock solutions of SA, H_2O_2, DMTU (H_2O_2 scavenger, Sigma, USA), CAT (Sigma, USA), and IMD (NADPH scavenger, Sigma, USA) were prepared in distilled water and then sterilized after filtration through 0.22 μm membrane. The resultant solutions with different concentrations were added in the media in accordance with the experimental design. In the control group, only distilled water with the same volume was added to substitute for the chemicals. DMTU, CAT, and IMD were added separately to the cell culture 30 min before SA treatment. All experiments were performed with three replications.

4.3. PAL Activity Assay. PAL activity was measured according to the method of Solecka and Kacperska [33] with some modifications. Fresh cultured calli were placed on filter paper in a Bucher funnel, filtered in vacuum, washed by distilled water, and filtered in vacuum again to remove the facial water. Two grams of calli were homogenized with 5 mL extraction buffer in a mortar. The homogenate was filtered through four-layer cheesecloth and centrifuged at 10000 rpm for 15 min at 4°C to get supernatant that would be used as a crude enzyme. The reaction mixture (3 mL) included 0.5 mL crude enzyme, 16 mM L-phenylalanine, 50 mM Tris-HCl buffer (pH 8.9), and 3.6 mM NaCl. The mixture was incubated at 37°C for 60 min and the reaction was stopped by 500 μL 6 M HCl. The resultant mixture was then centrifuged (12,000 ×g, 10 min). The absorbance was measured at 290 nm before and after incubation. The enzyme activity (U) was calculated by the following equation:

$$\mathrm{PAL}\left(U \cdot g^{-1}\mathrm{FW} \cdot h^{-1}\right) = \frac{A_{290} \times v_T \times v}{0.01 \times V_s \times \mathrm{FW} \times t}, \quad (1)$$

where V_t represents the total volume of enzyme solution (mL); FW is the fresh weight of calli; V_s is the volume of

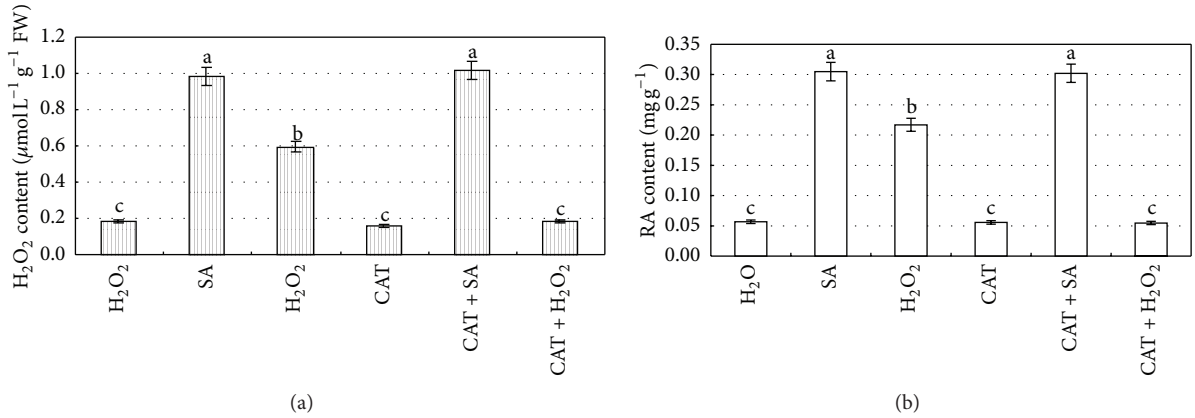

Figure 4: Influences of CAT (a scavenger of H_2O_2) on the generation of H_2O_2 (a) and the biosynthesis of RA (b) in the suspension cultured cells treated by SA and/or exogenous H_2O_2. 6-day-old suspension cultured cells treated with CAT (100 U) 30 min before SA treatment were harvested at 8 h (for H_2O_2 analysis) and 2 d (for RA analysis) later, and the H_2O_2 and rosmarinic acid contents were then determined. The SA concentration is 22.5 mg/L. The exogenous H_2O_2 concentration is 10 mM. Values are means of three independent experiments. Bars represented standard errors. Different lowercase letters represent the significant differences between the concentrations of H_2O_2 (a) and RA (b) after each treatment at the level of 5%.

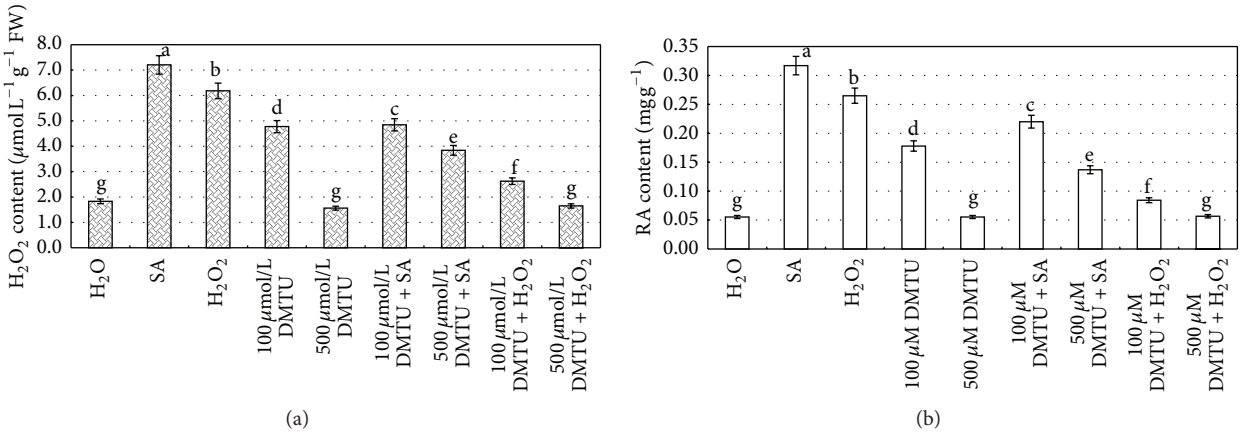

Figure 5: Inhibition of DMTU on exogenous SA in the generation of intracellular H_2O_2 (a) and the biosynthesis of RA (b) in suspension cultured cells. 8-day-old suspension cultured cells treated with DMTU 30 min before exogenous H_2O_2 and/or SA treatment as indicated were harvested at 8 h (for H_2O_2 analysis) and 2 d (for RA analysis) later, and the H_2O_2 and Sal B contents were then determined. The Salicylic acid concentration is 22.5 mg/L. The exogenous H_2O_2 concentration is 10 mM. Values are means of three independent experiments. Bars represented standard errors. Different lowercase letters represent the significant differences between the contents of H_2O_2 (a) and Sal B (b) after each treatment at the level of 5%.

the enzyme solution sampled (mL); ν is the total volume of the reaction solution (mL); and t is the reaction time (h).

4.4. Determination of Hydrogen Peroxide. Hydrogen peroxide was determined by the method of Li et al. [34]. The calli (0.2-0.3 g) were homogenized with 5 mL acetone precooled under 4°C and then ground to homogenate on the ice. The mixture was centrifuged at 12,000 rpm for 10 min at 4°C. The supernatant (2 mL) was mixed quickly with 0.5 mL 5% titanium sulfate, and ammonia solution (2 mL) was added and homogenized. The resultant mixtures were then centrifuged again; the supernatant was discarded. The precipitate (the titanium-hydro peroxide complex) was dissolved in 5 mL 2 M sulfuric acid, and the supernatant absorbance was measured at 415 nm, and the content of hydrogen peroxide was calculated.

4.5. RA Extraction and HPLC Analysis. The *S. miltiorrhiza* cells were collected from cell cultures by centrifugation at 1200 rpm, and then dried at 47.5°C in an oven till constant weight. The dried cells (0.05 g) were put into a test tube with a stopper, and the extraction was conducted with aqueous methanol (70 : 30, methanol : water) for 45 min in an ultrasonic bath. The extract was filtered through a 0.22 μm membrane and the filtrate was obtained for detection.

The content of RA was quantified by HPLC (Shimadzu, model SCL-10AVPTM equipped with UV/Vis absorbance detector, 150 mm × 4.6 mm shim-pack column,

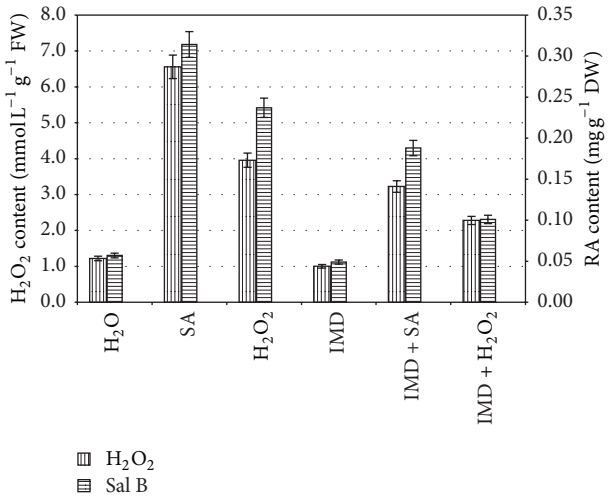

Figure 6: Inhibition of IMD on exogenous H_2O_2 and/or SA in the generation of intracellular H_2O_2 and the biosynthesis of RA in suspension cultured cells. 8-day-old suspension cultured cells treated with IMD 30 min before exogenous H_2O_2 and/or SA treatment as indicated were harvested at 8 h (for H_2O_2 analysis) and 2 d (for RA analysis) later, and the H_2O_2 and Sal B contents were then determined. The Salicylic acid concentration is 22.5 mg/L. The exogenous H_2O_2 concentration is 10 mM. The IMD concentration is 100 μM. Values are means of three independent experiments. Bars represented standard errors.

and LC-ATVP pump). The mobile phase was acetonitrile : water : phosphate (25 : 75 : 0.1, v/v/v). The flow rate was 1 mL/min and the injection amount was 10 μL. The detection wavelength was 285 nm and the column temperature was 25°C.

5. Conclusions

SA is an effective elicitor inducing RA accumulation in *S. miltiorrhiza* cell cultures, which can act independently or synergistically with H_2O_2. The intracellular H_2O_2 acts as a signal molecule to participate in RA accumulation in response to SA elicitation.

Conflict of Interests

The authors declare that there is no conflict of interests regarding the publication of this paper.

Authors' Contribution

Wenfang Hao and Hongbo Guo contributed equally to this work.

Acknowledgments

The authors gratefully acknowledge the funding and support from the Natural Science Foundation (no. 31170274) and from National Forestry Public Welfare Industry Research Project (no. 20120406).

References

[1] B. Guo, Y. C. Liang, Y. G. Zhu, and F. J. Zhao, "Role of salicylic acid in alleviating oxidative damage in rice roots (*Oryza sativa*) subjected to cadmium stress," *Environmental Pollution*, vol. 147, no. 3, pp. 743–749, 2007.

[2] Q. Hayat, S. Hayat, M. Irfan, and A. Ahmad, "Effect of exogenous salicylic acid under changing environment: a review," *Environmental and Experimental Botany*, vol. 68, no. 1, pp. 14–25, 2010.

[3] J. F. Dat, C. H. Foyer, and I. M. Scott, "Changes in salicylic acid and antioxidants during induced thermotolerance in mustard seedlings," *Plant Physiology*, vol. 118, no. 4, pp. 1455–1461, 1998.

[4] H. M. Kang and M. E. Saltveit, "Chilling tolerance of maize, cucumber and rice seedling leaves and roots are differentially affected by salicylic acid," *Physiologia Plantarum*, vol. 115, no. 4, pp. 571–576, 2002.

[5] O. Borsani, V. Valpuesta, and M. A. Botella, "Evidence for a role of salicylic acid in the oxidative damage generated by NaCl and osmotic stress in Arabidopsis seedlings," *Plant Physiology*, vol. 126, no. 3, pp. 1024–1030, 2001.

[6] A. Metwally, I. Finkemeier, M. Georgi, and K.-J. Dietz, "Salicylic acid alleviates the cadmium toxicity in barley seedlings," *Plant Physiology*, vol. 132, no. 1, pp. 272–281, 2003.

[7] A. Pastírová, M. Repčák, and A. Eliašová, "Salicylic acid induces changes of coumarin metabolites in *Matricaria chamomilla* L," *Plant Science*, vol. 167, no. 4, pp. 819–824, 2004.

[8] Y. D. Wang, Y. J. Yuan, and J. C. Wu, "Induction studies of methyl jasmonate and salicylic acid on taxane production in suspension cultures of *Taxus chinensis* var. mairei," *Biochemical Engineering Journal*, vol. 19, no. 3, pp. 259–265, 2004.

[9] Y. Zhang, Y. Wang, S. C. Jiang, M. Z. Zhang, F. H. Li, and M. P. Zhang, "Cloning of the differential expression fragment from ginseng culture induced by salicylic acid," *Genomics and Applied Biology*, vol. 28, pp. 245–250, 2009.

[10] J. Dong, G. Wan, and Z. Liang, "Accumulation of salicylic acid-induced phenolic compounds and raised activities of secondary metabolic and antioxidative enzymes in *Salvia miltiorrhiza* cell culture," *Journal of Biotechnology*, vol. 148, no. 2-3, pp. 99–104, 2010.

[11] H. Yin, A. Kjaer, X. C. Fretté et al., "Chitosan oligosaccharide and salicylic acid up-regulate gene expression differently in relation to the biosynthesis of artemisinin in *Artemisia annua* L," *Process Biochemistry*, vol. 47, no. 11, pp. 1559–1562, 2012.

[12] J. A. Martín, A. Solla, M. C. García-Vallejo, and L. Gil, "Chemical changes in Ulmus minor xylem tissue after salicylic acid or carvacrol treatments are associated with enhanced resistance to Ophiostoma novo-ulmi," *Phytochemistry*, vol. 83, pp. 104–109, 2012.

[13] M. E. Alvarez, R. I. Pennell, P.-J. Meijer, A. Ishikawa, R. A. Dixon, and C. Lamb, "Reactive oxygen intermediates mediate a systemic signal network in the establishment of plant immunity," *Cell*, vol. 92, no. 6, pp. 773–784, 1998.

[14] S. Neill, R. Desikan, and J. Hancock, "Hydrogen peroxide signalling," *Current Opinion in Plant Biology*, vol. 5, no. 5, pp. 388–395, 2002.

[15] A. Levine, R. Tenhaken, R. Dixon, and C. Lamb, "H_2O_2 from the oxidative burst orchestrates the plant hypersensitive disease resistance response," *Cell*, vol. 79, no. 4, pp. 583–593, 1994.

[16] C. S. Bestwick, I. R. Brown, M. H. R. Bennett, and J. W. Mansfield, "Localization of hydrogen peroxide accumulation during the hypersensitive reaction of lettuce cells to *Pseudomonas syringae* pv phaseolicola," *Plant Cell*, vol. 9, no. 2, pp. 209–221, 1997.

[17] Z. Chen, H. Silva, and D. F. Klessig, "Active oxygen species in the induction of plant systemic acquired resistance by salicylic acid," *Science*, vol. 262, no. 5141, pp. 1883–1886, 1993.

[18] T. Janda, G. Szalai, K. Rios-Gonzalez, O. Veisz, and E. Páldi, "Comparative study of frost tolerance and antioxidant activity in cereals," *Plant Science*, vol. 164, no. 2, pp. 301–306, 2003.

[19] Y. J. Yuan, C. Li, Z. D. Hu, and J. C. Wu, "Signal transduction pathway for oxidative burst and taxol production in suspension cultures of *Taxus chinensis* var. mairei induced by oligosaccharide from Fusarium oxysprum," *Enzyme and Microbial Technology*, vol. 29, no. 6-7, pp. 372–379, 2001.

[20] M. Xu and J. Dong, "O^{2-} from elicitor-induced oxidative burst is necessary for triggering phenylalanine ammonia-lyase activation and catharanthine synthesis in *Catharanthus roseus* cell cultures," *Enzyme and Microbial Technology*, vol. 36, no. 2-3, pp. 280–284, 2005.

[21] K. T. Hung, D. G. Cheng, Y. T. Hsu, and C. H. Kao, "Abscisic acid-induced hydrogen peroxide is required for anthocyanin accumulation in leaves of rice seedlings," *Journal of Plant Physiology*, vol. 165, no. 12, pp. 1280–1287, 2008.

[22] M. Perassolo, C. V. Quevedo, V. D. Busto, A. M. Giulietti, and J. R. Talou, "Role of reactive oxygen species and proline cycle in anthraquinone accumulation in *Rubia tinctorum* cell suspension cultures subjected to methyl jasmonate elicitation," *Plant Physiology and Biochemistry*, vol. 49, no. 7, pp. 758–763, 2011.

[23] "Chinese Pharmacopoeia Commission," Pharmacopoeia of the People's Republic of China, Beijing, China, 2010.

[24] M. Jiao, R. Cao, H. Chen, W. Hao, and J. Dong, "Effects of salicylic acid on synthesis of rosmarinic acid and related enzymes in the suspension cultures of *Salvia miltiorrhiza*," *Shengwu Gongcheng Xuebao/Chinese Journal of Biotechnology*, vol. 28, no. 3, pp. 320–328, 2012.

[25] C. K. Auh and T. M. Murphy, "Plasma membrane redox enzyme is involved in the synthesis of O^{2-} and H_2O_2 by Phytophthora elicitor-stimulated rose cells," *Plant Physiology*, vol. 107, no. 4, pp. 1241–1247, 1995.

[26] J. Foreman, V. Demidchik, J. H. F. Bothwell et al., "Reactive oxygen species produced by NADPH oxidase regulate plant cell growth," *Nature*, vol. 422, no. 6930, pp. 442–446, 2003.

[27] C. An and Z. Mou, "Salicylic acid and its function in plant immunity," *Journal of Integrative Plant Biology*, vol. 53, no. 6, pp. 412–428, 2011.

[28] R.-Q. Zhang, H.-H. Zhu, H.-Q. Zhao, and Q. Yao, "Arbuscular mycorrhizal fungal inoculation increases phenolic synthesis in clover roots via hydrogen peroxide, salicylic acid and nitric oxide signaling pathways," *Journal of Plant Physiology*, vol. 170, no. 1, pp. 74–79, 2013.

[29] K. Zitta, P. Meybohm, B. Bein et al., "Salicylic acid induces apoptosis in colon carcinoma cells grown in-vitro: influence of oxygen and salicylic acid concentration," *Experimental Cell Research*, vol. 318, no. 7, pp. 828–834, 2012.

[30] S. Mandal, I. Kar, A. K. Mukherjee, and P. Acharya, "Elicitor-induced defense responses in *Solanum lycopersium* against *Ralstonia solanacearum*," *The Scientific World Journal*, vol. 2013, Article ID 561056, 9 pages, 2013.

[31] S. Mandal, N. Mallick, and A. Mitra, "Salicylic acid-induced resistance to *Fusarium oxysporum* f. sp. lycopersici in tomato," *Plant Physiology and Biochemistry*, vol. 47, no. 7, pp. 642–649, 2009.

[32] Y. Wang, C. C. Dai, Y. W. Zhao, and Y. Peng, "Fungal endophyte-induced volatile oil accumulation in *Atractylodes lancea* plantlets is mediated by nitric oxide, salicylic acid and hydrogen peroxide," *Process Biochemistry*, vol. 46, no. 3, pp. 730–735, 2011.

[33] D. Solecka and A. Kacperska, "Phenylpropanoid deficiency affects the course of plant acclimation to cold," *Physiologia Plantarum*, vol. 119, no. 2, pp. 253–262, 2003.

[34] S. W. Li, L. Xue, S. Xu, H. Feng, and L. An, "Hydrogen peroxide acts as a signal molecule in the adventitious root formation of mung bean seedlings," *Environmental and Experimental Botany*, vol. 65, no. 1, pp. 63–71, 2009.

Hindawi Publishing Corporation
The Scientific World Journal
Volume 2014, Article ID 437684, 12 pages
http://dx.doi.org/10.1155/2014/437684

Review Article

A Meta-Analysis of the Bacterial and Archaeal Diversity Observed in Wetland Soils

Xiaofei Lv,[1,2] Junbao Yu,[1] Yuqin Fu,[1,2] Bin Ma,[1] Fanzhu Qu,[1] Kai Ning,[1,2] and Huifeng Wu[1]

[1] *Key Laboratory of Coastal Zone Environmental Processes and Ecological Remediation, Yantai Institute of Coastal Zone Research (YIC), Chinese Academy of Sciences (CAS), Shandong Provincial Key Laboratory of Coastal Zone Environmental Processes, YICCAS, Yantai 264003, China*
[2] *University of Chinese Academy of Sciences, Beijing 100049, China*

Correspondence should be addressed to Junbao Yu; junbao.yu@gmail.com

Received 22 February 2014; Revised 10 April 2014; Accepted 24 April 2014; Published 28 May 2014

Academic Editor: Xu Gang

This study examined the bacterial and archaeal diversity from a worldwide range of wetlands soils and sediments using a meta-analysis approach. All available 16S rRNA gene sequences recovered from wetlands in public databases were retrieved. In November 2012, a total of 12677 bacterial and 1747 archaeal sequences were collected in GenBank. All the bacterial sequences were assigned into 6383 operational taxonomic units (OTUs 0.03), representing 31 known bacterial phyla, predominant with Proteobacteria (2791 OTUs), Bacteroidetes (868 OTUs), Acidobacteria (731 OTUs), Firmicutes (540 OTUs), and Actinobacteria (418 OTUs). The genus *Flavobacterium* (11.6% of bacterial sequences) was the dominate bacteria in wetlands, followed by Gp1, *Nitrosospira*, and *Nitrosomonas*. Archaeal sequences were assigned to 521 OTUs from phyla Euryarchaeota and Crenarchaeota. The dominating archaeal genera were *Fervidicoccus* and *Methanosaeta*. Rarefaction analysis indicated that approximately 40% of bacterial and 83% of archaeal diversity in wetland soils and sediments have been presented. Our results should be significant for well-understanding the microbial diversity involved in worldwide wetlands.

1. Introduction

Wetlands, which were estimated to be 45% of the total value of global natural ecosystems [1], are one of the most important terrestrial ecosystems and distribute in all regions throughout the world including Antarctica [2]. Microbiomes in wetlands play an important role in biogeochemical processes and microbial activities are crucial to the functions of wetland systems [3–8]. Moreover, microbial diversity is essential for exploiting potential of microbial resources from the wetland ecosystems [9–13]. It is crucial and necessary to understand the overall survival microorganisms in wetlands. Bacteria and archaea have been widely studied with respect to their biodiversity in natural and constructed wetlands [14–17]. Initial studies employed traditional culture-dependent methods and resulted in the discovery of plenty of new bacterial and archaeal taxa [18]. Employing kinds of molecular biology methods, increasing evidences have suggested that the structures of microbial communities are related to soil processes, such as cloning and sequencing of 16S rRNA genes, denaturing gradient gel electrophoresis (DGGE), terminal restriction fragment length polymorphism (T-RFLP), and quantitative PCR [4, 8, 19–23]. Cloning and sequencing of 16S rRNA genes have been widely used for their identification of potential known and unknown microbes [24]. Plenty of studies have examined the microbial diversity in wetlands using relatively large (>200 sequences) 16S rRNA clone libraries [4, 20, 25]. However, most studies to date have focused on individual wetland ecosystem [16, 26–28]. Many of the datasets published contain a small number of cloned sequences (generally >100), thus revealing only a small portion of the full diversity present in wetlands [10, 11, 29, 30]. The focus of some studies is limited to particular microbial group [31, 32]. In addition, there are many sequences recovered from wetlands with no additional information which were deposited into GenBank without being reported

yet. High-throughput sequencing technologies, such as 454-pyrosequencing and ion torrent, were used to analyze the microbiomes in wetlands [30, 33–35]. These methods can produce huge datasets of short sequence reads. However, the length of these reads is too short to classify. Currently, there is no consensus on the size or nature of the microbial diversity generally found in wetlands. As a result, the understanding of the microbiomes in wetlands is fragmented and likely biased. This knowledge gap of microbiomes in wetlands will hamper the efficiency and stability of wetlands ecosystems. Few of the collective overviews of the microbial diversity in global wetlands are found up to date. The purposes of the study are to (1) perform a meta-analysis of all publicly available 16S rRNA gene sequences identified from various wetlands to provide a collective appraisal of the microbial diversity in wetland ecosystem, (2) make an effort to estimate the current coverage of the microbial diversity in wetlands, and (3) identify particular gaps in the knowledge and understanding of the microbial populations involved in wetlands.

2. Methods

2.1. Sequence Data Collection. Initial sequence sets were obtained from the GenBank (http://www.ncbi.nlm.nih.gov) and RDP (Release 10, http://rdp.cme.msu.edu) databases using the search terms ("wetland" OR "marsh" OR "fen") AND "soil" AND "16S" on November 11, 2012. Non-16S rRNA sequences from GenBank were removed by checking the name of sequences. All 16S rRNA gene sequences from two databases were merged. Duplicate sequences identified based on accession numbers were removed. Mallared was used for checking sequences with vector nucleotides or chimera (http://www.softsea.com/review/Mallard.html). The 16S rRNA gene sequences of *Escherichia coli* (accession number: U00096) and *Methanothermobacter thermoautotrophicus* (accession number: AE000666) were selected as reference sequences for bacteria and archaea, respectively. In order to avoid uncertainties in comparing and classifying short sequences, sequences shorter than 250 bp were removed from the dataset which have few or no sequence overlap. The remaining sequences comprised the redacted composite dataset used in this work.

2.2. Phylogenetic Analysis. Sequences were aligned with Kalign [36] and classified into taxonomic ranks using the RDP Classifier with default settings [37]. Based on the output classifications from the RDP Classier, treemaps were constructed using the treemap packages in R. The dataset was divided into the following groups based on the classifications: Archaea, Bacteria, Proteobacteria, Actinobacteria, Firmicutes, Acidobacteria, Bacteroidetes, Chloroflexi, and the collected "minor phyla" of bacteria that comprised sequences not assigned to any of the aforementioned phyla. Distances matrices of aligned sequences were computed within ARB using Jukes-Cantor correction [38]. Individual distance matrices were analyzed using Mothur [39] to cluster OTUs, generated rarefaction curves, and estimated the expected maximum species richness complementary to the ACE and Chao1 richness. Unless otherwise stated, the genetic distance ≤0.03 was used to define species-level OTUs. The distance cut-off for other taxonomic ranks was set as follows: 0.05, genus; 0.10, family; 0.15, class/order; and 0.2, phylum. All the estimated asymptotes of the rarefaction curve were determined through R package monomol (https://github.com/binma/monomol) [40]. The coverage percentages were calculated as described by Nelson et al. [41].

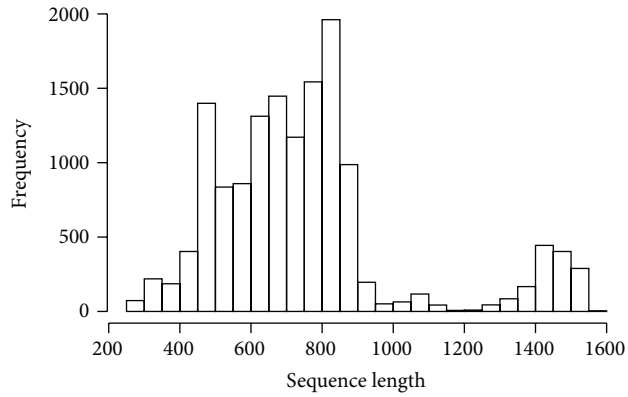

Figure 1: Distribution of the length of retrieved 16S rRNA sequences.

2.3. Accession Numbers. The accession numbers for all sequences analyzed in this study were available from the corresponding author. The sequences were currently maintained in an in-house ARB database of 16S rRNA gene sequences for wetlands. A copy of this database and the sequence alignment were also available by request from the corresponding author.

3. Results and Discussion

This study was conducted as a meta-analysis ground on publicly available 16S rRNA gene sequences recovered from wetland soils worldwide. The sequences dataset collected from Genbank and RDP database was analyzed no matter their previously assigned taxonomic information or other analyses.

To address the long-term question of understanding microorganisms from wetland soil habitats, this study first aimed at characterizing prokaryotic communities inhabiting wetland soils. The prokaryotic microorganisms from wetland soil habitats drive the biogeochemical cycles of elements and may be a source of novel halophilic enzymes. Thus, we studied the diversity of prokaryotic microorganisms from wetland soils with meta-analysis approach.

3.1. Data Summary. Totally 14318 sequences longer than 250 bp were retrieved from GenBank and RDP databases. The sequences were mostly about 800 bp long, followed by approximately 600 bp (Figure 1). Interestingly, there is a small submit of sequence length between 1400 bp and 1600 bp. The 12583 bacterial sequences were assigned to 6383 OTUs, while the 1735 archaeal sequences were assigned to 521 OTUs (Table 1 and Figure 1). The most abundant bacterial and

Table 1: Diversity statistics for Archaea, Bacteria, and "Major" phylum groups. Coverage = #OTUs/rarefaction estimate; OTU and abundance were calculated using a 0.03 dissimilarity cut-off.

Group	Total sequences	Unclassified to phylum	Number of OTUs	ACE	Chao1	Rarefaction estimation	Current coverage (%)
Bacteria	12583	none	6383	30581	17176	15768	41
Pro	5763		2791	12472	7245	6811	40
Act	783		418	2280	1088	1033	46
Aci	1345		731	2972	1693	1602	28
Fir	973		540	3595	1856	1915	54
Bact	2244		868	2700	1887	1601	59
Archaea	1735	none	521	1131	884	883	83
Eur	925		418	681	505	504	62
Cre	810		197	442	311	320	41

archaeal OTU contained 143 sequences and 113 sequences, respectively. Over 90% bacterial sequences were classified within five phyla, namely, Proteobacteria, Bacteroidetes, Acidobacteria, Firmicutes, and Actinobacteria (Figure 2). The remaining sequences were classified within 26 "minor" phyla, of which Chloroflexi, Planctomycetes, Cyanobacteria, and Verrucomicrobia were the only "minor" phyla with representation 1% of all bacterial sequences.

Of the archaeal sequences analyzed, all of them were classified within two phyla: Euryarchaeota and Crenarchaeota, representing 925 and 810 sequences, respectively.

3.2. Bacteria

3.2.1. Proteobacteria. The Proteobacteria was the largest and most diverse phylum in the present dataset. It comprised a total of 5637 sequences, approximately 44.8% of the bacterial sequences, assigned to 466 known genera. There are 2791 OTUs generated, with a Simpson diversity index of 0.0020. All six classes within the Proteobacteria were represented, but the Delta-, Gamma-, Beta-, and Alphaproteobacteria together represented over 99% of the proteobacterial sequences (Figure 3). The classes Epsilonproteobacteria and Zetaproteobacteria were extremely rare, represented by 43 and 1 sequences, respectively, indicating a low recovery rate in most of wetlands.

Classes in Proteobacteria showed various tendencies in different wetlands. The wide distribution of Gammaproteobacteria and Deltaproteobacteria in marine sediment has been documented, and most of them were involved in sulfur reduction under anaerobic conditions [4]. In comparison, a high abundance of Alphaproteobacteria and Betaproteobacteria appeared in freshwater sediment, and it is significantly correlated with pH and nutrients [34]. Some genera of Betaproteobacteria were confirmed to inhabit extremely alkaline wetland filled with historic steel slag [42]. The Epsilonproteobacteria is relatively abundant at oxic-anoxic interfaces such as intertidal wetland [43].

Deltaproteobacteria was the largest class in the phylum, with 1627 sequences (28.9% of the proteobacteria). *Geobacter* of family Geobacteraceae was the most abundant genus (9.8% of the Deltaproteobacteria) in Deltaproteobacteria. It was abundant in the rhizosphere and has been widely known as a kind of Fe (III)-reducing bacterium [44]. The followed abundant genera were *Deltaproteobacteria*, *Desulfosarcina*, *Desulfopila*, *Desulfovibrio*, *Desulfonema*, and *Desulfobacterium*, which represented greater than 1.0% of proteobacterial sequences. All of them were sulfate-reducing bacteria, and their distributions were influenced by salinity and plant nutrient [45]. They played important roles in the metabolism of nitrogen, phosphorus, sulfur, and some organic compounds in wetland systems [18, 46]. *Anaeromyxobacter* was also the genus owning more than 1.0% proteobacterial sequences. As a kind of facultative bacteria, its unique respiratory reduction of nitrate and nitrite to ammonia was not linked to its ability to reduce nitrous oxide to nitrogen gas [47].

For the class Gammaproteobacteria, 1456 sequences were identified. It was the second largest class in Proteobacteria. Approximately 12.6% of gammaproteobacterial sequences (184 sequences) were assigned to the genus *Rhodanobacter* of family Xanthomonadaceae. This genus might be engaged in acidic denitrification in wetland soils [3]. The following abundant genera were *Thioprofundum* and *Methylobacter*, accounting for 8.9% (129 sequences) and 8.0% (108 sequences) of gammaproteobacterial sequences, respectively. *Thioprofundum* was recently considered as a mesophilic, facultatively anaerobic, sulfur-oxidizing bacterial strain [48]. *Methylobacter* was reported as dominating in the Zoige wetland where the centers of methane emission were [24]. However, it was not affected by nitrogen leached from the catchment area in boreal littoral wetlands [9]. The other genera representing more than 1.0% proteobacteria sequences were *Ectothiorhodosinus*, *Pseudomonas*, and *Steroidobacter*. *Pseudomonas* was one of the widely studied PAH-degrading bacteria; it spread widely in contaminated wetlands environment [29] and was predominant microbial populations in the constructed wetland for nitrobenzene wastewater [32].

The 1420 betaproteobacterial sequences were identified in Proteobacteria. The genus *Nitrosomonas* was the predominant genera with 222 assigned sequences, while the genus *Nitrosospira* was the second abundant genus with 217 sequences. They were also the first and second most abundant proteobacterial genera, and both of them belonged to the family Nitrosomonadaceae which were well known as the main

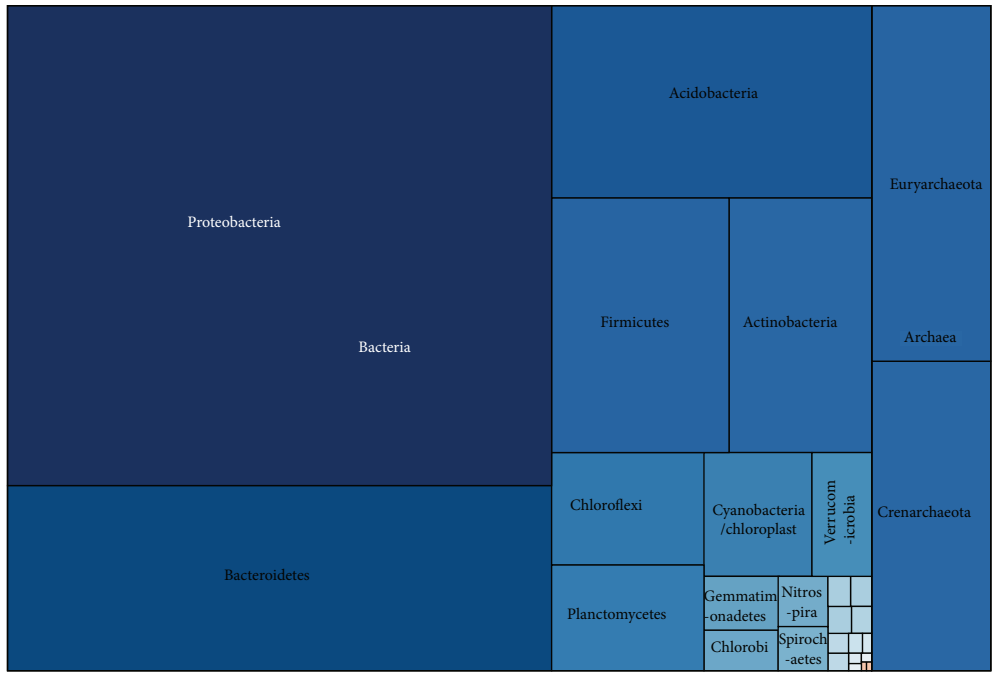

Figure 2: Treemap of observed prokaryotic taxons shown in their hierarchical order. Treemap showing taxonomic ranking of all taxa for all retrieved sequences. The size of each box is proportional to the number of sequences assigned to that taxon with respect to the entire dataset. The placement of boxes is arbitrary with respect to boxes within the same taxonomic rank and does not correspond to any form of phylogeny or relatedness.

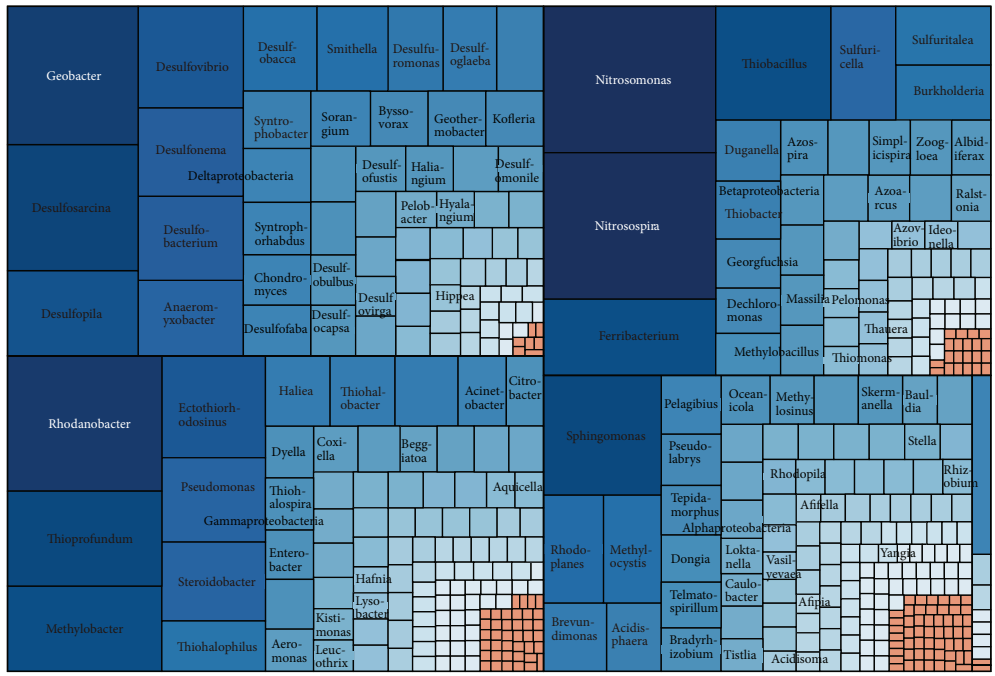

Figure 3: Treemap of observed Proteobacteria taxons shown in their hierarchical order.

ammonia-oxidizing microorganisms contributing to N_2O production in wetlands and sediments [31, 49, 50]. The genera *Ferribacterium*, *Thiobacillus*, and *Sulfuricella* owned more than 1.0% of proteobacterial sequences.

The fourth largest proteobacterial class was Alphaproteobacteria, with 1090 sequences (over 19.3%). The dominating genus *Sphingomonas* in class Alphaproteobacteria was widely distributed in wetland and sediments, due to its ability to survive in low concentrations of nutrients, as well as to metabolize a wide variety of carbon sources [7, 51]. Except for *Sphingomonas* which contains over 2.0% of the proteobacterial sequences (122 sequences), other genera of Alphaproteobacteria represented less than 1.0% proteobacteria sequences.

3.2.2. Bacteroidetes. Bacteroidetes was the second abundant phylum in the present dataset, including 2244 sequences (nearly 17.8% of all bacterial sequences), which were assigned to 109 known genera, with 868 OTUs and a Simpson diversity index of 0.0007 (Figure 4). A plenty of Bacteroidetes strains isolated from wetland soils and sediments were reported to be anaerobic and saprophytic representative bacteria [52, 53]. Highlighting the unevenness of the phylum, over 70% of all the Bacteroidetes sequences (12.8% of all bacterial sequences) were assigned to class Flavobacteria. As a common heterotrophic obligate aerobe, Flavobacteria was the second largest class in the dataset. It is widespread in various wetlands, even in swine wastewater lagoon and constructed wetlands [54, 55]. The class Sphingobacteria was represented by only 491 sequences, while the class Bacteroidia was represented by only 75 sequences. "Undefined Bacteroidetes" comprised 65 sequences.

The most frequently observed genus in Flavobacteria was *Flavobacterium* (1459 sequences), which was also the most abundant bacterial genus in this dataset. A number of species of *Flavobacterium* have been isolated from rhizosphere of wetland [52, 53].

3.2.3. Acidobacteria. Acidobacteria was the third largest phylum in our dataset, including 1345 sequences assigned to 29 genera. Acidobacteria is a new phylum, whose members are physiologically diverse and ubiquitous in soils, but are underrepresented in culture at present. There were 731 OTUs identified, with a Simpson diversity index of 0.0031 (Figure 5). Just over 90% of all the acidobacterial sequences (9.7% of all bacterial sequences) were assigned to 21 unclassified groups, only 130 sequences represented to class Holophagae. In total, nearly 40% of the Acidobacteria sequences were able to be classified to Gp1, which was the second largest class of bacteria. The following classes were group Gp3 and then group Gp6, with 196 and 116 sequences, respectively. As the reports, Acidobacteria group was more abundant in natural wetlands than in created wetlands [10, 34], especially in freshwater sediment [34]. Acidobacteria has been reported as the largest division in the active layer and the associated permafrost of a moderately acidic wetland in Canada [11]. Future studies are needed to examine the interrelations of environmental parameters with Acidobacteria and individual populations within subgroups [56].

3.2.4. Firmicutes. The fourth largest phylum was the Firmicutes, assigned into 973 sequences and 540 OTUs with a Simpson diversity index of 0.0041 (Figure 6). As saprophytic microbes, some members of Firmicutes are known to produce endospores under stressful environmental conditions such as in intertidal sediment [34], extremely alkaline (pH > 12) constructed wetland [42].

In total, about 45% of the Firmicutes sequences were classified to the class Clostridia, and nearly 36% were classified into the class Bacilli. The Clostridia (sulfite-reducing bacteria) is an anaerobic and highly polyphyletic bacterium, while Bacilli can be obligate aerobes or facultative anaerobes. There was a long record of evidence to suggest that both of them were the abundant taxa in sewage sludge [57]. Some species of them exhibit great ability to degrade hydrocarbons in crude oil contaminated wetland ultisol [6]. Within the class Bacilli, two primary genera were *Bacillus* and *Pasteuria*, representing 107 and 98 sequences, respectively. While in Clostridia, genus *Stricto* was the most abundant genus, with 56 sequences.

The class Negativicutes represented 178 sequences. The genus *Succinispira* represented over 70% of sequences in Negativicutes. The genus *Succinispira*, the most abundant genus in Firmicutes, was capable of decarboxylating succinate in anaerobic conditions. The class Erysipelotrichia represented only three sequences.

3.2.5. Actinobacteria. As the fifth abundant phylum, Actinobacteria represented 783 sequences, clustered into 418 OTUs, with a Simpson diversity index of 0.0054. All of Acidobacteria sequences were classified to the class Actinobacteria and over 66% of them belonged to order Actinomycetales (Figure 7). Actinobacteria can be terrestrial or aquatic, playing an important role in the decomposition of organic materials. Although understood primarily as soil bacteria, they might be more abundant in freshwaters [10, 57].

Mycobacterium (103 sequences) was the most frequently observed genus in Actinobacteria. It has been widely detected from contaminated soil or sediments [51]. Some species of *Mycobacterium* were the dominant PAH-degraders and played an important role in degrading PAHs in contaminated mangrove sediments [7]. The following abundant genera were *Aciditerrimonas*, *Conexibacter*, *Arthrobacter*, and *Ilumatobacter*. The rest of genera were less than 5% of actinobacterial sequences.

3.2.6. Minor Phyla. In addition to the five phyla described above, 26 minor phyla with 1601 sequences were also observed based on the dataset. Of these minor phyla, only the phyla Chloroflexi (2.96%), Planctomycetes (2.77%), Cyanobacteria (2.28%), and Verrucomicrobia (1.28%) represented more than 1% of all the bacterial sequences and accounted for over 73% of all minor phyla sequences (Figure 1).

Some known genera were represented in these "minor phyla." The most abundant of the minor phyla, Chloroflexi, comprised 372 sequences. Members of the Chloroflexi are generally found in intertidal sediment and moderately acidic wetland [11, 13, 34, 58]. Planctomycetes was the second most abundant of the minor phyla, to which 349 sequences were assigned. A number of genera of the Planctomycetes, which were once thought to occur primarily in aquatic environments, have been discovered in wetlands [12, 29]. As the third most abundant minor phyla, Cyanobacteria occupy a broad range of habitats across all latitudes. They are widespread in freshwater, marine, and even in the most extreme niches such as hot springs and hypersaline bays [12, 59, 60]. Evidence suggests that Verrucomicrobia are abundant within the environment and important. The species of Verrucomicrobia have been identified and isolated from fresh water and soil environments [61].

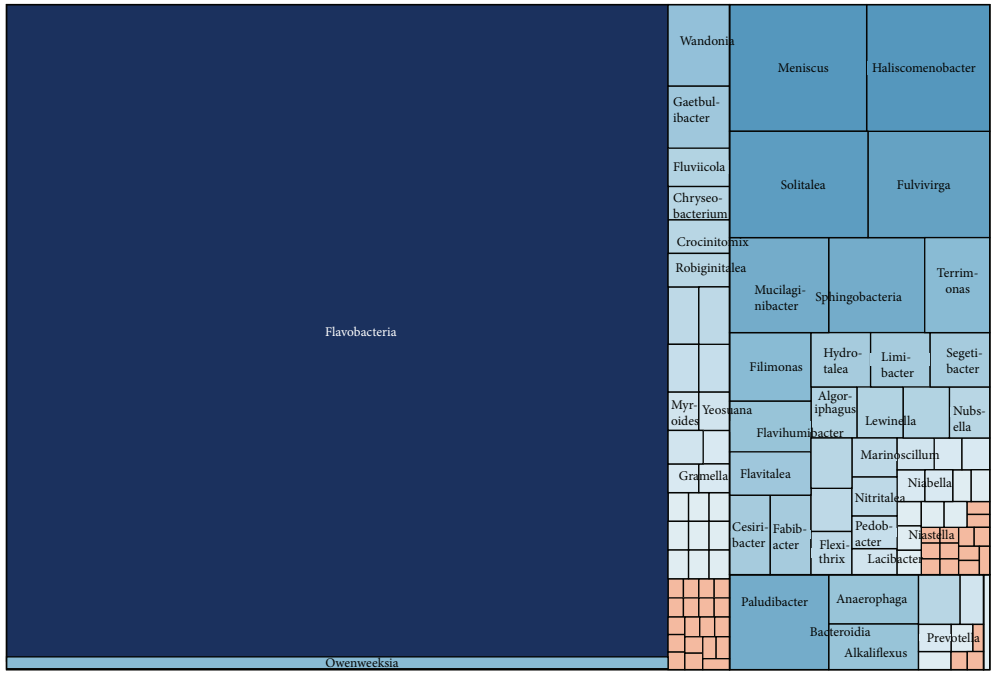

Figure 4: Treemap of observed Bacteroidetes taxons shown in their hierarchical order.

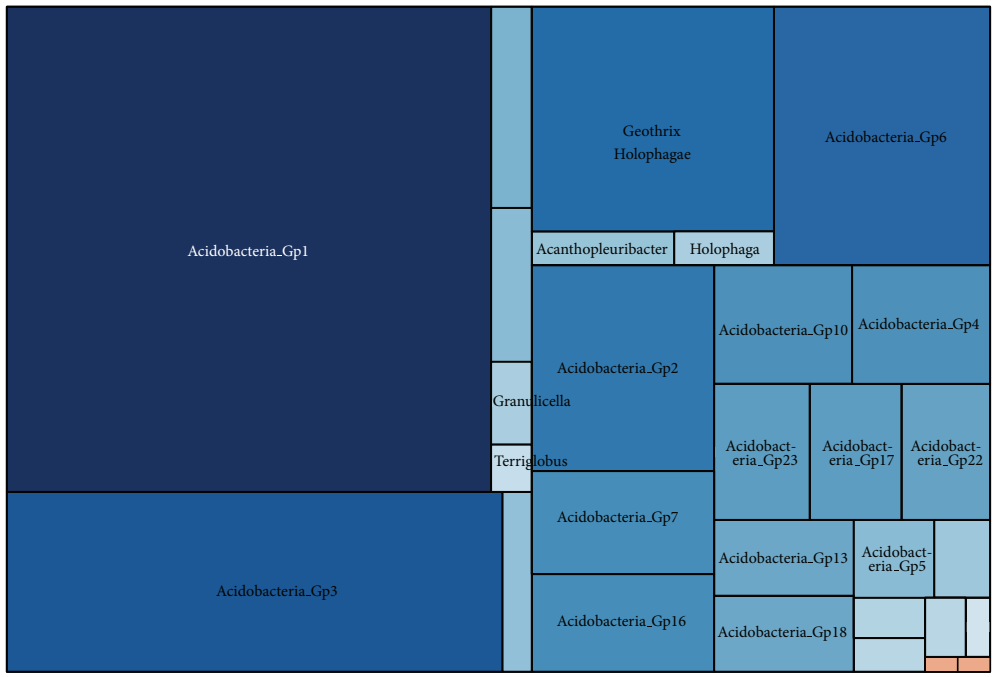

Figure 5: Treemap of observed Acidobacteria taxons shown in their hierarchical order.

3.3. Archaea

3.3.1. Euryarchaeota. Euryarchaeota comprised 925 sequences, approximately 53.3% archaeal sequences. They were clustered into 418 OTUs with a Simpson diversity index of 0.0054 (Figure 8). The majority (70.9%) of Euryarchaeota sequences were assigned to the methanogenic class Methanomicrobia (656 sequences). The class Thermoplasmata comprised 132 sequences, while the class Methanobacteria comprised 75 sequences. Only 59 sequences were classified into class Halobacteria. Classes Archaeoglobi and Methanopyri represented only 2 and 1 sequences, respectively.

Methanomicrobia contributes a large proportion of methane emission in wetlands, no matter in cold area or in subtropical places [19, 62]. As seen in Figure 6, the most predominate Methanomicrobia genus (223 sequences)

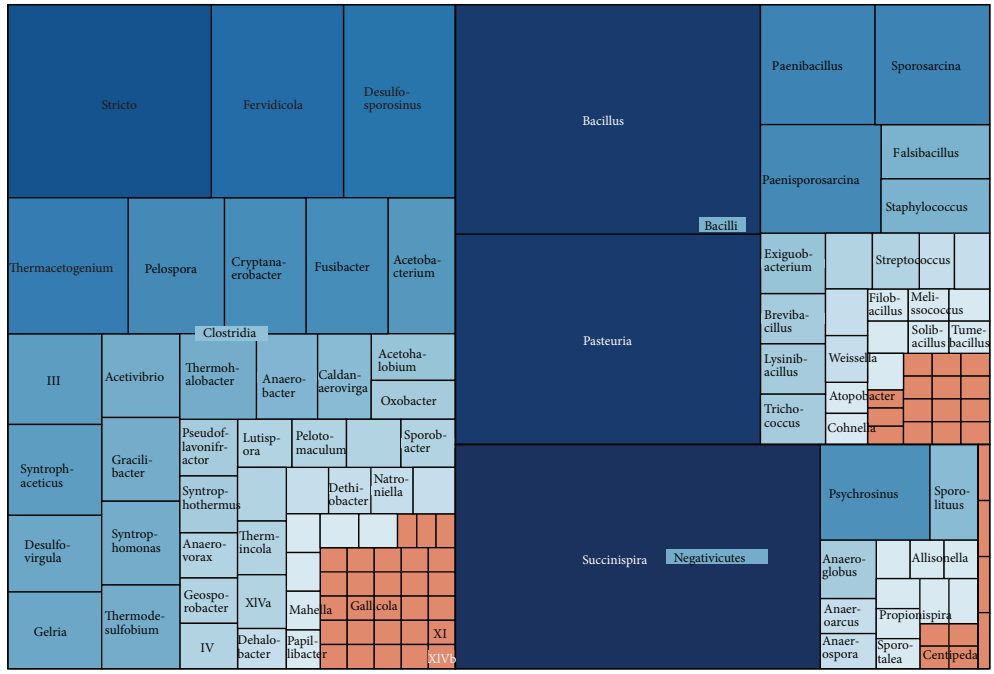

Figure 6: Treemap of observed Firmicutes taxons shown in their hierarchical order.

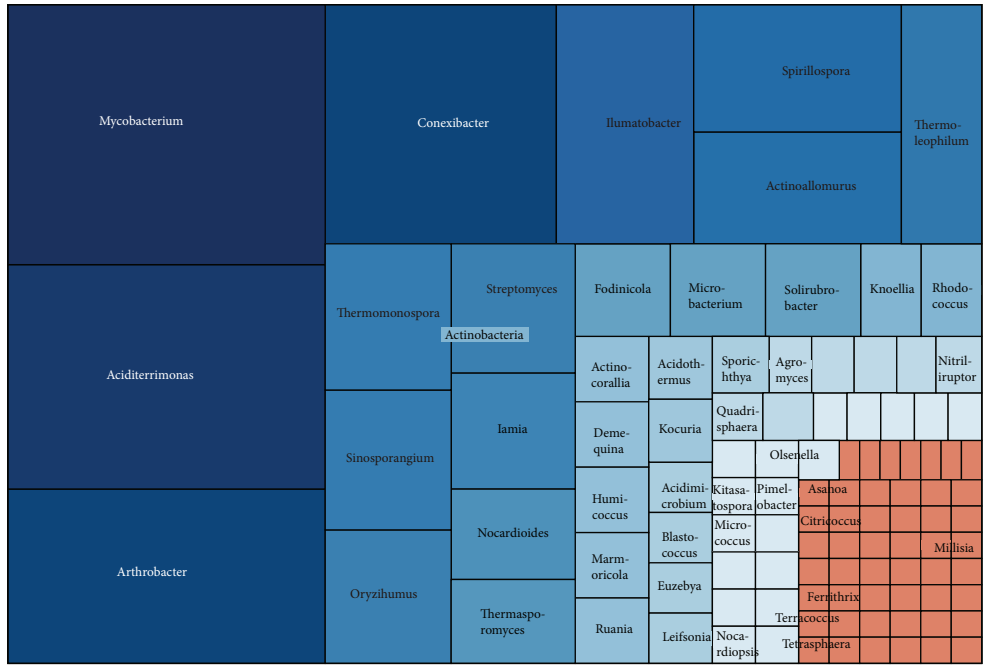

Figure 7: Treemap of observed Actinobacteria taxons shown in their hierarchical order.

was *Methanosaeta* (formerly *Methanothrix*), which was also the second most abundant archaeal genus. It was reported precisely as the dominant acetoclastic methanogen in the high arctic wetlands [63]. The methanogens genera *Methanosarcina*, *Methanocella*, *Methanolinea*, and *Methanoregula* each represented nearly 10% of Euryarchaeota sequences. The other 12 genera were only represented by a small number of sequences in the dataset.

The largest genus in class Thermoplasmata was *Thermogymnomonas* (120 sequences), which was detected widely even at low pH wetlands. It was known as a kind of iron-oxidizing microorganisms [64]. The rest 12 sequence of Euryarchaeota were assigned to genus *Ferroplasma*, an anaerobic and acidophilic archaea, which coupled to the reduction of ferric iron [5]. Of the class Methanobacteria, there were two genera, *Methanobacterium* and *Methanosphaera*, with 57 and

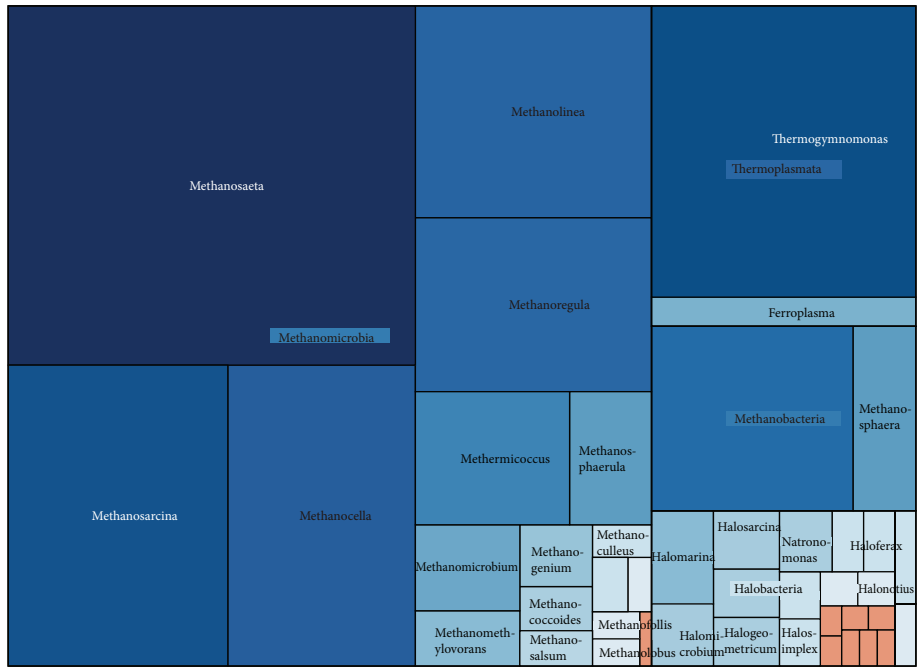

Figure 8: Treemap of observed Euryarchaeota taxons shown in their hierarchical order.

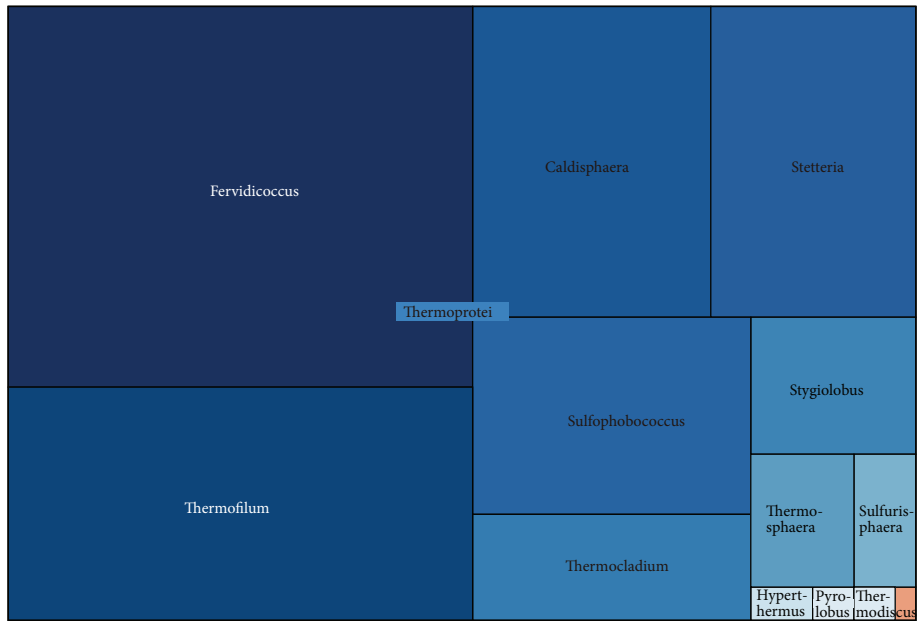

Figure 9: Treemap of observed Crenarchaeota taxons shown in their hierarchical order.

18 sequences, respectively. Both of these genera were detected from water and sediments of a high-altitude athalassohaline wetland [25]. As a facultative anaerobic archaea, Halobacteria was common in most environments where large amounts of salt, moisture, and organic material are available [25].

3.3.2. Crenarchaeota. Crenarchaeota owned less abundant sequences than Euryarchaeota in the dataset, with 810 sequences. Crenarchaeota diversity was lower, with only 197 OTUs generated and a Simpson diversity index of 0.0443. It suggested that Crenarchaeota was more related to aerobic metabolisms in the water and surface sediment [65].

All of the Crenarchaeota sequences were assigned to the class Thermoprotei (Figure 9). As the reports, class Thermoprotei dominated in archaeal phyla in Pacific influenced sediments, while Methanomicrobia inhabited in methane-containing Atlantic influenced sediments [58]. Within the class, 258 sequences were classified to the genera *Fervidicoccus*. *Fervidicoccus* was the most abundant genera in archaeal

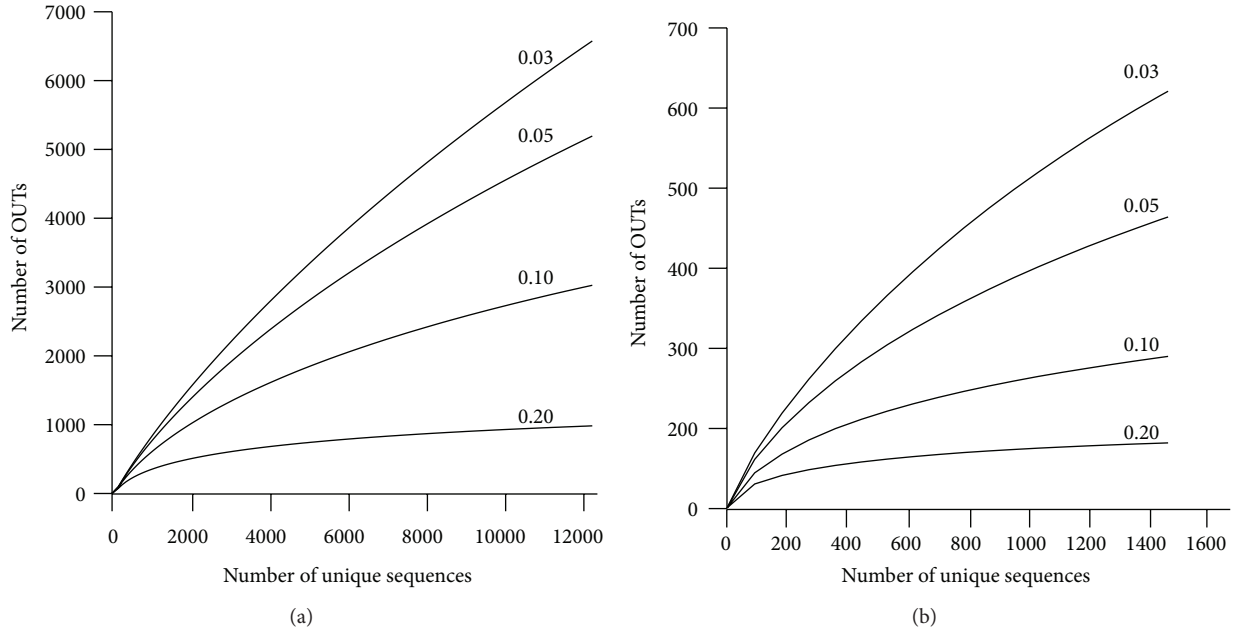

Figure 10: Rarefaction curve for the Archaea (a) and Bacteria (b) with different dissimilarity cut-off.

and has been cultivated and characterized widely. The following abundant genera in this phylum were *Thermofilum* (19.5%), *Caldisphaera* (13.3%), and *Stetteria* (11.5%). The other genera sequences were less than 10%.

3.4. Diversity Estimates. For all of the bacterial groups, the ACE value of richness was the greatest, while the majority of corresponding rarefaction estimates were the lowest (Table 1). Similar with rarefaction estimates, the ACE and Chao1 estimate the maximum species richness for an OUT definition. However, the richness estimates derived from the rarefaction curves differed less from the Chao1 estimate, comparing with those from ACE estimates. The richness estimates derived from ACE differed greatly (72~120%) for Bacteria, Proteobacteria, Acidobacteria, Firmicutes, and Actinobacteria, while the corresponding estimates for the Bacteroidetes, Archaea, Euryarchaeota, and Crenarchaeota were less than 70% different.

The present results showed that the coverage of microbial diversity in wetlands was remaining rather low. Rarefaction analysis of Bacteria showed that only sampling at the phylum (0.20 phylogenetic distance) level has begun to reach a horizontal plateau. The other sampling at the taxonomic ranks was still projecting upward (Figure 10 and Table 2). At the species (0.03 phylogenetic distance) level, only 41% of the expected diversity has been revealed. The estimates of current coverage suggest that of Bacteria was less than that of Actinobacteria, Bacteroidetes, and Firmicutes, greater than that of Acidobacteria. Coverage rate of Proteobacteria was similar to that of the Bacteria. For the archaea, the coverage of diversity was greater than bacteria, but still low compared to estimated richness. There was about 59% of the expected diversity revealed at the species level. The estimates of current coverage of Euryarchaeota and Crenarchaeota were much greater than that of Archaea. As the results of rarefaction analysis and diversity statistics, it was obvious that the known bacterial and archaeal diversity in wetlands were incomplete below the phylum level. Nevertheless, the global microbial diversity in wetlands revealed in this study had ability to serve as a framework for future studies of alpha and beta diversity. More specifically, the collected sequence dataset could give a hand on detecting and quantifying specific groups of either bacteria or archaea at the nucleotide level. Additionally, these studies will greatly advance the ecology of individual microbia collected in the dataset.

Table 2: Estimates of current taxonomic coverage for Archaea and Bacteria.

Distance	Number of Current OTUs	Rarefaction estimation	Coverage[a] (%)
Archaea			
0.03	521	883	59
0.05	364	587	62
0.10	190	278	68
0.20	82	91	90
Bacteria			
0.03	6383	15768	40
0.05	5042	9854	51
0.10	2937	4617	63
0.20	954	1118	85

[a]Coverage = number of OTUs/rarefaction estimate.

Sufficient coverage and depth were provided to explore an individual sample or compare multiple samples through multiplexing, with the developing of second generation sequencing technologies. Moreover, new sequences dataset could

be added to the composite datasets analyzed in this study to increase our knowledge on the diversity of this ecosystem. The knowledge on the diversity may shine light on the understanding of the microbiomes of wetlands and define the significance of individual microbia. It is also suited for continuous following of the succession variation of the diversity of wetlands. However, the beta diversity was hardly determined because most of studies could not contain large sequence datasets and detailed information with same methodologies and sequence submission criteria. A "core group" was defined after analyzing seven municipal sludge digesters [66]. Although distinct microbiomes are possibly being selected under a unique environment, only a small number of "core OTUs" can be found among the large numbers of OTUs identified. Systematic studies examining multiple wetlands designs with great depth of coverage should help further define the "core microbiomes" in wetlands.

Now that analysis of 16S rRNA gene sequences can provide insight into the functional diversity of wetlands, the metabolic functions of organisms are getting more concerned. For a good comprehension of the metabolic capacities of these organisms, metagenomic studies techniques such as SIP and MAR-FISH should be used more frequently. Cultivation-based studies are also needed to define the functions of uncharacterized species of bacteria and archaea in wetlands.

4. Conclusions

The present dataset generated from GenBank and RDP databases was largely dominated by Proteobacteria. Approximately 40% of sequences and OTUs belonged to Proteobacteria. Our results showed that (1) nearly 56% of the archaeal and 45% of the bacterial species-level diversity in wetlands have been witnessed; (2) sequences from the bacterial phyla Proteobacteria, Bacteroidetes, Chloroflexi, Firmicutes, Actinobacteria, and archaeal class were well represented by the available sequences and the corresponding microorganisms were probably important participants in the wetland environments; (3) the global diversity contains numerous groups for which there was no close cultured representative, especially the majority of sequences assigned to the phyla Chloroflexi and Bacteroidetes. Therefore future studies should utilize multiple approaches to characterize the microbial diversity and its function in wetlands.

Conflict of Interests

The authors declare that there is no conflict of interests regarding the publication of this paper.

Authors' Contribution

Xiaofei Lv, Junbao Yu, and Yuqin Fu contributed equally to this work.

Acknowledgments

The authors would like to thank the Project of National Science & Technology Pillar Program in "12th Five Year" period (2011BAC02B01), National Natural Science Foundation for Distinguished Young Scholar of Shandong Province (no. JQ201114), the National Science Foundation of China (41301333), and the CAS/SAFEA International Partnership Program for Creative Research Teams "Representative environmental processes and resources effects in coastal zone." They also would like to thank the Yellow River Delta Wetland Ecological Experimental Station, CAS, for providing experimental and residential place for this study.

References

[1] R. Costanza, R. d'Arge, R. de Groot et al. et al., "The value of the world's ecosystem services and natural capital," *Nature*, vol. 387, no. 6630, pp. 253–260, 1997.

[2] A. D. Jungblut, S. A. Wood, I. Hawes, J. Webster-Brown, and C. Harris, "The pyramid trough wetland: environmental and biological diversity in a newly created Antarctic protected area," *FEMS Microbiology Ecology*, vol. 82, no. 2, pp. 356–366, 2012.

[3] R. N. van den Heuvel, E. van der Biezen, M. S. M. Jetten, M. M. Hefting, and B. Kartal, "Denitrification at pH 4 by a soil-derived Rhodanobacter-dominated community," *Environmental Microbiology*, vol. 12, no. 12, pp. 3264–3271, 2010.

[4] S. Lenk, J. Arnds, K. Zerjatke, N. Musat, R. Amann, and M. Mußmann, "Novel groups of Gammaproteobacteria catalyse sulfur oxidation and carbon fixation in a coastal, intertidal sediment," *Environmental Microbiology*, vol. 13, no. 3, pp. 758–774, 2011.

[5] N. B. Justice, C. Pan, R. Mueller et al. et al., "Heterotrophic archaea contribute to carbon cycling in low-pH, suboxic biofilm communities," *Applied and Environmental Microbiology*, vol. 78, no. 23, pp. 8321–8330, 2012.

[6] R. C. John, A. Y. Itah, J. P. Essien, and D. I. Ikpe, "Fate of nitrogen-fixing bacteria in crude oil contaminated wetland ultisol," *Bulletin of Environmental Contamination and Toxicology*, vol. 87, no. 3, pp. 343–353, 2011.

[7] C. Guo, L. Ke, Z. Dang, and N. F. Tam, "Temporal changes in Sphingomonas and Mycobacterium populations in mangrove sediments contaminated with different concentrations of polycyclic aromatic hydrocarbons (PAHs)," *Marine Pollution Bulletin*, vol. 62, no. 1, pp. 133–139, 2011.

[8] B. Hu, L. Shen, X. Lian et al. et al., "Evidence for nitrite-dependent anaerobic methane oxidation as a previously overlooked microbial methane sink in wetlands," *Proceedings of the National Academy of Science*, vol. 111, pp. 4495–4500, 2014.

[9] H. M. Siljanen, A. Saari, L. Bodrossy, and P. J. Martikainen, "Effects of nitrogen load on the function and diversity of methanotrophs in the littoral wetland of a boreal lake," *Frontiers in Microbiology*, vol. 3, p. 39, 2012.

[10] R. M. Peralta, C. Ahn, and P. M. Gillevet, "Characterization of soil bacterial community structure and physicochemical properties in created and natural wetlands," *Science of the Total Environment*, vol. 443, pp. 725–732, 2012.

[11] R. C. Wilhelm, T. D. Niederberger, C. Greer, and L. G. Whyte, "Microbial diversity of active layer and permafrost in an acidic wetland from the Canadian high arctic," *Canadian Journal of Microbiology*, vol. 57, no. 4, pp. 303–315, 2011.

[12] R. Prasanna, L. Nain, A. K. Pandey, and A. K. Saxena, "Microbial diversity and multidimensional interactions in the rice ecosystem," *Archives of Agronomy and Soil Science*, vol. 58, no. 7, pp. 723–744, 2012.

[13] M. E. Farias, M. Contreras, M. C. Rasuk et al., "Characterization of bacterial diversity associated with microbial mats, gypsum evaporites and carbonate microbialites in thalassic wetlands: tebenquiche and La Brava, Salar de Atacama, Chile," *Extremophiles*, vol. 18, no. 2, pp. 311–329, 2014.

[14] Y. F. Wang and J. D. Gu, "Higher diversity of ammonia/ammonium-oxidizing prokaryotes in constructed freshwater wetland than natural coastal marine wetland," *Applied Microbiology and Biotechnology*, vol. 97, no. 15, pp. 7015–7033, 2013.

[15] H. Schmidt and T. Eickhorst, "Spatio-temporal variability of microbial abundance and community structure in the puddled layer of a paddy soil cultivated with wetland rice (*Oryza sativa L.*)," *Applied Soil Ecology*, vol. 72, pp. 93–102, 2013.

[16] C. J. Decker and R. Parker, "Analysis of double-stranded RNA from microbial communities identifies double-stranded RNA virus-like elements," *Cell Reports*, vol. 7, no. 3, pp. 898–906, 2014.

[17] M. Bouali, E. Pelletier, S. Chaussonnerie, D. le Paslier, A. Bakhrouf, and A. Sghir, "Characterization of rhizosphere prokaryotic diversity in a horizontal subsurface flow constructed wetland using a PCR cloning-sequencing based approach," *Applied Microbiology and Biotechnology*, vol. 97, no. 9, pp. 4221–4231, 2013.

[18] P. Vladár, A. Rusznyák, K. Márialigeti, and A. K. Borsodi, "Diversity of sulfate-reducing bacteria inhabiting the rhizosphere of Phragmites australis in Lake Velencei (Hungary) revealed by a combined cultivation-based and molecular approach," *Microbial Ecology*, vol. 56, no. 1, pp. 64–75, 2008.

[19] G. Zhang, J. Tian, N. Jiang, X. Guo, Y. Wang, and X. Dong, "Methanogen community in Zoige wetland of Tibetan plateau and phenotypic characterization of a dominant uncultured methanogen cluster ZC-I," *Environmental Microbiology*, vol. 10, no. 7, pp. 1850–1860, 2008.

[20] S. Kato, T. Itoh, and A. Yamagishi, "Archaeal diversity in a terrestrial acidic spring field revealed by a novel PCR primer targeting archaeal 16S rRNA genes," *FEMS Microbiology Letters*, vol. 319, no. 1, pp. 34–43, 2011.

[21] J. Tang, X. Ding, L. Wang et al., "Effects of wetland degradation on bacterial community in the Zoige Wetland of Qinghai-Tibetan Plateau (China)," *World Journal of Microbiology and Biotechnology*, vol. 28, no. 2, pp. 649–657, 2012.

[22] Z.-Y. Wang, Y.-Z. Xin, D.-M. Gao, F.-M. Li, J. Morgan, and B.-S. Xing, "Microbial community characteristics in a degraded wetland of the yellow river delta," *Pedosphere*, vol. 20, no. 4, pp. 466–478, 2010.

[23] B. Ma, X. Lv, A. Warren, and J. Gong, "Shifts in diversity and-community structure of endophytic bacteria and archaea across root, stem and leaf tissues in the common reed, Phragmites australis, along a salinity gradient in a marine tidal wetland of northern China," *Antonie van Leeuwenhoek International Journal of General and Molecular Microbiology*, vol. 104, pp. 759–768, 2013.

[24] J. Yun, G. Zhuang, A. Ma, H. Guo, Y. Wang, and H. Zhang, "Community structure, abundance, and activity of methanotrophs in the Zoige wetland of the Tibetan Plateau," *Microbial Ecology*, vol. 63, no. 4, pp. 835–843, 2012.

[25] C. Dorador, I. Vila, F. Remonsellez, J. F. Imhoff, and K.-P. Witzel, "Unique clusters of Archaea in Salar de Huasco, an athalassohaline evaporitic basin of the Chilean Altiplano," *FEMS Microbiology Ecology*, vol. 73, no. 2, pp. 291–302, 2010.

[26] Y. F. Wang, Y. Y. Feng, X. J. Ma, and J. D. Gu, "Seasonal dynamics of ammonia/ammonium-oxidizing prokaryotes in oxic and anoxic wetland sediments of subtropical coastal mangrove," *Applied Microbiology and Biotechnology*, vol. 97, no. 17, pp. 7919–7934, 2013.

[27] A. F. Scavino, Y. Ji, J. Pump, M. Klose, P. Claus, and R. Conrad, "Structure and function of the methanogenic microbial communities in Uruguayan soils shifted between pasture and irrigated rice fields," *Environmental Microbiology*, vol. 15, no. 9, pp. 2588–2602, 2013.

[28] C. Dorador, I. Vila, K. P. Witzel, and J. F. Imhoff, "Bacterial and archaeal diversity in high altitude wetlands of the Chilean Altiplano," *Fundamental and Applied Limnology*, vol. 182, no. 2, pp. 135–159, 2013.

[29] M. A. Khan, "Environmental contamination of Hokersar Wetland Waters in Kashmir Himalayan Valley, India," *Journal of Environmental Science and Engineering*, vol. 52, no. 2, pp. 157–162, 2010.

[30] B. A. Frank-Fahle, E. Yergeau, C. W. Greer, H. Lantuit, and D. Wagner, "Microbial functional potential and community composition in permafrost-affected soils of the NW Canadian Arctic," *Plos ONE*, vol. 9, no. 1, Article ID e84761, 2014.

[31] S. S. Domingos, S. Dallas, L. Skillman, S. Felstead, and G. Ho, "Nitrogen removal and ammonia-oxidising bacteria in a vertical flow constructed wetland treating inorganic wastewater," *Water Science and Technology*, vol. 64, no. 3, pp. 587–594, 2011.

[32] Y. Lin, J. Yin, J. Wang, and W. Tian, "Performance and microbial community in hybrid Anaerobic Baffled Reactor-constructed wetland for nitrobenzene wastewater," *Bioresource Technology*, vol. 118, pp. 128–135, 2012.

[33] Y. Yu, H. Wang, J. Liu et al., "Shifts in microbial community function and structure along the successional gradient of coastal wetlands in Yellow River Estuary," *European Journal of Soil Biology*, vol. 49, pp. 12–21, 2012.

[34] Y. Wang H Sheng, Y. He, J. Wu, Y. Jiang, N. Tam, and H. Zhou, "Comparison of the levels of bacterial diversity in freshwater, intertidal wetland, and marine sediments by using millions of illumina tags," *Applied and Environmental Microbiology*, vol. 78, no. 23, pp. 8264–8271, 2012.

[35] E. Yergeau, J. R. Lawrence, S. Sanschagrin, M. J. Waiser, D. R. Korber, and C. W. Greer, "Next-generation sequencing of microbial communities in the Athabasca River and its tributaries in relation to oil sands mining activities," *Applied and Environmental Microbiology*, vol. 78, no. 21, pp. 7626–7637, 2012.

[36] T. Lassmann and E. L. L. Sonnhammer, "Kalign—an accurate and fast multiple sequence alignment algorithm," *BMC Bioinformatics*, vol. 6, article 298, 2005.

[37] J. R. Cole, B. Chai, R. J. Farris et al., "The Ribosomal Database Project (RDP-II): sequences and tools for high-throughput rRNA analysis," *Nucleic Acids Research*, vol. 33, pp. D294–D296, 2005.

[38] D. L. Cohen and R. R. Townsend, "Is there added value to adding ARB to ACE inhibitors in the management of CKD?" *Journal of the American Society of Nephrology*, vol. 20, no. 8, pp. 1666–1668, 2009.

[39] P. D. Schloss, S. L. Westcott, T. Ryabin et al., "Introducing mothur: open-source, platform-independent, community-supported software for describing and comparing microbial communities," *Applied and Environmental Microbiology*, vol. 75, no. 23, pp. 7537–7541, 2009.

[40] B. Ma and J. Gong, "A meta-analysis of the publicly available bacterial and archaeal sequence diversity in saline soils," *World Journal of Microbiology & Biotechnology*, vol. 29, no. 12, pp. 2325–2334, 2013.

[41] M. C. Nelson, M. Morrison, and Z. Yu, "A meta-analysis of the microbial diversity observed in anaerobic digesters," *Bioresource Technology*, vol. 102, no. 4, pp. 3730–3739, 2011.

[42] G. S. Roadcap, R. A. Sanford, Q. Jin, J. R. Pardinas, and C. M. Bethke, "Extremely alkaline (pH > 12) ground water hosts diverse microbial community," *Ground Water*, vol. 44, no. 4, pp. 511–517, 2006.

[43] H. F. dos Santos, J. C. Cury, F. L. do Carmo et al., "Mangrove bacterial diversity and the impact of oil contamination revealed by pyrosequencing: bacterial proxies for oil pollution," *PLoS ONE*, vol. 6, no. 3, Article ID e16943, 2011.

[44] G. Imfeld, C. E. Aragonés, I. Fetzer et al., "Characterization of microbial communities in the aqueous phase of a constructed model wetland treating 1,2-dichloroethene-contaminated groundwater," *FEMS Microbiology Ecology*, vol. 72, no. 1, pp. 74–88, 2010.

[45] M. Miletto, A. Loy, A. M. Antheunisse, R. Loeb, P. L. E. Bodelier, and H. J. Laanbroek, "Biogeography of sulfate-reducing prokaryotes in river floodplains," *FEMS Microbiology Ecology*, vol. 64, no. 3, pp. 395–406, 2008.

[46] Y. H. Li, J. N. Zhu, Z. H. Zhai, and Q. Zhang, "Endophytic bacterial diversity in roots of Phragmites australis in constructed Beijing Cuihu Wetland (China)," *FEMS Microbiology Letters*, vol. 309, no. 1, pp. 84–93, 2010.

[47] R. A. Sanford, D. D. Wagner, Q. Wu et al., "Unexpected nondenitrifier nitrous oxide reductase gene diversity and abundance in soils," *Proceedings of the National Academy of Sciences of the United States of America*, vol. 109, no. 48, pp. 19709–19714, 2012.

[48] K. Mori, K.-I. Suzuki, T. Urabe et al., "*Thioprofundum hispidum* sp. nov., an obligately chemolithoautotrophic sulfur-oxidizing gammaproteobacterium isolated from the hydrothermal field on Suiyo Seamount, and proposal of *Thioalkalispiraceae* fam. nov. in the order *Chromatiales*," *International Journal of Systematic and Evolutionary Microbiology*, vol. 61, part 10, pp. 2412–2418, 2011.

[49] J. Wu, J. Zhang, W.-L. Jia, H.-J. Xie, and R. R. Gu, "Nitrous oxide fluxes of constructed wetlands to treat sewage wastewater," *Huan Jing Ke Xue*, vol. 30, no. 11, pp. 3146–3151, 2009.

[50] A. Tietz, R. Hornek, G. Langergraber, N. Kreuzinger, and R. Haberi, "Diversity of ammonia oxidising bacteria in a vertical flow constructed wetland," *Water Science and Technology*, vol. 56, no. 3, pp. 241–247, 2007.

[51] C.-H. Li, H.-W. Zhou, Y.-S. Wong, and N. F.-Y. Tam, "Vertical distribution and anaerobic biodegradation of polycyclic aromatic hydrocarbons in mangrove sediments in Hong Kong, South China," *Science of the Total Environment*, vol. 407, no. 21, pp. 5772–5779, 2009.

[52] M. Liu, Y. H. Li, Y. Liu et al., "*Flavobacterium phragmitis* sp. nov., an endophyte of reed (*Phragmites australis*)," *International Journal of Systematic and Evolutionary Microbiology*, vol. 61, part 11, pp. 2717–2721, 2011.

[53] Y.-P. Xiao, W. Hui, J.-S. Lee, K. C. Lee, and Z.-X. Quan, "*Flavobacterium dongtanense sp. nov.*, isolated from the rhizosphere of a wetland reed," *International Journal of Systematic and Evolutionary Microbiology*, vol. 61, part 2, pp. 343–346, 2011.

[54] X. Dong and G. B. Reddy, "Nutrient removal and bacterial communities in swine wastewater lagoon and constructed wetlands," *Journal of Environmental Science and Health A: Toxic/Hazardous Substances and Environmental Engineering*, vol. 45, no. 12, pp. 1526–1535, 2010.

[55] G. Jin and T. R. Kelley, "Characterization of microbial communities in a pilot-scale constructed wetland using PLFA and PCR-DGGE analyses," *Journal of Environmental Science and Health A: Toxic/Hazardous Substances and Environmental Engineering*, vol. 42, no. 11, pp. 1639–1647, 2007.

[56] A. Naether, B. U. Foesel, V. Naegele et al., "Environmental factors affect *Acidobacterial* communities below the subgroup level in grassland and forest soils," *Applied and Environmental Microbiology*, vol. 78, no. 20, pp. 7398–7406, 2012.

[57] G. Zhang, Q. Zhao, Y. Jiao, K. Wang, D.-J. Lee, and N. Ren, "Efficient electricity generation from sewage sludge usingbiocathode microbial fuel cell," *Water Research*, vol. 46, no. 1, pp. 43–52, 2012.

[58] L. J. Hamdan, R. B. Coffin, M. Sikaroodi, J. Greinert, T. Treude, and P. M. Gillevet, "Ocean currents shape the microbiome of Arctic marine sediments," *ISME Journal*, vol. 7, no. 4, pp. 685–696, 2012.

[59] O. Choi, A. Das, C.-P. Yu, and Z. Hu, "Nitrifying bacterial growth inhibition in the presence of algae and cyanobacteria," *Biotechnology and Bioengineering*, vol. 107, no. 6, pp. 1004–1011, 2010.

[60] A. Barberán and E. O. Casamayor, "Global phylogenetic community structure and β-diversity patterns in surface bacterioplankton metacommunities," *Aquatic Microbial Ecology*, vol. 59, no. 1, pp. 1–10, 2010.

[61] K. Yu and T. Zhang, "Metagenomic and metatranscriptomic analysis of microbial community structure and gene expression of activated sludge," *Plos ONE*, vol. 7, no. 5, Article ID e38183, 2012.

[62] M. Utsumi, S. E. Belova, G. M. King, and H. Uchiyama, "Phylogenetic comparison of methanogen diversity in different wetland soils," *Journal of General and Applied Microbiology*, vol. 49, no. 2, pp. 75–83, 2003.

[63] L. Høj, R. A. Olsen, and V. L. Torsvik, "Archaeal communities in High Arctic wetlands at Spitsbergen, Norway (78∘N) as characterized by 16S rRNA gene fingerprinting," *FEMS Microbiology Ecology*, vol. 53, no. 1, pp. 89–101, 2005.

[64] E. González-Toril, Á. Águilera, V. Souza-Egipsy, E. L. Pamo, J. S. España, and R. Amils, "Geomicrobiology of La Zarza-Perrunal acid mine effluent (Iberian Pyritic Belt, Spain)," *Applied and Environmental Microbiology*, vol. 77, no. 8, pp. 2685–2694, 2011.

[65] K. C. Costa, J. B. Navarro, E. L. Shock, C. L. Zhang, D. Soukup, and B. P. Hedlund, "Microbiology and geochemistry of great boiling and mud hot springs in the United States Great Basin," *Extremophiles*, vol. 13, no. 3, pp. 447–459, 2009.

[66] D. Rivière, V. Desvignes, E. Pelletier et al., "Towards the definition of a core of microorganisms involved in anaerobic digestion of sludge," *ISME Journal*, vol. 3, no. 6, pp. 700–714, 2009.

Hindawi Publishing Corporation
The Scientific World Journal
Volume 2014, Article ID 487961, 5 pages
http://dx.doi.org/10.1155/2014/487961

Research Article

Distribution Characteristic of Soil Organic Carbon Fraction in Different Types of Wetland in Hongze Lake of China

Yan Lu[1,2] and Hongwen Xu[1]

[1] *School of Urban and Environmental Science, Huaiyin Normal University, Huai'an 223300, China*
[2] *Jiangsu Key Laboratory for Eco-Agricultural Biotechnology around Hongze Lake, Huai'an 223300, China*

Correspondence should be addressed to Hongwen Xu; hongwen_xu@163.com

Received 10 May 2014; Accepted 13 May 2014; Published 22 May 2014

Academic Editor: Hongbo Shao

Soil organic carbon fractions included microbial biomass carbon (MBC), dissolved organic carbon (DOC), and labile organic carbon (LOC), which was investigated over a 0–20 cm depth profile in three types of wetland in Hongze Lake of China. Their ecoenvironmental effect and the relationships with soil organic carbon (SOC) were analyzed in present experiment. The results showed that both active and SOC contents were in order reduced by estuarine wetland, flood plain, and out-of-lake wetland. Pearson correlative analysis indicated that MBC and DOC were positively related to SOC. The lowest ratios of MBC and DOC to SOC in the estuarine wetland suggested that the turnover rate of microbial active carbon pool was fairly low in this kind of wetland. Our results showed that estuarine wetland had a strong carbon sink function, which played important role in reducing greenhouse gas emissions; besides, changes of water condition might affect the accumulation and decomposition of organic carbon in the wetland soils.

1. Introduction

Wetland played a key role in the global cycles of carbon, which had important function in the global carbon balance and climate change mitigation [1–3]. Carbon cycle process in different types of wetland could provide basis for further understanding of the mechanism of carbon sources and sinks in terrestrial ecosystem [4–6]. Decrease of carbon storage and vegetation biomass in wetland soils might release more carbon into atmosphere, thus causing the increase of atmospheric carbon dioxide concentration [7–10]. Meanwhile, global warming could accelerate decomposition of soil organic matter and release of carbon into atmosphere, which would further strengthen the trend of global warming [11, 12]. Original alteration in soil organic carbon pool of wetland occurred mainly on the part easily to be decomposed and mineralized, that is, activated carbon [13]. Soil activated carbon was referred to the part of the organic carbon with poor stability and higher activity for plants and soil microorganisms [14]. Soil microbial biomass carbon (MBC) and dissolved organic carbon (DOC) were important characteristic indicators for expressing the activity of active soil organic carbon pool [15]. Although active organic carbon was just a very small part of total carbon, its sizes and turnover rates were of great importance to the content and recycling of soil available nutrients, and it was directly related to greenhouse gas emissions [16]. Therefore, exploring the changes of soil active organic carbon in different types of wetland was helpful in achieving deep understanding of the characteristics of wetland soil organic carbon and the response to climate change.

Hongze Lake (33°06′N~33°40′N, 118°10′E~118°55′E) is the fourth largest fresh water lake in China. It is located in the northwest of Jiangsu province, and its water area is 1597 km^2. The lake and the surrounding area have composed a relatively intact inland wetland as typical lake wetland of China. Differences might exist in soil carbon pool due to various hydrological conditions and vegetation for kinds of wetland. Although researches on soil carbon in wetland have been well documented, limited systematic investigations focus on different types of natural lakes wetland soil carbon and their ecological environment effect. In order to study the distribution characteristics of different types of wetland soil active organic carbon about Hongze Lake Wetland, MBC,

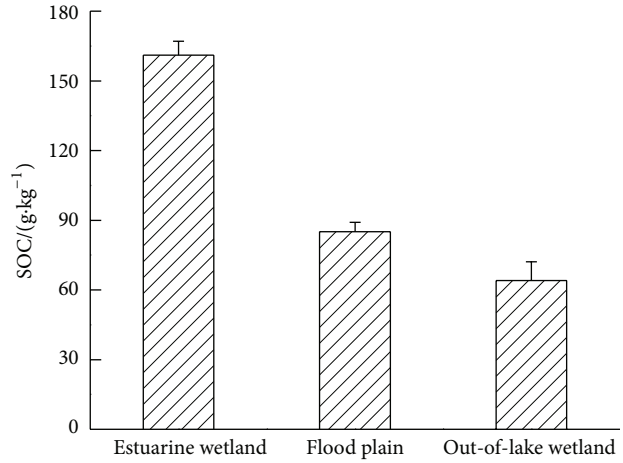

Figure 1: Changes of SOC content under different types of wetland in Hongze Lake of China.

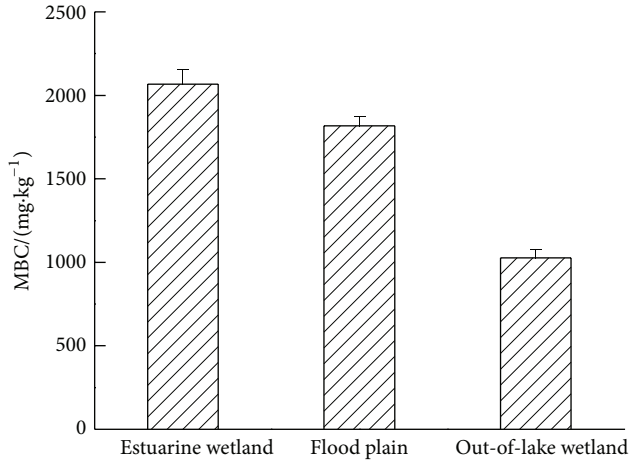

Figure 2: Changes of MBC content under different types of wetland in Hongze Lake of China.

soluble organic carbon (SOC), DOC, labile organic carbon (LOC), and their ecological environment effects were studied in the present experiment.

The objective of this research was to study the role which different types of wetland soil active organic carbon played in the biogeochemical cycle and thereby to provide a theoretical basis for a good deal of insight into biogeochemical cycle mechanism of wetland soil carbon.

2. Material and Methods

2.1. Experimental Design. The experimental site is located at Hongze Lake, China. Three sample plots were selected in south, east, and west bank of Hongze Lake Wetland (representing Estuary wetland, flood plain, and out of lake wetland, separately). The research sample point of three types of wetlands was chosen in the middle of April 2012, and the indicators related to surface vegetation distribution and hydrological conditions were observed and recorded. Soil of 0–20 cm depth was collected into a sterile bag by using the multipoint-mix-sampling method; the soil samples were taken back to the laboratory quickly and divided into two parts. One part was refrigerated under 4°C, which was used to measure soil water content, DOC, and MBC. Another part of the soil sample was just put in the air and taken through a 0.25 mm sieve after being dried and grinded. The latter part was applied to the analysis of SOC and LOC.

2.2. Measurements. Soil organic carbon was determined by taking potassium dichromate volumetric method. MBC was measured using chloroform fumigation-K_2SO_4 extraction method. TOC instrument was used to determine DOC concentration. Content of LOC estimation was performed according to the method of potassium permanganate oxidation.

2.3. Data Analysis. The data was analyzed by one-way analysis of variance (ANOVA) followed by Duncan's test at 0.05 significance level to compare the means using SPSS 16.0 for Windows.

3. Results

3.1. Distribution Characteristics of Soluble Organic Carbon. Soil was considered as a carbon source and sink; if organic matter content in soil reduced by one percent, atmospheric CO_2 concentration would increase by 5 mg·m^{-3}. The difference between soil texture and number of vegetation types would lead to variety of input and output of organic matter and causing differences in SOC content. Figure 1 showed the change trend of SOC content at 0–20 cm depth in three kinds of typical natural wetlands. It also could be seen that the SOC content in the estuary wetland had the peak value with 161.67 g·kg^{-1}, which was significantly higher than that of two other types of wetlands. SOC content of wetland soil depended largely on the circulation and decomposition rate of vegetation annually. Estuary wetland was under flooded condition all the year round, resulting in the slow decomposition of organic residue, which caused accumulating of SOC. A seasonal depletion that occurred in flood plain, aerobic microorganisms, and soil enzyme hydrolysis could bring about higher decomposition of organic matter than estuarine wetland when it was not flooding [17]. However, ventilation condition in flood plain was relatively poor compared with out-of-lake wetland. Therefore, the organic carbon content of flood plain was fairly higher than the latter.

3.2. Distribution Characteristics of Microbial Biomass Carbon. MBC was referred to the internal carbon in live bacteria, fungi, algae, and soil animals whose volume was less than 5–105 μm^3; it accounted for only a small portion of total carbon in soil; however, it was the most active section in soil organic matter [18]. Besides, it was taken on as the main driving force for decomposition of nutrient pool [19–21]. As an important source of soil nutrients, it correlated closely with cycling of the nutrients such as C, N, P, and S [22]. Changes of MBC

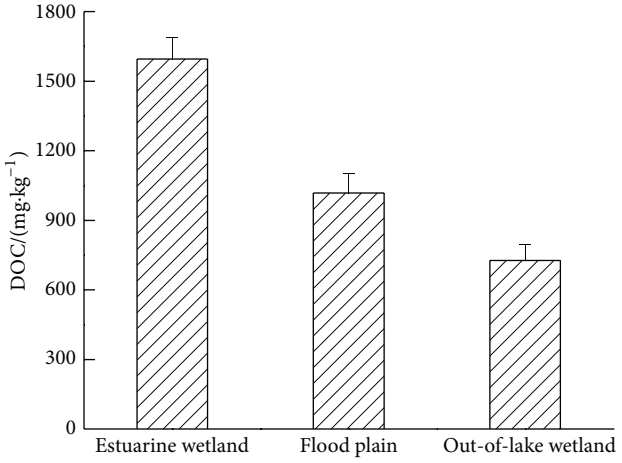

Figure 3: Changes of DOC content under different types of wetland in Hongze Lake of China.

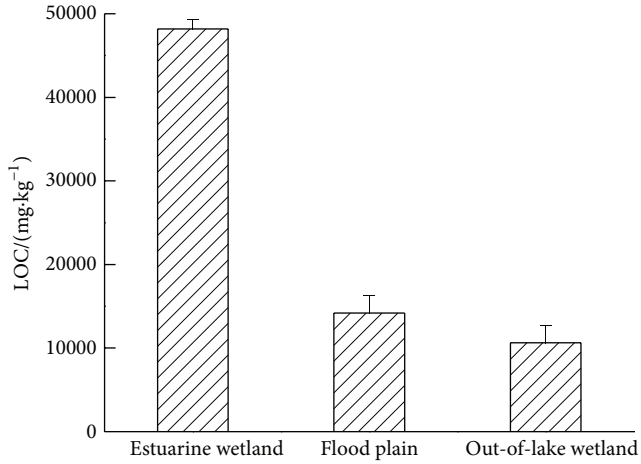

Figure 4: Changes of LOC content under different types of wetland in Hongze Lake of China.

were in accordance with SOC, and significant difference of MBC content in soil of three different types of wetland was found in present experiment (Figure 2) ($P < 0.01$). Positive relationship was found between soil MBC content and SOC content of three kinds of wetland ($r = 0.823$, $P < 0.05$). The ratio of MBC and SOC reflected the conversion efficiency from the organic matter into MBC, which could imply the turnover rate of biologically active soil organic carbon pool. The specific value of MBC/SOC of estuary wetland, flood plain, and out-of-lake wetland was 1.28%, 2.12%, and 1.6%, which suggested that flooded condition could inhibit aerobic microbial activity.

3.3. Distribution Characteristics of Dissolved Organic Carbon. DOC mainly originated from the recent humus of plant litter and soil organic matter, which included a series of organic matter from simple organic acids to the complex of macromolecular substances, such as humic acid and fulvic acid [23–25]. And it was taken as organic carbon source directed using for soil microbes, and affecting the transformation, migration, and degradation of soil organics and inorganics [26–28]. The formation, migration, and transformation of DOC in the wetland had important influence on soil carbon flux [29]. Similar changing trend in DOC and MBC in 0–20 cm of soil appeared in Figure 3, and ANOVA analysis showed that the DOC content of estuarine wetland was significantly higher than that of flood plain and out-of-lake wetland ($P < 0.01$). This was due to the flooded condition of estuary wetland, which could improve the dissolution of soil organic carbon and the dispersion of soil aggregate [30, 31]. Pearson correlation suggested that it was significantly and positively related to DOC and SOC of the three different types of wetland soil ($r = 0.872$, $P < 0.01$), which indicated that SOC was the main source of DOC. The ratio of DOC to SOC of estuary wetland, flood plain, and out-of-lake wetland was 0.09%, 1.19%, and 1.12% individually. The lowest proportion that occurred in estuarine wetland would declare the lower turnover rate of biological active soil organic carbon pool in estuary wetland.

3.4. Distribution Characteristics of Labile Organic Carbon. Soil LOC content and the ratio of LOC to SOC were the indexes to reflect the stability of soil carbon. And the two indexes of estuarine wetland soil were significantly higher than that of flood plain and out-of-lake wetland (Figure 4). Positively significant correlation between LOC and SOC in different types of wetland soil was found in present experiment ($r = 0.952$, $P < 0.01$); thus, the quantity of SOC could determine the abundance of LOC. The higher the proportion of LOC/SOC was, the worse the stability was. Special hydrological conditions of wetland would make the anaerobic environment; when hydrological conditions changed from anaerobic into aerobic environment, huge LOC would be decomposed and consumed by microbes [32, 33].

4. Conclusions

From this study, we concluded that estuarine wetland had fairly important environmental function in the greenhouse gas emissions reduction and the climate change mitigation. And we supported the speculation that variation in water condition would have a real impact on the accumulation and decomposition of organic carbon in the wetland soils.

Conflict of Interests

The authors declare that there is no conflict of interests regarding the publication of this paper.

Acknowledgments

This work was supported by the National Natural Science Foundation of China (41201559; 41301314) and the Natural Science Foundation of Jiangsu province (BK2011412).

References

[1] N. Saintilan, K. Rogers, D. Mazumder, and C. Woodroffe, "Allochthonous and autochthonous contributions to carbon accumulation and carbon store in southeastern Australian coastal wetlands. Estuarine," *Coastal and Shelf Science*, vol. 128, no. 10, pp. 84–92, 2014.

[2] J. Q. Gao, G. C. Lei, X. W. Zhang, and G. X. Wang, "Can $\delta^{13}C$ abundance, water-soluble carbon, and light fraction carbon be potential indicators of soil organic carbon dynamics in Zoigê wetland?" *Catena*, vol. 119, no. 8, pp. 21–27, 2014.

[3] M. Liu, Z. J. Zhang, Q. He, H. Wang, and X. Li, "Jonathan Schoer Exogenous phosphorus inputs alter complexity of soil-dissolved organic carbon in agricultural riparian wetlands," *Chemosphere*, vol. 95, pp. 572–580, 2014.

[4] A. C. Barbera, M. Borin, A. Ioppolo, G. L. Cirelli, and C. Maucieri, "Carbon dioxide emissions from horizontal subsurface constructed wetlands in the Mediterranean Basin," *Ecological Engineering*, vol. 64, no. 3, pp. 57–61, 2014.

[5] W. Yang, H. Zhao, X. L. Chen, S. L. Yin, X. Y. Chen, and S. Q. An, "Consequences of short-term C_4 plant Spartina alterniflora invasions for soil organic carbon dynamics in a coastal wetland of Eastern China," *Ecological Engineering A*, vol. 61, no. 12, pp. 50–57, 2013.

[6] J. Wang, C. Song, X. Wang, and Y. Song, "Changes in labile soil organic carbon fractions in wetland ecosystems along a latitudinal gradient in Northeast China," *Catena*, vol. 96, pp. 83–89, 2012.

[7] Q. S. Lu, Z. Q. Gao, Z. H. Zhao, J. C. Ning, and X. L. Bi, "Dynamics of wetlands and their effects on carbon emissions in China coastal region—case study in Bohai Economic Rim," *Ocean & Coastal Management*, vol. 87, no. 1, pp. 61–67, 2014.

[8] L. Huo, Z. Chen, Y. Zou, X. Lu, J. Guo, and X. Tang, "Effect of Zoige alpine wetland degradation on the density and fractions of soil organic carbon," *Ecological Engineering*, vol. 51, pp. 287–295, 2013.

[9] X. Yang, W. Ren, B. Sun, and S. Zhang, "Effects of contrasting soil management regimes on total and labile soil organic carbon fractions in a loess soil in China," *Geoderma*, vol. 177-178, pp. 49–56, 2012.

[10] J. Beringer, S. J. Livesley, J. Randle, and L. B. Hutley, "Carbon dioxide fluxes dominate the greenhouse gas exchanges of a seasonal wetland in the wet-dry tropics of northern Australia," *Agricultural and Forest Meteorology*, vol. 182-183, no. 12, pp. 239–247, 2013.

[11] D. S. Jenkinson, D. E. Adams, and A. Wild, "Model estimates of CO_2 emissions from soil in response to global warming," *Nature*, vol. 351, no. 6324, pp. 304–306, 1991.

[12] L. X. Yang and J. J. Pan, "Progress in the study of measurements of soil active organic carbon pool," *Chinese Journal of Soil Science*, vol. 35, no. 4, pp. 502–506, 2004 (Chinese).

[13] J. Q. Gao, H. Ouyang, and J. H. Bai, "Vertical distribution characteristics of soil labile organic carbon in Ruoergai wetland," *Journal of Soil and Water Conservation*, vol. 20, no. 1, pp. 76–79, 2006 (Chinese).

[14] H. Shen, Z. Y. Cao, and Z. Y. Hu, "Characteristics and ecological effects of the active organic carbon in soil," *Chinese Journal of Ecology*, vol. 18, no. 3, pp. 32–38, 1999 (Chinese).

[15] B. C. Liang, M. Schnitzer, C. M. Monreal, A. F. MacKenzie, P. R. Voroney, and R. P. Beyaert, "Management-induced change in labile soil organic matter under continuous corn in eastern Canadian soils," *Biology and Fertility of Soils*, vol. 26, no. 2, pp. 88–94, 1998.

[16] J. Z. Ni, J. M. Xu, and Z. M. Xie, "The size and characterization of biologically active organic carbon pool in soils," *Plant Nutrition and Fertilizer Science*, vol. 7, no. 1, pp. 56–63, 2001 (Chinese).

[17] Q. Liang, R. T. Gao, B. D. Xi, Y. Zhang, and H. Zhang, "Long-term effects of irrigation using water from the river receiving treated industrial wastewater on soil organic carbon fractions and enzyme activities," *Agricultural Water Management*, vol. 135, no. 3, pp. 100–108, 2014.

[18] T. H. Anderson and K. H. Domsch, "Application of eco-physiological quotients (qCO_2 and qD) on microbial biomasses from soils of different cropping histories," *Soil Biology and Biochemistry*, vol. 22, no. 2, pp. 251–255, 1990.

[19] Z. H. Shang, Q. S. Feng, G. L. Wu, G. H. Ren, and R. J. Long, "Grasslandification has significant impacts on soil carbon, nitrogen and phosphorus of alpine wetlands on the Tibetan Plateau," *Ecological Engineering*, vol. 58, no. 2, pp. 170–179, 2013.

[20] X. Wang, C. Song, X. Sun, J. Wang, X. Zhang, and R. Mao, "Soil carbon and nitrogen across wetland types in discontinuous permafrost zone of the Xiao Xing'an Mountains, northeastern China," *Catena*, vol. 101, pp. 31–37, 2013.

[21] X. Ye, A. J. Wang, and J. Chen, "Temporal-spatial variation and source analysis of carbon and nitrogen in a tidal wetland of Luoyuan Bay," *Acta Ecologica Sinica*, vol. 33, no. 3, pp. 150–157, 2013.

[22] Y. Lu, H. W. Xu, and C. C. Song, "Effects of plants on N_2O emission in freshwater marsh ecosystem," *Journal of Food, Agriculture and Environment*, vol. 10, no. 1, pp. 662–666, 2012.

[23] C. Mu, H. Lu, B. Wang, X. Bao, and W. Cui, "Short-term effects of harvesting on carbon storage of boreal Larix gmelinii-Carex schmidtii forested wetlands in Daxing'anling, northeast China," *Forest Ecology and Management*, vol. 293, no. 4, pp. 140–148, 2013.

[24] H. Wu, D. P. Batzer, X. Yan, X. Lu, and D. Wu, "Contributions of ant mounds to soil carbon and nitrogen pools in a marsh wetland of Northeastern China," *Applied Soil Ecology*, vol. 70, pp. 9–15, 2013.

[25] J. N. Sun, B. C. Wang, G. Xu, and H. B. Shao, "Effects of wheat straw biochar on carbon mineralization and guidance for large-scale soil quality improvement in the coastal wetland," *Ecological Engineering*, vol. 62, no. 1, pp. 43–47, 2014.

[26] J. R. Burford and J. M. Bremner, "Relationships between the denitrification capacities of soils and total, water-soluble and readily decomposable soil organic matter," *Soil Biology and Biochemistry*, vol. 7, no. 6, pp. 389–394, 1975.

[27] J. Z. Ni, J. M. Xu, and Z. M. Xie, "Advances in soil water-soluble organic carbon research," *Ecology and Environment*, vol. 12, no. 1, pp. 71–75, 2003 (Chinese).

[28] M. M. Wander, S. J. Traina, B. R. Stinner, and S. E. Peters, "Organic and conventional management effects on biologically active soil organic matter pools," *Soil Science Society of America Journal*, vol. 58, no. 4, pp. 1130–1139, 1994.

[29] C. C. Song, Y. Y. Wang, and B. X. Yan, "The changes of the soil hydrothermal condition and the dynamics of C, N after the mire tillage," *Environmental Science*, vol. 25, no. 3, pp. 168–172, 2004 (Chinese).

[30] Z. P. Li, T. L. Zhang, and B. Y. Chen, "Dynamics of soluble organic carbon and its relation to mineralization of soil organic carbon," *Acta Pedologica Sinica*, vol. 41, no. 4, pp. 544–552, 2004 (Chinese).

[31] A. O. Olaleye, T. Nkheloane, R. Mating et al., "Wetlands in Khalong-la-Lithunya catchment in Lesotho: soil organic carbon contents, vegetation isotopic signatures and hydrochemistry," *Catena*, vol. 115, no. 4, pp. 71–78, 2014.

[32] Y. Zhang, Y. Li, L. Wang et al., "Soil microbiological variability under different successional stages of the Chongming Dongtan wetland and its effect on soil organic carbon storage," *Ecological Engineering*, vol. 52, pp. 308–315, 2013.

[33] Y. Hu, L. Wang, Y. S. Tang et al., "Variability in soil microbial community and activity between coastal and riparian wetlands in the Yangtze River estuary-Potential impacts on carbon sequestration," *Soil Biology and Biochemistry*, vol. 70, no. 1, pp. 221–228, 2014.

Hindawi Publishing Corporation
The Scientific World Journal
Volume 2014, Article ID 912083, 11 pages
http://dx.doi.org/10.1155/2014/912083

Research Article

Soil Phosphorus Forms and Profile Distributions in the Tidal River Network Region in the Yellow River Delta Estuary

Junbao Yu,[1] Fanzhu Qu,[1,2] Huifeng Wu,[1] Ling Meng,[3] Siyao Du,[3] and Baohua Xie[1]

[1] *Key Laboratory of Coastal Environmental Processes and Ecological Remediation, Yantai Institute of Coastal Zone Research (YIC), Chinese Academy of Sciences (CAS), Shandong Provincial Key Laboratory of Coastal Environmental Processes, YICCAS, Yantai, Shandong 264003, China*
[2] *University of Chinese Academy of Sciences, Beijing 100049, China*
[3] *College of Environmental Science and Engineering, Ocean University of China, Qingdao, Shandong 266100, China*

Correspondence should be addressed to Junbao Yu; junbao.yu@gmail.com

Received 21 February 2014; Revised 7 April 2014; Accepted 14 April 2014; Published 20 May 2014

Academic Editor: Xu Gang

Modified Hedley fraction method was used to study the forms and profile distribution in the tidal river network region subjected to rapid deposition and hydrologic disturbance in the Yellow River Delta (YRD) estuary, eastern China. The results showed that the total P (P_t) ranged from 612.1 to 657.8 mg kg^{-1}. Dilute HCl extractable inorganic P (P_i) was the predominant form in all profiles, both as absolute values and as a percentage of total extracted P_i. The NaOH extractable organic P (P_o) was the predominant form of total extracted P_o, while Bicarb-P_i and C.HCl-P_o were the lowest fractions of total extracted P_i and P_o in all the P forms. The Resin-P concentrations were high in the top soil layer and decreased with depth. The Pearson correlation matrix indicated that Resin-P, Bicarb-P_i, NaOH-P_i, and C.HCl-P_i were strongly positively correlated with salinity, TOC, Ca, Al, and Fe but negatively correlated with pH. The significant correlation of any studied form of organic P (Bicarb-P_o, NaOH-P_o, and C.HCl-P_o) with geochemical properties were not observed in the study. Duncan multiple-range test indicated that the P forms and distribution heterogeneity in the profiles could be attributed to the influences of vegetation cover and hydrologic disturbance.

1. Introduction

Phosphorus (P), as a limiting nutrient, is one of the major plant nutrient elements second in importance to nitrogen (N) in terms of nutrient requirements for increased plant biomass production in ecosystem [1]. In its biogeochemical cycle, P is typically eroded from upland sources and transported, along with the sediment to which it is attached, to a final receiving water body [2, 3]. Before reaching the ocean, overland flow and runoff may travel through most of tidal wetlands, which are complex, dynamic, and continually changing due to the action of wind, currents, tides, and waves. Phosphorus in tidal river network region typically exists in many complex chemical forms, while investigations of P biogeochemistry often partition the pool of P into its labile and refractory components, especially with regard to soil P availability for plant or phytoplankton growth [4].

Meanwhile, most methods for available P determination attempt to quantify P solubility using different extractions, but few of those were related to P supply rates and relevant to plant uptake [5, 6]. To overcome this limitation, Hedley et al. [7] developed a method to extract P using a series of successively stronger reagents. At each step of the fractionation scheme, extracts could be assigned a role that could be used to characterize a chemical form of P. The sequential fractionation, in which the pool of soil P is partitioned into inorganic, organic, and microbial forms [8], can differentiate the plant-available forms (Resin-P_i, Bicarb-P_i, and Bicarb-P_o) and refractory forms (NaOH-P_i, NaOH-P_o, D.HCl-P_i, C.HCl-P_i, C.HCl-P_o, and Residual-P). Many previous studies have used the sequential fractionation scheme developed by Hedley, which was successfully used to separate forms of organically bound soil phosphorus from the geochemically

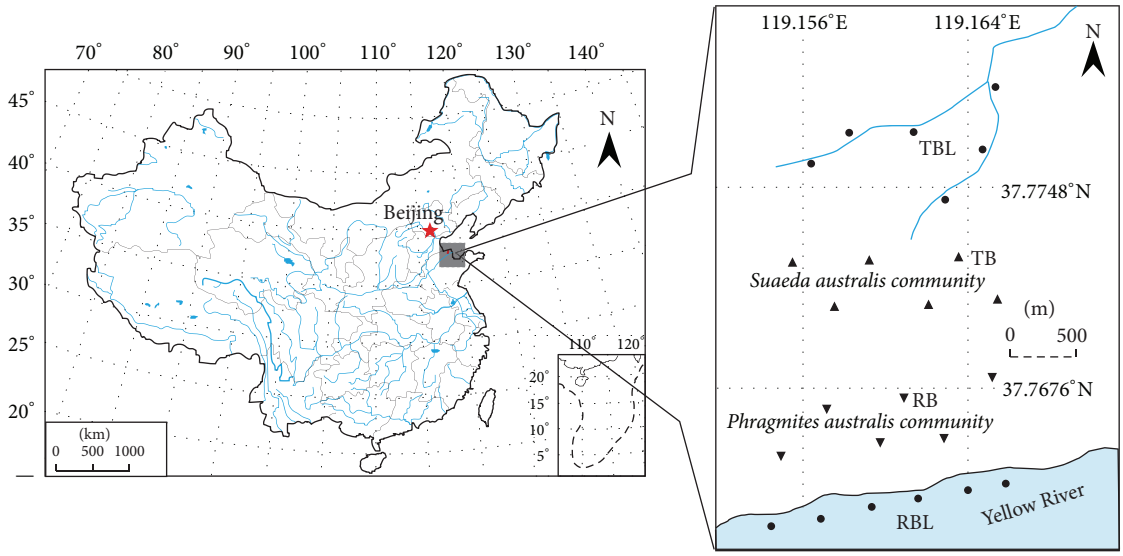

Figure 1: The tidal river network region in the Yellow River Delta estuary and sampling plots in wetlands (including bare river bed (BRB), river bank (RB), tidal bank (TB), and tidal creek bed (TCB)).

bound fractions [9], to successfully describe the contribution of biological processes to the concentrations and disposition of P pools across a gradient of mineral weathering and soil development [10]. Among the studies reviewed, there are rare systematic studies of sequentially extractable P fractions in the tidal river network soils reported and no concerned documentation of the relationship between P forms of tidal wetlands and their chemical soil properties is available, especially for the soils in the tidal river network region of the Yellow River Delta (YRD) estuary in the east part of China.

The Yellow River, whose basin was the birthplace of ancient Chinese civilization, is one of the essential rivers for China's very existence. The YRD is the youngest natural coastal wetland ecosystem and the most intensive land-ocean interaction region among the large river deltas in the world [11]. The typical characteristics of the YRD are rapid deposit and fast evolution because the sediment load delivered into the sea accounts for 6% of the global rivers' sediment load into the sea [12]. Thus the Yellow River is regarded as the largest contributor of fluvial sediment load compared to the oceans in the world. The net increase of delta shoreline length was ~61.64 km with annual increase of ~1.81 km, and the net extension of area was ~309.81 km^2 with rate of ~9.11 $km^2\ yr^{-1}$ within 34 years (1976–2009) [13].

The ability of wetlands to act as sinks for certain chemicals, sediments, and nutrients has been one of the main motivating factors for wetland protection. For the past few years, there are many studies focusing on the landscape pattern [14–16], biodiversity conservation [16], ecological restoration [17], and wetland evolution [11, 18] of the YRD. Unfortunately, few studies focused on the soil P forms and the relation of P distribution with vegetation cover and hydrologic disturbance in coastal areas [19–22]. In the present study, soil phosphorus forms and profile distributions in the tidal river network region were studied. Our objectives were (a) to fill a void of information on P forms of the tidal river network region soils, (b) to investigate the differences of contents and distribution of P forms of soils in river and tidal creek bed and bank by the sequential extraction procedure according to a modified Hedley fraction, (c) to correlate the content of P forms with basic chemical soil properties, and (d) to establish general differences in P forms and availability influence by vegetation cover and hydrologic disturbance.

2. Material and Methods

2.1. Study Area. The studied tidal river network region (Figure 1) is located in the Yellow River Delta Natural Reserve (37°35′–38°12′N, 118°33′–119°20′E) established in 1992 by the State Council of China, which is between the Bohai Gulf and the Laizhou Bay in eastern China. As a wetland type reserve, which is well protected for the important habitat, breeding, or stopover place for the birds in China, it holds the most extensive, integrated, and youngest wetland ecosystem in the warm temperate zone of China. Due to deposition of lots of sand and mud carried by water of the Yellow River from the Loess Plateau, the main soil is typical saline alluvial soil (Fluvisols, FAO). The natural vegetation is salt-tolerant plants and aquatic plants. The predominant species in the tidal river network region are *Phragmites australis* and *Suaeda heteroptera* Kitag. This region is subjected to warm temperate continental monsoon climate with distinctive seasons and rainy summer. Average annual sunshine hours are 2590–2830 h, average annual temperature is 11.7–12.8°C, and the frost-free period is about 196 d. The average annual precipitation is 530–630 mm with nearly 70% of the precipitation falling mainly in summer, while the evaporation is 1900–2400 mm and the drought index is up to 3.56 [17].

2.2. Soil Collection. In order to examine the forms and distribution of soil phosphorus in the tidal river network

region in the YRD estuary, along the Yellow River and a tidal creek, four soil sampling plots were collected for study on 27 April in 2011. The plots were demonstrated as follows: (1) bare river bed (BRB), which was in the Yellow River bed with no vegetation cover; (2) river bank (RB), which was on the river bank with *Phragmites australis* as dominated species cover; (3) tidal bank (TB), which was on the tidal creek with *Suaeda heteroptera* Kitag. as dominated species cover; and (4) tidal creek bed (TCB), which was in the tidal creek bed with no vegetation cover. In each plot, 6 replicate soil samples were collected using a stainless-steel slide hammer with an inner diameter of 3.5 cm. Each collected core was sectioned at 10 cm interval of 0–60 cm depth. The soil samples were stored immediately in polyethylene plastic bags after collection in the field. All soil samples were air-dried, grounded using a mortar and pestle, and then sieved 0.850 mm and 0.150 mm sieves prior to laboratory analysis.

2.3. Laboratory Analyses and Statistical Methods. A 0.5000 g soil sample was placed in a 50 mL plastic centrifuge tube with 30 mL of deionized water and the freely exchangeable fractions were removed by anion exchange resin in the chloride form. The plant available and moderately labile pool was extracted with $NaHCO_3$ (0.5 M, pH = 8.5) and 0.1 M NaOH, whereas 1 M HCl removed the Ca-associated portion, since Fe- or Al-associated P that might remain unextracted after the NaOH extraction is insoluble in acid. Hot concentrated HCl was used to separate organic P (P_o) from inorganic P (P_i) in stable residual fractions. The residue left after the hot concentrated HCl extraction is unlikely to contain anything but highly recalcitrant P_i pool which can be digested with concentrated H_2SO_4 and H_2O_2 at 360°C. To determine total P in 0.5 M $NaHCO_3$, 0.1 M NaOH, and concentrated HCl, extracts of dissolved organic matter were oxidized with ammonium persulfate before P analysis. A volume of 5 mL of solution was injected into a 50 mL volumetric flask. 0.5 g ammonium persulfate and 10 mL 0.9 M H_2SO_4 were weighed into the flask containing 5 mL of the $NaHCO_3$ and NaOH extracts. The extracts were then autoclaved for 60 min ($NaHCO_3$ and concentrated HCl) and 90 min (NaOH). Inorganic P in the 0.5 M $NaHCO_3$ and 0.1 M NaOH extracts was determined by acidifying 10 mL aliquot in a 50 mL centrifuge tube with 6 mL and 1.6 mL of 0.9 M H_2SO_4 at 0°C for 30 min to precipitate OM. The OM was removed by carefully decanting the supernatant after centrifuging at 16000 rpm for 10 min. Organic P was estimated as the difference between total P and P_i. The P concentration in the supernatant was determined by a Tu-1810 spectrophotometer (PERSEE, China), using the ascorbic acid molybdenum blue method described by Murphy and Riley [23]. The P fractionation procedure has been described in detail by Tiessen and Moir [24].

To analyze for pH, soil moisture (SM), soil salinity, and total organic carbon (TOC), the representative samples of dried and sieved soil were delivered to Yantai Institute of Coastal Zone Research, Chinese Academy of Sciences. Soil pH was measured with a Beckman pH meter with combination electrode (soil : water ratio = 1 : 5) and salinity was quantified with a conductivity bridge. Cutting ring and oven dry method was used to measure SM. TOC was measured using a LECO CN2000 combustion gas analyzer (AOAC International 1997). Al, Fe, and Ca in acid digested extract were measured by ICPS-7500 (Manufactured by Shimadzu, Japan).

The chemical analyses were performed at the Key Laboratory of Wetlands Ecology and Environment, Yantai Institute of Coastal Zone Research, Chinese Academy of Sciences. The P forms against concentrations of basic chemical properties and Duncan multiple-range test about P factions in the four plots were conducted using the Pearson correlation method. Correlation analyses and Duncan multiple-range test were conducted with SPSS 18.0 (SPSS, Inc. 2010).

3. Results and Discussion

3.1. General Characteristics of the Soils in the Tidal River Network Region. The mean pH of the tidal river network region soils which varied from 8.7 to 9.2 was strongly alkaline. The mean proportion of SM which ranged from 20.7 to 25.1% was high water content and the mean salinity which ranged from 0.4 to 22.2% was mainly hypersaline. Meanwhile, SM and salinity exhibited increasing gradients from the Yellow River bed to a tidal creek bed, which was primarily caused by the regionally geological, geochemical, and hydrologic conditions. The content of TOC ranged from 0.3 to 1.3% (Table 1), while the contents of Ca, Al, and Fe ranged 3.7–6.2%, 5.6–7.6%, and 2.4–4.1%, respectively (Table 1). Related research has also found that the soil characteristics in this region have low nutrients and high salinity [25]. These soils were characterized with low organic matter. Because the sediment to which they were attached in the YRD came from Loess Plateau by long transportation via the Yellow River, the organic matter was lost during the long transportation. These tidal river network region soils in the YRD estuary are classified as young hydromorphic alluvia (Fluvents) formed on fluvo-marine deposits. As a newborn estuarine coastal wetland, it was characterized by poor soil development with high soil salinity and low nutrient availability and only covered by salt-tolerant plant communities.

3.2. Distribution of Soil Phosphorus Fractions. Previous studies about the phosphorus fractions in an acid soil continuously fertilized with mineral and organic fertilizers revealed that the potential information about the distribution of soil P pools could help us to well understand the sinks and sources of P in the soil [26]. Related study has evaluated the mean total P fractions ranging from 471.1 to 694.9 mg kg^{-1} in the newly formed wetland soils in the Yellow River Delta [20]. In these soils in the tidal river network region, the mean content of total P (P_t) was ranked as TCB (mean, 657.8 mg kg^{-1}) > RB (mean, 649.2 mg kg^{-1}) > TB (mean, 636.3 mg kg^{-1}) ≫ BRB (mean, 612.1 mg kg^{-1}) (Table 2). The P_t concentrations were larger in the top and bottom layers than those in the middle layers in all the soil profiles with an exception of BRB. The minimum value of P_t occurred in 20–30 cm layer in RB and TB, 30–40 cm layer in TCB, but 50–60 cm layer

Table 1: General characteristics of the soils in the tidal river network region.

Soil	Depth (cm)	pH	SM (%)	Salinity (%)	TOC (%)	Ca (%)	Al (%)	Fe (%)
BRB	0–10	8.9 (0.08)	21.4 (1.40)	2.2 (1.22)	0.6 (0.25)	4.5 (0.86)	6.2 (0.70)	3.2 (0.52)
	10–20	9.1 (0.05)	21.1 (0.19)	0.7 (0.22)	0.5 (0.13)	4.3 (0.31)	6.3 (0.33)	2.8 (0.22)
	20–30	9.1 (0.12)	21.9 (0.40)	0.7 (0.37)	0.4 (0.11)	4.1 (0.06)	6.0 (0.10)	2.6 (0.08)
	30–40	9.2 (0.07)	22.6 (0.36)	0.5 (0.24)	0.3 (0.05)	4.0 (0.05)	5.8 (0.14)	2.5 (0.10)
	40–50	9.1 (0.10)	23.9 (0.49)	0.5 (0.07)	0.3 (0.06)	3.8 (0.38)	5.7 (0.32)	2.4 (0.09)
	50–60	9.2 (0.07)	24.5 (0.45)	0.4 (0.03)	0.3 (0.09)	3.7 (0.39)	5.6 (0.35)	2.5 (0.05)
RB	0–10	8.8 (0.28)	21.0 (1.83)	4.4 (4.32)	1.2 (0.18)	4.9 (0.50)	6.7 (0.46)	3.2 (0.46)
	10–20	8.8 (0.32)	20.7 (0.71)	4.7 (4.65)	0.7 (0.51)	4.7 (1.26)	6.5 (0.95)	3.0 (0.95)
	20–30	8.7 (0.24)	21.3 (0.83)	4.9 (3.92)	0.7 (0.19)	4.4 (0.53)	6.3 (0.36)	2.8 (0.42)
	30–40	8.8 (0.17)	21.9 (0.86)	3.9 (2.48)	0.4 (0.13)	4.2 (0.13)	6.0 (0.19)	2.6 (0.15)
	40–50	8.8 (0.14)	22.2 (0.70)	4.9 (2.51)	0.9 (0.66)	5.2 (1.54)	6.8 (0.94)	3.2 (0.82)
	50–60	8.9 (0.10)	22.3 (0.28)	4.4 (2.39)	0.7 (0.26)	5.3 (1.48)	6.8 (0.90)	3.2 (0.79)
TB	0–10	8.7 (0.05)	21.3 (1.19)	20.3 (1.12)	1.3 (0.11)	5.4 (0.20)	6.8 (0.24)	3.5 (0.06)
	10–20	8.9 (0.13)	21.7 (0.88)	9.6 (0.81)	1.0 (0.36)	5.6 (0.51)	6.9 (0.20)	3.7 (0.57)
	20–30	8.8 (0.06)	22.4 (0.96)	9.1 (0.17)	0.7 (0.12)	4.9 (0.49)	6.4 (0.31)	3.1 (0.45)
	30–40	8.8 (0.10)	23.0 (0.79)	9.4 (2.72)	0.7 (0.12)	4.9 (0.55)	6.5 (0.61)	3.2 (0.40)
	40–50	8.9 (0.16)	23.3 (0.58)	8.8 (2.14)	0.8 (0.32)	5.4 (0.74)	6.9 (0.55)	3.4 (0.57)
	50–60	8.9 (0.08)	24.4 (0.38)	7.9 (0.59)	0.9 (0.53)	5.0 (0.22)	6.6 (0.14)	3.2 (0.12)
TCB	0–10	8.7 (0.04)	20.9 (0.16)	22.2 (1.41)	1.0 (0.19)	6.1 (0.50)	7.5 (0.21)	3.1 (1.23)
	10–20	8.8 (0.10)	21.5 (0.56)	11.7 (1.50)	1.2 (0.13)	6.2 (0.41)	7.6 (0.29)	4.1 (0.36)
	20–30	8.9 (0.03)	22.2 (0.74)	9.5 (0.98)	1.1 (0.39)	5.6 (0.74)	7.2 (0.64)	3.6 (0.54)
	30–40	8.8 (0.10)	24.0 (0.32)	14.7 (5.90)	0.9 (0.23)	5.9 (0.56)	7.4 (0.53)	3.9 (0.36)
	40–50	8.9 (0.12)	24.6 (0.47)	9.6 (1.01)	0.9 (0.17)	5.6 (0.51)	7.2 (0.53)	3.6 (0.45)
	50–60	8.8 (0.06)	25.1 (0.63)	10.0 (1.95)	0.8 (0.22)	5.5 (0.92)	7.2 (0.78)	3.6 (0.66)

Table 2: Mean soil phosphorus concentrations by fraction in tidal river network region soils listed as mg P kg^{-1} soil. Means were averaged from 18 soil samples in each type. Duncan multiple-range test was conducted with 17 degrees of freedom. The signification of different forms of phosphorus was described in [8].

P extract	BRB	RB	TB	TCB	Geochemical significance	Ecological significance
Resin-P	9.6^{c}	11.0^{c}	14.6^{b}	16.6^{a}	Nonoccluded, rapid turnover	Plant available
Bicarb-P_i	4.2^{c}	4.9^{bc}	5.8^{b}	7.1^{a}		Easily plant available,
Bicarb-P_o	30.0^{b}	40.8^{a}	17.7^{c}	37.6^{a}		Easily mineralized
NaOH-P_i	4.0^{b}	5.4^{a}	5.7^{a}	6.2^{a}	Nonoccluded, slow turnover	Lesser plant available
NaOH-P_o	32.0^{b}	43.9^{a}	25.7^{bc}	22.1^{c}		
D.HCl-P_i	420.2^{a}	417.4^{a}	423.5^{a}	414.6^{a}	Occluded, slow turnover	Not directly plant available
C.HCl-P_i	45.0^{c}	61.6^{b}	73.8^{a}	78.0^{a}		
C.HCl-P_o	30.1^{a}	22.0^{c}	22.7^{bc}	28.6^{ab}		
Residual-P	36.9^{c}	42.0^{b}	46.9^{a}	47.1^{a}		
P_i	520.0^{c}	542.4^{b}	570.2^{a}	569.5^{a}		
P_o	92.1^{b}	106.7^{a}	66.1^{c}	88.2^{b}		
P_t	612.1^{c}	649.2^{ab}	636.3^{b}	657.8^{a}		

The a, b, c represent significant differences between means for groups, while means for groups in homogeneous subsets are displayed as ab and bc ($P = 0.05$, $n = 18$).

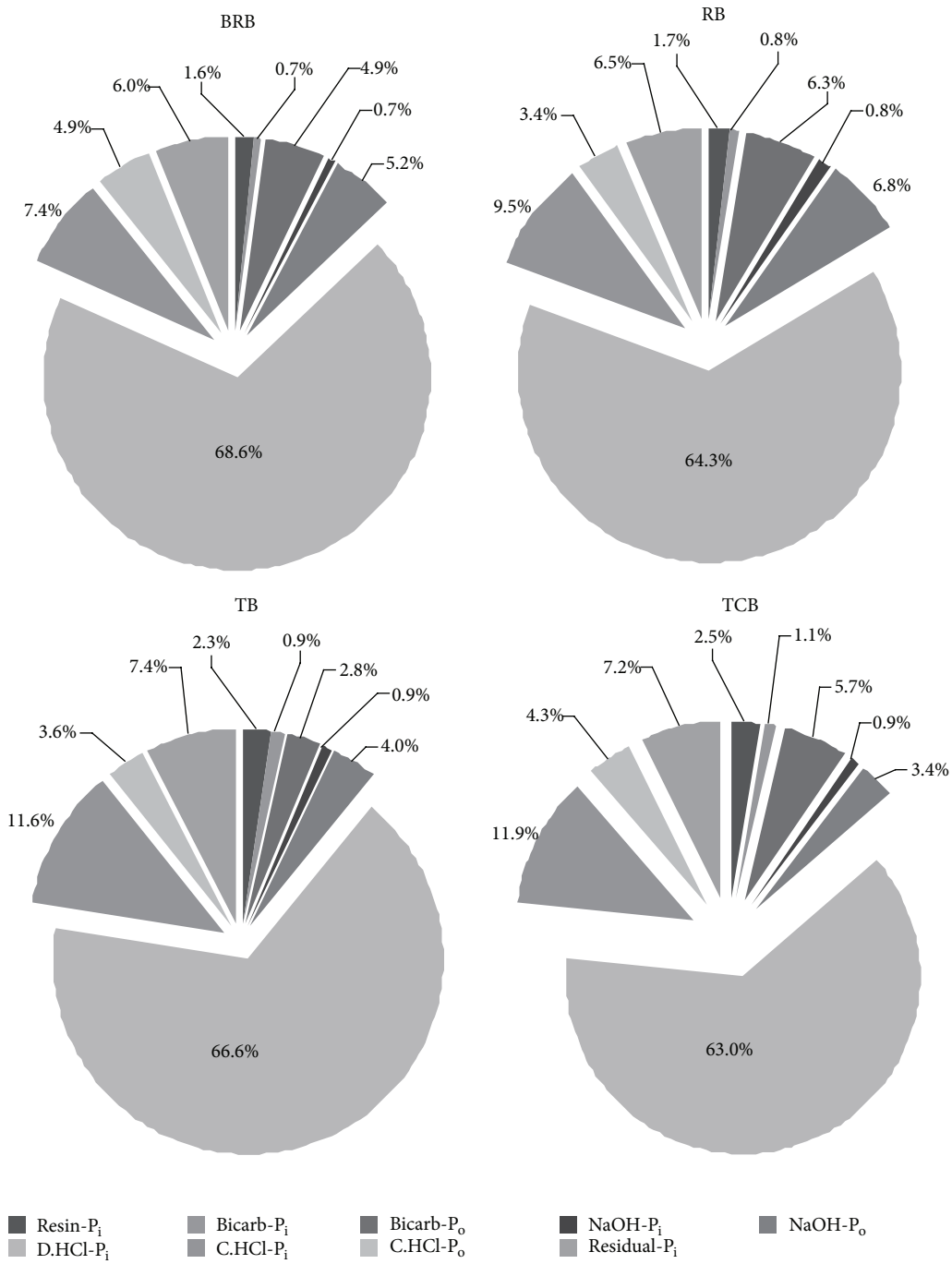

Figure 2: Soil P fractions in BRB, RB, TB, and TCB soils (P fractions including Resin-P, Bicarb-P_i, NaOH-P_i, D.HCl-P_i, C.HCl-P_i, Bicarb-P_o, NaOH-P_o, C.HCl-P_o, and Residual-P).

in BRB (Table 3 and Figure 3). Duncan multiple-range test indicated a marked difference among TCB, TB, and BRB, while the differences between TCB and RB, TB and RB were not significant (Table 2). The mean content of inorganic P forms with Resin-P, Bicarb-P_i, NaOH-P_i, D.HCl-P_i, C.HCl-P_i, and Residual-P (recalcitrant P_i) ranged 9.6–16.6, 4.2–7.1, 4.0–6.2, 414.6–423.5, 45.0–78.0, and 36.9–47.1 mg kg^{-1}, respectively (Table 2) while the mean content of organic P forms with Bicarb-P_o, NaOH-P_o, and C.HCl-P_o ranged 30.0–40.8, 22.1–43.9, and 22.0–30.1 mg kg^{-1}, respectively (Table 2). In all the soils, total inorganic P was the predominant part and accounted for 82.7–90.9%.

The plant available P fractions—Resin P and Bicarb-P_i/P_o—summed to 7.2% of total P in the BRB and 8.8% in the RB, meanwhile 6.0% of total P in the TB and 9.3% in the TB (Table 2). Resin-P is reasonably well defined as freely

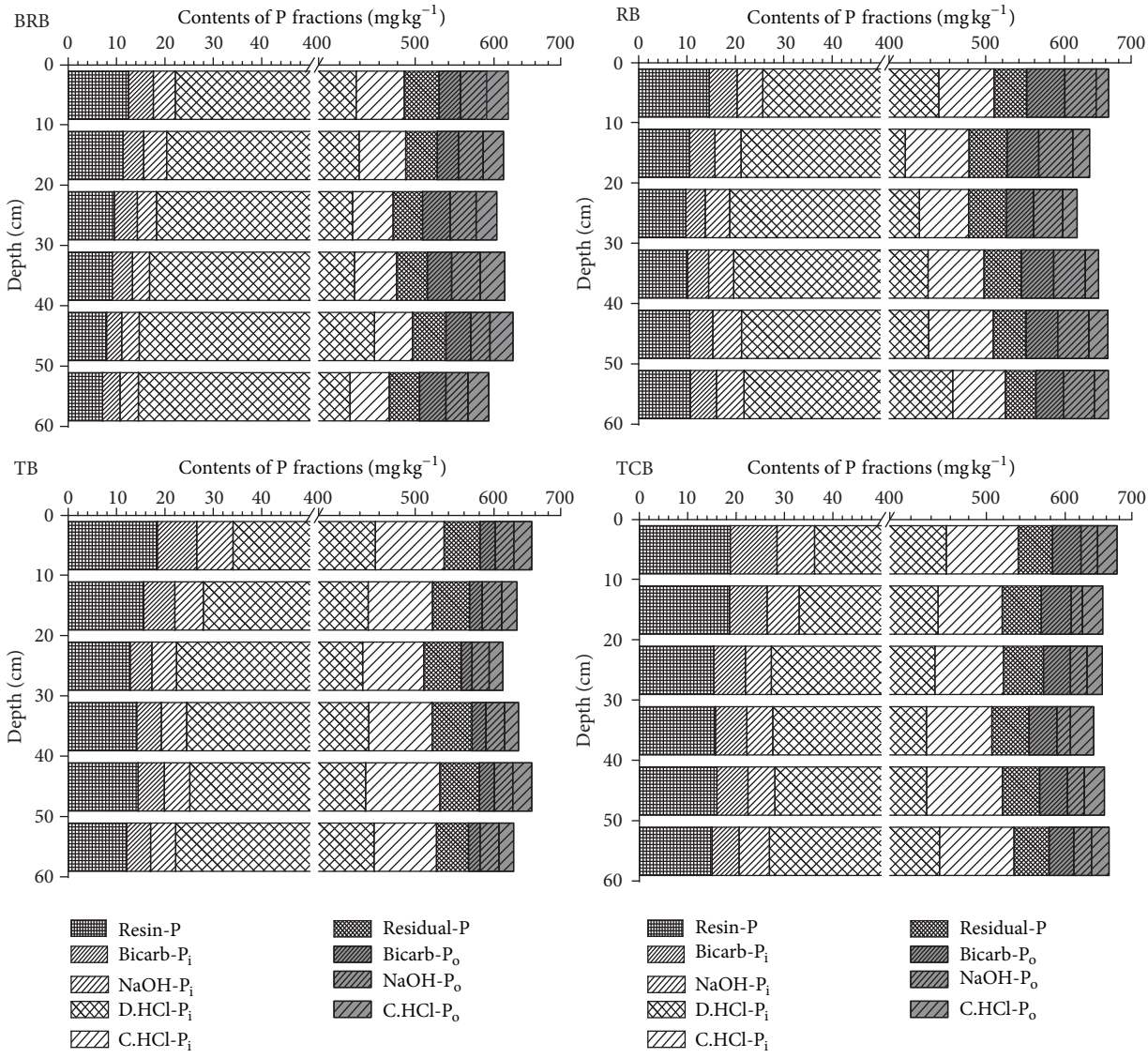

Figure 3: P fractions distribution in BRB, RB, TB, and TCB soil profiles (P forms including Resin-P, Bicarb-P_i, NaOH-P_i, D.HCl-P_i, C.HCl-P_i, Bicarb-P_o, NaOH-P_o, C.HCl-P_o, and Residual-P).

exchangeable P_i, since the resin extract does not chemically modify the soil solution. The mean content of Resin-P was ranked as TCB (16.6 mg kg^{-1}, 2.5%) ≫ TB (14.6 mg kg^{-1}, 2.3%) ≫ RB (11.0 mg kg^{-1}, 1.7%) > BRB (9.6 mg kg^{-1}, 1.6%) (Table 2 and Figure 2). In all profiles, the Resin-P concentrations were high in the top soil layer and decreased with depth (Table 3 and Figure 3). The most likely contributor to the effect of exchanging on Resin-P in the tidal river network region was salinity, which was an important feature of coastal wetlands that can affect P sorption.

Bicarbonate extracts a P_i fraction, which is likely to be plant available, since the chemical changes introduced are minor and somewhat representative of root action respiration. Bicarb-P_o, which is easily mineralisable, is also likely to represent similar pools. The mean content of Bicarb-P_i which was ranked as TCB (7.1 mg kg^{-1} g, 1.1%) ≫ TB (5.8 mg kg^{-1}, 0.9%) > RB (4.9 mg kg^{-1}, 0.8%) > BRB (4.2 mg kg^{-1}, 0.7%) (Table 2 and Figure 2) was the lowest fraction of total extracted P_i. The mean contents of Bicarb-P_o of TB, BRB, TCB, and RB were 17.7 mg kg^{-1}, 30.0 mg kg^{-1}, 37.6 mg kg^{-1}, and 40.8 mg kg^{-1}, respectively, in soil profiles. *Suaeda heteroptera* Kitag., as pioneer plant community in TB in newly from coastal wetland, significantly enhanced the easily mineralisable P_o and increased P availability.

NaOH extractable P (NaOH-P_i + NaOH-P_o) in the soil profiles averaged 36.0 mg kg^{-1} in BRB soils, 49.3 mg kg^{-1} in RB soils, 31.4 mg kg^{-1} in TB soils, and 28.36 mg kg^{-1} in TCB soils (Table 2). NaOH-P_o (mean: 3.4–6.8% of P_t) was the predominant form of total extracted P_o (Figure 2). The depth distribution of Bicarb-P_i and NaOH-P_i in BRB, TB, and TCB was large in top soil and decreased with depth. The distributions in RB profiles showed that

Table 3: Mean content (mg kg^{-1}) of P forms of the tidal river network region soil profiles in the Yellow River Delta estuary.

Soil	Depth (cm)	Resin-P	Bicarb-P_i	NaOH-P_i	D.HCl-P_i	C.HCl-P_i	Residual-P	Bicarb-P_o	NaOH-P_o	C.HCl-P_o	P_i	P_o	P_t
BRB	0–10	12.5	5.2	4.5	414.1	51.3	41.0	26.6	34.9	30.4	528.6	102.5	620.5
	10–20	11.3	4.3	4.8	418.8	50.0	37.1	26.5	32.6	27.9	526.2	96.2	613.3
	20–30	9.5	4.7	4.0	414.5	42.4	33.4	33.7	33.5	28.2	508.6	100.6	604.0
	30–40	9.1	4.2	3.6	417.7	44.5	35.4	29.6	37.2	33.9	514.5	102.2	615.1
	40–50	7.9	3.1	3.6	440.5	41.8	39.9	31.9	25.7	32.5	536.9	97.5	627.1
	50–60	7.1	3.6	3.8	415.5	40.8	34.3	31.8	28.3	27.6	505.1	94.4	592.9
RB	0–10	14.6	5.8	5.3	423.1	61.1	40.2	50.6	44.9	19.0	550.0	135.7	664.5
	10–20	10.5	5.3	5.4	394.1	65.9	44.5	39.8	46.5	23.8	525.7	130.8	635.8
	20–30	9.8	4.0	5.0	410.2	51.6	44.5	33.7	38.9	20.3	525.1	117.1	618.0
	30–40	10.1	4.4	5.2	418.2	60.4	44.9	42.1	44.4	19.7	543.1	131.4	649.3
	40–50	10.5	4.8	5.9	417.1	70.6	40.1	41.8	44.3	28.2	549.0	126.1	663.3
	50–60	10.7	5.4	5.7	441.6	60.2	38.2	37.0	44.4	21.0	561.8	119.5	664.1
TB	0–10	18.4	8.2	7.5	421.9	78.7	46.4	20.7	26.6	26.4	581.1	93.7	654.8
	10–20	15.6	6.5	5.9	420.6	71.8	46.7	16.8	27.2	21.6	567.1	90.7	632.7
	20–30	12.8	4.5	5.1	420.5	67.2	46.3	14.1	22.7	19.1	556.4	83.1	612.4
	30–40	14.2	5.1	5.2	424.8	70.7	50.4	18.7	25.9	20.1	570.4	95.0	635.1
	40–50	14.5	5.4	5.3	420.8	83.5	50.8	20.5	25.8	28.3	580.3	97.0	654.9
	50–60	12.1	5.0	5.2	432.4	70.6	40.6	15.2	26.0	20.7	565.8	81.8	627.8
TCB	0–10	18.8	9.7	7.7	419.6	82.4	44.3	40.1	24.3	29.7	582.5	108.6	676.5
	10–20	18.7	7.7	6.6	414.2	71.3	49.3	40.6	15.9	30.1	567.9	105.8	654.5
	20–30	15.4	6.5	5.4	416.7	75.9	50.9	36.5	24.0	22.5	570.8	111.4	653.8
	30–40	15.8	6.5	5.4	407.7	71.1	45.6	36.8	18.7	33.4	552.0	101.2	640.9
	40–50	16.0	6.4	5.6	407.6	83.2	47.0	37.5	23.9	29.7	565.8	108.4	656.9
	50–60	15.0	5.6	6.2	421.9	84.2	45.3	33.8	25.8	26.1	578.3	104.9	664.0

the low concentration of Bicarb-P_i was encountered at 20–30 cm depth and the high concentration of NaOH-P_i was encountered at 50–60 cm depth of the soil (Table 3 and Figure 3). Meanwhile, we did not observe vertical variation trends of Bicarb-P_o and NaOH-P_o and marked differences in the same profile were not shown.

Dilute HCl extractable inorganic P (D.HCl-P_i) (mean: 63.0–68.6% of P_t) was the predominant form in all profiles, both as absolute values and as a percentage of total extracted P_i. Dilute HCl extractable P was clearly defined as inorganic P associated with Ca [5]. There were no significant vertical differences with respect to the soil D.HCl-P_i profiles in all the four profiles (Figure 3). The D.HCl-P_i is the predominant form (mean: 394.1–441.6 mg kg^{-1}; 63.0%–68.6%), both as absolute values and as a percentage of total extracted P, which suggests that a relatively high proportion of inorganic P is in no-directly plant available forms. The depth distribution of D.HCl-P_i in all profiles showed little differences in top soil and dramatically increased in bottom soil. The maximum content of D.HCl-P_i in RB, TB, and TCB occurred in 50–60 cm layer and in 40–50 cm layer in BRB profile (Table 3).

The hot concentrated HCl extractable P_i (C.HCl-P_i) and Residual-P were ranked as TCB (78.0 mg kg^{-1}, 11.9%, and 47.1 mg kg^{-1}, 7.2%) > TB (73.8 mg kg^{-1}, 11.6%, and 46.9 mg kg^{-1}, 7.4%) ≫ RB (61.6 mg kg^{-1}, 9.5%, and 42.0 mg kg^{-1}, 6.5%) > BRB (45.0 mg kg^{-1}, 7.4%, and 36.9 mg kg^{-1}, 6.0%) (Table 2 and Figure 2). Meanwhile, the content of the hot concentrated HCl extractable P_o (C.HCl-P_o, mean: 3.4–4.9%), which was the lowest fraction of total extracted P_o in all the P forms, was ranked as BRB (30.1 mg kg^{-1}, 4.9%) > TCB (28.6 mg kg^{-1}, 4.3%) ≫ TB (22.7 mg kg^{-1}, 3.6%) > RB (22.0 mg kg^{-1}, 3.4%) (Table 2 and Figure 2). Meanwhile, there were no significant vertical differences with respect to the soil C.HCl-P_i/P_o and Residual-P profiles (Figure 3).

3.3. Phosphorus Forms Related to Soil Geochemical Properties. The correlation analysis results showed that the Resin-P, Bicarb-P_i, OH-P_i, and C.HCl-P_i were strongly positively correlated with salinity (r = 0.76, 0.69, 0.61, and 0.64, resp.), TOC (r = 0.63, 0.65, 0.62, and 0.58, resp.), Ca (r = 0.75, 0.74, 0.60, and 0.72, resp.), Al (r = 0.75, 0.71, 0.54, and 0.73, resp.), and Fe (r = 0.65, 0.63, 0.48, and 0.63, resp.) but negatively correlated with pH (r = 0.48, 0.45, 0.60, and 0.50, resp.) (Table 4). The availability of P in most ecosystems depends on soil properties that regulate P availability, such as mineralogy of the parent material, leaching rates, and soil texture [27]. Part of the reason for the observed correlations might be that,

Table 4: Pearson correlation coefficients between P fractions and soil geochemical properties.

Sites		Pearson correlation								
		Resin-P	Bicarb-P_i	NaOH-P_i	D.HCl-P_i	C.HCl-P_i	Bicarb-P_o	NaOH-P_o	C.HCl-P_o	Residual-P
BRB ($n = 18$)	pH	−0.66**								
	SM	−0.77**								
	Salinity	0.50*								
	TOC	0.59*	0.64**							
	Ca	0.65**				0.78**				
	Al	0.59*				0.74**				
	Fe	0.73**	0.56*			0.76**				
RB ($n = 18$)	pH			−0.66**				0.61**	−0.58*	−0.58*
	SM	−0.47*	−0.49**							
	Salinity		0.54**						0.55*	
	TOC	0.59*	0.75**	0.61**						
	Ca	0.48*	0.79**	0.76**		0.55**			0.48*	
	Al	0.54*	0.83**	0.73**		0.53**			0.49*	
	Fe	0.59*	0.86**	0.73**		0.51**			0.50*	
TB ($n = 18$)	pH									
	SM			−0.54**						
	Salinity	0.53*	0.60**	0.77**						
	TOC	0.45*	0.60**	0.66**						
	Ca	0.59**	0.71**			0.72**			0.50*	
	Al	0.59**	0.61**			0.82**	0.45*		0.51*	
	Fe	0.64**	0.80**			0.67**			0.46*	
TCB ($n = 18$)	pH			−0.50*						
	SM	−0.47*	−0.49**							
	Salinity		0.54**	0.48*						
	TOC									
	Ca	0.50*	0.79**		0.50*		0.51**	0.55*		
	Al	0.51*	0.83**		0.51*		0.57**	0.51*	0.55*	
	Fe									
All ($n = 72$)	pH	−0.48**	−0.45**	−0.60**		−0.50**				−0.41**
	SM							−0.28*		
	Salinity	0.76**	0.69**	0.61**		0.64**		−0.36**		0.43**
	TOC	0.63**	0.65**	0.62**		0.58**				0.34**
	Ca	0.75**	0.74**	0.60**		0.72**				0.36**
	Al	0.75**	0.71**	0.54**		0.73**				0.36**
	Fe	0.65**	0.63**	0.48**		0.63**				0.33**

*Significant at the 0.05 level (2-tailed).
**Significant at the 0.01 level (2-tailed).

in alkaline soils, P fixation which is biologically unavailable in many wetlands is governed by the activities of Ca and Mg [28–30]. We defined that forms of Bicarb-P_i and NaOH-P_i in soils represent a continuum of Fe- and Al-associated P extractable with high pH (8.7–9.2). Correlation and regression analyses showed that the amorphous and free Fe/Al oxides, in the newly formed wetland soils, were the crucial chemical factors ascribed to the soil P retention and release capacity [20].

Although the dilute extractable inorganic P has been clearly defined as Ca-associated P, D.HCl-P_i was not correlated with soil geochemical properties in our study (Table 4). Meanwhile, no significant correlations were found between organic P fractions (Bicarb-P_o, NaOH-P_o, and C.HCl-P_o) and soil geochemical properties. All of the above results indicated that the there were actually links between P forms in estuarine coastal soils and the intensity of plant salt tolerance.

This appearance was attributed to the fact that the formation of newborn coastal wetland in the YRD is only 35 years (1976–2011). Meanwhile, the soils in the wetland were formed from sediment eroded from the upland soils on the Loess Plateau and deposited in the Yellow River estuary. Deposition is usually episodic rather than smoothly continuous and this newborn wetland is still also influenced by water coming from the Yellow River and ocean tide [11, 13].

3.4. Vegetation Effects on the P Forms for Tidal River Network Region. Plants growing on tidal wetland are exposed to a number of extreme conditions, such as high wind velocities, drastic temperature fluctuations, high potential evapotranspiration, salt spray, low levels of soil nutrients, and burial in sediment [31, 32]. Vegetation has been proven to improve the soil P dynamics and availability [33–35]. Our results showed some clear differences between RB covered by *Phragmites australis* and TB covered by *Suaeda heteroptera* Kitag. (Table 2). The mean content of Resin-P, C.HCl-P_i, Residual-P, and total inorganic P of TB soils (14.6 mg kg^{-1}, 73.8 mg kg^{-1}, 46.9 mg kg^{-1}, and 570.2 mg kg^{-1}, resp.) was higher than those of RB soils (11.0 mg kg^{-1}, 61.6 mg kg^{-1}, 42.0 mg kg^{-1}, and 542.4 mg kg^{-1}, resp.), while the mean content of Bicarb-P_o, NaOH-P_o, and total organic P of TB soils (17.7 mg kg^{-1}, 25.7 mg kg^{-1}, and 66.1 mg kg^{-1}, resp.) was less than those of RB soils (40.8 mg kg^{-1}, 43.9 mg kg^{-1}, and 106.7 mg kg^{-1}, resp.). Furthermore, there was no significant difference in mean content of Bicarb-P_i, NaOH-P_i, D.HCl-P_i, C.HCl-P_o, and total P of TB and RB. Vegetation cover also influenced the correlation coefficients between above P_i fractions and soil geochemical properties in the tidal river network region. The coefficients of RB covered by *Phragmites australis* and TB covered by *Suaeda heteroptera* Kitag. were higher than those of BRB and TCB with no vegetation cover. The results support the view that the soil P content varies with vegetation covers and have actually indicated links between the P forms in tidal wetland soils and the intensity of plant salt tolerance.

3.5. Hydrologic Disturbance Effects on the P Forms for Tidal River Network Region. Disturbance and stress are not uniformly high within coastal systems but exhibit strong gradients in physical disturbance, water availability, soil pH, nutrient level, and salinity [36]. Hydrology has been shown to influence a wetland soil ability to sorb [37, 38]. Berretta and Sansalone investigated the transport and partitioning of P to particulate matter fractions in runoff from a landscaped and biogenically loaded car park in Gainesville, FL (GNV), and found that P is predominantly bound to particulate matter (PM) fractions and the transport of each of PM and P fractions was influenced by separate hydrologic parameters [39]. Salinity was found to account for a significant proportion of variance in the phosphorus sorption index data [40]. Li et al. [15] simulated the effects of water level and salinity on nitrogen and phosphorus in salt marsh soils of the Yellow River Delta. Results showed that total nitrogen and total phosphorus contents accumulated in surface soils in each sampling date and that they are significantly affected by soil organic matter and salinity. Under such tidal-river conditions, water and salt of soil play a dominant role in the geochemical property in the area. In present research, it is also shown that SM and salinity significantly changed the phosphorus fractions in soils. Generally, the mean Resin-P, Bicarb-P_i/P_o, NaOH-P_i/P_o, C.HCl-P_i, Residual-P, and total P_i/P_t concentrations were TCB (seawater mainly influenced soil, higher value of SM and salinity) $\gg$ BRB (freshwater mainly influenced soil, lower value of SM and salinity) and there was no significant difference found in mean content of D.HCl-P_i, C.HCl-P_o, and total P_o (Table 4). The results also support the view that the soil P availability can increase by increasing salinity [41–43].

4. Conclusions

Our results proved that the modified Hedley fraction was effective in differentiating inorganic and organic P forms in this tidal river network region. The phosphorus in the investigated region exists in many complex chemical forms, which differ markedly in profile distribution in the four sampling plots. The P_t ranged from 612.1 to 657.8 mg kg^{-1}. D.HCl-P_i was the predominant form of total extracted P_i and NaOH-P_o was the predominant form of total extracted P_o, while Bicarb-P_i and C.HCl-P_o were the lowest fractions of total extracted P_i and P_o, respectively, in all the P forms. The Pearson correlation matrix showed that Resin-P, Bicarb-P_i, NaOH-P_i, and C.HCl-P_i were strongly positively correlated with soil salinity, TOC, Ca, Al, and Fe, while all forms of organic P (Bicarb-P_o, NaOH-P_o, and C.HCl-P_o) did not show any significant correlation with geochemical properties. Duncan multiple-range test indicated the P forms and distribution heterogeneity in the profiles can be attributed to the influences of different vegetation cover and hydrologic disturbance. The estimated distribution of different soil P fractions presented in the tidal river network region will be useful for wetland evolution that includes P as a limiting element in biological production by providing initial estimates of the available soil P for plant uptake and microbial utilization. Meanwhile, further investigation should be made to explore P availability and transformation dynamics in the soil under hydrologic disturbance.

Conflict of Interests

The authors declare that there is no conflict of interests regarding the publication of this paper.

Acknowledgments

The authors would like to thank the Project of National Science & Technology Pillar Program in "12th Five Year" period (2011BAC02B01), National Natural Science Foundation for Distinguished Young Scholar of Shandong Province (no. JQ201114), and the CAS/SAFEA International Partnership Program for Creative Research Teams—"Representative environmental processes and resources effects in coastal zone." The authors also would like to thank the Yellow River Delta Wetland Ecological Experimental Station, CAS, for providing experimental and residential place for this study.

References

[1] P. H. Doering, C. A. Oviatt, B. L. Nowicki, E. G. Klos, and L. W. Reed, "Phosphorus and nitrogen limitation of primary production in a simulated estuarine gradient," *Marine Ecology Progress Series*, vol. 124, no. 1–3, pp. 271–287, 1995.

[2] G. M. Pierzynski, G. F. Vance, and J. T. Sims, *Soils and Environmental Quality*, CRC Press, Boca Raton, Fla, USA, 2005.

[3] F. J. Stevenson and M. A. Cole, *Cycles of Soils: Carbon, Nitrogen, Phosphorus, Sulfur, Micronutrients*, John Wiley & Sons, New York, 1999.

[4] E. T. Levy and W. H. Schlesinger, "A comparison of fractionation methods for forms of phosphorus in soils," *Biogeochemistry*, vol. 47, no. 1, pp. 25–38, 1999.

[5] M. R. Carter and E. G. Gregorich, *Soil Sampling and Methods of Analysis*, Taylor & Francis, Boca Raton, Fla, USA, 2008.

[6] M. Li, J. Zhang, G. Q. Wang, H. J. Yang, M. J. Whelan, and S. M. White, "Organic phosphorus fractionation in wetland soil profiles by chemical extraction and phosphorus-31 nuclear magnetic resonance spectroscopy," *Applied Geochemistry*, vol. 33, pp. 213–221, 2013.

[7] M. J. Hedley, J. W. B. Stewart, and B. S. Chauhan, "Changes in inorganic and organic soil phosphorus fractions induced by cultivation practices and by laboratory incubations," *Soil Science Society of America Journal*, vol. 46, no. 5, pp. 970–976, 1982.

[8] A. F. Cross and W. H. Schlesinger, "A literature review and evaluation of the Hedley fractionation: applications to the biogeochemical cycle of soil phosphorus in natural ecosystems," *Geoderma*, vol. 64, no. 3-4, pp. 197–214, 1995.

[9] A. F. Cross and W. H. Schlesinger, "Biological and geochemical controls on phosphorus fractions in semiarid soils," *Biogeochemistry*, vol. 52, no. 2, pp. 155–172, 2001.

[10] G.-P. Wang, Z.-L. Zhai, J.-S. Liu, and J.-D. Wang, "Forms and profile distribution of soil phosphorus in four wetlands across gradients of sand desertification in Northeast China," *Geoderma*, vol. 145, no. 1-2, pp. 50–59, 2008.

[11] Q. Ye, S. Chen, Q. Chen et al., "Spatial-temporal characteristics in landscape evolution of the Yellow River Delta during 1855–2000 and a way out for the Yellow River estuary," *Chinese Science Bulletin*, vol. 51, pp. 197–209, 2006.

[12] J. D. Milliman and J. P. M. Syvitski, "Geomorphic/tectonic control of sediment discharge to the ocean: the importance of small mountainous rivers," *The Journal of Geology*, vol. 100, no. 5, pp. 525–544, 1992.

[13] J. Yu, Y. Fu, Y. Li et al., "Effects of water discharge and sediment load on evolution of modern Yellow River Delta, China, over the period from 1976 to 2009," *Biogeosciences*, vol. 8, no. 9, pp. 2427–2435, 2011.

[14] C. Song and G. Liu, "Application of remote sensing detection and gis in analysis of vegetation pattern dynamics in the Yellow River Delta," *Chinese Journal of Population, Resources and Environment*, vol. 6, no. 2, pp. 62–69, 2008.

[15] S.-N. Li, G.-X. Wang, W. Deng, Y.-M. Hu, and W.-W. Hu, "Influence of hydrology process on wetland landscape pattern: a case study in the Yellow River Delta," *Ecological Engineering*, vol. 35, no. 12, pp. 1719–1726, 2009.

[16] W. Ouyang, X. Wang, F. Hao, and R. Srinivasan, "Temporal-spatial dynamics of vegetation variation on non-point source nutrient pollution," *Ecological Modelling*, vol. 220, no. 20, pp. 2702–2713, 2009.

[17] B. Cui, Q. Yang, Z. Yang, and K. Zhang, "Evaluating the ecological performance of wetland restoration in the Yellow River Delta, China," *Ecological Engineering*, vol. 35, no. 7, pp. 1090–1103, 2009.

[18] H. Fan, H. Huang, and T. Zeng, "Impacts of anthropogenic activity on the recent evolution of the Huanghe (Yellow) River delta," *Journal of Coastal Research*, vol. 22, no. 4, pp. 919–929, 2006.

[19] L. L. Wang, M. Ye, Q. S. Li, H. Zou, and Y. S. Zhou, "Phosphorus speciation in wetland sediments of Zhujiang (Pearl) River Estuary, China," , *Chinese Geographical Science*, vol. 23, no. 5, pp. 574–583, 2013.

[20] G. Xu, H. B. Shao, J. N. Sun, and S. X. Chang, "Phosphorus fractions and profile distribution in newly formed wetland soils along a salinity gradient in the Yellow River Delta in China," *Journal of Plant Nutrition and Soil Science*, vol. 175, no. 5, pp. 721–728, 2012.

[21] G. Pan, M. D. Krom, M. Y. Zhang et al. et al., "Impact of suspended inorganic particles on phosphorus cycling in the Yellow River (China)," *Environmental Science & Technology*, vol. 47, no. 17, pp. 9685–9692, 2013.

[22] J. N. Sun, G. Xu, H. B. Shao, and S. H. Xu, "Potential retention and release capacity of phosphorus in the newly formed wetland soils from the yellow river delta, China," *Clean-Soil Air Water*, vol. 40, no. 10, pp. 1131–1136, 2012.

[23] J. Murphy and J. P. Riley, "A modified single solution method for the determination of phosphate in natural waters," *Analytica Chimica Acta*, vol. 27, pp. 31–36, 1962.

[24] H. Tiessen and J. Q. Moir, "Characterization of available P by sequential extraction," in *Soil Sampling and Methods of Analysis*, pp. 293–306, Taylor & Francis, Boca Raton, Fla, USA, 2008.

[25] J. Yu, X. Chen, Z. Sun et al., "The spatial distribution characteristics of soil nutrients in new-born coastal wetland in the Yellow River delta," *Acta Scientiae Circumstantiae*, vol. 30, no. 4, pp. 855–861, 2010.

[26] S. Verma, S. K. Subehia, and S. P. Sharma, "Phosphorus fractions in an acid soil continuously fertilized with mineral and organic fertilizers," *Biology and Fertility of Soils*, vol. 41, no. 4, pp. 295–300, 2005.

[27] A. Mishra, J. K. Tripathi, P. Mehta, and V. Rajamani, "Phosphorus distribution and fractionation during weathering of amphibolites and gneisses in different climatic setups of the Kaveri river catchment, India," *Applied Geochemistry*, vol. 33, pp. 173–181, 2013.

[28] R. E. Masto, M. Mahato, V. A. Selvi, and L. C. Ram, "The effect of fly ash application on phosphorus availability in an acid soil," *Energy Sources A: Recovery Utilization and Environmental Effects*, vol. 35, no. 23, pp. 2274–2283, 2013.

[29] D. M. Paiva, C. L. Walk, and A. P. McElroy, "Influence of dietary calcium level, calcium source, and phytase on bird performance and mineral digestibility during a natural necrotic enteritis episode," *Poultry Science*, vol. 92, no. 12, pp. 3125–3133, 2013.

[30] M. C. W. M. Wadu, V. K. Michaelis, S. Kroeker, and O. O. Akinremi, "Exchangeable calcium/magnesium ratio affects phosphorus behavior in calcareous soils," , *Soil Science Society of America Journal*, vol. 77, no. 6, pp. 2004–2013, 2013.

[31] M. A. Maun, "Adaptations of plants to burial in coastal sand dunes," *Canadian Journal of Botany*, vol. 76, no. 5, pp. 713–738, 1998.

[32] Z. Sun, X. Mou, G. Lin, L. Wang, H. Song, and H. Jiang, "Effects of sediment burial disturbance on seedling survival and growth of Suaeda salsa in the tidal wetland of the Yellow River estuary," *Plant and Soil*, vol. 337, no. 1, pp. 457–468, 2010.

[33] N. C. Tuchman, D. J. Larkin, P. Geddes, R. Wildova, K. Jankowski, and D. E. Goldberg, "Patterns of environmental change associated withTypha xglauca invasion in a Great Lakes coastal wetland," *Wetlands*, vol. 29, no. 3, pp. 964–975, 2009.

[34] K. M. B. Boomer and B. L. Bedford, "Groundwater-induced redox-gradients control soil properties and phosphorus availability across four headwater wetlands, New York, USA," *Biogeochemistry*, vol. 90, no. 3, pp. 259–274, 2008.

[35] G. Bonanomi, M. Rietkerk, S. C. Dekker, and S. Mazzoleni, "Islands of fertility induce co-occurring negative and positive plant-soil feedbacks promoting coexistence," *Plant Ecology*, vol. 197, no. 2, pp. 207–218, 2008.

[36] E. Balestri and C. Lardicci, "The impact of physical disturbance and increased sand burial on clonal growth and spatial colonization of Sporobolus virginicus in a coastal dune system," *PLoS ONE*, vol. 8, no. 8, Article ID e72598, 2013.

[37] J. R. Axt and M. R. Walbridge, "Phosphate removal capacity of palustrine forested wetlands and adjacent uplands in Virginia," *Soil Science Society of America Journal*, vol. 63, no. 4, pp. 1019–1031, 1999.

[38] R. M. Chambers and W. E. Odum, "Porewater oxidation, dissolved phosphate and the iron curtain: iron-phosphorus relations in tidal freshwater marshes," *Biogeochemistry*, vol. 10, no. 1, pp. 37–52, 1990.

[39] C. Berretta and J. Sansalone, "Hydrologic transport and partitioning of phosphorus fractions," *Journal of Hydrology*, vol. 403, no. 1-2, pp. 25–36, 2011.

[40] G. L. Bruland and G. DeMent, "Phosphorus sorption dynamics of hawaii's coastal wetlands," *Estuaries and Coasts*, vol. 32, no. 5, pp. 844–854, 2009.

[41] L. E. Fox, S. L. Sager, and S. C. Wofsy, "The chemical control of soluble phosphorus in the Amazon estuary," *Geochimica et Cosmochimica Acta*, vol. 50, no. 5, pp. 783–794, 1986.

[42] W. A. House, "The physico-chemical conditions for the precipitation of phosphate with calcium," *Environmental Technology*, vol. 20, no. 7, pp. 727–733, 1999.

[43] P. V. Sundareshwar and J. T. Morris, "Phosphorus sorption characteristics of intertidal marsh sediments along an estuarine salinity gradient," *Limnology and Oceanography*, vol. 44, no. 7, pp. 1693–1701, 1999.

Hindawi Publishing Corporation
The Scientific World Journal
Volume 2014, Article ID 765907, 10 pages
http://dx.doi.org/10.1155/2014/765907

Research Article

Soil Characteristic Comparison of Fenced and Grazed Riparian Floodplain Wetlands in the Typical Steppe Region of the Inner Mongolian Plateau, China

Lixin Wang,[1] Huamin Liu,[2] Yuhong Liu,[1,3] Jianwei Li,[1,4] Hongbo Shao,[3] Wei Wang,[2] and Cunzhu Liang[2]

[1] *College of Environment and Resources, Inner Mongolia University, Hohhot 010021, China*
[2] *College of Life Sciences, Inner Mongolia University, Hohhot 010021, China*
[3] *Yantai Institute of Coastal Zone Research, Chinese Academy of Sciences, Yantai 264003, China*
[4] *BERIS Engineering and Research Corporation, Baotou 014010, China*

Correspondence should be addressed to Yuhong Liu; yhliu@yic.ac.cn and Hongbo Shao; shaohongbochu@126.com

Received 19 March 2014; Accepted 24 March 2014; Published 19 May 2014

Academic Editor: Xu Gang

In recent decades, degradation of ecosystem in the steppe region of the Inner Mongolia Plateau, especially in riparian floodplain wetlands, has become a significant ecological crisis. Not uncommonly, with the increasing of livestock in the Inner Mongolian steppe region, a riparian floodplain wetland is becoming a hotspot area of grazing for local herdsmen. Hence, it is essential to understand degradation mechanisms of riparian floodplain wetland ecosystems caused by extensive grazing. In this study, the spatial distribution of soil compaction, salinity, total nitrogen, total phosphorus, organic carbon, and microbial biomass C and N were investigated. The results showed that grazing led to an increase in soil compaction and soil surface salinity, which significantly lowered levels of total N, P, and TOC in the soil surface. Grazing decreased soil microbial biomass C and N concentration in the lower riparian floodplain wetland, whereas it significantly increased soil microbial biomass C and N concentration in the higher riparian floodplain wetland. Elevation differences in the riparian floodplain wetland increased spatial heterogeneity in the soil and thus resulted in different influence of grazing on wetland soils and ecosystem. Therefore, elevation differences and grazing intensity were the main factors controlling soil characteristics in the riparian floodplain wetland of this region.

1. Introduction

The restoration and degradation characteristics of degraded riparian wetlands have become an important subject in wetland ecological studies [1–4]. Presently, most studies focused on decreases in wetland area and species succession, underlying degradation mechanisms affected by climate change [5, 6], land use [5–8], and overgrazing [9–14], and changes in nutrient composition of degraded wetlands [15–18].

With the increasing of livestock in the Inner Mongolian steppe region, grazing intensity also increased, which led to grassland degradation at various degrees [19, 20] and greatly decreases productivity [21, 22], hence existing pastures for grazing were not big enough to supply enough food for the livestock, and local people were transferring their livestock from grasslands to adjacent riparian floodplain wetlands [23, 24]. As a result, vegetation and soil physical and chemical properties of riparian floodplain wetland began to degrade, and riparian floodplain wetland ecosystem health was affected by grazing intensity. Although grazing effects on typical steppe ecosystems have been thoroughly studied, which includes biodiversity, grassland productivity, soil physical and chemical properties, and changes in the succession of degraded plant communities [24–31], few studies were carried on the influences of grazing on adjacent riparian wetland soil and their underlying mechanisms of degradation in this region.

In this study, a fenced conservation and a degraded grazing riparian floodplain wetland with similar initial

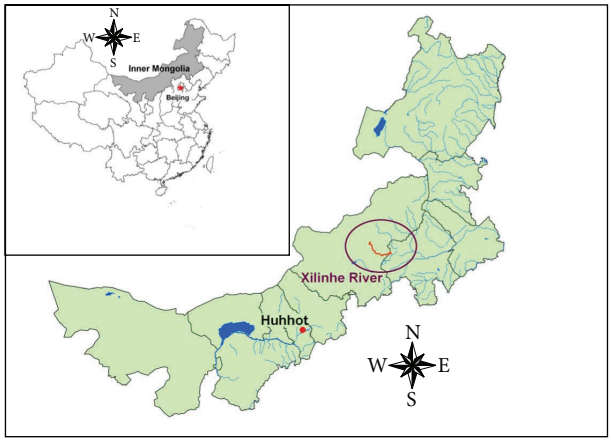

Figure 1: Location of Xilin River in Inner Mongolia, China.

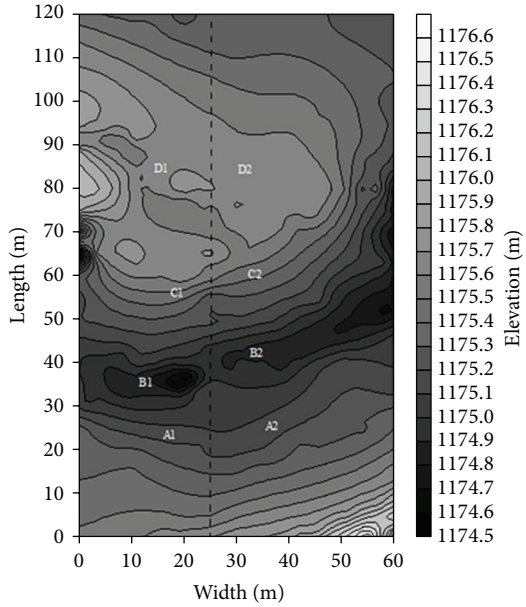

Figure 2: Topographical map of the study sites.

environmental conditions were chosen as experiment sites in the riparian floodplain wetland of the Xilin River in the typical steppe region in the Inner Mongolian Plateau. Soil properties and its nutrient contents of grazed and fenced river floodplain wetlands were investigated, and these characteristics were compared in order to provide a theoretical foundation for sustainable development and managing of wetland natural resources in the steppe regions of the Inner Mongolian Plateau. We hypothesized that (1) direct grazing and trampling would increase soil compaction and decrease soil carbon content and (2) various elevations would affect levels of inundation in riparian floodplain wetland, and this would change distribution of grazing intensity, whereas vegetation compositions and soil properties in different locations of floodplain wetland also would be altered accordingly.

2. Study Areas

The Xilin River, one of the major inland rivers, flows from southeast to northwest, and its floodplain with a total area of 10,000 km^2 is located at the eastern edge of the Xilingol High Plain in the middle of the Inner Mongolian Plateau (Figure 1). The elevation of the Xilin River watershed varies from 1,000 m to 1,500 m and decreases from east to west. The climate in the Xilin River watershed is described as a continental temperate steppe climate. The vegetation consists of typical steppe vegetation and the soil is mainly dark Kastanozems and light Kastanozems. The local economy is livestock-based.

Experiment sites, including grazed site and fenced site, were designed in the floodplain of the middle reach of the Xilin River 500 m away from the west of the Inner Mongolian Grassland Ecosystem Research Station of the Chinese Academy of Sciences with an elevation of 1,177 m (43°37′40″ N, 116°41′11″ E). Overgrazing and trampling caused by nearby livestock existed on the degraded grazed site, whereas the fenced site was enclosed to exclude grazing livestock. The two sites were separated by a fence (at 35 m on the x-axis in Figure 2) and had similar initial environmental conditions. To eliminate the influence of microtopography on soil physical and chemical properties, wetland soil characteristics at locations A, B, C, and D with similar topography were compared in the two sites (Figure 2). The species compositions of the fenced and grazed wetland were listed in Table 1.

3. Methods

3.1. Field Sampling and Laboratory Analysis. The samples of wetland soil were collected from 0–10 cm, 10–20 cm, 20–30 cm, 30–40 cm, and 40–50 cm by a soil auger with three replicates at each depth during the growing season in 2010. Soil compaction was measured by using the Soil Hardness Meter 6110 FS. Three soil samples obtained by cutting ring with a volume of 100 cm^3 were taken to the laboratory and dried at 108°C until constant weight in order to measure soil bulk density. Soil samples from different depths, from which plant tissues were removed, were air-dried and the remaining soil materials were then sieved through a 2 mm filter. About one-fourth of each sample was ground using a globe grinder RetschRM100, passed through a number 100 sieve (d = 150 μm), and then stored in glass vials for analyzing its chemical and physical properties. Soil total nitrogen (N) content, soil total phosphorus (P) content, and soil organic carbon (TOC) were measured by using a UDK 142 + DK20 Kjeltec Auto Analyzer, the Molybdenum blue colorimetric method [32], and a Liqui TOC analyzer (Germany) [33], respectively. C and N contents of soil microbial biomass were determined by using the chloroform fumigation-K_2SO_4 extraction method [34]. Soil salinity was tested by using a Spectrum 2265 FS [35], and pH was determined using a Spectrum IQ150 [36].

Table 1: The composition of plant community in the study sites.

Topography	Fenced			Grazed		
	Plant community	Plant height (cm)	Aboveground biomass (g/m^2)	Plant community	Plant height (cm)	Aboveground biomass (g/m^2)
Low floodplain wetlands	*Glyceria spiculosa* + *Poa subfastigiata* (A1)	40.66 ± 12.99	415.31 ± 128.84	*Carex appendiculata* + *Geranium vlassowianum* (A2)	18.63 ± 8.07	329.44 ± 40.17
	Carex. appendiculata + *Eleocharis valleculosa* (B1)	47.57 ± 17.07	889.49 ± 57.96	*Leymus chinensis* + *Melilotus officinalis* (B2)	38.67 ± 21.76	483.09 ± 181.44
Transition zone	*Carex. appendiculata* + *Glyceria spiculosa* (C1)	34.26 ± 10.46	467.92 ± 144.35	*Glyceria spiculosa* + *Agrostis gigantea* (C2)	14.03 ± 7.49	262.56 ± 94.45
High floodplain wetlands	*Leymus chinensis* + *Carex korshinskii* (D1)	26.07 ± 21.49	251.41 ± 126.04	*Leymus chinensis* + *Artemisia tanacetifolia* (D2)	15.43 ± 9.72	138.77 ± 24.23

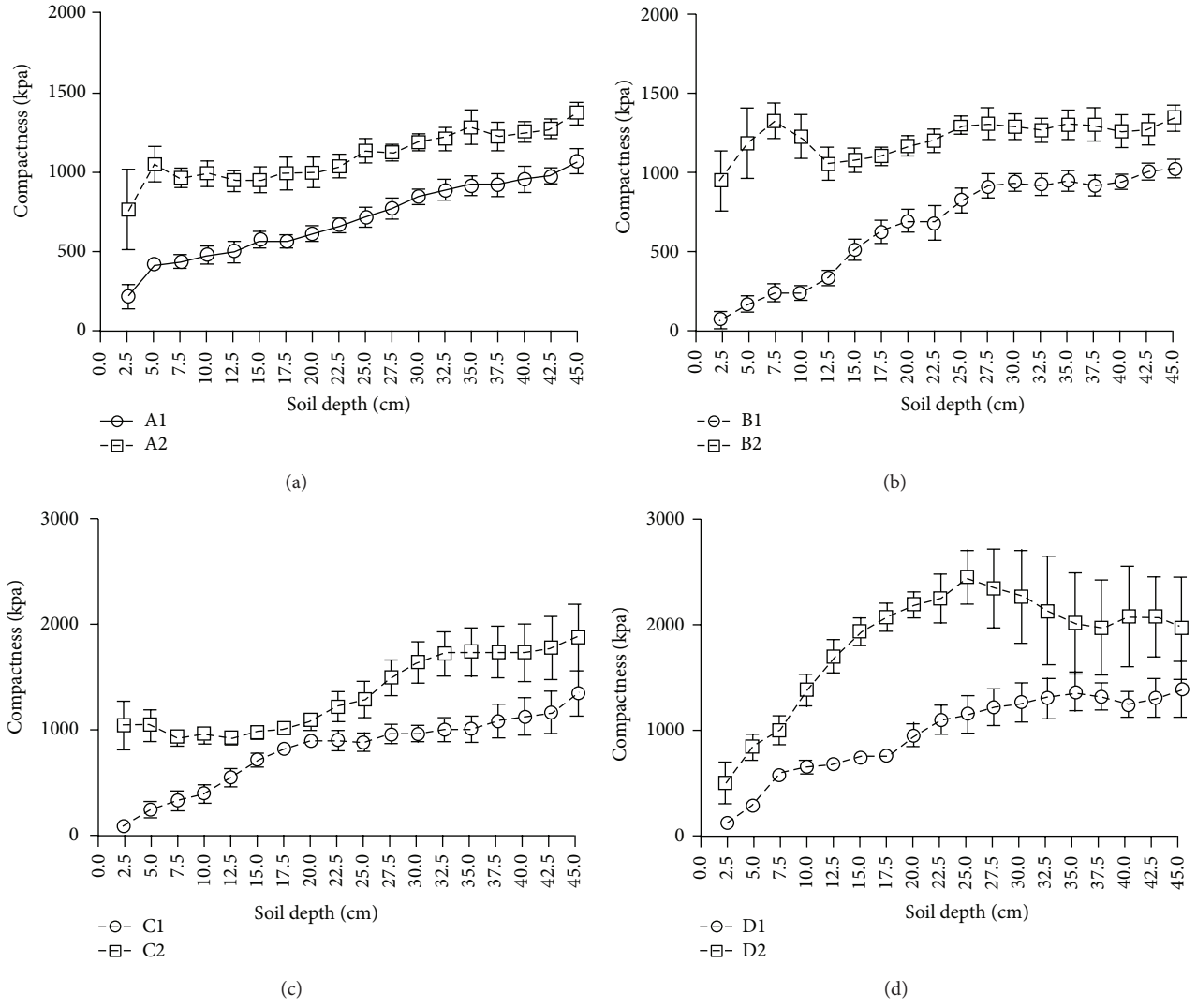

Figure 3: Spatial distribution of soil compaction.

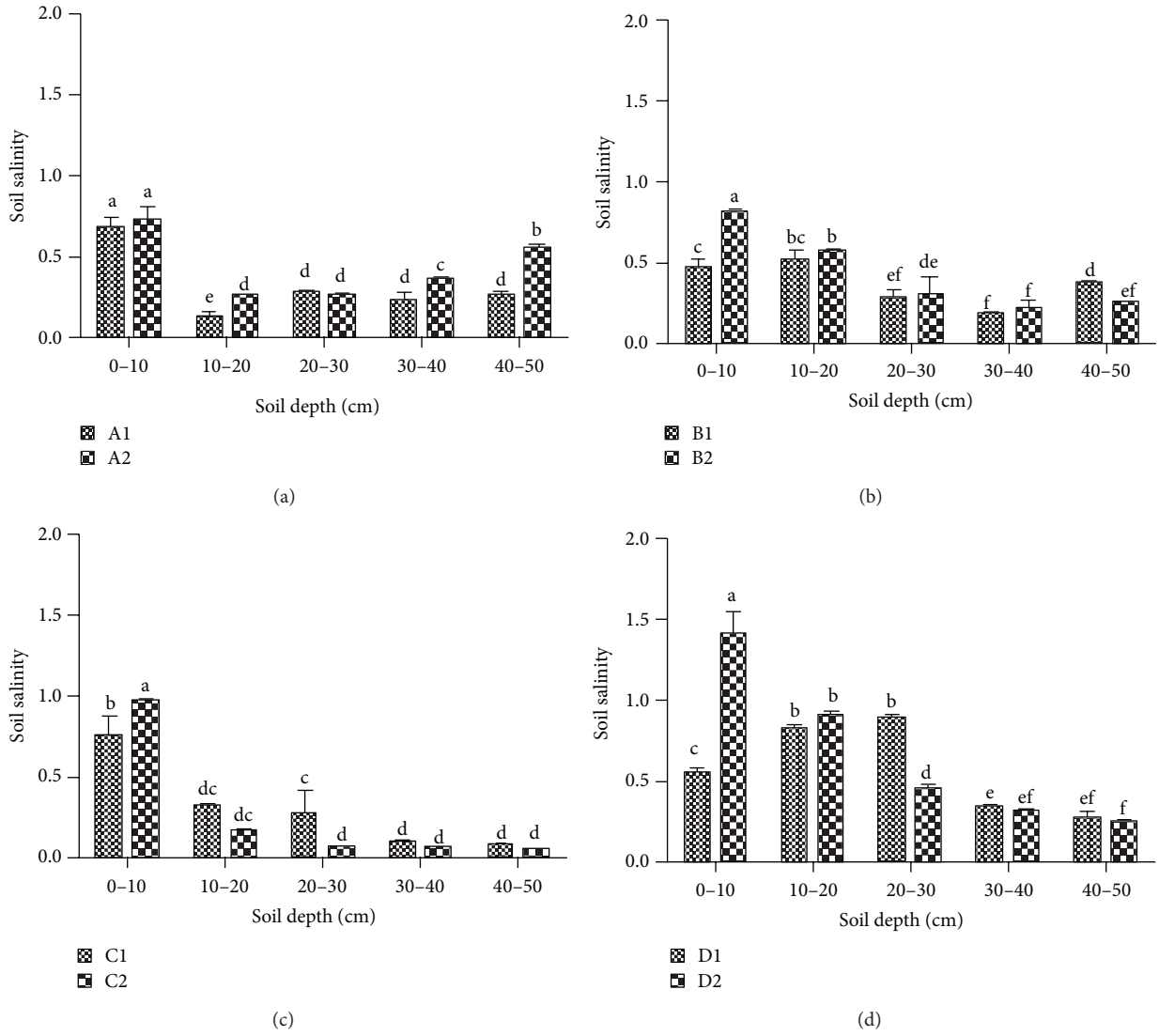

Figure 4: Spatial distribution of soil salinity.

3.2. Data Analysis. Data processing of soil compaction, soil nutrient, and soil microbial biomass C and N were performed using Microsoft Excel 2007 and GraphPad Prism 5.0.

One-way ANOVA was used to evaluate the differences among soil salinity of the grazed and fenced floodplain wetlands by SPSS 16.0.

4. Results

4.1. Comparison of Soil Compaction in Fenced and Grazed Wetlands. Grazing increased soil compaction (Figure 3), especially in the soil outside the fence. The soil compaction layer found in the A2 association was located at a depth of 5 cm from the soil surface, and the level of compaction increased with depth. The soil compaction layer found in the B2 association existed at a depth of 7.5 cm from the soil surface, and the level of soil compaction did not change much with depth. No soil compaction layer was found in the C2 and D2 association. Soil compaction in C2 association increased with depth. The greatest compaction in D2 was located at a depth of 27.5 cm. There were similar trends that soil compaction increased with depth in A1, B1, C1, and D1 association of fenced wetlands. Generally, the soil compaction in wetlands C and D was more than in wetlands A and B.

4.2. Spatial Distribution of Soil Salinity in Fenced and Grazed Wetlands. Soil salinity of the top 0–10 cm in the grazed sites was significantly greater than that of the fenced sites except for the same salinity in sites A1 and 2, while there were no significant differences in soil salinity of most other soil layers in grazed and fenced sites (Figure 4). Generally, with soil depth increasing, soil salinity decreased in fenced and grazed sites.

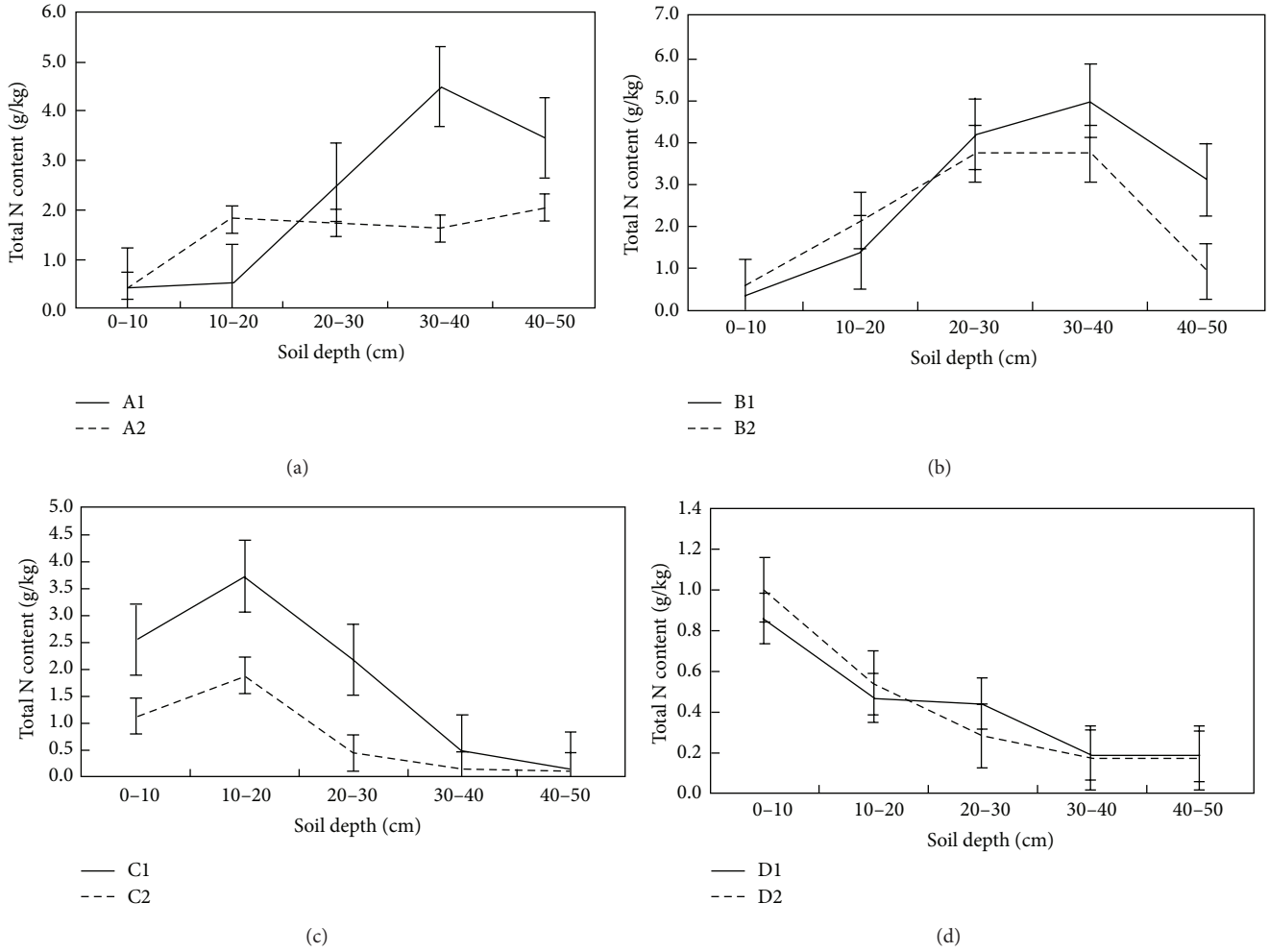

Figure 5: Spatial distribution of soil total N content.

4.3. Spatial Distribution of Soil Total N, Soil Total P, and Soil Organic C. The soil total C, N, and P vertical profiles were similar at the fenced and grazed sites except for in the associations of A1 and A2, hence grazing did not affect the vertical distribution of soil total N and P; that is, Maximum soil total C, N, and P content was found at a depth of 20–40 cm in B1 and B2, at a depth of 10–20 cm in C1 and C2, and at a depth of 0–10 cm in D1 and D2, whereas Maximum soil total C, N, and P content in A1 was different from in A2 (Figures 5, 6, and 7).

4.4. Comparison of Soil Microbial Biomass C and N. In the low elevation floodplain wetlands A and B, soil microbial biomass C and N content of the grazed site was greater than that of the fenced site. However, in the transition zone and the high elevation floodplain wetlands C and D, soil microbial biomass C and N content of the grazed site was significantly lower than that of the fenced site (Figure 8). Moreover, contents in soil microbial biomass C and N in the high elevation wetlands C and D were more than in the low elevation wetlands A and B.

5. Discussion

Some studies have reported that grazing and trampling increased soil compaction and soil salinity (e.g., [37, 38]), changed nutrient conditions (e.g., [39–41]), and resulted in a smaller size of individual wetland plant with lower biomass [42–44]. These phenomena also existed in our study results.

Our study further proved that grazing increased soil compaction in the grazed wetland more significantly than in the fenced wetland. Moreover, a compaction layer was formed in the soil surface of sites A2 and B2, while no soil compaction layers were found in the fenced wetlands. This was because undecomposed remains of plant litters accumulated fast in sites A and B, and trampling of livestock caused these remains to form a compaction layer. The large pores in the wetland soil are the main passage for transporting water, the reduction of which limits the transportation of water and nutrients to the roots [45, 46]. Generally, trampling reduced soil pore space in the wetland and increased soil compaction [38, 47, 48]. In the grazed sites A to D, grazing and trampling reduced soil pore space and lowered soil water content in site D more than in

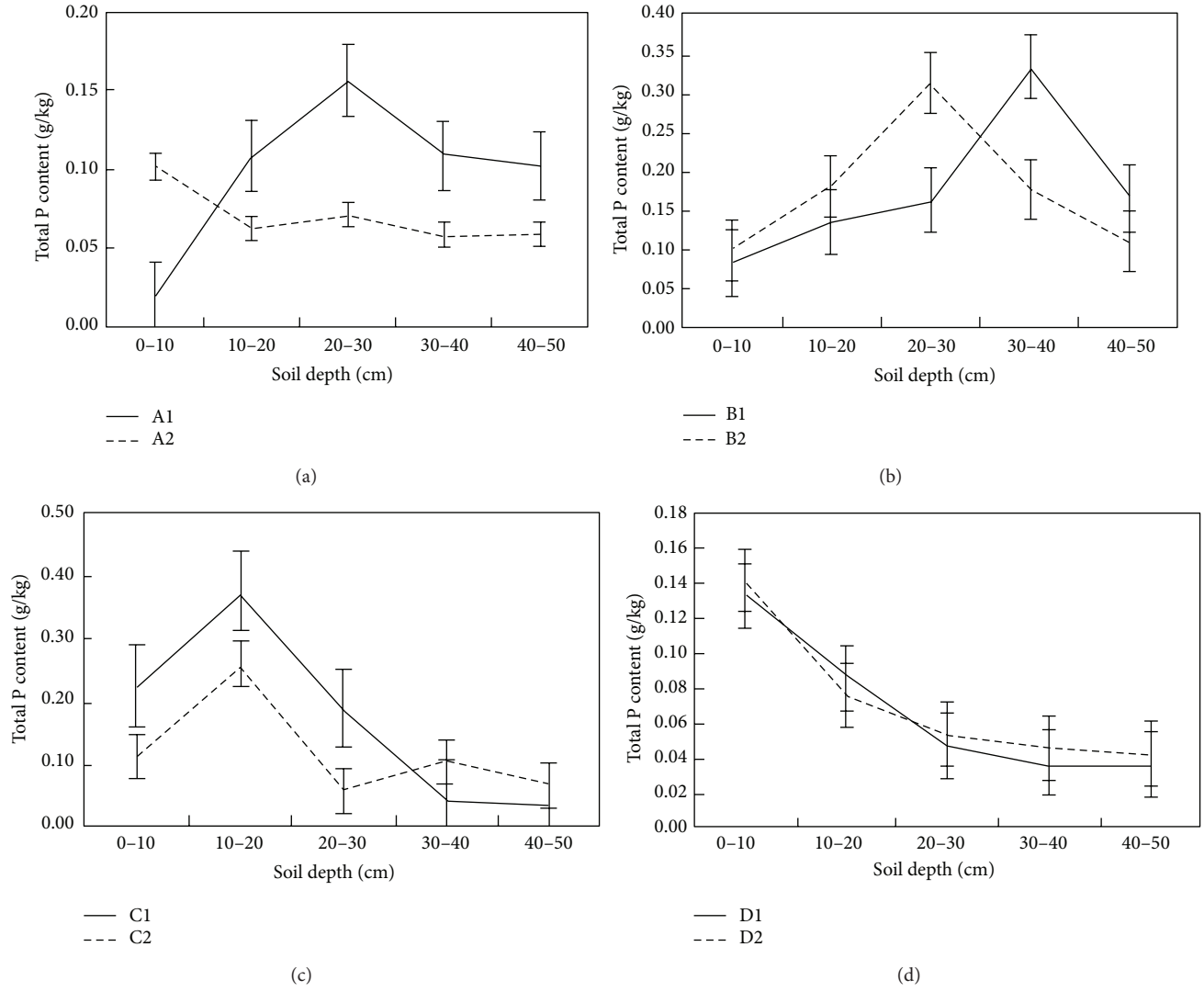

Figure 6: Spatial distribution of soil total P content.

the other sites, which were critical in changing soil physical properties.

Some studies investigated the response of wetland plants to grazing and found that reactions were dependent on hydrological conditions and grazing intensity [9, 49–51]. Soil water content was thus the main limiting factor for plant productivity [21, 52], and Pietola et al. [53] found that trampling at wetter conditions made surface soil looser and increased the air permeability and saturated hydraulic conductivity, while in deeper soil layers it was contrary. In this study, the floodplain wetlands A to D showed distinctive characteristics in the variety of soil compaction with increasing depth under the influence of grazing, and especially in site D, grazing effects were similar to the findings of Pietola et al. [53]. Grazing could decrease litter accumulation and cause plant functional types change, and heavy grazing would produce higher salinity and less biomass [37], which were obvious in our studies. Our studies further showed that grazing promoted the accumulation of soil salinity of the top 0–10 cm, and C, N, and P accumulation increased from shallow soil in sites D and C to deep soil on sites A and B. This was attributed to a decrease in soil water content from sites A and B to site D, which was caused by elevation of different sites. Moreover, compositions of plant species varied from sites A to D, and the abundance of tall and rhizomatous species decreased. The phenomenon of individual plant miniaturization revealed that grazing disturbed plant growth. Hence, depressional wetlands such as sites A and B in riparian floodplain benefited from organic C and nutrient accumulation and increased plant species richness.

The shift in elevation of riparian floodplain wetlands added to the spatial heterogeneity of wetland soil, which was also shown in the variations of soil microbial biomass C and N in this study. Grazing intensity increased soil microbial biomass C and N clearly [54, 55] and stagnant flood conditions also decreased microbial biomass [56], which explained that higher soil microbial biomass C and N existed in the higher elevation wetlands C and D for their higher

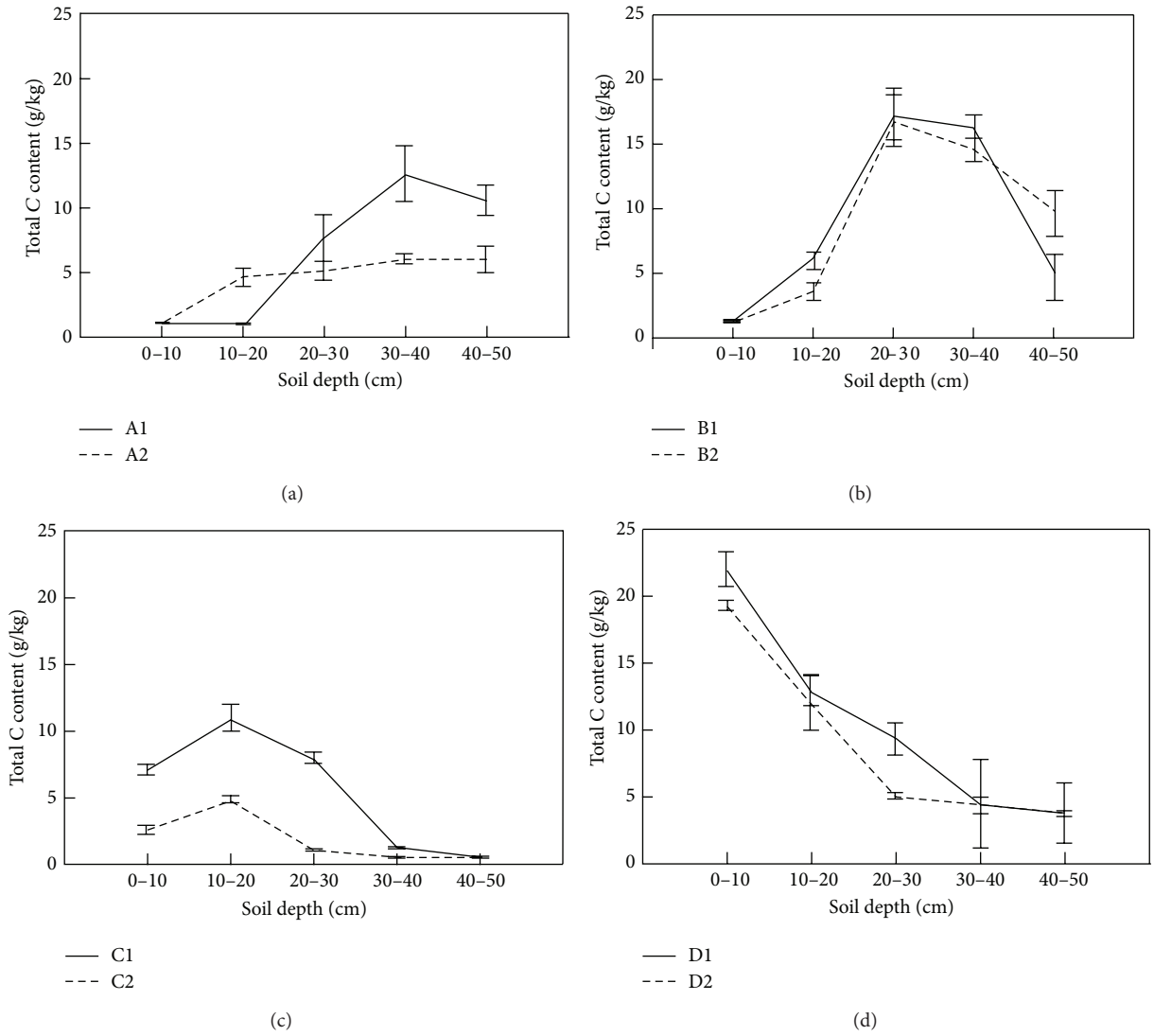

Figure 7: Spatial distribution of soil total C content.

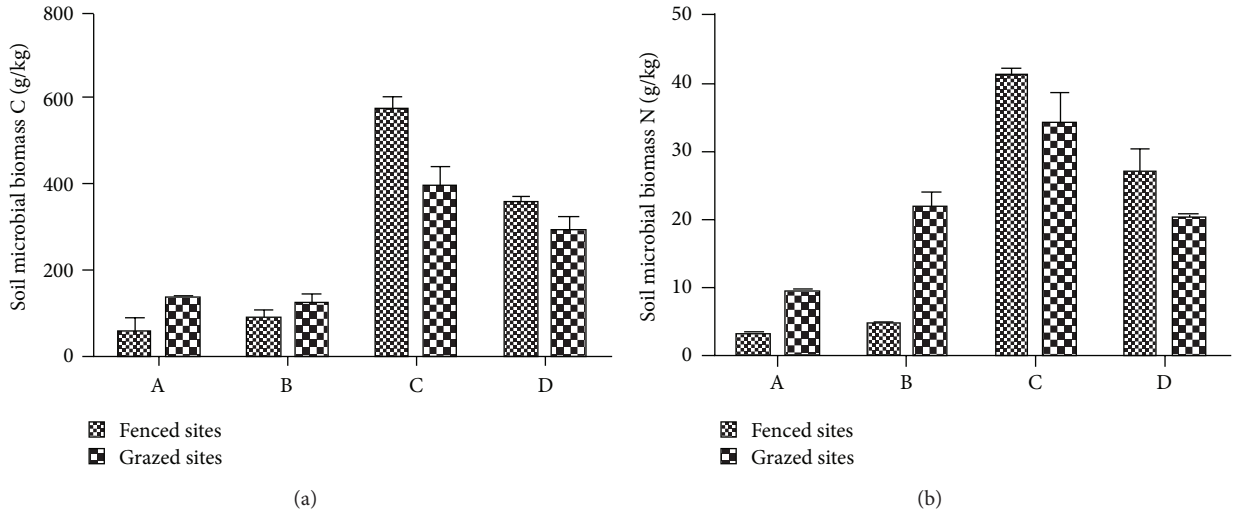

Figure 8: Spatial distribution of soil microbial biomass C and N.

grazing intensity and fewer inundation. The decrease in the number of soil pores limited the growing space for microbes and decreased microbial respiration [57]. The reduction in microbes broke efficient belowground cycles and thus lowered belowground productivity, that is, less root biomass [58, 59]. This phenomenon was obvious in sites C and D. If extensive grazing still continued, plant productivity of the riparian wetland would further decrease and eventually result in extreme ecosystem degradation [19, 29]. Wetland degradation caused less water infiltration, greater surface runoff, and more soil nutrient loss [60–63]. Therefore, grazing also lowered soil total N and total P content in the wetland [37, 64].

All of these changes of the wetland soil resulting from grazing were consistent with the responses of typical degraded steppe to grazing, including lower soil nutrient contents, more compact soil with a compaction layer at the soil surface, and salinized soil [65–69]. Therefore, we should realize the importance of conserving wetland and grassland ecosystems in Xilin River riparian floodplain wetland and strengthen the management of grazing to restore ecosystem health of riparian floodplain wetland.

6. Conclusion

Comparison of the soil in the fenced and grazed riparian floodplain wetland in the steppe region of the Inner Mongolian Plateau showed that grazing and trampling from livestock resulted in a more compact soil with a surface compaction layer and less TOC, total N, and total P concentration. Overgrazing produced more exposed soil surfaces, greater soil surface salinity with a tendency towards salinization, and degradation of wetland vegetation. However, variable elevations of riparian floodplain wetlands formed greater spatial heterogeneity in wetland soil and vegetation composition, and thus different topographical characteristics displayed in the influence of grazing on riparian floodplain wetland. Additionally, wetland plant communities at a higher elevation location in riparian floodplain wetland endured more grazing pressures.

Conflict of Interests

The authors declare that there is no conflict of interests regarding the publication of this paper.

Authors' Contribution

Lixin Wang and Huamin Liu contributed to the work in the paper equally.

Acknowledgments

This study was supported by the National Key Basic Research Program of China (no. 2014CB138802), the National Key Technology R&D Program of China (nos. 2011BAC02B03 and 2013BAC09B03), and the National Natural Science Funds of China (nos. 31060076 and 41261009).

References

[1] P. Dugan, *Wetlands in Danger*, Mitchell Beazley, London, UK, 1992.

[2] K. D. Schuyt, "Economic consequences of wetland degradation for local populations in Africa," *Ecological Economics*, vol. 53, no. 2, pp. 177–190, 2005.

[3] J. B. Zedler, "Progress in wetland restoration ecology," *Trends in Ecology and Evolution*, vol. 15, no. 10, pp. 402–407, 2000.

[4] J. Bai, B. Cui, H. Cao, A. Li, and B. Zhang, "Wetland degradation and ecological restoration," *The Scientific World Journal*, vol. 2013, Article ID 523632, 2 pages, 2013.

[5] P. Banaszuk and A. Kamocki, "Effects of climatic fluctuations and land-use changes on the hydrology of temperate fluviogenous mire," *Ecological Engineering*, vol. 32, no. 2, pp. 133–146, 2008.

[6] K. L. Erwin, "Wetlands and global climate change: the role of wetland restoration in a changing world," *Wetlands Ecology and Management*, vol. 17, no. 1, pp. 71–84, 2009.

[7] J. Álvarez-Rogel, F. J. Jiménez-Cárceles, M. J. Roca, and R. Ortiz, "Changes in soils and vegetation in a Mediterranean coastal salt marsh impacted by human activities," *Estuarine, Coastal and Shelf Science*, vol. 73, no. 3-4, pp. 510–526, 2007.

[8] Z. Luan and D. Zhou, "Impacts of intensified agriculture developments on marsh wetlands," *The Scientific World Journal*, vol. 2013, Article ID 409439, 10 pages, 2013.

[9] W. M. Jones, L. H. Fraser, and P. J. Curtis, "Plant community functional shifts in response to livestock grazing in intermountain depressional wetlands in British Columbia, Canada," *Biological Conservation*, vol. 144, no. 1, pp. 511–517, 2011.

[10] P. Laffaille, J.-C. Lefeuvre, and E. Feunteun, "Impact of sheep grazing on juvenile sea bass, Dicentrarchus labrax L., in tidal salt marshes," *Biological Conservation*, vol. 96, no. 3, pp. 271–277, 2000.

[11] Y. S. Olsen, A. Dausse, A. Garbutt, H. Ford, D. N. Thomas, and D. L. Jones, "Cattle grazing drives nitrogen and carbon cycling in a temperate salt marsh," *Soil Biology and Biochemistry*, vol. 43, no. 3, pp. 531–541, 2011.

[12] M. A. Reid, R. Ogden, and M. C. Thoms, "The influence of flood frequency, geomorphic setting and grazing on plant communities and plant biomass on a large dryland floodplain," *Journal of Arid Environments*, vol. 75, no. 9, pp. 815–826, 2011.

[13] R. J. Reimold, R. A. Linthurst, and P. L. Wolf, "Effects of grazing on a salt marsh," *Biological Conservation*, vol. 8, no. 2, pp. 105–125, 1975.

[14] N. Rossignol, A. Bonis, and J.-B. Bouzillé, "Consequence of grazing pattern and vegetation structure on the spatial variations of net N mineralisation in a wet grassland," *Applied Soil Ecology*, vol. 31, no. 1-2, pp. 62–72, 2006.

[15] Z.-Y. Wang, Y.-Z. Xin, D.-M. Gao, F.-M. Li, J. Morgan, and B.-S. Xing, "Microbial community characteristics in a degraded wetland of the Yellow River Delta," *Pedosphere*, vol. 20, no. 4, pp. 466–478, 2010.

[16] D. Moreno-Mateos, M. E. Power, F. A. Comín, and R. Yockteng, "Structural and functional loss in restored wetland ecosystems," *PLoS Biology*, vol. 10, no. 1, Article ID e1001247, 2012.

[17] I. Douterelo, R. Goulder, and M. Lillie, "Soil microbial community response to land-management and depth, related to the degradation of organic matter in English wetlands: implications for the in situ preservation of archaeological remains," *Applied Soil Ecology*, vol. 44, no. 3, pp. 219–227, 2010.

[18] H. M. Yao, J. Bai, and Z. Zhang, "Variations of soil organic matter and nutrients in degenerated wetland in response to ecological restoration in shuangtaizi erstuary, Northeast China," *Advanced Materials Research*, vol. 664, pp. 48–54, 2013.

[19] W. J. Li, S. H. Ali, and Q. Zhang, "Property rights and grassland degradation: a study of the Xilingol Pasture, Inner Mongolia, China," *Journal of Environmental Management*, vol. 85, no. 2, pp. 461–470, 2007.

[20] D. M. Williams, "Grassland enclosures: catalyst of land degradation in Inner Mongolia," *Human Organization*, vol. 55, no. 3, pp. 307–313, 1996.

[21] Y. Z. Gao, M. Giese, S. Lin, B. Sattelmacher, Y. Zhao, and H. Brueck, "Belowground net primary productivity and biomass allocation of a grassland in Inner Mongolia is affected by grazing intensity," *Plant and Soil*, vol. 307, no. 1-2, pp. 41–50, 2008.

[22] Y. Bai, L. Li, Q. Wang, L. Zhang, Y. Zhang, and Z. Chen, "Changes in plant species diversity and productivity along gradients of precipitation and elevation in the Xilin River Basin, Inner Mongolia," *Acta Phytoecologica Sinica*, vol. 24, no. 6, pp. 667–673, 2000.

[23] J. W. Li, L. X. Wang, W. Wang, C. Z. Liang, and H. M. Liu, "Characterization of degradation of wetland plant communities on floodplain in typical steppe region of Inner Mongolia Plateau, China," *Chinese Journal of Plant Ecology*, vol. 36, no. 1, pp. 10–18, 2012.

[24] H. Olff and M. E. Ritchie, "Effects of herbivores on grassland plant diversity," *Trends in Ecology and Evolution*, vol. 13, no. 7, pp. 261–265, 1998.

[25] P. Adler, D. Raff, and W. Lauenroth, "The effect of grazing on the spatial heterogeneity of vegetation," *Oecologia*, vol. 128, no. 4, pp. 465–479, 2001.

[26] H. Olff and M. E. Ritchie, "Effects of herbivores on grassland plant diversity," *Trends in Ecology and Evolution*, vol. 13, no. 7, pp. 261–265, 1998.

[27] A. Altesor, M. Oesterheld, E. Leoni, F. Lezama, and C. Rodríguez, "Effect of grazing on community structure and productivity of a Uruguayan grassland," *Plant Ecology*, vol. 179, no. 1, pp. 83–91, 2005.

[28] B. Peco, I. de Pablos, J. Traba, and C. Levassor, "The effect of grazing abandonment on species composition and functional traits: the case of dehesa grasslands," *Basic and Applied Ecology*, vol. 6, no. 2, pp. 175–183, 2005.

[29] P. Schönbach, H. Wan, M. Gierus et al., "Grassland responses to grazing: effects of grazing intensity and management system in an Inner Mongolian steppe ecosystem," *Plant and Soil*, vol. 340, no. 1, pp. 103–115, 2011.

[30] A. Zemmrich, M. Manthey, S. Zerbe, and D. Oyunchimeg, "Driving environmental factors and the role of grazing in grassland communities: a comparative study along an altitudinal gradient in Western Mongolia," *Journal of Arid Environments*, vol. 74, no. 10, pp. 1271–1280, 2010.

[31] Z. Luan, Z. Wang, D. Yan, G. Liu, and Y. Xu, "The ecological response of carex lasiocarpa community in the riparian wetlands to the environmental gradient of water depth in sanjiang plain, Northeast China," *The Scientific World Journal*, vol. 2013, Article ID 402067, 7 pages, 2013.

[32] M. A. Tabatabai and W. A. Dick, "Simultaneous determination of nitrate, chloride, sulfate, and phosphate in natural waters by ion chromatography," *Journal of Environmental Quality*, vol. 12, no. 2, pp. 209–213, 1983.

[33] A. Braun, M. Wolter, F. Zadrazil, G. Flachowsky, C. Mba, and L. V. Griensven, "Bioconversion of wheat straw by Lentinus tuber-regium and its potential utilization as food, medicine and animal feed," in *Science and Cultivation of Edible Fungi*, A. Van Griensven and A. A. Balkema, Eds., pp. 549–558, 2000.

[34] E. D. Vance, P. C. Brookes, and D. S. Jenkinson, "An extraction method for measuring soil microbial biomass C," *Soil Biology and Biochemistry*, vol. 19, no. 6, pp. 703–707, 1987.

[35] Y. Li, T. Wang, J. Li, and Y. Ao, "Effect of phosphorus on celery growth and nutrient uptake under different calcium and magnesium levels in substrate culture," *Horticultural Science*, vol. 37, no. 3, pp. 99–108, 2010.

[36] K. E. Segarra, *Source or Sink? Analysis of Narragansett Bay's Carbon Cycle*, Brown University, 2002.

[37] L. M. Teuber, N. Hoelzel, and L. H. Fraser, "Livestock grazing in intermountain depressional wetlands-effects on plant strategies, soil characteristics and biomass," *Agriculture Ecosystems & Environment*, vol. 175, pp. 21–28, 2013.

[38] A. J. Belsky and D. M. Blumenthal, "Effects of livestock grazing on stand dynamics and soils in upland forests of the Interior West," *Conservation Biology*, vol. 11, no. 2, pp. 315–327, 1997.

[39] R. A. Golluscio, A. T. Austin, G. C. García Martínez, M. Gonzalez-Polo, O. E. Sala, and R. B. Jackson, "Sheep grazing decreases organic carbon and nitrogen pools in the patagonian steppe: combination of direct and indirect effects," *Ecosystems*, vol. 12, no. 4, pp. 686–697, 2009.

[40] E. S. Bakker, H. Olff, M. Boekhoff, J. M. Gleichman, and F. Berendse, "Impact of herbivores on nitrogen cycling: contrasting effects of small and large species," *Oecologia*, vol. 138, no. 1, pp. 91–101, 2004.

[41] J. D. Reeder and G. E. Schuman, "Influence of livestock grazing on C sequestration in semi-arid mixed-grass and short-grass rangelands," *Environmental Pollution*, vol. 116, no. 3, pp. 457–463, 2002.

[42] J. Zimmermann, S. I. Higgins, V. Grimm, J. Hoffmann, and A. Linstädter, "Grass mortality in semi-arid savanna: the role of fire, competition and self-shading," *Perspectives in Plant Ecology, Evolution and Systematics*, vol. 12, no. 1, pp. 1–8, 2010.

[43] G.-L. Wu, G.-Z. Du, Z.-H. Liu, and S. Thirgood, "Effect of fencing and grazing on a Kobresia-dominated meadow in the Qinghai-Tibetan Plateau," *Plant and Soil*, vol. 319, no. 1-2, pp. 115–126, 2009.

[44] W. Wang, C. Z. Liang, Z. L. Liu, and D. Y. Hao, "Mechanism of degradation succession in Leymus chinensis + Stipa grandis steppe community," *Acta Phytoecologica Sinica*, vol. 24, no. 4, pp. 468–472, 2000.

[45] J. J. Drewry, J. A. H. Lowe, and R. J. Paton, "Effect of sheep stocking intensity on soil physical properties and dry matter production on a Pallic Soil in Southland," *New Zealand Journal of Agricultural Research*, vol. 42, no. 4, pp. 493–499, 1999.

[46] J. M. Warren, J. R. Brooks, M. I. Dragila, and F. C. Meinzer, "In situ separation of root hydraulic redistribution of soil water from liquid and vapor transport," *Oecologia*, vol. 166, no. 4, pp. 899–911, 2011.

[47] D. H. McNabb, A. D. Startsev, and H. Nguyen, "Soil wetness and traffic level effects on bulk density and air-filled porosity of compacted boreal forest soils," *Soil Science Society of America Journal*, vol. 65, no. 4, pp. 1238–1247, 2001.

[48] M. A. Wheeler, M. J. Trlica, G. W. Frasier, and J. D. Reeder, "Seasonal grazing affects soil physical properties of a montane riparian community," *Journal of Range Management*, vol. 55, no. 1, pp. 49–56, 2002.

[49] J. E. Austin, J. R. Keough, and W. H. Pyle, "Effects of habitat management treatments on plant community composition and biomass in a Montane wetland," *Wetlands Ecology and Management*, vol. 27, no. 3, pp. 570–587, 2007.

[50] R. W. Lucas, T. T. Baker, M. K. Wood, C. D. Allison, and D. M. Vanleeuwen, "Riparian vegetation response to different intensities and seasons of grazing," *Journal of Range Management*, vol. 57, no. 5, pp. 466–474, 2004.

[51] T. T. Schulz and W. C. Leininger, "Differences in riparian vegetation structure between grazed areas and exclosures," *Journal of Range Management*, vol. 43, no. 4, pp. 295–299, 1990.

[52] W. Webb, S. Szarek, W. Lauenroth, R. Kinerson, and M. Smith, "Primary productivity and water use in native forest, grassland, and desert ecosystems," *Ecology*, vol. 59, no. 6, pp. 1239–1247, 1978.

[53] L. Pietola, R. Horn, and M. Yli-Halla, "Effects of trampling by cattle on the hydraulic and mechanical properties of soil," *Soil and Tillage Research*, vol. 82, no. 1, pp. 99–108, 2005.

[54] K.-H. Wang, R. McSorley, P. Bohlen, and S. M. Gathumbi, "Cattle grazing increases microbial biomass and alters soil nematode communities in subtropical pastures," *Soil Biology and Biochemistry*, vol. 38, no. 7, pp. 1956–1965, 2006.

[55] R. D. Bardgett, D. K. Leemans, R. Cook, and P. J. Hobbs, "Seasonality in the soil biota of grazed and ungrazed hill grasslands," *Soil Biology and Biochemistry*, vol. 29, no. 8, pp. 1285–1294, 1997.

[56] I. M. Unger, A. C. Kennedy, and R.-M. Muzika, "Flooding effects on soil microbial communities," *Applied Soil Ecology*, vol. 42, no. 1, pp. 1–8, 2009.

[57] P. Jouquet, G. Huchet, N. Bottinelli, T. D. Thu, and T. T. Duc, "Does the influence of earthworms on water infiltration, nitrogen leaching and soil respiration depend on the initial soil bulk density? A mesocosm experiment with the endogeic species Metaphire posthuma," *Biology and Fertility of Soils*, vol. 48, no. 5, pp. 561–567, 2012.

[58] M. Luke McCormack and C. W. Fernandez, "Measuring and modeling roots, the rhizosphere, and microbial processes belowground," *The New phytologist*, vol. 192, no. 3, pp. 573–575, 2011.

[59] P. M. Haygarth, R. D. Bardgett, and L. M. Condron, "Nitrogen and phosphorus cycles and their management," in *Gregory Soil Conditions and Plant Growth*, P. H. Gregory and S. Nortcliff, Eds., pp. 132–159, John Wiley & Sons, 2012.

[60] C. Huang, J. Bai, H. Shao et al., "Changes in soil properties before and after wetland degradation in the Yellow River Delta, China," *CLEAN-Soil, Air, Water*, vol. 40, no. 10, pp. 1125–1130, 2012.

[61] K. Ballantine, R. Schneider, P. Groffman, and J. Lehmann, "Soil properties and vegetative development in four restored freshwater depressional wetlands," *Soil Science Society of America Journal*, vol. 76, no. 4, pp. 1482–1495, 2012.

[62] L. Huo, Z. Chen, Y. Zou, X. Lu, J. Guo, and X. Tang, "Effect of Zoige alpine wetland degradation on the density and fractions of soil organic carbon," *Ecological Engineering*, vol. 51, pp. 287–295, 2013.

[63] J. Bai, H. Ouyang, R. Xiao et al., "Spatial variability of soil carbon, nitrogen, and phosphorus content and storage in an alpine wetland in the Qinghai-Tibet Plateau, China," *Australian Journal of Soil Research*, vol. 48, no. 8, pp. 730–736, 2010.

[64] J. Reader and C. Craft, "Comparison of wetland structure and function on grazed and ungrazed salt marshes," *Journal of the Elisha Mitchell Scientific Society*, vol. 115, no. 4, pp. 236–249, 1999.

[65] R. S. Lavado, J. O. Sierra, and P. N. Hashimoto, "Impact of grazing on soil nutrients in a Pampean grassland," *Journal of Range Management*, vol. 49, no. 5, pp. 452–457, 1996.

[66] S. Yong-Zhong, L. Yu-Lin, C. Jian-Yuan, and Z. Wen-Zhi, "Influences of continuous grazing and livestock exclusion on soil properties in a degraded sandy grassland, Inner Mongolia, northern China," *Catena*, vol. 59, no. 3, pp. 267–278, 2005.

[67] A. B. Frank, D. L. Tanaka, L. Hofmann, and R. F. Follett, "Soil carbon and nitrogen of Northern Great Plains grasslands as influenced by long-term grazing," *Journal of Range Management*, vol. 48, no. 5, pp. 470–474, 1995.

[68] G. Pineiro, J. M. Paruelo, M. Oesterheld, and E. G. Jobbágy, "Pathways of grazing effects on soil organic carbon and nitrogen," *Rangeland Ecology and Management*, vol. 63, no. 1, pp. 109–119, 2010.

[69] X. M. Shi, X. G. Li, C. T. Li, Y. Zhao, Z. H. Shang, and Q. Ma, "Grazing exclusion decreases soil organic C storage at an alpine grassland of the Qinghai-Tibetan Plateau," *Ecological Engineering*, vol. 57, pp. 183–187, 2013.

Hindawi Publishing Corporation
The Scientific World Journal
Volume 2014, Article ID 412183, 7 pages
http://dx.doi.org/10.1155/2014/412183

Research Article

Effects of Different Vegetation Zones on CH_4 and N_2O Emissions in Coastal Wetlands: A Model Case Study

Yuhong Liu,[1,2] Lixin Wang,[1] Shumei Bao,[1] Huamin Liu,[3] Junbao Yu,[2] Yu Wang,[4] Hongbo Shao,[1,2] Yan Ouyang,[4] and Shuqing An[4]

[1] *College of Environment and Resources, Inner Mongolia University, Hohhot 010021, China*
[2] *Key Laboratory of Coastal Zone Environmental Processes, Yantai Institute of Coastal Zone Research, Chinese Academy of Sciences, Yantai 264003, China*
[3] *College of Life Sciences, Inner Mongolia University, Hohhot 010021, China*
[4] *The Institute of Wetland Ecology, School of Life Science, Nanjing University, Nanjing 210093, China*

Correspondence should be addressed to Lixin Wang; lx_wimu@163.com and Hongbo Shao; shaohongbochu@126.com

Received 8 March 2014; Accepted 21 March 2014; Published 29 April 2014

Academic Editor: Xu Gang

The coastal wetland ecosystems are important in the global carbon and nitrogen cycle and global climate change. For higher fragility of coastal wetlands induced by human activities, the roles of coastal wetland ecosystems in CH_4 and N_2O emissions are becoming more important. This study used a DNDC model to simulate current and future CH_4 and N_2O emissions of coastal wetlands in four sites along the latitude in China. The simulation results showed that different vegetation zones, including bare beach, *Spartina* beach, and *Phragmites* beach, produced different emissions of CH_4 and N_2O in the same latitude region. Correlation analysis indicated that vegetation types, water level, temperature, and soil organic carbon content are the main factors affecting emissions of CH_4 and N_2O in coastal wetlands.

1. Introduction

Methane (CH_4) and nitrous oxide (N_2O) are important active greenhouse gases contributing to global warming [1, 2]. Contributions of CH_4 and N_2O to global warming are 21 and 310 times of CO_2 [3] and occupy about 15% and 5% of greenhouse effects [4], respectively. Moreover, the two kinds of gases in the atmosphere are growing at 3% and 0.22% per year, respectively [5]. As an important source and sink of greenhouse gases, the coastal wetland ecosystems are important in the global carbon and nitrogen cycle and global climate change. Since coastal wetlands belong to the ecologically fragile zone [6], it is important to understand the relationships between vegetation characteristics and CH_4 and N_2O emissions.

Many studies on CH_4 and N_2O emissions in natural wetlands are carried out since the 1990s and focus on their emissions, absorptions, spatial and temporal variations, and environmental factors. Although the effects of vegetation features on CH_4 and N_2O emissions from wetland ecosystems worldwide have been investigated (e.g., [7–9]), these studies in our country are still relatively weak. In China, greenhouse gas emission flux and the effects of environmental factors are mainly concentrated on *Phragmites* wetland of the Sanjiang plain [10] and in the southern mangrove coastal wetlands [11, 12]. Recently, the spatial and temporal variations of N_2O and CH_4 fluxes associated with abiotic sediment parameters are quantified in the coastal marsh dominated by *Suaeda salsa* in the Yellow River estuary [13], and the effects of *different vegetation, Spartina alterniflora* and *Phragmites australis,* on CH_4 and N_2O emissions are investigated by using experimental mesocosms [9]. However, these studies do not compare roles of vegetation zone in different areas in CH_4 and N_2O emissions and future variations of CH_4 and N_2O emissions in coastal wetlands of China.

In this study, denitrification-decomposition (DNDC) model was used to simulate wetland biogeochemistry processes and its response to global warming in the four sites

of coastal zone distributing along the latitude. By simulation analysis, the following research questions were focused on the following.

(1) Are there differences in effects of different vegetation zones on CH_4 and N_2O emissions of coastal wetlands in different sites along latitude?

(2) How will CH_4 and N_2O emissions change with increasing temperature in coastal wetlands?

2. Materials and Methods

2.1. Study Areas. Four coastal wetlands were chosen in Sheyang, Dongtai, and Nantong of Jiangsu province and Chongming of Shanghai city (Figure 1). Each coastal wetland was divided into the bare beach, *Spartina* beach, and *Phragmites* beach according to vegetation type distribution.

Coastal zone of Jiangsu is affected by marine and continental climate. Average annual temperature is about 15°C. Average annual rainfall increases gradually from north to south, and average annual relative humidity decreases from south to north.

Chongming in Shanghai city is affected by subtropical marine monsoon climate. Average annual temperature is about 16°C, and average annual rainfall is about 1,030 mm.

2.2. Description of DNDC Model. The DNDC model takes denitrification and decomposition as the main processes applied in soil carbon and nitrogen biogeochemical cycles [14]. DNDC model has been applied in agriculture, forest, and grassland research worldwide for calculating soil carbon sequestration and greenhouse gas emissions [15]. This model consists of six submodels including soil, climate, plant growth, decomposition of organic matter, nitrification, denitrification, and fermentation process. Input variables of this model are soil properties, climate conditions, and agricultural production measures, and output variables are daily C and N content in soil and plant, soil temperature, and humidity data at different levels, and output variables are the emissions flux of CO_2, CH_4, N_2O, and NO.

2.3. Acquisition of Meteorological Data. Daily observation meteorological data in 1988 (for 80s) and 2004 (for 00s) are obtained from "China Meteorological Data Sharing Service System" (http://cdc.cma.gov.cn/). According to input data requirements, the daily maximum temperature (°C), the daily minimum temperature (°C), the rainfall data (cm), and other correlated data are turned into text format (ASCII encoding) and ready for input into the model. Future meteorological data are calculated by IPCC simulations.

2.4. Collection of Soil Parameters. Land use type and soil texture in this study are wetlands and silt loam, respectively, which were set directly in the options of DNDC model. Soil bulk density, soil pH, and surface soil organic carbon (SOC) content are obtained from literatures and field measurements measured in 2004. By inputting these soil data, the model would give other corresponding soil data, and default data would be used in this study.

2.5. Collection of Plant Physiological Parameters. In this paper, plant types included no plant (bare beach), *Spartina,* and *Phragmites*, which were not listed in the DNDC model. Therefore, we chose "0 Fallow" of the DNDC model to simulate a bare beach, while *Spartina* and *Phragmites* were created as new plant options. The two plant physiological parameters including biomass, C\N, LAI, and water requirement, for this model, were collected by literatures and field measurements in 2004.

2.6. Hydrological Data Preparation. The DNDC model provides four patterns to simulate the influence of flooding, including irrigation, rain-fed, observed water-table data, and empirical parameters. This study adopted observed water-table data pattern. Tidal data were obtained from tidal tables of the Yellow Sea and Bohai Sea, in 2004 and 1990, and Xiaoyang, Lvsi, Sheshan, and Sheyang port were chosen as tidal stations for Dongtai, Nantong, Chongming, and Sheyang, respectively. Every 10-day tidal height and tidal height datum of the port and the elevation of different wetlands were used to calculate the water levels of bare beach, *Spartina* beach, and *Phragmites* beach, which were made into water level table finally.

3. Results

3.1. Comparison of CH_4 and N_2O Annual Emission Flux of Different Beaches. The annual CH_4 emission flux of different beaches including Sheyang, Dongtai, Nantong, and Chongming has a similar trend between 80s and 00s (Figure 2), and similar phenomenon occurred for N_2O emission flux (Figure 3). The order of CH_4 emission ability in different beaches is *Spartina* beach > *Phragmites* beach > bare flat, while for N_2O the order is *Phragmites* beach > *Spartina* beach > bare flat (Figures 2 and 3). *Spartina alterniflora* and *Phragmites australis* increase CH_4 and N_2O emission fluxes contrasting with bare beach, which suggests that the vegetation type is one of the important factors affecting warm gas emission. CH_4 emission ability of *Spartina* beach is higher than *Phragmites* beach, while N_2O emission ability is contrary.

3.2. Comparison of Future CH_4 and N_2O Annual Emission Flux. Based on Figures 4 and 5, CH_4 and N_2O emission flux of three different coastal wetlands increase with increasing time from the present situation to 2100 in four study sites, which is consistent with the predicted trend of rising temperature (Figure 6). For different beaches, CH_4 emission flux of *Spartina* beach (MC) is > *Phragmites* beach (LW) > bare flat (GT), and N_2O emission flux of *Phragmites* beach is > *Spartina* beach > bare beach.

In different sites, CH_4 emission flux of CM and SY in MC and GT beach is higher than DT and NT, while on LW beach this trend is contrary. For N_2O emission flux, NT is the highest while SY is the lowest.

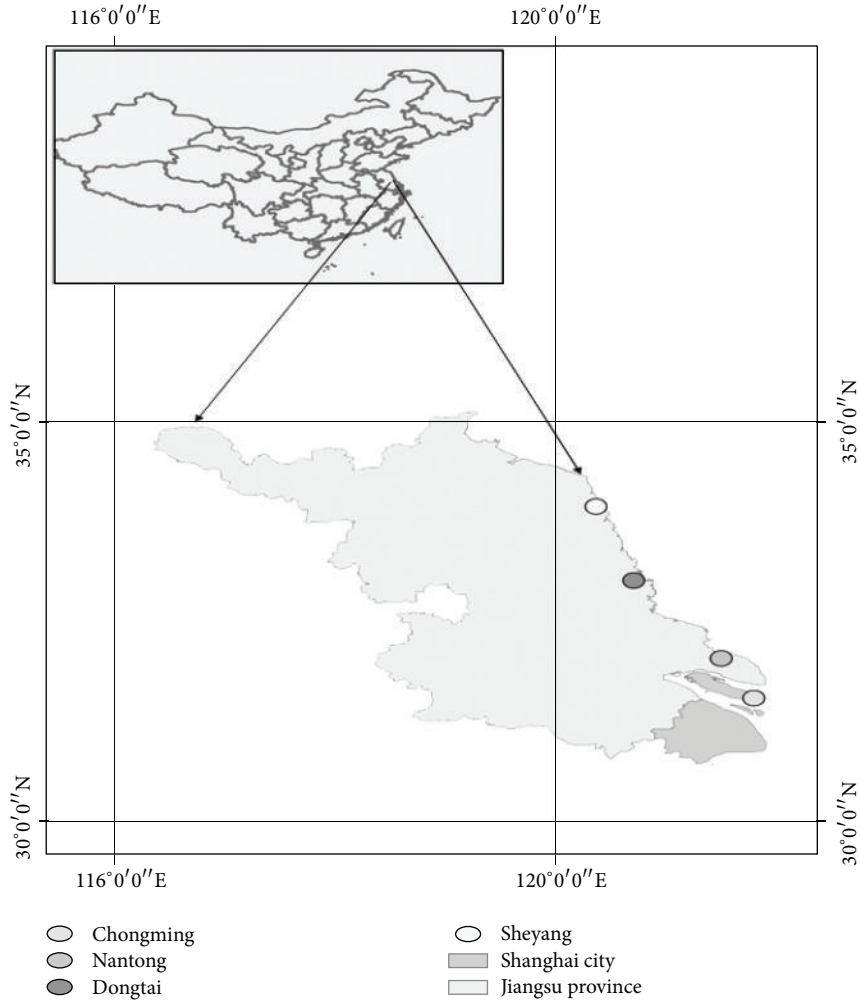

Figure 1: Locations of different sampling sites.

3.3. Roles of Different Factors in CH_4 and N_2O Emissions. By correlation analysis, CH_4 and N_2O emission flux are significantly correlated with soil organic carbon content ($R = 0.97$, $R = 0.695$ ($P < 0.01$), resp.) and with maximum biomass of per unit area ($R = 0.822$, $P < 0.01$; $R = 0.821$, $P < 0.01$). Soil pH has a significant correlation with CH_4 emission flux ($R = 0.362$, $P < 0.05$) and N_2O emission flux ($R = 0.402$, $P < 0.05$). CH_4 and N_2O emission flux have significant negative correlation with average water level ($R = -0.261$, $P < 0.05$; $R = -0.630$, $P < 0.01$).

Study results show that CH_4 emission flux in coastal wetland has significant correlation with temperature ($R = 0.707$, $P < 0.01$) and also is affected significantly by rainfall ($R = 0.379$, $P < 0.05$). N_2O emission flux is positively correlated with temperature ($R = 0.768$, $P < 0.01$); however, N_2O flux and total annual precipitation have no relevance.

4. Discussions

4.1. Roles of Similar Vegetation Distribution Zone in CH_4 and N_2O Emissions in Coastal Wetland along Latitude. Some studies showed that the emission of trace gases from wetlands was controlled by multiple factors like soil temperature, hydrology, and vegetation (e.g., [16–20]). Our study also indicated that vegetation, soil characteristics, and climate conditions affected emissions of CH_4 and N_2O in coastal wetlands. Moreover, it was noticeable that, at different sites along latitude, similar CH_4 and N_2O emission patterns were found, which was caused by similar vegetation distribution zone including bare beach, *Spartina* beach, and *Phragmites* beach in coastal wetlands. This indicated that vegetation was an important factor affecting greenhouse gas emission [21]. Van der Nat and Middelburg [22] found that gas emissions were affected collectively by vegetation type and species composition in tidal marshes, and increasing CH_4 flux was achieved by improvement of organic substrates and transportation of plant aerenchyma reducing oxidation of methane [23, 24]. Windham and Ehrenfeld [25] pointed out that, in two different tidal areas dominated by reeds and cattails, CH_4 emissions had some obvious differences. Exotic-species invasions affecting the vegetation structure of wetland ecosystems [25] would change the input of organic matter to soil [26]. Cheng et al. [9] reported that CH_4 emissions were significantly correlated with plant biomass and stem

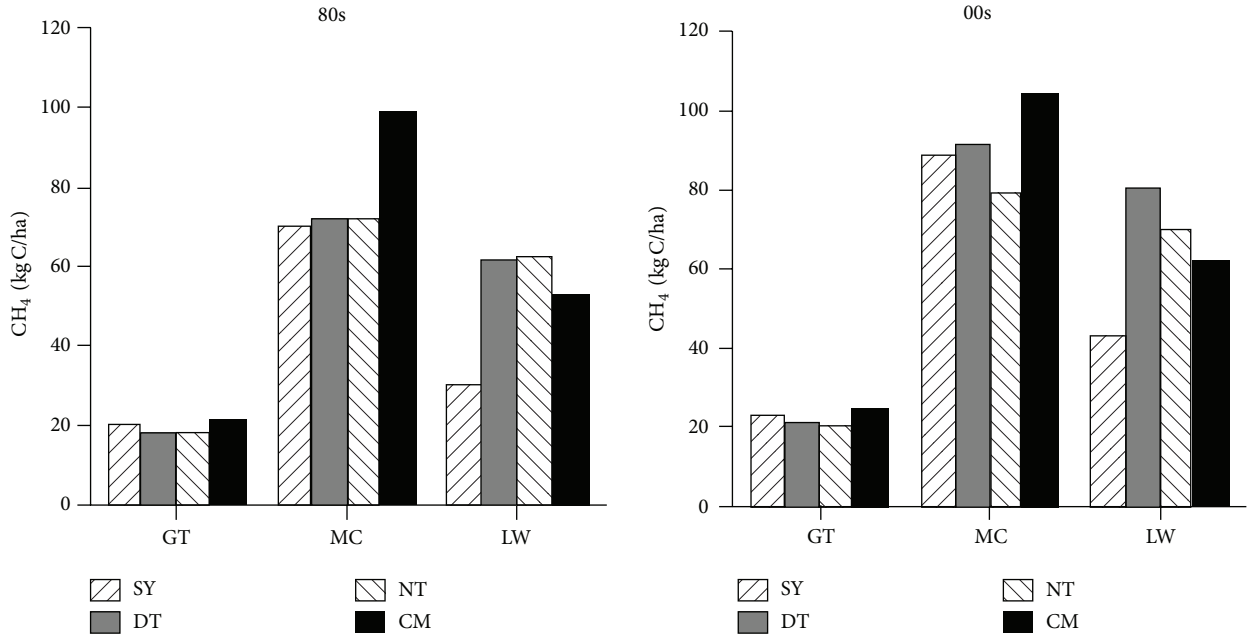

Figure 2: Comparison of CH_4 emission flux of different beach in 80s and 00s (SY, DT, NT, and CM represent Sheyang, Dongtai, Nantong, and Chongming, resp.; GT, MC, and LW represent bare beach, *Spartina* beach, and *Phragmites* beach, resp.).

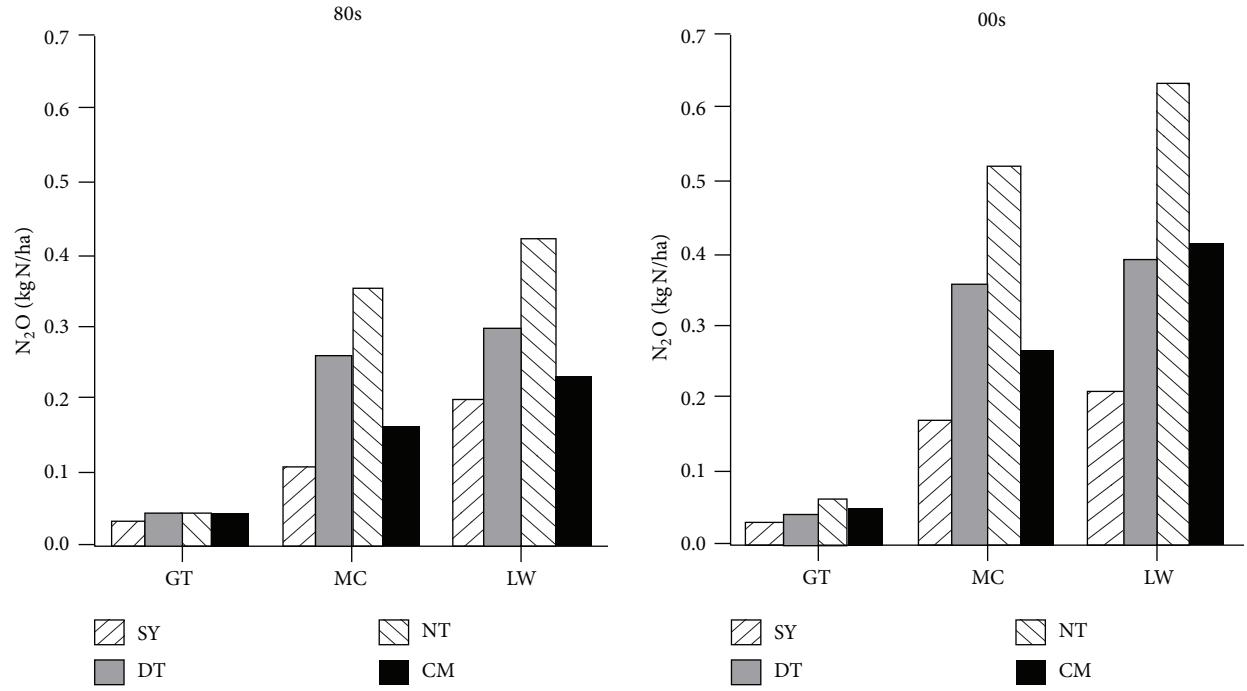

Figure 3: Comparison of N_2O emission flux of different beach in 80s and 00s (SY, DT, NT, and CM represent Sheyang, Dongtai, Nantong, and Chongming, resp.; GT, MC, and LW represent bare beach, *Spartina* beach, and *Phragmites* beach, resp.).

density for *Spartina* and *Phragmites,* while N_2O emissions were not accorded with this trend. Our model study also showed that, in a vegetation gradient zone, the effects of exotic-species *Spartina* on CH_4 emissions were more than native species *Phragmites* for its higher biomass and organic matter. However, this phenomenon did not exist in N_2O emission [27]. This was attributed to different mechanisms of CH_4 and N_2O emissions. Therefore, different vegetation distribution in coastal wetland was actually an important factor during the processes of CH_4 and N_2O emissions.

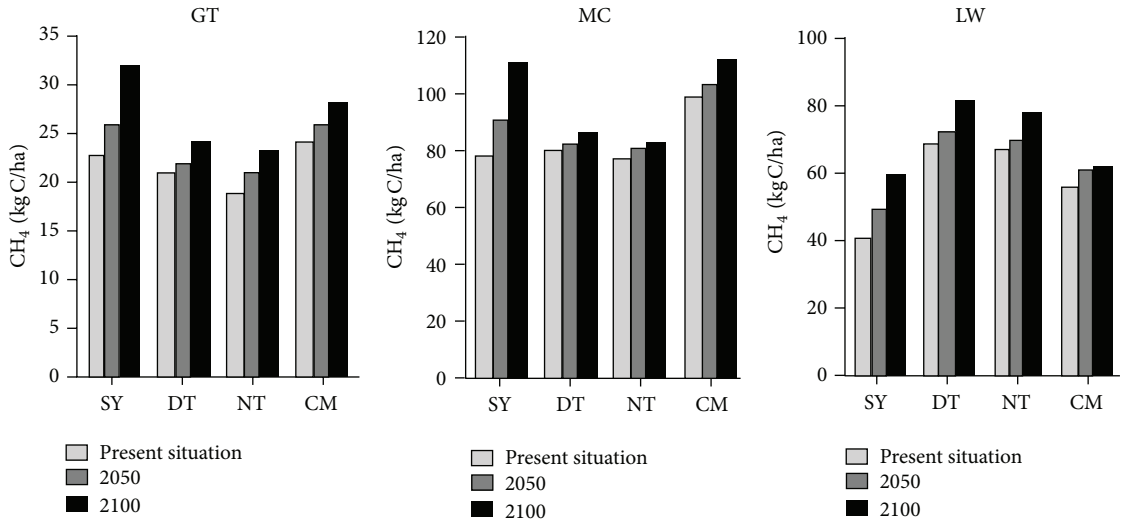

Figure 4: Comparison of present (average CH_4 emission flux of 80s and 00s) and future CH_4 emission flux of different vegetation zones at different locations.

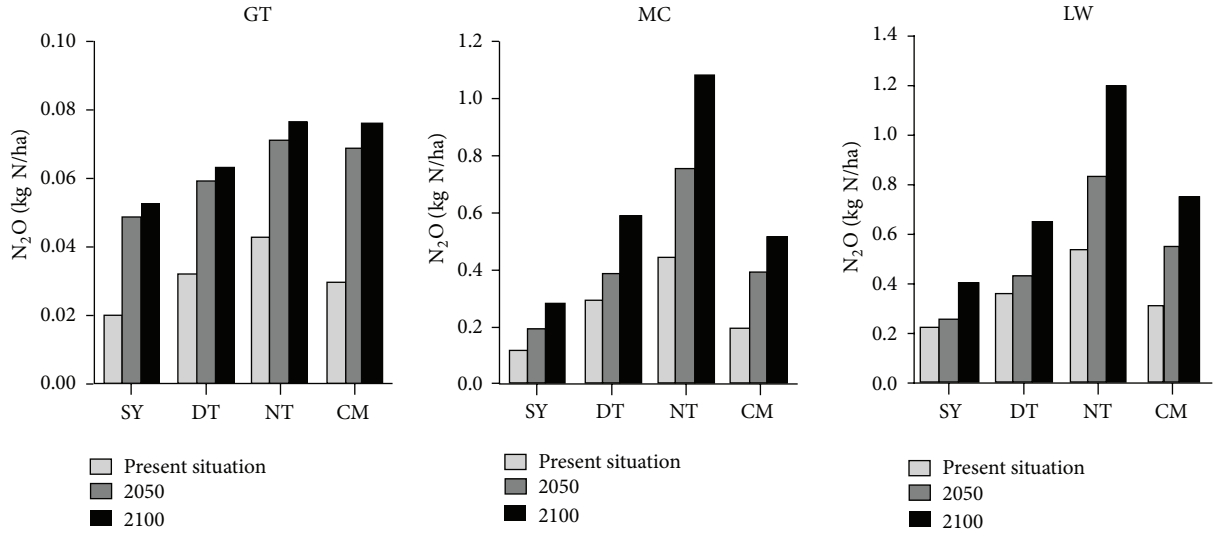

Figure 5: Comparison of present (average N_2O emission flux of 80s and 00s) and future N_2O emission flux of different vegetation zones at different locations.

4.2. Effects of Temperature on CH_4 and N_2O Emissions. The changes between present and future CH_4 and N_2O emission flux in the same site were mainly due to future temperature higher than present temperature. Temperature, especially soil temperature, played a very important role in CH_4 production and emission. Soil temperature directly affected the quantity, structure, and activity of a series of microflora that were involved in the process of the methane production and oxidation [7] and methane transport in soil [28]. Huttunen et al. [29] found that the correlation between CH_4 emission flux and peat surface temperature was most significant in all factors in the northern peatland, and incubation experiments also proved this relationship [30]. Our study results also showed that CH_4 emission flux in coastal wetland had significant correlation with temperature.

Hotness, humidity, and high carbon and nitrogen content of the soil were the best environment for N_2O production. The temperature was an important environmental factor in soil N_2O production and emission, but its relationship with N_2O emission was still controversial. Luo et al. [31] argued that temperature affected soil nitrification and denitrification, and Dorland and Beauchamp [32] found that, while temperature varied from −2°C to 25°C, the amount of the square root of the denitrification had a linear relationship with temperature. However, some studies also suggested that the temperature impact was not obvious. This study was consistent with the result of [33] that N_2O flux was positively correlated with temperature.

Comparisons of CH_4 and N_2O flux in different locations were complex. Multiple factors could cause the regional

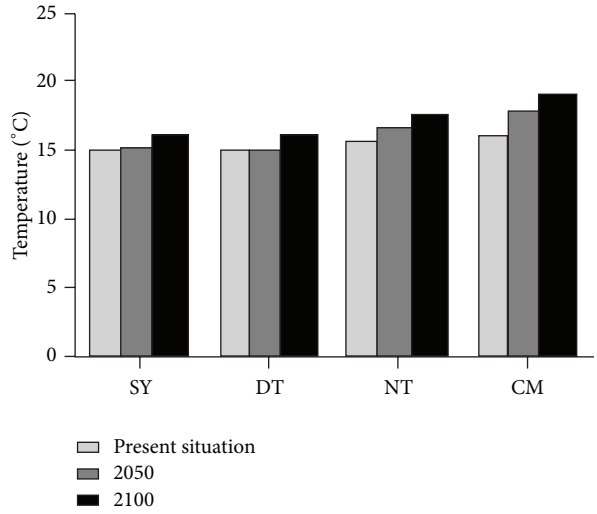

Figure 6: Comparison of present (average temperature of 80s and 00s) and future average annual temperature at different locations.

difference, such as temperature, rainfall, water level, and soil pH (e.g., [34, 35]).

5. Conclusions

By simulating CH_4 and N_2O emissions in the coastal wetlands by DNDC model, CH_4 emission ability of *Spartina* beach in three different vegetation zones was the highest, while the highest N_2O emission ability existed in *Phragmites* beach. This trend was very similar in the different sites including Sheyang, Dongtai, Nantong, and Chongming. By correlation analysis, CH_4 and N_2O emission fluxes were positively correlated with soil organic carbon content, temperature, and maximum biomass of per unit area and were negatively correlated with average water level. Comparisons of CH_4 and N_2O flux in different locations were complex, which were caused by multiple factors, such as temperature, rainfall, water level, and soil pH.

Conflict of Interests

The authors declare that they have no conflict of interests regarding the publication of this paper.

Authors' Contribution

Yuhong Liu and Lixin Wang contributed to this work equally.

Acknowledgments

This study was supported by the National Key Basic Research Program of China (no. 2014CB138802), National Key Technology R&D Program of China (nos. 2011BAC02B03 and 2013BAC09B03), the National Natural Science Funds of China (no. 31060076, 41261009), and the National Basic Research Program of China (no. 2013CB430405).

References

[1] IPCC, *Climate Change: The Scientific Basis*, Cambridge University Press, New York, NY, USA, 2001.

[2] D. Song, M. R. Su, J. Yang, and B. Chen, "Greenhouse gas emission accounting and management of low-carbon community," *The Scientific World Journal*, vol. 2012, Article ID 613721, 6 pages, 2012.

[3] IPCC, *Climate Change: The Physical Science Basis*, Cambridge University Press, Cambridge, UK, 2007.

[4] J. E. Hansen and A. A. Lacis, "Sun and dust versus greenhouse gases: an assessment of their relative roles in global climate change," *Nature*, vol. 346, no. 6286, pp. 713–719, 1990.

[5] S. Ghosh, D. Majumdar, and M. C. Jain, "Methane and nitrous oxide emissions from an irrigated rice of North India," *Chemosphere*, vol. 51, no. 3, pp. 181–195, 2003.

[6] X. L. Zhang, P. Y. Li, P. Li, and X. Y. Xu, "Present conditions and prospects of study on coastal wetlands in China," *Advances in Marine Science*, vol. 23, no. 1, pp. 83–91, 2005 (Chinese).

[7] J. P. Schimel and J. Gulledge, "Microbial community structure and global trace gases," *Global Change Biology*, vol. 4, no. 7, pp. 745–758, 1998.

[8] L. Kutzbach, D. Wagner, and E.-M. Pfeiffer, "Effect of microrelief and vegetation on methane emission from wet polygonal tundra, Lena Delta, Northern Siberia," *Biogeochemistry*, vol. 69, no. 3, pp. 341–362, 2004.

[9] X. L. Cheng, R. H. Peng, J. Q. Chen et al., "CH_4 and N_2O emissions from *Spartina alterniflora* and *Phragmites australis* in experimental mesocosms," *Chemosphere*, vol. 68, no. 3, pp. 420–427, 2007.

[10] G. H. Huang, Y. X. Li, G. X. Chen, Y. C. Yang, and C. W. Zhao, "Influence of environmental factors on CH_4 emission from Reed Wetland," *Chinese Journal of Environmental Science*, vol. 22, no. 1, pp. 1–5, 2001.

[11] M. A. K. Khalil, R. A. Rasmussen, M.-X. Wang, and L. Ren, "Emissions of trace gases from Chinese rice fields and biogas generators: CH_4, N_2O, CO, CO_2 chlorocarbons, and hydrocarbons," *Chemosphere*, vol. 20, no. 1-2, pp. 207–226, 1990.

[12] Y. Ye, C. Y. Lu, P. Lin, F. Y. Tan, and Y. S. Huang, "Diurnal change of CH_4 fluxes from esturine mangrove wetlands," *Acta Oceanologica Sinica*, vol. 22, no. 3, pp. 103–109, 2000 (Chinese).

[13] Z. G. Sun, L. L. Wang, H. Q. Tian, H. H. Jiang, X. J. Mou, and W. L. Sun, "Fluxes of nitrous oxide and methane in different coastal *Suaeda salsa* marshes of the Yellow River estuary, China," *Chemosphere*, vol. 90, no. 2, pp. 856–865, 2013.

[14] C. Li, S. Frolking, and T. A. Frolking, "A model of nitrous oxide evolution from soil driven by rainfall events: 1. Model structure and sensitivity," *Journal of Geophysical Research: Atmospheres*, vol. 97, no. 9, pp. 9759–9776, 1992.

[15] C. S. Li, "Modeling terrestrial ecosystems, complex systems and complexity," *Science*, vol. 1, no. 1, pp. 49–57, 2004 (Chinese).

[16] H. Kang, C. Freeman, and M. A. Lock, "Trace gas emissions from a north Wales fen—role of hydrochemistry and soil enzyme activity," *Water, Air, and Soil Pollution*, vol. 105, no. 1-2, pp. 107–116, 1998.

[17] H. Rusch and H. Rennenberg, "Black alder (*Alnus glutinosa* (L.) Gaertn.) trees mediate methane and nitrous oxide emission from the soil to the atmosphere," *Plant and Soil*, vol. 201, no. 1, pp. 1–7, 1998.

[18] Y. Ye, C. Y. Lu, and P. Lin, "Methane production, oxidation, transportation rate and pool in sediments of an *Avicennia marina* mangrove at Dongyu, Xiamen," *Journal of Oceanography in Taiwan Strait*, vol. 20, no. 2, pp. 236–244, 2001 (Chinese).

[19] N. Fenner, D. J. Dowrick, M. A. Lock, C. R. Rafarel, and C. Freeman, "A novel approach to studying the effects of temperature on soil biogeochemistry using a thermal gradient bar," *Soil Use and Management*, vol. 22, no. 3, pp. 267–273, 2006.

[20] J. L. Morse, M. Ardón, and E. S. Bernhardt, "Greenhouse gas fluxes in southeastern US coastal plain wetlands under contrasting land uses," *Ecological Applications*, vol. 22, no. 1, pp. 264–280, 2012.

[21] M. Hirota, Y. Senga, Y. Seike, S. Nohara, and H. Kunii, "Fluxes of carbon dioxide, methane and nitrous oxide in two contrastive fringing zones of coastal lagoon, Lake Nakaumi, Japan," *Chemosphere*, vol. 68, no. 3, pp. 597–603, 2007.

[22] F.-J. van der Nat and J. J. Middelburg, "Methane emission from tidal freshwater marshes," *Biogeochemistry*, vol. 49, no. 2, pp. 103–121, 2000.

[23] M. Roura-Carol and C. Freeman, "Methane release from peat soils: effects of *Sphagnum* and *Juncus*," *Soil Biology and Biochemistry*, vol. 31, no. 2, pp. 323–325, 1999.

[24] H. Brix, B. K. Sorrell, and P. T. Orr, "Internal pressurisation and convective gas flow in some emergent freshwater macrophytes," *Limnology and Oceanography*, vol. 37, no. 7, pp. 1420–1433, 1992.

[25] L. Windham and J. G. Ehrenfeld, "Net impact of a plant invasion on nitrogen-cycling processes within a brackish tidal marsh," *Ecological Applications*, vol. 13, no. 4, pp. 883–896, 2003.

[26] J. G. Ehrenfeld, P. Kourtev, and W. Huang, "Changes in soil functions following invasions of exotic understory plants in deciduous forests," *Ecological Applications*, vol. 11, no. 5, pp. 1287–1300, 2001.

[27] L. H. Zhang, L. P. Song, L. W. Zhang, H. B. Shao, X. B. Chen, and K. Yan, "Seasonal dynamics in nitrous oxide emissions under different types of vegetation in saline-alkaline soils of the Yellow River Delta, China and implications foreco-restoring coastal wetland," *Ecological Engineer*, vol. 61, pp. 82–89, 2013.

[28] W. X. Ding, Z. C. Cai, and D. X. Wang, "Preliminary budget of methane emissions from natural wetlands in China," *Atmospheric Environment*, vol. 38, no. 5, pp. 751–759, 2004.

[29] J. T. Huttunen, H. Nykänen, J. Turunen, and P. J. Martikainen, "Methane emissions from natural peatlands in the northern boreal zone in Finland, Fennoscandia," *Atmospheric Environment*, vol. 37, no. 1, pp. 147–151, 2003.

[30] J. A. MacDonald, D. Fowler, K. J. Hargreaves, U. Skiba, I. D. Leith, and M. B. Murray, "Methane emission rates from a northern wetland: response to temperature, water table and transport," *Atmospheric Environment*, vol. 32, no. 19, pp. 3219–3227, 1998.

[31] J. Luo, R. W. Tillman, and P. R. Ball, "Factors regulating denitrification in a soil under pasture," *Soil Biology and Biochemistry*, vol. 31, no. 6, pp. 913–927, 1999.

[32] S. Dorland and E. G. Beauchamp, "Denitrification and ammonification at low soil temperatures," *Canadian Journal of Soil Science*, vol. 71, no. 3, pp. 293–303, 1991.

[33] W. B. Xv, W. P. Liu, and G. S. Liu, "Effect of temperature on N_2O emissions from sub-tropical upland soils," *Acta Pedologica Sinica*, vol. 8, no. 1, pp. 1–8, 2002.

[34] Z. Q. Luan, Z. X. Wang, D. D. Yan, G. H. Liu, and Y. Y. Xu, "The ecological response of *Carex lasiocarpa* community in the riparian wetlands to the environmental gradient of water depth in Sanjiang Plain, Northeast China," *The Scientific World Journal*, vol. 2013, Article ID 402067, 7 pages, 2013.

[35] Z. Dai, C. C. Trettin, C. Li, H. Li, G. Sun, and D. M. Amatya, "Effect of assessment scale on spatial and temporal variations in CH_4, CO_2, and N_2O fluxes in a forested Wetland," *Water, Air, and Soil Pollution*, vol. 223, no. 1, pp. 253–265, 2012.

Hindawi Publishing Corporation
The Scientific World Journal
Volume 2014, Article ID 517020, 7 pages
http://dx.doi.org/10.1155/2014/517020

Research Article

Multivariate-Statistical Assessment of Heavy Metals for Agricultural Soils in Northern China

Pingguo Yang,[1] Miao Yang,[2] Renzhao Mao,[3] and Hongbo Shao[4,5]

[1] *Shanxi Normal University, Linfen 041000, China*
[2] *Shanxi Agricultural University, Taigu 030801, China*
[3] *Center for Agricultural Resources Research, Institute of Genetics and Developmental Biology, Chinese Academy of Sciences, Shijiazhuang 050021, China*
[4] *Key Laboratory of Coastal Biology & Bioresources Utilization, Yantai Institute of Coastal Zone Research, Chinese Academy of Sciences (CAS), Yantai 264003, China*
[5] *Institute for Life Sciences, Qingdao University of Science & Technology (QUST), Qingdao 266042, China*

Correspondence should be addressed to Hongbo Shao; shaohongbochu@126.com

Received 26 March 2014; Revised 4 April 2014; Accepted 5 April 2014; Published 16 April 2014

Academic Editor: Xu Gang

The study evaluated eight heavy metals content and soil pollution from agricultural soils in northern China. Multivariate and geostatistical analysis approaches were used to determine the anthropogenic and natural contribution of soil heavy metal concentrations. Single pollution index and integrated pollution index could be used to evaluate soil heavy metal risk. The results show that the first factor explains 27.3% of the eight soil heavy metals with strong positive loadings on Cu, Zn, and Cd, which indicates that Cu, Zn, and Cd are associated with and controlled by anthropic activities. The average value of heavy metal is lower than the second grade standard values of soil environmental quality standards in China. Single pollution index is lower than 1, and the Nemerow integrated pollution index is 0.305, which means that study area has not been polluted. The semivariograms of soil heavy metal single pollution index fitted spherical and exponential models. The variable ratio of single pollution index showed moderately spatial dependence. Heavy metal contents showed relative safety in the study area.

1. Introduction

Soils are critical environments where rock, biology, air, and water interface. Soil pollution has become an important environmental issue in China owing to rapid economic development and industrialization and increasing reliance on agrochemicals in the last few decades [1–3]. Soil heavy metal contents are not only the serious environmental issue but also frequency related to agricultural soil utilization problem [4–6]. Soil heavy metals could be necessary or beneficial to plants at certain levels but toxic when exceeding specific threshold [7–11]. If these elements are absorbed by the plants through the root system, they may enter the food chain and become toxic to humans and animals. The ecological importance of soil heavy metals is closely related to human health due to their high ecological transference potential.

For agricultural soils, the main pollution sources of heavy metals are due to activities such as irrigation using wastewater, pesticides, agricultural fertilizers, and organic manure, disposal of urban and industrial wastes, and atmospheric pollution from motor vehicles and the combustion of fossil fuels. Heavy metals in agricultural soil have become higher than background levels. It has also become a hot spot for the study of the international soil environment science research and ensured its sustainability.

Multivariate statistical approaches including principal component analysis (PCA) and cluster analysis (CA) are the statistical tools used in the elaboration pollution [12, 13]. It has been reported that PCA methods have been widely used in geochemical applications to identify soil pollution sources and distinguish natural versus anthropic contribution [14, 15]. CA is often used coupled to PCA to check results and group

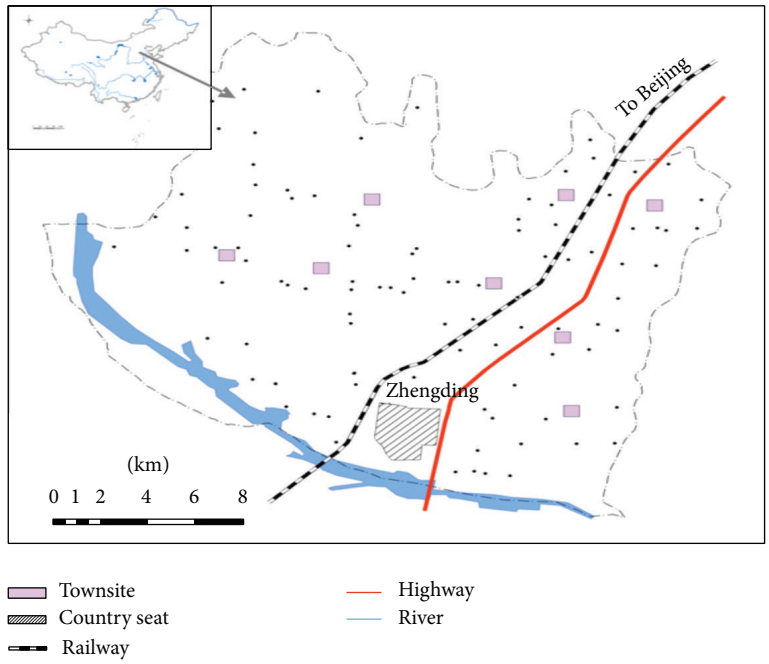

Figure 1: Map of the studied area and sampling locations.

individual parameters and variables [16–20]. The methods of geostatistics use the stochastic theory of spatial correlation for both interpolation and for apportioning uncertainty [21]. Geostatistics is based on the theory of a regionalized variable which uses the technique of semivariogram to measure the spatial variability of a regionalized variable and provides the input parameters for the spatial interpolation of kriging [22, 23]. Geostatistics can also be used to assess the risk of exceeding critical values (regulatory thresholds, soil quality criterion) at unsampled locations and to simulate the spatial distribution of attribute values [21].

The present study is focused on the suburban area of Shijiazhuang city. Zhengding has formed an industrial structure consisting of Shijiazhuang airport, electronic, petrochemical, and highly traffic density undergone a rapid transition from a traditionally agricultural-based to an increasingly industrial-based economy in the last 30 years which could enhance the risk of metal contamination through food chain in the region as heavy metals may enter and accumulate in agricultural soils through atmospheric deposition and irrigation. Early studies in the study area indicated the spatial variability of heavy metal distribution [17].

The study was to analyze possible sources of these heavy metals by multivariate statistical techniques and to assess soil heavy metal contamination using single pollution index and integrated pollution index to identify spatial distribution of single pollution index of soil heavy metal through geostatistical analysis.

2. Materials and Methods

2.1. Study Region and Soil Sampling. The study is focused on the suburban area of Shijiazhuang city, northern China. The region is well known for intense industrial and commercial activities. Soil samples were collected from 100 locations in the Zhengding, an administrative district covering 468 km^2 with a population of around 467,000 people. This area has a continental monsoon climate with an average annual temperature 13°C, and an average precipitation of 530 mm. The altitude levels range from 65 m to 105 m within the study area. The main soil type is carbonate cinnamon and Chao soil according to China soil classification system. The samples were collected from agricultural areas (mostly wheat, cereals, and vegetables). The coordinates of sampling locations were recorded with GPS. The sampling locations are shown in Figure 1.

2.2. Soil Analyses. Each sample consists of 10 soil cores (0–20 cm) depth, 1 kg ca total weight, which was collected from within a 10 × 10 m area with the central point corresponding to the defined position for the sample. All of the samples were air-dried at room temperature and sieved by a 2 mm mesh and stored in polyethene plastic bags for subsequent sample analysis. Metal concentrations for Cu, Zn, Ni, Pb, Cr, Hg, As, and Cd were analyzed after complete dissolution using a mixture of HNO_3-HF-$HCLO_4$ and heated in a microwave digestion system, using appropriate atomic absorption spectrometric techniques [17]. The accuracy of the procedure was determined by analyzing the certified reference material GB 7475-87 (National Institute of Standards and Technology, China). Quality controls involved analysis of random samples, blank samples, and national standard samples each time.

2.3. Assessment of Soil Contamination. The assessment of soil heavy metal contamination in agro-ecosystem is often the choice of single pollution index (Pi) and the Nemerow

Table 1: Total variance and component matrixes (three factors selected) for heavy metals.

(a) Total variance explained

Component	Initial eigenvalues			Extraction sums of squared loadings			Rotation sums of squared loadings		
	Total	% of variance	Cumulative %	Total	% of variance	Cumulative %	Total	% of variance	Cumulative %
1	2.700	33.752	33.752	2.700	33.752	33.752	2.187	27.338	27.338
2	1.464	18.304	52.056	1.464	18.304	52.056	1.639	20.484	47.822
3	1.264	15.797	67.853	1.264	15.797	67.853	1.602	20.030	67.851
4	0.893	11.160	79.013						
5	0.630	7.871	86.884						
6	0.479	5.987	92.871						
7	0.362	4.523	97.394						
8	0.208	2.600	100.000						

(b) Component matrixes

Element	Component matrix			Rotated component matrix		
	PC1	PC2	PC3	PC1	PC2	PC3
Cu	0.838	0.231	0.117	**0.648**	0.585	0.086
Zn	0.804	0.236	−0.325	**0.875**	0.207	0.008
Ni	0.549	−0.593	0.335	0.125	0.367	**0.785**
Pb	0.317	0.028	0.727	−0.153	**0.756**	0.182
Cr	0.692	−0.355	−0.148	0.565	0.114	0.544
Hg	−0.041	0.850	0.101	0.085	0.319	**−0.791**
As	0.428	0.381	0.380	0.205	**0.637**	−0.156
Cd	0.536	0.096	−0.572	**0.771**	−0.166	0.013

integrated pollution index (P). Generally P_i is defined as the ratio of the heavy metal concentration C_i to the second grade standard values according to the Chinese soil environmental quality standards S_i (GB15618-1995) [24]:

$$P_i = \frac{C_i}{S_i}. \quad (1)$$

When $P_i < 1$, there is no metal pollution; otherwise, if $P_i \geq 1$, it means pollution happens.

The Nemerow integrated pollution index P considers not only the mean values of all considered metals but also the maximum value of P_i [25]. P is determined by the mean value P_{ave} and the maximum P_{max} as the following equation:

$$P = \sqrt{\frac{{P_{max}}^2 + {P_{ave}}^2}{2}}. \quad (2)$$

2.4. Statistical Analysis. Multivariate statistical including principal component analysis (PCA), cluster analysis (CA), and geostatistical analysis are powerful tools for distinguishing pollution sources. Semivariograms model for each single pollution index considered elements (Cu, Zn, Ni, Pb, Cr, and Hg) using geostatistics. Classic statistical analyses were processed using SPSS19.0 software. Geostatistical modeling software Variowin 2.2 was used for the calculation of semivariogram of soil heavy metal single pollution index.

3. Results and Discussion

3.1. Principal Component Analysis. Summary statistics and normal test of Zhengding datasets were performed and the results were present [17]. PCA can be used to reduce data and to extract a smaller number of independent factors (principal components) to find the relationship among observed variables [16–18]. Principal component analysis (PCA) was applied in the study to have high quality experimental results. The PCA based results for soil heavy metals are listed in Table 1. According to the initial eigenvalues, three principal components are selected, accounting for over 67.8% of the total variance. The eigenvalues of the three first extracted factors are greater than one. All of the elements are consequently well represented by these three principal components.

The initial component matrix for heavy metals indicates that Cu, Zn, and Cd are associated, showing high values in the first principal component (PC1) which explains 27.3% of the total variance and loads heavily on Cu (0.65), Zn (0.88), and Cd (0.77). Cu and Zn values are controlled by a long-term anthropic activity such as pesticides. The second principal component (PC2) includes univocally Pb and As, which accounts for 20.5% of the total variance. Common sources of lead in soils are manure, sewage sludge, lead-arsenate pesticides, vehicle exhausts, and industrial fumes. The study area has a high vehicular traffic density, constituted by Zhengding international airport and several important railways, expressway

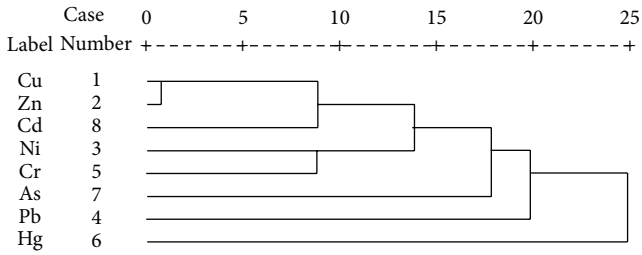

FIGURE 2: Dendrogram results from Pearson correlation coefficients of hierarchical cluster analysis for heavy metals.

(http://www.en.wikipedia.org/wiki/zhengding), for leaded gasoline widely used. The third principal component (PC3) is correlated very strongly with Hg loading (−0.79) and also by Ni loading (0.79), accounting for 20% of the total variance.

Long-term and extensive use of pesticides in farmland may cause heavy metals such as copper, nickel, zinc, and cadmium to accumulate in the topsoil [26, 27]. Common sources of lead in soils include car exhausts, manure, sewage sludge, and coal burning. Cd is present in fossil fuel such as coal and oil and having no functions in plants or animals or human body. In addition, normal agricultural practices may cause enrichment of heavy metals. These practices are an important source of Zn, Cu, and Cd due to the application of manure or inorganic fertilizers. Thus in Table 1, the relationship among all of the eight variables is clearly revealed.

3.2. Cluster Analysis. Although not substantially different from PCA, CA could be used as an alternative method to confirm results and provide grouping of variables [5]. The heavy metals concentration data were calculated using the hierarchical clustering with SPSS software. Figure 2 shows the CA results for the heavy metals as a dendrogram in the study area. This figure shows three clusters. (1) Cu, Zn, and Cd are very well correlated with each other. The farming area has had several decades of intensive tillage, long-term fertilizer and pesticide application might be a major source of accumulated heavy metals in the study area, (2) which is associated with Pb and As. Pb is mostly found in automobile battery in sufficient amount; excessive intake Pb can damage the nervous, skeletal, circulatory, enzymatic, endocrine, and immune systems of human body. (3) Ni and Hg are commonly associated in a number of rock types or soil parent materials. The analyzed results are in good accordance with the findings of the PCA analysis.

3.3. Hazard Assessment of Soil Heavy Metals. Table 2 shows that the mean contents of Zn, Hg, and Cd exceed soil background values, but they are still lower than the Grade II criteria, which mean that the three metal elements are mainly affected by anthropogenic sources. The mean value of soil Zn 69.96 mg/kg was higher than its background value 62.0 mg/kg but it did not exceed the limiting content 300 mg/kg of SEPA. The average value of Cd 0.15 mg/kg was higher than its background value 0.075 mg/kg. Phosphate fertilizers have been well known as the major external source of soil Cd [26, 27]. Especially Hg is 3.49 times the background value and mainly originated from industry and traffic sources. Cu, Ni, Pb, Cr, and As concentrations are lower than or approximately equal to their corresponding background values, which indicates that these elements are dominated by natural sources and human activities.

The heavy metal concentrations in Zhengding agricultural soil are compared with the data reported from other areas in the world in Table 2 [6, 14, 17, 20]. The mean content of Cu and As is lower than that for other areas. The average values of Pb, Hg, and Cd are similar to those of Beijing and Tianjin, but lower than in other areas. The mean concentration of Cu, Pb, Cr, As, and Cd was lower than those reported by Hu, and within the range reported by Qiao.

The Chinese Environmental Quality Standard for soils (GB 15618-1995) [24] and the soil background values of Hebei were adopted to evaluate the pollution degree. The soil is mainly alkaline in the investigated area. Grade II criteria for soil quality are established to protect agricultural production and to maintain human health. Across the investigated area, a wide range of soil heavy metal concentrations have been measured.

The analyzed results indicate that all of the metal concentrations are below the Environmental Protection Administration for soil in China. The P_i of soil heavy metals and the Nemerow P values, range, median values, and CV in the 100 topsoil samples are shown in Table 3. On average, the P_i indices for Cu, Zn, Ni, Pb, Cr, Hg, As, and Cd were 0.212, 0.233, 0.417, 0.054, 0.231, 0.076, 0.246, and 0.246, respectively. Different heavy metal concentrations of single pollution index are in an order of Ni > Cd = As > Zn > Cr > Cu > Hg > Pb. The single pollution index showed that the Ni pollution intensity was strong. Cd, Cr, and Pb are considered as the most important environmental pollutants in agricultural soils because of the potential harmful effects they may have on food quality and health of soil.

The Nemerow integrated pollution index (P) in this area is 0.305, which is lower than 1, meaning that heavy metal exposure through the food chain does not have considerable consequence and is generally safe.

3.4. Semivariogram Analysis. The semivariogram model of soil heavy metal single pollution index at both orientations is given in Figure 3. Theoretical models were then employed to interpret the experimental semivariograms and the model with the best fitting was chosen [22]. P_{Ni} and P_{Cr} were fitted with the exponential model, and the other four heavy metal single pollution indexes were all best fitted with the spherical model.

The attributes of the semivariograms for each soil heavy metal single pollution index were also summarized in Table 4. All of the Nug/Sill ratios were less than 59.74%, indicating random heterogeneity. The nugget effect may be caused by random factors such as data deviations, agricultural activities, or sample density. Nugget contributions highlighted the stronger spatial correlation in Table 4. The range of semivariograms for soil heavy metal single pollution index ranged from 0.0384 km to 0.1192 km. This confirmed the rational of the sampling density.

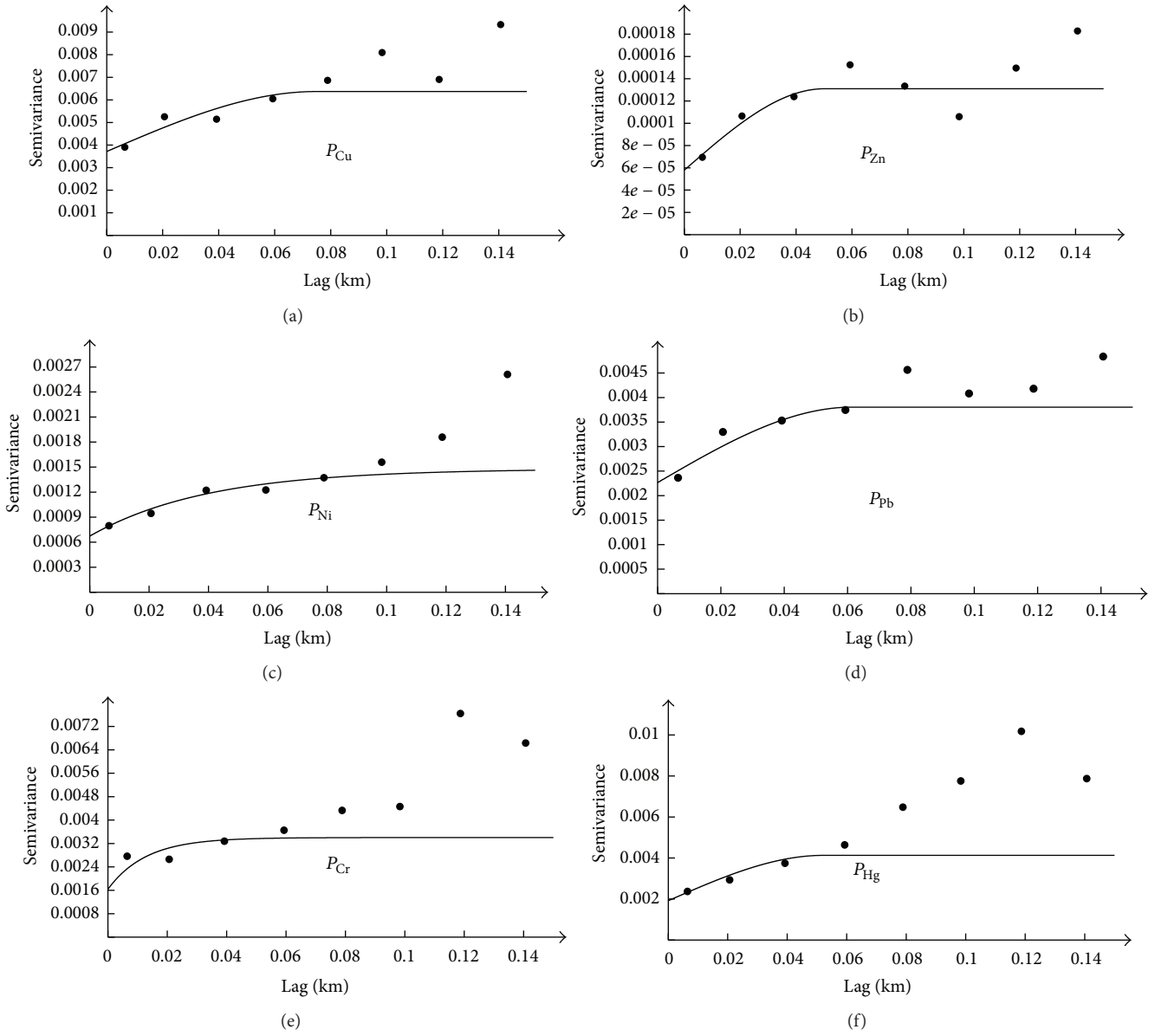

Figure 3: Semivariograms model of soil heavy metal single pollution index.

Table 2: A summary of heavy metal concentrations in agricultural soil for various areas (mg/kg).

Area	Cu	Zn	Ni	Pb	Cr	Hg	As	Cd	References
Zhengding	21.22	69.96	25.04	18.80	57.77	0.08	6.16	0.15	This study
Background value	21.7	62.0	28.8	20.0	63.9	0.023	12.1	0.075	Yang et al. (2009) [18]
Grade II	100	300	60	350	250	1.0	25	0.6	SEPA (1995) [24]
Beijing	26.08	61.18	24.01	18.81	67.77	0.079	7.68	0.24	Hu et al. (2004)
Beijing, Tianjin	28.2	71.0	NA	18.7	52.3	0.092	7.9	0.145	Qiao et al. (2011) [15]
Alicante	22.5	52.8	20.9	22.8	26.5	NA	NA	0.34	Micó et al. (2006) [6]
Ebro	17.3	57.5	20.5	17.5	20.3	0.036	NA	0.42	Rodriguez et al. (2006)
Huizhou	21.82	66.15	20.52	65.38	43.01	0.24	12.76	0.12	Cai et al. (2012) [9]

Grade II (the value for protection of agricultural production and human health).

Table 3: Descriptive statistics of soil heavy metals pollution indices.

Variable	P_i								P
	Cu	Zn	Ni	Pb	Cr	Hg	As	Cd	
Min.	0.111	0.154	0.215	0.035	0.131	0.018	0.087	0.15	0.091
Max.	0.332	0.293	0.608	0.117	0.354	0.374	0.396	0.483	0.521
Mean	0.212	0.233	0.417	0.054	0.231	0.076	0.246	0.246	0.305
Kurt.	1.403	0.430	−0.283	9.317	1.959	9.669	0.177	3.142	1.968
Skew.	0.352	0.073	−0.185	2.108	0.762	2.769	−0.116	1.476	0.086
St.d	0.034	0.024	0.077	0.011	0.035	0.060	0.060	0.067	0.121
C.V.	16.04	10.30	18.47	20.37	15.15	78.95	24.39	27.24	39.67

St.d: standard deviation, C.V.: coefficient variation.

Table 4: Spatial correlation for heavy metals.

	Model	Nugget C_0	Sill $C + C_0$	$C_0/(C + C_0)$ (%)	Range (km)
P_{Cu}	Spherical	0.0037	0.0064	58.40	0.0746
P_{Zn}	Spherical	$5.8e-05$	0.0001	44.25	0.05
P_{Ni}	Exponential	0.0007	0.0015	45.58	0.1192
P_{Pb}	Spherical	0.0023	0.0038	59.74	0.0613
P_{Cr}	Exponential	0.0016	0.0034	48.24	0.0384
P_{Hg}	Spherical	0.0019	0.0041	46.49	0.0521

4. Conclusions

The single pollution index, integrated pollution index, and sources of the heavy metals Cu, Zn, Ni, Pb, Cr, Hg, As, and Cd in agricultural topsoil samples collected from Zhengding have been investigated in this work. The mean values of single pollution index and integrated pollution index are less than 1 in the area.

The mean values of Zn, Ni, Pb, Cr, Hg, As, and Cd in the analysed soils do not exceed the limited second grade criteria environmental quality standard for soils in China (GB 15618-1995), which means that the soil in this area is not polluted. Only Zn, Hg, and Cd present higher values in some cases. The mean values of soil Zn, Hg, and Cd were higher than the, respectively, background values. Agrochemical inputs may play the most important role for the input of Zn and Cd. The risk of Hg and Cd accumulation requires further attention and monitoring.

Multivariate statistics is found to be a powerful tool to identify the main factors determining the variability of geochemical data and interpret the measurement results. Variation of Cu, Zn, and Cd concentrations is controlled by anthropogenic intense agriculture activities. The concentrations of Pb and As in agricultural soil are abnormalities mainly affected by aerial deposits from gasoline exhausts, while the concentrations of Ni and Hg in agricultural soil are mainly affected by natural parent material and human activities.

Conflict of Interests

The authors declare that there is no conflict of interests regarding the publication of this paper.

Acknowledgments

The authors are grateful for the financial support of the National Natural Science Foundation of China (no. 31272258) and the Natural Science Foundation of Shanxi Province (no. 2010011044). The authors wish to thank Gao Yunfeng for assistance with soil sampling and lab analysis. They also acknowledge the valuable comments of the anonymous reviewers.

References

[1] S. S. Huang, Q. L. Liao, M. Hua et al., "Survey of heavy metal pollution and assessment of agricultural soil in Yangzhong district, Jiangsu Province, China," *Chemosphere*, vol. 67, no. 11, pp. 2148–2155, 2007.

[2] Y. X. Song, J. F. Ji, Z. F. Yang et al., "Geochemical behavior assessment and apportionment of heavy metal contaminants in the bottom sediments of lower reach of Changjiang River," *Catena*, vol. 85, no. 1, pp. 73–81, 2011.

[3] H. R. Zhao, B. C. Xia, C. Fan, P. Zhao, and S. Shen, "Human health risk from soil heavy metal contamination under different land uses near Dabaoshan Mine, Southern China," *Science of the Total Environment*, vol. 417-418, pp. 45–54, 2012.

[4] R. Garcia, I. Maiz, and E. Millan, "Heavy metal contamination analysis of roadsoils and grasses from Gipuzkoa (Spain)," *Environmental Technology*, vol. 17, no. 7, pp. 763–770, 1996.

[5] F. A. Nicholson, S. R. Smith, B. J. Alloway, C. Carlton-Smith, and B. J. Chambers, "An inventory of heavy metals inputs to agricultural soils in England and Wales," *Science of the Total Environment*, vol. 311, no. 1–3, pp. 205–219, 2003.

[6] C. Micó, L. Recatalá, M. Peris, and J. Sánchez, "Assessing heavy metal sources in agricultural soils of an European Mediterranean area by multivariate analysis," *Chemosphere*, vol. 65, no. 5, pp. 863–872, 2006.

[7] B. J. Alloway, "The origins of heavy metals in soils," in *Heavy Metals in Soils*, B. J. Alloway, Ed., pp. 38–57, Blackie Academic and Professional, London, UK, 1995.

[8] A. Facchinelli, E. Sacchi, and L. Mallen, "Multivariate statistical and GIS-based approach to identify heavy metal sources in soils," *Environmental Pollution*, vol. 114, no. 3, pp. 313–324, 2001.

[9] L. M. Cai, Z. C. Xu, M. Ren et al., "Source identification of eight hazardous heavy metals in agricultural soils of Huizhou, Guangdong Province, China," *Ecotoxicology and Environmental Safety*, vol. 78, pp. 2–8, 2012.

[10] G. Wu, H. B. Kang, X. Zhang, H. B. Shao, L. Y. Chu, and C. Ruan, "A critical review on the bio-removal of hazardous heavy metals from contaminated soils: issues, progress, eco-environmental concerns and opportunities," *Journal of Hazardous Materials*, vol. 174, no. 1–3, pp. 1–8, 2010.

[11] P. Yang, M. Yang, and H. Shao, "Magnetic susceptibility and heavy metals distribution from risk-cultivated soil around iron-steel plant, China," *Clean-Soil, Air, Water*, vol. 40, no. 6, pp. 615–618, 2012.

[12] A. Hani and E. Pazira, "Heavy metals assessment and identification of their sources in agricultural soils of Southern Tehran, Iran," *Environmental Monitoring and Assessment*, vol. 176, no. 1–4, pp. 677–691, 2011.

[13] W. Huang, R. Campredon, J. J. Abrao, M. Bernat, and C. Latouche, "Variation of heavy metals in recent sediments from Piratininga Lagoon (Brazil): interpretation of geochemical data with the aid of multivariate analysis," *Environmental Geology*, vol. 23, no. 4, pp. 241–247, 1994.

[14] S. Dragović and N. Mihailović, "Analysis of mosses and topsoils for detecting sources of heavy metal pollution: multivariate and enrichment factor analysis," *Environmental Monitoring and Assessment*, vol. 157, no. 1–4, pp. 383–390, 2009.

[15] M. Qiao, C. Cai, Y. Huang, Y. Liu, A. Lin, and Y. Zheng, "Characterization of soil heavy metal contamination and potential health risk in metropolitan region of northern China," *Environmental Monitoring and Assessment*, vol. 172, no. 1–4, pp. 353–365, 2011.

[16] K. L. Hu, F. R. Zhang, Y. Z. Lu, R. Wang, and Y. Xu, "Spatial distribution of concentrations of soil heavy metals in Daxing county, Beijing," *Acta Scientiate Circumstantiae*, vol. 24, no. 3, pp. 463–469, 2011.

[17] F. Ruiz, M. L. González-Regalado, J. Borrego, J. A. Morales, J. G. Pendón, and J. M. Muñoz, "Stratigraphic sequence, elemental concentrations and heavy metal pollution in Holocene sediments from the Tinto-Odiel Estuary, southwestern Spain," *Environmental Geology*, vol. 34, no. 4, pp. 270–278, 1998.

[18] P. Yang, R. Mao, H. Shao, and Y. Gao, "The spatial variability of heavy metal distribution in the suburban farmland of Taihang Piedmont Plain, China," *Comptes Rendus-Biologies*, vol. 332, no. 6, pp. 558–566, 2009.

[19] A. Franco-Uría, C. López-Mateo, E. Roca, and M. L. Fernández-Marcos, "Source identification of heavy metals in pastureland by multivariate analysis in NW Spain," *Journal of Hazardous Materials*, vol. 165, no. 1–3, pp. 1008–1015, 2009.

[20] R. J. Yao, J. S. Yang, P. Gao, H. B. Shao, X. B. Chen, and S. P. Yu, "Multivariate simulation and assessment of three dimensional spatial patterns of coastal soil salinity using ancillary variables," *Fresenius Environmental Bulletin*, vol. 22, no. 1, pp. 39–52, 2013.

[21] E. H. Isaaks and R. M. Srivastava, *An Introduction to Applied Geostatistics*, Oxford University Press, New York, NY, USA, 1989.

[22] R. J. Yao, J. S. Yang, and H. B. Shao, "Accuracy and uncertainty assessment on geostatistical simulation of soil salinity in a coastal farmland using auxiliary variable," *Environmental Monitoring and Assessment*, vol. 185, no. 6, pp. 5151–5164, 2013.

[23] P. Goovaerts, "A coherent geostatistical approach for combining choropleth map and field data in the spatial interpolation of soil properties," *European Journal of Soil Science*, vol. 62, no. 3, pp. 371–380, 2011.

[24] SEPA, "State environmental protection administration of China," Environmental Quality Standard for Soils GB15618-1995, SEPA, Beijing, China, 1995.

[25] Z. P. Yang, W. X. Lu, Y. Q. Long, X. H. Bao, and Q. C. Yang, "Assessment of heavy metals contamination in urban topsoil from Changchun City, China," *Journal of Geochemical Exploration*, vol. 108, no. 1, pp. 27–38, 2011.

[26] Y. B. Huang, Y. B. Lan, S. J. Thomson, A. Fang, W. C. Hoffmann, and R. E. Lacey, "Development of soft computing and applications in agricultural and biological engineering," *Computers and Electronics in Agriculture*, vol. 71, no. 2, pp. 107–127, 2010.

[27] H. B. Shao, Ed., *Metal Contamination: Sources, Detection and Environmental Impact*, Nova Science, New York, NY, USA, 2012.

Hindawi Publishing Corporation
The Scientific World Journal
Volume 2014, Article ID 821781, 9 pages
http://dx.doi.org/10.1155/2014/821781

Research Article

Effects of Urbanization Expansion on Landscape Pattern and Region Ecological Risk in Chinese Coastal City: A Case Study of Yantai City

Di Zhou,[1,2] Ping Shi,[1] Xiaoqing Wu,[1] Jinwei Ma,[3] and Junbao Yu[1]

[1] *Key Laboratory of Coastal Environment Processes and Ecological Remediation and Shandong Provincial Key Laboratory of Coastal Zone Environmental Processes, YICCAS, Yantai Institute of Coastal Zone Research, Chinese Academy of Sciences, Yantai 264003, China*
[2] *University of Chinese Academy of Sciences, Beijing 100049, China*
[3] *Linqu First Middle School Shandong, Linqu 262600, China*

Correspondence should be addressed to Ping Shi; pshi@yic.ac.cn and Junbao Yu; junbao.yu@gmail.com

Received 22 February 2014; Revised 13 March 2014; Accepted 13 March 2014; Published 10 April 2014

Academic Editor: Hong-bo Shao

Applied with remote sensing, GIS, and mathematical statistics, the spatial-temporal evolution characteristics of urbanization expansion of Yantai city from 1974 to 2009 was studied. Based on landscape pattern metrics and ecological risk index, the landscape ecological risk from the landscape pattern dynamics was evaluated. The results showed that the area of urban land increased by 189.77 km^2 with average expansion area of 5.42 km^2 y^{-1} from 1974 to 2009. The urbanization intensity index during 2004–2009 was 3.92 times of that during 1974–1990. The land use types of urban land and farmland changed greatly. The changes of landscape pattern metrics for land use patterns indicated that the intensity of human activities had strengthened gradually in study period. The landscape ecological risk pattern of Yantai city shaped half-round rings along the coastline. The ecological risk index decreased with increase of the distance to the coastline. The ratio of high ecological risk to subhigh ecological risk zones in 2009 was 2.23 times of that in 1990. The significant linear relationship of urbanization intensity index and regional ecological risk indicated that the anthropological economic activities were decisive factors for sustainable development of costal ecological environment.

1. Introduction

It is common that the urbanization expansion is rapid in the world, especially in the developing countries where there are about 70% of the world's largest cities [1–3]. The urbanization has boosted rapidly in China since the reform and opening-up in the 1980s. The urbanized area in Yangtze River Delta region increased exponentially during 1979–2008 [4]. According to the report of the National Bureau of Statistics in 2012, the urbanization ratio of China has increased by 1.35% per year from 2002 to 2011. By the end of 2011, the total urban population has been about 690.69 million people and the urbanization ratio was about 51.27%. The human development report 2013 of the United Nations Development Programme predicted that the urban population of China will be 1000 million people and the urbanization ratio will be 70% in 2030. Up to now, more than 40% of population and more than 70% of cities are widely distributed in China's coastal areas [5] where many coastal economic zones are set up and have become the preferred destination for millions of internal migrants and overseas investors [6]. Some studies indicated that the urbanization ratio will increase to 60% in 2020 in the eastern coastal provinces and cities of China [7].

The rapid development of urbanization expansion and heavy burden of human activities have impaired ecosystem functions in coastal areas [8–12]. From the view of landscape ecology, urbanization is the process in which land use/cover landscape changes from natural landscape which is mainly made of water, soil, and vegetation to manmade landscape which is mainly composed of cement, asphalt, chemical materials, and metal [13, 14]. Meanwhile, the change of land use/cover landscape pattern could be interpreted as the

changes of patch shape, area, quality, and spatial combination [15, 16]. Rapid urbanization has been companied by more drastic changes of land use types, disorderly landscape layout, and fragile ecological environment [14, 16, 17]. Therefore, the problems of landscape pattern change and region ecological risk under urbanization expansion in China have drawn the increasing attention of the ecologists [4–10]. The technologies of RS and GIS have become important methods to identify the potential eco-environmental influences and guide urban planning management [3, 15, 18–22]. The previous researches in China mainly focused on large cities distributed in the Yellow River [23], the Yangtze River [24, 25], Pearl River Delta [9, 26], and the Ring-Bohai Region [27–29]. Few studies have focused on landscape pattern and region ecological risk under urbanization expansion in the small and medium-sized coastal cities [30–32]. In the study, Yantai city, which was one of the 14 coastal open economy cities in China, was selected to study the impacts of urbanization expansion on the landscape pattern change and regional ecological risk for the small and medium-sized coastal cities. The objectives of the present study were to reveal (1) dynamic changes and spatial characteristics of landscape pattern and the regional ecological risk and (2) the relationship between urbanization intensity index and regional ecological risk based on the analysis of urbanization expansion in Yantai city.

2. Materials and Methods

2.1. Description of the Study Area. Yantai city (119°34′–121°57′E, 36°16′–38°23′N) is located at the northeast tip of Shandong Peninsula bordering on the Bohai Sea and the Yellow Sea (Figure 1). It covers an area of 13746.50 km^2 with the coastline of 909.00 km. The mountain, mound, plain, and the marsh land are about 36.6%, 39.7%, 20.8%, and 2.9% of total area, respectively. Average annual precipitation is 651.90 mm and mean annual temperature is 11.8°C. The total population was 6.96 million in 2010 based on the 6th population census data of China. The gross domestic product (GDP) was about 490.68 billion Chinese YUAN according to the government work report of Yantai City in 2011. With the improvement of comprehensive competitiveness, Yantai city has been an important economic zone of the Ring-Bohai Region.

Five districts of Yantai city, that is, Zhifu District, Laishan District, Mouping District, Fushan District, and Economic and Technological Development Zone (Development Zone), were selected for the study (Figure 1). The study area (121°15′–121°56′E, 37°04′–37°38′N) covers an area of 2721.04 km^2 and the total population is about 2.22 million in 2010. With rapid economic development and enormous population growth, large area agricultural land has been occupied by nonagricultural lands and urban landscape pattern resulting from urbanization expansion in the past years.

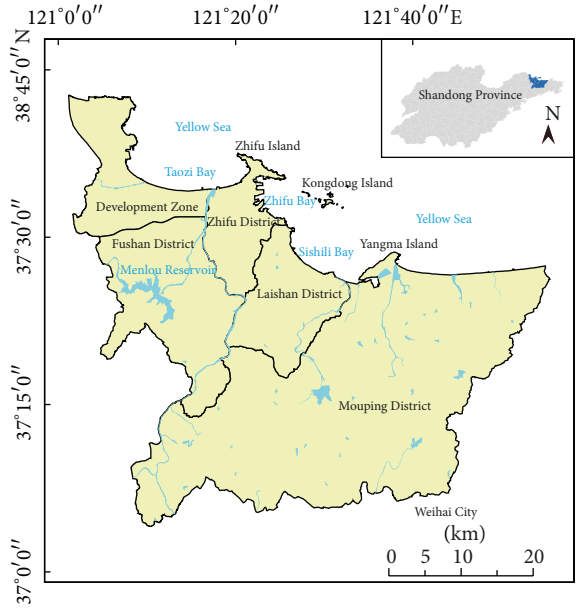

Figure 1: Location map of the study area.

2.2. Data Sources and Processing

2.2.1. Remote Sensing Image Interpretation. The spatial data was obtained from five-period remote sensing images June 2, 1990 (TM), September 20, 1995 (TM), June 12, 2000 (ETM), November 9, 2004 (TM), and July 15, 2009 (TM). In addition, administrative division maps, traffic map, topographic map (1 : 100,000) in 1974, topographic map (1 : 50,000) in 2000, and land use planning of Yantai city were used for secondary data. The five period remote sensing images of 1990, 1995, 2000, 2004, and 2009 were used to study the spatial-temporal evolution characteristics of urbanization expansion in Yantai city. Three period images of 1990, 2000, and 2009 were applied for the analysis of the land-use landscape pattern characteristics and region ecological risk.

The topographic maps of Yantai city, geometric correction of Landsat TM remote sensing images had been conducted by using ArcGIS 9.3. The error was controlled within 0.5 pixels. All images were classified by combing supervised classification with visual interpretation and the interpretation results were resampled in spatial resolution (30 m).

According to the Chinese national standard of Status of Land Use Classification (GB/T 21020-2007), the land use types of the study area were divided into urban land, farmland, orchard, forestland, grassland, water body, other construction land (industrial land, mine land, and port land), and other object land (unused land, barren land). Based on land use interpretation results which were corrected by field survey, the classification error rate was lower than 5% of the land use actual change.

2.2.2. Urbanization Expansion. The urbanization intensity index (I_{ue}) was used to analyze the urbanization expansion intensity from 1974 to 2009. The equation was as follows:

$$I_{ue} = \frac{\Delta U_i \times 100}{TLA \times \Delta t}, \quad (1)$$

Table 1: Description of landscape pattern metrics.

Index	Equation		Ecological significance
Largest Patch Index (LPI)	$\mathrm{LPI} = \frac{\max a_{ij}}{A}(100)$	(i)	To indicate ratio of the largest patch area to total landscape area
Fractal Dimension Index (FD)	$\mathrm{FD} = \frac{2\ln(l/k)}{\ln(A)}$	(ii)	To reflect the complexity of self-similarity of a patch
Shannon's Diversity Index (SHDI)	$H = -\sum_{i=1}^{m}(p_i \ln p_i)$	(iii)	To reflect landscape heterogeneity
Shannon's Evenness Index (SHEI)	$E = -\sum_{i=1}^{m}\frac{(p_i \ln p_i)}{\ln m}$	(iv)	To indicate even degree of different landscape types
Dominance Index (Dominance)	$\mathrm{Do} = \ln m + \sum_{i=1}^{m}(p_i \ln p_i)$	(v)	To what extent several principal landscape types control whole landscape
Contagion Index (CONTAG)	$\mathrm{CONTAG} = \left[1 + \frac{\sum_{h=1}^{m}\sum_{i=1}^{m}[(p_i)(g_{hi}/\sum_{i=1}^{m} g_{hi})][\ln(p_i)(g_{hi}/\sum_{i=1}^{m} g_{hi})]}{2\ln(m)}\right](100)$	(vi)	To express the agglomeration degree among different landscape types

I : patch type; j: number of patch; A: the total area; a_{ij}: the area of patch ij; l: patch perimeter; k: a constant, as to grid map, k equals to 4; g_{hi}: contiguity number among patch h and patch i; p_i: the area ratio of class i; m: quantity of region landscape types.

where I_{ue} is urbanization intensity index, ΔU_i is expansion area of urban land during a certain period, TLA is the total area of the research area, and Δt is time span of a certain duration.

2.2.3. Landscape Pattern Metrics. The six landscape metrics of Largest Patch Index (LPI), Fractal Dimension Index (FD), Shannon's Diversity Index (SHDI), Shannon's Evenness Index (SHEI), Dominance Index (Dominance), and Contagion Index (CONTAG) were selected for landscape pattern analysis. As a measure of landscape heterogeneity, SHDI is especially sensitive to the nonbalanced distribution of all patch types in the landscape. SHEI is applied to indicate the diversity of different landscapes or a certain landscape in different periods, which results in maximum evenness. As such, evenness could be the complement of dominance. Contagion Index is related to edge density and can measure the clumping trends of the patches. The higher the CONTAG is, the more homogeneous and contiguous the spatial pattern is. The Fragstats 3.3 was adopted to calculate and analyze landscape pattern metrics. Expressions and ecological significance of metrics in the present study are given in Table 1 [33–38].

2.2.4. Ecological Risk Assessment. The ecological risk index (ERI) [39] (2) was adopted to assess the spatial difference of comprehensive ecological risk in the various land use types under urbanization expansion:

$$\mathrm{ERI} = \sum_{i=1}^{N}\frac{A_i}{A}w_i, \tag{2}$$

where ERI is ecological risk index; i is land use type; A_i is area of land i; A is the total area of research area; w_i which is the comprehensive ecological risk intensity reflected by i is determined by the method of the analytic hierarchy process (AHP) for each land use type. The values of w_i for urban land, farmland, orchard, forestland, grassland, water body, other construction land, and other object land are 0.29, 0.13, 0.11, 0.03, 0.05, 0.04, 0.20, and 0.07, respectively.

Based on the geostatistical analysis module of ArcGIS 9.3, the studied area was divided into 370 sampling grid units with the size of 3 km × 3 km to establish the evaluation unit of ecological risk after equidistant partition. The ecological risk index values were calculated in each grid units. The spherical model method was applied to control test fitting results. Together with ordinary Kriging method for data interpolation, the regional ecological risks in 1990–2009 were evaluated. Finally, with calculating results of the urbanization intensity index and variation of ecological risk of the evaluation unit, the regression analysis method was used for the quantitative relationship between urban spatial expansion and regional ecological risk.

3. Results and Discussion

3.1. The Spatial-Temporal Evolution Characteristics of Urbanization Expansion. The urbanization process in Yantai city speeded up sharply since the reform and opening-up policy (1980s) (Figures 2 and 3). The area of urban land occupied 29.43 km^2 and only distributed in the center of Zhifu District and Muping District in 1974. The urban area increased 52.81 km^2 from 29.43 km^2 in 1974 to 82.24 km^2 in 1990. Meanwhile, as an important coastal city in China, the port industry developed rapidly, such as the construction of Yantai Port in Zhifu District. Therefore, urban land not only expanded to the northern and western part of Zhifu District, but also appeared in the connection between Zhifu District and Development Zone (Figure 2). The rapid development of urbanization expansion occurred in period of 1990–2009.

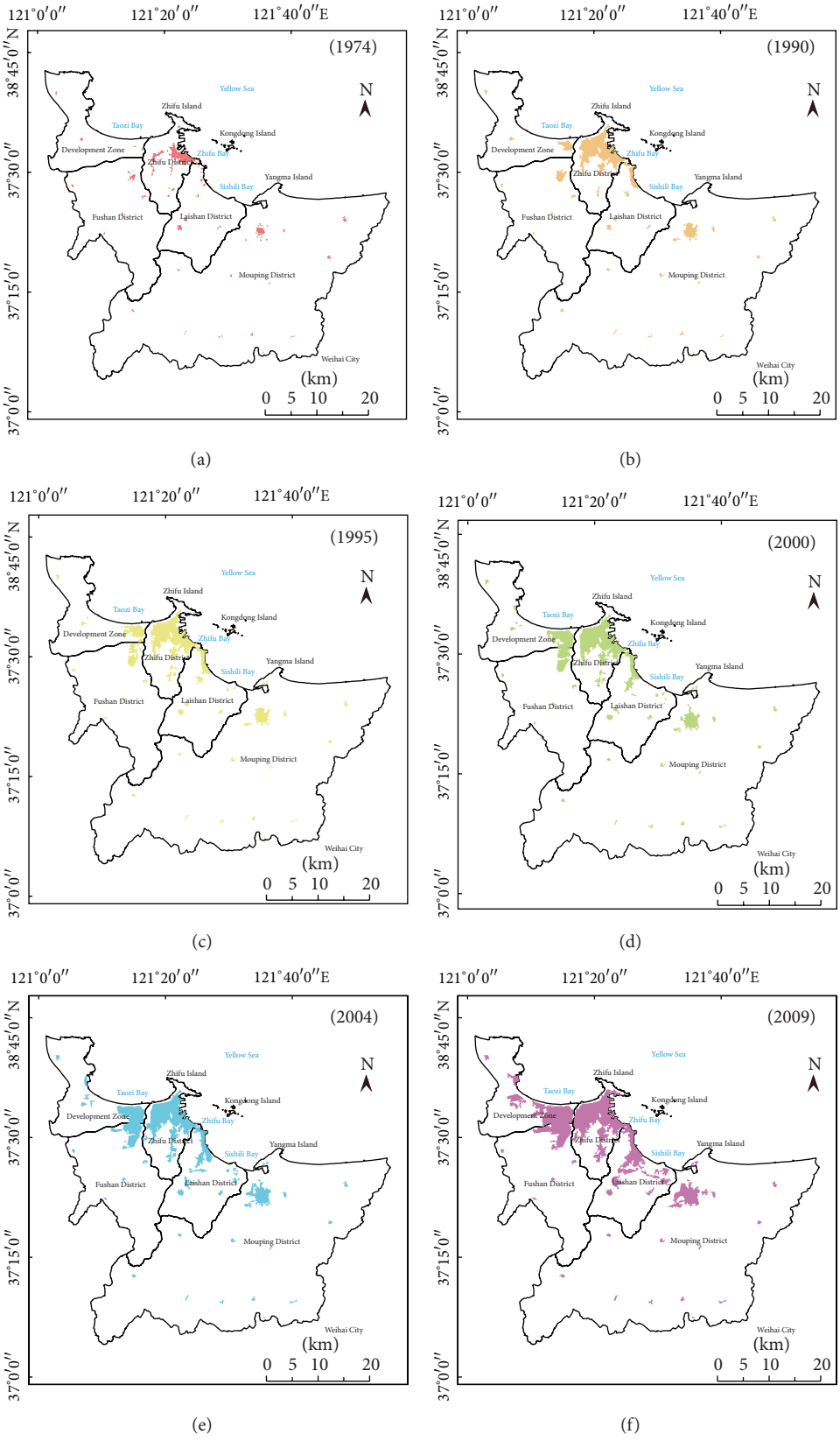

Figure 2: Spatial distribution of urban land in the study area.

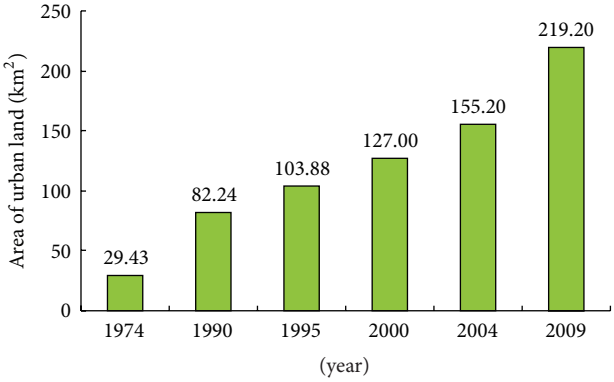

Figure 3: Area of urban land during the period of 1974–2009.

Table 2: Urbanization extension in Yantai city in different historical periods.

Different period	Extension area (km^2)	Annual expansion area ($km^2\ y^{-1}$)	Urbanization intensity index
1974–1990	52.81	3.30	0.12
1990–2000	44.76	4.48	0.16
2000–2009	92.20	10.24	0.38
1974–2009	189.77	5.42	0.20

The area of urban land expanded to 127.00 km^2 in 2000 and 219.20 km^2 in 2009, respectively (Figure 3). Restricted by geographical limit, the distribution of urban land in Zhifu District began to spread to Zhifu Island (northern part of Zhifu District) and Huangwu Town (southern part of Zhifu District) after 1990. Because of the migration of Yantai municipal government from Zhifu District to Laishan District since 2000, the Laishan District has become a new hot spot of urban land expansion. In addition, the study area had been well served with traffic facilities including Laishan Airport, Yantai-Weihai highway, Tongjiang-Sanya highway, 010 National Highway, and 204 National Highway. The Shanhai Road which was constructed in 2003 has connected Fushan District, Zhifu District, and Laishan District. Meanwhile, the port industry (such as Bajiao Port in Development Zone) and a series of coastal leisure planning related coastal tourism economy developed quickly in the study area. Therefore, urban land in Yantai city expanded dramatically from coastline to inland region during 2000 and 2009.

The area of urban land of Yan city increased by 189.77 km^2 with annual expansion area of 5.42 km^2 and Urbanization Intensity Index of 0.20 during 1974–2009 (Table 2). The urbanization process during studied period can be divided into three stages, that is, initial stage (1974–1990), development stage (1990–2000), and rapid expansion stage (2000–2009) (Table 2). The urbanization expansion rate was 3.30 $km^2\ y^{-1}$ and there were about 52.81 km^2 changed to urban land during 1974–1990. The urban extension rate (4.48 $km^2\ y^{-1}$) in the next ten years of 1990–2000 was obviously higher than that in the initial stage. Since 2000, the urban expansion started with a sharp speed of 10.28 $km^2\ y^{-1}$ which was more than two times of 1990–2009, because of the rapid economic development and insistent population growth in this stage. The urban extension area reached to 92.20 km^2 within 10 years, and the values of urbanization intensity index were 0.12, 0.16 and 0.30 in stages of 1974–1990, 1990–2000, and 2000–2009 (Table 2), respectively. The high value of urbanization intensity index in 2000–2009 indicated that the urban expansion was great in this period.

The urbanization expansion and landscape pattern change were influenced by many factors, such as geographical location, population, economic policy, resources, and transportation [25, 40]. The coastal location advantages played an important role in urbanization expansion [8, 9]. The spatial distribution of urban land expanded along the coastline (Figure 2). Influenced by port economy, the distribution of urban land in the study area from 1974 to 1990 was formed with the spatial construction of "one center," which was similar with the urbanization process of many coastal cities which depended on port economy in the world [26, 41]. In the studied area, The GDP increased from 4.69 billion YUAN in 1990 to 155.30 billion YUAN in 2009; the total population grew about 0.70 million from 1990 (1.41 million) to 2009, resulting in about 137 km^2 urban land increase (Table 2) and about 237 km^2 farmland lost during this period (Table 3). The fast speed urbanization expansion started since 2000. From 2000 to 2009, the area of urban land added 92.20 km^2 and urbanization intensity index was 0.38. Meanwhile, the urban space had transformed to axial expansion that developed from compact nutty to dispersed groups (Figure 2), which was similar with the axial expansion of Shanghai city between 1979 and 2000 [25]. Furthermore, with the ideology changes of urban construction policy [42] and transportation construction [25], the urban land of Yantai city has expanded to inner regions with the T-shape along the coastline (Figure 2), then has gradually aggregated from dispersed. In recent years, the agglomeration growth pattern of urbanization expansion became more and more obvious.

3.2. Analysis of Land Use/Cover and Landscape Pattern Changes. The dominant land use in study area in 1990 was farmland (48.45%), forestland (24.17%), and grassland (7.91%), the sum of which was more than 80% of the total area (Table 3). The urban land covered only 82.24 km^2 (Figure 3), no more than 3% of the total area. In 2000, farmland and grassland had reduced to 1173.11 km^2 and 163.72 km^2, respectively, while the areas of urban land, orchard, forestland, water body, and other construction land increased greatly. Compared to 1990, the orchard, urban land, and forestland increased by 92.44 km^2, 44.76 km^2, and 40.03 km^2, respectively (Table 3). A similar pattern of land use/cover change trend was found in 2009. Farmland continued shrinking to 1081.05 km^2 and grassland decreased to 25.21 km^2 from 2000 to 2009. The fastest growth of land uses was urban land instead of orchard with an increase of 92.20 km^2 within 10 years. Many studies reported that the acceleration of urbanization expansion was the main driving force for decrease

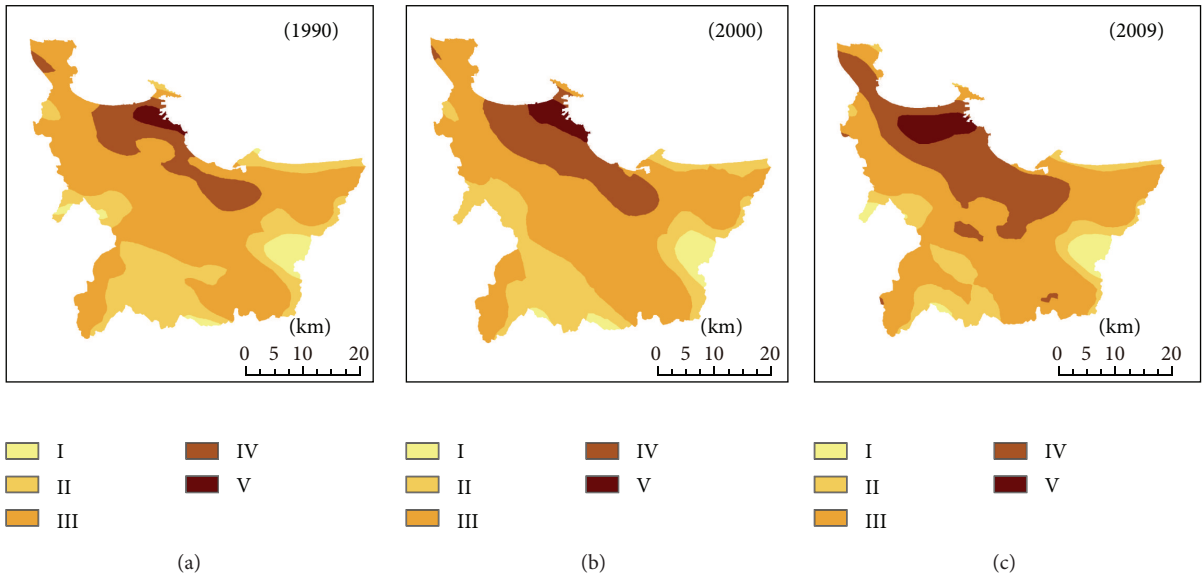

Figure 4: Spatial distribution of ecological risk in 1990–2009 ((I) low ecological risk, (II) sublow ecological risk, (III) moderate ecological risk, (IV) subhigh ecological risk, and (V) high ecological risk).

Table 3: Area and percentage of land use types in Yantai city from 1990 to 2009.

LUCC type	1990		2000		2009	
	Area (km^2)	Percentage (%)	Area (km^2)	Percentage (%)	Area (km^2)	Percentage (%)
Urban land	82.24	3.02	127.00	4.67	219.20	8.06
Farmland	1318.33	48.45	1173.11	43.11	1081.05	39.73
Orchard	182.76	6.72	275.20	10.11	308.15	11.32
Forestland	657.62	24.17	697.65	25.64	662.41	24.34
Grassland	215.11	7.91	163.72	6.02	138.51	5.09
Water body	79.72	2.93	89.21	3.28	87.80	3.23
Other construction land	131.34	4.83	150.05	5.51	180.65	6.64
Other object land	53.92	1.98	45.10	1.66	43.27	1.59

Table 4: Dynamic change of landscape metrics from 1990 to 2009.

Year	LPI	FD	SHDI	SHEI	Dominance	CONTAG
1990	23.32	1.0671	1.55	0.71	0.29	54.49
2000	22.20	1.0679	1.62	0.74	0.26	52.72
2009	20.35	1.0682	1.68	0.76	0.24	51.26

of farmland and green land [14, 31, 40, 43]. Farmland was the largest land use type in the study area (Table 3). During the period 1990–2009, the area of urban land increased greatly (about 137 km^2) and farmland decreased from 1318.33 km^2 in 1990 to 1081.05 km^2 in 2009 (Figure 3 and Table 3). The result was similar with another Chinese coastal city, Longkou city [31]. Due to development of fruit economy, part of farmland was transformed into orchard (Table 3). The area of forestland increased from 1990 to 2000 because of the implementation of "returning farmland to forestland and grassland" project, while decreasing from 2000 to 2009 due to human activities increase and ecology degradation. In contrast, the forestland, water body, and other object land tented to decrease and most of lost areas had been transformed into maritime industrial land and tourism land.

The calculation results of landscape metrics which indicate landscape pattern change showed that the LPI decreased from 23.32 in 1990 to 20.35 in 2009 (Table 4), indicating that the dominant landscape of farmland had declined. Due to the strengthen of human interferences, the study area showed more fragmented landscapes, fewer large patches, which caused the Dominance and CONTAG decrease and FD increase during 1990–2009 (Table 4). Meanwhile, the urban land rapidly expanded from the urban center to the surrounding areas and then aggregated to a new large patch. The increase of SHDI and SHEI from 1990 to 2009 indicated that the landscape shapes in the study area had become more and more complex because of human activities [8].

3.3. Analysis of Regional Ecological Risk. Using the Natural Breaks classification method [21], the ecological risk was grouped into five grades, that is, low ecological risk (I),

Table 5: Area of different level ecological risk from 1990 to 2009.

Ecological risk grade	1990	2000	2009	1990	2000	2009
	Area (km^2)			Area proportion (%)		
Low ecological risk region	92.97	91.47	88.47	3.42	3.36	3.25
Sublow ecological risk region	654.59	629.28	388.12	24.07	23.14	14.27
Moderate ecological risk region	1633.04	1550.90	1487.92	60.05	57.03	54.72
Subhigh ecological risk region	300.94	386.22	650.65	11.07	14.2	23.93
High ecological risk region	37.79	61.47	104.18	1.39	2.26	3.83

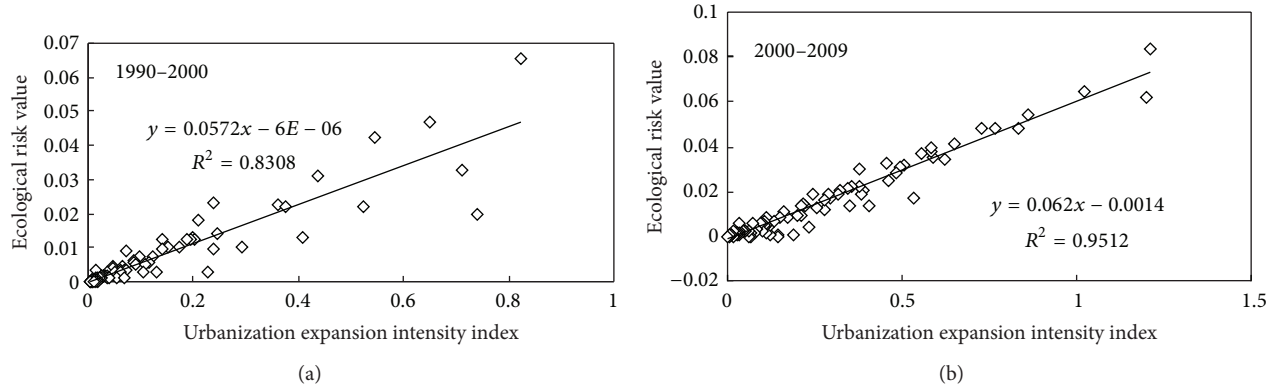

Figure 5: The relationship between urbanization intensity index and region ecological risk.

sublow ecological risk (II), moderate ecological risk (III), subhigh ecological risk, and (IV) and high ecological risk (V), according to the ecological risk index. The results showed that the high and subhigh ecological risk areas are mainly distributed in the urban land, while low and sublow ecological risk areas appeared in forestland and grassland with high vegetation coverage (Figure 4). In addition, the ecological risk level decreased with the distance to the coastline increase. From 1990 to 2009, the moderate ecological risk level was major, and the proportions of subhigh and sublow ecological risk changed obviously in study area (Figure 4 and Table 5). The areas of moderate and sublow ecological risk decreased to 145.12 km^2 and 266.47 km^2 from 1990 to 2009, respectively. The low ecological risk area reduced to 4.5 km^2. On the contrary, the area of high ecological risk increased from 37.79 km^2 in 1990 to 61.47 km^2 in 2000 and expanded rapidly to 104.18 km^2 in 2009. The high ecological risk region mainly distributed along the coastline of Zhifu District and expanded westward to Fushan District and Development Zone (Figure 4). The area of subhigh ecological risk in 2009 was 2 times higher than that in 1990 and expanded to inner region from inshore region (Table 5 and Figure 4). The ecological security in the coastal zone was largely influenced by urbanization expansion and land use change [8, 16, 32, 44]. As the sensitive area in land-ocean interactions zone, Yantai city is located in the integrated high ecological risk area of the Ring-Bohai Region [16, 45]. In this study, the area of high and subhigh ecological risk region increased rapidly and extended eastward and westward along the coastline with layered distribution and the area of moderate and sublow ecological risk region reduced under the development of urbanization expansion (Figure 4). Such changes, especially the increasing trend of high ecological risk, were also observed in the coastal economic developing zone of Jinzhou Bay in Liaoning Province and Yancheng coastal area in Jiangsu Province [29, 45]. Previous studies predicted that more and more farmland and coastal water of Yantai city will be lost in the next 40 years due to the acceleration of urbanization process; a series of coastal development activities and reclamation projects would enhance the regional ecological risk [32]. The significant positive linear relationship between the urbanization intensity index and regional ecological risk index both in 1990–2000 and 2000–2009 with the determination coefficient (R^2) of 0.831 and 0.951, respectively, (Figure 5) was observed in the study, which obviously supported these prediction results. The results of this study suggested that the scientific urban development plan and rational coastal management measures should be implemented in order to reduce the ecological risk brought from urbanization expansion.

4. Conclusions

With economic development and population growth, the process of urbanization of Yantai city had accelerated obviously and the area of urban land increased quickly. The area of urban land increased about 137 km^2 and about 237 km^2 farmland lost during the period of 1990–2009. The distribution of urban land showed a T-shape along the coastline extent to inner regions. The area of high ecological risk increased rapidly and the moderate and sublow ecological

risk decreased from 1990 to 2009. The high and subhigh ecological risk areas mainly distributed in the urban land and the ecological risk level decreased with the distance to the coastline increase. The significant positive relation between urbanization intensity and regional ecological risk was found in the study.

Conflict of Interests

The authors declare that there is no conflict of interests regarding the publication of this paper.

Authors' Contribution

Di Zhou, Ping Shi, and Junbao Yu contributed equally to this work.

Acknowledgments

The authors are grateful for the support from the Project of the Young Scientist Fund of National Natural Science Foundation of China (30800149) and the Public Science and Technology Research Funds Projects of Ocean (201005009).

References

[1] B. Cohen, "Urbanization in developing countries: current trends, future projections, and key challenges for sustainability," *Technology in Society*, vol. 28, no. 1-2, pp. 63–80, 2006.

[2] J. Li, X. Wang, X. Wang, W. Ma, and H. Zhang, "Remote sensing evaluation of urban heat island and its spatial pattern of the Shanghai metropolitan area, China," *Ecological Complexity*, vol. 6, no. 4, pp. 413–420, 2009.

[3] P. K. Mallupattu and J. R. S. Reddy, "Analysis of land use/land cover changes using remote sensing data and GIS at an Urban Area, Tirupati, India," *The Scientific World Journal*, vol. 2013, Article ID 268623, 6 pages, 2013.

[4] C. Li, J. X. Li, and J. G. Wu, "Quantifying the speed, growth modes, and landscape pattern changes of urbanization: a hierarchical patch dynamics approach," *Landscape Ecology*, vol. 28, no. 10, pp. 1875–1888.

[5] L. Liu and H. Han, "Research on countermeasures of coastal zone management," *Marine Development and Management*, no. 6, pp. 51–55, 2007.

[6] M. Chen, X. Han, and S. Liu, "The effects of reclamation and sustainable development on coastal zone in Shanghai. China," *Soft Science Magzine*, no. 12, pp. 115–120, 2000.

[7] G. Zhou and S. Jia, "The persuit of best benefit for urban land utilization—the study on the allocation of land resource under urbanization accelerating stage," *China Land*, no. 12, pp. 1250–1256, 2001.

[8] T. Lin, X. Xue, L. Shi, and L. Gao, "Urban spatial expansion and its impacts on island ecosystem services and landscape pattern: a case study of the island city of Xiamen, Southeast China," *Ocean and Coastal Management*, vol. 81, pp. 90–96, 2013.

[9] X. Li, T. Lin, G. Zhang, L. Xiao, Q. Zhao, and S. Cui, "Dynamic analysis of urban spatial expansion and its determinants in Xiamen Island," *Journal of Geographical Sciences*, vol. 21, no. 3, pp. 503–520, 2011.

[10] Y. Cai, H. Zhang, W. Pan, Y. Chen, and X. Wang, "Urban expansion and its influencing factors in natural wetland distribution Area in Fuzhou City, China," *Chinese Geographical Science*, vol. 22, no. 5, pp. 568–577, 2012.

[11] X. Xu, H. Peng, and Q. Xu, "Land resource conflicts and coordination in fast urbanized coastal zone: a case study of the Shandong peninsula," *Acta Scientiarum Naturalium Universitatis Pekinensis*, vol. 42, no. 4, pp. 527–533, 2006.

[12] W. P. Chang, S. J. Wu, W. C. Chang, and H. C. Kuo, "Population-based study of the association between urbanization and Kawasaki disease in Taiwan," *The Scientific World Journal*, vol. 2013, Article ID 10.1155/2013/169365, 4 pages, 2013.

[13] A. A. A. Al-Manni, A. S. A. Abdu, N. A. Mohammed, and A. E. Al-Sheeb, "Urban growth and land use change detection using remote sensing and geographic information system techniques in Doha City, State of Qatar," *Arab Gulf Journal of Scientific Research*, vol. 25, no. 4, pp. 190–198, 2007.

[14] A. Merlotto, M. C. Piccolo, and G. R. Bertola, "Urban growth and land use/cover change at Necochea and Quequen cities, Buenos Aires province, Argentina," *Revista de Geografia Norte Grande*, no. 53, pp. 159–176, 2012.

[15] Y. Li, X. Zhu, X. Sun, and F. Wang, "Landscape effects of environmental impact on bay-area wetlands under rapid urban expansion and development policy: a case study of Lianyungang, China," *Landscape and Urban Planning*, vol. 94, no. 3-4, pp. 218–227, 2010.

[16] N. Zhou and S. Zhao, "Urbanization process and induced environmental geological hazards in China," *Natural Hazards*, vol. 67, no. 2, pp. 797–810, 2013.

[17] G. Pigeon, A. Lemonsu, N. Long, J. Barrié, V. Masson, and P. Durand, "Urban thermodynamic island in a coastal city analysed from an optimized surface network," *Boundary-Layer Meteorology*, vol. 120, no. 2, pp. 315–351, 2006.

[18] X. Wu, Y. Hu, H. He, R. Bu, and M. Feng, "Research for scenarios simulation of future urban growth and land use change in Shenyang City," *Geographical Research*, vol. 28, no. 5, pp. 1264–1275, 2009.

[19] X. Qin, X. Duan, and J. Yang, "Scenario simulation of urban land use allocation and scheme evaluation based on GIS: a case study of Taicang City," *Acta Geographica Sinica*, vol. 65, no. 9, pp. 1121–1119, 2010.

[20] Y. Lin, W. Chen, Q. Yu, Y. Zhang, and W. Ma, "A simulation of the urban expansion in Shanghai and its environmental impact," *Acta Scientiae Circumstantiae*, vol. 31, no. 1, pp. 206–216, 2011.

[21] Y. Zhang, G. Lei, J. Lin, and H. Zhang, "Spatiotemporal change and its ecological risk of landscape pattern in different spatial scales in Zhalong Nature Reserve," *Chinese Journal of Ecology*, vol. 31, no. 5, pp. 1250–1256, 2012.

[22] T. F. Stepinski, P. Netzel, and J. Jasiewicz, "LandEx—a GeoWeb tool for query and retrieval of spatial patterns in land cover datasets," *IEEE Journal of Selected Topics in Applied Earth Observations and Remote Sensing*, vol. 7, no. 1, pp. 257–266, 2014.

[23] D. Guo, "Analysis of spatial-tempo features of land use of Bohai Sea sealine buffer zones in the recent Yellow River Delta," *Transactions of the Chinese Society of Agricultural Engineering*, vol. 22, no. 4, pp. 53–57, 2006.

[24] C. Y. Ji, Q. Liu, D. Sun, S. Wang, P. Lin, and X. Li, "Monitoring urban expansion with remote sensing in China," *International Journal of Remote Sensing*, vol. 22, no. 8, pp. 1441–1455, 2001.

[25] J. Yin, Z. Yin, H. Zhong et al., "Monitoring urban expansion and land use/land cover changes of Shanghai metropolitan

area during the transitional economy (1979–2009) in China," *Environmental Monitoring and Assessment*, vol. 177, no. 1–4, pp. 609–621, 2011.

[26] L. Hua, X. Li, L. Tang, K. Yin, and Y. Zhao, "Spatio-temporal dynamic analysis of an island city landscape: a case study of Xiamen Island, China," *International Journal of Sustainable Development and World Ecology*, vol. 17, no. 4, pp. 273–278, 2010.

[27] D. Li, A. Zhang, and S. Zhang, "Characteristics and driving forces analysis of residential area expansion in the north of Shandong Peninsula coastal area," *Journal of Natural Resources*, vol. 23, no. 4, pp. 612–618, 2008.

[28] L. Guo, D. Wang, J. Qiu, L. Wang, and Y. Liu, "Spatio-temporal patterns of land use change along the Bohai Rim in China during 1985–2005," *Journal of Geographical Sciences*, vol. 19, no. 5, pp. 568–576, 2009.

[29] B. Gao, X. Li, Z. Li, W. Chen, X. He, and S. Qi, "Assessment of ecological risk of coastal economic developing zone in Jinzhou Bay based on landscape pattern," *Acta Ecologica Sinica*, vol. 31, no. 12, pp. 3441–3450, 2011.

[30] J. Zhang, X. Chang, and Y. Song, "Analysis of land use change and landscape pattern change in coastalzone in Taozi Bay of Shandong Peninsula," *Areal Research and Development*, vol. 27, no. 3, pp. 108–112, 128, 2008.

[31] A. Zhang, D. Li, D. Wang, and G. Jiang, "Aanlysis of land use dynamic changes and its driving forces in the north of Shandong Peninsula: taking Longkou as an example," *Economic Geography*, vol. 27, no. 6, pp. 1007–1010, 2007.

[32] J. Ma, X. Wu, D. Zhou, and Z. Wang, "Scenario simulation of urban spatial expansion and its ecological risks assessment in coastal zones," *Resources Science*, vol. 34, no. 1, pp. 185–194, 2012.

[33] J. Wu, *Landscape Ecology: Pattern, Process, Scale and Hierarchy*, Higher Education Press, Beijing, China, 2nd edition, 2000.

[34] J. Sun, C. Lan, H. Xia, and K. Xin, "Analysis on landscape pattern of Guigang City based on QuickBird imagery," *Chinese Journal of Ecology*, vol. 25, no. 1, pp. 50–54, 2006.

[35] Q. Wang and S. Zheng, "Changes of landscape pattern evolvement in Hefei City based on GIS in recent 50 years," *Journal of Anhui Agricultural Sciences*, vol. 36, no. 23, pp. 10112–10115, 2008.

[36] X. Wang, D. Xiao, R. Bu, and Y. Hu, "Analysis on land scape pat-terns of Liaohe Delta wetland," *Acta Ecologica Sinica*, vol. 17, no. 3, pp. 317–323, 1997.

[37] H. Shi, K. Yu, Y. Feng, X. Dong, H. Zhao, and X. Deng, "RS and GIS- based analysis of landscape pattern changes in urban-rural ecotone: a case study of Daiyue District, Tai' an City, China," *Journal of Landscape Research*, vol. 4, no. 9, pp. 20–23, 2012.

[38] X. Wang, L. Ning, J. Yu, R. Xiao, and T. Li, "Changes of urban wetland landscape pattern and impacts of urbanization on wetland in Wuhan City," *Chinese Geographical Science*, vol. 18, no. 1, pp. 47–53, 2008.

[39] L. Yuan, W. Gong, Y. Dang, and Z. Long, "Study on ecological risk of land use in urbanization watershed based on RS and GIS: a case study of Songhua River watershed in Harbin Section," *Asian Agriculture Reaserch*, vol. 5, no. 3, pp. 61–65, 69, 2013.

[40] Y. Liu, L. Wang, and H. Long, "Spatio-temporal analysis of land-use conversion in the eastern coastal China during 1996–2005," *Journal of Geographical Sciences*, vol. 18, no. 3, pp. 274–282, 2008.

[41] R. Bhagyanagar, B. M. Kawal, G. S. Dwarakish, and S. Surathkal, "Land use/land cover change and urban expansion during 1983–2008 in the coastal area of Dakshina Kannada district, South India," *Journal of Applied Remote Sensing*, vol. 6, no. 1, Article ID 063576, 2012.

[42] J. Xu, B. Liao, Q. Shen, F. Zhang, and A. Mei, "Urban spatial restructuring in transitional economy—changing land use pattern in Shanghai," *Chinese Geographical Science*, vol. 17, no. 1, pp. 19–27, 2007.

[43] C. Duran, H. Gunek, and E. K. Sandal, "Effects of urbanization on agricultural lands and river basins: case study of Mersin (South of Turkey)," *Journal of Environmental Biology*, vol. 33, no. 2, pp. 363–371, 2012.

[44] Y. Lu, L. Xu, Z. Ma, L. Yan, and X. Xu, "Ecological risk assessment of five provinces around the Bohai Sea Chinese," *Journal of Ecology*, vol. 31, no. 1, pp. 227–234, 2012.

[45] X. Sun and H. Liu, "The effect of land use on landscape ecological risk in Yancheng coastal area, Jiansu Province," *Remote Sensing for Land and Resources*, no. 3, pp. 140–145, 2011.

Hindawi Publishing Corporation
The Scientific World Journal
Volume 2014, Article ID 949213, 8 pages
http://dx.doi.org/10.1155/2014/949213

Research Article

Wet and Dry Atmospheric Depositions of Inorganic Nitrogen during Plant Growing Season in the Coastal Zone of Yellow River Delta

Junbao Yu,[1] Kai Ning,[1,2] Yunzhao Li,[1,2] Siyao Du,[3] Guangxuan Han,[1] Qinghui Xing,[1,2] Huifeng Wu,[1] Guangmei Wang,[1] and Yongjun Gao[4]

[1] *Key Laboratory of Coastal Zone Environmental Processes and Ecological Remediation, Yantai Institute of Coastal Zone Research (YIC), Chinese Academy of Sciences (CAS) and Shandong Provincial Key Laboratory of Coastal Zone Environmental Processes, YICCAS, Yantai 264003, China*
[2] *University of Chinese Academy of Sciences, Beijing 100049, China*
[3] *College of Environmental Science and Engineer, Ocean University of China, China*
[4] *Department of Geosciences, University of Houston, Houston, TX 77204, USA*

Correspondence should be addressed to Junbao Yu; junbao.yu@gmail.com

Received 22 February 2014; Revised 15 March 2014; Accepted 15 March 2014; Published 1 April 2014

Academic Editor: Hong-bo Shao

The ecological problems caused by dry and wet deposition of atmospheric nitrogen have been widespread concern in the world. In this study, wet and dry atmospheric depositions were monitored in plant growing season in the coastal zone of the Yellow River Delta (YRD) using automatic sampling equipment. The results showed that SO_4^{2-} and Na^+ were the predominant anion and cation, respectively, in both wet and dry atmospheric depositions. The total atmospheric nitrogen deposition was ~2264.24 mg m^{-2}, in which dry atmospheric nitrogen deposition was about 32.02%. The highest values of dry and wet atmospheric nitrogen deposition appeared in May and August, respectively. In the studied area, NO_3^-–N was the main nitrogen form in dry deposition, while the predominant nitrogen in wet atmospheric deposition was NH_4^+–N with ~56.51% of total wet atmospheric nitrogen deposition. The average monthly attribution rate of atmospheric deposition of NO_3^-–N and NH_4^+–N was ~31.38% and ~20.50% for the contents of NO_3^-–N and NH_4^+–N in 0–10 cm soil layer, respectively, suggested that the atmospheric nitrogen was one of main sources for soil nitrogen in coastal zone of the YRD.

1. Introduction

It is well known that nitrogen is an important nutrient in terrestrial and marine ecosystems. The primary production, the nutrient cycling, and the biodiversity in natural ecosystems were great limited by the availability of reactive nitrogen [1–5]. The global reactive nitrogen production rate increased from approximately 15 Tg N yr^{-1} in 1860 to 187 Tg N yr^{-1} in 2005; more than half of total was deposited onto the ground [6]. Atmospheric nitrogen deposition has become a large source of nitrogen for terrestrial and aquatic ecosystems worldwide [7]. The atmospheric nitrogen deposition can affect the soil nitrogen balance, which probably results in some negative effects on terrestrial and marine ecosystems [8–10] through eutrophication and acidification [11]. Nitrogen entering the soil-plant system has been a main factor for the nitrogen cycle of ecosystem [12]. Atmospheric nitrogen deposition has frequently been observed to increase soil carbon (C) storage in natural ecosystems [13, 14]. Some studies tried to build relations between atmospheric depositions and nitrogen concentration in moss and proved that mosses could serve as biological indicators for atmospheric nitrogen depositions [15]. Therefore, the atmospheric nitrogen deposition has become an increasingly important source for reactive nitrogen entering to the coastal ecosystems and contributed to the coastal nitrogen budget [5].

The ecological problems caused by dry and wet deposition of atmospheric nitrogen have widespread concern in the

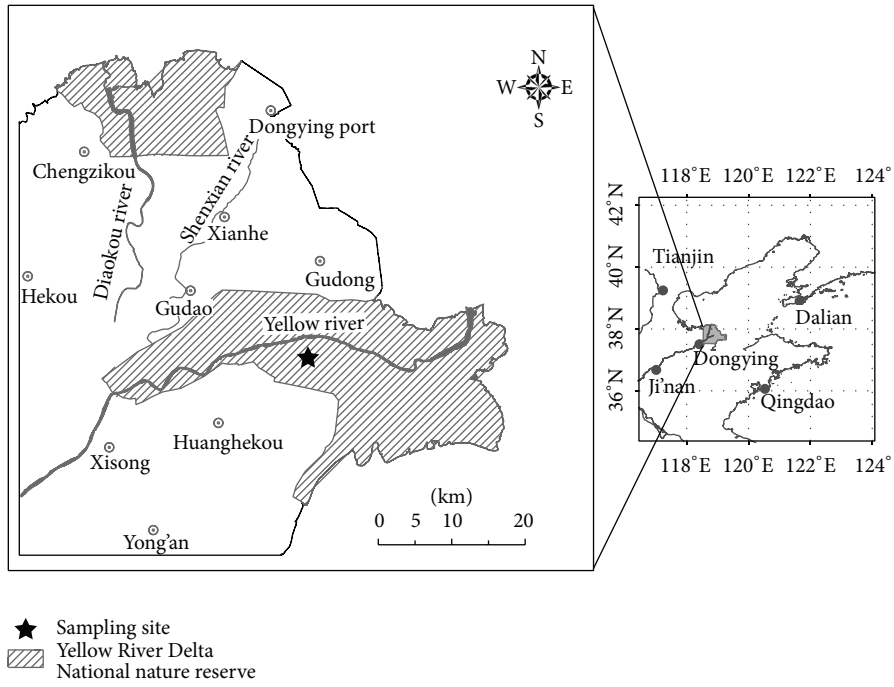

Figure 1: The location of the Yellow River Delta and sampling sites.

world. In recent decades, high rates of atmospheric nitrogen deposition have been reported in Europe [16], East Asia [17], North America [18], and Northern and Southeastern China [19, 20]. The National Atmospheric Deposition Program (NADP) was built to oversee the long-term sampling and analysis of precipitation across the United States, Puerto Rico, and the Virgin Islands [21], and the dry deposition was monitored by networks in Europe (EMEP), North America (CASTNET), and East Asia (EANET). As the largest developing country, China has consumed more than 24 Tg year^{-1} fertilizer N in recent years, which is ~30% of total fertilizer N used worldwide [22]. In addition, livestock production in China has increased greatly since the late 1980s. The amount of NH_3 volatilization from wastes of domestic animals (manure and urine) is even higher than that from fertilizer use in China [23]. Furthermore, the transport network and traffic have increased rapidly since the 1980s in China, resulting in increasing NO_x emissions by 62% [24]. 70–80% of the emitted nitrogen was deposited to the land or water surface as wet and dry deposition [11]. Nitrogen deposition was the highest over Southern China and exhibited a decreasing gradient from Southern to Western and Northern China. The anthropogenic activities were the main reason for the nitrogen deposition increase [25]. Therefore, China is now a hotspot for nitrogen deposition according to recent modeling studies [7, 25, 26]. However, the magnitude of atmospheric deposition of various N species in China remains uncertain because of a paucity of measurements and quantitative knowledge [19, 27]. Previous studies of atmospheric nitrogen deposition in China have considered the wet and the dry deposition separately [28, 29] and most monitored locations were in agricultural areas and cities [19, 22]. Few measurements have focused on both the wet and the dry deposition of individual nitrogen species in coastal wetlands. In this study, the dry and wet nitrogen deposition was monitored using automatic sampling equipment in coastal wetland of the Yellow River Delta (YRD) which is one of intensive agricultural regions and rapidly economic developing regions in China. The objectives of the present study were to (1) determine the composition and amount in dry and wet atmospheric nitrogen deposition, (2) reveal the monthly variation of nitrogen (wet/dry) deposition in growing season, and (3) assess the contribution of atmospheric nitrogen inputs to local soil.

2. Materials and Methods

2.1. Study Area Description. The sampling sites (118°58′E, 37°45′N) located at the Yellow River Delta Ecology Research Station of Coastal Wetland, Chinese Academy of Sciences (Figure 1), which is in the Yellow River DeltaNational Nature Reserve. All around the sampling sites was wide open without buildings. The climate in study area is warm temperate continental monsoon climate. It is arid and windy in spring, hot and rainy in summer, cool and sunny in autumn, and less snowy and dry in winter [30]. The annual average temperature is ~12.1°C, the annual average precipitation is ~551.6 mm, and the annual average evaporation is ~1962 mm. More than 85% of plants are the aquatic vegetation and halophytic vegetation in study region. The *Suaeda salsa* and *Phragmites communis Trin* are predominant plants and widely distributed [27].

2.2. Sampling. The dry and wet atmospheric depositions were monitored in plant growing season from May to November in 2012. The samples were collected using SCJ-302 model automatic sampling equipment (Qingdao Xuanhui Instruments & Equipment Co. Ltd, China). The sensitivity of the equipment was 0.05 mm/h. The automatic sampling equipment stops the dry atmospheric deposition collection with a lid covered and starts to collect the wet atmospheric depositions sample within 60 seconds of rainfall event beginning. As soon as the precipitation ceased, the head covering covered over the wet atmospheric deposition collection buckets and rotated to collect the dry atmospheric deposition. Meanwhile, the TE525 tipping bucket gauge (Texas Electronics, USA) which was anchored 0.7 m above the ground was used to monitor precipitation. In this study, the method of Balestrini et al. [31] was used for sample collection. According to national atmospheric environmental monitoring criterions, the solution of ethylene glycol was used at the surface of collection bucket to collect the dry atmospheric deposition samples.

The dry atmospheric deposition samples were collected monthly and wet atmospheric deposition samples were collected after each precipitation event. In the monitoring period, the surface soils (0–10 cm) in atmospheric deposition monitoring sites were collected monthly.

2.3. Analytical Procedures. The wet and dry deposition samples were taken to the laboratory for chemical analysis. The water-soluble ions (Na^+, K^+, Ca^{2+}, Mg^{2+}, NH_4^+, Cl^-, NO_3^-, and SO_4^{2-}) were measured by ICS3000 ion chromatograph (Dionex, USA). Total inorganic nitrogen (TIN) was considered as the sum of ammonium nitrogen (NH_4^+–N) and nitrate nitrogen (NO_3^-–N). The number of ions and nitrogen content per unit area for wet and dry deposition samples was calculated using cross-sectional area and volume of wet and dry atmospheric deposition collection buckets.

The air-dried soil samples which collected in monitoring sites were extracted in 2 mol/L KCl. Then the contents of NH_4^+–N and NO_3^-–N were analyzed by a flow-injection autoanalyzer (Seal-Branlubbe AA3, Seal Germany). The soil volume weight was measured by cutting ring method.

2.4. Statistic Analyses. The data were statistically analyzed by the descriptive statistics and personal correlation coefficient. The significance was defined if the probability value (P) of a test is less than 0.05.

3. Results and Discussion

3.1. Results

3.1.1. Ionic Composition and Ion Concentrations in Atmospheric Deposition. The major cations and anions of ionic compositions were Na^+ and SO_4^{2-} in dry and wet atmospheric deposition in the YRD, respectively (Figure 2). The predominant cation in dry atmospheric deposition was Na^+ (71.34%), followed by Ca^{2+} (16.24%) and NH_4^+ (9.29%). These three cations accounted for more than 95% of the total cations in dry atmospheric deposition, while the total number of K^+ and Mg^{2+} was less than 5%. The major anions in dry atmospheric deposition were SO_4^{2-} and NO_3^-, which were more than 93% of the number of the total anions (Figure 2(a)). Ionic composition in wet atmospheric deposition was similar to that in dry deposition. Compared to the dry atmospheric deposition, the proportions of Ca^{2+} (30.42%) and NH_4^+ (14.26%) in wet atmospheric deposition were relative high. SO_4^{2-} constituted ~77.86% of the total cation numbers and was also the predominant anion in wet atmospheric deposition (Figure 2(b)).

The significant relations of the total number of anions and the total number of cations were observed in both dry atmospheric depositions ($P < 0.005$) and wet atmospheric depositions ($P < 0.0001$) (Figure 2). The correlation coefficients (R^2) were 0.86 and 0.80, respectively.

3.1.2. Monthly Variations of Atmospheric Nitrogen Depositions. The main type of nitrogen in dry deposition was NO_3^-–N (~57.21%). The maximum values of TIN and NO_3^-–N in dry atmospheric deposition were 139.99 mg m^{-2} and 113.89 mg m^{-2}, respectively, which was observed in May (Table 1 and Figure 3(a)). The main nitrogen in wet deposition was NH_4^+–N which accounted for ~56.51%. The high content of NH_4^+–N in wet deposition was observed from June to August when the rainfall was abundant (Figure 3(b)). There was a significant positive relationship between the content of NH_4^+–N in wet deposition and precipitation in the study ($R^2 = 0.90$). In addition, the fertilizer was widely used in this period. High temperature accelerated ammonia volatilization in wetland ecosystem and large quantity ammonia application caused the content of NH_4^+–N to increase. Therefore the peaks of precipitation (~297.3 mm) and the content of NH_4^+–N (452.24 mg m^{-2}) in wet deposition occurred simultaneously in August (Figure 3(b)). However the content of NO_3^-–N in wet deposition varied with precipitation was not obvious. During the study period, the contributions of NO_3^-–N and that of NH_4^+–N to total atmospheric deposition were ~48% and ~52%, respectively (Table 1).

The dry and wet atmospheric nitrogen depositions were ~32% and ~68% of the total atmospheric nitrogen deposition, respectively (Table 1). The content of nitrogen in dry deposition was the highest in May when the wind was strong in spring in the YRD. With the precipitation increasing and wind becoming weak in summer, the proportion of wet nitrogen deposition increased (Figure 4). When the peak of precipitation occurred in August, the content of wet nitrogen deposition achieved the maximum value (675.64 mg m^{-2}), of which the contribution reached 85.88%. With the precipitation decreasing dramatically from September, contribution of wet nitrogen deposition to the total atmospheric nitrogen deposition gradually declined (Figure 4). Further analysis revealed that there was significant positive relationship between nitrogen content in wet deposition and the precipitation ($R^2 = 0.82$) (Figure 5).

3.1.3. Contribution of Atmospheric Deposition for Soil Nitrogen. The average contents of NO_3^-–N and NH_4^+–N in topsoil (0–10 cm) were 493.49 mg m^{-2} and 822.36 mg m^{-2}, respectively (Table 2). The attribution rates of atmospheric

Table 1: The monthly variation of atmospheric nitrogen deposition.

Month	Dry deposition		Wet deposition		NO_3^-–N		NH_4^+–N		TIN (mg m^{-2})
	N content (mg m^{-2})	% of TIN	N content (mg m^{-2})	% of TIN	Content (mg m^{-2})	% of TIN	Content (mg m^{-2})	% of TIN	
May	139.99	53.68	120.79	46.32	178.55	68.47	82.23	31.53	260.78
Jun.	103.62	27.39	274.77	72.61	242.70	64.14	135.69	35.86	378.39
Jul.	119.84	30.04	279.03	69.96	175.42	43.98	223.44	56.02	398.87
Aug.	111.12	14.12	675.64	85.88	280.22	35.62	506.54	64.38	786.76
Sep.	77.70	41.99	107.34	58.01	97.72	52.81	87.32	47.19	185.03
Oct.	91.66	60.89	58.88	39.11	77.15	51.25	73.38	48.75	150.54
Nov.	81.00	77.98	22.88	22.02	32.37	31.17	71.50	68.83	103.87
Total	724.92	32.02	1539.32	67.98	1084.13	47.88	1180.11	52.12	2264.24

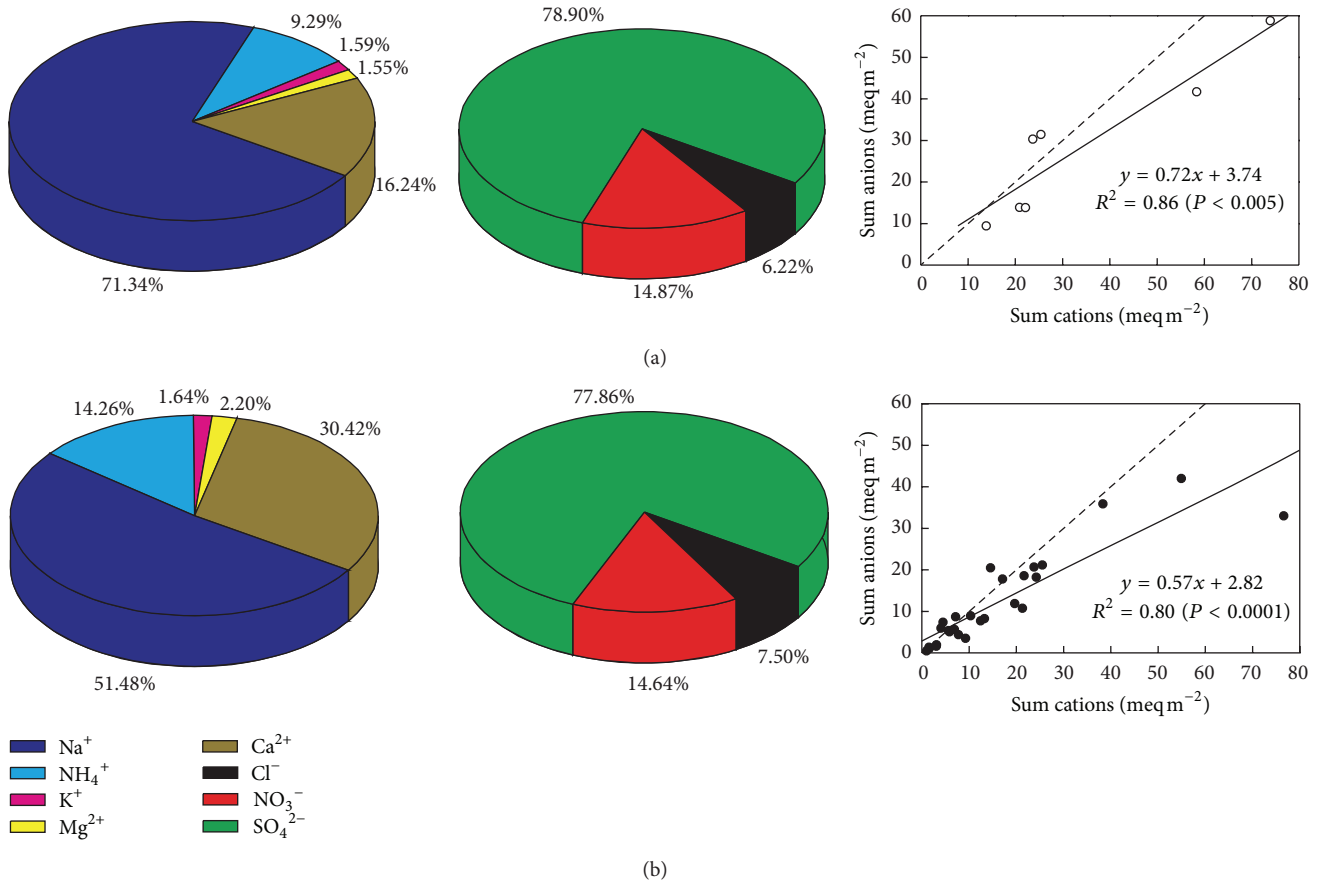

Figure 2: The percentage of water-soluble ions and the ionic balance in dry (a) and wet (b) atmospheric deposition.

NO_3^-–N and NH_4^+–N depositions ranged 3.73%–80.18% and 4.77%–77.47%, respectively. The maximum of attribution rates of atmospheric NO_3^-–N and NH_4^+–N deposition for that in topsoil both appeared in August (80.18% and 77.47%, resp.) (Table 2). The high attribution rates of atmospheric NO_3^-–N deposition for topsoil nitrogen reached 78.04% in May, while that of NH_4^+–N was the lowest (no more than 5%). On the contrary, the attribution rates of atmospheric NO_3^-–N deposition for topsoil nitrogen was the lowest in November (3.73%), while that of NH_4^+–N reached 20.83%. The average monthly attribution rates of atmospheric deposition of NO_3^-–N and NH_4^+–N for corresponding nitrogen in 0–10 cm soil layer in the plant growing season were about 31.38% and 20.50%, respectively (Table 2).

3.2. Discussions. The ionic composition of atmospheric depositions varied in different regions [12, 26, 31]; that is, Ca^{2+} and SO_4^{2-} were the most abundant cation and anion in urban Beijing [32] and Northern Italy [31]. By contrast, the predominant cation and anion in wet and dry atmospheric

Table 2: Atmospheric N deposition contributes to N inputs to local soil.

Month	Topsoil		Atmospheric deposition	
	NO_3^-–N (mg m^{-2})	NO_4^+–N (mg m^{-2})	% of NO_3^-–N content in topsoil	% of NO_4^+–N content in topsoil
May	228.78	1722.77	78.04	4.77
Jun.	706.59	976.09	34.35	13.90
Jul.	786.59	602.23	22.30	37.10
Aug.	349.47	653.89	80.18	77.47
Sep.	281.27	816.33	34.74	10.70
Oct.	234.77	641.91	32.86	11.43
Nov.	866.97	343.27	3.73	20.83
Average	493.49	822.36	31.38	20.50

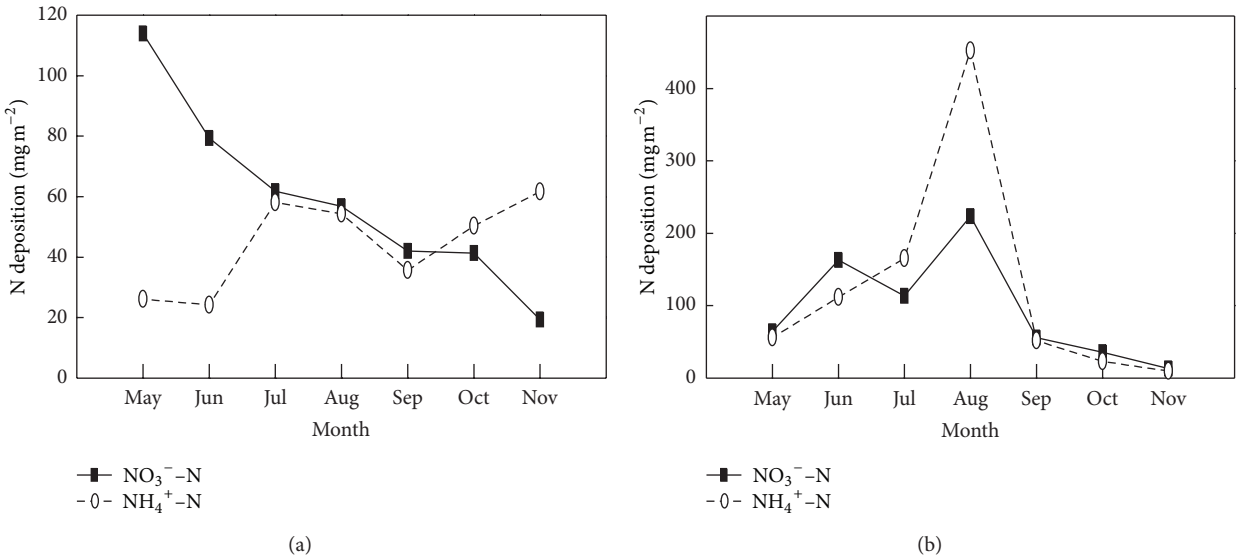

Figure 3: The monthly variations of NO_3^-–N and NH_4^+–N in dry (a) and wet (b) atmospheric depositions.

depositions in the YRD were Na^+ and SO_4^{2-}, respectively (Figure 2). It was closely related to that high salt content in fluvoaquic soil and saline soil which were widely distributed in the YRD [27, 33]. Our results showed that the most ratios of anions to cations in atmospheric deposition were less than 1, probably due to some anions such as F^-, Br^- and short chain organic anions were not measured in this study [34, 35].

The atmospheric nitrogen deposition has been of great concern since 1980s, mainly due to acid rain and its negative effect on ecosystem [36–38]. Previous studies reported that the atmospheric nitrogen deposition only in growing season (2264.24 mg N m^{-2}) was higher than total nitrogen deposition for the whole year [39]. To agree with that, a large amount of nitrogen deposition was received in coastal zone of the YRD from May to November (Table 1). The wet nitrogen deposition mainly occurred from June to August (Figure 4) because of precipitation (Figure 5). The wet atmospheric nitrogen deposition was more than 2 times of dry atmospheric nitrogen deposition in study region, which was similar with previous results in coastal zone of Barnegat Bay (>80%) [40].

Dentener and Crutzen [41] reported that anthropogenic emissions from domestic animals, fertilizer application, and biomass burning were thought to be the largest source of NH_4^+–N in atmospheric deposition. The monthly variations of atmospheric NH_4^+–N deposition results showed that both dry and wet atmospheric NH_4^+–N depositions were high in July and August (Figures 3(a) and 3(b)) when amount of fertilizer is applied for croplands. Another peak dry atmospheric NH_4^+–N deposition appeared in autumn (Figure 3(a)) probably because of the biomass burning in field. The dry atmospheric NO_3^-–N deposition was decreased from spring to autumn and the maximum values (113.89 mg m^{-2}) appeared in May (Figure 3(a)). Its reason is probably that the NO_3^-–N of dry atmospheric deposition was strongly influenced by petrochemical industrial pollution which is transferred by wind from Dongying city. However the high NO_3^-–N of wet atmospheric deposition occurring in August (Figure 3(b)) was much related precipitation (Figure 5). The similar results were also reported in several studies monitored at similar latitude in China [22, 42]. The seasonal variation of NH_4^+/NO_3^- ratio could reflect the deposited nitrogen source [43]. Compared with the developed region, the average NH_4^+/NO_3^- ratio in atmospheric nitrogen deposition in this study (~1.16) was much less than that in Beijing area and Liaohe River Plain of Northeast China [22, 43] and similar to that in

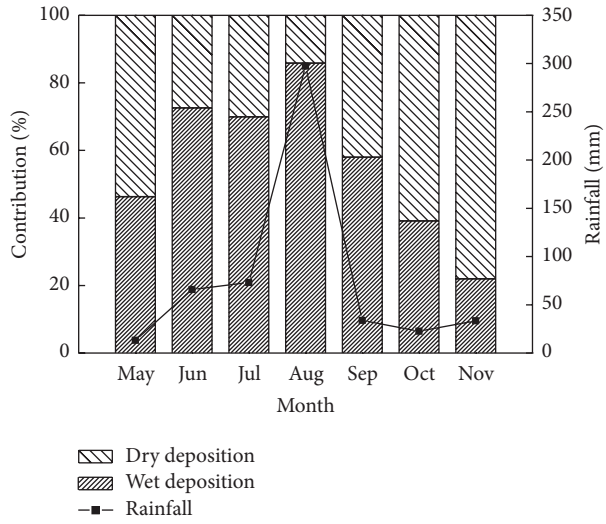

Figure 4: The variation of contributions of wet and dry deposition.

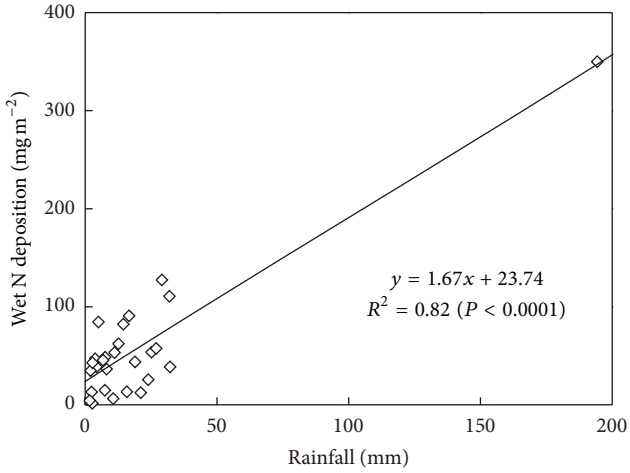

Figure 5: Relationship between precipitation and the content of nitrogen in wet deposition.

central New York [44] and Europe [11], suggested that the atmospheric nitrogen deposition in this region was affected by both agricultural activities and industrial activities.

Atmospheric nitrogen deposition has become a large source of nitrogen for terrestrial and aquatic ecosystems worldwide [7]. The total amount of nitrogen deposition and other environment-derived nitrogen in China was up to 18 Tg N year^{-1}, equal to approximately 60% of the national nitrogen fertilizer consumption [9]. Atmospheric inputs of bioavailable nitrogen represented an imbalanced contribution to the new production of 8–20% in the Mediterranean coast of Israel [45]. The average monthly attribution rates of atmospheric deposition of NO_3^-–N and NH_4^+–N were about 31.38% and 20.50% for the contents of NO_3^-–N and NH_4^+–N in 0–10 cm soil layer, respectively (Table 2), suggesting that the atmospheric nitrogen deposition was one of the main sources of soil nitrogen in coastal wetland ecosystem in the YRD.

4. Conclusions

The cation of Na^+ and anion of SO_4^{2-} were major ionic compositions in dry and wet atmospheric deposition in the YRD. There were the significant relations of the total number of anions and the total number of cations in both dry atmospheric depositions ($P < 0.005$) and wet atmospheric depositions ($P < 0.0001$), respectively. The main form of atmospheric nitrogen input was wet deposition which accounted for 67.98% of the total atmospheric nitrogen deposition. Both dry and wet atmospheric NH_4^+–N depositions were high in July and August. The NO_3^-–N of dry atmospheric deposition was decreased from spring to autumn. There was a significant positive relationship between wet atmospheric nitrogen deposition and precipitation. The average NH_4^+/NO_3^- ratio in atmospheric nitrogen deposition indicated that the atmospheric nitrogen deposition in this region was affected by both agricultural activities and industrial activities. Our results suggested that the atmospheric nitrogen deposition was one of the main sources of soil nitrogen in coastal wetland ecosystem in the YRD.

Conflict of Interests

The authors declare that there is no conflict of interests regarding the publication of this paper.

Acknowledgments

The authors are grateful for the support from the Project of National Science & Technology Pillar Program in "12th Five Year" period (2011BAC02B01), the National Natural Science Foundation for Distinguished Young Scholar of Shandong Province (no. JQ201114), and the CAS/SAFEA International Partnership Program for Creation Research Team. They thank the Yellow River Delta Ecology Research Station of Coastal Wetland, CAS, for the help of field work.

References

[1] J. D. Aber, K. J. Nadelhoffer, P. Steudler, and J. M. Melillo, "Nitrogen saturation in northern forest ecosystems," *Bioscience*, vol. 39, no. 6, pp. 378–386, 1989.

[2] N. J. P. Owens, J. N. Galloway, and R. A. Duce, "Episodic atmospheric nitrogen deposition to oligotrophic oceans," *Nature*, vol. 357, no. 6377, pp. 397–399, 1992.

[3] R. Bobbink, M. Hornung, and J. G. M. Roelofs, "The effects of air-borne nitrogen pollutants on species diversity in natural and semi-natural European vegetation," *Journal of Ecology*, vol. 86, no. 5, pp. 717–738, 1998.

[4] S. V. Krupa, "Effects of atmospheric ammonia (NH3) on terrestrial vegetation: a review," *Environmental Pollution*, vol. 124, no. 2, pp. 179–221, 2003.

[5] R. A. Duce, J. LaRoche, K. Altieri et al., "Impacts of atmospheric anthropogenic nitrogen on the open ocean," *Science*, vol. 320, no. 5878, pp. 893–897, 2008.

[6] N. Gruber and J. N. Galloway, "An Earth-system perspective of the global nitrogen cycle," *Nature*, vol. 451, no. 7176, pp. 293–296, 2008.

[7] J. N. Galloway, A. R. Townsend, J. W. Erisman et al., "Transformation of the nitrogen cycle: Recent trends, questions, and potential solutions," *Science*, vol. 320, no. 5878, pp. 889–892, 2008.

[8] P. A. Matson, W. H. McDowell, A. R. Townsend, and P. M. Vitousek, "The globalization of N deposition: ecosystem consequences in tropical environments," *Biogeochemistry*, vol. 46, no. 1–3, pp. 67–83, 1999.

[9] X. Liu, L. Song, C. He, and F. Zhang, "Nitrogen deposition as an important nutrient from the environment and its impact on ecosystems in China," *Journal of Arid Land*, vol. 2, no. 2, pp. 137–143, 2010.

[10] Q. G. Wang, S. B. Li, P. Jia, C. J. Qi, and F. Ding, "A review of surface water quality models," *Scientific World Journal*, vol. 2013, Article ID 231768, 7 pages, 2013.

[11] K. W. T. Goulding, N. J. Bailey, N. J. Bradbury et al., "Nitrogen deposition and its contribution to nitrogen cycling and associated soil processes," *New Phytologist*, vol. 139, no. 1, pp. 49–58, 1998.

[12] W. A. H. Asman, M. A. Sutton, and J. K. Schjørring, "Ammonia: emission, atmospheric transport and deposition," *New Phytologist*, vol. 139, no. 1, pp. 27–48, 1998.

[13] M. Griepentrog, S. Bode, P. Boeckx, F. Hagedorn, A. Heim, and M. W. I. Schmidt, "Nitrogen deposition promotes the production of new fungal residues but retards the decomposition of old residues in forest soil fractions," *Global Change Biology*, vol. 20, no. 1, pp. 327–340, 2014.

[14] J. B. Wang, T. C. Zhu, H. W. Ni, H. X. Zhong, X. L. Fu, and J. F. Wang, "Effects of elevated CO_2 and nitrogen deposition on ecosystem carbon fluxes on the sanjiang plain wetland in Northeast China," *PLoS ONE*, vol. 8, no. 6, 2013.

[15] W. Schroder, R. Pesch, S. Schonrock, H. Harmens, G. Mills, and H. Fagerli, "Mapping correlations between nitrogen concentrations in atmospheric deposition and mosses for natural landscapes in Europe," *Ecological Indicators*, vol. 36, pp. 563–571, 2014.

[16] N. B. Dise and R. F. Wright, "Nitrogen leaching from European forests in relation to nitrogen deposition," *Forest Ecology and Management*, vol. 71, no. 1-2, pp. 153–161, 1995.

[17] T. Endo, H. Yagoh, K. Sato et al., "Regional characteristics of dry deposition of sulfur and nitrogen compounds at EANET sites in Japan from 2003 to 2008," *Atmospheric Environment*, vol. 45, no. 6, pp. 1259–1267, 2011.

[18] M. E. Fenn, M. A. Poth, J. D. Aber et al., "Nitrogen excess in North American ecosystems: predisposing factors, ecosystem responses, and management strategies," *Ecological Applications*, vol. 8, no. 3, pp. 706–733, 1998.

[19] Y. Pan, Y. Wang, G. Tang, and D. Wu, "Wet and dry deposition of atmospheric nitrogen at ten sites in Northern China," *Atmospheric Chemistry and Physics*, vol. 12, no. 14, pp. 6515–6535, 2012.

[20] J. Cui, J. Zhou, Y. Peng, Y. Q. He, H. Yang, and J. D. Mao, "Atmospheric wet deposition of nitrogen and sulfur to a typical red soil agroecosystem in Southeast China during the ten-year monsoon seasons (2003–2012)," *Atmospheric Environment*, vol. 82, pp. 121–129, 2014.

[21] D. Lamb and J. van Bowersox, "The national atmospheric deposition program: an overview," *Atmospheric Environment*, vol. 34, no. 11, pp. 1661–1663, 2000.

[22] X. Liu, X. Ju, Y. Zhang, C. He, J. Kopsch, and Z. Fusuo, "Nitrogen deposition in agroecosystems in the Beijing area," *Agriculture, Ecosystems and Environment*, vol. 113, no. 1–4, pp. 370–377, 2006.

[23] A. F. Bouwman, L. J. M. Boumans, and N. H. Batjes, "Estimation of global NH_3 volatilization loss from synthetic fertilizers and animal manure applied to arable lands and grasslands," *Global Biogeochemical Cycles*, vol. 16, no. 2, 2002.

[24] D. G. Streets and S. T. Waldhoff, "Present and future emissions of air pollutants in China: SO_2, NO_x and CO," *Atmospheric Environment*, vol. 34, no. 3, pp. 363–374, 2000.

[25] Y. Jia, G. Yu, N. He et al., "Spatial and decadal variations in inorganic nitrogen wet deposition in China induced by human activity," *Scientific Reports*, vol. 4, Article ID 3763, 2014.

[26] F. Dentener, J. Drevet, J. F. Lamarque et al., "Nitrogen and sulfur deposition on regional and global scales: a multimodel evaluation," *Global Biogeochemical Cycles*, vol. 20, no. 4, Article ID GB4003, 2006.

[27] Q. He, B. S. Cui, X. S. Zhao, H. L. Fu, X. Xiong, and G. H. Feng, "Vegetation distribution patterns to the gradients of water depth and soil salinity in wetlands of Yellow River Delta, China," *Wetland Science*, vol. 5, no. 3, pp. 208–214, 2007.

[28] J. Shen, A. Tang, X. Liu, A. Fangmeier, K. T. W. Goulding, and F. S. Zhang, "High concentrations and dry deposition of reactive nitrogen species at two sites in the North China Plain," *Environmental Pollution*, vol. 157, no. 11, pp. 3106–3113, 2009.

[29] Y. Zhang, X. J. Liu, A. Fangmeier, K. T. W. Goulding, and F. S. Zhang, "Nitrogen inputs and isotopes in precipitation in the North China Plain," *Atmospheric Environment*, vol. 42, no. 7, pp. 1436–1448, 2008.

[30] J. Yu, X. Wang, K. Ning et al., "Effects of Salinity and Water Depth on Germination of Phragmites australis in Coastal Wetland of the Yellow River Delta," *Clean-Soil Air Water*, vol. 40, no. 10, pp. 1154–1158, 2012.

[31] R. Balestrini, L. Galli, and G. Tartari, "Wet and dry atmospheric deposition at prealpine and alpine sites in northern Italy," *Atmospheric Environment*, vol. 34, no. 9, pp. 1455–1470, 2000.

[32] Y. Y. Cai, F. M. Yang, K. B. He, Y. L. Ma, O. Tomoaki, and T. Shigeru, "Characteristics of water-soluble ions in dry deposition in urban Beijing," *China Environmental Science*, vol. 31, no. 7, pp. 1071–1076, 2011.

[33] J. Yu, Y. Li, G. Han et al., "The spatial distribution characteristics of soil salinity in coastal zone of the Yellow River Delta," *Environmental Earth Sciences*, 2013.

[34] F. Zhang, J. Zhang, H. Zhang, N. Ogura, and A. Ushikubo, "Chemical composition of precipitation in a forest area of Chongqing, Southwest China," *Water, Air, and Soil Pollution*, vol. 90, no. 3-4, pp. 407–415, 1996.

[35] R. Mosello and G. A. Tartari, "Formiate and acetate in wet deposition at Pallanza (NW Italy) in relation to major ion concentrations," *Water, Air, and Soil Pollution*, vol. 63, no. 3-4, pp. 397–409, 1992.

[36] N. van Breemen and H. F. G. van Dijk, "Ecosystem effects of atmospheric deposition of nitrogen in The Netherlands," *Environmental Pollution*, vol. 54, no. 3-4, pp. 249–274, 1988.

[37] E. D. Schulze, "Air pollution and forest decline in a spruce (Picea abies) forest," *Science*, vol. 244, no. 4906, pp. 776–783, 1989.

[38] S. E. Schwartz, "Acid deposition: unraveling a regional phenomenon," *Science*, vol. 243, no. 4892, pp. 753–763, 1989.

[39] Y. Luo, X. Yang, R. J. Carley, and C. Perkins, "Atmospheric deposition of nitrogen along the Connecticut coastline of Long Island Sound: a decade of measurements," *Atmospheric Environment*, vol. 36, no. 28, pp. 4517–4528, 2002.

[40] Y. A. Gao, "Atmospheric nitrogen deposition to Barnegat Bay," *Atmospheric Environment*, vol. 36, no. 38, pp. 5783–5794, 2002.

[41] F. Dentener and P. J. Crutzen, "A three-dimensional model of the global ammonia cycle," *Journal of Atmospheric Chemistry*, vol. 19, no. 4, pp. 331–369, 1994.

[42] Z. Fang and X. Zhao, "Dynamic changes of atmospheric nitrogen wet deposition in Qingdao," *Journal of Soil and Water Conservation*, vol. 27, no. 1, pp. 263–266, 2013.

[43] W. Yu, C. Jiang, Q. Ma, Y. Xu, H. Zou, and S. Zhang, "Observation of the nitrogen deposition in the lower Liaohe River Plain, Northeast China and assessing its ecological risk," *Atmospheric Research*, vol. 101, no. 1-2, pp. 460–468, 2011.

[44] T. J. Fahey, C. J. Williams, J. N. Rooney-Varga et al., "Nitrogen deposition in and around an intensive agricultural district in central New York," *Journal of Environmental Quality*, vol. 28, no. 5, pp. 1585–1600, 1999.

[45] B. Herut, M. D. Krom, G. Pan, and R. Mortimer, "Atmospheric input of nitrogen and phosphorus to the Southeast Mediterranean: sources, fluxes, and possible impact," *Limnology and Oceanography*, vol. 44, no. 7, pp. 1683–1692, 1999.

Hindawi Publishing Corporation
The Scientific World Journal
Volume 2014, Article ID 952051, 8 pages
http://dx.doi.org/10.1155/2014/952051

Research Article

Ecological Effects of Roads on the Plant Diversity of Coastal Wetland in the Yellow River Delta

Yunzhao Li,[1,2] Junbao Yu,[1] Kai Ning,[1,2] Siyao Du,[3] Guangxuan Han,[1] Fanzhu Qu,[1,2] Guangmei Wang,[1] Yuqin Fu,[1,2] and Chao Zhan[1,2]

[1] *Key Laboratory of Coastal Zone Environmental Processes and Ecological Remediation, Yantai Institute of Coastal Zone Research (YIC), Chinese Academy of Sciences (CAS) and Shandong Provincial Key Laboratory of Coastal Zone Environmental Processes, YICCAS, Yantai, Shandong 264003, China*
[2] *University of Chinese Academy of Sciences, Beijing 100049, China*
[3] *College of Environmental Science and Engineering, Ocean University of China, Qingdao, Shandong 266100, China*

Correspondence should be addressed to Junbao Yu; junbao.yu@gmail.com

Received 22 February 2014; Revised 14 March 2014; Accepted 14 March 2014; Published 31 March 2014

Academic Editor: Hong-bo Shao

The 26 sample sites in 7 study plots adjacent to asphalt road and earth road in coastal wetland in the Yellow River Delta were selected to quantify plant diversity using quadrat sampling method in plant bloom phase of July and August 2012. The indice of β_T and Jaccard's coefficient were applied to evaluate the species diversity. The results showed that the plant diversities and alien plants were high in the range of 0–20 m to the road verge. There were more exotics and halophytes in plots of asphalt roadside than that of earth roadside. However, proportion of halophytes in habitats of asphalt roadsides was lower than that of earth roadside. By comparing β-diversity, there were more common species in the asphalt roadsides than that in the earth roadsides. The similarity of plant communities in studied plots of asphalt roadsides and earth roadsides increased with increasing the distance to road verge. The effect range of roads for plant diversity in study region was about 20 m to road verge. Our results indicate that the construction and maintenance of roads in wetland could increase the plant species diversities of communities and risk of alien species invasion.

1. Introduction

Roads are common artificial infrastructures, but high density roads rarely appear in wetlands. However, the study interests of road ecology in the wetland are growing [1–3]. Construction and maintenance of roads have modified the natural wetland landscape and might result in many ecological effects (or ecological risks) [4–6]. Generally, there are six primary ecological effects of roads, that is, (1) habitat loss [7], (2) disturbance [8, 9], (3) corridor [10, 11], (4) mortality [12], (5) barrier [13], and (6) behavior modification [14–16]. The ecological effects of roads can be divided into effects in construction period and short term effects and long term effects in operation period [17, 18]. Therefore, it is difficult to evaluate accurately ecological effects of road on ecosystem because of comprehensive results [19–22]. The roads construction and existence have shown deleterious effects on a variety of ecosystems [1, 23, 24] and often noted by ecologists for their far-reaching negative consequences to ecosystem structures and flows [10, 22, 24–27]. Meanwhile, some road effects are beneficial to ecosystems though they are hard to confirm [22]. For example, ecologists have found that the positive feedbacks, for example, regional climate change, and the amount of forest fragmentation and deforestation directly related to the construction of roads [28, 29]. Actually, it is true that roads and roads edges provide resources for some species, particularly small mammals and insects [7, 17, 24]. In some cases, roads were found to have been acted as essential corridors for survival, movement, and propagation [7, 24, 30]. The wetland vegetation, one of the three most important elements of wetlands [31, 32], is greatly affected by the disturbance of road. The previous studies in the YRD reported that the high species richness and biodiversity were observed adjacent to the road verge [33]. Besides the distance from the road verge, the width, noise, vehicle traffic levels of road, and highway density also could influence the plant

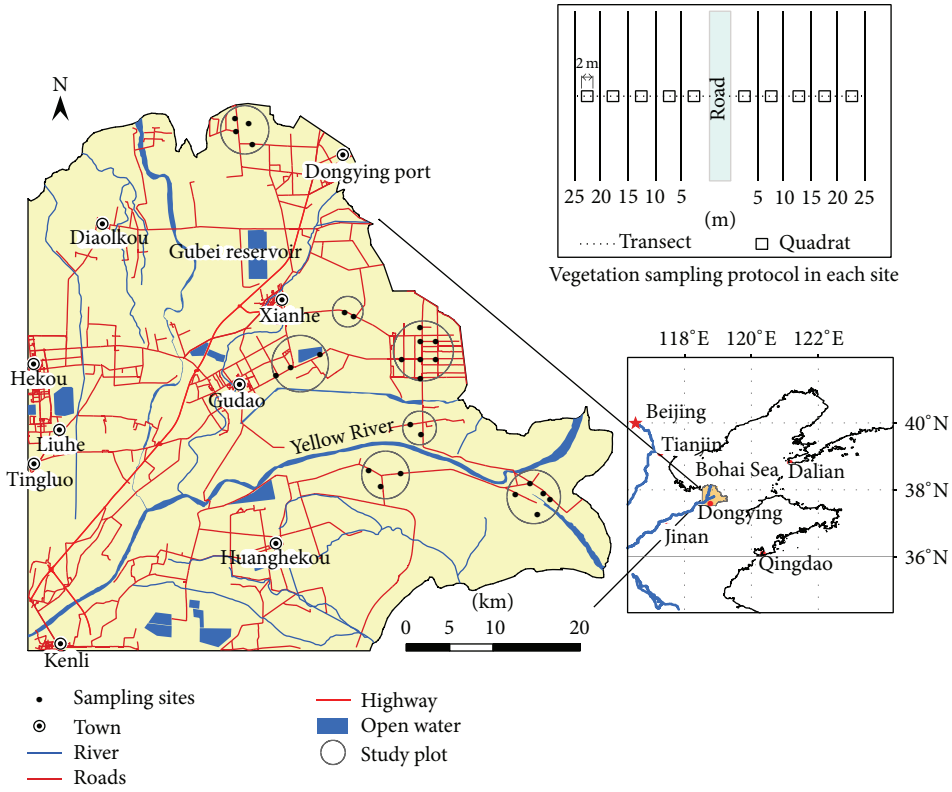

Figure 1: Location of the study area and sampling sites in the Yellow River Delta.

community anyway [4, 24, 34]. In addition, the natural wetland landscape and the water-salt migration in coastal wetland could be changed by road, which might result in changes of the environment of vegetation growth [23, 35, 36]. Previous studies reported that there was heavy metals accumulation in road verge soils, which might influence plants adjacent to road indirectly [37–40]. It was also believed that construction and maintenance of roads might alter nutrient levels, bulk density, and moisture of soils and led to a high soil concentration of nitrogen at roadside verges [41, 42]. Roads altered flows of materials in the landscape and changed levels of available resources, such as water, light, and nutrients of ecosystems [24], and thus affected the plant communities. Therefore, it could not be affirmed that the road effects are positive or not briefly before evaluating the road effects objectively as much as possible. To implement this objective, the YRD wetland was selected as a suitable place to evaluate the effects of road on vegetation distribution in coastal wetlands because the high density of roads was constructed for oil exploitation.

There are several types of roads, for example, asphalt road, cement road, and earth road for oil exploitation in the YRD wetland which is a short-formed and protogenous ecosystem with various kinds of wetland plants [43], resulting in dividing the wetland into patches. Our assumption is that the wetland plants might be impacted by different kinds of roads, resulting in differences of community composition and biodiversity appearing in verges of the different types of road. With this assumption, the wetland plant communities beside the road verges of asphalt road and earth road which were representative road types in the study region were surveyed using quadrat sampling method in plant bloom phase. The objectives of this study are to reveal (1) the composition changes of plant communities in the habitats adjacent to the asphalt roads and earth roads and (2) how the plant biodiversity is affected by roads.

2. Materials and Methods

2.1. Description of the Study Area. The study area is located in the YRD, eastern China (Figure 1). The regional climate is a temperate semihumid continental monsoon climate and the average annual precipitation in the study area is 530–630 mm, of which 70% is in the summer [44, 45]. Evaporation is strong and the ratio of evaporation to precipitation is about 3 : 1 [46]. The YRD is a flat floodplain with a plain slope of 0.0001 and an area less than 10 m in elevation [47]. Swamp and salt marsh are widespread in the study area and the predominant natural wetland plants are *Phragmites australis, Tamarix chinensis,* and *Suaeda salsa*. The oil exploitation is the major human activity in the natural wetland region where there are few settlements. There was about 2035.5 km of asphalt road built for oil exploitation from 1963 to 2002 in the YRD.

2.2. Sampling Sites and Methods. The 26 sample sites in 7 study plots adjacent to asphalt road and earth road in coastal wetlands were selected to quantify plant communities using

quadrat sampling method in plant bloom phase of July and August 2012 (Figure 1). The selected study plots were plain and far from human settlements and seashore as well as the Yellow River to weaken the impacts from slope, irrelevant human activities, the sea and river. By referring to the species-area curve established by Zeng et al. [33], the 2 m × 2 m quadrats were adopted for sampling. Two transects with opposite directions perpendicular to a selected road were made in each site. The five quadrats were arranged at 0–5 m, 5–10 m, 10–15 m, 15–20 m, and 20–25 m to the road verge in each transect (Figure 1). The presence, name, coverage, number, and dominance of all vascular plants were surveyed and recorded at each quadrat.

2.3. Data Analysis. To reveal the composition of wetland plant communities in the road verges, the proportion of halophytes and exotics in all plants was calculated. The occurrence frequencies of all recorded plants were compared to determine the most common species.

β-diversity, which is the variation in species composition among localities [48], was used to detect changes of communities in studied plots with distance to road verges. The indice of β_T which was described by Wilson and Shmida [49] was adopted to implement in this study:

$$\beta_T = \frac{[g(H) + l(H)]}{2\alpha}, \quad (1)$$

where $g(H)$ and $l(H)$ are the numbers of species gained and lost, respectively, along a (habitat) gradient and α is the average number of species found within the community samples.

The Jaccard's coefficient (J) which may be expressed in several ways [50] was used to compare the similarity of plants composition among localities:

$$J = \frac{c}{a + b - c}, \quad (2)$$

where c is the number of species common to both sites, a is the number of species in the first plot (with high species), and b is the number of species in the second plot (with low species).

In addition, independent-sample Student's t-test was used to evaluate the effects of regional disparity on number of species applying the software of SPSS 18.0 [51].

3. Results and Discussion

3.1. Comparison of Plant Species in the Asphalt Roadside and Earth Roadside. A total of 48 plant species with an incidence of 10–90% for eighteen species were found within 25 m to the roadsides during investigation (Table 1). The observed species belonged to 22 families. The best-represented families were Gramineae (8), Compositae (7), Chenopodiaceae (5), and Leguminosae (4). The most common species were *Phragmites australis* (Cav.) Trin. ex Steud., *Suaeda salsa* (L.) Pall., *Tamarix chinensis* Lour., *Sonchus oleraceus* L., *Artemisia argyi* Levl. et Van., and *Imperata cylindrica* (L.) Beauv.Eight species (17%) were identified as exotics and 36 (75%) as halophytes. The most abundant life form was herb, of which

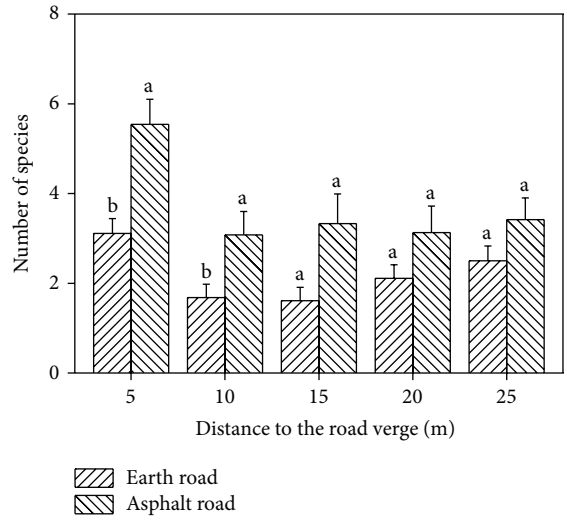

Figure 2: Number of species in plots of asphalt roadsides and earth roadsides. Letters above error bar of each column indicate significant difference at the $P < 0.05$ level for Student's t-test.

40 species (83%) were observed. The total observed plant species in this study was about half of previous identified results (100 species) in the same region [33, 52], because of the attributions of the different sampling sites location, roadside conditions, and anthropogenic impacts. The sampling sites in the previous study mainly located in both sides of truck road in the central part of the YRD where the conditions of soil and freshwater for plant were much better than those in present plots. In addition, some special plants were purposefully planted in truck road verges to maintain the roadbed and the high vehicle flow increased the spread of exotics, resulting in higher alien plants in previous study [33, 52] than this study. Agreeing with previous studies [33, 52, 53], the herbaceous plants with high proportion of halophytes were high and ligneous plants were few in the communities of roadsides in the YRD (Table 1).

The mean value of species in the asphalt roadside was larger than that in the earth roadside regardless of distance from road verges (Figure 2). The differences of number of species were significant within 0–10 m from road edge between the earth road and the asphalt road (Figure 2). Generally, the number of exotics decreased with distance increase to the road edge and those in asphalt roadside were greater than that in earth roadside regardless of distance from road verge (Figure 3). 24 (80%) and 30 (77%) halophytes were found in the earth road verge and the asphalt road verge, respectively (Table 1). The number of halophytes in the asphalt roadside was greater than that in the earth roadside. However, the proportion of halophytes in all plant species in the asphalt roadside was smaller than that in the earth roadside (Figure 4). The differences of environment and the anthropogenic activities of the asphalt roadside and earth roadside were mainly responsible for the plant species difference. The truck numbers and human being activities in the asphalt road are much more than the earth road. Based on the survey results, the vehicle traffic flow in asphalt roads

Table 1: List of plant species distributed in roadsides (range of 25 m) of the Yellow River Delta during our investigation.

Species	Family	Plots of earth roadside	Plots of asphalt roadside	Halophyte	Exotics	Life form
Amaranthus retroflexus	Amaranthaceae		Y			Herb
Amaranthus viridis	Amaranthaceae	Y	Y	Y	Y	Herb
Rhus typhina L.	Anacardiaceae		Y		Y	Arbor
Apocynum venetum L.	Apocynaceae	Y	Y	Y		Shrub
Metaplexisjaponica (Thunb.) Makino	Asclepiadaceae	Y		Y		Liane
Cynanchum chinense R. Br.	Asclepiadaceae	Y	Y	Y		Liane
Atriplex centralasiatica Iljin	Chenopodiaceae	Y		Y		Herb
Chenopodium hybridum L.	Chenopodiaceae	Y		Y	Y	Herb
Suaeda salsa (L.) Pall.	Chenopodiaceae	Y	Y	Y		Herb
Suaeda glauca (Bunge) Bunge	Chenopodiaceae	Y	Y	Y		Herb
Kochiascoparia (L.) Schrad.	Chenopodiaceae	Y		Y		Herb
Cirsium maackii Maxim.	Compositae		Y			Herb
Taraxacum mongolicum Hand.-Mazz.	Compositae		Y	Y		Herb
Artemisia argyi Levl. et Van.	Compositae	Y	Y	Y		Herb
Scorzonera mongolica Maxim.	Compositae		Y	Y		Herb
Artemisia capillaris	Compositae	Y		Y		Herb
Sonchus oleraceus L.	Compositae	Y	Y	Y		Herb
Dendranthema indicum (L.) Des Moul.	Compositae	Y	Y	Y		Herb
Pharbitis nil (L.) Choisy	Convolvulaceae		Y	Y		Herb
Convolvulus arvensis L.	Convolvulaceae		Y		Y	Herb
Cuscuta chinensis Lam.	Convolvulaceae	Y	Y	Y	Y	Cancerroot
Cyperus rotundus L.	Cyperaceae	Y				Herb
Carex tristachya Thunb.	Cyperaceae	Y	Y			Herb
Ephedra sinica Stapf	Ephedraceae Dumortier		Y	Y		Herb
Imperata cylindrica (L.) Beauv.	Gramineae	Y	Y	Y		Herb
Triarrhena sacchariflora (Maxim.) Nakai	Gramineae	Y				Herb
Setaria viridis (L.) Beauv.	Gramineae		Y	Y		Herb
Chloris virgata Sw.	Gramineae		Y	Y		Herb
Alopecurus aequalis Sobol.	Gramineae	Y				Herb
Phragmites australis (Cav.) Trin. ex Steud.	Gramineae	Y	Y	Y		Herb
Aeluropus sinensis (Debeaux) Tzvel.	Gramineae	Y	Y	Y		Herb
Calamagrostis epigeios (L.) Roth	Gramineae		Y	Y		Herb
Leonurus artemisia (Laur.) S. Y. Hu	Labiatae		Y	Y		Herb
Melilotus officinalis	Leguminosae		Y	Y	Y	Herb
Robinia pseudoacacia	Leguminosae		Y			Arbor
Medicago sativa L.	Leguminosae	Y	Y	Y		Herb
Glycine soja Sieb. et Zucc.	Leguminosae	Y	Y	Y		Herb
Humulus scandens	Moraceae	Y	Y	Y		Herb
Epilobium hirsutum L.	Onagraceae	Y	Y	Y		Herb
Limonium bicolor (Bag.) Kuntze	Plumbaginaceae	Y		Y		Herb
Polygonum orientale L.	Polygonaceae		Y	Y		Herb
Polygonum lapathifolium L.	Polygonaceae	Y	Y			Herb
Portulaca oleracea L.	Portulacaceae		Y	Y		Herb
Salix matsudana	Salicaceae	Y	Y			Arbor
Veronica didyma Tenore	Scrophulariaceae		Y		Y	Herb
Datura stramonium Linn.	Solanaceae		Y	Y	Y	Herb
Tamarix chinensis Lour.	Tamaricaceae	Y	Y	Y		Shrub
Typha orientalis	Typhaceae	Y	Y	Y		Herb

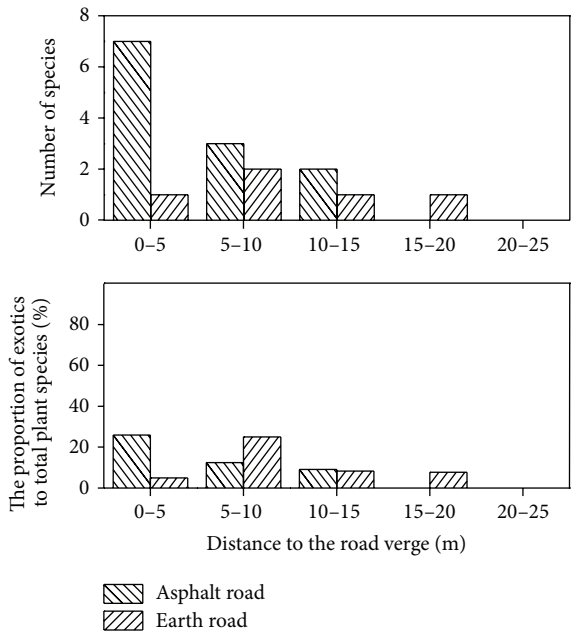

Figure 3: Number and proportion of alien plant species in plots of asphalt roadsides and earth roadsides.

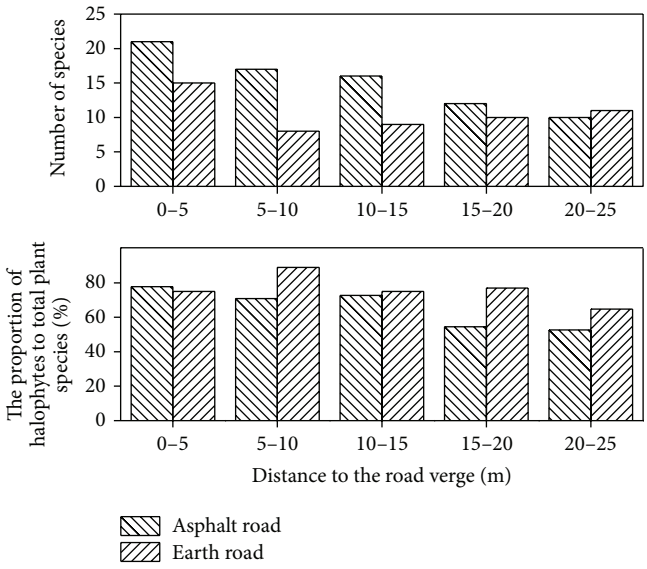

Figure 4: Number and proportion of halophytes in plots of asphalt roadsides and earth roadsides.

was about 5–8 times higher than that in earth roads, resulting in both the native and the alien plants species in the plots of asphalt roadside being more abundant than that of the earth roadside within a certain distance from sampling site to road (Figures 2 and 3). Furthermore, in order to protect the road and avoid soil-water loss, the vegetation beside the asphalt road was removed first, and then different species of trees and bushes were planted. The removal of habitats and vegetation were soon replaced by new settlers, resulting in more edges in landscape and more niches in communities in the asphalt roadside [4, 18, 54].

3.2. Effects of Roads on Plant Communities. Roads increased the contacts between plant communities [24] and the anthropogenic activities near roadsides had great impacts on species [3, 4]. In this study, there were 39 species, of which thirty-two species (82%) were categorized as herbs (Table 1) and were found in 24 sampling transects in the asphalt roadsides, while there were 30 species of which 24 species (80%) were grassland species and were observed in 28 sampling transects in the earth roadsides (Table 1). Additionally, three and seven alien plants were found near the earth roadside and the asphalt road verge, respectively (Table 1). The exotics accounted for no more than 30% of total plants in both asphalt roadside and earth roadside (Figure 3). With the distance to the road edge being increased, the numbers of both saline plants and their proportion in all plants decreased (Figure 4). The results were similar to some previous study results [33, 41, 52]. The road was regarded as dispersal corridor and conduit for vegetation [24, 30, 55–57]. It is believed that roads promoted the dispersal of plant propagules along roadsides [33]. Because of the easy movement of wind, water runoff, and animals by roads, the numerous seeds were carried and deposited along roads by those carriers [4, 58]. Therefore, plants with high dispersal capacities could preferentially occupy their living spaces along roadsides [56, 59, 60]. Furthermore, the dispersal of native and alien plants was affected directly by the vehicle traffic flow and vectors. Roadsides do provide better growth conditions and are good habitat to vegetation [61, 62]. Construction and maintenance of road altered the physical and chemical environment of plant communities [4, 5]. The alterations of light conditions, soil nutrients, and water availability were remunerative for plant communities, thus increasing the survival opportunities for most plants [61, 62]. Additionally, the elevation of most roadbeds was 1-2 meters higher than that of around wetlands in the YRD, which was a great benefit in salt reducing. The areas of roadsides have become refuges to many nonhalophytes. As a result, both native and alien plant species in roadsides were more abundant than wetland far away from road verge and the proportion of halophytes in the road verges was much lower than in wetland habitats (Table 1 and Figure 4).

3.3. Diversity of Plant Communities in Roadside. The variation of β_T index showed different patterns between asphalt roadside and earth roadside (Figure 5 and Table 2). The β_T index of the plant communities decreased gradually with distance to road verge in the spots adjacent to asphalt road. While the variation of β_T showed an inverse "N" shape with the distance from plant communities to earth roadside, increased the β_T index in study sites adjacent to earth roadside was larger than that adjacent to asphalt roadside within 20 meters to road verge (Figure 5). The similarity of communities was completely different between the spots of asphalt roadside and earth roadside (Figure 5). The Jaccard's coefficient gradually increased with increase of

Table 2: Matrix of β-diversity indices measured by numerical data from sampling sites.

Distance of sampling sites from road (m)	0–5	5–10	10–15	15–20	20–25
Asphalt roadside					
0–5	×	0.4581	0.5445	0.5751	0.5672
5–10		×	0.3361	0.5408	0.5308
10–15			×	0.3949	0.4494
15–20				×	0.3291
20–25					×
Earth roadside					
0–5	×	0.4946	0.5403	0.5342	0.5242
5–10		×	0.4639	0.6117	0.6082
10–15			×	0.4753	0.4689
15–20				×	0.2362
20–25					×

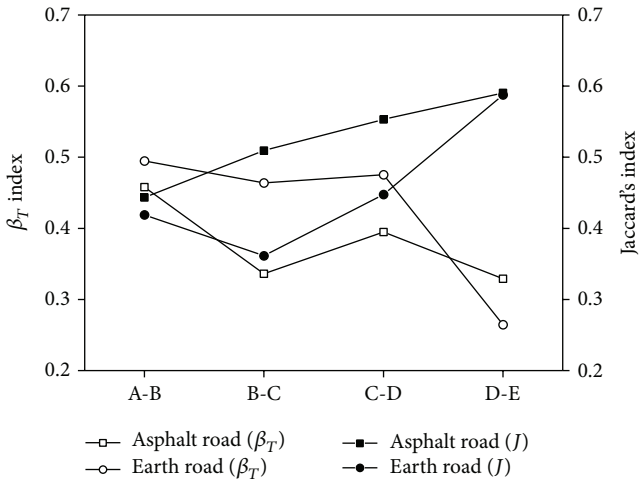

Figure 5: Characteristic of β_T index and Jaccard's coefficient in plots of the asphalt roadsides and earth roadsides. A: plant communities in plots of 0–5 m to road verge; B: plant communities in plots of 5–10 m to road verge; C: plant communities in plots of 10–15 m to road verge; D: plant communities in plots of 15–20 m to road verge; E: plant communities in plots of 20–25 m to road verge.

the distance from study plot to roadside in the asphalt road verge. However, The Jaccard's coefficient of plant communities in the earth roadside decreased originally and then increased with the distance from study plots to earth roadside increasing (Figure 5). The values of the Jaccard's coefficient in the study plots adjacent to earth roadside were smaller than that adjacent to asphalt roadside within 20 meters from road verge (Figure 5). As soon as the distances of study plots to roadside were more than 20 m, the values of the Jaccard's coefficient in the plots of earth roadside were approximate to that in the asphalt roadside (Figure 5). Our results indicated that both β_T index and Jaccard's coefficient, which provide different but equally illuminating views of biodiversity [63, 64], were adopted in this study. The β_T of plant communities in roadsidetended to decrease, while Jaccard's coefficient increased, with the distance increasing from sampling plots to road verge in asphalt roadsides (Figure 5). Some previous studies indicated that construction and maintenance of roads did a lot of negative effects to plant communities [24, 65, 66] because most communities were destroyed during construction of roads, leaving few survival plants. The patterns of β_T and Jaccard's coefficient indicated low ebb in plant communities within 5 to 15 m of earth roadsides (Figure 5). Actually, during investigation and sampling, the bare land and open water were the most common landscape types in 5 to 15 m away from earth in the YRD. While the sampling sites were more than 20 m away from road verges, the plant communities in both asphalt roadsides and earth roadsides indicated little differences.

4. Conclusions

The biodiversity of plant communities are deeply affected by roads in the YRD. The high plant species, especially exotics, was observed in the range of 0–20 m to the road verge. There were more plant species and exotics in the asphalt roadsides than that in the earth roadsides. However, the proportion of halophytes in plant communities in the earth roadsides was higher than that in the asphalt roadsides. The analysis results of β-diversity showed that there were more common species in the asphalt roadsides than that in the earth roadsides. The similarity of plant communities in studied plots of asphalt roadsides and earth roadsides increased with the increasing distance to road verge. The effected distance of roads on plant diversity was limited within 20 m to road verge. Our results indicate that the construction and maintenance of roads in wetland could increase the plant species diversities of communities and risk of alien species invasion.

Conflict of Interests

The authors declare that there is no conflict of interests regarding the publication of this paper.

Authors' Contribution

Yunzhao Li, Kai Ning, and Junbao Yu contributed equally to this work.

Acknowledgments

The authors are grateful for support from the Project of National Science & Technology Pillar Program in "12th Five Year" period (2011BAC02B01 and 2012BAC19B08), the National Natural Science Foundation for Distinguished Young Scholar of Shandong Province (JQ201114), and the CAS/SAFEA international partnership program for creation research team. The authors thank the Yellow River Delta Ecology Research Station of Coastal Wetland, CAS, for the help in field work.

References

[1] C. S. Findlay and J. Bourdages, "Response time of wetland biodiversity to road construction on adjacent lands," *Conservation Biology*, vol. 14, no. 1, pp. 86–94, 2000.

[2] F. S. Bernardino Jr. and G. H. Dalrymple, "Seasonal activity and road mortality of the snakes of the Pa-Hay-Okee wetlands of Everglades National Park, USA," *Biological Conservation*, vol. 62, no. 2, pp. 71–75, 1992.

[3] C. Scott Findlay and J. Houlahan, "Anthropogenic correlates of species richness in southeastern Ontario wetlands," *Conservation Biology*, vol. 11, no. 4, pp. 1000–1009, 1997.

[4] R. T. T. Forman and L. E. Alexander, "Roads and their major ecological effects," *Annual Review of Ecology and Systematics*, vol. 29, pp. 207–231, 1998.

[5] S. C. Trombulak and C. A. Frissell, "Review of ecological effects of roads on terrestrial and aquatic communities," *Conservation Biology*, vol. 14, no. 1, pp. 18–30, 2000.

[6] J. L. Frair, E. H. Merrill, H. L. Beyer, and J. M. Morales, "Thresholds in landscape connectivity and mortality risks in response to growing road networks," *Journal of Applied Ecology*, vol. 45, no. 5, pp. 1504–1513, 2008.

[7] R. E. Brock and D. A. Kelt, "Influence of roads on the endangered Stephens' kangaroo rat (*Dipodomys stephensi*): are dirt and gravel roads different?" *Biological Conservation*, vol. 118, no. 5, pp. 633–640, 2004.

[8] L. L. Kerley, J. M. Goodrich, D. G. Miquelle, E. N. Smirnov, H. B. Quigley, and M. G. Hornocker, "Effects of roads and human disturbance on Amur tigers," *Conservation Biology*, vol. 16, no. 1, pp. 97–108, 2002.

[9] A. Pauchard and P. B. Alaback, "Influence of elevation, land use, and landscape context on patterns of alien plant invasions along roadsides in protected areas of south-central Chile," *Conservation Biology*, vol. 18, no. 1, pp. 238–248, 2004.

[10] R. W. Tyser and C. A. Worley, "Alien flora in grasslands adjacent to road and trail corridors in Glacier National Park, Montana, (USA)," *Conservation Biology*, vol. 6, no. 2, pp. 253–262, 1992.

[11] L. A. Tigas, D. H. van Vuren, and R. M. Sauvajot, "Behavioral responses of bobcats and coyotes to habitat fragmentation and corridors in an urban environment," *Biological Conservation*, vol. 108, no. 3, pp. 299–306, 2002.

[12] R. L. Mumme, S. J. Schoech, G. E. Woolfenden, and J. W. Fitzpatrick, "Life and death in the fast lane: demographic consequences of road mortality in the Florida Scrub-Jay," *Conservation Biology*, vol. 14, no. 2, pp. 501–512, 2000.

[13] C. K. Dodd Jr., W. J. Barichivich, and L. L. Smith, "Effectiveness of a barrier wall and culverts in reducing wildlife mortality on a heavily traveled highway in Florida," *Biological Conservation*, vol. 118, no. 5, pp. 619–631, 2004.

[14] P. F. Develey and P. C. Stouffer, "Effects of roads on movements by understory birds in mixed-species flocks in Central Amazonian Brazil," *Conservation Biology*, vol. 15, no. 5, pp. 1416–1422, 2001.

[15] A. Seiler, "Ecological effects of roads: a review," *Introductory Research Essay*, vol. 9, pp. 1–40, 2001.

[16] M. Bhattacharya, R. B. Primack, and J. Gerwein, "Are roads and railroads barriers to bumblebee movement in a temperate suburban conservation area?" *Biological Conservation*, vol. 109, no. 1, pp. 37–45, 2002.

[17] B. Deckers, P. de Becker, O. Honnay, M. Hermy, and B. Muys, "Sunken roads as habitats for forest plant species in a dynamic agricultural landscape: effects of age and isolation," *Journal of Biogeography*, vol. 32, no. 1, pp. 99–109, 2005.

[18] I. F. Spellerberg, "Ecological effects of roads and traffic: a literature review," *Global Ecology and Biogeography Letters*, vol. 7, no. 5, pp. 317–333, 1998.

[19] Lyon, "Road effects and impacts on wildlife and fisheries," in *Proceedings of the Forest Transportation Symposium*, USDA Forest Service, Casper, Wyo, USA, 1985.

[20] R. Elvik, "To what extent can theory account for the findings of road safety evaluation studies?" *Accident Analysis & Prevention*, vol. 36, no. 5, pp. 841–849, 2004.

[21] L. Ries, R. J. Fletcher Jr., J. Battin, and T. D. Sisk, "Ecological responses to habitat edges: mechanisms, models, and variability explained," *Annual Review of Ecology, Evolution, and Systematics*, vol. 35, pp. 491–522, 2004.

[22] A. E. Lugo and H. Gucinski, "Function, effects, and management of forest roads," *Forest Ecology and Management*, vol. 133, no. 3, pp. 249–262, 2000.

[23] J. A. Jones, F. J. Swanson, B. C. Wemple, and K. U. Snyder, "Effects of roads on hydrology, geomorphology, and disturbance patches in stream networks," *Conservation Biology*, vol. 14, no. 1, pp. 76–85, 2000.

[24] A. W. Coffin, "From roadkill to road ecology: a review of the ecological effects of roads," *Journal of Transport Geography*, vol. 15, no. 5, pp. 396–406, 2007.

[25] W. E. Rickard Jr. and J. Brown, "Effects of vehicles on arctic tundra," *Environmental Conservation*, vol. 1, no. 1, pp. 55–62, 1974.

[26] L. W. Carr and L. Fahrig, "Effect of road traffic on two amphibian species of differing vagility," *Conservation Biology*, vol. 15, no. 4, pp. 1071–1078, 2001.

[27] L. Fahrig, J. H. Pedlar, S. E. Pope, P. D. Taylor, and J. F. Wegner, "Effect of road traffic on amphibian density," *Biological Conservation*, vol. 73, no. 3, pp. 177–182, 1995.

[28] W. F. Laurance and G. Bruce Williamson, "Positive feedbacks among forest fragmentation, drought, and climate change in the Amazon," *Conservation Biology*, vol. 15, no. 6, pp. 1529–1535, 2001.

[29] T. Enoki, B. Kusumoto, S. Igarashi, and K. Tsuji, "Stand structure and plant species occurrence in forest edge habitat along different aged roads on Okinawa Island, southwestern Japan," *Journal of Forest Research*, vol. 19, no. 1, pp. 97–104, 2014.

[30] H. J. W. Vermeulen, "Corridor function of a road verge for dispersal of stenotopic heathland ground beetles Carabidae," *Biological Conservation*, vol. 69, no. 3, pp. 339–349, 1994.

[31] L. M. Cowardin and F. C. Golet, "US Fish and Wildlife Service 1979 wetland classification: a review," *Vegetatio*, vol. 118, no. 1-2, pp. 139–152, 1995.

[32] L. M. Cowardin, *Classification of Wetlands and Deepwater Habitats of the US*, Diane Publishing, Washing, DC, USA, 1979.

[33] S.-L. Zeng, T.-T. Zhang, Y. Gao et al., "Effects of road age and distance on plant biodiversity: a case study in the Yellow River Delta of China," *Plant Ecology*, vol. 212, no. 7, pp. 1213–1229, 2011.

[34] P. G. Angold, "The impact of a road upon adjacent heathland vegetation: effects on plant species composition," *Journal of Applied Ecology*, vol. 34, no. 2, pp. 409–417, 1997.

[35] T. Qin, *Landscape Analysis of Yellow River Delta Based on Road Network—A Case Study of Dongying City*, Shandong Agricultural University, Ji'nan, China, 2012.

[36] S. Godefroid and N. Koedam, "The impact of forest paths upon adjacent vegetation: effects of the path surfacing material

on the species composition and soil compaction," *Biological Conservation*, vol. 119, no. 3, pp. 405–419, 2004.

[37] T.-W. Wang, C.-F. Cai, Z.-X. Li, Z.-H. Shi, and G.-H. Liu, "Simulation of distribution pattern of heavy metals in road verge soils using neural network; a case study of modern Yellow River Delta," *Acta Ecologica Sinica*, vol. 29, no. 6, pp. 3154–3162, 2009.

[38] C. Pagotto, N. Rémy, M. Legret, and P. Le Cloirec, "Heavy metal pollution of road dust and roadside soil near a major rural highway," *Environmental Technology*, vol. 22, no. 3, pp. 307–319, 2001.

[39] A. Christoforidis and N. Stamatis, "Heavy metal contamination in street dust and roadside soil along the major national road in Kavala's region, Greece," *Geoderma*, vol. 151, no. 3-4, pp. 257–263, 2009.

[40] X. J. Zuo, D. F. Fu, and H. Li, "Variation characteristics of mercury in speciation during road runoff for different rainfall patterns," *Clean: Soil, Air, Water*, vol. 41, no. 1, pp. 69–73, 2013.

[41] N. A. Auerbach, M. D. Walker, and D. A. Walker, "Effects of roadside disturbance on substrate and vegetation properties in arctic tundra," *Ecological Applications*, vol. 7, no. 1, pp. 218–235, 1997.

[42] A. M. Truscott, S. C. F. Palmer, G. M. McGowan, J. N. Cape, and S. Smart, "Vegetation composition of roadside verges in Scotland: the effects of nitrogen deposition, disturbance and management," *Environmental Pollution*, vol. 136, no. 1, pp. 109–118, 2005.

[43] F.-Y. Wang, R.-J. Liu, X.-G. Lin, and J.-M. Zhou, "Arbuscular mycorrhizal status of wild plants in saline-alkaline soils of the Yellow River Delta," *Mycorrhiza*, vol. 14, no. 2, pp. 133–137, 2004.

[44] X. Zhang, S. Ye, P. Yin, and D. Chen, "Characters and successions of natural wetland vegetation in Yellow River Delta," *Ecology and Environmental Sciences*, vol. 18, no. 1, pp. 292–298, 2009.

[45] H. Fang, G. Liu, and M. Kearney, "Georelational analysis of soil type, soil salt content, landform, and land use in the Yellow River Delta, China," *Environmental Management*, vol. 35, no. 1, pp. 72–83, 2005.

[46] Y. Guan, G. Liu, and J. Wang, "Regionalization of salt-affected land for amelioration in the Yellow River Delta based on GIS," *Acta Geographica Sinica*, vol. 56, no. 2, pp. 198–205, 2001.

[47] C. Shi, L. You, B. Li, Z. Zhang, and O. Zhang, "Natural consolidation of deposits and its consequences at the Yellow River Delta," *Scientia Geographica Sinica*, vol. 23, no. 2, pp. 174–181, 2003.

[48] R. H. Whittaker, "Evolution and measurement of species diversity," *Taxon*, vol. 21, pp. 213–251, 1972.

[49] M. V. Wilson and A. Shmida, "Measuring beta diversity with presence-absence data," *Journal of Ecology*, vol. 72, no. 3, pp. 1055–1064, 1984.

[50] R. Real and J. M. Vargas, "The probabilistic basis of Jaccard's index of similarity," *Systematic Biology*, vol. 45, no. 3, pp. 380–385, 1996.

[51] R. Carver and J. G. Nash, *Doing Data Analysis with SPSS: Version 18.0*, Cengage Learning, Singapore, 2011.

[52] Z. Li, H. Wang, S. Liu, G. Song, and J. Gao, "Analysis about the biodiversity of Yellow River Delta," *Ecology and Environment*, vol. 15, no. 3, pp. 577–582, 2006.

[53] S. Zhu, W. Wang, Y. Wang, and K. Shan, "Wetland restoration and biodiversity conservation in the Yellow River Delta Nature Reserve," *Journal of Beijing Foresty University*, vol. 33, no. 2, pp. 1–5, 2011.

[54] C. H. Greenberg, S. H. Crownover, and D. R. Gordon, "Roadside soils: a corridor for invasion of xeric scrub by nonindigenous plants," *Natural Areas Journal*, vol. 17, no. 2, pp. 99–109, 1997.

[55] P. M. Tikka, H. Högmander, and P. S. Koski, "Road and railway verges serve as dispersal corridors for grassland plants," *Landscape Ecology*, vol. 16, no. 7, pp. 659–666, 2001.

[56] J. L. Gelbard and J. Belnap, "Roads as conduits for exotic plant invasions in a semiarid landscape," *Conservation Biology*, vol. 17, no. 2, pp. 420–432, 2003.

[57] Q. Tang, G. F. Liang, X. L. Lu, and S. Y. Ding, "Effects of corridor networks on plant species composition and diversity in an intensive agriculture landscape," *Chinese Geographical Science*, vol. 24, no. 1, pp. 93–103, 2014.

[58] W. M. Lonsdale and A. M. Lane, "Tourist vehicles as vectors of weed seeds in Kakadu National Park, Northern Australia," *Biological Conservation*, vol. 69, no. 3, pp. 277–283, 1994.

[59] S. L. Flory and K. Clay, "Invasive shrub distribution varies with distance to roads and stand age in eastern deciduous forests in Indiana, USA," *Plant Ecology*, vol. 184, no. 1, pp. 131–141, 2006.

[60] S. F. McCracken and M. R. J. Forstner, "Oil Road effects on the anuran community of a high canopy Tank Bromeliad (*Aechmea zebrina*) in the upper Amazon Basin, Ecuador," *PLoS ONE*, vol. 9, no. 1, Article ID e85470, 2014.

[61] R. Z. Watkins, J. Chen, J. Pickens, and K. D. Brosofske, "Effects of forest roads on understory plants in a managed hardwood landscape," *Conservation Biology*, vol. 17, no. 2, pp. 411–419, 2003.

[62] L. A. Parendes and J. A. Jones, "Role of light availability and dispersal in exotic plant invasion along roads and streams in the H.J. Andrews Experimental Forest, Oregon," *Conservation Biology*, vol. 14, no. 1, pp. 64–75, 2000.

[63] C. A. Lozupone, M. Hamady, S. T. Kelley, and R. Knight, "Quantitative and qualitative β diversity measures lead to different insights into factors that structure microbial communities," *Applied and Environmental Microbiology*, vol. 73, no. 5, pp. 1576–1585, 2007.

[64] G. Stirling and B. Wilsey, "Empirical relationships between species richness, evenness, and proportional diversity," *American Naturalist*, vol. 158, no. 3, pp. 286–299, 2001.

[65] I. Keller, W. Nentwig, and C. R. Largiadèr, "Recent habitat fragmentation due to roads can lead to significant genetic differentiation in an abundant flightless ground beetle," *Molecular Ecology*, vol. 13, no. 10, pp. 2983–2994, 2004.

[66] J. L. Gelbard and S. Harrison, "Roadless habitats as refuges for native grasslands: interactions with soil, aspect, and grazing," *Ecological Applications*, vol. 13, no. 2, pp. 404–415, 2003.